7th LARGE IGNEOUS PROVINCES CONFERENCE
AUG 28 - SEPT 8, 2019
TOMSK, RUSSIA

7-th International Science Conference

Large Igneous Provinces

THROUGH EARTH HISTORY: MANTLE PLUMES, SUPERCONTINENTS, CLIMATE CHANGE, METALLOGENY AND OIL-GAS, PLANETARY ANALOGUES

Tomsk, Russia, 28-th August – 8-th September 2019



Abstract Volume

МИНИСТЕРСТВО НАУКИ И ВЫСШЕГО ОБРАЗОВАНИЯ РОССИЙСКОЙ ФЕДЕРАЦИИ

НАЦИОНАЛЬНЫЙ ИССЛЕДОВАТЕЛЬСКИЙ

ТОМСКИЙ ГОСУДАРСТВЕННЫЙ УНИВЕРСИТЕТ

Attraction of the leading scientists to Russian institutions of higher learning, research organizations of the governmental academies of sciences, and governmental research centers of the Russian Federation

7th LARGE IGNEOUS PROVINCES CONFERENCE
SEPTEMBER 2-5, 2019
TOMSK, RUSSIA

25 YEARS RFBR

Laboratory of Geochronology and Geodynamics
Tomsk State University

LARGE IGNEOUS PROVINCES THROUGH EARTH HISTORY: MANTLE PLUMES, SUPERCONTINENTS, CLIMATE CHANGE, METALLOGENY AND OIL-GAS, PLANETARY ANALOGUES (LIP – 2019)

Abstract volume of the 7 International Conference
Tomsk, Russia, 28 August – 8 September 2019

КРУПНЫЕ ИЗВЕРЖЕННЫЕ ПРОВИНЦИИ В ИСТОРИИ ЗЕМЛИ: МАНТИЙНЫЕ ПЛЮМЫ, СУПЕРКОНТИНЕНТЫ, КЛИМАТИЧЕСКИЕ ИЗМЕНЕНИЯ, МЕТАЛЛОГЕНИЯ, ФОРМИРОВАНИЕ НЕФТИ И ГАЗА, ПЛАНЕТЫ ЗЕМНОЙ ГРУППЫ (КИП – 2019)

Тезисы VII Международной конференции
Томск, Россия 28 августа – 8 сентября 2019

УДК 552.3
ББК Д342.56

Large Igneous Provinces through earth history: mantle plumes, supercontinents, climate change, metallogeny and oil-gas, planetary analogues. Abstract volume of the 7 International Conference. Tomsk: CSTI Publishing house, 2019. 204 c.

For specialists in the field of geology, tectonics, mineralogy, geochronology, petrology, mineralogy, geochemistry, climatology.

Abstracts are presented in the original edition.

The conference was supported by the Government of the Russian Federation (project 14.Y26.31.0012), grants of RFBR (project 19-05-20130).

Scientific Editors: Ernst R.E., Vrublevskii V.V., Gladkochub D.P., Gertner I.F., Dobretsov N.L., Izokh A.E., Krasnova T.S., Kruk N.N., Kuzmin M.I., Tishin P.A., Tsygankov A.A., Chernyshov A.I.

Крупные изверженные провинции в истории земли: мантийные плюмы**, суперконтиненты, климатические изменения, металлогения, формирование нефти и газа, планеты земной группы.** Тезисы 7 Международной конференции. Томск: Изд-во Томского ЦНТИ, 2019. 204 с.

Для специалистов в области геологии, тектоники, минерагении, геохронологии, петрологии, минералогии, геохимии, климатологии.

Материалы представлены в авторской редакции.

Конференция поддержана грантами Правительства Российской Федерации (проект № 14. Y26.31.0012) и Российского фонда фундаментальных исследований (проект № 19-05-20130).

Редакционная коллегия: Эрнст Р.Э., Врублевский В.В., Гладкочуб Д.П., Гертнер И.Ф., Добрецов Н.Л., Изох А.Э., Краснова Т.С., Крук Н.Н., Кузьмин М.И., Тишин П.А., Цыганков А.А., Чернышов А.И.

ISBN 978-5-89702-456-8
DOI 10.17223/9785897024568

Dear colleges!

We welcome you to the 7th International Large Igneous Provinces (LIP) conference, at Tomsk State University, Tomsk, Siberia, Russia. We continue the tradition that began in 2007 in Novosibirsk, of gathering every two years to discuss the latest in LIPs research. Subsequent conferences were in Novosibirsk, Russia (2009), Irkutsk, Russia (2011), Hanoi, Vietnam (2013), Irkutsk, Russia (2015), Chengdu, China (2017). The initial conferences focused on the LIP record of Asia, but the focus shifted to the global LIP record, starting with the 2017 conference. This current 7th International LIPs conference has more than 158 delegates from 12 different countries and the topics cover the full breadth of modern LIPs research.

Welcome to beautiful and exciting Siberia, and for those of you attending a field trip, you will see the natural beauty firsthand. Welcome to Tomsk, a lovely and impressive university town with 6 universities and 100,000 students, representing over 20% of the population. Welcome to Tomsk State University, the host for the conference, and an esteemed classical university founded in 1878.

For our international delegates, if this is your first time to Siberia, we are sure you will be back again. For all our delegates, Russian and international we wish you productive interactions with each other, leading to new and expanded collaborations in the rapidly growing field of LIPs.

28 August 2019, Russia, Tomsk
Regards, Organizing Committee

Дорогие коллеги!

Мы рады приветствовать вас на 7-ой Международной конференции «Крупные изверженные провинции» (КИП), которая проходит в Томском государственном университете, (Томск, Сибирь, Россия). Мы продолжаем традицию, которая началась в 2007 году в Новосибирске. Предыдущие конференции проходили в Новосибирске, Россия (2009 г.), Иркутске, Россия (2011 г.), Ханое, Вьетнам (2013 г.), Иркутске, Россия (2015 г.), Чэнду, Китай (2017 г.). На большинстве этих мероприятий обсуждались результаты изучения КИП в Азии, но начиная с конференции 2017 года акцент сместился на глобальный тренд исследований КИП. 7-я Международная конференция собрала более 150 делегатов из 12 стран мира. Тематика докладов отражает весь спектр современных исследований КИП.

Добро пожаловать в красивую и завораживающую Сибирь! Для тех из вас, кто принимает участие в экскурсиях, будет возможность воочию увидеть естественную красоту этого края. Добро пожаловать в Томск, прекрасный университетский город, где в 6 университетах обучаются 100 000 студентов, что составляет около 20 % населения. Добро пожаловать в классический Томский государственный университет, основанный в 1878 году.

Для наших международных участников, если вы впервые в Сибири, мы уверены, что вы вернетесь снова. Мы желаем нашим участникам, как российским, так и международным, плодотворного взаимодействия друг с другом, новых совместных проектов и расширению сотрудничества в быстро растущей области исследований КИП.

28 августа 2019, Россия, Томск
С уважением, Организационный комитет

RECONSTRUCTING PRIMARY KIMBERLITE MELT COMPOSITIONS: INSIGHTS FROM MELT INCLUSIONS

Abersteiner A.[1], Kamenetsky V. S.[1,3], Goemann K.[2], Kamenetsky M.[1]

[1]*University of Tasmania, Hobart, Australia*
[2]*Central Science Laboratory, Hobart, Australia*
[3]*Institute of Experimental Mineralogy RAS, Chernogolovka, Russia*

Introduction

Kimberlites represent some of rarest and most volumetrically insignificant manifestations of igneous rocks, where they originate from deepest derived (>150km) mantle magmas. This deep origin in conjunction with their intermittent relationship with diamonds and mantle xenoliths renders kimberlites an invaluable tool for examining the composition and nature of the subcontinental lithospheric mantle. However, reconstructing the composition of primary kimberlite melts is challenging, as kimberlite rocks are no longer considered to be representative of the original melts that were generated at depth. This is due to: i) assimilation and entrainment of mantle and crustal xenoliths and wall-rock interaction during ascent and emplacement, ii) volatile (H_2O, CO_2) exsolution and degassing, iii) magma differentiation, and iv) syn- and post-magmatic alteration (i.e. serpentinisation). Therefore, elucidating kimberlite melt compositions is an essential step in understanding their petrogenesis.

This study presents a summary of detailed petrographic, geochemical and melt/fluid inclusion data of relatively well-preserved coherent kimberlites from localities worldwide (South Africa, Russia, Canada, Finland). New insights into the composition and evolution of kimberlitic melts prior to post-magmatic processes, which shows that kimberlite rocks originated from silicate-carbonate or even carbonatitic melts that were more enriched in alkalis/alkali-earths and halogens.

Methodology

Samples were prepared as thin sections and polished epoxy mounts using kerosene as a lubricant to avoid the dissolution of water soluble minerals. Mineralogical, textural and inclusion analyses were untaken using optical microscopy, scanning electron microscope (SEM) equipped with an energy-dispersive X-ray spectrometer (EDS), as well as electron microprobe (EMP) and Raman spectrometry at the Central Science Laboratory (CSL) at the University of Tasmania.

Results

To circumvent the effects of secondary alteration in kimberlite rocks, which is pervasive in the majority of studied samples, analyses of different generations (primary, pseudosecondary and secondary) of multiphase melt inclusions entrapped in various xenocrystic (e.g., olivine, Cr-diopside, picroilmenite) and magmatic (olivine, spinel, perovskite, monticellite, apatite and carbonates) minerals was conducted. Although melt inclusions are extremely heterogeneous in daughter mineral assemblages, there were consistently shown across all localities and studied minerals to be composed of Ca-Mg- and Na-K-Ba-Sr- carbonates, Na-K-chlorides, F-bearing halides, phosphates, sulphates/sulphides and oxides. In contrast, silicate minerals are rare or absent.

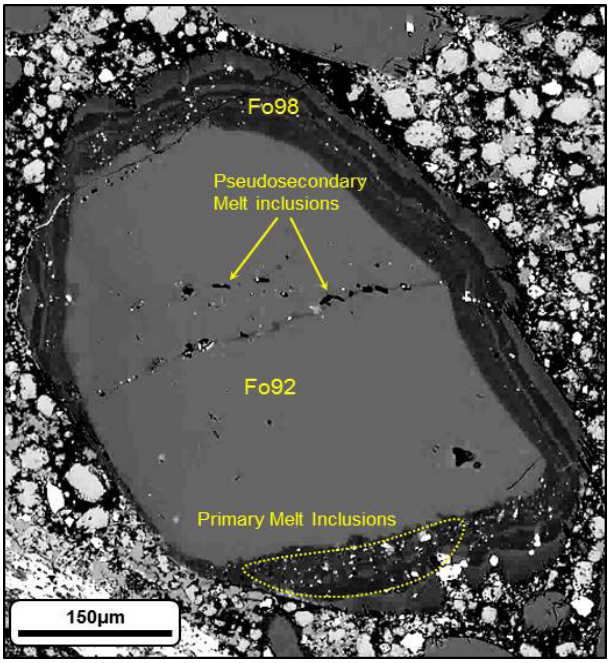


Figure 1. Back-scatter electron (BSE) image of an olivine phenocryst with an Mg-rich rind and primary and pseudosecondary melt inclusions.

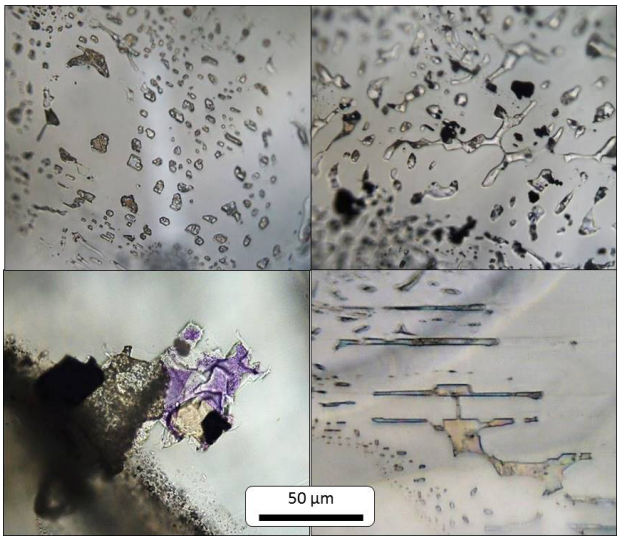


Figure 2. Transmitted light image of inclusions in olivine.

Conclusions

The combined study of melt inclusions in xenocrystic and magmatic kimberlitic minerals from localities worldwide have all demonstrated a consistent trend, which shows that they interacted and/or entrapped a variably differentiated aluminosilicate- and H_2O-poor, Ca-Mg-, halogen- (F, Cl) and alkali- (Na, K) bearing melt, that contained varying amounts of alkali-earths (Ba, Sr), phosphorus and sulphur (Kamenetsky et al., 2004, 2012; Abersteiner et al., 2018). This composition may be a more suitable candidate for primary/parental kimberlite melt compositions, as opposed to the classical 'ultramafic and H_2O-bearing' model which is based on whole-rock analyses, which are unable to fully discern numerous contamination processes or the loss of phases during emplacement (e.g., le Roex et al., 2003).

Experimental studies have similarly suggested that kimberlite melts must have originally contained much lower SiO_2 contents and higher abundances of carbonates. A carbonate-rich kimberlite melt model may assist in explaining certain aspects rheological aspects of petrogenesis, such as fast magma ascent rates and relatively low temperatures of crystallization.

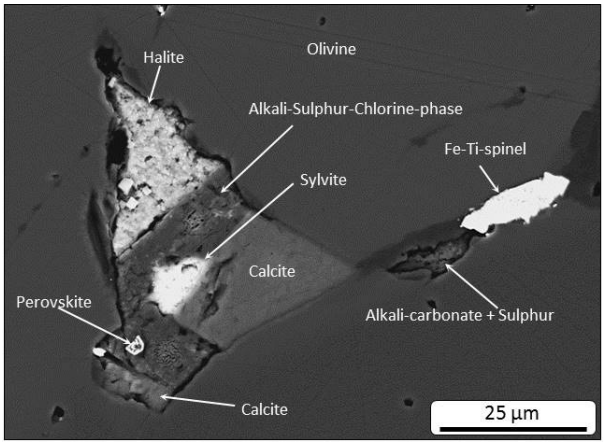


Figure 2. BSE image of a multiphase melt inclusion in olivine.

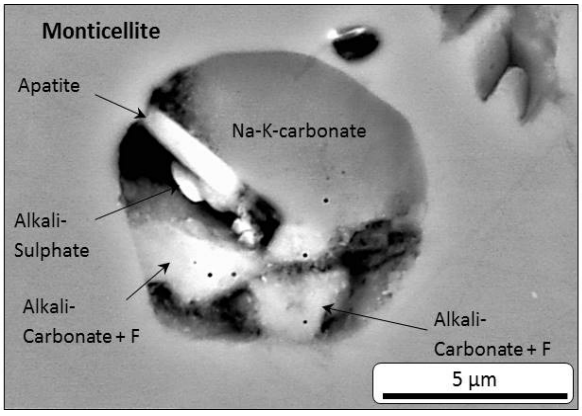


Figure 3. BSE image of a multiphase melt inclusion in monticellite.

The instability and rapid degradation of many of these daughter minerals hosted in studied melt inclusions (e.g., alkali-carbonates and chlorides) upon exposure to water or the atmosphere may explain their paucity in the kimberlite groundmass. It is likely that any water-soluble alkali-carbonate or chloride phase that crystallised in the kimberlite groundmass was subsequently removed by infiltrating serpentinising fluids, similar to the rapid mineralogical changes that occur in freshly erupted natrocarbonatite lavas, such as at Oldoinyo Lengai (Zaitsev and Keller, 2006), or alternatively these components were exsolved during emplacement.

Acknowledgements

This study and was supported by an Australian Postgraduate Award (APA) and the Max Banks Research

Scholarship in Earth Sciences. This work was supported by funding from the Institute of Volcanology and Seismology, Far East Branch, Russian Academy of Sciences.

References

1. Abersteiner, A., Kamenetsky, V. S., Golovin, A. V., Goemann, K., Kamenetsky, M. (2019) Was crustal contamination involved in the formation of the serpentine-free Udachnaya-East kimberlite? New insights into parental melts, liquidus assemblage and effects of alteration. Journal of Petrology 59:1467-1492.
2. Brooker, R., Sparks, R., Kavanagh, J., Field, M. (2011) The volatile content of hypabyssal kimberlite magmas: some constraints from experiments on natural rock compositions. Bulletin of Volcanology 73, 959-981.
3. Kamenetsky, M.B., Sobolev, A.V., Kamenetsky, V.S., Maas, R., Danyushevsky, L.V., Thomas, R., Pokhilenko, N.P., Sobolev, N.V. (2004) Kimberlite melts rich in alkali chlorides and carbonates: A potent metasomatic agent in the mantle. Geology 32:845-848.
4. Kamenetsky, V.S., Kamenetsky, M.B., Golovin, A.V., Sharygin, V.V., Maas, R. (2012) Ultrafresh salty kimberlite of the Udachnaya-East pipe (Yakutia, Russia): A petrological oddity or fortuitous discovery? Lithos 152:173-186.
5. le Roex, A.P., Bell, D.R., Davis, P. (2003) Petrogenesis of Group I Kimberlites from Kimberley, South Africa: Evidence from Bulk-rock Geochemistry. Journal of Petrology 44:2261-2286.
6. Zaitsev, A., Keller, J. (2006) Mineralogical and chemical transformation of Oldoinyo Lengai natrocarbonatites, Tanzania. Lithos 91:191-207.

PRELIMINARY DATA ON THE CONNECTION OF THE CA. 150 MA LIPS WITH THE BAZHENOV FORMATION (WESTERN SIBERIA)

Afonin I. V.[1], Tishin P. A.[1], Hitarova A. V.[1], Ernst R. E.[1,2], Kudamanov A. V.[3]

[1] *Tomsk State University, Tomsk, Russia*
[2] *Carleton University, Ottawa, Canada*
[3] *Tyumen Petroleum Research Center LLC, Tyumen, Russia*

Keywords: *Bazhenov suite, black shales, LIP, Western Siberia*

Introduction

During the Phanerozoic eon, there are periods of oceanic ecological crisis (Ernst et al., 2017; Jenkyns, 2010; Kerr, 1998; Meyer et al., 2008), the so-called Oceanic Anoxic Events (OAE), which are characterized by low oxygen content or its complete absence in the surface and bottom layers of the waters of the sedimentation basins. The appearance of OAEs is associated with the activity of the LIPs (Jones et al., 2016; Self et al., 2015) and is determined by three main parameters: the volume of gas release, its composition (H_2O, CO_2, CH_4, SO_2, and halogens) and the height of the gas ejection. The larger the event, the greater the climatic and the environmental change. It is noted in the work of Wignall (2001), that perhaps the duration of short-term impulses that extend up to single volcanic streams is more important than the overall volume of LIP volcanism.

OAEs are clearly identified by the accumulation of black shale strata that emphasize reductive, oxygenless environments (Kerr, 1998). Except for the fundamental aspect, black shale is connected with a practical one — their oil and gas potential.

Almost every manifestation of black shale in the Phanerozoic eon is comparable to the activity of the LIP (Jenkyns, 2010; Ernst and Youbi, 2017; Zhang et al., 2018). Kimmeridgian oil and gas fields aged 155-146 Ma (Kerr, 1998) haves an age correlation with the Sorachi plateau in the western Pacific ocean (Kimura et al., 1994), the Shatsky Rise (Ernst et al., 2017; Heydolph et al., 2014; Sager et al., 2013), and the NW Australian margin event (Rohrman, 2013; Ernst, 2014).

The Bazhenov suite was formed in the close age range (152-145 million years ago) in Western Siberia, which suggests a connection with the above described events. The suite is a group of oil-source rocks composed of carbonate, clay and siliceous formations. The object of the study was the hydrocarbon deposit of the Krasnoleninsky arch (Khanty-Mansiysk). Within the deposit, sediments of the Bazhenov suite were sampled by 4 wells up to 40 m.

The main research methods were petrography (210 samples), XRF (414 samples) and XRD (414 samples). Analytical work was carried out in the Geodynamics and Geochronology Laboratory of Tomsk State University.

Results

According to the results of the multi-disciplinary studies, a four-member structure of the Bazhenov suite was established. The boundaries between the members were identified by significant changes in the physical and chemical parameters of the sedimentation basin waters. Each of the identified cycles (packs) is characterized by clear divides and is emphasized by the identified petrographic, mineralogical and petrochemical associations.

The base of the section is composed of siliceous-clay and carbonate-clay-silica rocks (1st pack), which are characterized by mineralogical (clay-quartz, carbonate-clay-quartz associations with minor pyrite contents) and petrochemical (aluminum-silicon and calcium-aluminum-silicon) associations. The formation of this section fragment took place in normal sea conditions in the outlying shelf environments.

The second pack is composed of clay-siliceous rocks with thin carbonate interlayers (clay-quartz and aluminum-silicon associations). The divide between the first and second packs is clearly traced by the appearance of barite, ichthyodetrite interlayer (local peaks of phosphorus oxide content) and a tuff layer in the section. These signs indicate the activity of the LIPs. This is expressed in the flow of sulfur dioxide (sulphate minerals) and carbon in the marine basin. The changes in the chemistry of the basin waters led to the decrease of various forms of life, and as a result ichthiodetrite accumulations were formed (mass death). Thus, the formation of the second pack took place under the conditions of the shelf zone in the basin, saturated with sulfur oxide and carbon, due to the activity of LIPs.

The third pack is represented by carbonate-clay-siliceous rocks and clay dolomites (calcite-clay-quartz and calcium-aluminum-silicon associations). The divide of the third pack corresponds to the appearance in the sections of the thick carbonate layer, which has at predominant calcite composition. Massive and abrupt precipitation of carbonate minerals is caused by strong contamination of the basin waters by carbon dioxide. Sulfate minerals are also noted, this may show that the SO_2 content abruptly increases in the environment of sedimentation. An increase of these gases content in water may be a consequence of active volcanic activity (Brand et al., 2015; Ernst and Youbi, 2017; Ganino et al., 2010). Also significant concentrations of ichthyodetritis are often associated with sections of sulphates, which indicates the mass death of marine organisms (Ernst and Youbi, 2017). Thus, a change in pH and Eh of water mode may be the result of significant climate change due to the activity of LIPs. After the formation of the carbonate pack is completed, a reduction of the acid-base and redox balance (short-term) of the sedimentation basin water is noted. During this period, normal-marine clay-siliceous rocks accumulate again.

The upper part of the suite (4th pack) is represented mainly by clay-siliceous rocks with a high content of organic matter and pyrite (pyrite-clay-quartz and sulfur-iron-aluminum-silicon associations). This indicates anoxic sedimentation conditions with a significant enrichment of organic matter (possibly

increasing the concentration of CH_4 in the waters) and with significant hydrogen sulfide contamination (the flow of SO_2 and H_2S) (Brand et al., 2015; Ernst and Youbi, 2017). The divide separating the third and fourth packs is determined by the layer containing the fragments of andesites. The combination of the facts of the presence of a volcanic layer and the strong reducing conditions of formation make it possible to quite clearly recognize the activity of LIPs at this time.

Conclusion

On the basis of the conducted studies, direct signs of volcanic activity were established — tuff interlayers and layers with andesitic fragments. Given the significant stratigraphic dissociation of these finds in the section, it is assumed that the activity of LIPs was of a pulsating nature. Another variant is the existence of several LIPs in the time of Bazhenov suite formation, which is emphasized by the various conditions of the formation of the selected packs.

Thus, it can be concluded that at the time of the Bazhenov suite the active LIP has existed (possibly the Sorachi (Kimura et al., 1994), Shatsky Rise (Sager et al., 2013; Heydolph et al., 2014; Ernst et al., 2017), Okhotsk (Bogdanov et al., 2002), Magellan Rise (Ernst and Youbi, 2017), Southeast African (Gohl et al., 2011), NW Australian Margin (Rohrman, 2013; Ernst, 2014), which had a strong effect on the lower and upper layers of the atmosphere (The Okhotsk and Magellan Rises, both being oceanic LIPs would also have a direct effect on ocean water compoisition), which resulted in climate change and, as a result, physical and chemical parameters of sedimentation basin, which is reflected in the accumulated sediment.

Acknowledgements

This work was conducted as a government task of the Ministry of Science and Higher Education of the Russian Federation, Project No. 5.9336.2017/P220.

References

1. Bogdanov N.A., Dobretsov N.L. (2002) The Okhotsk volcanic oceanic plateau. Russian Geology and Geophysics 43:87-99
2. Brand U., Blamey N.J.F., Griesshaber E., Posenato R., Angiolini L., Azmy K., Farabegoli E., Came R.E., (2015) Methane hydrate: killer cause of Earth's greatest mass extinction. Palaeoworld 25:496-507
3. Ernst R.E. (2014) Large Igneous Provinces. Cambridge University Press., 653 p.
4. Ernst R.E., Youbi N. (2017) How Large Igneous Provinces affect global climate, sometimes cause mass extinctions, and represent natural markers in the geological record. Palaeogeography, Palaeoclimatology, Palaeoecology 478:30–52
5. Ganino C., Arndt N.T. (2010) Climate changes caused by degassing of sediments during the emplacement of large igneous provinces: reply. Geology 38:211
6. Gohl K., Uenzelmann-Neben G., Grobys N. (2011) Growth and dispersal of a Southeast African large igneous province. South African Journal of Geology 114: 379-386
7. Heydolph K., Murphy D.T., Geldmacher J., Romanova I.V., Greene A., Hoernle K., Weis D., Mahoney J. (2014) Plume versus plate origin for the Shatsky Rise oceanic plateau (NW Pacific): insights from Nd, Pb and Hf isotopes. Lithos:49–63
8. Jenkyns H.C. (2010) Geochemistry of Oceanic Anoxic Events. Geochemistry, Geophysics Geosystems 11:23–33
9. Kerr A.C (1998) Oceanic plateau formation: a cause of mass extinction and black shale deposition around the Cenomanian–Turonian boundary. Journal of the Geological Society 155:619–626
10. Kimura G., Sakakibara M., Okamura M. (1994) Plumes in central Panthalassa? Deductions from accreted oceanic fragments in Japan. Tectonics 13:905–916
11. Meyer K.M., Kump L.R. (2008) Oceanic euxinia in Earth history: causes and consequences. Earth and Planetary Science Letters 36:251-288
12. Rohrman M. (2013) Intrusive large igneous provinces below sedimentary basins: An example from the Exmouth Plateau (NW Australia) Journal of Geophysical Research: Solid Earth 118:1–11
13. Sager W.W., Zhang J.C., Korenaga J., Sano T., Koppers A.A.P., Widdowson M., Mahoney J.J. (2013) An immense shield volcano within the Shatsky Rise oceanic plateau, north- west Pacific Ocean. Nature Geoscience 6:976–981.
14. Self S., Glaze L.S., Schmidt A., Mather T.A. (2015) Volatile release from flood basalt eruptions: understanding the potential environmental effects. Volcanism and Global Environmental Change 11:164–176
15. Wignall P.B. (2001) Large igneous provinces and mass extinctions. Earth Sci. Rev. 53:1–33
16. Zhang S-H., Ernst R.E., Pei J-L., Zhao Y., Zhou M-F., Hu G-H. (2018) A temporal and causal link between ~1380 Ma large igneous provinces and black shales: Implications for the Mesoproterozoic time-scale and paleoenvironment. Geology 46: 963-966

500 MILLION YEARS OF VOLCANISM AND SEDIMENTATION ON THE NEOARCHAEAN TO EARLY PALAEOPROTEROZOIC KAAPVAAL CRATON: THE VENTERSDORP, ONGELUK AND HEKPOORT LIPS

Altermann W., Humbert F., de Kock M.

University of Johannesburg, Geology Department, UPPM Group, PO Box 524 Auckland Park, Johannesburg, 2006, South Africa

Keywords: *Volcano-Sedimentary Sequences, South African LIPS, Archean and Proterozoic Rifts*

Introduction

The petrologic and geochemical properties of magmatic rocks of the Neoarchaean Ventersdorp Supergroup and the early Palaeoproterozoic Ongeluk and Hekpoort formations show astonishing similarities over the enormous time span of more than 500 million years (myr). Moreover, these Large Igneous Provinces represent episodes of widespread continental magmatism and cratonic-epeiric basin sedimentation (Eriksson et al. 2006; Altermann and Lenhardt, 2012; Humbert et al.2019).

Results

The Ventersdorp Supergroup is the most extensive LIP of the Kaapvaal Craton and may probably be subdivided into several desecrate LIP events, or pronounced pulses between ca. 2.78 and 2.70 Ga (Altermann and Lenhardt, 2012; Cornell et al. 2017) at different parts of the craton. This long lasting magmatism was largely related to continental rift systems producing also thick sedimentary piles of coarse to fine, clastic and volcaniclastic, but also minor carbonate rocks, in lacustrine to terrestrial environments (Van der Westhuizen et al. 1991).

The Ventersdorp Supergroup, is the thickest (>5000 m) succession of multiple volcanic pulses with continental flood basalts, andesitic to felsic volcanics, and associated sedimentary rocks extending across an area greater than 300,000 km^2. It is subdivided into three stratigraphic units: the basal Klipriviersberg Group and the overlying Platberg and Pniel groups, with some locally developed stratigraphic equivalents, like the Sodium Group.

During the period of ca. 2.7 to 2.4 Ga magmatic activity was of lesser importance on the Kaapvaal Craton and erosion and/or chemical and siliciclastic sedimentation dominated the geological record.

The two Proterozoic formations, the older Ongeluk and the younger Hekpoort, are parts of the Transvaal Supergroup which rests unconformably on the Ventersdorp Spgr. They crop out in different sub-basins (Griqualand West and Transvaal respectively) and are separated by ca. 200 myr of differing sedimentary evolution in these regional Transvaal basin compartments.

The basaltic magmatism of the Ongeluk Fm, at ca. 2.43 Ga (Gumsley et al. 2017) and of the Hekpoort Fm, at 2.23 Ga (Schröder et al. 2016) may represent progressive differentiation series from a single parental magma. The degree of crustal assimilation is however strongly inconsistent with the extrusion order across these period of 200 myr.

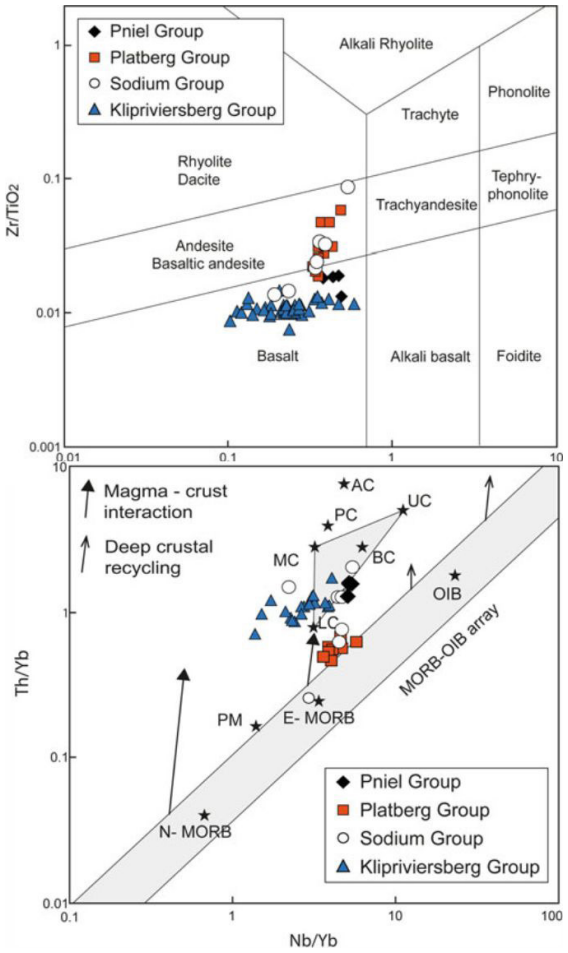


Figure 1. Classification of the Ventersdorp lavas and the Th/Yb–Nb/Yb ratio: LC = Lower Crust, MC = Middle Crust, UC = Upper Crust, BC = Bulk Crust, PC = Phanerozoic Crust, AC = Archaean Crust

The Ongeluk Formation in Griqualand West is characterized by an up to 900 m-thick succession of massive basaltic andesites, pillow lavas and hyaloclastites indicating terrestrial and subaqueous extrusions on the early Proterozoic glacial deposits of the Magkanyene Formation. The contact to the glacial base is sometimes conformable and in other places unconformable.

The Hekpoort Fm in the Transvaal is of basaltic to basaltic andesite flows and minor localized volcaniclastics, in total up to 1100 m thick and with little sedimentary intercalations. It extruded on the fluvial Boshoek Fm of fine, pebbly sandstone to conglomerates and underlying quartzites.

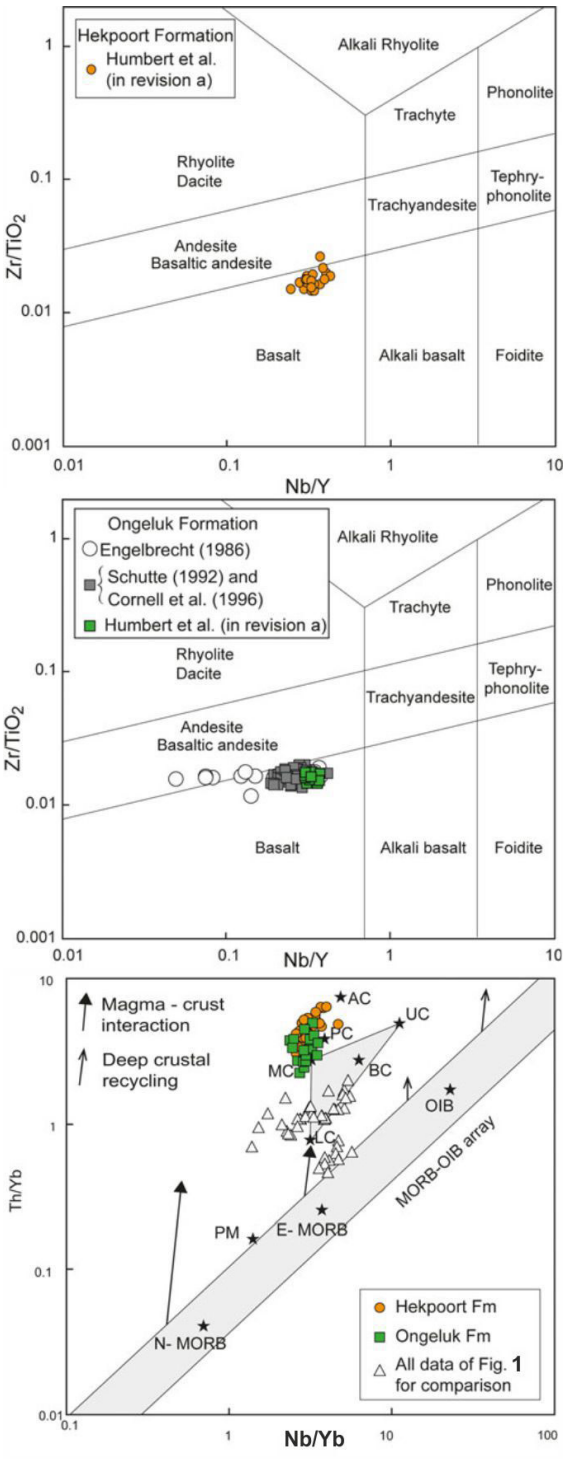


Figure 2. Classification diagram of the Hekpoort and Ongeluk lavas and Th/Yb–Nb/Yb ratios. For abbreviations see Fig. 1 (Humbert et al. 2019).

The trace element patterns of the Ventersdorp, Hekpoort and Ongeluk samples show similar 'arc-like' geochemical signature which is probably linked to the magma source. As discussed previously (Eriksson et al. 2006; Humbert et al. 2019) a 'subduction-related' origin of these lavas is however unlikely. The arc-like signatures are represented by negative Nb–Ta anomalies likely related to metasomatism of the sub-continental lithospheric mantle by past subductions.

Conclusions

The Ventersdorp Supergroup exhibits a polyphased volcanic history, unlike the Hekpoort and Ongeluk formations, which are uniform and share remarkably similar geochemical signatures. Despite of differences in volumes, age and geochemistry, the data suggest that an important subduction event marked the Archaean-Proterozoic boundary in the Kaapvaal craton (Humbert et al. 2019). Nevertheless, the magmatic events of the Ventersdorp Supergroup, Ongeluk Formation and Hekpoort Formation cannot be linked to any marked tectonic events and thus may represent failed rifting events grounded in mantle dynamics.

References

1. Altermann W., Lenhardt N. (2012) The volcano-sedimenatry succession of the Archean Sodium Group, Ventersdorp Supergroup, South Africa: Volcanology, sedimentology and geochemistry. Precambrian Research, 214-215: 60-81.
2. Cornell D.H, Meintjies P.G., Van der Westhuizen W.A., Frei D. (2017) Microbeam U–Pb Zircon dating of the Makwassie and Goedgenoeg formations in the Ventersdorp Supergroup of South Africa. S Afr J Geol 120:525–540. https://doi.org/10.25131/gssajg.120.4.525
3. Eriksson P.G., Altermann W., Hartzer F.J. (2006) The Transvaal Supergroup and Precursors. Chapter 10. In: Johnson M.R., Annhaeusser C.R. Thomas R.J. (Editors): The Geology of South Africa. Geol. Society of South Africa. 237-260.
4. Gumsley A.P., Chamberlain K.R., BleekeW., Söderlund U., de Kock M.O., Larsson E.R., Bekker A. (2017) Timing and tempo of the Great Oxidation Event. Proc Natl Acad Sci USA 114:1811–1816
5. Humbert F., de Kock M.O., Lenhardt N., Altermann W. (2019) Neoarchaean to Early Palaeoproterozoic Within-Plate Volcanism of the Kaapvaal Craton: Comparing the Ventersdorp Supergroup and the Ongeluk and Hekpoort Formations (Transvaal Supergroup). In Kröner A., Hofmann A. (eds): The Archaean Geology of the Kaapvaal Craton, Southern Africa, Springer Nature Switzerland AG. 277-302. DOI: 10.1007/978-3-319-78652-0_11.
6. Schröder S., Beukes N.J., Armstrong R.A. (2016) Detrital zircon constraints on the tectonostratigraphy of the Paleoproterozoic Pretoria Group, South Africa. Precambrian Res 278:362–393
7. Van der Westhuizen WA, De Bruiyn H., Meinties PG (1991) The Ventersdorp Supergroup; an overview. J Afr Earth Sci 13:83–105.

EMPLACEMENT OF BASHKIRIAN MEGAZONE RIPHEAN INTRUSIVE BODIES (SOUTH URALS) BASED OF PALEOMAGNETIC DATA

Anosova M.[2], Latyshev A.[1,2], Khotylev A.[2]

[1] Schmidt institute of the Physics of the Earth RAS, Moscow, Russia,
[2]Geological Faculty, Lomonosov Moscow State University, Moscow, Russia
Mai.anosova@yandex.ru

We present the results of the study of the basic dikes and sills, which cut Early-Riphean sedimentary formations and the Berdyaush pluton of the Southern Urals. The studied objects are located in the core of the Bashkirian megazone (near the towns of Kusa, Bakal and Berdyaush) and related to the Riphean stage of rift magmatism of the East European craton (Ernst et al., 2006).

The measurements of the anisotropy of magnetic susceptibility demonstrate three types of the magnetic fabric. About 40% of the studied objects demonstrate the "normal" type of the AMS ellipsoid, when the minimal axis K3 is normal to the contact of intrusion and the other two axis lie in the dike plane. In other sites we found either inverse magnetic fabric, when the maximal axis K1 is normal to the dike plane, or intermediate fabric, when the middle axis K2 is orthogonal to the contact of intrusion. Also, in some sites the dispersed fabric was observed. When the K1 axis lies in the dike plane, we were able to reconstruct the magma flow lineation. Axis K1 is flat and it has a North-Eastern orientation near the Kusa town. We assume that magma propagated from SW to NE direction parallel to the Bakal-Satka regional fault, because the central part of the Mashak rift, active at the beginning of the middle Riphean, was located to the Southwest. The dikes related to the Berdyaush pluton demonstrate the shallow magma transport from the west to the east. We propose a model under which Berdyash pluton was formed in shear zones of local extension near Bakal-Satka fault and magma intruded along the extrension fractures. Thus, the Bakal-Satka fault acted as the long-lived magma feeding zone, which controlled the emplacement of basic dikes and the Berdyaush pluton itself in Riphean. At the same time, the intrusion of sills near the Kusa area was controlled the regional stretching zone parallel to the Bakal-Satka fault.

As a result of paleomagnetic investigation of the basic intrusions, we obtained the new paleomagnetic pole for the high-temperature component of remanence: N=8, Plong=163.0, Plat=8.1, A95=4.3. Taking into account the age obtained for one of the bodies - 1349±11 Ma (U-Pb (SHRIMP) for zircons), our pole is located between the published poles for 1265 and 1458 Ma for the East European craton (Salminen., 2007; Buchan et al., 2000).

There was no significant rotation of the block, since, according to the proposed model, the intrusion of the studies dikes occurred along the vertical separation cracks, and the dikes are vertical at the present.

This result is the important contribution to the development of APWP of the East European craton in the Mesoproterozoic and can be used in the reconstruction of the "Columbia" supercontinent breakup.

Besides, we found component of remanence which can be attributed to the Later Paleozoic remagnetization during the Uralian collision event. The directions of this component are similar in remote areas of the Bashkirian megazone. this indicates the absence of relative movements of Bashkirian megazone blocks after the Late Paleozoic.

This work was supported by RFBR (project № 17-05-01121) and the Ministry of Education and Science RF (project № 14.Z50.31.0017).

References

1. Buchan K.L., Mertanen S., Park R.G., Pesonen L.J., Elming S.-A., Abrahamsen N., Bylund G., 2000. Comparising the drift of Laurentia and Baltica in the Proterozoic: the importance of key palaeomagnetic poles. Tectoniphisics 319 (3), 167–198.
2. Ernst, R.E., Pease, V., Puchkov, V.N., Kozlov, V.I., Sergeeva, N.D., Hamilton, M. Geochemical characterization of Precambrian magmatic suites of the Southeastern margin of the East European Craton, Southern Urals, Russia // Геологический сб.№ 5. /под ред. В.Н. Пучкова, Р.Ф. Абдрахманова, И.Б. Серавкина / ИГ УрО РАН. 2006 № 5. С. 1–45.
3. Salminen, J., Pesonen, L.J., 2007. Palaeomagnetic and rock magnetic study of the Mesoproterozoic sill, Valaam island, Russian Karelia. Precambrian Res. 159, 212–230.

THE EARLY STAGES OF SILICATE-SULFIDE IMMISCIBILITY AT CRYSTALLIZATION OF PRIMITIVE CUMULATES IN LAYERED INTRUSIONS (EXEMPLIFIED BY THE YOKO-DOVYREN MASSIF IN NORTHERN TRANSBAIKALIA)

Ariskin A. A.[1,2], Pshenitsyn I. V.[1], Danyushevsky L. V.[3], Fiorentini M. L.[4], Nikolaev G. S. [2], Kislov E. V. [5]

[1]*Lomonosov Moscow State University, Moscow, Russia, ariskin@rambler.ru*
[2]*Vernadsky Institute, Moscow, Russia*
[3]*School of Physical Sciences and CODES, University of Tasmania, Hobart, Australia*
[4]*Centre for Exploration Targeting, Perth, Australia*
[5]*Geological Institute, Siberian Branch of the RAS, Ulan-Ude, Russia*

Keywords: *original sulfide composition, layered intrusion, COMAGMAT modeling*

Introduction

Geology and mineralization. The 3.4 km thick Yoko-Dovyren massif (hereinafter YDM) is the largest layered intrusion of the Upper Riphean Synnyr-Dovyren volcano-plutonic complex located in Northern Transbaikalia, Russia. Gabbroic dykes and ultramafic sills below its lower contact include a diversity of net-textured to massive sulfide ores, composing a sub-economic Baikal Cu-Ni deposit (Kislov, 1998).

Other types of low-sulfide and ore mineralization include: (1) rare Mss-like sulfide clusters within the lower chilled zone of the YDM, (2) Ni-rich sulfides disseminated in the lower plagioperidotite and plagiodunite, (3) Mss-like to Cu-rich PGM-containing sulfides occurred in the lower troctolite, (4) Cu-PGE rich anorthosites of the Main Reef (in a transition zone between troctolite and olivine gabbro), and (5) pyrrhotite-rich PGE-depleted sulfides in Pig-containing gabbronorite near the roof of the YDM (Ariskin et al., 2018a). In addition, sporadic PGE- to Au-rich sulfide occurrences took place in leucogabbro situated between the Main Reef and the near-roof horizon.

In this paper, we present newly acquired data on concentrations of precious metals, chalcogens (Se, Te), and base metals in rocks and sulfides throughout a completed cross-section of the Dovyren intrusion. Focusing on sulfide-bearing rocks and Cu–Ni ores from the bottom portion of the YDM, it is shown that positive covariations between Pd, Pt, Au, S, and Te in the samples highlight sulfide control on the behavior of these elements related to the accumulation of essentially Fe–Ni sulfide liquids at a magmatic stage.

Combining their geochemistry with COMAGMAT-5 modeling (Ariskin et al., 2018b), the first estimate of the original immiscible sulfide is presented. The protosuldide composition is proposed to be a precursor of Mss-like to Cu-PGE rich (Iss-like) sulfide compositions observed in PGM-containing low-sulfide horizons of the YDM.

Observations

Chemostratigraphy of the Dovyren rocks. Concentrations of precious metals, chalcogens, and base metals in representative rocks were determined at Acmelabs (Vancouver, Canada) and Geolabs (Sudbury, Canada): to analyze PGE+Au ICP-MS was used following fire assay fusion by standard methods (Fig. 1).

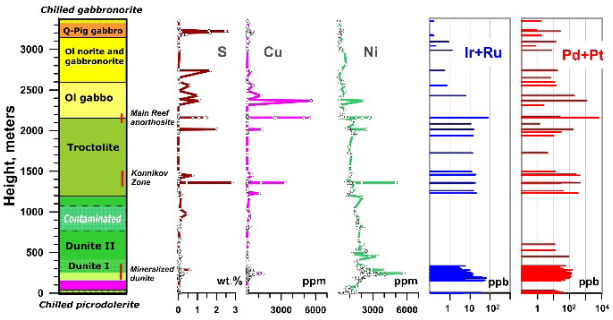


Fig. 1. Chemostratigraphy of S, base metals, IPGE and PPGE in the Yoko-Dovyren intrusion.

Positive correlations Pd vs. S and Pt vs. Te evidence a distinct sulfide control on the concentration and (probably) transport of PPGE through specific parts of the Dovyren magma chamber (Fig. 2).

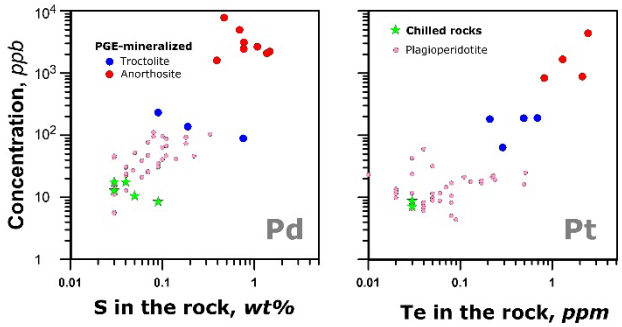


Fig. 2. Pd and Pt vs. S and Te in the main types of rocks

Natural sulfide compositions. We follow the conclusion that 100%-sulfides (whole-rock compositions normalized to the amount of sulfides) are the best approximation of a bulk sulfide in a particular rock (Ariskin et al., 2018c). In this case, the most primitive protosulfide composition can be evaluated by comparison of the 100%-sulfides from basal ultramafics with results of thermodynamic modeling of the sulfide immiscibility in primitive olivine cumulates (Ariskin et al., 2018bc).

Geochemistry of primitive sulfides

To recover probable evolution of an original immiscible sulfide liquid, we used the COMAGMAT-5 model allowing for calculation of closed system crystallization of a chilled

picrodolerite from the lower contact of YDM. The proposed most primitive Ol-orthocumulate contains 0.05 wt. % S and 24.4 wt. % MgO. Sulfide immiscibility was found to occur at T~1248°C, i.e. ~40°C below the magma emplacement temperature (Ariskin et al., 2016). Combining these results with known sulfide-silicate melt partition coefficients, the chemical evolution of the immiscible sulfide is calculated. The modeled trajectory has been compared with average 'most primitive 100%-sulfides' from a chilled olivine gabbronorite and basal plagioperidotites. As a result, modeled compositions match most primitive sulfide compositions observed in the basal zone of the YDM. This gave rise to the estimate of the most probable original sulfide composition, which is consistent with 3.4 wt% Cu, ~10 ppm Pd, ~5.7 ppm Pt, ~1.2 ppm Au, and ~19 ppm Te.

Geochemistry of sulfides from the Konnikov Zone

Detailed sampling of lower troctolites in the interval ~100-500 m above the dunite/troctolite boundary revealed a number of sulfide-mineralized samples, which contained disseminated round silicate-sulfide clusters, several cm to ~10 cm in diameter, see Fig. 1 (Ariskin et al., 2018a). In thin sections, these heterogeneous schlieren displayed typical orthomagmatic intercumulus sulfides filling the pore space between olivine and plagioclase. Similar to the Main PGE Reef, chalcopyrite and cubanite accounted for ~75-80% of the total sulfide in the samples. As many as 60 PGM grains (1 to 40 mm in size) were identified in samples from this occurrence. These PGM-assemblages are mostly composed of tellurides and bismuthotellurides of Pd, Ag, Pt, and Pb (moncheite, paolovite, atokite, merenskyite, michenerite $Pd_2(Bi,Te)$, kotulskite Pd(Te,Pb,Bi), telargpalite $(Pd,Ag)_3Te$). Other minerals include alloys/amalgams, such as electrum (Au-Ag), tetraferro-platinum (PtFe), and potarite (PdHg). LA-ICP-MS analyses of pentlandite from these samples demonstrated high concentrations of all PGE with the notable exception of Pt (all values in ppm): Pd 23.1±7.2, Rh 23.1±7.2, Ru 7.5±4.7, Os 4.2±3.3, and Ir 6.7±4.0.

Another type of the sulfide mineralization is represented by pegmatoid varieties occurred in thin veins of feldspar-rich large-grained troctolite cutting hosting massive rocks. Chemical features of the 100%-sulfides for both types are displayed in Fig. 3. These data clearly demonstrate two different geochemical types of sulfides, relatively enriched and depleted in PGE, Cu, Au and Te. Note that the primitive sulfide composition discussed above is in between these types. This seems to be indicative of a protosulfide melt (which is very similar to that from the basal part of YDM) can be considered as a precursor split to these two chemically different types.

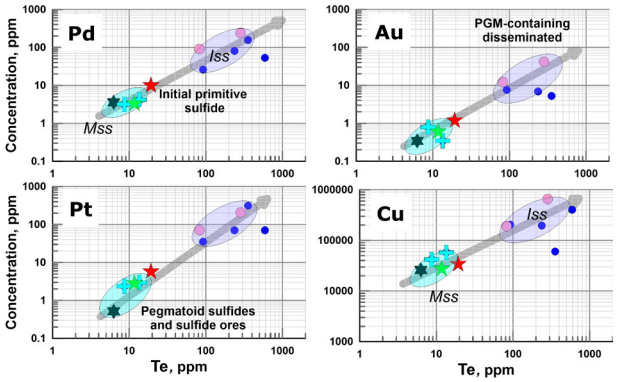


Fig. 3. The most primitive sulfide liquid (red star) and two types of sulfides from the Konnikov Zone.

Conclusions

The primitive sulfide composition estimated for the basal zone of the Dovyren intrusion may be considered as a valid approximation of an initial sulfide liquid in lower troctolites. Chemical relations in Fig. 3 argue for a crystallization history of this precursor resulted in Mss-like and Iss-like derivatives.

Acknowledgements

We acknowledge support from the Russian Science Foundation (RSF, grant No. 16-17-10129).

References

1. Ariskin, A.A., Kislov, E.V., Danyushevsky, L.V. et al. (2016) Cu-Ni-PGE fertility of the Yoko-Dovyren layered massif (Northern Transbaikalia, Russia): thermodynamic modeling of sulfide compositions in low mineralized dunite based on quantitative sulfide mineralogy. Mineralium Deposita 51: 993-1011.
2. Ariskin A., Danyushevsky L., Nikolaev G. et al. (2018a) The Dovyren Intrusive Complex (Southern Siberia, Russia): Insights into dynamics of an open magma chamber with implications for parental magma origin, composition, and Cu-Ni-PGE fertility. Lithos 302-303: 242-262.
3. Ariskin A.A., Bychkov K.A., Nikolaev G.S., Barmina G.S. (2018b) The COMAGMAT-5: Modeling the effect of Fe-Ni sulfide immiscibility in crystallizing magmas and cumulates. Journal of Petrology 59: 283-298.
4. Ariskin A.A, Nikolaev G.S., Danyushevsky L.V. et al. (2018c) Genetic interpretation of the distribution of PGE and chalcogens in sulfide-mineralized rocks from the Yoko-Dovyren layered intrusion. Geochemistry International 56 (13): 1322-1340.

IS THERE A TRACK OF THE ICELAND PLUME BENEATH GREENLAND?

Artemieva I. M.

University of Copenhagen, Denmark
China University of Geosciences, Wuhan, China

Keywords: *Lithosphere, heat flux, Iceland hotspot track*

Introduction

Lithosphere thermal structure in Greenland is poorly known and models based on seismic and magnetic data are inconsistent, while growing awareness in the fate of the ice sheet in Greenland requires reliable constraints on geothermal heat flux (GHF) from the Earth's interior in the region where conventional heat flux measurements are nearly absent. The lithosphere structure of Greenland remains controversial, while its geological evolution is constrained by direct observations in the narrow ice-free zone along the coasts. The effect of the Iceland hotspot on the lithosphere structure is also debated.

Results

A new method for modeling the thermal structure of the lithosphere, termed thermal isostasy, is used to calculate upper mantle temperature anomalies, lithosphere thickness, and GHF in Greenland (Artemieva, 2019). The method is based on analysis of topography deviations from the expected correlation between the Moho depth and topography. Anomalous topography is interpreted as caused by thermal anomalies in the lithosphere and by variations in the lithosphere thermal thickness. The new method allows for recovering the lithosphere thermal structure with a high lateral resolution and for testing the results by comparing the predicted and measured heat flux. To verify the model results, the predicted GHF values are compared to available measurements and show a good agreement.

Thick (200-270 km) cratonic lithosphere of SW Greenland with GHF of ca. 40 mW/m^2 thins to 180-190 km towards central Greenland without a clear boundary between the Archean and Proterozoic blocks, and the deepest lithosphere keel is observed beneath the largest kimberlite province in West Greenland. The NW-SE belt with an anomalously thin (100-120 km) lithosphere and GHF of 60-70 mW/m^2 crosses north-central Greenland from coast to coast and it may mark the Iceland hotspot track. In East Greenland this anomalous belt merges with a strong GHF anomaly of >100 mW/m^2 in the Fjordland region. The anomaly is associated with a strong lithosphere thinning, possibly to the Moho, that requires advective heat transfer such as above active magma chambers, which would accelerate ice basal melting. The anomaly may extend 500 km inland with possibly a significant contribution of ice melt to the ice-drainage system of Greenland.

Conclusions

East Greenland has anomalous crustal structure, thin (50–100 km) lithosphere, high mantle temperatures and a strong GHF anomaly of >100 mW/m2 centered in the Fjordland region. Thermal anomaly cannot be explained by conductive heat transfer and requires advective heat transfer such as above active magma chambers, that may significantly enhance basal ice melting. A possible extent of the anomaly ca. 500 km inland may have strong consequences for a contribution of ice melt to the ice-drainage system in central Greenland.

The anomalous belt with a 100–120 km thick lithosphere and increased GHF that extends from the NW coast towards East Greenland may result from the passage of the Iceland hotspot, which may have been "stocked" in the Fjordland region of East Greenland.

Acknowledgements

Research supported by grant DFF-1323-00053 of the Danish Fund for Independent Research (DFF-FNU).

References

1. Artemieva I.M., 2019. Lithosphere thermal thickness and geothermal heat flux in Greenland from a new thermal isostasy method. Earth Science Reviews, 188, 469-481, https://doi.org/10.1016/j.earscirev.2018.10.015

My papers may be downloaded from: lithosphere.info

KIMBERLITE MAGMATISM AND LITHOSPHERIC STRUCTURE

Artemieva I. M.

University of Copenhagen, Denmark
China University of Geosciences, Wuhan, China

Keywords: *Lithosphere mantle, kimberlites, mantle density, metasomatism, gravity modeling*

Introduction

Kimberlite-type magmatism is typical of stable continental lithosphere of Precambrian cratons. This is paradoxical since "stable" regions are not expected to be subject to any tectono-magmatic events at all. Furthermore, it has recently been proposed that kimberlite magmatism may be associated with mantle plumes (Torsvik et al., 2010; Tappe et al, 2016).

Geodynamic origin of kimberlite-type magmatism remains speculative and the proposed models range from plate tectonics processes to plume-lithosphere interaction. No matter the origin, kimberlite magmatism should lead to a significant modification of the cratonic lithosphere, which otherwise is expected to have a unique thickness (>200 km) and unique composition (dry and depleted in basaltic components). Magmatic reworking of the Precambrian lithosphere may include magmatic underplating at the base of the crust, thermal thinning, and metasomatism of the lithospheric mantle. These processes are clearly reflected in the thermal, density, and seismic velocity structure of the cratonic lithosphere.

Results

Based on a joint interpretation of geophysical data, such as thermal, seismic tomography, and gravity data, I demonstrate a significant lateral and vertical heterogeneity in the structure of the crust and the lithospheric mantle of cratons worldwide (Artemieva, 2009; Cherepanova and Artemieva, 2015; Artemieva and Vinnik, 2016). This heterogeneity reflects the extent of the lithosphere reworking by both a large-scale (e.g. Siberian LIP) and kimberlite-type magmatism. The results (compared to petrological studies of mantle-derived xenoliths) indicate that kimberlite regions have different composition of the lithospheric mantle than the "intact" cratons. There are no significant differences in lithospheric thickness between kimberlite regions and intact cratonic lithosphere. Therefore, lithosphere modification is caused primarily by mantle metasomatism, and kimberlites of different ages (e.g. Group I and II kimberlites in Kaapvaal) may sample mantle of a significantly different composition. The results may provide a new strategy for diamond prospecting, since statistically, diamondiferous kimberlites tend to erupt through a low-density, depleted lithosphere, while non-diamondiferous kimberlites are more typical of a highly metasomatised cratonic mantle.

Closely related to the problem of kimberlite magmatism, the isopycnicity hypothesis states that the lithospheric mantle of ancient platforms has a unique composition such that high density due to low lithosphere temperature is nearly compensated by low-density composition of old cratonic mantle. This hypothesis is supported by petrological studies of mantle xenoliths hosted in kimberlite magmas. However, the representativeness of the kimberlite sampling may be questioned, given that any type of magmatism is atypical for stable regions. In the Siberian craton, geochemically studied kimberlite-hosted xenoliths sample exclusively those parts of the mantle where the isopycnic condition is satisfied, while the pristine lithospheric mantle, which has not been affected by magmatism, has a significantly lower density than required by isopycnicity. This discovery allows us to conclude that our knowledge on the composition of cratonic mantle is incomplete and that it is biased by kimberlite sampling which provides a deceptive basis for the isopycnicity hypothesis (Artemieva et al., 2019).

Conclusions

Kimberlite regions have different composition of the lithospheric mantle than the "intact" cratons.

Our knowledge on the composition of cratonic mantle is biased by kimberlite sampling which provides a deceptive basis for the isopycnicity hypothesis.

Acknowledgements

Research supported by grant DFF-1323-00053 of the Danish Fund for Independent Research (DFF-FNU).

References

1. Artemieva I.M., Thybo H., Cherepanova Y., 2019. Isopycnicity of cratonic mantle restricted to kimberlite provinces. Earth Planet. Sci. Lett., 505, 13-19.
2. Artemieva I.M., Vinnik L.P., 2016. Density structure of the cratonic mantle in southern Africa: 2. Correlations with kimberlite distribution, seismic velocities and Moho sharpness. Gondwana Res., 36, 14-27.
3. Artemieva I.M., 2009. The continental lithosphere: Reconciling thermal, seismic, and petrologic data. Lithos, 109, 23-46.
4. Cherepanova Y. and Artemieva I.M., 2015. Density heterogeneity of cratonic lithospheric mantle: A case study of the Siberian craton. Gondwana Res., 28, 1344-1360.
5. Tappe S., et al., 2016. Plates or plumes in the origin of kimberlites: U/Pb perovskite and Sr-Nd-Hf-Os-C-O isotope constraints from the Superior craton (Canada). Chem.Geology, doi: 10.1016/j.chemgeo.2016.08.019
6. Torsvik, T.H., Burke, K., Steinberger, B., Webb, S.J., Ashwal, L.D., 2010. Diamonds sampled by plumes from the core-mantle boundary. Nature 466, 352–355.

NEW ILP TASK FORCE (2019-2024): LITHOSPHERIC STRUCTURE AND MINERAL RESOURCES

Artemieva I. M.[1], Dong S-W.[2], Ernst R. E.[3]

[1] *University of Copenhagen, Denmark; China University of Geosciences, Wuhan, China*
[2] *SINOPROBE, CAGS (Beijing) and Nanjing University (China)*
[3] *Tomsk University (Russia) and Carleton University (Ottawa, Canada)*

Keywords: *Lithosphere structure, mineral resources*

Introduction

Geological, geodynamic and tectonic processes that define and control the lithosphere structure and evolution are closely related to deposition of minerals, many of which occur only in specific lithospheric settings. Recent technological shifts and the depletion of mineral resources put pressure on the mineral exploration industry which is experiencing a boom in activity over the past decade. This boom is also associated with breakthroughs in mineral exploration which build on new fundamental results in geophysics, geochemistry, and geodynamics.

Significant efforts are being put forward internationally and nationally, e.g. at the scales of national geological surveys, to bridge mineral exploration and the academic community. However, the results of the academic research are not used at full by the mining industry. On the other side, a significant part of the fundamental research does not target practical application of the results by the mineral exploration community and the step between the academic result and its possible application is often missing.

New ILP Task Force

The objective of the new ILP Task Force (2019-2024) is to provide a new framework for mineral exploration targeting. This requires detailed knowledge on the lithosphere-scale structure, including detailed knowledge of the crust, together with the improved and enhanced understanding of the impact of various plate tectonics and mantle dynamics processes on the lithosphere composition and architecture.

The new ILP Task Force will focus primarily on magmatic ore deposits on continents, which are mostly associated with large igneous provinces, continental collisional orogens, Precambrian cratons, and paleo-subduction systems. Other tectonic settings, such as the Arctic shelf, may also be included as a sub-task of the new Task Force.

Magmatic ore deposits are formed during crystallization of a magma. They are linked to magmatic processes associated with either plate tectonic settings (collisional orogens and subduction systems), or with mantle hotspots and plumes (large igneous provinces); some may also be associated with large-scale impacts that cause intensive lithosphere heating and melting. All these processes create and modify the structure and composition of the crust and the lithosphere mantle, and therefore can be recognized by high-resolution geophysical models. Geological data combined with geochemical studies provides constraints on geodynamic processes responsible for formation and deposition of ore deposits. These processes can be tested by numerical modeling which provides important constraints on the details of magmatic processes and their impact on the lithosphere structure and composition.

Conclusions

The goal of the new Task Force fits the mission of the ILP in:

- addressing the connections between the deep Earth ore-forming processes, lithosphere structure and mineral deposits at the near-surface;
- building on interdisciplinary research which includes collaboration between geology, geophysics and geochemistry;
- building on the integration of geophysical imaging of the crustal and upper mantle structure with tectonic reconstruction of processes that form and modify the lithosphere and with geodynamic modeling of these processes.

We invite a broad international geoscience community to join us in the new ILP Task Force !

GREAT OXIDATION EVENT IN THE EARLY PALEOPROTEROZOIC AND ITS IMPACT ON THE SECULAR TRENDS IN SEDIMENT-HOSTED MINERAL DEPOSITS

Bekker A.

Department of Earth and Planetary Sciences, University of California, Riverside, CA 92521 USA; e-mail: andreyb@ucr.edu

Keywords: *GOE; U and V deposits; iron formations; manganese deposits; sulfate evaporites; copper stratiform deposits; phosphorites*

Introduction

The first irreversible rise of atmospheric oxygen and large-scale oxygenation of shallow-marine settings during the Great Oxidation Event (GOE) between ~2.43 and 2.32 Ga had a profound impact not only on surface environments, but also on processes involved in the origin of sediment-hosted mineral deposits. The GOE introduced free oxygen as an abundant component to surface environments resulting in a large-scale delivery of redox-sensitive elements such as U, Mo, Re, and V as well as sulfate to the oceans from the continents via oxidative continental weathering. Associated increase in the Gross Primary Productivity (GPP) produced fresh organic matter to trap dissolved redox-sensitive elements from the oceans in anoxic and euxinic settings and in subsurface from basinal fluids. Remineralization of organic matter in deep-marine settings utilizing newly introduced oxidants released P that was upwelled onto continental margins to form phosphorite deposits for the first time in Earth's history. Ocean iron and manganese cycles changed dramatically across the GOE in response to stronger redox gradients between shallow and deep oceans. The oldest sulfate evaporites were deposited at the early stage of the GOE, starting at ~2.4 Ga, and enhanced ability of basinal fluids to transport base metals as chlorine and sulfate complexes.

U and V deposits

It has been recognized for almost 100 years that the Archean sedimentary successions contain detrital redox-sensitive minerals such as uraninite, pyrite, and siderite, whereas sedimentary successions deposited during or after the GOE contain red beds. Detrital pyrite and uraninite occur in sedimentary units as young as ~2.45 Ga immediately below the stratigraphic level recording the initiation of the GOE. Redox-front U and V deposits, reflecting U and V transport in the oxidized state and trapping via reduction on contact with carbonaceous matter or pyrobytumens, appeared with the GOE (e.g., natural nuclear reactors hosted in the Francevillian Series of Gabon).

Iron Formations

Typical Archean Banded Iron Formations disappeared from the rock record during the GOE except for the spatially restricted sites proximal to high-temperature hydrothermal venting. Instead, shallow-marine, Granular Iron Formations became prominent in the rock record, which in turn were succeeded by ironstones of the Phanerozoic.

Manganese deposits

Mn deposits are typically hosted in the Archean BIFs and carbonates deposited before the GOE and affected by tropical weathering (e.g., India and Brazil). During the GOE thick and high-grade Mn deposits (e.g., Hotazel Mn deposit in South Africa and Nsuta and correlative deposits in West Africa) were precipitated as Mn-oxides in upwelling zones with high biological productivity on continental margins, recording for the first time efficient separation of Fe and Mn. Mn oxides were converted to Mn-carbonates during early diagenesis when organic matter was remineralized. The source of Mn, whether from high-temperature hydrothermal venting or anoxic terrigenous sediments via Mn-shuttle, is still debated and could be unique to each deposit.

Sulfate evaporites

Sulfate evaporites are missing in the Archean sedimentary record, but appear at the very early stage of the GOE once oxidative continental weathering became a widespread surface process. Most carbonate successions deposited during the Lomagundi carbon isotope excursion (>2.22-2.06 Ga) bear pseudomorphs and layers of sulfate evaporites. Although economically unimportant, dissolution of these evaporites during their burial and circulation of basinal fluids provided a critical media to transport base metals to their depositional sites.

Copper stratiform deposits

Copper stratiform deposits are unknown in the Archean sedimentary successions, but appear in the rock record for the first time at the very early stage of the GOE. Several factors are important for copper stratiform deposit to be formed: 1) sources of metals: typically from leaching of mafic volcanic and intrusive rocks; 2) intense fluid circulation driven by a hydrological head at high mountains; 3) basinal brines, derived from evaporite dissolution and rich in Cl and sulfate to form chlorine and sulfate complexes with base metals; and 4) a redox front (e.g., carbonaceous shales) to reduce sulfate and trap base metals as sulfides.

Phosphorites

Sedimentary phosphorites are also unknown from the Archean rock record and appear for the first time at the end of the Lomagundi carbon isotope excursion at ~2.06 Ga in association with carbonaceous shales. Although P is not a redox-sensitive element, P cycle was affected by the GOE as it depends on oxidants to remineralize organic matter in the deep oceans (to release P) and abundance of Fe(II) to scavenge P on oxidation to Fe-oxyhydroxides. Major, economic phosphate deposits appear at the late stage of the Paleoproterozoic in India in association with stromatolitic dolostones.

Discussion

The GOE has been linked to the gradual cooling of the mantle, emergence of large landmasses, and assembly of the low-latitude positioned supercraton, eventually resulting in the emplacement of massive and multiple LIPs at the beginning of the Paleoproterozoic (Gumsley et al., 2017; Bindeman et al., 2018). Enhanced weathering of juvenile volcanics under these conditions increased nutrient flux to the oceans, ushering the GOE. The long-term change that followed brought about the Earth's surface environments we have experience with now – oxygenated atmosphere and oceans. This change propagated into less appreciated, and yet critical changes to the sediment-hosted mineralizing systems replacing the Archean style of mineralization with that typical for the Proterozoic and Phanerozoic.

GEOCHEMISTRY OF SUPRA-SUBDUCTION, MORB AND OIB MAGMATISM IN OPHIOLITIC FRAGMENTS OF THE DZHIDA TERRAIN (NORTHERN MONGOLIA AND SOUTHERN SIBERIA)

Belyaev V. A., Gornova M. A., Karimov A. A., Medvedev A. Y.

Institute of Geochemistry SB RAS, Irkutsk, Russia, belyaev_vasya@mail.ru

In this contribution, we summarize published and new geochemical data on mafic rocks from ophiolites of the Dzhida terrain of the Central Asian Orogenic Belt, located in Northern Mongolia and South of Buryatia Republic of Russia. The Dzhida terrain is considered as an island arc terrain, containing ophiolites, differentiated basalt-andesite-dacite-rhyolite series, turbidite, accreted seamounts, and gabbro-tonalite-plagiogranite intrusions. The layered gabbro of Buguriktai ophiolite massif intruded at 560±5 Ma (hereafter U-Pb age of zircon) (Elbaev et al., 2018). Gabbro and granitoids with island-arc geochemical characteristics intruded at 560-570 and 504±2, 506±1 Ma (Gordienko et al., 2007, 2015). All rock associations are intruded by collisional granites at 490±2 to 477±6 Ma (Gordienko et al., 2012).

Ophiolite complexes and separate ultramafic massifs form linear trends within Dzhida terrain. The ophiolites are dismembered, in places some parts of typical ophiolite cross-section (such as mantle peridotites, cumulates, gabbro, sheeted dikes, lavas) may lack. Here we interpret geochemistry of ophiolitic basalts from four localities: Dzhidot (Buryatia), Uri-Gol, Bayangol, and Alag-Tsari-Gol (Mongolia), focusing on normalized REE and multi-element patterns, Nb/Yb–Th/Yb (Pearce, 2008), and Nb-Th (Saccani, 2015) systematics.

Gordienko et al. (2007) described two accreted paleo-seamounts (guiots), namely Dzhidot and Uri-Gol. Simonov et al. (2014) reported chemical composition of both paleo-seamounts. There are two types of Dzhidot basalts. The first type has REE pattern identical to those in N-MORB, but exhibits negative anomalies of Nb and Zr, making it similar to IAT. The second type shows REE and trace-element patterns parallel to those in OIB, with contents of Th, Nb, LREE varying from E-MORB to OIB. Similarly, Uri-Gol basalts show two different trace-element patterns. One type is IAT with negative anomalies of Nb, slight enrichment in Th and LREE, level of HREE lower than in N-MORB. The second type is N-MORB with characteristic trace-element pattern. It should be noted that alkaline basalts with rather high TiO_2 and P_2O_5 reaching levels of OIB were reported by Il'in (1982) for Uri-gol locality, but no recent trace-element data are available for those samples in literature.

The Bayangol (Narmandal) ophiolite association contains boninites and calc-alkaline basalts. According to our data, the boninites are of high-Ca type with U-shaped REE pattern, relative enrichment in Th, Pb, Sr, Zr, Hf. Their trace-element composition is close to those of high-Ca boninites from Troodos (Cyprus). Calc-alkaline basalts show high concentrations of Th, LREE, Pb, Sr, negative anomalies of Nb, Zr, Hf, Ti. Their composition is close to island-arc CAB. Based on major-element data of Il'in (1982), calc-alkaline basalts are found not only in Bayangol locality, but also widespread across the Dzhida terrain.

The Alag-Tsari-Gol ophiolite basalts (Medvedev et al., 2008) show two geochemical types. The first has trace-element patterns parallel to N-MORB, but at lower levels. Enrichment in Pb and Sr is notable. These basalts can result from melting of MORB-type mantle affected by subduction fluids. The second type is enriched in Th and LREE, with slight negative anomalies of Nb and Ti. Althouth Alag-Tsari-Gol basalts are similar to Narmandal CAB in REE systematics, they have less prominent Nb anomaly and are more close to N-MORB – OIB array in Nb/Yb–Th/Yb space. Thus, enriched Alag-Tsari-Gol basalts can be regarded as enriched or anomalous BABB.

The supra-subduction basaltic magmatism dominates within the Dzhida terrain. Uri-Gol IAT and Bayangol CAB are typical manifestation of island arc magmatism. Dzhidot and Alag-Tsari-Gol N-MORB show subduction fluid signatures and can be similar to fore-arc-basalts (FAB) erupted during subduction initiation. Bayangol boninites formed either during the subduction initiation event or in back-arc basin. Alag-Tsari-Gol enriched BABB probably formed in the same basin. Dzhidot OIB can be interpreted as seamount accreted during subduction of oceanic crust (Gordienko et al., 2007; Simonov et al., 2014). Alternatively, they can represent OIB magmatism in back-arc basin or rear-arc. We claim that reconsideration of geochemistry of ophiolitic basalts is needed to re-evaluate the tectonic evolution of the Dzhida terrain.

References

1. Elbaev, A.L., Gordienko, I.V., Bayanova, T.V., Gorokhovskiy, D.V., Orsoev, D.A., Badmantsyrenova, R.A., Zarubina, O.V., 2018. U-Pb age and geochemical

characteristics of ultramafic-mafic rocks of the Dzhida zone ophiolite association (Southwestern Transbaikalia). Doklady Earth Sciences 478, 208-210.
2. Gordienko, I.V., Filimonov, A.V., Mininia, O.R., Gornova, M.A., Medvedev, A.Ya., Klimuk, V.S., Elbaev, A.L., Tomurtogoo, O., 2007. Dzhida island-arc system in the Paleoasian Ocean: structure and main stages of Vendian-Paleozoic geodynamic evolution. Russian Geology and Geophysics 48, 91-106.
3. Gordienko, I.V., Kovach, V.P., Elbaev, A.L., Kotov, A.B., Sal'nikova, E.B., Reznitskii, L.Z., Yakovleva, S.Z., Anisimova, I.V., 2012. Collisional granitoids of the Dzhida zone of the Central Asian Fold Belt, Southwestern TRansbaikalia: age and conditions of the formation. Petrology 20, 40-58.
4. Gordienko, I.V., Gorokhovskiy, D.V., Elbaev, A.L., Bayanova, T.B., 2015. New data on the Early Paleozoic gabbroid and granitoid magmatism age within the Dzhida zone of Caledonides (Southwestern Tranbaikalia, North Mongolia). Doklady Earth Sciences 463, 817-821.
5. Il'in, A.V., 1982. Late Precambrian-Cambrian geological evolution of southern Siberia and Mongolia. Nauka, Moscow (in Russian).
6. Medvedev, A.Ya., Gordienko, I.V., Gornova, M.A., Al'mukhamedov, A.I., 2008. Geochemistry of metavolcanics in the Southern Hovsgul area (Northern Mongolia): geodynamic implications. Russian Geology and Geophysics 49, 245-253.
7. Pearce, J.A., 2008. Geochemical fingerprinting of oceanic basalts with applications to ophiolite classification and the search for Archean oceanic crust. Lithos 100, 14-48.
8. Saccani, E., 2015. A new method of discriminating different types of post-Archean ophiolitic basalts and their tectonic significance using Th-Nb and Ce-Dy-Yb systematics. Geoscience Frontiers 6, 481-501.
9. Simonov, V.A., Gordienko, I.V., Stupakov, S.I., Medvedev, A.Ya., Kotlyarov, A.V., Kovyazin, S.V., 2014. Conditions of basalt formation in the Dzhida zone of the Paleoasian Ocean. Russian Geology and Geophysics 55, 929-940.

LARGE IGNEOUS EVENTS IN THE ALPHA REGIO (V-32) QUADRANGLE, VENUS

Bethell E. M.[1], Ernst R. E.[1,2], Samson C.[1,3]

[1]*Department of Earth Sciences, Carleton University, Ottawa, ON, Canada*
[2]*Faculty of Geology and Geography, Tomsk State University, Tomsk, Russia*
[3]*Department of Construction Engineering, École de Technologie Supérieure, Montréal, Canada*

Keywords: *Venus, Planetary Geology, Geology*

Introduction

The Alpha Regio (V-32) quadrangle, Venus, is bounded by the coordinates 0°-30° E, 0°-25° S and covers an area of nearly 8 million km2. The V-32 quadrangle contains a diverse range of geological terrains and features. The central northern area of the quadrangle is a region of low-lying volcanic plains named Tinatin Planitia; the southwestern corner is dominated by Alpha Regio, a highland containing tessera terrain after which the quadrangle is named. Tectono-magmatic features include two major fracture belts and several coronae. Detailed geological mapping of the V-32 quadrangle at a scale of 1:2,500,000 has revealed numerous localized geological units within regions previously grouped as generalized global units (Bethell et al., 2019b). Geological units were grouped into the following categories: 1) volcanic edifice and flow material, comprising mostly localized units mapped as distinct volcanic flows; 2) corona material, comprising units associated with the formation of coronae; 3) plains material, comprising regional volcanic units that do not have identified sources; 4) structural terrains, comprising units with extensive structural deformation, and 5) tessera material, comprising units associated with tessera terrain. This abstract will focus on the results of this geological mapping effort that are relevant to large igneous provinces (LIPs).

Volcanic Plains

Plains material is the most extensive group of geological units, encompassing 55% of the surface area of the quadrangle. The majority of the areas identified as plains material were previously mapped by Ivanov and Head (2011) in their global geological map of Venus as shield plains, and lower and upper regional plains, which are globally correlated units. Our mapping approach attempted to resolve as many discernable sub-units as possible within the plains, using subtle differences in radar properties in combination with cross-cutting relationships of post-emplacement structures. Rather than grouping all mapped materials with similar radar properties into singular regional units, units with similar properties that were separated by large distances (sometimes 1000s of kms) were also distinguished as separate sub-units as these materials cannot be confidently geologically correlated using the available data. An example of this approach in mapping plains material is illustrated in the region bounded by 16°-23° E, 0°-3° S, which was mapped as lower regional plains by Ivanov and Head (2011). Here, we have mapped three distinct units: ridged plains material unit 3 (pr3), ridged plains material unit 4 (pr4), and smooth plains material unit 1 (ps1). Units pr3 and pr4 are characterized by intermediate radar brightness and the presence of pervasive wrinkle ridges, whereas ps1 is characterized by relatively lower radar backscatter (appearing "radar-dark"). Many NNW-SSE trending extensional structures are visible within unit pr4. At the boundary between units pr4 and ps1, there is a subtle difference in radar brightness and the abrupt truncation of the extensional structures in unit pr4, suggesting that unit ps1 is distinctly younger than unit pr4 and has flooded and obscured the extensional

structures. Units pr4 and pr3, while belonging to the same major unit, are distinguished as sub-units due to the absence of NNW-SSE trending extensional structures in unit pr3 and a slightly higher radar backscatter.

In total, plains material in the V-32 quadrangle was mapped as 8 major units that were further subdivided into 27 sub-units. The recognition of subtle differences in the surface properties and relative ages of Venus' volcanic plains is relevant to the debate on the style of Venus' resurfacing, namely whether the resurfacing was catastrophic (resurfacing of the entire planet over a short duration) or steady-state (continuous, more localized resurfacing). Structural cross-cutting relationships that indicate age variations in plains material at local scales would seem to favour a more steady-state resurfacing style.

Coronae

Units designated as corona material cover 10% of the surface area of the V-32 quadrangle. Several previously unrecognized volcanic flow units inferred to be associated with coronae have been recognized. Detailed mapping of structures associated with coronae has also increased the recognized extent of several coronae in the quadrangle, notably Cybele (from 480 km to 670 km), Fatua (from 310 km to 870 km), and Thermuthis (from 330 km to 1250 km) coronae (Stofan et al., 1992; Bethell et al., 2019a,b).

Three flow units (Fatua Corona flow material units 1 (cmF1), 2 (cmF2), and 3 (cmF3)) have been mapped that are interpreted to be associated with Fatua Corona, corresponding to a combined surface area of 327,512 km^2. These volcanic flows extend well beyond the rim of the corona; unit cmF1 extends to a distance of over 600 km from the southeastern edge of the corona rim. Assuming a volcanic flow thickness of 10 m (Roberts et al., 1992), the corresponding volume of these flow units is 3,275 km^3. Combining the estimated volume of these flow units with previous estimates on the upper limit of the intrusive volume of radiating dykes associated with Fatua Corona (approximately 57,000 km^3) leads to a total igneous volume estimate of 60,275 km^3. However, this estimate does not take into account additional igneous material which may be associated with volcanic constructs in the corona's interior, or with circumferential dykes and/or other intrusive bodies, such as layered intrusions. The assumption of a 10 m flow thickness may also be an underestimation of the true flow thickness, which is not ascertainable with the available data. With the consideration of these potential additional sources of igneous material, Fatua Corona may meet the volume criteria (100,000 km^3) of a LIP (Coffin and Eldholm, 1992; Bryan and Ernst, 2008; Ernst, 2014). Additionally, Fatua Corona has been classified in the global corona catalogue of Venus by Stofan et al. (1992) as volcanic category 2 (moderate associated volcanism). The recognition of its three associated volcanic flow units may warrant its re-classification to volcanic category 3 (extensive associated volcanism).

Digitate Flows

An approximately 1400 km long series of layered digitate volcanic flows is located in the central western area of the quadrangle. Where possible, individual flows were mapped, but were grouped into four generalized sub-units based on their radar brightness: digitate flow material units 1 (fd1; radar-bright), 2 (fd2; intermediate radar brightness), 3 (fd3; radar-dark), and 4 (fd4; moderately radar-dark to intermediate radar brightness). The combined surface area of these flows is 426,589 km^2; they cover 5% of the surface area of the quadrangle. With the assumption of a 10 m flow thickness (Roberts et al., 1992), the total volume would be 4,266 km^3. However, the full extent of the flows is not represented here as they extend into the neighbouring V-43 (Carson) quadrangle to the west. Based on the topography and the morphology of flow lobes, we interpret the general flow direction to be roughly eastward. At present, no source has been identified for these flows, although they may belong to a much larger flow field extending across the V-32 and V-43 quadrangles, and possibly at the scale of fluctüs.

Conclusions

Detailed geological mapping in the V-32 quadrangle has identified a number of previously unrecognized geological units and extended the sizes of several features. Mapping of plains material using subtle differences in radar properties in combination with structural cross-cutting relationships has revealed a number of sub-units with varying ages that were previously grouped as singular units. Structures and several volcanic flow units associated with coronae have been identified, leading to increased size estimates for several coronae. In particular, estimates of the volume of igneous material associated with Fatua Corona suggest the feature may be of LIP scale, although the timescale of its formation is unknown. A portion of a large field of volcanic flows that extends into a neighbouring quadrangle has also been mapped. This flow field may be at the scale of a fluctus.

Acknowledgements

This work was funded by a National Sciences and Engineering Research Council of Canada (NSERC) Discovery grant (grant number 315825, awarded to REE). REE was partially supported by a Ministry of Education and Science of the Russian Federation grant (grant number 14.Y26.31.0012).

References

1. Bethell, E.M., Ernst, R.E., and Samson, C. 2019a. Re-Evaluating the Structure of Thermuthis Corona through Detailed Geological Mapping: The Second Largest Corona on Venus? LPSC L, Abstract #1462.
2. Bethell, E.M., Ernst, R.E., and Samson, C. 2019b. Geology of the Alpha Regio (V-32) Quadrangle, Venus. Journal of Maps 15:2, 474-486.
3. Bryan, S.E., and Ernst, R.E. 2008. Revised Definition of Large Igneous Provinces (LIPs). Earth Science Reviews 86, 175-20.
4. Coffin, M.F., and Eldholm, O. 1992. Volcanism and Continental Break-Up; A Global Compilation of Large Igneous Provinces. Geological Society Special Publications 68, 17-30.
5. Ernst, R.E. 2014. Large Igneous Provinces. Cambridge University Press.
6. Ivanov, M.A., and Head, J.W. 2011. Global Geological Map of Venus. Planetary and Space Science 59, 1559-1600.

IMPROVED U-PB DATING OF THE CA. 450 MA SUORDAKH MAFIC EVENT IN EASTERN SIBERIA WILL TEST WHETHER THIS IS THE MISSING LIP RELATED TO END-ORDOVICIAN MASS EXTINCTION: PROGRESS REPORT

Chamberlain K. R.[1,4], Khudoley A. K.[2,4], Ernst R. E.[3,4], Prokopiev A. V.[5]

[1]*Dept. of Geol. and Geophy., Univ. of Wyoming, Laramie WY USA 82071*
[2]*Geol. Dept., St. Petersburg State Univ., St. Petersburg, Russia*
[3]*Dept. Earth Sci., Carleton Univ., Ottawa, Canada 82071*
[4]*Faculty of Geology and Geography, Tomsk State University, Tomsk 634050, Russia*
[5]*Diamond & Precious Metal Geol. Inst., Russian Acad. of Sci., Yakutsk, Rep. Sakha (Yakutia), 677980, Russia*

Keywords: *U-Pb dating, baddeleyite, secondary ion mass spectrometry, Suordakh sills, Ordovician*

Introduction

The Suordakh north-south trending mafic dikes and associated sills are currently recognized over an area of 11,000 km^2 in the Verkhoyansk region of eastern Siberia (Figure 1), but candidates are possible over an area that is approximately 500 km long and 80 km wide (Khudoley et al. 2013). "Moreover, the intensity of magmatic activity increases northward and eastward, although in both directions the Paleozoic rocks of the Sette–Daban Range are obscured by the Carboniferous siliciclastic units of the Verkhoyansk Complex" (Khudoley et al. 2013) and so the full extent could plausibly reach Large Igneous Province (LIP) scale (minimum of 100,000 km^2; Ernst, 2014).

Recent in-situ secondary ion mass spectrometry (SIMS) U-Pb baddeleyite dates (Schmitt et al. 2010; Chamberlain et al., 2010; Khudoley et al. 2013; Chamberlain, unpublished data) coupled with an ID-TIMS U-Pb baddeleyite date (Khudoley et al. 2001), establish that the Suordakh swarm is ca. 450 Ma. The precisions on the existing dates are low enough however, that there could be several discrete magmatic events within the sampled dikes and sills, with additional events ca. 420 Ma and 380 Ma. Ongoing research is focussed on 1) improving the precisions of ages on existing samples from ±10% to ±1% or better, 2) collecting samples from nearby regions to test for the areal extent of the events, and 3) studying the composition and tectonic setting of the Suordakh mafic intrusions.

Higher precisions on the ages of the Ordovician-Silurian mafic intrusions will: 1) determine how many events are present and 2) determine the temporal relationships, if any, between these intrusions and phases of the end-Ordovician extinction.

Results

Six mafic dike and sill samples from Sette-Daban range were collected in 2004 and have preliminary in-situ SIMS U-Pb baddeleyite dates of 457±34 to 379±27 Ma, based on 2 to 8 spot analyses each. Twenty-five or more additional target grains have been identified in each sample using improved mapping techniques. Re-analysis of one sample, X04-14-1, based on 40 new SIMS spots has established a date of 467±18 Ma (Fig. 1), improving both the precision and accuracy on magmatism. The previous date of 379±27 Ma for this sample was based on only 3 analyses, all of which are interpreted to have had some Pb loss discordance based on the new data (Fig. 1).

Twenty-five additional samples were collected in 2017 and 2018 and thin sections are being mapped to determine whether they are dateable. If any of these samples have baddeleyite grains that are >20 microns in size, the baddeleyite will be separated by the Söderlund method (Söderlund and Johansson, 2002), then dated by higher precision, dissolution, isotope dilution, thermal ionization mass spectrometry (ID-TIMS). Preliminary ID-TIMS data from one sample demonstrate more discordance than the corresponding SIMS data however, so resolving the intrusive ages of the Suordakh magmatism may require a combination of dating by both methods.

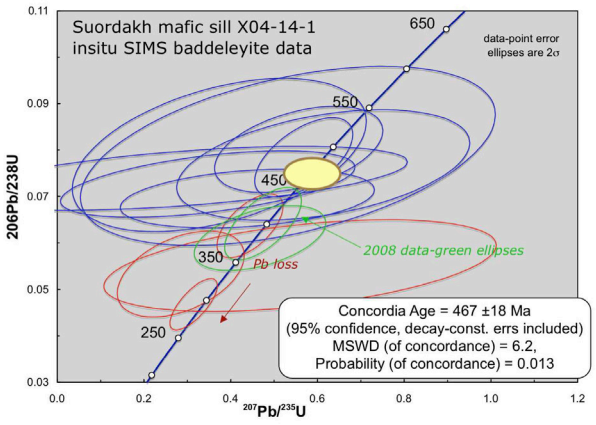


Figure 1. Concordia plot of SIMS spot analyses from Suordakh mafic sill sample X04-14-1 using the CAMECA 1290 at Univ. California at Los Angeles (UCLA), USA. Analyses were from baddeleyite grains (5 to 20 microns in diameter) in polished thin sections using 3x3-micron rastered ion beam spots. The Concordia Age (Ludwig 1998) of 8 high-quality analyses (blue ellipses) is 467±18 Ma (solid yellow ellipse). Data from 4 other spots (red ellipses) are interpreted to reflect varying degrees of Pb loss as they produced a range of younger $^{206}Pb/^{238}U$ dates than the cluster at 467 Ma. The preliminary data collected in 2008 (green ellipses) are also interpreted to reflect Pb loss; the preliminary date from those analyses, 379±27 Ma is now interpreted to be inaccurate. The baddeleyite grains have evidence of post-magmatic alteration to zircon, so data from 40 spot analyses were filtered by Th/U and % radiogenic ^{206}Pb to ensure that the date is based on pure baddeleyite domains.

Conclusions

The end-Ordovician glaciation event and its mass extinction has been an anomaly since it is the sole major mass extinction that is not yet associated with a LIP (Ernst 2014). The temporal link between LIPs and other extinction events is robust. Many major, and some minor, LIP events occur within several million years or less of global extinctions (e.g. Courtillot and Renne 2003; Wignall 2005; Ernst 2014; Bond and Grasby 2016; Ernst and Youbi, 2017). The most compelling examples are currently the Deccan (c. 66 Ma), Central Atlantic Magmatic Province (CAMP; 201 Ma), and the Siberian Trap

(252 Ma) LIPs, whose current dating overlaps precisely in age to the Cretaceous–Tertiary, Triassic–Jurassic, and Permian–Triassic boundary extinctions, respectively (Blackburn et al. 2013; Burgess and Bowring 2015; Schoene et al. 2010, 2015). Improving the age precisions on the Suordakh mafic event will test whether this is the missing LIP for the end-Ordovician extinction.

Acknowledgements

This study is partly supported by RNF grant 18-17-00240 of the Russian Federation.

References

1. Blackburn, T.J., Olsen, P.E., Bowring, S.A., McLean, N.M., Kent, D.V., Puffer, J., McHone, G., Rasbury, E.T., Et-Touhami, M. (2013). Zircon U–Pb geochronology links the end-Triassic extinction with the Central Atlantic Magmatic Province. Science, 340: 941–945.
2. Bond, D.P.G., Grasby, S.E. (2016) On the causes of mass extinctions, Palaeogeography, Palaeoclimatology, Palaeoecology (2016), doi: 10.1016/j.palaeo.2016.11.005
3. Burgess, S.D., Bowring, S.A. (2015). High-precision geochronology confirms voluminous magmatism before, during and after Earth's most severe extinction. Science Advances, 28, v. 1, no. 7, e1500470, doi: 10.1126/sciadv.1500470.
4. Courtillot, V., Renne, P.R. (2003). On the ages of flood basalt events. Comptes Rendus Géoscience, v. 335, p. 113–140.
5. Ernst, R.E. and Youbi, N. (2017). How Large Igneous Provinces affect global climate, sometimes cause mass extinctions, and represent natural markers in the geological record. Palaeogeography, Palaeoclimatology, Palaeoecology, 478, pp.30-52.
6. Ernst, R.E. (2014) Large Igneous Provinces. Cambridge University Press, 653 p.
7. Khudoley, A.K., Kropachev, A.P., Heaman, L.M., Zhuravlev, D.Z., Gur'ev, G.A. 2001b. Early Paleozoic magmatism of the Sette Daban, southern Verkhoyansk region, southeastern Yakutia. Doklady Earth Sciences, v. 378, no. 4, pp. 392-395.
8. Khudoley, A.K., Prokopiev, A.V., Chamberlain, K.R., Ernst, R., Jowitt, S.M., Malyshev, S.V., Zaitsev, A.I., Kropachev, A.P., Koroleva, O.V., (2013). Early Paleozoic mafic magmatic events on the eastern margin of the Siberian Craton. Lithos 174, 44–56.
9. Ludwig, K.R., 1998. On the treatment of concordant uranium-lead ages. Geochimica et Cosmochimica Acta, 62(4), pp.665-676.
10. Schoene, B., Guex, J., Bartolini, A., Schaltegger, U., Blackburn, T.J. (2010). Correlating the end-Triassic mass extinction and flood basalt volcanism at the 100 ka level. Geology, v. 38; no. 5; p. 387–390.
11. Schoene, B., Samperton, K.M., Eddy, M.P., Keller, G., Adatte, T., Bowring, S.A., Khadri, S.F.R., Gertsch, B. (2015). U-Pb geochronology of the Deccan Traps and relation to the end-Cretaceous mass extinction. Science, v. 347 no. 6218 pp. 182-184.
12. Söderlund, U. and Johansson, L., 2002, A simple way to extract baddeleyite (ZrO_2). Geochemistry, Geophysics, Geosystems (G^3), v. 3, n. 2, 10.1029/2001GC000212, ISSN: 1525-2027.
13. Wignall, P.B. (2005). The link between large igneous province eruptions and mass extinctions. Elements, v. 1, p. 293–297.

CHEMICAL WEATHERING OF LESOTHO HIGHLANDS BASALT

Chen Y.[1], Hedding D. W. [2], Li G-J.[1], Li X-M.[1], Wu W-H.[1]

[1]MOE Key Laboratory of Surficial Geochemistry, Department of Earth and Planetary Sciences, Nanjing University, Nanjing 210023, China
[2]Department of Geography, University of South Africa, Pioneer Avenue, Florida 1710, South Africa
E-mail: chengyang@nju.edu.cn

Basaltic terrains contribute a significant component to the global silicate weathering flux despite its limited areal coverage. A strong correlation between chemical weathering flux and climatic factors such as temperature in volcanically inactive basaltic fields implies that weathering of basalt might have played an important role in maintaining the habitability of the Earth and the balance of the geological carbon cycle. However, the low erosion rate of flood basalt provinces on tectonically quiescent cratons, where the clear climate dependence of weathering rate has been observed, implies a 'supply-limited' weathering regime where weathering flux is controlled by physical erosion rather than climate. This work tests the weathering limitation regime of flood basalts by investigating the weathering flux of the Lesotho Highlands where an extremely low rate of denudation has been registered. Stream chemistry of the rivers in the Lesotho Highlands shows typical characteristics of basalt weathering with Ca and Mg as the dominant cations and HCO_3^- as the dominant anion. Strong spatial and seasonal variability of solute concentration, possibly linked to dilution effect, has been observed. However, the giant Katse reservoir of the Lesotho Highland Water Project effectively averages the spatial and seasonal variability of the solute concentration. The average solution concentration and the long-term runoff monitoring of the Katse catchment give an average atmospheric CO_2 consumption rate of $0.259\pm0.024 \times 10^6$ mol/km^2/yr. The chemical weathering flux requires a minimum chemical alteration rate that is close to the total denudation rate, indicating congruent weathering and thus a 'supply-limited' weathering regime. Nevertheless, the chemical weathering rate of the Lesotho Highlands is still consistent with the global correlation between the rate of basalt weathering and temperature. Rock detachment and thus denudation, controlled by chemical weathering, is suggested to reconcile the paradox between the observed temperature dependence of chemical weathering rate and the 'supply-limited' weathering regime.

PILLOW LAVAS OF KAROO LIP FORMED MANY LEAGUES UNDER THE SEA

de Wit M. J., Linol B., Furnes H., Valashiya K.

AEON, Mandela University, South Africa; 2. Department Earth Science, University of Bergen, Norway

Small fragments of volcanic sequences of the ca. 183Ma Karoo Large Igneous Province (KLIP) are preserved across continental regions of southern Africa and linked to equivalents of the Ferrar Large Igneous Province (FLIP) of Antarctica and farther east to Tasmania. The best exposures of the KLIP sequences occur along the escarpments of Eastern Cape (Drakensberg) and the Lesotho highlands where the volcanics overlie Lower Jurassic sedimentary rocks of the desert-like Clarens Formation (Fig. 1). Whilst regional contacts between these sediment and volcanic sequences are described as conformable, albeit with local disconformities, time-gabs between the rock sequences are unquantified. The most accurate zircon dating of tuffs in sediments (Pronksberg bentonites 60 m below the Clarens) and of KLIP volcanism range between 5-20 million years. Tuffs and volcanoclastics (ranging up to near 500 m thick) occur also along the contact between the Clarens aeolinites and the KLIP volcanics. In places, the volcanoclastics are 'intruded' by volcanic tubes, and overlain by pillow lavas. Such pillow lavas were described in the 1970s by Brian Lock and his collaborators, but have not been documented in detail since. Our new fieldwork has identified pillow lavas in many contacts between the tuffs and lavas across the Figure 1. Geology of Karoo intrusive and volcanic rocks, with locations of pillow lavas highlighted in green.entire region of the Karoo volcanics (Figs. 1 and 2).

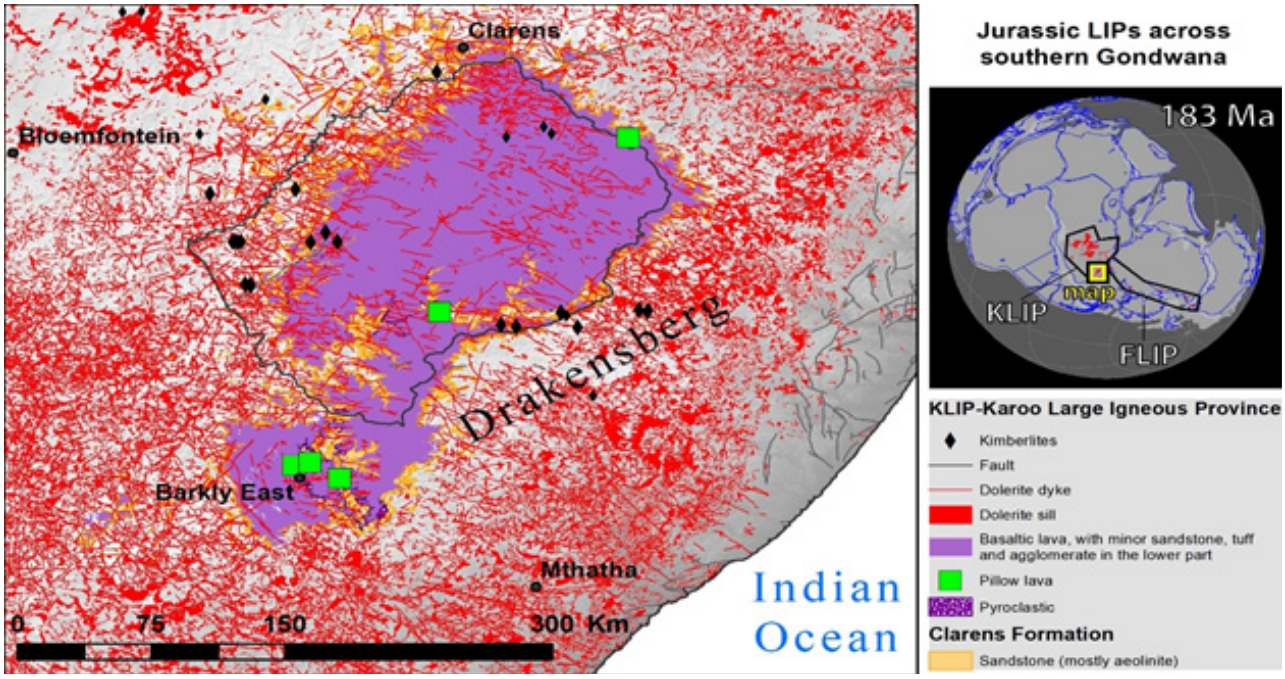


Figure 1. Geology of Karoo intrusive and volcanic rocks, with locations of pillow lavas highlighted in green.



Figure 2. Right – pillow lavas outcrop – highlighted the pillow on left with vesicle calculations

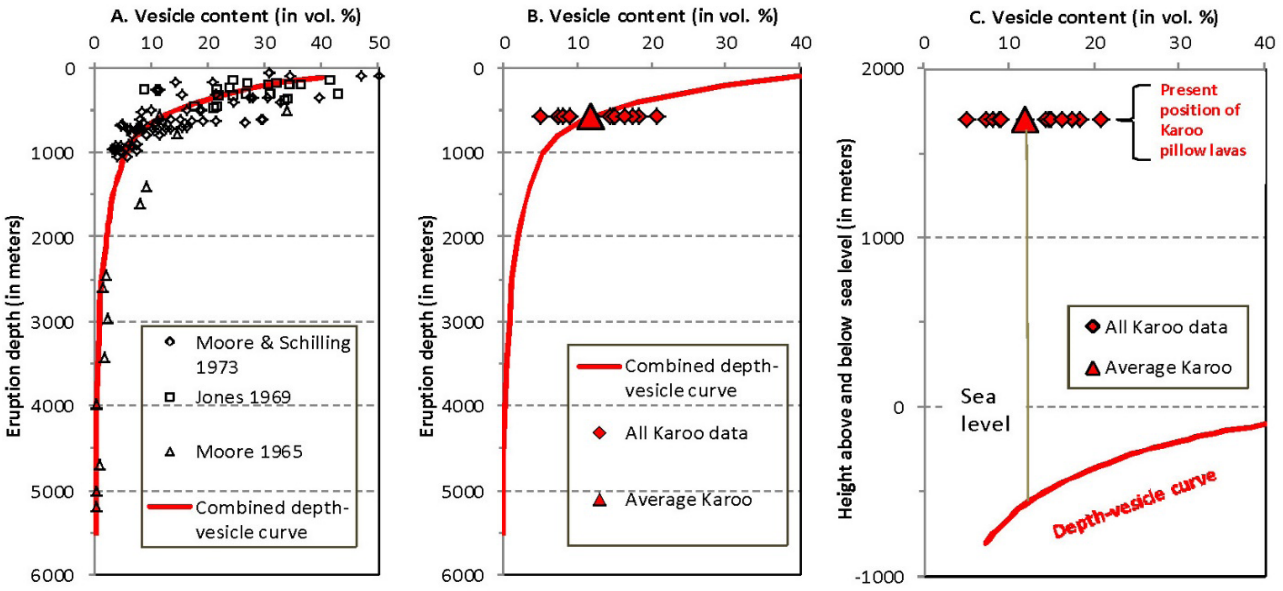


Figure 3. Diagrams showing the relationship between vesicle content in pillow lavas and depth of eruption. A. Depth-vesicle content curve based on the combined data of Moore (1965), Jones (1969), and Moore & Schilling (1973). B. The range and average vesicle content of the Karoo pillow lavas superimposed on the depth-vesicle diameter curve, indicating a water depth of eruption of ca. 500 m. C. The present position of the pillow lavas is ca. 1700 m above sea level, and the paleo-position of the pillow lavas ca. 500 m below sea level.

Vesicularity (content and size) and geochemistry of these pillow lavas reveal they originated below 500 m of saline water (Fig. 3). Since their present minimum position is 1750 m above sea level, the KLIP volcanics have been uplifted some 2250 m since the pillow lavas were erupted. The pillow lavas are cut also by dolerite systems drilled more than 4 km below sea level. Thus, the intrusions cut a vertical crust of more than 6 km.

Geochemistry of the major oxides and trace elements of the pillow lavas reveal they define tholeiitic basalt with minor basaltic andesite, similar to KLIP dolerite intrusions. The Karoo pillow lavas, like most of the other KLIP basalts, define Th/Yb-ratios well above the mantle array and the majority Ti-V resemble mid-oceanic ridge basalt (MORB) and alkaline basalts; and the Nb/Yb-Th/Yb data reveal subduction-related components. Initial $^{87}Sr/^{86}Sr$ data range between 0.707438 and 0.710462, and εNd_{183} values range between -4.43 and -5.86. These ranges are relatively small compared with previously published isotope data of KLIP and FLIP. The Nd-Sr isotope data for the pillow lava samples would indicate that the primary magma assimilated ca. 10-15% of continental crust. Anomalously high values of Th and U suggest that in additions to granitic crust KLIP magma also reacted with deep-level organic-rich shale, as has been confirmed from drill core data.

Most of the initial $^{87}Sr/^{86}Sr$ ratios of the pillow lavas presented in this work scatter around ca. 0.708, which is also the value of Jurassic seawater. There is also clear relationship of increase in the $\delta^{18}O$ values concomitantly with increasing alteration. This is well-known feature at low-temperature alteration, when basalts are altered to high- $\delta^{18}O$ bearing minerals such as clays and zeolites, thus stripping ^{18}O by mass balance from seawater. It is most likely therefore that the basaltic pillow lavas and hyaloclastites altered under low-temperature conditions in seawater. However, the consistent loss of Na_2O, comparable to the trend as seen in subglacial, freshwater-altered hyaloclastites (in Iceland), may indicate some geochemical modification in freshwater environment.

Thus, it appears that the early parts of the KLIP volcanics erupted in relatively (500 m) deep water. This was either a lake system, of similar depths to Lake Tanganyika, or, more likely, a rift system with fragmented continental lithosphere surrounded by ocean spreading domains, such as at the open-end of the East African rift across the Afar. Present uplift data shows that shortly thereafter (by 183 Ma), KLIP uplifted above sea level; and by 120-140 Ma reached heights of 2 km or more. These new findings have major implications for geodynamic models that focus on both the uplift and continental separation history of Gondwana.

References

1. Jones, J.G., 1969. Pillow lavas as depth indicators. American Journal of Science 267, 181-195.
2. Moore, J.G., 1965. Petrology of deep-sea basalts near Hawaii. American Journal of Science 263, 40-52.
3. Moore, J.G., Schilling, J-G., 1973. Vesicles, water, and sulfur in Reykjanes Ridge basalts. Contributions to Mineralogy and Petrology 41, 105-118.

MID-PROTEROZOIC LARGE IGNEOUS PROVINCES AND ENVIRONMENTAL PERTURBATION

Diamond C. W. [1], Ernst R. E. [2,3], Zhang S-H.[4], Lyons T. W.[1]

[1]Department of Earth Sciences and NASA Astrobiology Institute, University of California Riverside, Riverside, CA 92521, USA
[2] Department of Earth Sciences, Carleton University, Ottawa, Ontario K1S 5B6, Canada
[3]Faculty of Geology and Geography, Tomsk State University, Tomsk 634050, Russia
[4]Institute of Geomechanics, Chinese Academy of Geological Sciences, MLR Key Laboratory of Paleomagnetism and Tectonic Reconstruction, Beijing 100081, China

During the Phanerozoic, the emplacement and weathering of some large igneous provinces (LIPs) have had profound implications for global climate and marine biogeochemical cycles. These effects have often included shallow marine anoxia, leading to metazoan extinction and enhanced burial of organic matter. These outcomes, however, stem from initial conditions unique to the Phanerozoic, and it is possible that similar LIP activity in the weakly oxygenated, bacterially dominated world of the Proterozoic would have led to different results. Here, we review the available geochemical data that underpin our perception of mid-Proterozoic (1.8-0.8 Ga) environmental conditions, emphasizing both the remarkable stability present in many records during this time and the few, apparently transient, departures from these baseline conditions. We will go on to consider feedbacks present in the Earth system that could have maintained stability over these billion years and highlight recent modeling attempts to narrow the range of environmental parameter space allowable during the time. One common result of these models is a requirement for low global productivity to maintain low atmospheric O_2. This low primary productivity is generally thought to have resulted from nutrient limitation associated with widespread anoxia in the deep ocean. Given this scenario, the weathering of a large amount of mafic material over a relatively short time span could have significantly perturbed global O_2 production. Finally, we will review an up to date record of continental LIP activity. While this record is naturally incomplete, existing remnants suggest a pulse of activity around 1.4 Ga, a time when multiple independent redox proxies point to transiently heightened biospheric O_2.

A NEW KEY PALEOMAGNETIC POLE FOR THE ~1.8 GA KAAPVAAL CRATON: IMPLICATIONS FOR THE PALEOPROTEROZOIC APPARENT POLAR WANDER AND RECONSTRUCTIONS

Djeutchou C., de Kock M.O., Wabo H.

Department of Geology, University of Johannesburg, PO Box 524, Auckland Park 2006, Johannesburg, Gauteng, South Africa. Corresponding author e-mail: djeutchoucdric@yahoo.fr

Keywords: *Dyke swarm, Kaapvaal craton, Columbia/Nuna supercontinent.*

Dykes are ideal targets for paleomagnetic studies because (i) they experienced a rapid cooling and represent snapshots of the Earth's magnetic field, (ii) they contain minerals which can be dated to establish their precise crystallization ages, (iii) they represent excellent time indicators of paleostress to infer plume-head impact on the crust which is pivotal for supercontinent reconstructions, (iv) individual dyke represents a single cooling unit, which limit site duplication like it can be the case for a single massive intrusion. In this study, two N-trending, one SE-trending and twenty-four NE-trending dolerite dykes intruding the Archean granitoid basement over an area of ~55 000 km^2 in the northeastern Kaapvaal craton were paleomagnetically sampled. High-stability magnetizations were isolated from twenty-seven dykes; seven of which yield precise baddeleyite U-Pb ages between 1.88 and 1.83 Ga. These remanences, which mostly occurred as positively inclined directions are interpreted as primary based on antipodal groupings as well as several positive baked contact tests. The existence of dual polarity primary remanence directions recorded by distant dykes, combined to available ages suggest that the 1.8 Ga magmatism is a widespread event in the Kaapvaal craton and involved multiple magma pulses. Combining the primary magnetization among sites and existing radiometric ages further allow us to evaluate the reversal rates of the Earth's magnetic field at the time interval spanned by the studied dykes and to constrain the existing magnetic barcode for the Kaapvaal craton. Slight grouping differences of mean sites confirm that the paleosecular variation has been adequately averaged out. Large groupings differences, however, cannot be explained by paleosecular variations and are interpreted in the context of the ~1.8 Ga true polar wander path previously reported from other cratons. Our primary directions are compiled with reliable existing results to provide the best-constrained yet developed ~1.8 Ga key paleomagnetic pole for the Kaapvaal craton. Our new key paleopole provides additional constraints for Kaapvaal craton's latitudinal drift in Paleoprotezoic, with which test the existing paleogeographic reconstructions for the Columbia/Nuna supercontinent.

2.5 GA MAFIC DYKES IN THE KOLA AND MURMANSK BLOCKS, EASTERN FENNOSCANDIA: COMPOSITION, PETROLOGY AND PALEOCONTINENTAL APPLICATION

Egorova S. V.[1], Stepanova A. V.[1], Salnikova E. B.[2], Larionova Y. O.[3], Arzamastsev A. A.[2,4], Samsonov A. V.[3], Veselovskiy R. V.[5,6]

[1]*Institute of Geology Karelian Science Centre, Petrozavodsk, Russia*
[2]*Institute of Precambrian Geology and Geochronology, Saint-Petersburg, Russia*
[3]*Institute of Geology of Ore Deposits, Petrography, Mineralogy and Geochemistry, Moscow, Russia*
[4]*Institute of the Earth Sciences, Saint-Petersburg State University, Russia*
[5]*Lomonosov Moscow State University, Moscow, Russia*
[6]*Institute of Physics of the Earth, Moscow, Russia*

Keywords. *Paleoproterozoic, mafic dykes, Kola block, Murmansk block, Mistassini event*

Reconstructions of supercontinents are usually based on the correlations of precisely dated magmatic and metamorphic events and paleomagnetic data (Ernst et al., 2013). In this context, large igneous provinces (LIPs) are useful because these short-lived plume-related mafic igneous events often mark a continental breakup and preserve primary paleomagnetic records.

Relicts of ca. 2505 Ma Mistassini LIP that have been recognized in several cratons (Ernst, 2014) include (1) mafic dyke swarms in the Superior, Hearn and Nain cratons in the Canadian Shield (Sandeman, 2013; Ernst, 2014); (2) layered intrusions, mafic volcanics and dykes in the Kola block (Amelin et al., 1995; Bayanova, 2004; Glebovitsky, 2005; Fedotov et al., 2012; Ciborowski et al., 2015); (3) gabbro-anortosite intrusions of the Belomorian mobile belt (Stepanova et al., 2017); (4) Shala and Avdeevo dykes in the southern Karelian craton (Bleeker et al., 2008).

A conjunction of the Early Paleoproterozoic mafic igneous provinces of the Canadian Shield and Eastern Fennoscandia have been proposed by L. Heaman (Heaman, 1995) and later followed by Bleeker and Ernst (Bleeker, Ernst 2006) in the Superia supercraton reconstruction. In the Superia reconstructions Kola and Karelia were considered as parts of a single Kola-Karelia continental block (Bleeker, Ernst, 2006).

Our new geochemical and Sm–Nd isotope data and baddeleyite U–Pb ID-TIMS dating results indicate that ca. 2505 Ma mafic dykes are widespread in the Kola and Murmansk blocks.

The olivine gabbronorite dykes occupy an area in the central part of the Kola block. Dyke margins are composed of olivine-porphyrite, whereas internal parts comprise medium- to coarse- grained massive olivine gabbronorite and melanogabbronorite. High concentrations of MgO (up to 20.23 wt. %), Cr (> 2000 ppm), Ni (> 700 ppm), relatively high SiO_2 (up to 53 wt.%) and low TiO_2 (<0.54 wt.%) content are characteristic feature of these dykes. The olivine gabbronorite have low contents of HFSE and exhibit fractionated REE patterns with LREE enrichment and HREE depletion ((La/Sm)n= 2.8–3.5, (Gd/Yb)n= 1.3-1.6). The U-Pb (ID-TIMS) baddeleyite concordant age of 2503±1 Ma from the Olenegorsky quarry Ol gabbronorite dyke define the crystallization age of the high-Mg dykes and is consistent with previous results (Layered…, 2004; Rodionov et al., 2014).

The quartz doleritic dykes are most widespread in the Kola-Murmansk region. These dykes vary in thickness from a few meters to a few tens of meters and form several NNE-trending swarms outcropping along Barents Sea coast from the Pechenga Bay to the Savikha Bay. Petrographically, dykes are uniform, their central parts are composed of fine-grained quartz-bearing and granophyre dolerite, dominated by plagioclase laths and ophitic clinopyroxene. Chemically, the dykes range in composition from low-Mg basite to diorite. All dykes are characterized by a strong depletion of Nb (Nb/Nb* = 0.17-0.41), have fractionated REE patterns ((La/Sm)n= 2.1–4.1, (Gd/Yb)n= 1.3-2.1) and negative εNdT values varying from -1.7 to -1.3. According to the U-Pb (ID-TIMS) baddeleyite age data the crystallization age of quartz doleritic dykes is 2505 Ma.

The pyroxene-plagioclase porphyrite dykes were found in the central part of the Kola block. Dyke thickness never exceeds 2 meters, therefore their margins and internal parts comprise similar fine-grained Px-Pl porphyrite (dolerite). Moderate MgO (6.1–6.7 wt. %), relatively high Al_2O_3 (15.8-17.1 wt. %) concentrations and low contents of HFSE, fractionated REE patterns ((La/Sm)n = 2.4–3.0, (Gd/Yb)n = 1.4–1.6) and negative εNd_T values (εNd_T= -2.3) are typical of pyroxene-plagioclase porphyrite.

Few olivine gabbro dykes were found in the Barents sea coastal part of the Murmansk block. The chilled margins of these dykes are composed of olivine-porphyrite, whereas cores are comprise medium-grained massive olivine microgabbro. The olivine gabbro are characterized by relatively low MgO (to 8.5 wt.%) and elevated TiO_2 (to 1.4 wt.%) concentrations. Depletion in HREE and Nb ((Gd/Yb)n=2.5–2.7; Nb/Nb*=0.38–0.40) combined with negative εNd_T values (varying from -0.28 to -0.62) are characteristic features of these rocks. The U-Pb (ID-TIMS) baddeleyite concordant age of 2505±4 Ma from the Varzina Bay dyke define the crystallization age of olivine gabbro dykes.

The geochronological, Nd isotopic and geochemical data indicate that ca. 2505 Ma mafic dykes in the Kola and Murmansk blocks could be subdivided into two petrological groups. The dykes of Group I include olivine gabbronorite, quartz dolerite and Px-Pl porphyrite. These rocks show great similarity with previously studied in the Kola block components of ca. 2505 Ma event. The olivine gabbronoritic dykes are analogues of layered intrusions of Monchegorsk area (Layered…, 1995). The quartz doleritic and Px-Pl porphyritic dykes are similar with andesibasalts of Seidorechka Fm, Imandra belt (Melezhik et al., 2013). MELTs modelling results suggest that Group I dykes, layered intrusions and mafic volcanics could be related via fractional crystallization of a single parental melt. The isotopic features of these group in-

dicate high degrees of crustal contamination.

The dykes of Group II comprise olivine gabbro dykes with distinct Nd isotopic and geochemical characteristics that have no clear analogues in the adjacent areas and recognized only in the north-eastern part of the Kola Peninsula. Their parental melts were probably generated via relatively low degrees of mantle melting in the garnet stability field and underwent relatively low degrees of crustal contamination that other components of ca. 2505 Ma event.

The analysis of geological, geochemical, geochronological and Nd isotopic data of studied dykes allow to conclude that:

2505 Ma mafic dykes are widespread both in Kola and Murmansk blocks. Wide area distribution, high-magnesium composition of the dykes and short duration of these event are evident for mantle plume-induced mantle melting on a wide area within Archean crustal blocks of the Fennoscandian Shield in the beginning of the Paleoproterozoic. 2505 Ma mafic dykes of Kola and Murmansk blocks could be subdivided into two groups, reflecting variations in degrees of mantle melting and crustal contamination.

Spatial and age data suggest that mafic dyke swarms in the Kola and Murmansk blocks could be considered as components of a ca. 2505 Ma Mistassini LIP. These data also suggest that Kola and Murmansk blocks were connected with Superior craton of the Canadian Shield in the beginning of the Paleoproterozoic. The center of the plume was probably located within the Kola block - in the area there most high-Mg (high-temperature) rocks occur. The Karelian craton, in this case, could be located on the periphery of the plume-affected area that caused a small volume of ca. 2505 Ma igneous rocks within this crustal segment.

This work was supported by the Russian Science Foundation (Grant 16-17-10260).

References

1. Amelin Y.V., Heaman L.M., Semenov V.S. (1995) U-Pb geochronology of layered mafic intrusions in the eastern Baltic Shield: implications for the timing and duration of Paleoproterozoic continental rifting. Precam. Res. 75: 31–46.
2. Bayanova T. B. (2004) Age of Reference Geological Complexes of the Kola Region and Duration of Magmatism Processes (in Russian). Nauka, St. Petersburg.1-172.
3. Bleeker W., Hamilton M.A., Ernst R.E., Kulikov V.S. (2008) The search for Archean-Paleoproterozoic supercratons: New constraints on Superior-Karelia-Kola correlations within supercraton Superia, including the first ca. 2504 Ma (Mistassini) ages from Karelia. Abstract for IGC33 meeting, Oslo, Norway.
4. Bleeker, W., Ernst, R. (2006) Short-lived mantle generated magmatic events and their dyke swarms: The key unlocking Earth's paleogeographic record back to 2.6 Ga. Dyke swarms — time markers of crustal evolution. 3–26.
5. Ciborowski T. J. R., Kerr A. C., Ernst R. E. et.al. (2015) The early proterozoic Matachewan Large Igneous Province: geochemistry, petrogenesis and implications for Earth evolution. Journal of petrology 56(8):1459-1494.
6. Ernst, R.E., Bleeker, W. (2010) Large igneous provinces (LIPs), giant dyke swarms, and mantle plumes: significance for breakup events within Canada and adjacent regions from 2.5 Ga to present. Canadian Journ. of Earth Sciences 47: 695-739
7. Ernst R.E., Bleeker W., Söderlund U., Kerr A.C. (2013) Large Igneous Provinces and supercontinents: Toward completing the plate tectonic revolution. Lithos 174: 1–14
8. Ernst R. (2014.) Large igneous provinces. Cambridge Univ. Press. 1-666
9. Fedotov Z.A., Bayanova T.B., Serov P.A. (2012) Spatio-temporal relationships of dike magmatism in the Kola region, the Fennoscandian Shield. Geotectonics 46: 412-426
10. Glebovitsky V.A. (Ed). (2005) Precambrian of the Baltic Shield (in Russian). St. Petersburg, Nauka Publ. 1-711.
11. Heaman, L.M. (1995) U–Pb dating of mafic rocks: past, present, and future. Geological Association of Canada – Mineralogical Association of Canada. Program with Abstracts, 20: A43.
12. Melezhik V.A. et al. (2013) 6.1 The Imandra/Varzuga Greenstone Belt. Reading the archive of Earth's oxygenation 6:1.
13. Layered intrusions of the Monchegorsk ore area. Part 1 (in Russian) (2004) Apatity: Kola research centre RAS. 177 p.
14. Sandeman H.A., Heaman L.M., LeCheminant A.N. (2013) The Paleoproterozoic Kaminak dykes, Hearne craton, western Churchill Province, Nunavut, Canada: Preliminary constraints on their age and petrogenesis. Precam. Res. 232: 119–139
15. Stepanova, A.V., Stepanov, V.S., Larionov, A.N., Azimov, P.Ya., Egorova, S.V., Larionova, Yu.O. (2017) 2.5 Ga Gabbro-anorthosites in the Belomorian Province, Fennoscandian Shield: Petrology and Tectonic Setting. Petrology 25(6): 566-591.
16. Rodionov N., Belyatsky B., Antonov A., Smolkin V., Sergeev S. (2014) Baddeleyite and zircon dating of gabbronorite rocks from the Early Proterozoic Monchegorsk Layered Mafite-Ultramafite Complex in the Kola Peninsula (Russia): evidence for very close synchronous magmatism. 7th International SHRIMP Workshop. National Institute of Polar Research, Japan. 26-31.

FRONTIERS IN LARGE IGNEOUS PROVINCE RESEARCH

Ernst R. E.

Department of Earth Sciences, Carleton University, Ottawa, Canada
Faculty of Geology and Geography, Tomsk State University, Tomsk, Russia

Keywords: *resource exploration, ore deposit, climate change, mass extinction, planetary geology, geochemistry*

Introduction

Large Igneous Provinces (LIPs) are huge volume, short duration volcanic/intrusive events often linked to mantle plumes, that occur every 20-30 million years and can rival plate tectonics in importance. LIPs have become an important research focus because they are an efficient tool for reconstructing Pre-Pangea supercontinents, provide insights into volcanism on other planets, caused dramatic climate change including mass extinctions throughout Earth history, and are growing in importance as a tool for finding new ore and also oil/gas deposits.

LIP definition and essential characteristics

LIPs represent large volume (>0.1 Mkm^3; frequently above 1 Mkm^3), mainly mafic (-ultramafic) magmatic events of intraplate affinity (based on tectonic setting and/or geochemistry) that occur in both continental and oceanic settings, and are typically either of short duration (<5 Ma; sometimes < 1 Ma) or consist of multiple short pulses that occur over a maximum of a few 10s of Ma (Ernst, 2014; Ernst and Youbi, 2017). They consist of volcanic packages (flood basalts) and a plumbing system of mafic dyke swarms, mafic sill complexes, layered mafic-ultramafic (M-UM) intrusions, and crustal magmatic underplates.

Continental LIPs are typically associated with minor silicic magmatism, but can also be associated with major silicic magmatic events termed Silicic LIPs (SLIPs) as well as carbonatites and kimberlites. LIPs occur at a variable rate that averages approximately every 20-30 Myr but with possible peaks associated with supercontinent breakup, back at least to 2.5 Ga. The rate of LIP occurrence in the Archean is less certain because of poorer preservation.

A variety of models have been proposed for LIP and other intraplate magmatism, including rifting, delamination, edge convection, melting of water enriched mantle; however, mantle plumes arguably have a role in the majority of LIPs

Paleocontinental reconstructions:

LIPs and especially their regional dyke swarms represent an efficient tool for constraining paleocontinental reconstructions: 1) comparison of LIP 'barcodes' can reveal which crustal blocks were nearest neighbors and over what time span; 2) reconstruction of coeval dyke swarm trends from different crustal blocks into giant linear, radiating and circumferential swarms, constrains the relative positioning of these blocks, and 3) LIP units are particularly reliable for paleomagnetic study for reconstructions (Bleeker and Ernst, 2006).

LIP Plumbing System

A new plumbing system model is proposed for plume-related continental LIPs linking flood basalts to a feeder system of sill provinces, dyke swarms (linear, radiating and circumferential), mafic-ultramafic intrusions (M-UM), a magmatic underplate at the base of the crust and ultimately to mantle source areas (Ernst et al. 2019).

Tracking geochemical batches

Magmas can have a number of discrete pathways into the crust from both asthenospheric and lithospheric sources before being distributed vertically and horizontally through the crust. Geochemistry, integrated with an understanding of the plumbing system framework, is key for tracking the progress of specific magma batches through the LIP plumbing system (e.g. Peate et al., 2008; Neumann et al., 2011). Furthermore, identification of geochemical pathways (between dykes, sill, volcanics, and layered intrusions) can lead to the identifying of "upstream" and "downstream" relationships.

Resource exploration targeting:

The relationships between LIPs and differing metallogenic systems (and also hydrocarbon and aquifer systems) can be condensed into five distinct, although partially overlapping classifications as a tool in exploration targeting (Ernst and Jowitt, 2013, 2017; ch. 16 Ernst, 2014), For instance, if a chalcophile element depleted intrusion is identified, then its identified "upstream" link would have potential for chalcophile element enrichment as an ore deposit.

Planetary analogues:

Large volume mafic magmatism on Venus, Mars, Mercury and the Moon, is an analogue for terrestrial LIPs (e.g. Head and Coffin, 1997; ch. 7 Ernst, 2014). Systematic comparison between terrestrial and planetary LIPs provides new insights for each (e.g. Ernst et al. 2017).

Climate change:

LIPs can have a significant global climatic effect as monitored by sedimentary trace and isotopic compositions that record paleo-seawater/atmosphere variations. Improved U-Pb dating (approaching 50,000 year resolution) for some LIPs is confirming a long-proposed mass extinction-LIP link. The most dramatic climatic effect is global warming due to greenhouse-gases from LIPs. Global cooling (and even global glaciations) can be caused by CO_2 drawdown through weathering of LIP-related basalts, and/or by sulphate aerosols. Ad-

ditional kill mechanisms that can be associated with LIPs include oceanic anoxia, ocean acidification, sea level changes, toxic metal input, essential nutrient decrease, all producing a complex web of catastrophic environmental effects (Ernst and Youbi, 2017; Bond and Grasby, 2017).

Integration of magmatic and sedimentary records

Increased understanding of the environmental effect of LIPs has created an opportunity for more systematic integration of LIPs (and other types of magmatic events) with the sedimentary record (with facies changes, and trace element and isotopic compositional excursions).

Defining natural chronostratigraphic Precambrian boundaries

Based on the robust array of environmental effects due to LIPs, as demonstrated in the Phanerozoic record, it is suggested that LIP events can be used to define natural chronostratigraphic boundaries in the Precambrian Era (e.g. Ernst and Youbi, 2017; Zhang et al. 2018).

Other frontiers

Additional frontier areas will be discussed.

Acknowledgments

This study is partly supported by grants:

RNF 18-17-00240 (assisting in characterizing LIPs of eastern margin of the Siberian craton), Mega-Grant 14.Y26.31.0012 (assisting in characterizing LIPs elsewhere in Russia, and Canadian NSERC CRDPJ 523131-17 (assisting in characterizing LIPs elsewhere in the world).

References

1. Bleeker, W., Ernst, R. 2006. Short-lived mantle generated magmatic events and their dyke swarms: the key unlocking Earth's paleogeographic record back to 2.6 Ga. In Hanski, E., et al. (eds.), Dyke Swarms – Time Markers of Crustal Evolution. London: Taylor and Francis/ Balkema, pp. 3–26.
2. Bond, D.P.G., Grasby, S.E., 2017. On the causes of mass extinctions. Palaeogeogr. Palaeoclimatol. Palaeoecol. 478, 3–29.
3. Ernst, R.E., 2014. Large Igneous Provinces. Cambridge University Press, 653 p.
4. Ernst R.E., Jowitt S.M., 2013, Large igneous provinces (LIPs) and metallogeny, in Colpron M., Bissig, T., Rusk, B.G., Thomspon, J.F.H., eds., Tectonics, metallogeny, and discovery: The North American Cordillera and similar accretionary settings: Society of Economic Geologists Special Publication, 17, 17-51.
5. Ernst, R.E., Youbi, N., 2017, How Large Igneous Provinces affect global climate, sometimes cause mass extinctions, and represent natural markers in the geological record: Palaeogeography, Palaeoclimatology, Palaeoecology, 478, 30–52.
6. Ernst, R.E., Buchan, K.L., Jowitt, S.M.. Youbi, N., 2017. Applying the terrestrial Large Igneous Province (LIPs) context to planetary intraplate magmatism. Lunar and Planetary Science Conference XLVIII, abstract 1373.
7. Ernst, R.E., Liikane, D.A., Jowitt, S.M., Buchan, K.L., Blanchard, J.A. 2019. A New Plumbing System Framework for Mantle Plume-Related Continental Large Igneous Provinces and Their Mafic-Ultramafic Intrusions. Journal of Volcanology and Geothermal Research (in review).
8. Head, J.W., Coffin, M.F., 1997, Large Igneous Provinces: a planetary perspective. in Mahoney, J.J., Coffin, M.F., eds., Large Igneous Provinces: Continental, Oceanic, and Planetary Flood Volcanism: AGU Geophysical Monograph, 100, 411–438.
9. Neumann, E.-R., Svensen, H., Galerne, C.Y., Planke, S., 2011. Multistage evolution of dolerites in the Karoo Large Igneous Province, Central South Africa: Journal of Petrology 52, 959–984.
10. Peate, D.W., Barker, A.K., Riishuus, M.S., Andreason, R., 2008. Temporal variations in crustal assimilation of magma suites in the East Greenland flood basalt province: Tracking the evolution of magmatic plumbing systems. Lithos 102, 179-197.
11. Zhang, S-H., Ernst, R.E., Pei, J-L., Zhao, Y., Zhou, M-F., Hu, G-H., 2018. A temporal and causal link between ~1380 Ma large igneous provinces and black shales: Implications for the Mesoproterozoic time-scale and paleoenvironment. Geology, 46, 963-966.

DEVONIAN BIOTIC CRISES AND LINKS TO LIPS

Ernst R. E.[1,2], Rodygin S. A.[2], Grinev O. M.[2]

[1]*Dept. Earth Sci., Carleton Univ., Ottawa, Canada 82071*
[2]*Faculty of Geology and Geography, Tomsk State University, Tomsk 634050, Russia*

Keywords: *biotic crises, LIPs, Devonian, anoxia*

Large Igneous Provinces (LIPs) are emerging as a significant driver of short duration climatic change including mass extinctions (e.g., Bond and Grasby, 2017; Ernst and Youbi 2017). We compare the record of LIPs against the timing of Devonian (and end-Silurian) biotic crises that are recorded in the numerous anoxia events throughout this period (Figs. 1, 2). The largest LIPs are two-pulse events at ca. 370 and ca. 360 Ma that are present in both Siberia (Yakutsk-Vilyui LIP) and Baltica (Kola-Dnieper LIP) and correlate with the Kellwasser anoxia events (end Frasnian) and Annulata or Dasber and Hangernberg anoxia events in the middle/late Famennian. The regionally significant Altai Sayan LIP is only approximately dated at c. 400 Ma and within uncertainties could be linked to either (or both?) the c. 405 Ma Chebbi or Atopus anoxia events near the basal Emsian (associated with graptolite extinction) or the c. 385-390 Ma group of anoxia events in the Eifelian or Givetian.

Additional magmatic events that are less precisely dated are: 1) the c. 0.45-.41 "Overstep volcanic-sedimentary events and 0.38–0.33 Maritimes (Magdalen) basin event of the Appalachian region of eastern Canada and adjacent US, 2) lower Devonian Selwyn basin alkaline magmatism of northwestern Canada, and 3) the Ordovician - late Silurian Soltan Maidan event and younger Devonian volcanics pulses of Iran. However, more precise dating is required for each of these before they can be usefully compared with the Devonian (late Silurian) biotic crisis record.

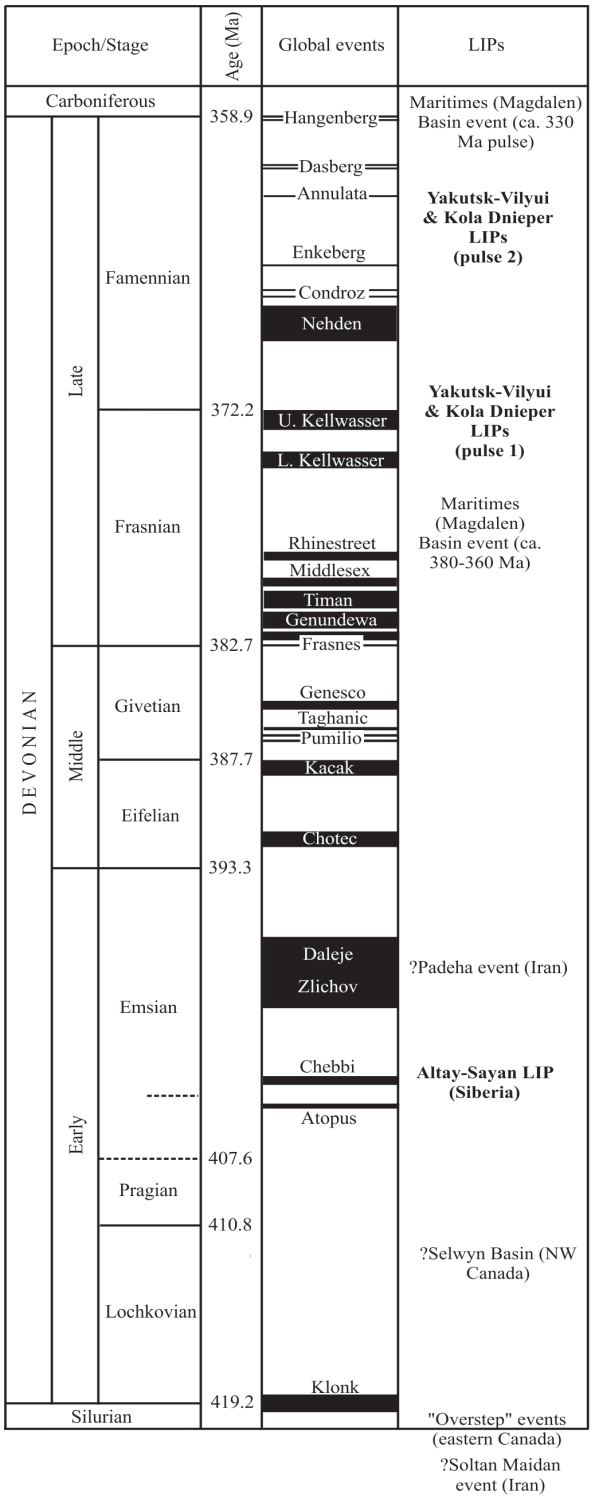


Figure 1. Potential correlations of Devonian (late Silurian) LIPs with black shale events and other biotitic crises. See text and Ernst et al. (2019) for more details.

Acknowledgements

This study is partly supported by RNF grant 18-17-00240 of the Russian Federation.

References

1. Bond, D.P.G., Grasby, S.E. (2017). On the causes of mass extinctions. Palaeogeography, Palaeoclimatology, Palaeoecology, v. 478, p. 3–29.
2. Ernst, R.E., Youbi, N. (2017). How Large Igneous Provinces affect global climate, sometimes cause mass extinctions, and represent natural markers in the geological record. Palaeogeography, Palaeoclimatology, Palaeoecology, v. 478, p. 30-52.
3. Ernst, R.E., Rodygin, S.A., Grinev, O.M. (2019) Large Igneous Provinces as probable trigger of Devonian biotic crises. Global and Planetary Change (in review)

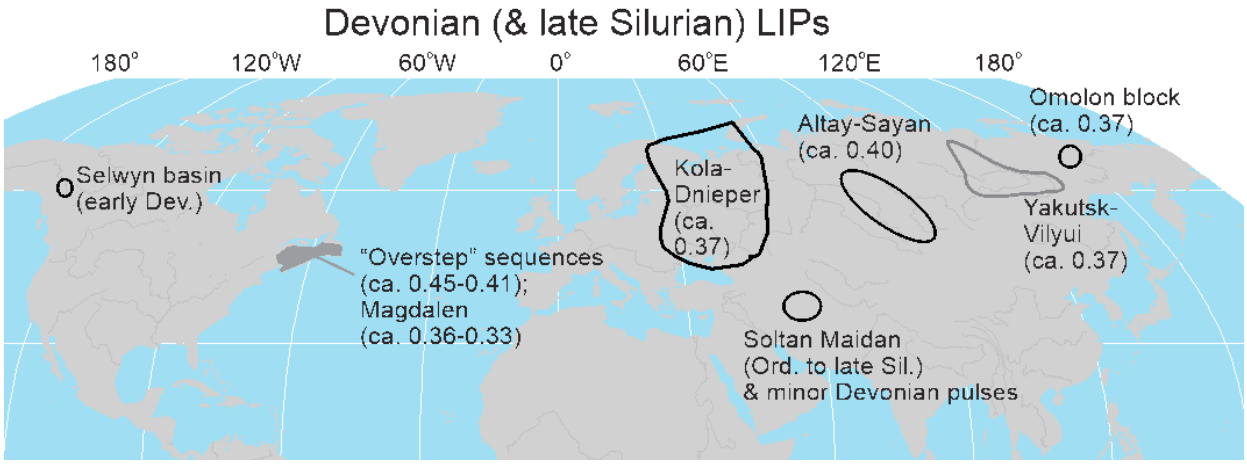


Figure 2: Distribution of LIPs and other important intraplate magmatism of Devonian (and late Silurian) age discussed in this abstract. After Ernst et al. 2019.

EARLY-MIDDLE DEVONIAN KAZAKHSTAN-ALTAI-SAYAN IGNEOUS PROVINCE: FACIES AND TECTONIC ASPECTS

Fedoseev G. S.

Sobolev Institute of Geology and Mineralogy SB RAS, Novosibirsk, Russia

Keyword: *MIP, mafic sillogenesis, rheological breccia*

Introduction

Large igneous provinces of basic composition emplaced on the continental and/or oceanic platforms are subdivided into two facies types: effusive and dike (Ernst, 2014). The dike-sill type is proposed to distinguish within the mobile (orogenic) belts. (Fedoseev, 2003). In the middle part of the Central Asian orogenic belt it is mapped on a vast territory that can be called as Kazakhstan-Altai-Sayan igneous province (KASIP). It covers an area from the southern spurs of the Urals to the southwestern margin of the Siberian platform extending for about 2000 km with an average width of about 450 km (Fig. 1). However, actually by the total volume of mafic magma including preceding products of pyroclastic volcanism of acid and intermediate composition, it does not conform to the classical LIPs and therefore it can be considered as a medium-scale province (KASMIP).

Results

According to the present concept, the KASMIP is a junction area of active continental margins of the Kazakhstan and Siberian paleocontinents. Evolving in the mode of a young platform, this area changed into a rift-like area. Therefore, the volcanogenic-sedimentary formations of the platform cover including mafic sills were fragmented into numerous blocks. The amount of mafic bodies in different formations varies widely. The total thickness of basalt-dolerite bodies in individual blocks vary widely and can frequently reach several tens of meters. On generally, this is in agreement with the hypothesis of the feasible existence of one or more sedimentary basins whose depocenters are preserved as the Minusa, Kuznetsk, Tuva, Agul, and other troughs (Krasnov et al., 2018).

The obtained new geological data are in contradiction with the traditional concept of the facies nature of mafic bedded bodies and the time of their formation. It turns out that they occur in KASMIP as sills (hypabyssal facies) rather than effusive flows and sheets (surface facies). It is not surprising, then, that the resumed discussion on the correct recognition of the effusive paleo flows and shallow sills are very timely (Makarenko, Kotel'nikov, 2018) The Minusa trough is undoubtedly a worthy area for its constructive development under the "field" conditions, a visit to which is provided for both excursions. This problem is actual when performing geological surveying works, which inevitably stimulates the development of internally consistent set of convergent, divergent and conditionally divergent (false valid) features for identifying the facies of the mapped mafic rocks. Two examples of divergent features of shallow sills are shown hereafter (Fig. 2).

The tectonic factor is of paramount importance among the cause and effect relationships when modeling the process of sill formation ("sillogenesis" in a broad sense). At the moment, there are three versions of the trigger mechanism of sillogenesis: a) undercompensation periods of the downwarping of the Earth's crust (after G.S. Fedoseev), b) decompression of dilatancy faults (after S.Yu. Kolodyazhnyi), c) intersection of the «basement/cover» border by the geochord (after M.G. Leonov), which were proposed in 2006, 2011, and 2013, respectively.

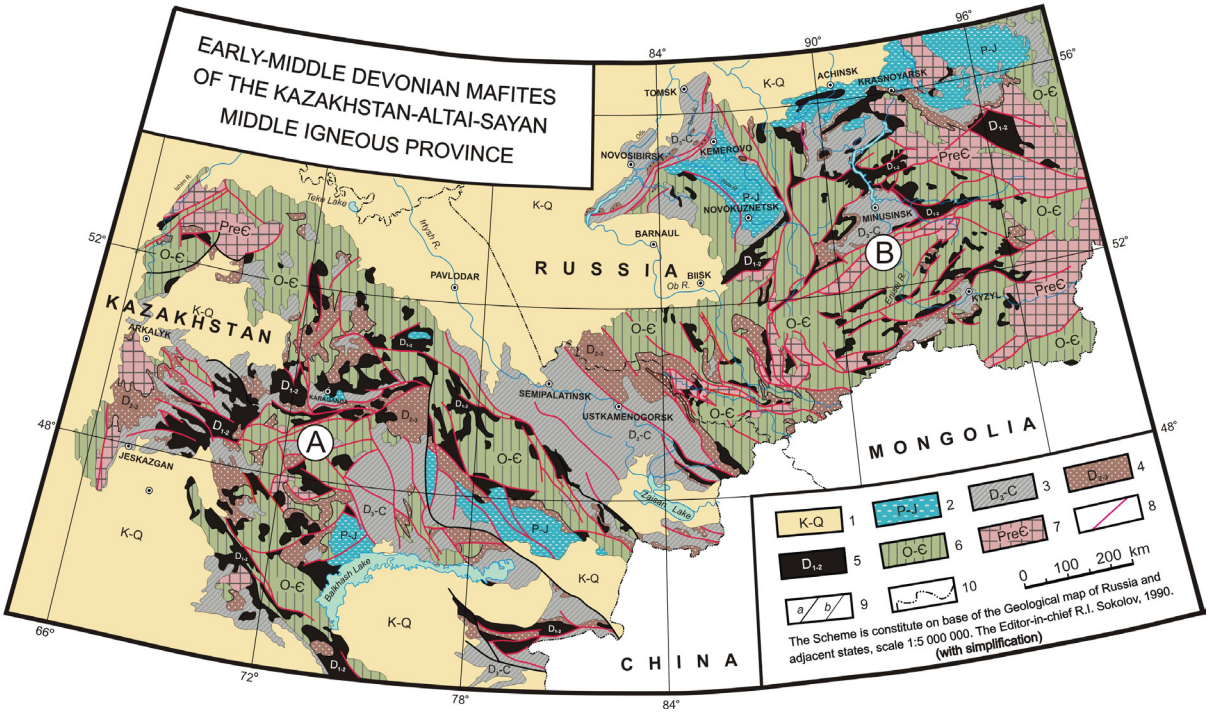


Fig. 1. Location of the Kazakhstan (A) and Altai-Sayan (B) areals.
1–5 – cover formations: 1–3 – terrigenous, 4 – volcanogenic-terrigenous, 5 – terrigenous-volcanogenic with dike-sill complexes; 6–7 – volcanogenic-terrigenous-carbonate formations of the basement; 8 – faults; 9 – formation boundaries: 9a – Devonian, 9b – other formations; 10 – state boundaries.

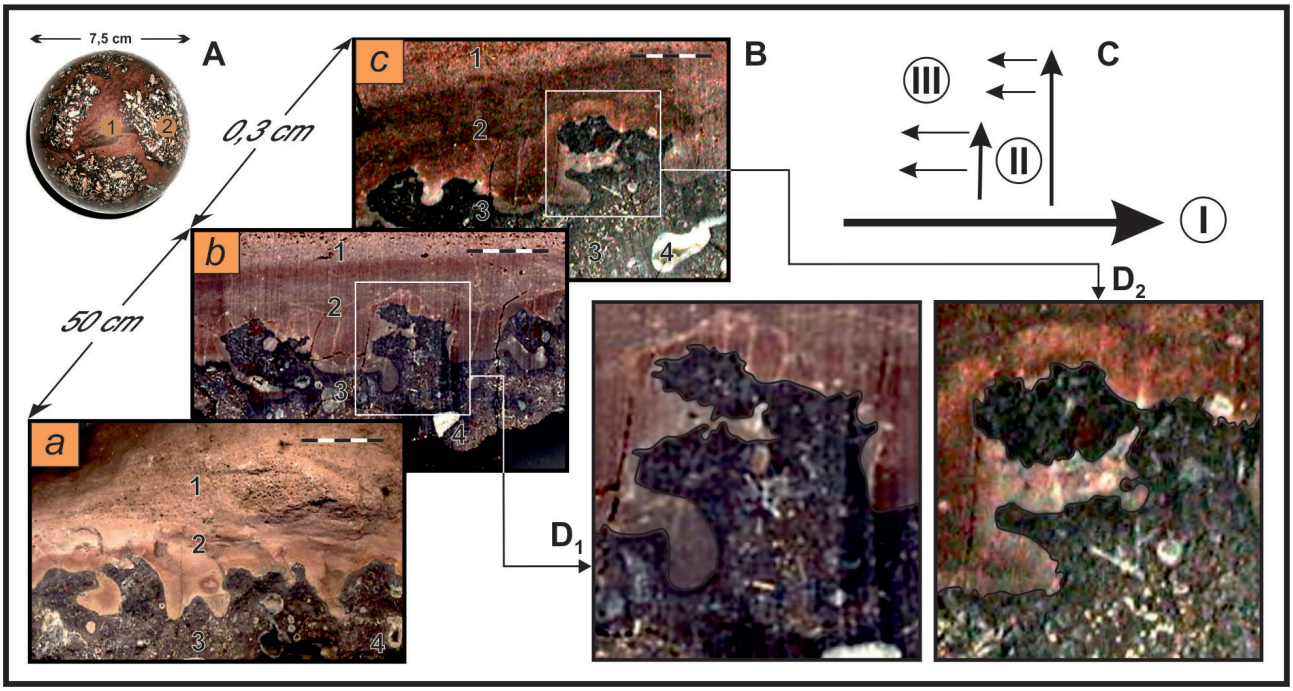


Fig. 2. The inversion-rheological breccia (A) and magmadiverticulas (B) in the Ust'-Koksa and Sisim sills, respectively; stages of diverticula formation (C) and section fragments (D_1, D_2). A: 1 – Early Devonian sandstone, 2 — fragments of plagioclase porphyrite, which previously (NB!) has intruded this sandstone (!); B: 1 – sandstone, 2 – siltstone, 3 – basalt, 4 – calcite amygdule; C: 1 – supposed direction of magma flow path during sill formation, II–III – directions of the first (II) and second (III) stages of the intrusion. Scale bar is 1 cm.

Conclusions

The development of the concept of sillogenesis is not an end in itself. An increased attention to this issue (as well as a critical attitude) is caused primarily by a number of direct and indirect consequences, which are both of theoretical and practical significance. The direct consequences deal with the improvement of the history of geological development and stratigraphic schemes, recognition of the antidromous scheme of "Byskar" magmatism, and reevaluation of potential metallogenic specialization. The indirect consequences include, apparently, the rift-like (non riftogenic) nature of KASMIP and the "sill" reason in explaining a global catastrophe due to short duration of trap formation in Siberia (Burgess et al., 2017). The authors relate a biospheric collapse with an abundant emplacement of mesoabyssal sills. However, their intrusion into Tungus basalts is doubtful.

Acknowledgements

I thank V.S. Gimon for the translation of these theses. This work was conducted under state assignment, project N 0330-20-16-001.

References

1. Burgess S.D., Muirhead J.D. & Bowring S.A. (2017) Initial pulse of Siberian Traps sills as the trigger of the end-Permian mass extinction. Nature Communications, 8; 164:https://www.nature. com/articles/s41467-017-00083-9
2. Fedoseev G.S. (2003) The concept of continental mafic sillogenesis. Current problems of formational analysis, petrology and ore content of igneous formations. Publishing house: Branch "GEO":348-349.
3. Ernst Richard E. (2014) Large Igneous Provinces (LIPs). Cambridge university press: 653.
4. Krasnov V.I., Fedoseev G.S., Ratanov L.S. (2018) The role of the byskarian series in geological structure and historical development of the Minusa trough. Geology and mineral resources of Siberia 4(36):8–21.
5. Makarenko N.A., Kotel'nikov A.D. (2018) Devonian magmatism of the Minusa trough in the light of two geological hypotheses – continental sillogenesis and alkaline-basic petrogenesis (based on scientific publications). Geology and mineral resources of Siberia 4(36):105–111.

THE DENSITY OF FAULTS OVER TRIASSIC RIFTS AND PALEOZOIC BLOCKS AT DIFFERENT OIL AND GAS FIELDS IN WESTERN SIBERIA

Galinsky K.[1], Zagorovsky Y.[1,2], Kobylinsky D.[2], Novikova L.[2]

[1] *Industrial University of Tyumen, Tyumen, Russia*
[2]*Gazprom geologorazvedka LLC, Tyumen, Russia*

Keywords: *West Siberian basin, rift, faults, seismic*

Introduction

The West Siberian sedimentary basin is of the riftogenic type, with Triassic rifts at its basement (Surkov, Zhero 1981; Ulmishek 2003). In the Triassic Western Siberia could become the ocean (Aplonov 1987, Rudkevich 1987).

The rifts are filled with heavy and magnetic rocks, there is a lot of basalt and other volcanic rocks in this structures. That is why, we can see the gravimetric and magnetic anomalies above them (Figure 1).

Nowadays we have 3D seismic data from most of the oil and gas fields in this huge petroleum basin. Using these data we can see fault systems in terrigenous rocks of Jurassic, Cretaceous, Paleogene.

3D seismic data from many oil and gas fields has shown that faults in the oil and gas bearing formations of West Siberian basin are arranged in chain systems. The direction of these faults is connected with the rift system of the basin. It turned out that the faults surfaces are curved as propellers. The surfaces of faults in many fields (Yety-Perovskoye, Gubkinskoye, Vyngapurovskoye, Vyngayakhinskoye etc.) and the mechanism of their formation were described by A.I. Timurziev with coauthors (Timurziev 2009; Gogonenkov et al. 2007). They are the result of twisting rocks with linear movements of the cover along the rifts.

Now we have new seismic data from other areas. Different oil and gas fields of Western Siberia have different history and number of faults. Some fields contain almost no faults, while others are very much broken. The folds have different amplitude. It is very interesting to compare the number of faults with the results of the thicknesses analysis and type of rocks of the pre-Jurassic base of the basin in different fields.

Results

One of the most fractured fields in Western Siberia is Medvezhye gas field (Figure 2). Medvezhy dome – quite ancient structure, it was formed before the Cenomanian, however, it had much smaller amplitude in those time (Figure 3). The basement is formed by metamorphic shales of Paleozoic.

Geochemical exploration shows that the faults are leaking methane and other hydrocarbons (Zavatsky, 2008).

At the Urengoy and Pestsovoye fields there are few big faults. The basement consists of basalt, and the arch was formed after the Cenomanian, there was a depression before Cenomanian here (Zagorovsky 2017).

There are very few faults at the Kharasavey gas field. Basement is uncovered, but the analysis of thicknesses shows us that it's a young (Neocomian) fold.

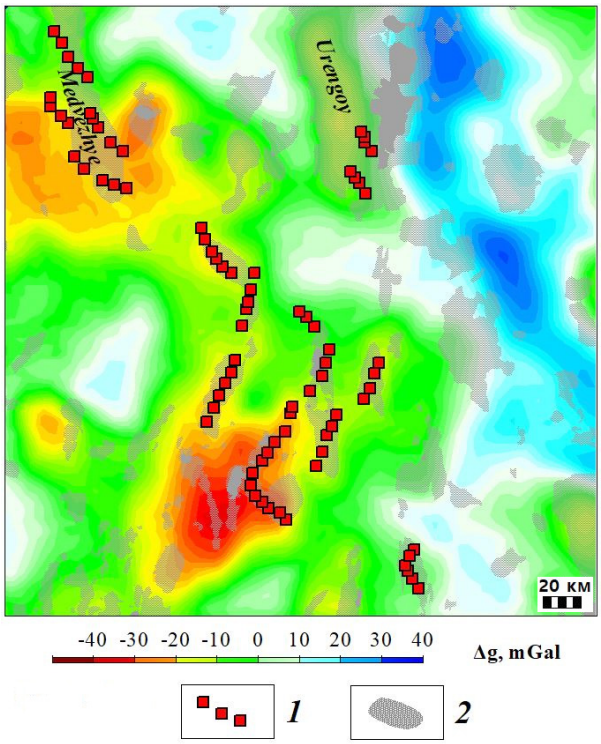


Figure 1. Gravity anomalies over Triassic rifts, position of the largest systems of faults (1), oil and gas fields (2)

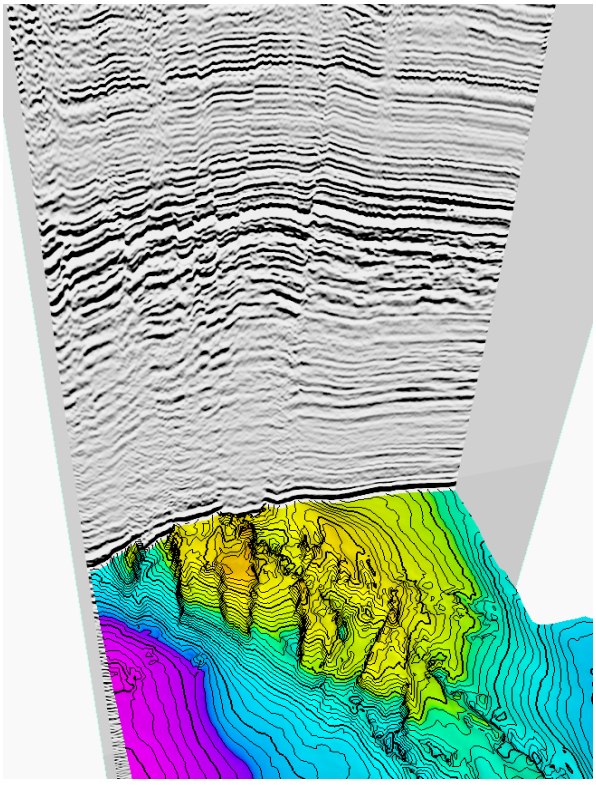


Figure 2. Faults on seismic time section across Medvezhye gas field, typical for Western Siberia system of faults

There is Bovanenkov gas field near Kharasavey. Bovanenkov dome is older than Kharasavey and there are typical chains of faults here. The basement is combined metamorphosed rocks of Paleozoic.

The Novoportov field, Yarudey and Suginsky arches are rich with faults like Medvezhye field (Sudakova 2019). The basement is formed by late Paleozoic dolomites, shales, volcanic rocks, breccia.

It is quite obvious that the greatest number of faults are formed at the central parts of more ancient arches where there are blocks of Paleozoic rocks.

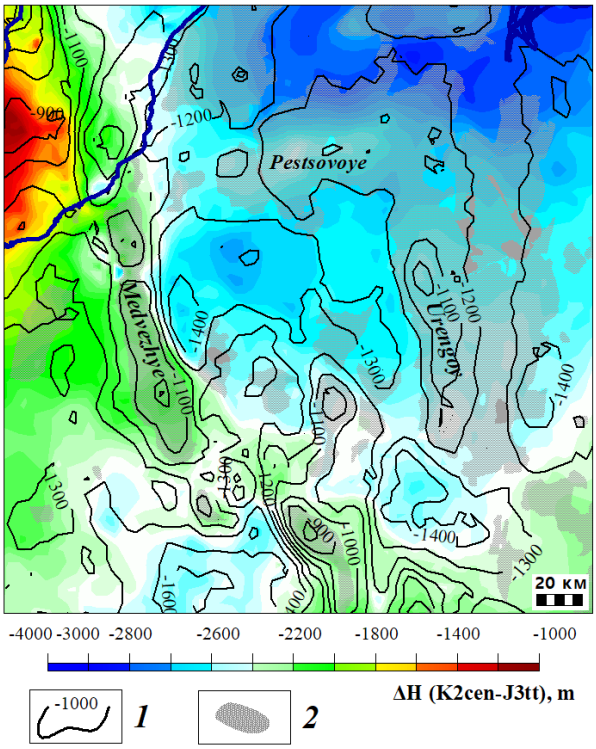


Figure 3. Thickness of the Cenomanian-Jurassic interval (Zagorovsky 2017); 1-top of Cenomanian depth/meters, 2-oil and gas fields

Conclusions

The fields with many faults formed at the fields where:

-there were active tectonic movements in the Neogene;

-the arch is pre-Cenomanian or pre-Jurassic;

-there is a block of Paleozoic rocks at the central part of the arch.

The rift system of Western Siberia take an active part in the geological history of this basin not only in the Triassic. In the Neogene, and probably in our days the stress in the sedimentary formations is controlled by the contact between the Paleozoic methamorphites and hard basalt bodies in the pre-Jurassic basement of the basin.

References

1. Aplonov S.V. (1987) Obsky ocean. Priroda, 12. 27-23.
2. Gogonenkov G.N., Kashik A.S., Timurziev A.I. (2007) Horizontal movement of the Foundation of Western Siberia. Oil and gas geology, 3. 3–11.
3. Rudkevich M.Ya. (1987) West Siberian basin - failed ocean. Priroda, 12. 24-27.
4. Sudakova V.V., Panasenko V. Yu., Naymushin A.G. (2019) A tectonic model for the structure of pre-jurassic sediments Suginsky small shaft, forecast of petroleum potential of the Paleozoic. Exposition Oil & Gas magazine, 1 (68), 11-16.

5. Surkov V.S., Zhero O.G. (1981) Basement and Development of the Platform Cover of the West Siberian Platform, Nedra, Moscow.
6. Timurziev A.I. (2009) Recent strike-slip tectonics in sedimentary basins: tectonophysic, and fluid-dynamic aspects (in connection with petroleum potential). Extended Abstract of Doctor (Geol.-Min.) Dissertation, Moscow.
7. Ulmishek G. F. (2003) Petroleum Geology and Resources of the West Siberian Basin, Russia. U.S. Geological Survey Bulletin 2201-G.
8. Zagorovsky Yu.A. (2017) The role of fluid dynamic processes in the formation and location of hydrocarbon deposits in the north part of Western Siberia. Candidate (Geol.-Min.) Dissertation, Tyumen.
9. Zavatsky M.D. (2008) Dependence of surface fields concentration of hydrocarbon gases on the oil content of the sedimentary cover within the West-Siberian oil and gas-bearing basin. Oil and Gas Studies, 2. 9-16.

LATEST PALEOPROTEROZOIC DYKE SWARMS OF THE SIBERIAN CRATON

Gladkochub D. P.[1], Donskaya T. V.[1], Ernst R. E.[2,3],
Söderlund U.[4], Kotov A. B.[5], Mazukabzov A. M.[1], Shokhonova M. N.[1]

[1]*Institute of the Earth's crust SB RAS, Irkutsk, Russian Federation*
[2]*Carleton University, Ottawa, Canada*
[3]*Tomsk State University, Tomsk, Russian Federation*
[4]*Lund University, Lund, Sweden*
[5]*Institute of Precambrian Geology and Geochronology RAS, St. Petersburg, Russian Federation*

Keywords: *Dolerite; dyke; geochemistry; Paleoproterozoic; Large Igneous Province; Siberian craton*

Introduction

The Latest Paleoproterozoic Timpton Large Igneous Province (LIP) of the Siberian craton, the center of which is located in the middle section of the Vilyuy river flow, includes the Chaya, Doros, Timpton-Algamay and Eastern Anabar swarms. Age of dykes is 1752 – 1759 Ma (Gladkochub et al., 2010; Ernst et al., 2016 and unpublished author's data). The dykes form an overall radiating swarm. We present new geochronological and geochemical data on a dolerite from the Chaya and Doros dyke swarms and discuss their origin and geodynamic interpretations.

Results

The Chaya dykes are located in the Baikal inlier, tracing more than 200 km. The dykes are sub-vertical with NNE trend in SW end of the dyke swarm and NE trend in the NE end of this swarm. Thicknesses of these dykes vary from few meters to 250 meters. U-Pb baddeleyite ages of the Chaya dykes are 1752 ± 6 and 1752 ± 3 Ma.

The Doros dykes and sills are situated in the western Aldan shield. Most of the dykes are NNW-NNE trending and some are ENE-NE trending. The dykes are up to 50 – 60 m thick. The thickness of mafic sills reaches 250 – 300 m. U-Pb baddeleyite age of the Doros dykes is 1757 ± 4 Ma.

The Chaya and Doros dykes are composed of fine to coarse grained dolerite. These dolerites consist of rock-forming plagioclase and clinopyroxene, minor orthopyroxenes hornblende, biotite, quartz.

The Chaya and Doros dykes demonstrate similar geochemical affinities. They are close to sub-alkaline basalts and basaltic andesites. They are characterized by low and moderate Ti, P, Nb, and moderate and high La and Th contents. Primitive mantle-normalized diagrams show that the Chaya and Doros dolerites are characterized by negative Nb-Ta, P and Ti anomalies. All analyzed samples are enriched in REE. Chondrite-normalized REE patterns of Chaya and Doros dolerites show a similar REE fractionation with $(La/Yb)_n = 2.5 – 9.3$. All dolerites demonstrate high $(Th/La)_{pm}$ ratios (> 1) and negative eNd(t) values. These dolerites could be produced from lithospheric mantle sources or crustal contaminated mantle sources.

The Chaya and Doros dyke swarms as well as other dyke swarms of the Timpton LIP were generated in an intracontinental extensional setting. We assume that this extension could have been caused by a rising mantle plume in the continental lithosphere of the Siberian craton. The location of the Chaya and Doros dyke swarms shows that they were generated and emplaced far from mantle plume centers. In this case, the dolerites were not produced from mantle plume-related source, and mantle plume supplied extra (additional) temperature and fluids to lithospheric mantle sources.

Conclusions

We conclude that 1.75–1.76 Ga Chaya and Doros dykes of the Timpton LIP of the Siberian craton are characterized by similar geochemical compositions and were generated from lithospheric mantle sources or crustal contaminated mantle sources in intracontinental extensional setting, which caused by a rising mantle plume.

Acknowledgements

This research was supported by grant 18-17-00101 from the Russian Science Foundation.

References

1. Ernst R.E., Hamilton M.A., Söderlund U., Hanes J.A., Gladkochub D.P., Okrugin A.V., Kolotilina T., Mekhonoshin A.S., Bleeker W., LeCheminant A.N., Buchan K.L., Chamberlain K.R., Didenko A.N. (2016) Long-lived connection between southern Siberia and northern Laurentia in the Proterozoic. Nature Geosciences 9(6):464-469.
2. Gladkochub D.P., Pisarevsky S.A., Ernst R., Donskaya T.V., Soderlund U., Mazukabzov A.M., Hanes J. (2010) Large Igneous Province of about 1750 Ma in the Siberian Craton. Doklady Earth Sciences 430(2):168-171.

MIDDLE PALEOZOIC BASITES OF THE VILYUI PALEORIFT AS DERIVATIVES OF PLUME-MAGMATIC INTERACTION

Gogoleva S. S., Tomshin M. D., Kopylova A. G.

Diamond and Precious Metals Geology Institute, Siberian Branch of the Russian Academy of Sciences, Yakutsk, Russia

Keywords: *Middle Paleozoic; 40Ar/39Ar geochronology; dike swarms; dolerites*

One of the most significant and interesting manifestations of magmatic activity is the Middle Paleozoic Vilyui sedimentary basin. Its rift origin, the wide occurrence of alkaline mafic magmatism was previously substantiated in a several of studies (Levashov 1975, Gaiduk 1988, Polyansky et al. 2013 and et.al).

Mantle magmatism associated with the formation of the Vilyui paleorift were controlled by the plume-lithosphere interaction. The source for plume-induced magmatism was melting of a relatively homogeneous mantle with the isotopic and geochemical signatures close to those of PREMA (Kiselev et al., 2005), and OIB. It was assumed that a high-temperature mantle plume, with a diameter of about 100 km, rose beneath the craton lithosphere (Polyansky et al., 2017). The partially molten material of the lithosphere mantle (Grachev, 1977) ascended in the form of a diapir. Underplating of magmas may have been promoted by the Moho boundary acting as a high-density barrier for rising melts. The accumulation of large volumes of melt at the crust–mantle boundary and subsequent spreading of magma beneath the base of the crust promoted crustal extention (rifting). Brittle failure of the crust gave rise to the zones of weakness, and the development of magma feedingьconduits that channeled magmatic melts to the upper structural levels.

According to the isotopic dating of basites ^{40}Ar / ^{39}Ar by the method, the sequence of their formation over ~ 18 million years is substantiated [Tomshin et al., 2016, 2018]. It began 380.7–378 million years ago with the formation of the southeastern part of the rift over the plume of the Kontai–Dzherba zone. The formation of dolerite sills occurs on an area of 250x80 km. Dike-like bodies are less common. The sills appear to have been intruded into horizontal or shallowly dipping Lower Paleozoic strata. Intrachamber magma fractionation processes gave rise to a variety of rock types, ranging in composition from ophitic dolerites and prismatic-ophitic gabbro-dolerites to troctolitic gabbro-dolerites containing up to 25% olivine. The rocks of the intrusions are prismatic-ophitic gabbro-dolerite consisting essentially of plagioclase ($An_{72–38}$), augite ($Wo_{40–43}En_{46–40}Fs_{18–15}$), olivine ($Fa_{35–23}$) and oxide ore minerals. The accumulation of large volumes of mafic magma at the crust–mantle boundary marks the earliest stages of crystal lization of this dike swarm, particularly, the crystallization of early plagioclase, which is present in almost all varieties of gabbro-dolerites of the Vilyui paleorift.

The outpouring of large volumes of mafic magma eventually leads to collapses of magma conduits. Further melting of new batches of material, including restites, occurs at depths of magma generation corresponding to the lithospheric mantle. The melt becomes enriched in TiO_2, P_2O_5, alkalis and a set of incompatible trace elements. The new lens of the melt rising at the Moho boundary spreads and thins westward. Simultaneously, the slip of the western flank of the Vilyui structure occurs in the same direction. The once existing local area of magma conduits begins to expand to the north of the Kontai–Dzherba structure. This results in the inception of a narrow zone of deep faults, which acted as conduits for the rising mafic magma in the form of gabbro-dolerite dikes and sills within the Vilyui–Markha swarm. This swarm extends for almost 700 km ranging in width from 30 km in the south to 150 km in the north. In the northern part, it changes its strike from mostly NE to E direction with the formation of swarm of en-echelon dikes. Paleomagnetic data indicate that this event was accompanied by a relative rotation of the Anabar–Angara block with respect to the Aldan block. This period was also marked by lithospheric extension and thinning, and the amount of extension of the mantle is greater than that of the crust (Polyansky et al., 2013). Magmatic activity in this dike swarm was associated with the intrusion of sills, chonoliths, dikes and eruptive vents of basic composition. All of them are intruded into sedimentary carbonate rocks of Cambrian and Ordovician age. Intrusions are characterized by poorly developed processes of intrachamber magma differentiation, as indicated by the presence of a single rock variety in each particular magmatic body. The rare exception is some magmatic bodies that were formed by melts experienced a protracted prechamber evolution at great depths along an anorthositic (Oleinikov and Tomshin, 1976). They contain anortosite gabbro-dolerite lenses and horizons. The results of the homogenization experiments on plagioclase-hosted melt inclusions showed that crystallization of the early plagioclase of anorthosite gabbro-dolerites occurred at temperatures of 1450–1470°C (Tomshin and Pankov, 1979) under reducing conditions at a pressure close to 12 kbar at depths of 35–40 km from the paleosurface. Under these conditions, pyrope–almandine garnets, chromian picotite, kyanite, corundum, moissanite, and a large group of native metals and intermetallic compounds crystallize simultaneously with the early anorthite–bitownite and chrysolite–forsterite (Oleinikov et al., 1980). The dominant type of intrusive rocks of the Vilyui–Markha dike swarm belt is prismatic-ophitic gabbro-dolerite. A distinctive feature of these rocks is the presence of quartz, a ubiquitous late-magmatic phase, which may account for 5– 6 vol.%. Most gabbro-dolerites contain 3–5% of early crystallizing phases such as bytownite ($An_{88–80}$), chrysolite– hyalosiderite ($Fa_{21–35}$) and less common magnesian clinopyroxene ($Wo_{35–37}En_{54–52}Fs_{11–12}$). The anorthositic gabbrodolerite usually contain the largest volume proportion of early plagioclase (18–25 vol.%). The intrachamber mineral paragenesis of gabbro-dolerites consists of plagioclase of a more felsic composition ($An_{78–44}$), augite ($Wo_{43–37}En_{49–41}Fs_{15–21}$), hortonolite ($Fa_{39–56}$), oxide ore minerals, and apatite.

The next phase of magmatic events is associated with the formation of the basites of the Chara–Sinsk dike swarm 362.1–364.2 million years ago. It began with a significant (8 Ma) lag behind previous events. The ascent and underplating of the next batch of magma beneath the crust leads to the intensive phase of crustal extension (rifting). This time (early Famennian) was the onset of the formation of the Vilyui paleorift valley. Directly above the plume, a new extensive (290 km across) zone of fractures was formed. The onset of magmatic activity in the Chara–Sinsk dike swarm was associated with the intrusion of sills and dikes of gabbro-dolerite and their quartz analogues. This stage was followed by the emplacement of subalkaline quartz gabbro-dolerites, which were replaced by quartz monzonite porphyries. The late stage of magmatic activity was represented by quartz syenite porphyries occurring as individual intrusions (Olekma stock) or later multiple dikes (Tomshin et al., 1985). Based on the example of these objects described a monzonitoid trend representing differentiation of a tholeiitic basaltic melt (Koroleva, 1991; Tomshinet al., 1985). The gabbro-dolerites are characterized by the constant content of early plagioclase (from 3–5 to 15%). In addition to early plagioclase ($An_{75–68}$), other phases that crystallized at the prechamber stage include chrysolite ($Fa_{21–24}$), magnesian augite ($Wo_{37}En_{52}Fs_{11}$), almandine and spessartine–almandine garnet, rutile, and moissanite. The phases representing the intrachamber stage of crystallization are more felsic plagioclase ($An_{58–33}$), more Fe-rich augite ($Wo_{36–38}En_{43}Fs_{21–19}$) and olivine ($Fa_{35–54}$), as well as hornblende, biotite, and micropegmatitic intergrowth of quartz and K-feldspar. In these dikes, the melts have evolved toward more Ti-, P-, and alkali-rich compositions with higher REE, HFSE, and LILE contents as a result of partial melting of more refractory mantle sources.

Conclusions

We present results of study of the basites of the Vilyui paleorift. Their $^{40}Ar/^{39}Ar$ isotopic ages were used to establish the sequence of their intrusion, which lasted ~18 Myr. Dolerite sills of the Kontai–Dzherba zone were the first crystallizing phase (378.0–380.7 Ma), which was followed by the intrusion of dikes of the Vilyui–Markha zone (372–373 Ma). Dikes of the Chara–Sinsk zone were the last crystalizing phase (362–364 Ma). The prolonged plume–lithosphere interaction resulted in the successive enrichment of basaltic melt with titanium, phosphorus, REE, HSFE, and LILE. Accumulation of the melt and formation of a magmatic lens at the crust–mantle boundary led to early crystallization of the melt at a depth of 35–40 km from the paleosurface under reducing conditions at a temperature of 1450–1470 ºC.

Acknowledgement

The work was done under research project of DMPGI SB RAS and was partly financially supported by grant 18-45-140043r_a from the Russian Foundation of Basic Research

References

1. Gaiduk, V.V. (1988) The Middle Paleozoic Vilyui Rift System [in Russian]. YaF SO AN USSR, Yakutsk.
2. Grachev, A.F. (1977) Rift Zones of the Earth [in Russian]. Nedra, Leningrad.
3. Koroleva, O.V. (1991) Peculiarities of composition and genesis of basic alkaline-silicic magmatite suites of the Siberian and Hindustan platforms, in: Polyakov, G.V. (Ed.), Siberian and Deccan Traps: Similarities and Differences [in Russian]. Nauka, Novosibirsk: 177–195.
4. Levashov, K.K. (1975) The Middle Paleozoic rift system of the eastern Siberian Platform. Soviet Geology, No. 10: 49–58.
5. Oleinikov, B.V., Tomshin, M.D. (1976) Deep differentiation of the magma of platform basites. Dokl. Akad. Nauk SSSR 231(1): 177–180.
6. Oleinikov, B.V., Tomshin, M.D., Okrugin, A.V. (1980) Petrological features of the prechamber evolution of magmas of platform basites. Izv. AN SSSR, Ser. Geol. 1: 62–71.
7. Polyansky, O.P., Prokopiev, A.V., Babichev, A.V., Korobeinikov, S.N., Reverdatto, V.V. (2013) The rift origin of the Vilyui basin (East Siberia), from reconstructions of sedimentation and mechanical mathematical modeling. Russian Geology and Geophysics (Geologiya i Geofizika) 54 (2): 121–137 (163–183).
8. Polyansky, O.P., Prokopiev, A.V., Koroleva, O.V., Tomshin, M.D., Reverdatto, V.V., Selyatitsky, A.Yu., Travin, A.V., Vasiliev, D.A. (2017) Temporal correlation between dike swarms and crustal extension in the Middle Paleozoic Vilyui rift basin (Siberian platform). Lithos: 282–283, 45–64.
9. Tomshin, M.D., Konstantinov, K.M., Prokopiev, A.V. (2016) The Middle Paleozoic Vilyui paleorift and the sequence of magmatic events, in: Proc. Conf. Geodynamic Evolution of the Lithosphere of the Central Asian Mobile Belt (from the Ocean to the Continent). Izd. IZK SB RAS, Irkutsk, Issue 14: 277–279.
10. Tomshin M.D., Kopylova A.G., Konstantinov K.M., Gogoleva S.S (2018) Basites of the Vilyui paleorift. Geochemistry and seguence of formation // Russian Geology and Geophysics.. V. 59. Iss.10: 1204–1216
11. Tomshin, M.D., Pankov, V.Yu. (1979) Melt inclusions in protocrystals of plagioclase from the Siberian traps and their petrogenetic significance, in: Mineralogy and Geochemistry of Kimberlite and Trap Rocks [in Russian]. Izd. YaF SO AN SSSR, Yakutsk: 100–106.
12. Tomshin, M.D., Oleinikov, B.V., Koroleva, O.V. (1985). Monzoitoid trend of deep evolution of the tholeiite-basalt series of melts on the Siberian platform, in: Petrological and Geochemical Features of the Abyssal Evolution of Kimberlite and Basite Systems [in Russian]. Izd. YaF SO AN SSSR, Yakutsk: 130–188.

CARBONATITE FLUID-EXPLOSIVE SYSTEM OF THE MIDDLE TIMAN

Golubeva I. I.

Institute of Geology, Komi Scientific Center, UB RAS

Keywords: *carbonatites, ultramafic dikes, fluid, explosions, rare earth mineralization, Middle Timan*

Introduction

Fluid-explosive sistem is allocated in the Middle Timan, including carbonatites, explosive ultramafic rocks of dike complex and alkaline metasomatites. Fluid-explosive sistem was formed due to the carbonatite magmatism and its fluid derivatives.

Results

Carbonatite magmatism of the Middle Timan manifested itself in the form of a relatively small stock with a diameter of about 250 × 400 m (Kostyukhin, 1987), while the impact area of the Na-Ca fluid flow generated from the carbonatite source is about 300 km2. Carbonatites are not spatially associated with any alkaline intrusive complexes or kimberlites. The enclosing rocks are the weakly metamorphosed terrigenous and terrigenous-carbonate rocks of the Chetlas and Bystrin series of the middle and upper Riphean.

The results of the carbonatite fluids exposure manifested themselves in the formation of the ultramafic fluid-explosive dikes and the separate ore bodies with rare-earth and rare-metal mineralization. The field of the spread of these formations is close to isometric areal. Timan carbonatites are characterized by high levels of the lanthanoid group (for example, the amount of La averages 3695 ppm), that is a specific feature and distinguishes these carbonatites from carbonatites of known carbonatite formations associated with deep metasomatic processing (Figure 1). The main carrier of lanthanides in Timan carbonatites is monazite. In exocontacts of carbonatite bodies, 10–60 m wide zones of disintegrated host rocks, formed as a result of the explosive separation of gases from a carbonatite melt, are recorded. Riphean brecciated meta-sedimentary rocks undergo fenitization and carbonation. Each stage of rock formation corresponds to a certain rare-metal and rare-earth mineralization. The final stage of the carbonatite body formation is characterized by tantalum-niobium and rare-earth mineralization (Kostyukhin, 1987).

Numerous explosive dikes (in the amount of about 2000) are concentrated in the form of groups, have a thickness of tens of centimeters to tens of meters, their length reaches 3 km. Dikes consist of the mantle minerals fragments (olivine, pyroxene, chromespinelide) and rocks (pyroxenite, less often peridotite), cemented by the metamorphic minerals aggregate - pyroxene, amphibole, carbonate, phlogopite. Large fenitized and carbonatized (sometimes fractured) fragments of host rocks are noted. At the final stage of the formation of fluid-explosive ultramafic breccia, metasomatic calcite and calcite-albite veins with rare-earth and rare-metal mineralization are formed by Ca-Na fluid impregnation (Golubeva, 2018). SrO admixture up to 9.43% is noted in vein calcite. Rare-metal and rare-earth mineralization in the calcite-albite veins of the dike complex is formed in the same way as in the carbonatite stock, at the stage of low-temperature carbonation.

In the field of explosive dike bodies propagation there are zones of diaclasses with a complex branched fissure system with fenitization occurrence. In six areas of the fenitized zones, high concentrations of rare-metal and rare-earth minerals are noted, they are identified as promising ore objects.

The isotope determinations of Rb-Sr of the total composition of fluid-explosive dikes rocks showed 820 ± 9 million years (Bryanchaninova, 2010). The age obtained by K/Ar and 40Ar/39Ar methods was determined by the phlogopite formed in carbonatites and explosive dikes during the post-magmatic stage. Age values in the range of 550 - 635 Ma (Kostyukhin, 1087; Udoratina, 2014)

In ultramafic fluid-explosive dikes, significant variations in the isotopic composition of carbon and oxygen in calcite were found: δ13C, ‰ = -7.2 – -4.4 and δ13O, = 8.5–20.7. The same significant spread of values of carbon isotopic composition (δ13C, ‰ = -6.5 - -3.6) and oxygen (δ13O, ‰ = 9.2 - 21.1) was found in the rocks of the carbonatite stokc, that reflects a long and multi-stage history of it formation (Shumilova, 2012).

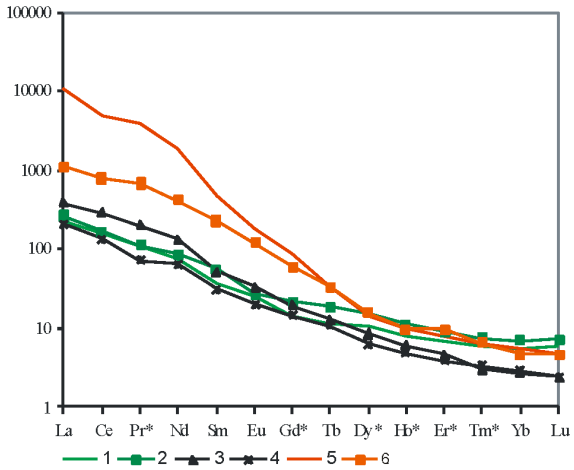


Figure 1. Spectrum of rare-earth elements normalized to the primitive mantle. 1 - fluid-explosive rocks of the Middle Timan dike complex, 2 - picrites of Maymecha-Kotui province, 3 - South African kimberlites, 4 - Kimberlites of Yakutia, 5 – Timan carbonatites, 6 - Kovdor carbonatites

Conclusions

Carbonatites, explosive ultramafic rocks of dike complex and associated alkaline metasomatites were identified as a common fluid-explosive sistem of carbonatite-alkaline type with mantle nature. The features of the explosive sistem of the Middle Timan reflect the migration of the carbonatite source from the mantle and the separation rate of the gas-liquid flow from the carbonatite magma. Vertical migration of carbonatite flow manifests itself in the repeated metasomatic impregna-

tion of Riphean shale, in explosive activity and in the intrusion of the carbonatite melt. At the first stage of carbonate-alkaline fluid-explosive system of the Middle Timan formation, in the front of the Ca-Na fluid flow, on the Riphean shale substrate, metasomatites were formed, composed of calcite, albite and alkaline colored minerals. At the second stage, due to a sharp drop of pressure and decompression, an explosive release of gases occurred from the carbonatite source, hacking into the Riphean strata and their metasomatized areas. At the third stage, carbonatite melt was introduced into the gas-shattered horizon and caused phlogopitization of host rocks and xenoliths.

A similar evolutionary history also corresponds the fluid- explosive alkaline rocks dike complex. The solid-gas fluidized mantle material was introduced in the form of dikes into the previously meta-somatically altered zone and mixed with hacked fragments of metasomatites and Riphean metasedimentary rocks. Xenogenic mantle material in the form of mineral fragments (pyroxene, olivine, chromespinelide) and rocks (pyroxenite and hornblendite) was transported by fluid flow from relatively shallow mantle horizons. The clastic material in the explosive dikes was cemented by low-temperature metasomatic minerals. At the next stage, as well as in the carbonatite stock, the rare-earth and rare-metal mineralization was generated in the formed fluid-explosive ultramafic rocks due to the incoming alkaline-carbonate hydrothermal solution from the cooling down carbonatite source.

References

1. Bryanchaninova N. I., Makeev A. B., Larionova Yu. O. (2010) Sm-Nd isotopic systematics of Middle Timan lamprophyres. New horizons in studying the processes of magma and ore formation.: 414 – 415
2. Golubeva I. I., Filippov V. N., Burtsev I.N. Metasomatic (2018) Rare-earth and rare-metal mineralization in ultramafic rocks of the dike complex on Middle Timan (Raising Chetlass). Modern Problems of Theoretical. experimental and applied mineralogy Syktyvkar: IG Komi Scientific Center, Ural Branch of the Russian Academy of Sciences: 278
3. Kostyukhin M. I., Stepanenko V. I. (1987) The Baikal Magmatism of the Kanino-Timan Region: Leningrad: Nauka: 232
4. Udoratina O.V., Travin A.V.(2014) Alkaline picrites of the Chetlas Middle Timan complex: Ar-Ar data. Ore potential of alkaline, kimberlite and carbonate magmatism. Moscow: 82 – 84.

GEOCHEMISTRY OF THE INTRUSIVE ROCKS OF THE SIBERIAN TRAP PROVINCE

Gongalsky B. I.[1], Krivolutskaya N. A.[2], Belyatsky B. V.[3], Dolgal A. S.[4], Makarieva E. M.[5]

[1]*Institute of Geology of Ore Deposits, Petrography, Mineralogy and Geochemistry RAS, Moscow, Russia*
[2]*Vernadsky Institute of Geochemistry and Analytical Chemistry RAS, Moscow, Russia*
[3]*A.P. Karpinsky Russian Geological Research Institute, St. Petersburg, Russia*
[4]*Perm State University, Perm, Russia*
[5]*Polar Marine Geological Exploration Expedition, St. Petersburg, Russia*

Keywords: *Siberian traps, platinum metals, geochemistry, deposits.*

Introduction

The connection of ore deposits with Large Igneous Provinces (LIPs) is one of the most important problems of geology, since they contain many deposits of strategic metals (Dobretsov, 2005; Ernst, 2014).The world's largest continental Siberian trap province is an example of a combination of a huge volume of basic rocks and Pt-Cu-Ni ores that provide 90% of the platinum group metals (PGE) and Ni in Russia. This metallogenic province is located in the Arctic zone of the province and includes deposits of the South Taimyr and Noril'sk area (Dodin, 2011; Malitch et al. 2017). Its high economic value raises the question of the possibility of new deposits discovering in other parts of the Siberian province and around the world. Meanwhile, the causes of localization of deposits in the north part of the province are rarely considered in genetic models and are still controversial (Rad'ko, 2016; Krivolutskaya et al. 2018).

To solve this problem we tried to identify specific features of the tectonic structure and magmatism of the northern zone of the Siberian province in comparison with the other areas including the Norilsk, Maimecha-Kotuy areas, Tunguska basin, Angara and Kulyumber river valleys. The research included a geochemical study of both volcanic and intrusive rocks: major components (XRF), trace elements (ICP-MS) and radiogenic isotopes Sr-Nd-Pb (TIMS).

Results

In this study our special attention was paid to intrusive rocks of the key areas. Analytical data demonstrate that the maximum composition diversity is typical of the intrusions located in the northern part of the province, namely the Norilsk, Maimecha-Kotuy and Taimyr areas. These rocks range from ultrabasic, alkaline and subalkaline to tholeiitic rocks of normal alkalinity. They have both mantle and crustal characteristics. The first intrusive type includes the Dyumtaleysky massif and a series of ultrabasic dikes and irregular bodies in Taymyr. These rocks are characterized by trace element patterns without Ta-Nb and Pb anomalies, with ε_{Nd} ranging from +3 to +5, and $^{87}Sr/^{86}Sr$ from 0.703 to 0.704 (Fig.). The second intrusive type (including the Norilsk intrusive complex) contains massifs with distinct Ta-Nb and Pb anomalies, ε_{Nd} varies from -9to +2, $^{87}Sr/^{86}Sr$ changes from 0.705 to 0.711. Major components in both types change significantly (wt%), i.e. MgO = 3-35, TiO_2 = 0.7-4.6, K_2O = 0.2-1.8. In contrary,

the intrusions of the southern part of the Siberian province (Tunguska basin; Angara and Kulyumber river valleys) represented by gabbro-dolerite sills (often with olivine) and combined in Katangsky, Kuzmovsky and Kurejsky intrusive complexes have a constant tholeiitic composition (wt%): 6-7 MgO, 1.6-1.8 TiO_2, 0.4-0.5 K_2O. Their isotope characteristics are following: ε_{Nd} = +1 to +2, $^{87}Sr/^{86}Sr$ =0.705-0.706. The composition of the intrusions from the southern part of the Siberian platform is close to the composition of the Norilsk intrusions excepting lower MgO and elevated TiO_2.

The difference in the rock compositions of northern and southern parts of the province could be explained by the difference in their tectonic position. According to geophysical data the northern part of the East Siberia is characterized by anomalous magnetic and gravitational

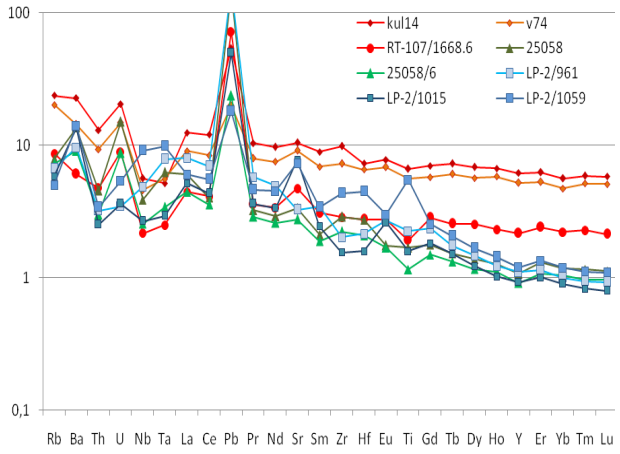


Figure. Spider-diagram for intrusive rocks of the Siberian trap province. Intrusions, lines colors: red – Kharaelakh, green – east Taimyr, blue-central Taimyr, brown – r. Kulyumber. Normalized after (Hofmann, 1989)

fields (Dolgal, 2012). It is suggested that these anomalies reflect the occurrence of large amount of basic-ultrabasic rocks within these blocks of crust and evidence of intense magmatic activity in this area in contrast to the southern part of the trap province. Thus, different tectonic regimes operated 251 Ma ago, rift and platform (Malitch.

The PGE-Cu-Ni deposits are concentrated only within zones where both regimes took place. These zones are paleorifts, the Yenisei-Khatanga and Norilsk-Igarka They are characterized by long-lasted development and their geological structure is a result of many geological processes.

Conclusions

Northern part of the Siberian trap province comprises many ultrabasic-basic intrusions varying in composition from peridotites to gabbro. This compositional diversity of this region is due to a specific tectonic development of this area in comparing with the southern part of the province

Acknowledgements

This work was supported by RFBR (project No. 18-05-70094)

References

1. Dobretsov N.L. (2005) The largest igneous provinces of Asia (250 Ma): Siberian and Emaishan traps (flood basalts) and associated granitoids: Russian Geology and Geophysics 9: 870-890
2. Dodin D.A., Zoloev K.K., Koroteev V.A., Chernyshov N. M. (2011) Platinum of Russia: state and prospects. Platinum of Russia 7:12-52 (In Russian)
3. Dolgal A.S. (2012) Realization of V.N. Strakhov ideas in interpretation of the geopotential fields. In: Academician V.N. Strakhov as Geophysics and Mathematics. Moscow, Nauka, 55-78 (In Russian)
4. Erinchek Y.M., Milshtein E.D., Kolesnik N.N. (2000) Deep structure and geodynamic of the Siberian platform kimberlite area. Regional Geology and Metallogeny 10:209-228 (In Rusian)
5. Ernst R.(2014) Large Igneous Provinces: Elsevire, 652
6. Hofmann A.W. (1988) Chemical differentiation of the Earth: The relationship between mantle, continental crust and ocean crust. Earth and Planet Science Letters 90: 297-314
7. Krivolutskaya N., Gongalsky B., Kedrovskaya T., Kubrakova I., Tyutyunnik O., Chikatueva V., Bychkova Ya., Kovalchuk E., Kononkova N., Yakushev A. (2018) Geology of the Western Flanks of the Oktyabr'skoe Deposit, Noril'sk District, Russia: Evidence of a Closed Magmatic System. Mineralium Deposita, 54:611-630
8. Malich K.N., Belousova E.A., Griffin W.L., Badanina I. Yu., Latypov R.M., Sluzhenikin S. F. (2017) New insights on the origin of ultramafic-mafic intrusions and associated Ni-Cu-PGE sulfide deposits of the Noril'sk and Taimyr provinces, Russia: evidence from radiogenic and stable isotope data. Processes and ore deposits of ultramafic-mafia magmas through space and time 7: 198-237
9. Rad'ko V.A. (2016) Facies of intrusive and volcanic magmatism in the Norilsk districts. St-Petersburg, VSEGEI, 285 (In Russian)

MULTI-DEPTH MAGMATIC CHAMBERS OF THE PALEOPROTEROZOIC ULTRAMAFIC-MAFIC MAGMATISM OF THE WESTERN PART OF THE ALDAN SHIELD

Gongalsky B. I.[1], Krivolutskaya N. A.[2],
Safonov Y. G. [1], Murashov K. Y. [1], Timashkov A. N.[3]

[1]*Institute of Geology of Ore Deposits, Petrography, Mineralogy and Geochemistry RAS, Moscow, Russia*
[2]*Vernadsky Institute of Geochemistry and Analytical Chemistry RAS, Moscow, Russia*
[3]*A.P. Karpinsky Russian Geological Research Institute, St. Petersburg, Russia*

Keywords: *Chineysky, Udokan, Unkur, copper, deposits.*

Introduction

The Northern Transbaikal region in the western Aldan Shield is one of the largest metallogenic provinces in Russia. The world-class Udokan copper deposit containing more than 27 Mt of identified Cu reserves, the Fe-Ti-V deposits with 30 Bt of hypothetical ore resources in the Chineysky massiv, the large Katugin Ta–Nb deposit, as well as PGE, Ag, Au, and U deposits and prospects are localized in this province (Fig. 1). All they were formed in the Paleoproterozoic, which is regarded as the most productive era for concentration of various metals. The ore deposits and prospects formed at different depths are now exposed at the surface and thus are accessible for comprehensive study. In addition to magmatic Fe–Ti–V oxide mineralization in the Chiney and Luktur layered mafic and ultramafic plutons, the primarily postmagmatic copper and noble-metal sulfide deposits are localized in the endo- and exocontact zones of these plutons. The giant Udokan sandstone-hosted copper deposit is distant from intrusive bodies and bears attributes of hydrothermal sulfide mineralization. The same can be said about the Pravoingamakitsky, Saku, Unkur, and other vein-type deposits. New genetic types have been revealed recently in layered plutons and their frameworks, e.g., Au–PGE–Cu and REE-U mineralization (Gongalsky, Krivolutskaya, 2019). Taken together, all these manifestations of magmatic activity and ore deposition make up the Udokan–Chiney ore-magmatic system.

Results

In contrast to many other shields of the world, the Aldan Shield and the Baikal Fold Region were involved in rifting from Early Precambrian to present time. The most important tectonomagmatic events in the region are marked by intrusion of mafic melts (Paleoproterozoic Chineysky Complex, Neoproterozoic Doros Complex, Mesozoic dikes and volcanic rocks, Neogene-Quaternary basaltic lava plateau and dikes). All the aforementioned rocks occur at the intersection of the northwestern tectonic sutures as splays of the Syulban Deep Fault and the near-latitudinal structural elements accompanying the Stanovoi Deep Fault.

The Chinesky pluton is a constituent of the transregional Yenisei–Aldan metallogenic belt extending from the southern framework of the Siberian Platform to the Taimyr Peninsula in the north. Both unique Ni–Cu–PGE deposits of the Noril'sk and Kodar–Udokan ore districts (Permian–Triassic and Paleoproterozoic, respectively) are situated in this belt. The Chineysky mafic-ultramafic pluton unique in distinct layering and rhythmic structure is comparable in the upper zone of Bushveld in petrography. The intrusive contacts between certain rock varieties, difference in their composition, structure, and texture allowed us to recognize the following rock groups related to four episodes of magma emplacement: (1) coarse-grained anorthosite and monzodiorite, (2) high-Ti gabbroic rocks, (3) low-Ti gabbroic rocks, (4) lamprophyres and fluid–magmatic brecciaT he Chineysky pluton is only a fragment of the large magmatic system. The Mylove pluton, which is cut through by Late Paleozoic granitic rocks of the Ingamakit Complex and then overlain by Neogene–Quaternary volcanic rocks of the Udokan lava plateau, is the major element of this system. The Mylove pluton is the center of radial mafic dykes

The large magmatic center controlled localization of hydrothermal, metasomatic, and other deposits. The U–REE occurrences and deposits recently discovered in the Chineysky pluton and its framework are coeval with leading types. The deep melts that rose from the upper mantle were partially accumulated at the cortex-mantle boundary (basaltic underlining) and determined the assimilation of the lower crust. The stresses associated with these processes led to rupture and rifting, which served as additional channels for introducing magmas. The formation of rift and supercritical troughs was accompanied by the development of stratified mafic plutons, which led to specific metallogeny and unique ore-bearing geodynamic systems, such as the largest ore deposits of Bushveld, Great Dyke, Stillwater and others. Paleoproterozoic magmatism is one of three major impulses of continental crust growth (Dobretsov, Buslov, 2005). The introduction of basites occurred against a background of post-collisional stretching, which followed the collision-accretion stage of the formation of the Siberian craton. (Gladkochub et al., 2012). Basite intrusions of the Chineysky complex are accompanied by swarms of dikes concentrated on the site of the Malove massif. This happened almost immediately after the crystallization of the gabbroids of the marginal zones in the eastern (Ar/Ar method 1880-16 million years, and the western parts of the Chineysky Massif (U-Pb method, 1867-3 million. The age of the years, highly titanic gabbroids of group 2 of 1858 ± 17 million years and of low-titanium gabbroids of the 3rd group of 1811±27 my was determined for zircons in SHRIMP-II (Gongalsky. 2015).

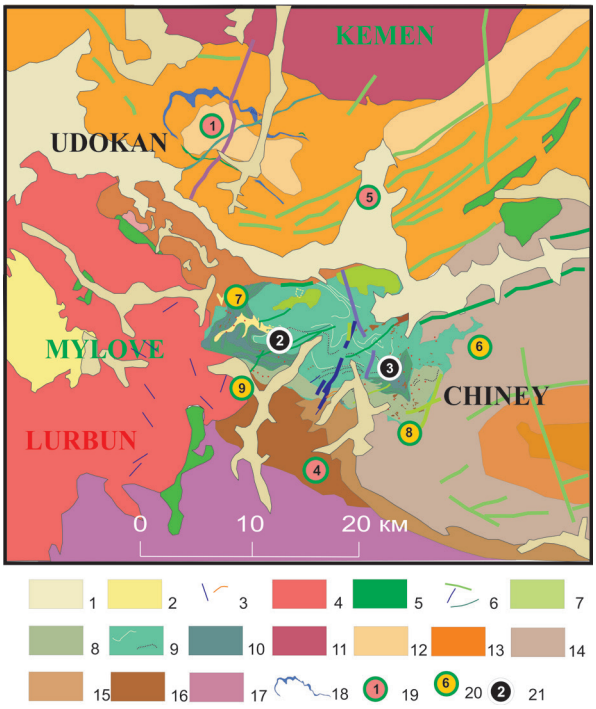


Figure 1. Geological map of the Udokan-Chiney district. (Modified after Chitageologia data).

1-Quaternary sediments; 2 - Neo-Quaternary volcanogenic deposits (Udokan lava plateau); 3 - Dikes of dacitic porphyries, granodiorite-porphyries, lamprophyres of Mesozoic (?) Age; 4-Granites and granodiorites of the Ingamakitsky (PZ3) complex; 5 - gabbrodiorites, gabbrodiabases of the Doros complex (R); 6 - dikes of the main composition of the Doros and Chinea complexes; 7-10 - Chineysky complex: 7- gabbrodiorites, monzodiorites of the upper edge series, 8 - gabbronorite series, 9 - leukogabbro series with layers of anorthosite (light line) and titanomagnetite (black dots); 10 - titanomagnetite-gabbro series; 11 - Kodar complex granites (PR_1); 12-16 - The sedimentary rocks of the Udokan series: 12-Naminga, 13-Sakukan, 14-Butun, 15-Alexandrov, 16-Chitkanda; 17-granitoids of the Kuanda (AR) complex. 18 - Ore horizon of the Udokan deposit, 19 - deposits in sedimentary rocks: 1-Udokan, 4-Pravoingamakitskoe, 5-Saku, 20 - Cu deposits of the Chineysky massif: 6-Rudny, 7-Kontaktovoy, 8-Verhnechneyakoe, 9- Skvoznoe; 21 - Fe-Ti-V deposits of the Chineysky massif; 2-Etyrko, 3-Magnitny.

The 3D model (Fig. 2) reflects main gravity structures where anorthosite-gabbronorite of Chiney and Luktur form positive (anticline) structures, between which there are the synclines (Unkur, Naminga). The latter contains the Udokan Cu-Ag-Fe and Unkur Cu-Ag deposits. The layered intrusions exposed on the surface represent the upper zones of high-density columns. The columns can be traced to a depth of about 20 km, making branches of a large magma chamber at a depth of about 20 km. The magmatic columns are zonal, gabbros, and gabbronorites dominating in the upper parts. Ultramafic rocks can be found at the lower levels of magmatic columns.

Conclusions

Dating rocks of the Chineysky, Luktursky (Gongalsky, Krivolutskaya, 2019), the Malozadoysky (Mekhonoshin et al., 2016) massifs of the Kalaro-Nimnyr swarm (Ernst et al., 2016) in the age range of 1811–1880 Ma suggests the existence in the Paleoproterozoic LIP. World-class deposits in the terrigenous and igneous rocks of the Udokan-Chineysky district have a common magmatic source of elements due to the prolonged fractionation of primary and contaminated magma from the lower crust, the formation of hydrothermal systems.

Acknowledgements

This work was supported by RFBR (project No. 17-05-01167, 18-05-70094)

References

1. Gongalsky B.I., Krivolutskaya N.A. (2019) World-class deposits of the Northeastern Transbaikalia, Siberia, Russia. Springer, Amsterdam, 321.
2. Gongalsky B.I. (2015) Deposits of the unique metallogenic province of Northern Transbaikalia. Moscow, VIMS: 248 (in Russian).
3. Dobretsov N.L., Buslov M.M. (2011) On the Problems of Foldbelt Geodynamics, Tectonics and Metallogeny. Russ Geol Geophys. 52(12):1911–1926.
4. D.P. Gladkochub, T.V. Donskaya, R. Ernst et al. (2012) Mafic Magmatism of the Siberian Craton during the Proterozoic. Geotektonika 4:28–41.
5. Ernst R.F, Hamilton M.A, Sцderlund U. et al. (2016) Long-lived connection of Siberia and northern Laurentia in the Proterozoic. Nat Geosci 9:464–469
6. Mekhonoshin A.S, Ernst R.E, Sцderlund U. et al. (2016) Relationship between platinun-bearing ultramafic-mafic intrusions and large igneous provinces (exemplified by the Siberian Craton). Russ Geol Geophys 57(5):1043–1057

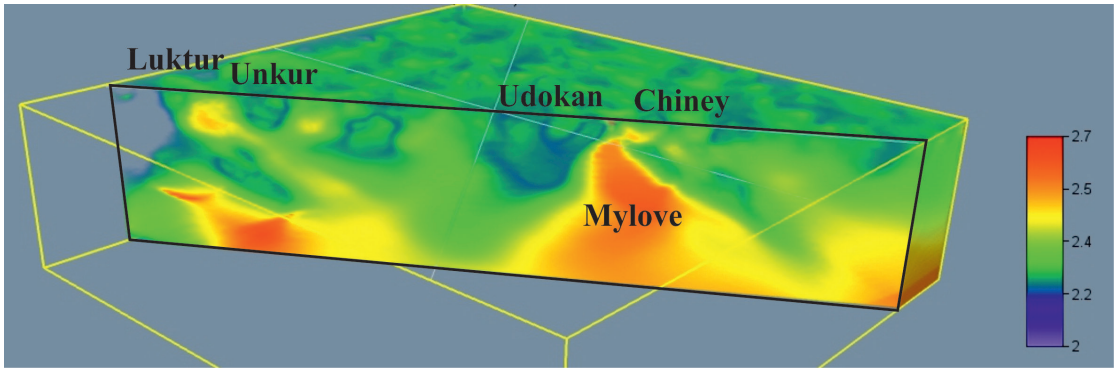


Figure 2. Cross section of gravity mass distribution across the Luktur and Chiney massifs and the Unkur and Naminga synclines with cupriferous sandstone deposits (Unkur and Udokan). Scale for gravity field is given in arbitrary. Vertical side 20 km, horizontal 65 km.

TECTONIC AND METALLOGENIC CONSEQUENCES OF THE EMEISHAN PLUME MANIFESTATION IN THE SOUTHEAST ASIA STRUCTURES

Goryachev N. A.[1,2], Izokh A. E.[3], Hoa T. T.[4]

[1]*North East Interdisciplinary Scientific Research Institute n.a.N.A.Shilo FEB RAS, Magadan, Russia*
[2]*A.P.Vinogradov Institute of Geochemistry SB RAS, Irkutsk, Russia*
[3]*V.S.Sobolev Institute of Geology and Mineralogy SB RAS, Novosibirsk, Russia*
[4]*Institute of Geosciences VAST, Ha Noi, Viet Nam*

In the geological history of Vietnam, an important place is occupied by the transition from the Paleozoic to the Mesozoic. It includes several stages of major tectonic events (Geology ..., 2011). According to modern data (Borisenko et al., 2008; Chen et al., 2014; Zaw et al, 2014; Nevolko et al., 2018), four stages of tectonic movements correspond within northern Vietnam in this period of time: 300-290, 253 -251, 245-220, 218-185 Ma. But in the stage of 260–250 Ma, there is clear evidence of the plume-related magmatic formation, which is a reflection of one of the largest events in South China orogenesis — the Emeishan plume magmatism (Hoa et al., 2008, 2016; Dobretsov et al., 2010). Its formation took place against the background of the interaction of the South China and Indochina tectonic blocks. This led to a complex tectonic interference of subduction and collision geodynamic settings with a plume formation environment on the edge of the continental block and the existence of various hypotheses on Indo-China tectonic evolution (Chen et al., 2014; Faure et al., 2018; Ngo et al., 2015; Shi et al., 2015; Wang et al., 2016; Zaw et al., 2014).

The tectonic effects of such a combination manifested themselves in different ways. On the one hand, this contributed to the development of subduction and the movement of the margin of the South China block in the direction of Simao (Wang et al., 2016). On the other hand, this led to the formation of zones of thrust formation on the eastern and southeastern flank of the South China block (Song Chay suture, and the belt of Cordillera type domes along the eastern edge of this block) (Faure et al., 2011, 2016, 2018; Roger et al., 2000, 2012; Vladimirov et al., 2018). In general, these movements contributed to Indo-Sinian collision and the formation of a variegated assemblages of igneous rocks (a combination of collisional S-granites with A-type and I-type granites with ultramafic-mafic association) (Wang et al., 2016; Faure et al., 2016; Shellnutt, Zhou , 2007; Shellnutt, Jahn, 2011) and a complex metallogenic association in the territory of modern North Vietnam (Hoa et al., 2008; Geology ..., 2011; Shi et al., 2015; Zaw et al., 2014). Reconstructions for a period of 260–250 Ma show that the well-known manifestations of the Emeishan plume magmatism of northwestern Vietnam are the southwestern flank of the Emeishan plume shifted along the Ailaoshan – Red River faults more than 300 km to the southeast in modern coordinates (Ali et al., 2010). Such a peculiar interference of tectonic events can explain both the specificity of the Emeishan plume itself (the small size, the relatively low amplitudes of the uplift (Ali et al., 2010)) and the structure of the Truong Son belt (the predominance of left-sided sutures on its northern flank, due to the complex history of the Ailao Shan suture zone (Wang et al., 2000; Lai, 2012) and right-sided on the southern flank, due to the pressure of the Kon Tum microcontinent (Faure et al., 2018; Lepvrier et al., 2008; Shi et al., 2015)).

Metallogenic consequences. The formation of the belt of mafic-ultramafic intrusions was accompanied by the formation of copper-nickel with PGE mineralization in center part of ELIP; a combination of orogenic gold mineralization with a plume origin antimony and gold-antimony mineralization, with a separate area of antimony mineralization and associated mercury on the flanks of the plume (Hoa et al., 2008; Dobretsov et al., 2010). Plume originated widespread copper and copper-nickel mineralization of the Permian-Triassic age, which, in combination with orogenic gold mineralization, causes complex non-zonal copper-gold metallogeny of large shear zones and gold-antimony metallogeny of thrust zones and erases signs of linear orogenic gold bearing.

Thus, in Permian-Triassic time, overlapping tectonic-magmatic events of different geodynamics occurred in the territory of North Vietnam, which led to the association of orogenic and plume formations and complex metallogeny within the territory of North Vietnam and affected a significant part of the Truong Son belt.

MORPHOTECTONICS AND THE EVOLUTION OF PLUM-RIFTOGENIC MAGMATISM OF GORYACHEGORSK VOLCANIC PLATEAU (KUZNETSKIY ALATAU)

Grinev O. M.[1], Vorontsov A. A.[2], Bogorodov A. A.[1], Adylbaev R. R.[1], Perfilova O. Y.[3], Grinev R. O.[1]

[1]*National Research Tomsk State University, Tomsk, Russia*
[2]*Vinogradov Institute of Geochemistry, SB RAS, Irkutsk, Russia*
[3]*Siberian Federal University, Krasnoyarsk, Russia*

Keywords: *Kuznetsk Alatau, Goryachegorskoye plateau, volcanics, Devonian, geochemistry, rifting*

Introduction

The Goryachegorsk volcanic plateau forms the western periphery of the adjacent Nazarovskaya and North Minusinsk Devonian depressions of the Minusinsk trough. The plateau volcanites transgressively overlap the fold-block Baikal-Salair construction of the northeastern part of the Kuznetsk Alatau. In the early Devonian, a classical volcano-plutonic alkaline-basic formation was formed here. Plutonic - alkaline-gabbroid part of it is first described systematically in the work (Grinev, 1990) and was further studied by O.M. Grinev, V.V. Vrublevsky, I.F. Gertner and other researchers. In 1982-1986 during the geological additional survey of 1:50 000 scale, the volcanic rocks were divided into three successively formed strata: the bazaryrskaya → bereshkaya → ashpanskaya (V.N. Markov et al., 1986). The strata were described in detail geologically-petrographically, but they were not studied as volcanic-tectonic structures (VTS) and also did not receive petro-geochemical certification. Researches of authors in the last 5-10 years fill this gap.

Results

Morphotectonics of the VTS Goryachegorsky plateau

One of the most important tasks in the study of paleovolcanic fields is to identify the types and primary appearance of the morphostructures composing the volcanic fields, which is directly related to the geodynamic setting of their formation. During the analysis of topobias, geological maps and satellite images, supported by field observations, it was found that within the Goryachegorsky Plateau there are three intergrown areal paleovolcanoes: the dome-ring Batanyul-Semenovsky and Sharypovsky and the dome Nichkuryupsk-Saralinsky (fig. 1). In addition, to the west and south of the plateau in the Kuznetsk Alatau, there are markedly eroded Palatninsk and Central Martayginskaya VTS. Within the last of these, most of the alkali-gabbroid plutons of the Kuznetsk-Alatau province are located. And to the east of the plateau within the west of the Severo-Minusinsk depression, Salbatskaya and Chebakovskaya (Chernozernaya) negative (synclinor) ring VTS are located, to which the Kopievskaya dome and the dome-ring Shirinskaya VTS are adjacent to the east. These morphostructures have approximately the same size with external diameters from 40 to 60–70 km (fig. 1).

To restore the initial appearance of the morphostructures, their structures and formations, the authors investigated the unique in terms of the set of nepheline bearing rocks Batanayul-Semenovskaya VTS. According to the constructed constructions, the VTS was a central-area areal volcano with an external diameter of 40–45 km and a cone-shaped structure of 3–5 km in height. The base of paleovulcano is composed of platobasalts of the bazyr stratum: subalkaline picrobasalts, trachybasalts, limited to leukobasalts 1.0–1.5 km thick.

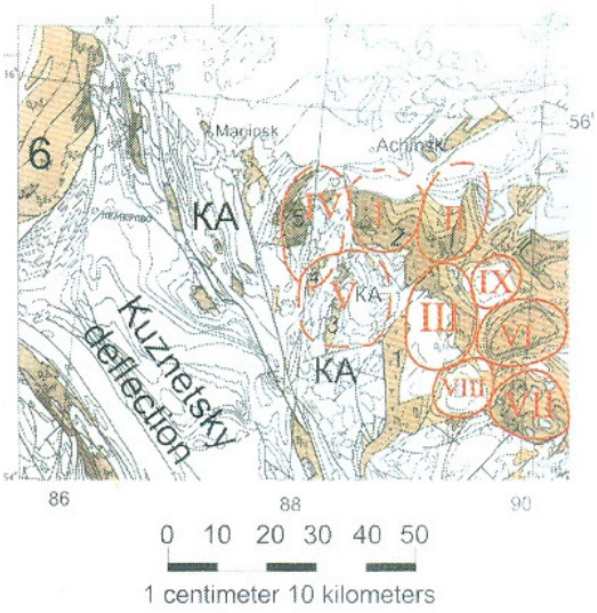


Figure 1. Tectonic scheme of the Devonian stage of development of the Kuznetsk Alatau (KA) and adjacent structures of the Minusinsk trough.

Structures of the Devonian paleorift: 1 – Saralinsky graben, 2 – Goryachegorsk volcanic plateau (north-western of the North Minusinsk depression), 3 – Rastai graben, 4 – Talanovsky graben, 5 Palatninskaya graben-syncline, 6 – The northern part of the Kolyvan-Tomsk folded area. Devonian ring morphostructures: I – Batanayul-Semenovskaya, II – Sharypovskaya, III – Nichkuryup-Saralinskaya, IV – Palatninskaya, V – Central Martayginskaya, VI – Kopyevskaya, VII – Shirinskaya, VIII – Chebakovskaya, IX – Salbat.

The middle part of the paleovolcano is composed of the bereshkaya stratum and has the most complex petrographic composition and structure. During its formation, there was a simultaneous eruption of sub-alkaline picrobasalts, trachybasalts, basalt trachyandesites, trachyandesites, trachytes and trachiriodocytes, as well as a series of alkaline differentiates; tefrits, phonotefrits, tefrifonolits and phonolits. Up to foidolitov varieties. At the same time, if bazaars are characterized by coarse-grained, cuesta-like relief of arcuate and radial types, then only fragments of low-grader, non-stretched, and arcuate small-crooked relief are found on the bereshkaya stratum, on which numerous structures of the central type and their clusters with a diameter of 1–3, 6–8 are laid. and up to 10–

12 km. On the whole, the circular range of the bereschkaya stratum has a diameter of about 24 km, and the thickness of volcanic rocks varies from 300–500 m to 3.0 km, depending on the scale of the MCT components. Some MCT have been intruded by the rod-dyke-shaped bodies of the main foidoliths and alkaline syenites, weakly exposed by erosion and accompanied by arenols of phenites.

The upper part of the building – ashpanskaya stratum, marks the final stage of volcanism. It has a substantially picrobasalt-trachybasalt and trachyte composition with limited participation of basanites and is closest in composition to the basyrites. The formation of the sequence is completed by subsurface subsidence, attenuation of volcanism, and substitution of volcanics up the section by red-colored terrigenous-sedimentary accumulations. The diameter of the ashpanite range is about 12 km with a thickness of about 1.0–1.5 km. In the present-day state of the Goryachegorskoye plateau, its strata are nested in each other along the system of arc and semicircular faults, occur at the same hypsometric level and are markedly eroded. During the middle-upper Devonian and Carboniferous, the most subsided northern and eastern periphery of the studied VTS and the entire plateau were covered with areal rhythmic lagoon-continental strata of the post-rift cover. The active stage of rifting in the area lasted about 10–15 Ma, was accompanied by three pulses of volcanism and was replaced by a long sub-platform regime D_{2-3}–C, and then P.

Evolution and geochemical features of volcanism

Subalkaline olivine-pyroxene picrobasalts and trachybasalts should be recognized as the original magma for the volcanites of the bazyrsky and ashpansky strata, and for the bereschky pyrobasalts and basanites. The processes of magma segregation cannot be excluded, especially if we compare the petrographic composition of volcanics with the rocks of the Kiya-Shaltyrsky and Goryachegorsk plutons.

Initially, differentiation of initial magmas for bazarites and ashpanites proceeded along a Fenner trend with a weak alkalinity and ended with the formation of a contrasting association, picrobasalt, trachybasalt-trachyte. Two differentiated series are characteristic of the Bereshsky stratum: trachybasalt-trachyte and alkaline tephrite-phonolitic. The Bowen trend clearly dominated here.

Geochemically, volcanites of all three strata and foidolite and alkaline-syenitic bodies penetrating them possess obvious geochemical affinity, as well as similarity with OIB. The spectra of their compositions in the diagrams were located between the OIB and E-MORB reference points, which clearly manifested themselves in the OIB and exceeded its values. At the same time, the spectra contain weakly pronounced Nb–Ta and Hf minima characteristic of IAB.

According to the Eu/Eu* index, all the rocks studied are mantle (0.78–1.07) and only trachyte (0.38–0.42) show significant influence of crustal matter.

On known discriminant triple and double geochemical diagrams, the compositions of volcanics fall into the fields of intra-plate continental basalts and basalts of destructive margins. They form compact ellipsoidal fields of figurative points at the OIB frame, slightly stretching in the direction of N-MORB and IAB. In the Condi diagram, rock composition points are located in the field of plume sources between the PM and OIB reference points. Early Devonian volcanic rocks of other areas of the Minusinsk zone have comparable characteristics (Grinev et al., 2016; Grinev et al, 2018; Vorontsov et al., 2013; 2015; 2017).

Conclusions

In the early Devonian, three impulses of sub-alkaline and alkaline basaltic volcanism manifested themselves within the Goryachegorsky Plateau and adjacent areas. As a result, an alkaline-basic volcano-plutonic Goryachegorsk formation was formed that was unique in petrographic composition. In its original form, the area had a multi-apex medium-high-mountain volcano-tectonic relief, in the form of a series of closely spaced volcanoes of the central type. The modern erosional surface of the plateau is about 4.8 thousand km^2 and an approximate volume of 12 thousand km^3.

The magma-generating system that formed the plateau had a branched-cellular structure of the feeding centers of the mantle foundation. The generation, differentiation and introduction of magmas into the limits of the crust has found a tectonic-magmatic pulse-wave character. The main source of primary magmas was the mantle-plume PREMA reservoir, which interacted during ascent with the asthenosphere mantle, and in the later differentials with the material of the earth's crust.

Acknowledgements

This work was conducted as task of RFBR, project No. 19-05-00300.

References

1. Grinev O.M. (1990). Evolution of alkaline gabbroid magmatism of the Kuznetsk Alatau. Abstract of diss. cand. geol.-mineral. sciences: 19 p.
2. Grinev. OM, Kotelnikov AD, Kaplun MV, Grinev R.O. (2016). Plume-rift-based early-evolution association of volcanic rocks of the Tashtypsky region Minuses. Correlation of altaids and uralides: magmatism, metamorphism, stratigraphy, geochronology, geodynamics and metallogeny: 60–62.
3. Grinev O.M., Grinev R.O., Bogorodov A.A., Adylbaev R.R. (2018). Material composition of the basalt-trachyte series of the Early Devonian of the Saralin graben-rift. IOP Cinference Series: Earth Enviromental Science 9: 1–9.
4. Vorontsov A.A., Fedoseev G.S., Andryushchenko S.V. (2013). Devonian volcanism of the Minusinsk depression of the Altai-Sayan rift region: geological, geochemical, isotope Sr-Nd characteristics and magmatic sources. Geology and geophysics 54 (9): 1283–1313.
5. Vorontsov A.A., Gazizova T.F., Yarmolyuk V.V., Fedoseev G.S., Travin A.V., Perfilova O.Y., Posokhov V.F. (2015). Differentiated volcanic association of the Minusa trough: mechanisms of formation and sources of melts, as exemplified by Batenevo rise. Petrology 23 (4): 353–375.
6. Vorontsov A.A., Perfilova O.Y., Buslov. M.M., Travin A.V., Makhlaev M.L., Dril S.I., Katraevskaya Ya.I. (2017). Plume magmatism in the northeast og Altay-Sayan area: stages, composition of sources, composition of sources, geodynamics (exemplified by the Minusa basin). Dokl. Earth Sci. 472 (4): 449–455.

PARAMETERS AND CLASSIFICATION OF THE DEVON RIFTOGENOUS ALTAI-SAYANSKY LIP

Grinev O. M.[1], Vorontsov A. A.[2], Ernst R. E.[3], Perfilova O. Y.[4]

[1]*National Research Tomsk State University, Tomsk, Russia*
[2]*Vinogradov Institute of Geochemistry, SB RAS, Irkutsk, Russia*
[3]*Carleton University, Ottawa, Canada*
[4]*Siberian Federal University, Krasnoyarsk, Russia*

Keywords: *Altai-Sayan region, large igneous provinces, Devonian, volcanism, riftogenesis*

Introduction

In the course of long-term studies of the Devonian magmatism of the Altai-Sayan folded region (ASFR) and the adjacent regions of Western Siberia and Western Mongolia in 80-90, a large transregional rift-continental system was installed and restored (Grinev, 1990; 1999; 2007; Vorontsov , 1994; Yarmolyuk, Vorontsov, 1993; Devonian ..., 1996, etc.). In the course of further study of rift magmatism, it was established that it has a plume nature and corresponds in scale to LIP. In the light of already established concepts, LIP is characterized by a number of manifestation parameters, allowing them to be classified into types and subtypes. This paper presents the main parameters of the manifestation of the Devonian rift-continental system (RCS), which allow not only to consider it as a paleotype LIP, but also to expand the existing ideas about these unique geological objects.

Results

Structural and tectonic position of the Devonian RCS

The structure under study was laid at the turn of the end of the Silurian-Early Devonian within the west-south-west border (in modern coordinates) of the Siberian Craton. For heterogeneous fold-block structures of this AR-PR-PZ_1 frame is characterized by a roughly zonal structure. In the direction from the craton to the west, the zone of metamorphic archaeid-proterozoid is replaced by a zone of Riphean-Cambrian folded structures and further Caledonian (O-S) structures. At the end of the Ordovician-Silurian, between the craton structures of the Russian, Siberian platforms and Kazakhstan, the Ural-Mongolian folded belt was laid and developed, and the Paleozoic Ocean corresponding to its beginning. In this context, the Devonian RCS occupied a marginal continental position. Using the inherited Precambrian structural seams separating uneven-age zones, she dissected the structures of the fold-block framing of the Siberian craton along almost its entire length.

The main morphostructures of the arch-rift system

In the structure of the RCS, two main types of morphostructures are distinguished: fragmentary developed depressive zones and the handful-like uplifts of the pre-rift base separating them. The structural framework of the system is formed by long-lived, activated in the Devonian, longitudinal transregional East-Sayan-Yenisei (eastern) and Kuznetsk-Alatausko-Kobdinsky (Western) lineaments, cut into approximately equal portions by transverse (transform) regional faults. Along the eastern and western lineaments in the early Devonian, depressive zones were laid, and between them a long arched uplift was formed, of which ASFR became the nuclear part. During the growth and split of the vault, the axial depressive zone of the RCS (Tuvinsko-Minusinsky) formed in its axial part. Further collapse of the arch led to the formation of the eastern and western handful-shaped uplifts, separating the axial depression zone from the adjacent marginal depression zones. Inside the zone, a series of transverse uplifts, dividing the deflections and depressions from each other along the strike, appeared.

Magmatism RCS, its composition and stages of formation

The morphostructure formation of paleorift was accompanied by active volcanism. The main arena of volcanic manifestations was depression zones, transverse elevations and nodes of their articulations. The framing horst-shaped uplifts were to a much lesser extent covered by volcanism. Within their limits, small and medium intrusive massifs, comagmatic to volcanics of adjacent structures, were mainly formed. It should be noted that the composition of volcanics is significantly influenced by their structural and tectonic position: the composition of volcanics and the set of their differentiates in the depressed zones and in the framing uplifts differ, as well as depending on the composition and structure of the pre-Devon rocks. So the eastern framing of the Minusinsky trough and its periphery are characterized by a wider development of lavas of acidic composition, and the western one, on the contrary, by the main one.

In terms of scale and volume, volcanism sharply dominates over the intrusive component of rift magmatism. In general terms, there are three stages (impulses) of volcanism associated with tectonics and sedimentogenesis of the RCS. The most early and active magmatism manifested itself mainly in the axial depression zone and engulfed the early Devonian. Signs of lateral migration of volcanism from the axial zone to the eastern and western, where its maximum falls at the end of the early-middle Devonian, are established.

The early stage of volcanism in the axial zone is characterized as plateau-basalt, represented by sub-alkaline picrobasalts, trachybasalts, trachyleucobasalts and basalt trachyandesites.

The middle stage is represented by a series of trachybasalts, basaltic trachiandesites — trachiandesibasalts, trachytes and trachyriodacytes. Along with it, alkaline series of tefrit-phonolites of sodium and potassium specificity of alkalinity (Martaiga, Sokol, Sopnyaya Sopka, etc.) appeared in local areas (subprovings) in parallel with it.

The final stage had trachybasal-trachyte, trachyryolite composition and a mild tephrite trend in the form of basanites.

A significant component of the volume of volcanics is a series of basalt sills and dikes.

The total time interval of the stages of manifestation of volcanism in the axial zone did not exceed 10-15 million

years. The duration of volcanism within the end of the early-middle Devonian of the eastern and western depression zones also corresponds to this interval.

The volcanites of the grabens and minor depressions of the framing uplifts and the periphery of the trough in the depressive zones are usually accompanied by a series of rod-like intrusions that are comagmatic in composition to the vulcanites: gabbro-syenitic, alkaline-gabbroid, alkaline-syenite-granite.

RCS dimensions and approximate volume of volcanic rocks

The total length of the RCS from north to south is about 2.5 thousand km with a width of 1.0-0.4 thousand km, which is about 1.5 million km^2 of the total area of the RCS.

The volume of volcanic rocks (effusive, sills, dikes) of the largest structural-depressive sites of paleorift volcanism, reaching the level of erosion and not less than 500 km^2 (Agulsky, Minusinsky, Delun-Yustydsky, Tuvinsky deflections, deflections and grabens of Gorny Altai, deflections and grabens framing Kuznetsk trough) is about 232 340 km^3. Considering that the area of the troughs is a multiple of the area of the listed volcanic fields that reach the surface, and many hundreds of structures with an area of tens and first hundreds km^2, as well as those not covered by the calculation of the depression of the buried West-Siberian part of the RCS and the structure of the volcanic belts of Central Mongolia The Devonian system can be at least 1 million km3, even without taking into account the erosion cut of the paleorift and the plutonic component of magmatism.

Geochemical parameters of volcanism

The most important features of the volcanic rocks of the axial rift zone are their geochemical proximity OIB, with the presence of weakly pronounced Nb-Ta and Hf minima. They belong to intraplate basalts and partially to basalts of the destructive margins of continents. According to the Eu/Eu* index, rocks are mantle (0.78–1.07), and medium and acidic species (0.38–0.42) show a significant presence of crustal matter. The dominant source of source magmas was the plume component. Thus, in general, the studied volcanics formed with the dominant mantle-plume PREMA – a source "diluted" with the asthenospheric mantle substance, which retains the geochemical recycling characteristics of the Baikal-Salair stages of the region's development, and in the later stages, the differentiates were enriched in core material.

Paleorift development scheme

The active tectonic-magmatic stage of the development of the early, early-middle Devonian RCS was replaced by a longer slab-syneclite stage of the upper Devonian, Carboniferous and Permian. During this stage, the largest depressions of the RCS were largely covered by terrigenous-sedimentary strata, and the open parts were eroded.

Conclusions

According to modern ideas about LIP, as reflected in the works of R.E. Ernst, M.E. Coffin, S.E. Bryan, H.C. Sheth et al., The Devonian RCS should be defined as an intraplate sub-rift-continental and substantially mafic province with a dominant extrusive nature. The rift fields of India and Western Australia can be considered as supposed analogues of it.

Acknowledgements

This work was conducted as task of RFBR, project No. 19-05-00300.

References

1. Grinev OM (1990). Evolution of alkaline gabbroid magmatism of the Kuznetsk Alatau. Abstract of diss. cand. geol.-mineral. sciences: 19 p.
2. Grinev OM (1999). Features of morphotectonics, magm ore genesis and gold-platinum-bearing rift-based framing systems of the Siberian platform. Structural analysis in geological research: Proceedings of the I International Seminar: 77–88.
3. Grinev OM (2007). Tuva-Minusinsk-West Siberian rift system: geology, morphotectonics, minerageny. TSU Bulletin 299: 185–193.
4. Grinev OM (2007). Siberian rift systems: study methodology, morphotectonics, minerageny: 434 p.
5. Devonian rift formations of the south of Siberia (1996). Ed. V.P. Parnachev, I.A. Vyltsan: 239 p.
6. Vorontsov A.A., Yarmolyuk V.V. (1992). Devonian magmatic associations with alkaline rocks of northwestern Mongolia. Geology and geophysics 8: 62–68.
7. Vorontsov A.A. Petrochemical characteristics of Devonian alkaline-alkaline magmatism of northwestern Mongolia. Geology and geophysics 34 (8): 117–124.
8. Vorontsov A.A. (1994). Geology and geochemistry of early Middle Devonian magmatic associations with alkaline rocks of North-West Mongolia. Abstract of diss. cand. geol.-mineral. sciences: 25 p.
9. Vorontsov A.A. (2007). The evolution of the Phanerozoic rift magmatism of Central Asia (on the example of the polychronic North-Mongolian-Zabayskal rift region): geochemistry, sources, geodynamics. Abstract of diss. cand. geol.-mineral. sciences: 41 p.

THE KALAHARI AND GRUNEHOGNA CRATONS, AND THEIR PLACEMENT WITHIN NEOPROTEROZOIC RODINIA, DEFINED BY NEW U-PB GEOCHRONOLOGY ON LARGE IGNEOUS PROVINCES

Gumsley A.[1,2,3], Sałacińska A.[4], Knoper M.[5], Mamuse A.[3], Chew D.[6], Söderlund U.[2,7], Kamo S.[8], Szopa K.[9], Ernst R. E.[10,11]

[1]*Institute of Geophysics, Polish Academy of Sciences, Warsaw, Poland.*
[2]*Department of Geology, Lund University, Lund, Sweden.*
[3]*Faculty of Mining and Mineral Processing Engineering, Midlands State University, Zvishavane, Zimbabwe.*
[4]*Institute of Geological Sciences, Polish Academy of Sciences, Warsaw, Poland.*
[5]*Department of Geology, University of Johannesburg, Johannesburg, South Africa.*
[6]*Department of Geology, Trinity College, Dublin, Ireland.*
[7]*Department of Geoscience, Swedish Museum of Natural History, Stockholm, Sweden.*
[8]*Department of Earth Sciences, University of Toronto, Toronto, Canada.*
[9]*Faculty of Earth Sciences, University of Silesia, Sosnowiec, Poland*
[10]*Department of Earth Sciences, Carleton University, Ottawa, Canada.*
[11]*Faculty of Geology and Geography, Tomsk State University, Tomsk, Russia*

Keywords: *Fingeren, Mutare, dyke swarm, Neoproterozoic, Rodinia*

The Grunehogna Craton of Dronning Maud Land in Antarctica and the Kalahari Craton of southern Africa are generally accepted to have been contiguous, in either close or far fit configurations, between 1.11 Ga and 0.18 Ga. In this study, dykes of the Fingeren dyke swarm in Grunehogna and dykes of the Mutare dyke swarm in Kalahari were dated using U-Pb on baddeleyite and apatite. The ages reveal similar mafic magmatism at ca. 720 Ma in both areas, which has not been reset by later metamorphic events. This confirms the relationship whereby Grunehogna is a rifted fragment of Kalahari, which was severed during the Jurassic breakup of Pangea into Africa and Antarctica. It also confirms a close fit between the cratons at ca. 720 Ma. The possibility that Kalahari was adjacent to north-western Laurentia during the Neoproterozoic should be considered, based on geological evidence. This includes shared magmatism at 790-780 Ma between the Gannoukouriep and Gunbarrel large igneous provinces (LIPs) as well as a connection between various LIPs at 730-710 Ma making the combined Franklin-Mutare-Fingeren-Irkutsk LIP one of the largest in geological history (also including Siberia), and an ideal trigger for the Cryogenian to Ediacaran glacial period that followed. Interplay between mantle plumes, LIPs, glaciation and Rodinia fragmentation likely led to the rise in free oxygen and multi-cellular life toward the Cambrian boundary.

Acknowledgements

Ashley Gumsley acknowledges financial support from the National Science Center in Poland (grant agreement no. UMO2016/23/P/ST10/02423). This grant has received funding from the Marie Sklodowska-Curie Actions COFUND2014 (grant agreement no. 665778). Anna Sałacińska acknowledges financial support from internal projects for young scientists (2018-2019) at the Institute of Geological Sciences, Polish Academy of Sciences, Warsaw in Poland.

ULKAN-BILYAKCHAN LIP (CA. 1.7 GA), SE SIBERIAN PLATFORM, ASSOCIATED TRIPLE JUNCTION RIFTING, AND ORE DEPOSITS

Guryanov V. A.[1], Ernst R. E.[2,3]

[1]*Kosygin Institute of Tectonics and Geophysics, FEB RAS, Khabarovsk, Russia;*
[2]*Department of Earth Sciences, Carleton University, Ottawa, Canada*
[3]*Faculty of Geology and Geography, Tomsk State University, Tomsk, Russia*

Keywords: *LIP, ore deposit, Siberia*

The Ulkan paleorift system (SE Siberia) has characteristics of a three-armed structure indicative of the intense rifting in response to hotspot activity; The triple junction appears as a zone that underwent intense intra-plate A-type alkaline-granitic magmatism in the Late Paleoproterozoic. (Guryanov, 2007; Guryanov et al., 2012; Larin, 2011; Guryanov & Peskov, 2017). The presence of both subalkaline granitoids and volcanic rocks (K-series) and alkaline granites, comendites and pantellerites (Na-series) intensely fractionated, is characteristic of the Ulkan anorogenic magmatism. A specific feature of these granites is that they contain iron-enriched ferromagnesian silicates, and alkaline granites that contain alkali amphibole and pyroxene and astrophyllite.

Globally, A-type granites are often associated with deposits of Sn, W, Be, Nb, Ta, REE, Au, U and Fe, such as Piting in Brazil, Thor Lake and Strange Lake in Canada, Zaiplats in South Africa, Katuginskoe of the Aldan-Stanovoi shield (Larin, 2011).

The Ulkan intraplate alkali-granite magmatism of the Ulkan massif is host to endogenous ore deposits unique in dimensions and diversity (Be, Ta, Nb, Zr, REEU, Au, Li, Sn, W, Mo, Ti and (Pt)) (Guryanov, 2007). Rare metal and rare earth

deposits are genetically associated with alkaline granites and their derivatives. Almost all of them occur in exocontact zones (adjacent host rock) of the Nygvagansky alkaline granite stock located in the central part of the Ulkan massif of subalkaline granitoids. The most important elements in these deposits are Be, Ta, Nb and REE. The U-Pb and Pb-Pb ages of REE deposits range from 1720 ± 23 to 1670 ± 70 Ma, closely matching the age of alkaline granites (Goroschko et al., 2006).

U-Pb zircons dating of the Early Precambrian crystalline basement rocks in the southern flanks of the Ulkan trough showed a range from 1769±9-1690±14 Ma (Guryanov et al. 2012). This intense tectonothermal reworking of crystalline basement rocks of the south-eastern Siberian Platform, is related to the development of the Ulkan, Bilyakchan and other proto-aulacogens; emplacement of voluminous intrusions of normal and alkaline granites, syenite, monzonite of the Ulkan, Nudymi and other complexes.

Komatiite dyke swarms and rare subalkaline granitic intrusions of the Ulkan complex can be traced on the southern periphery of the Ulkan trough among Archean granulites and anorthosites of the Dzhugdzhur block (Guryanov, 2007). Economic sulfide copper-nickel mineralisation with platinum-group elements (PGE) is found to be komatiite- associated. Estimates for the age of komattite are 1690+14, 1700+12, 1710+10, 1720+12 and 1730+15 Ma (Kun-Manie Cu-Ni deposit; U-Pb SHRIMP-II age on zircons Guryanov et al., 2016).

It appears evident that in the south-eastern part of the Aldan-Stanovoy shield there occurred tectonic and metamorphic events at 1.77 - 1.69 Ga accompanied by intense metamorphism (up to granulite facies) of Archean anorthosites of the Old Dzhugdzhur complex and enclosing rocks.

References

1. Goroschko M. V., Malyshev Yu. Ph., Kirillov V. E. Uranium Metallogeny of the Russian Far East. Moscow: Nauka, 2006. 372 p. [in Russian].
2. Guryanov V.A. Geology and metallogeny of the Ulkan area (Aldan – Stanovoy Shield)// Vladivostok: Dal`nauka, 2007. 227 p. [in Russian].
3. Guryanov V.A., Roganov G.V., Zelepugin V.N., Rozinov M.I. and Saltykova T.E. "Isotopic – geochronological studies of zircons from the Early Precambrian rocks of the southeastern Aldan – Stanovoy Shield: new results, their geological interpretation," Russ. J. Pac. Geol. 6 (2), 97 – 113 (2012).
4. Guryanov V.A., Peskov A. Yu. Ulkan paleorift structure in the south-eastern environs of the Siberian Platform: Age, Conditions, Sources, and Geodinamic Setting// Geosciences Research.Vol. 2, No. 2, 2017, p. 59-71.
5. Larin A.M. Rapakivi granites and associated rocks. – St. Petersburg: Nauka. 2011. 402 pp. [in Russian].

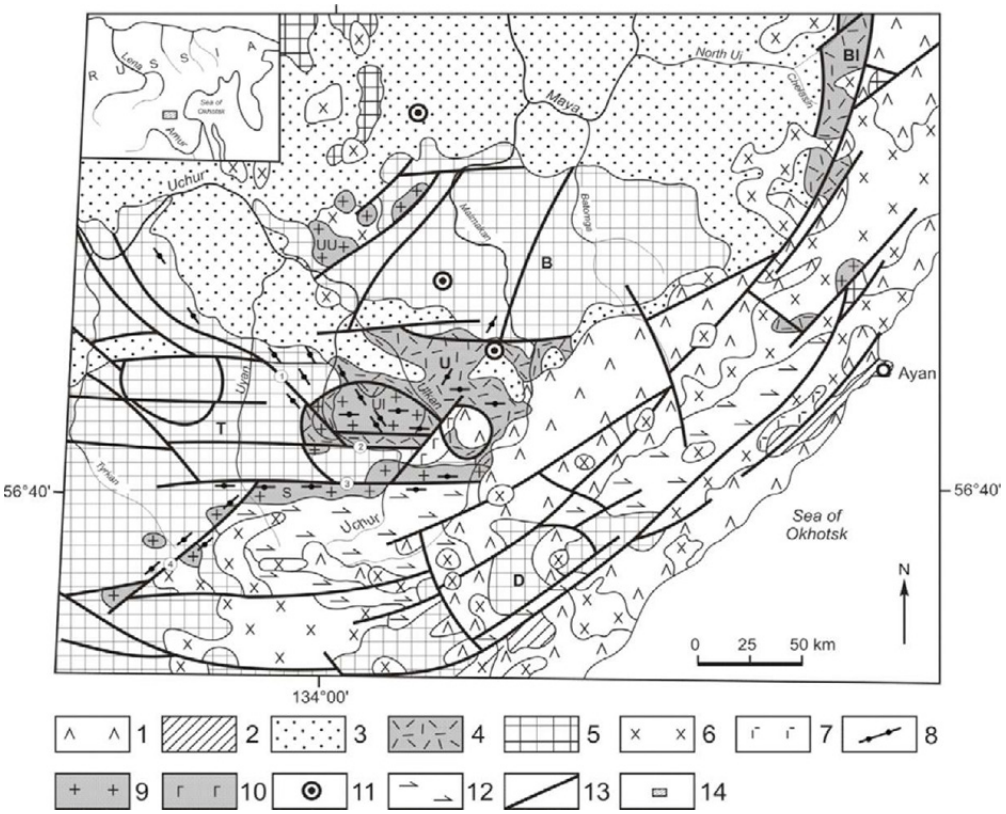


Fig. Geological map of southeastern margin of the Siberian Platform (Guryanov, 2007).

1 - Cretaceous volcanics of Okhotsk-Chukotka volcanic belt; 2 - Paleozoic terrigenous and carbonate sequences of Ayan-Shevli Pericratonic Trough; 3 - Cambrian-Mesoproterozoic volcanic-sedimentary and terrigenous-carbonate rocks of Uchur-Maya Plate; 4 - Paleoproterozoic Ulkan (U) and Bilyakchan (Bl) volcanic-sedimentary troughs; 5 - Archean crystalline rocks of Siberian Platform basement: Batomga (B), Tyrkan (T), and Dzhugdzhur (D) blocks; 6 - Cretaceous granitoid plutons; 7 - Paleozoic gabbroic rocks; 8-11 - Paleoproterozoic intrusions: 8 - basic dykes of the Maimakan Complex, 9 - granitic rocks of Ulkan Complex, 10 - gabbroic rocks of Gekundan Complex, 11 - ultramafic rocks of Konder Complex; 12 - anorthosite of Old Dzhugdzur Complex; 13 - fault; 14 - studied area (inset). Faults (numbers in circles): 1 - Uchur-Elgetei; 2 - North Uchur; 3 - South Uchur; 4 - Ukikan. Plutons (letters in figure): Ul, Ulkan; S, South Uchur; UU, Upper Ugayan.

PRELIMINARY COMMENTS ON THE ELEMENTAL AND ISOTOPE GEOCHEMISTRY OF THE EQUAMP MAFIC ROCKS (SOUTH AMERICA)

Hollanda M. H. B. M.[1], Macêdo Filho A. A.[1], Oliveira A.L.[1], Negri F. A.[2], Archanjo C. J.[1], de Castro D. L.[3], Dantas A. R.[1]

[1]*University of São Paulo, São Paulo, Brazil*
[2]*Institute of Geology, State Environmental Office, São Paulo, Brazil*
[3]*Federal University of Rio Grande do Norte, Natal, Brazil*

Keywords: *Gondwana break-up, Early Cretaceous, Tholeiitic magmatism, EQUAMP, Subcontinental lithospheric mantle, NE Brazil*

Introduction

This work is part of an ongoing project recently started that deals on the characterization of a hitherto unknown large igneous province in NE South America. The formation of the Equatorial Atlantic Magmatic Province (EQUAMP; Hollanda et al. 2018) was related to the disruption of the West Gondwana and resulting opening of the Equatorial Atlantic Ocean during the Early Cretaceous. EQUAMP comprises only intrusive bodies, which are mafic sills and dike swarms intruding, respectively, Paleozoic sedimentary rocks of the Parnaíba basin and the Precambrian basement of the Borborema Province, both in NE Brazil. En-echelon dikes form the main products of EQUAMP. They constitute a ca. 1,000 km-long arcuate swarm, which is parallel to the present-day continental E-and NE-trending Atlantic margins, and at least two other sub-sets of about 250-300 km in length, also extending parallel to the Atlantic coastline. Sills, in turn, occurs exclusively along the eastern side of the Parnaíba basin. From the available geophysical data, the major volume of magma representing EQUAMP is stored in sub-surface rather than exposed at surface.

Major and trace element geochemistry was carried out on a set of nearly 200 samples, of which 116 of sills and 72 of dikes, whereas Sr-Nd isotope analyses were made for a hundred samples chosen after the geochemical classification. Integration and interpretation of all data are still at early stage, the reason why we would introduce here only a brief account of the chemical characterization of EQUAMP.

Results

Classification and fractional crystallization

Mafic dikes and sills are mainly represented by medium- to fine-grained diabases. In a few sites, coarse-grained rocks are spatially associated with the diabases, and are characterized by centimeter-sized acicular crystals of augite in a plagioclase-rich groundmass. Petrographically, these rocks are defined as leucogabbros. The majority of the samples consist of unaltered to slightly weathered (LOI ≤ 1.5%) rocks, with minor evidence of degassing (i.e., amigdales or vesicles). They are all silica-oversaturated tholeiites, grouped into (1) subalkaline, low TiO2 (< 2 wt.%; P2O5 < 0.2 wt.%) basaltic andesites, and (2) subalkaline to transitional high TiO2 (= 2.1–4.5 wt.%; ; P2O5 > 0.2 wt.%) magmas including basalts to (trachy)dacites. The more evolved magmas are represented by the leucogabbros (mostly dacites in composition). Fractional crystallization is an important process in the high-Ti tholeiites, and their chemical variability is controlled by progressive removal of olivine and Ca-rich (augite) pyroxene, magnetite and ilmenite. Ilmenite, in fact, starts to decrease only at MgO ~3.5 wt. %. Plagioclase and apatite are not critical fractioning phases in these magmas. Contrarily, ilmenite and magnetite (and also apatite) do not fractionate during crystallization of the low-Ti magmas, their chemical variation being mainly controlled by discrete fractionation of plagioclase, Ca-rich pyroxene and olivine.

Isotope and trace element geochemistry

Trace element characteristics of the EQUAMP magmas are shown in chondrite-normalized diagrams. One important feature to be highlighted is the depletion in Nb(-Ta) relative to La (Nb/La ~0.61) and other lithophile elements (such as Th, U, Ba), which is not a characteristic of typical OIBs. The high-Ti tholeiites are more enriched in incompatible elements (100 times CHUR; LaN/YbN > 11) when compared with the low-Ti magmas, while these latter clearly experienced some extent of crustal contamination. High and low-Ti tholeiites also differentiate by their isotope compositions, mainly concerning to Nd. The high-Ti tholeiites have less radiogenic compositions (εNdt=130 from ~-3.4 to -2.1) than the low-Ti (from ~ -2.3 to-1.1), while the initial $^{87}Sr/^{86}Sr$ ratios of the uncontaminated samples (regardless the Ti content) are usually lower than 0.706300. Only two basalts that are part of one sill to the north and other to the south present depleted Sr-Nd compositions, which are 0.703520/εNd=+3.32 and 0.703431/ εNd= +6.13, respectively.

Conclusions

A preliminary examination of the data shows a clear distinction into two tholeiitic groups based on Ti (and P) contents, trace elements and isotope compositions. Although the interpretation still demands further deepening, it appears that the continental lithospheric mantle have participated as a major source for generation of the EQUAMP magmas. Thus, it is mandatory to think of what mechanisms would have triggered mantle melting during the Equatorial Atlantic opening.

Acknowledgements

This work has been funded by Fundação de Amparo a Pesquisa no Estado de São Paulo – FAPESP, project No. 2017/08423-9.

PLUME-RIDGE INTERACTION IN THE SOUTH CHINA SEA

Huang X-L., Yang F., Xu Y-G.

State Key Laboratory of Isotope Geochemistry, Guangzhou Institute of Geochemistry, Chinese Academy of Sciences, Guangzhou 510640, China

Keywords: *plume-ridge interaction; crystallization temperature; MORB; olivine-spinel pairs; South China Sea*

Introduction

The South China Sea (SCS) is a western Pacific marginal sea situated at the junction of Eurasian, Indo-Australian, and Philippine-Pacific plates. It has been speculated that a mantle plume might have triggered the opening of the SCS or interacted with mid-ocean ridge system of the SCS. Testing the hypothesis of the mantle plume triggering the opening of the South China Sea (SCS) and its interaction with the spreading ridge is important for understanding the dynamics for evolution of the SCS. In general, the potential temperature of the mantle at mid-ocean ridges is much lower than that associated with LIPs. If the opening of the SCS was triggered by an upwelling plume or the spreading was impacted/enhanced by a mantle plume, the volcanism produced at spreading ridges is expected to capture the signature of plume mantle. In this study, we collected the mid-ocean ridge basalt and basaltic glass from the Hole U1431E of IODP Expedition 349 located near the extinct ridges in the East Subbasin of SCS, calculated the crystallization temperature for the olivine-spinel pairs using the Al-in-olivine thermometry (Coogan et al., 2014), and then estimated the potentially highest crystallization temperature of primitive olivine, which allows to test the existence of plume-ridge interaction and the role mantle plume played for the opening of the SCS.

Results

This study examined nearly primitive olivine (Fo = 83.1–85.9) and spinel (Cr# = 27.8–49.7%) in sea floor basalts and glassy samples collected from the Hole U1431E of IODP Expedition 349 with aims of estimating the crystallization temperature. The application of the Al-in-olivine thermometer yields crystallization temperature for the studied samples varying from 1208±16°C to 1275±14°C with mean value of 1247±16°C. When extrapolating to Fo = 90 and spinel Cr# = 49.7, the crystallization temperature of primitive olivine is about 1350 °C, which is much higher than that of global MORB but comparable to that of Iceland OIB.

Conclusions

Mantle potential temperature at the extinct ridge of the SCS at ~16 Ma is much higher than that beneath a normal mid-ocean ridge, manifesting the mantle plume-ridge interaction during the last spreading of the SCS, which is also evidenced by high Ni olivines and the elevated Pb isotope composition for the N-MORB at U1431E. However, the thickness of the oceanic crust in the SCS is mostly less than 10 km, and there is not seamount chains or volcanic lineaments toward any direction either, indicating a non-classic plume. Another line of evidence for a non-classic plume comes from its location that is distal from the two large low shear velocity provinces (LLSVPs). The plume was likely generated by subducting slabs into the lower mantle in regions surrounding the SCS (Wang et al., 2013), which has been demonstrated by 3D geodynamic modelling (Zhang & Li, 2018). We proposed that the plume impacted on the SCS might contain large amounts of recycled oceanic crust in the form of eclogite, and then be low buoyant. Such a low-buoyancy mantle plume was ponded in the mantle transition zone and would have produced secondary plumes by heating the surrounding mantle (Dannberg & Sobolev, 2015).

Acknowledgements

This work was financially supported by the National Natural Science Foundation of China (NSFC Projects 41625007, 41890812).

References

1. Coogan, L.A., Saunders, A.D., Wilson, R.N., 2014. Aluminum-in-olivine thermometry of primitive basalts: Evidence of an anomalously hot mantle source for large igneous provinces. Chemical Geology 368, 1–10.
2. Dannberg, J., Sobolev, S.V., 2015. Low-buoyancy thermochemical plumes resolve controversy of classical mantle plume concept. Nature Communications 6960. https://doi.org/10.1038/ncomms7960.
3. Wang, X.C., Li, Z.X., Li, X.H., Li, J., Xu, Y.G., Li, X.H., 2013. Identification of an ancient mantle reservoir and young recycled materials in the source region of a young mantle plume: Implications for potential linkages between plume and plate tectonics. Earth and Planetary Science Letters 377–378, 248–259.
4. Yang F., Huang X.L., Xu Y.G., He P.L., 2019. Plume-ridge interaction in the South China Sea: Thermometric evidence from Hole U1431E of IODP Expedition 349. Lithos, 324–325, 466–478.
5. Zhang, N., Li, Z.X., 2018. Formation of mantle "lone plumes" in the global downwelling zone — Amultiscale modelling of subduction-controlled plume generation beneath the South China Sea. Tectonophysics 723, 1–13.

THE DIABASE SILLS IN THE OUTER ZONE OF THE EMEISHAN LARGE IGNEOUS PROVINCE SW CHINA: PETROGENESIS AND TECTONIC IMPLICATIONS

Huang Y.[1,2], He C.[1], Chen N-S.[1,3], Xia B.[1]

[1] *School of Earth Sciences, China University of Geosciences, Wuhan 430075, Hubei, China*
[2] *Geological Surveying Academy of Guizhou Province, Guiyang 550081, Guizhou, China*
[3] *Global Tectonic Center of China University of Geosciences, Wuhan 430074, Hubei, China*

Keywords: *diabasic sill, high-Ti and low-Ti rocks, petrogenesis, tectonic evolution, Emeishan LIP, SW China.*

Compositionally and texturally zoned diabase dykes and sills occur in the outer zone of the Emeishan Large Igneous Province (ELIP) in the southern Guizhou Province of South China Here we investigate a representative diabase sill in the Luodian region through detailed petrology, whole rock geochemistry, zircon U-Pb geochronology and Hf isotopes and clinopyroxene mineral compositions with a view to understand the petrogenesis and tectonic implications. The diabasic sill formed as composite zoned sub-volcanic intrusion that is characterized by gabbros and diabases in the inner zone and amygdaloidal diabases sporadically in the chilled zone within the upper sill margin. The diabasic and gabbroic rocks are composed of quartz-free and quartz-bearing groups. The quartz-free group shows low SiO_2 (45.7 wt.%–49.5 wt.%), moderate MgO (5.66 wt.%–7.88 wt.%), high TiO_2 (2.54 wt.%–3.65 wt.%), and Ti/Y values (536–747), corresponding to high-Ti type rocks. The quartz-bearing group has higher SiO_2 (49.8 wt.%–50.9 wt.%) and lower MgO (4.23 wt.%–4.74 wt.%), higher TiO_2 (3.16 wt.%–3.63 wt.%), but lower Ti/Y values (399–419) than the quartz-free group ones, and thus belong to the low-Ti type. Both groups of rocks are enriched in LREE and LILE with negative Nb-Ta anomalies, and show broad tholeiitic affinity. The precursor magma of the high-Ti rocks might have originated from a source composed of mantle plume and subcontinental lithosphere mantle components, with minor crustal contamination during ascending. The magma of the low-Ti rocks was produced by mingling of the high-Ti diabasic rocks with minor injected intermediate-acidic magma plugs or blebs, suggesting magma mingling as one of the effective ways to change the high-Ti to low-Ti rocks of the ELIP. The diabasic sill underwent a rapid cooling event probably in response to a rapid uplift tectonic, which probably occurred in the waning stage of ELIP during transition between the middle and late Permian after the domal uplift induced by the mantle-plume or in the Late Jurassic.

U-PB GEOCHRONOLOGY OF THE BAMBUYKA ALKALINE ROCKS (TRANSBAIKALIA, RUSSIA)

Izbrodin I. A.[1], Doroshkevich A. G.[1,2], Khubanov V. B.[1], Rampilov M. O.[1], Lastochkin E. I.[1]

[1]*Geological Institute SB RAS, Ulan-Ude, Russia, izbrodin@ginst.ru*
[2]*V.S. Sobolev Institute of Geology and Mineralogy SB RAS, Novosibirsk, Russia, doroshkevich@igm.nsc.ru*

Keywords: *Nepheline-bearing and nepheline-garnet-bearing syenites, geochronological data, Late Paleozoic magmatism*

Introduction

The precision geochronological data of most alkaline massifs of the Vitim plateau indicate repeated intrusions of alkaline rocks into a single developing structure. There were three stages of alkaline magmatic activity 520-486 306-280 and 261-242 Ma (Doroshkevich et al., 2018). This paper presents results of geochronological (U-Pb LA ICP-MS) studying of the Bambuyka massif.

Results

The Bambuyka alkaline massif is located in the middle of the Bambuyka River (left feeder of the Vitim River) 70 km above the mouth. The massif intrudes Lower and Middle Cambrian carbonate sediments and confined to the crossing of sublatitudinal and northwestern faults. According to Litvinovsky (1973) the massif was emplaced by one stage, and different rocks of eastern and western bodies which are divided by the river were formed due to magmatic differentiation and magmatic alteration processes. The massif is 15 km^2, thus the east body (6*1.8 km) is composed by gabbro and gabbro-pyroxenite. The body is cut by dykes of granites, pegmatites (amazonitic) and stock of leucocratic granites. The west body (4*1.5 km) is mostly composed by alkaline syenites which contain small bodies of nepheline syenites with gradual contact between them. There are garnet-bearing syenites near-contact parts of the west body. Total size of outcrop varies from some meters to 150 m, at the same time the garnet contents were increasing. There are aegirine-bearing and cancrinite-bearing varieties among the nepheline syenites.

Zircons from the aegirine-bearing (Bam-485), albitized (Bam-350) and garnet-bearing (Bam-349) nepheline syenites of the west body and from gabbro (Bam-461) of the east body were sampled for isotopic dating. In cathodoluminescence image the zircons from syenites have dark domains which were not recrystallized, and pale overgrowth rims or have heterogeneous parts with irregular alteration of pale and dark

domains. In some case there are inclusions of K-feldspar, albite, pyroxene, biotite, scapolite, titanite less pyrochlore and apatite. The local dating by LA-ICP-MS of unaltered dark and pale domains of the zircons from the nepheline syenites (Bam-458) shows analytically same ages. The concordant age is 291.0±1.8 Ma. There are two age groups (288±2.4 and 267±2.5 Ma) and single values in the range of 240-255 Ma for zircons from the garnet-bearing syenites.

Zircons from the albitized syenites are characterized by partially (zonal) porous structure. The concordant $^{207}Pb/^{206}Pb$ age is 274±1.7 Ma. Zircons from the gabbros are small (less than 100 μm) crystals with oscillatory zoning. The concordant age is 269.9±0.77 Ma.

Conclusion

Thus, the obtained ages indicate a time gap between alkaline syenites and gabbros of the Bambuyka massif (291 and 269 Ma respectively) and disprove a one stage emplacement of the massif; however this conclusion needs additional geochemical and petrological studies. At the same time, albitization is most likely related with the gabbro emplacement, which is evidenced by the age spectra (the albitized syenites – 274 Ma and the garnet-bearing syenites – 267 Ma). The age of the rocks is similar to the main stage of alkaline magmatism (311-294 Ma) of the Vitim plateau and the Sinnyr complex (Izbrodin et al., 2017; Doroshkevich et al., 2018).

Acknowledgements

The geochronological study of the rocks were supported by the Russian Foundation for Basic Research (Project no. 17-05-00309-a).

References

1. Doroshkevich A.G., Izbrodin I.A., Rampilov M.O., Ripp G.S., Lastochkin E.I., Khubanov V.B. (2018). Permo-Triassic stage of alkaline magmatism in the Vitim plateau (western Transbaikalia). Russian Geology and Geophysics 59:1061–1077
2. Izbrodin I.A., Doroshkevich A.G., Rampilov M.O., Ripp G.S., Lastochkin E.I., Khubanov V.B., Posokhov V.F., Vladykin N.V. 2017 Age and mineralogical and geochemical parameters of rocks of the China alkaline massif (western Transbaikalia). Russian Geology and Geophysics 58:903–921
3. Litvinovsky B.A. New data on the conditions of the formation of holy carriers (on the example of the garnet syenites of the Bambu intrusion, Vitim plateau) // Geology and Geophysics 1:42-51

SYNCOLLISION AND SYNSHEARING ULTRAMAFIC-MAFIC ASSOCIATIONS OF WESTERN MONGOLIA, CHINE AND NORTH VIETNAM

Izokh A. E.[1,2],Polyakov G. V.[1], Hoa T. T.[3]

[1] V.S. Sobolev Institute of Geology and Mineralogy SB RAS, Novosibirsk, Russia
[2] Novosibirsk State University, Novosibirsk, Russia
[3] Institute of Geological Sciences, NCNST, Ha Noi, Vietnam.

***Keywords**: LIP, Syncollision, synshearing ultramafic-mafic associations*

Introduction

Recently, in addition to the tectonics of lithospheric plates, involving significant movements of the blocks of the Earth's crust, plume tectonics has been actively developing. Ultramafic-mafic magmatism of Large Igneous Provinces is closely associated with deep mantle plumes. In the Altai-Sayan folded region in Western Mongolia, ultramafic-mafic magmatism corresponds to the Early Paleozoic, Devonian, Permian (Tarim) and Permo-Triassic LIP. In Permian-Triassic time in North Vietnam, ultramafic-mafic magmatism is associated with the Emeishan LIP. A specific feature of the Early Paleozoic LIP is that the mantle and crust magmatism manifests itself synchronously with the accretion-collision processes. At the same time, obduction of island-arc and back-arc associations on the Precambrian blocks is recorded.

Results

In the event of collisions of terranes of various types in the zones of obduction of ophiolites, differentiated ultrabasic-basic intrusions are widespread, breaking through the ophiolite sequence. The isotope-geochronological studies have shown that the age of these intrusions corresponds to the time of ophiolite obduction and is synchronous with the age of the granite-gneiss domes that accompany collision processes (Khain, Amelin, Izokh, 1995). Geological and isotopic data indicate that the introduction of these intrusions occurred in the ancient continental crust, on which a package of tectonic covers had already been pulled, with the surface of the main disruptions marked by the covers of ophiolites (Fedorovsky et al., 1995).

An example of syncollisional ultramafic-mafic association in the Lake zone of Western Mongolia is the Khairkhan dunite-troctolite-gabbro intrusion. It is located in the central part of the island-arc Lake zone. The sedimentary rocks of the Early Cambrian Burgasutai suite composed of mainly coarse-clastic terrigenous sediments with rare intercalations of carbonates serve as enclosures for the massif. In the internal structure of the massif two main complexes are distinguished - layered series and marginal zone. Rocks of the layered series form the central part of the massif, exposing mainly on the eastern slope of the ridge. Stratification has a

northwest strike, consistent with the long axis of the massif visible in plan. The series is composed of the horizons of plagiodunites, troctolites, olivine gabbros, and gabbronorites with a subordinate number of anorthosites. In the lower half of the stratified series, mesotroctoliths (to melanotroctolites) prevail, in the upper half - olivine gabbronorites, meso- and leukotroctoliths; small horizons of olivine gabbro enriched with titanomagnetite appear.

The marginal zones is manifested quite distinctly in the Khairkhan massif. It is fragmentary distributed along the periphery of the array, while its apparent thickness reaches in some areas more than 1 km. The marginal facies are composed mainly of non-olivine gabbronorites, alternating to contact with quartz-containing amphibole gabbronorites.

Of particular interest in the structure of the stratified array series is the horizon of taxitic gabbroids and the associated horizon of orbicular rocks. Outcrops of taxitic rocks can be traced almost through the entire massif along the eastern slope of the ridge, in accordance with stratification. The apparent thickness of the horizon is variable, and usually ranges from 30-100 meters. Taxitic gabbroids are characterized by chaotically located leucocratic and melanocratic isolations of various sizes (from 1–2 to 20 cm), breaks, bends, and folds of thin layering. Structures that apparently have arisen as a result of visco - plastic deformations are observed.

Above the section, directly above taxitic gabbroids, there is a horizon of orbicular rocks, with a capacity of up to 15 meters. Orbicules are spherical zonal formations, up to 30–40 centimeters in size in the pepperer. In the structure of most of them, two zones stand out: the outer, represented by radially oriented olivine crystals and (or) clinopyroxene, the space between which is filled with small grains of plagioclase, and the inner zone of anorthosite composition, often with large (up to 5-6 mm) crystals. Less commonly, multilayer orbicles with a variable number (up to 8–10) of layers of different thickness and composition are found. Petrographically, orbicular rocks are represented by the same troctolites and olivine gabbros as in the “normal” stratified series. The composition of minerals in orbiculi, their gabbroids and troctolites varies slightly. Orbicules usually occupy up to 40–50% of the volume; however, in certain areas, where they are in close contact and mutually deformed, their volume fraction reaches about 80%.

Synmagmatic plastic and shear deformations are widely manifested in the rocks of the massif, both at the macro and at the micro level. They are expressed in crushing of the elements of stratification into small folds of various amplitudes (usually up to the first tens of centimeters), often turning into taxitic sites and zones of disruption. The greatest number of such structural elements is characteristic of the upper part of the stratified series, including the horizons of orbicular and taxitic gabbroids and troctolites. These features indicate fairly intense tectonic processes that accompanied not only the direct intruding, but also the further formation of the array.

The features of the mineralogical-petrographic and petrochemical composition, as well as the geochemical features of the stratified rocks of the Khairkhan massif are typical of stratified gabbroids characteristic of the island-arc paleosystems. At the same time, the geological data (breakthrough of the Lower Cambrian molasses), the geochronological age of gabbro (511 Ma), the presence of synmagmatic viscous-plastic deformations make it possible to classify the formation of an array as an accretion-collision stage of development of the CASP. The convergence of the material characteristics of the Khairkhan massif and island-arc gabbroids is explained by the melting of the same supersubduction mantle, but in different geodynamic modes.

The heating of the asthenosphere and lithospheric mantle due to the deep mantle plumes is associated with the formation of large-amplitude shear zones. In East Kazakhstan and in Western China, the Irtysh shear zone, which was previously regarded as a way out of the Precambrian basement, is among such examples. The time of metamorphism and shear deformations corresponds to the Tarim Large Igneous Province (285 Ma). In Eastern Kazakhstan, in Dzungaria and in Western Mongolia, this stage is characterized by the extensive development of ultramafic-mafic magmatism, accompanied by Cu-Ni mineralization. At the same time, some ultramafic-mafic massifs (Huangshandong) are characterized by rhombus-shaped forms, which is characteristic of syn-shear intrusions confined to large-amplitude shear zones.

Recently, works have appeared that testify to the active participation of mantle magmas in collisional processes, including those in shear zones associated with a collision. The shear zone of the Ailao Shan-Red River (ASRR) in Vietnam attracts the attention of researchers, since its formation is associated with a Hindustan collision with Eurasia. Geochronological studies of the metamorphic rocks of this zone showed that they were formed in the Late Oligocene – Early Miocene (25–35 Ma). However, the thermal history and tectonic evolution of the ASRR shear zone is considered without taking into account the high-temperature mantle magmatism, which, as shown by our research, has repeatedly manifested itself during its formation. In the study of the ASRR zone in North-West Vietnam, amphibolites, amphibole gabbros, pyroxenites, and peridotites were studied in several intersections among garnet-sillimanite-biotite gneisses and blastomilonites. The individual bodies of lherzolites, olivine pyroxenites and pyroxenites previously discovered here were assigned to the Bao A complex, which was compared with the Proterozoic stratified gabbroids of the southern framing of the ASRR zone. Other researchers attribute the same rocks to the metamorphic formations of the Day Nui Con Voi zone.

Geological, mineralogical, petrographic and petrogeochemical data show that lherzolites, websterites and amphibole gabbro zones of ASRR form a single lherzolite-websterite-gabbro association of differentiated intrusive bodies. According to the petrographic composition and the composition of the minerals, two facies of the depth of formation of these rocks are distinguished. Amphibole gabbroids with garnet, as well as websterites and lherzolites with high alumina contents in pyroxenes crystallized at a depth corresponding to a pressure of at least 6 kbar. Whereas the amphibole gabbros of the Bao Yen and Yen Bai areas are characterized by a lower level of depth of their formation. Ultrabasic rocks and gabbroids have complementary geochemical characteristics, which indicates their comagmatic. Isotopic studies allow us to outline several stages in the formation of the ultrabasic-basic association of the ASRR zone. Garnet amphibole gabbros and peridotites of the May A range (49–42 Ma) correspond to the early stage, the introduction of which took place in deep conditions prior to the exhumation of the shear zone material. The younger datings (35 Ma) were obtained for the amphibole gabbro in the marginal part of the May A shear zone and for the websterite from the Veit Tri region, which coincides

with the formation of lamproites of the Fansipan province. The youngest age (25 Ma) was obtained for amphibole gabbroids, the formation of which took place in shallower conditions, probably after exhumation. The basic magmatism of the ASRR zone ends with the introduction of gabbro-dolerite dikes. The presented materials testify to the manifestation of a mantle ultrabasic-basic magmatism synchronous with shear movements in the Shong-Khong zone, and thus substantially complement the known tectonic constructions.

Acknowledgements

This work was conducted as a government task of the Ministry of Education and Science of the Russian Federation

References

1. Fedorovskiy V.S., Vladimirov A.G., Khain E.V., Kargapolov S.A., Gibsher A.S., Izokh A.E. Tectonics, metamorphism and magmatism of the Caledonide collision zones of Central Asia. // Geotectonics, No. 3, 1995, p. 3-22.
2. Izokh AE, Chan Chong Khoa, Polyakov GV, Ngo Thi Phuong, Travin A.V. Cineknematic ultramafic-basic magmatism of the Shong-Hong zone (Vietnam). Reports of the Academy of Sciences, 2004, v.397, No. 3, p. 1-5.
3. Izokh AE, Vishnevsky A.V.,. Shelepaev R.A., .Polyakov G.V., Gertner I.F., Vrublevsky V.V. Khairkhansky dunite-troctolite-gabbro massif (Lake zone of Western Mongolia) - an example of syncollisional middle Cambrian gabbroids // "Petrology of magmatic and metamorphic complexes": Proceedings of the X All-Russian Petrographic Conference with international participation, Tomsk, Tomsk CSTI, 2018, p. 169-175.
4. Khain E.V., Amelin Yu.V., Izokh A.E. Sm-Nd data on the age of ultrabasic-basite complexes in the zone of obduction of Western Mongolia. Dokl RAS t. 341, No. 6, 1995, p. 791-796.

LARGE IGNEOUS PROVINCES (LIPS) AND METALLOGENY; PUTTING LIP-RELATED MINERAL DEPOSITS INTO A LIP FRAMEWORK CONTEXT

Jowitt S. M.[1], Ernst R. E.[2,3]

[1]Department of Geoscience, University of Nevada Las Vegas, Las Vegas, NV 89154-4010, USA.
[2]Department of Earth Sciences, Carleton University, Ottawa, Canada
[3]Faculty of Geology and Geography, Tomsk State University, Tomsk, Russia

Keywords: *Large Igneous Provinces, metallogeny, mineralization, hydrothermal, economic geology*

Introduction

Large Igneous Province (LIP) events involve the transport of a significant amount of energy and metals from the Earth's mantle to the crust and are directly involved in (e.g. magmatic sulfide systems), drive (e.g. hydrothermal systems driven by the heat involved in LIP events) or otherwise causatively influence a variety of differing metallogenic systems (e.g. the weathering of LIP rocks to generate residual bauxite or laterite deposits; Ernst and Jowitt, 2013). These events can also directly affect the maturation of hydrocarbon source rocks and the formation of oil and gas reservoirs and are genetically related to the development of some important aquifer systems.

This presentation provides an overview of the key links between LIP events and the formation of mineral deposits, including those that form during metallogenic events that occur significantly after the formation of the LIP involved in this mineral deposit genesis. Combining these links with the development of a plumbing framework for LIPs (Ernst et al., in press) allows the development of targeting strategies focused on the sections of LIPs that are known to host or be associated with differing types of mineral deposits.

Links between LIP events and metallogeny

LIPs are genetically associated with a wide variety of different mineral deposit types, including magmatic sulfide Ni-Cu-platinum group element (PGE), iron oxide-copper-gold (IOCG), orogenic gold, Al-bauxites, and Ni-Co laterites, as well as water and hydrocarbon resources (Ernst and Jowitt, 2013). These associations can be distilled into five distinct types of relationship, with the caveat that these relationships may overlap both temporally and spatially:

(1) LIP magmas that directly generate mineralization, such as orthomagmatic Ni-Cu-PGE sulfides or Nb-Ta-REE and diamonds associated with LIP-related carbonatites and kimberlites, respectively.

(2) LIP magmas that provide energy, fluids, and/or metals for ore types such as hydrothermal volcanogenic massive sulfide (VMS) and iron oxide-copper-gold (IOCG) deposits.

(3) LIP rocks (particularly sills and dykes) that acted as barriers to fluid flow and/or as reaction zones that control mineralizing events (e.g. during the formation of some Au deposits), acted as structural traps within hydrocarbon systems, or formed impermeable barriers that controlled water flow and hence aquifer formation.

(4) Surficial effects, such as the weathering of LIP rocks to form Ni–Co laterites and Al bauxites from exposed LIP mafic-ultramafic rocks in tropical climates and residual Nb, Ta, and REE laterites from LIP-associated carbonatites; and

(5) Indirect links between LIPs and ore deposits, where LIP-related continental breakup generates distal compression and transpression in the plate tectonic circuit that can lead to the formation of orogeny-related deposits, such as orogenic Au mineralization.

LIP events also enable the reconstruction of Precambrian supercontinents and the tracing of areas of metallogenic

and hydrocarbon endowment between presently separated but formerly contiguous crustal blocks. However, although knowledge of these links is useful in e.g. regional exploration targeting and can inform and direct more localized exploration, what is needed is a combination of knowledge of these relationships and their relative timing with information relating to the location of these mineral deposits within the LIP system. For example, PGE-dominated magmatic sulfide mineralization is generally (but not always) located within deep-seated layered intrusions within the LIP plumbing system, whereas magnetite-related hydrothermal vent complex mineralization is generally located in near-surface environments, reflecting the genetic processes that formed these types of mineral deposit. This linking of spatial and genetic knowledge will allow the identification of key areas within given LIP systems for mineral exploration.

Metallogeny in a LIP framework context

A recent paper by Ernst et al. (in press) outlined the plumbing system of LIPs and the various forms of igneous units that form during continental LIP events. These magmatic components include flood basalts and associated different types of giant mafic dyke swarms, mafic sill provinces, lower crustal magmatic underplates, mafic-ultramafic (M–UM) intrusions, associated silicic magmatism (mainly related to the melting of lower crustal material as a result of heating by M-UM magmas), and associated carbonatites and kimberlites. This research outlined a plumbing system framework for plume-related LIPs that included all of these components, enabling the tracking of magma batches and their geochemical evolution, the interpretation of deep crustal LIP-related geophysical signatures, and more. In addition, this model has implications for mineral exploration and the use of the fivefold classification outlined above. Several examples of this are outlined below.

Magmatic sulfide mineralization is the best-known type of mineral deposit associated with LIP events and involves the transfer of chalcophile elements from deep in the mantle to the crust by high degree partial melts (e.g. Jowitt et al., 2014). The S-saturation of these magmas generates immiscible magmatic sulfides that can be concentrated to form economic Ni-Cu-PGE mineral deposits. Combining knowledge of these processes with the plumbing systems of LIPs can enable the tracking of chalcophile element variations that provide evidence of mineralizing processes, enabling improved identification of areas for targeted mineral exploration (e.g. Ernst and Jowitt, 2013, 2017). These areas include staging M–UM chambers, key locations for differentiation, crustal contamination, and the potential generation of magmatic sulfides, as well as linked intrusions where magma dynamics can cause the segregation of denser magmatic sulfides from the less dense transporting magma.

Other magma chambers within LIP systems can differentiate in situ or may be the site of magma mixing as new batches of M-UM magma are added to the chamber. Both of these processes can lead to S-saturation as exemplified by the LIP-related Skaergaard and Bushveld intrusions, respectively. The in situ differentiation of magmas within these chambers can also form other types of mineralization, such as gabbroic Fe-Ti-V mineralized intrusions that, if exposed by erosion, can represent viable exploration targets.

The upper sections of LIP plumbing systems can also be associated with mineralization, as exemplified by sills that intrude sedimentary basins and are often associated with hydrothermal vent complexes. These complexes record the interaction of sill magmas with volatile-rich sedimentary rocks, producing zones of brecciation that reach the surface from depths of up to 9 km and are linked with both magnetite mineralization as well as hydrocarbon potential (e.g. Ernst and Jowitt, 2013).

This lecture will outline the key relationships and links between LIP events, the formation of LIP-related mineral resources, and the identification of key metallogenic locations within LIP systems, all of which can be used to enhance mineral exploration strategies for a range of LIP-related and hosted mineral resources.

Conclusions

LIP events are genetically associated with the formation of a wide range of mineral deposits both during and after the events themselves. These mineral deposits are located within different areas of LIPs depending on the geological processes that generate individual classes of deposit. Combining this knowledge with a newly developed plumbing framework for LIP systems will enable more focused targeting for LIP-related mineral deposits.

Acknowledgements

REE partially supported from Mega-Grant 14.Y26.31.0012 of the government of the Russian Federation, and Canadian grant NSERC-CRDPJ 523131-17

References

1. Ernst R.E., Jowitt S.M., 2013. Large igneous provinces (LIPs) and metallogeny, in Colpron M., Bissig, T., Rusk, B.G., and Thompson, J.F.H., eds., Tectonics, metallogeny, and discovery: The North American Cordillera and similar accretionary settings: Society of Economic Geologists Special Publication, v. 17, p. 17-51.
2. Ernst, R.E., Jowitt, S.M., 2017. Multi-commodity, multiscale exploration targeting using the Large Igneous Province record. In: Wyche, S. and Witt, W.K. (eds.) TARGET 2017, Perth, Australia: Abstracts. Geological Survey of Western Australia, Record 2017/6, p. 41-44.
3. Ernst, R.E., Liikane, D.A., Jowitt S.M., Buchan, K.L., Blanchard J.A., 2019. A New Plumbing System Framework for Plume-Related Continental Large Igneous Provinces and Their Mafic-Ultramafic Intrusions. Journal of Volcanology and Geothermal Research, in press.
4. Jowitt, S.M., Ernst, R.E., 2013. Geochemical assessment of the metallogenic potential of Proterozoic LIPs of Canada. Lithos, 174: 291–307.
5. Jowitt, S.M., Williamson, M.C., Ernst, R.E., 2014. Geochemistry of the 130 to 80 Ma Canadian High Arctic large igneous province (HALIP) event and implications for Ni-Cu-PGE prospectivity. Economic Geology, 109: 281-307.

GEOCHRONOLOGY, GEOCHEMISTRY AND EXTENT OF THE 1998 MA MINTO-POVUNGNITUK LIP

Kastek N.[1], Ernst R. E.[1,2], Cousens B. L.[1]

[1]*Department of Earth Sciences, Carleton University, 1125 Colonel By Drive, Ottawa, ON K1S 5B6, Canada*
[2]*Faculty of Geology and Geography, Tomsk State University, 36 Lenin Ave, Tomsk 634050, Russia*

A recent U-Pb baddeleyite age of 1998 ± 6 Ma has been obtained for the main flood basalt sequence (Beauparlant Formation) of the Povungnituk Group of the Cape Smith belt, on the northern Superior craton, North America.

This age has regional significance because it matches the previously obtained 1998 ± 2 Ma age for the Watts Group (Purtuniq) ophiolite of the northern Cape Smith Belt and the 1998 ± 2 Ma U-Pb age of the Minto dykes intruding the Superior craton to the south.

Additional units can be linked to the dated units of the LIP. The Eskimo Formation (Belcher Islands) has been paleomagnetically linked to the Minto dykes and the lower lavas of the Roberts Lake Syncline (northeastern Superior craton) have been geochemically linked to the Povungnituk Group. Together these coeval units suggest widespread, short duration, large igneous province (LIP) magmatism that covered an area of >400,000 km^2 and has been termed the Minto-Povungnituk LIP (Figure 1).

Geochemical comparison between the units that erupted on, or have been transported onto, the northern margin of the Superior craton with the units within the craton to the south allows the Minto-Povungnituk LIP to be divided into two spatially separate geochemical domains with different mantle source characteristics. The northern domain, comprising the Povungnituk Group, Roberts Lake Syncline and Watts Group, shows mixing between a depleted mantle source and a more enriched mantle plume-sourced melt. The southern domain comprising the Minto dykes and the paleomagnetically linked Eskimo Formation shows signs of an even more enriched source, while these magmas also show the effect of crustal contamination.

Two distinct source mechanisms can be responsible for the observed geochemical differences between the two domains. First, a difference in lithospheric sources, where melting of different portions of Superior craton lithosphere caused the different melt signatures in the interior of the craton. In this case magmatism in the two domains is only related by having the same heat source (e.g., a mantle plume) interpreted to be located on the northwestern side of the northern Superior craton. Second, two distinct deep mantle sources that remained separated within the ascending plume. This is analogous to some current hotspots interpreted to sample both large low shear velocity provinces (LLSVPs) and adjacent ambient deep mantle. This latter interpretation would allow for the use of bilateral chemistry in LIPs as a potential tool for the recognition and mapping of the LLSVP boundaries throughout Earth's history.

References

1. Baragar,W.R.A., 2007. Geology, Sleeper Islands, Eastern Hudson Bay, Nunavut. Geological Survey of Canada, Map 2114A, scale 1 : 75 000.
2. Buchan, K.L., Mortensen, J.K., Card, K.D., Percival, J.A., 1998. Paleomagnetism and U–Pb geochronology of diabase dyke swarms of Minto block, Superior Province, Quebec, Canada. Canadian Journal of Earth Sciences 35, 1054–1069.
3. Chandler, F.W., 1984. Metallogenesis of an early Proterozoic foreland sequence, eastern Hudson Bay. Canada. Journal of the Geological Society London 141, 299–313.
4. Clark, T., Wares, R., 2006. Lithotectonic and metallogenic synthesis of the new Québec Orogen (Labrador Trough). MM 2005-01, Ministère des Ressources naturelles, de la Faune et des Parcs, Québec, 180 pp.
5. Maurice, C., David, J., O'Neil, J., Francis, D., 2009. Age and tectonic implications of Paleoproterozoic mafic dyke swarms for the origin of 2.2Ga enriched lithosphere beneath the Ungava Peninsula, Canada. Precambrian Research 174, 118–163.
6. St-Onge, M.R., Henderson, I., Baragar,W.R.A., 2004. Geology, Cape Smith Belt and adjacent domains, Ungava Peninsula, Quebec-Nunavut. Geological survey of Canada. Open File 4930 (scale 1:300 000).

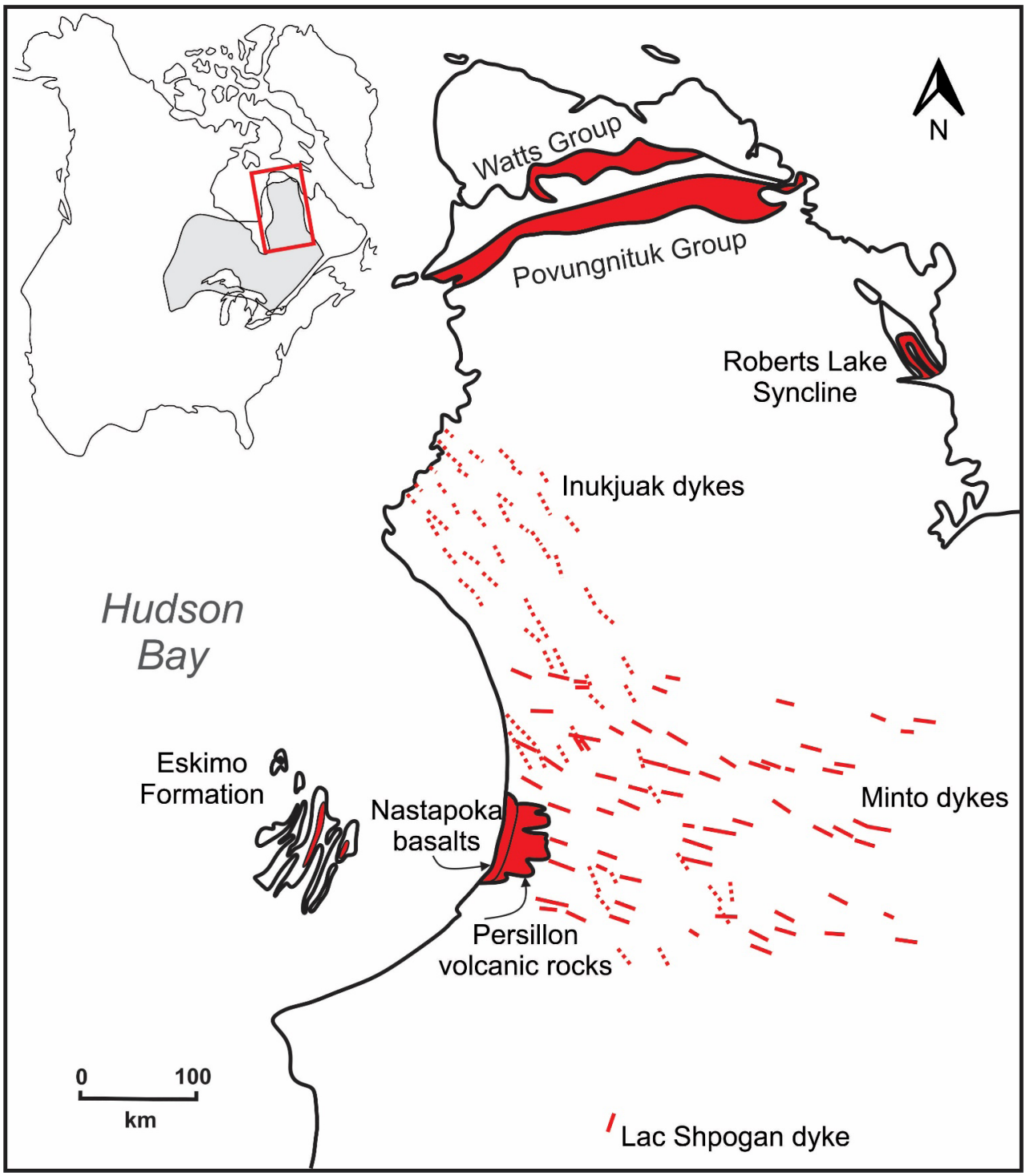


Figure 1. Map showing coeval magmatic units of the ca. 1998 Ma Minto-Povungnituk large igneous province. Inspired by Chandler (1984); Buchan et al. (1998); St. Onge et al. (2004); Clark and Wares (2006); Baragar (2007); Maurice et al. (2009).

DO TESSERA TERRAINS ON VENUS EXHIBIT EROSIONAL FEATURES?

Khawja S.[1], Ernst R. E.[1,2], Samson C.[1,3]

[1]*Department of Earth Sciences, Carleton University, Ottawa, Canada,*
[2] *Faculty of Geology and Geography, Tomsk State University, Tomsk, Russia,*
[3] *Department of Construction Engineering, École de Technologie Supérieure, Montréal, Canada*

Keywords: *Venus, Tesserae, Erosion, Climate Change*

Introduction

Tesserae, also known as complex ridge terrains, occupy approximately 8% of Venus' surface, forming continent-like units (crustal plateaus) embayed by adjacent volcanic plains (Bindschadler and Head, 1991). Tesserae consist of at least two sets of intersecting lineaments (e.g. ridges and grooves), and are a result of tectonic deformation of a precursor terrain (Basilevsky and Head, 1998). However, the nature of that precursor terrain, as well as the causes and mechanisms of deformation are still under debate (Hansen and Willis, 1996; Gilmore and Head, 2018). Recent models (e.g. Way et al., 2016) suggest Earth-like conditions on Venus prior to a major period of flood volcanism and associated hyper-global warming. A key test of this model is to investigate the tessera terrains in detail before the period of flood volcanism and search for evidence of erosion which would be indicative of pre-global warming conditions.

Erosion on Tesserae

There are three major reasons to expect erosional features in tessera terrains:

1. Climate models suggest that Venus could have had Earth-like habitable conditions until at least ca. 0.72 Ga, therefore the occurrence of water erosion would be expected before that time period (Way et al., 2016).
2. The tectonic complexity of tesserae (e.g., Hansen and Willis, 1996) would suggest deformation at depth followed by unroofing and exposure at the surface. This hypothesis would need to be evaluated by modeling the deformation of mafic and felsic units under a range of atmospheric pressure and temperature conditions.
3. Some present-day topographic variations observed in tesserae are potentially consistent with erosion (e.g. Ernst et al., 2019) although other causes should be considered.

The present research will concentrate on the third point by assessing the causes of observed topographic variations in tesserae. It will focus on the implications of erosion via water and/or ice. The possibility of wind erosion is also addressed.

Topographic Models

We consider three models to explain topographic variations in tesserae (Fig. 1). The first two models address whether the topography can be explained as primary topography, caused by folding or faulting, without any subsequent erosion. The third model require erosional mechanisms (Fig. 1d).

Methodology

All the SAR (synthetic aperture radar) images and topography data used in this research are from NASA's Magellan 1990-1994 mission. Topographic data have poor vertical and horizontal resolutions of 100 m and 50 km, respectively. Higher resolution stereo topographic maps were recently produced from combining Cycle 1 and 3 Magellan SAR data (Herrick et al., 2012) and have an improved horizontal resolution of 1-2 km and a vertical resolution of 50-100 m. However, even this slightly improved vertical resolution is not sufficient because the uncertainties are of comparable scale to the observed topographic variations.

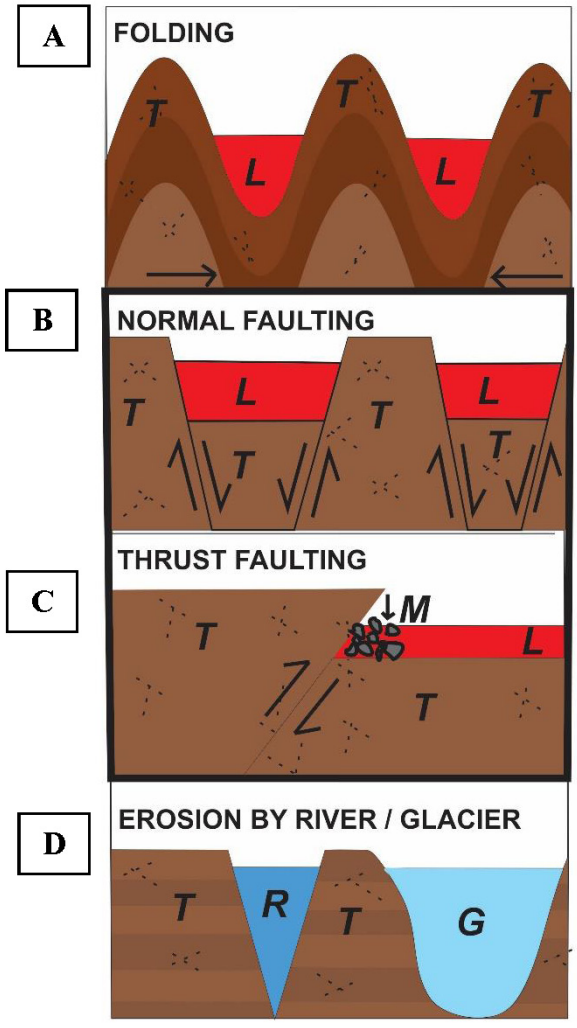


Figure 1: Schematic diagrams of three topographic models to explain topographic variations: folding (A), faulting (normal (B)/thrust (C)), and erosion by river/glacier (D). T = tessera, L = lava flooding, M = mass wasting, R = river erosion, G = glacial erosion.

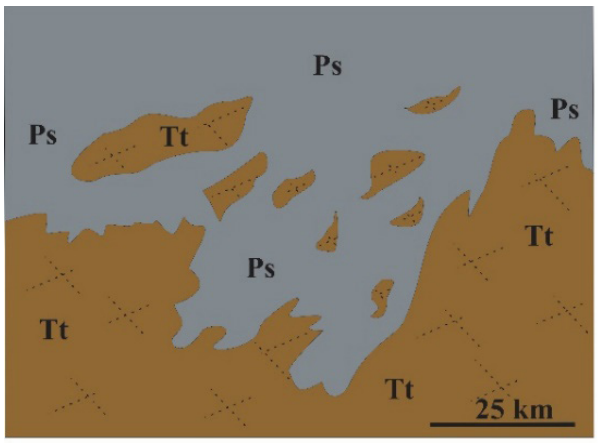


Figure 2: Schematic diagram of tessera terrain (Tt) partially flooded by lava flows of plains unit (Ps).

To circumvent the problem, we are using observations of tesserae that are partially flooded by lava flows (Fig. 2). We assume that lavas have flooded these areas to approximately the same level, and that therefore the lava flooding represent a relatively precise horizontal datum (analogous to sea level). Higher elevation areas are located above this datum.

Results

We examine two Magellan images of tesserae (Figs. 3, 4) that are partially flooded and consider the topography against the three end-member models (Fig. 1).

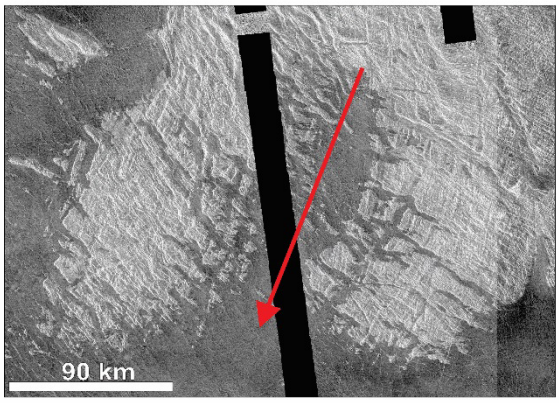


Figure 3: Magellan SAR image (48.2E, 4.4S) from the southern part of Salus Tessera (light grey), showing a re-entrant (red arrow) that has been flooded by younger plains lavas (dark grey).

Figure 3 shows flooding in a re-entrant. The only alternative to an erosional origin for this structure is a primary syncline (Ernst et al., 2019). However, in such a folding model the adjacent anticlinal portions should exhibit no structures in the absence of erosion (cf. Fig. 1a) which is at odds with observations (Fig. 3). Figure 4 shows an irregular pattern of tesserae high ground (above the lava flooding datum). In this case, the linear structures on the tesserae tend to be oblique to the trend of the flooding.

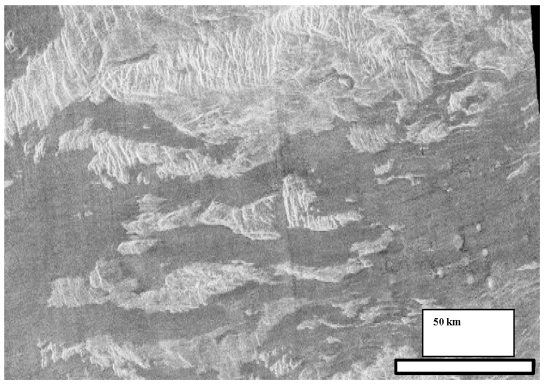


Figure 4: Magellan SAR image (61.7E, 6.5S) showing segments of tesserae (light grey) surrounded by plains unit (dark grey).

Discussion

In the areas displayed in Figures 3 and 4, there is weak evidence for the pattern of elevated topography being related to anticlines or domes, or to thrust fault uplift or normal faulting. Therefore, erosion is a viable alternative for explaining the topography in these two tesserae examples.

Wind erosion on Earth produces aeolian features such as terrestrial dunes, yardangs, and similar features are observed on Venus (Greeley et al., 1997). However, wind erosion will not cause tens to hundreds of metres of the topographic variations that we observe in tesserae (Khawja et al., 2019).

If primary folding and faulting, and wind erosion are ruled out, then the cause of the topographic variations in tesserae could be liquid water or ice erosion. We are currently doing a more systematic investigation of tesserae to identify additional examples that could be consistent with water or ice erosion.

References

1. Basilevsky A.T. & Head J.W. (1998) JGR, 103.E4, 8531-8544.
2. Bindschadler D.L. & Head J.W. (1991) JGR, 96.B4, 5889-5907. Ernst et al. (2019) LPSC 50, #238.
3. Gilmore M.S. & Head J.W. (2018) PSS, 154, 5-20. Greeley et al. (1997) JGR, 97(E8), 13319-13345.
4. Hansen V.L. & Willis J.A. (1996) Icarus, 123.2, 296-312. Herrick et al. (2012) TAG, 93(12), 125-126.
5. Khawja S. et al. (2019) LPSC 50 #1967. Way et al. (2018) GRL, 43, 8376–8383.

MESOPROTEROZOIC MAGMATISM OF THE WESTERN SLOPE OF THE SOUTHERN URALS

Khotylev A. O.

Lomonosov Moscow State University, Moscow, Russia

Keywords: *Riphean, Bashkirian meganticlinorium, Southern Urals, dyke swarms, gabbro*

Introduction

One of the largest stages of rifting and related magmatic activation in Late Proterozoic history of development of western slope of the Southern Urals is Middle Riphean, or "Mashak" stage. On Lower-Middle Riphean boundary under conditions of tension, which probably accompanied the breakup of Columbia (Nuna) supercontinent, there was formation of Berdyaush massif of rapakivi granites (1388-1368 Ma, [Ronkin et al., 2016]), Kusinsky-Kopansky complex of metagabbro, metapyroxenites and granites (1379-1353 Ma), and a range of smaller massifs. The dyke swarms of Kurgass dolerite complexes and Bulandikhinsky picrite complexes were intruded. Contrast volcanic series of Mashak and Kuvash suites were formed simultaneously with them (1381-1380 Ma, Puchkov et. al., 2014). Occurrence of Mashak magmatism is known also on the inner part of East-European craton – there are dolerite sills (1391-1382 Ma, [Puchkov et. al., 2013]).

This work is devoted to the geochemical features of the Kurgass dike complex of gabbro and dolerite. Originally Kurgass complex was distinguished in 1948 by V.A. Ivanova with colleagues in the most southern part of Bashkirian meganticlinorium within Kurgass anticline, where it is represented by multi-tiered dolerite sills in Yushin suite (Lower Riphean). Although originally the complex was distinguished on the far south of the Bashkirian meganticlinorium, dykes and sills of Early to Middle Riphean age are widespread throughout all western slope of the Southern Urals and also refer to Kurgass complex.

Results

The rocks of the Kurgass complex are characterized by 46-52% SiO_2, 0.5-1.4% K_2O, 1-2.8% Na_2O, and total alkalinity up to 4.5% with a slight predominance of Na_2O over K_2O - which generally corresponds to gabbro of normal and slightly increased alkalinity. The complex is characterized by a moderately high and non-uniform content of titanium oxide: for most of the included bodies it is 1.9-2.5%, but for individual differences it is only 0.5-0.7% TiO_2. The bodies of low-Ti gabbroids do not currently have isotopic datings, but they have very similar petrographic characteristics and geological position, which suggests that they are of Middle Riphean age. Also for the rocks of the Kurgass complex, as a whole, a higher content of MgO is distinguishing: 6-8% for the majority of representatives, and up to 18% in certain differences. In the rocks of similar gabbro complexes this value is: Poval'nensky (upper part of Middle Riphean) 4-7%; Suim (Early Riphean) 5-7%; Inzer (Upper Riphean) 3-8% of MgO [Khotylev et al., 2017]. The contents of MgO and TiO_2 are connected by a fairly clear negative dependence, but it is not typical for rift volcanic serials (for example, East African Rift System. The contents of other petrogenic oxides are within the field of normal gabbro values: 9-17% Al_2O_3, 9-10% FeOT, 0.1-0.2% P_2O_5. The CaO content is low - 2.5-11% - apparently, due to increased magnesia.

According to the pattern of the distribution of rare-earth and trace elements, the rocks of the complex occupy an intermediate position between E-MORB and OIB. The normalized values for HREEs are even less than in MORB and OIB, which may indicate melting at considerable depths in the garnet stability zone, since it collects these components. A negative Ta-Nb anomaly, which is characteristic of the vast majority of gabbroids of the Bashkirian meganticlinorium, is invariably present [Nosova et al., 2012; Kovalev, 2008], but the depletion of Zr and Hf is extremely weak. Enrichment with lead and all large-ion elements in the part of the samples is most likely due to bringing from host rocks - according to the author's data, the contents of these components, even within the same body without petrological zoning, can change by almost an order. The fluctuations in strontium content are usually regulated by the amount of plagioclase. Sharp depletion of uranium and enrichment of barium of a range of samples is, most likely, the result of metasomatism. The division into two groups - high-titanium and high-magnesian - is also expressed in the distribution of the trace elements: high-titanium differences are more enriched by the entire spectrum of trace elements and practically do not have a positive lead anomaly. Low-titanium, magnesium-rich differences are relatively depleted in trace elements, more often have a positive lead anomaly, are more depleted in Ta, Nb, Zr, Hf than high-titanium ones.

An important trend is clearly indicated for the chemical composition of rock. Northern bodies of kurgass complex (which located at Taratash block and its framing) are low-magnesian (2-5% MgO) and high-Si (more then 55-56% SiO_2). They change by dykes with higher contents of MgO (more than 15% MgO) and with low SiO_2 concentration (42-50%) to the south, in Bakal-Satka. Also, the value of the ratio La / Yb decreases from north to south: from 20-30 on the Taratash salient to 5-8 in the Bakal region.

Today, there are 5 precision isotopic datings for the dykes of the Kurgass complex, obtained by modern methods: 1385 ± 1.4 (U-Pb, baddeleyite, [Ernst et al, 2006]), 1360 ± 9 ($^{40}Ar/^{39}Ar$, biotite, [Ernst et al, 2008]), 1318 ± 10 ($^{40}Ar/^{39}Ar$, [Khotylev, 2018]) and 1349 ± 11 (U-Pb, zircon, [Khotylev, 2018]) 1365.6±6.6 Ma (U-Pb, zircon, our new dates) – i.e., the formation of the complex occurred at the end of the Early and the beginning of the Middle Riphean. Therefore, the duration of the entire riftogenic process (if to assume that the formation of the Kurgass complex on its entire length was connected with the Mashak rifting) is no less than 65 million years, which is comparable to the duration of the entire Cenozoic.

Conclusions

We think, that such a change in the composition of Kurgass complex rocks is associated with a decrease in the degree of melt differentiation from south to north. Long-term differentiation in the north led to the fact that the main phases crystallized in the intermediate magma chambers, and the silica accumulated in the melt. And to the south, the melts were rising with a smaller number of intermediate stops and did not differentiate. As a result, in the southern parts of the rock closer to the basalts and picrites in composition.

Different degrees of differentiation associated with the disclosure of the rift system. In the northern part there was a termination of the rift (with large crust) and because only dikes of the Kurghass complex were formed there. And in the south in the central part of the rift (with thin crust), contrasting volcanic rocks of the Mashak and Kuvash Formations of the Middle Riphean were formed. Thus, the Mashak rift system was wide in the south and narrow in the north. As for the age of the complex, judging by the isotopic data, it was formed simultaneously with the volcanics of the Mashak province. All these displays of magmatism are associated with the disintegration of the Mesoproterozoic supercontinent Columbia [Rogers and Santosh, 2002] or Nuna [Evans and Mitchell, 2011].

Acknowledgements

The studies were carried out with the support of the RFBR grant № 17-05-01121.

References

1. Ковалев С.Г. Позднедокембрийский рифтогенез в истории развития западного склона Южного Урала // Геотектоника. 2008. № 2. С. 68–79.
2. Носова А.А., Сазонова Л.В., Каргин А.В. и др. Мезопротерозойская внутриплитная магматическая провинция Западного Урала: основные петрогенетические типы пород и их происхождение // Петрология. 2012. Т. 20, № 4. С. 392–428.
3. Пучков В.Н. Дайковые рои Урала и ассоциирующие с ними магматические комплексы // Геотектоника. 2012. № 1. С. 42–52.
4. Пучков В.Н. Плюмы в геологической истории Урала // Бюл. МОИП. Отд. геол. 2013. Т. 88, № 4. С. 64–73.
5. Ронкин Ю.Л., Тихомирова М., Маслов А.В. 1380 млн лет LIP Южного Урала: прецизионные U-Pb-ID-TIMS-ограничения // Доклады АН. 2016. Т. 468. № 5. С. 674–769.
6. Хотылев А.О. Эволюция позднедокембрийского магматизма северной части Башкирского мегантиклинория: автореф. дисс. … канд. геол.-мин. наук: 25.00.01 – М., 2018. 24 с.
7. Хотылев А.О., Тевелев Ал.В., Мосейчук В.М., Бычков А.Ю., Девишева Н.Б. Суимский и кургасский рифейские дайковые комплексы: состав и петрологические особенности (Южный Урал, Башкирский мегантиклинорий) // Бюл. МОИП. Отд. геол. 2017. Т. 92, № 5. С. 3-14
8. Эрнст Р.Э., Хейнс Дж.А., Пучков В.Н. и др. Рекогносцировочное Ar-Ar датирование протерозойских долеритовых даек и силлов в Сибири и на Южном Урале: идентификация новых крупных магматических провинций и использование при реконструкции суперконтинента Нуна (Коламбия) // Мат-лы XLI Тектонического совещания. /отв. ред. Ю.В. Карякин/ Т. 2. М.: ГЕОС, 2008. С. 492–496.
9. Ernst R.E., Pease V., Puchkov V.N., Kozlov V.I., Sergeeva N.D., Hamilton M. Geochemical characterization of Precambrian magmatic suites of the Southeastern margin of the East European Craton, Southern Urals, Russia // Геологический сб. № 5. /под ред. В.Н. Пучкова, Р.Ф. Абдрахманова, И.Б. Серавкина / ИГ УрО РАН. 2006 № 5. С. 1–45.
10. Evans D., Mitchell R. Assembly and breakup of the core of Paleoproterozoic– Mesoproterozoic supercontinent Nuna // Geology. 2011. http://dx.doi.org/10.1130/G31654.1.
11. Rogers J.J.W., Santosh M.. Configuration of Columbia, a Mesoproterozoic Supercontinent // Gondwana Res. 2002. V.5. P. 5–22.

EVOLUTION OF MANTLE MAGMATISM IN LATE PALEOZOIC IN EASTERN KAZAKHSTAN: THE EVIDENCE OF TARIM LIP APPEARANCE

Khromykh S. V.[1,2], Izokh A. E.[1,2], Kotler P. D.[1,2], Semenova D. V.[1]

[1]Institute of Geology and Mineralogy SB RAS, Novosibirsk, Russia
[2]Novosibirsk State University, Novosibirsk, Russia

Keywords: *Central Asia, Eastern Kazakhstan, mafic magmatism, Tarim LIP …*

Introduction

The territory of Eastern Kazakhstan is a part of Altai collision system that was formed in Late Paleozoic during interaction between Siberian and Kazakhstan continents. These processes took place during the general closure of the Paleo-Asian Ocean and the formation of the Central Asian Orogenic Belt (Windley et al., 2007; Xiao et al., 2010). In Altai collision system the accretion-collision stage began at the and of Early Carboniferous (330-325 Ma) and finished in Early Permian (280 Ma). We performed geochemical and geochronological studies of all accretion-collision mafic-ultramafic associations of East Kazakhstan (Khromykh et al., 2013, 2018, 2019). It allowed us to ascertain the evolution of mantle sources, and to determine the indicators of the appearance of the Tarim large eruptive province in this territory..

Results

Comparison of geochemical compositions of mafic-ultramafic associations shows that from early to late mafic rocks get rich with titanium, alkalis and incoherent elements (K_2O, P_2O_5, REE, Zr, Hf, Nb, Ta). The contents of alumina and calcium in early associations are markedly higher than in later ones. MgO contents do not directly correlate with age, and most likely reflect the degree of melting of the mantle substrates or the degree of differentiation of primary magmas. Different types of mantle sources differing in the contents of Ti, K, P, REE and HFSE may be distinguish from a comparison of the MgO content with other indicator components.

It is possible to distinguish three stages of the mantle magmatism in the evolution of the Altai accretion-collision system based on geochronological data.

1st stage, the Early Carboniferous, ~ 330 Ma. Mafic magmatism was associated with subduction under the active margin of the Kazakhstan continent. A depleted mantle melting in the presence of a significant amount of hydrous fluid was the source of mafic magmas. This magmatism ceased with the cessation of subduction and the closure of the ocean basin.

2nd stage, the middle of Late Carboniferous, 317-311 Ma. Manifestations of mafic magmatism indicate the permeability of the lithosphere: first along large shear fault systems (gabbro massifs in Irtysh Shear Zone (317-313 Ma) and dike belts of NE strike in Zharma zone (315 Ma). The basalt and andesite effusions in local extensions such as pull-apart (Daubai volcanic basin and other) was second (311 Ma). This indicates the collapse of the orogenic structure, and deeper (and less depleted) mantle sources underwent partial melting during this stage.

3rd stage, the Early Permian, 297-267 Ma. It s the post-orogenic stage that characterized with synchronous scaled granite magmatism. Early Permian mafic complexes are significantly enriched with incoherent components, which indicates that a non-depleted mantle source was involved in partial melting. Early Permian magmatism manifested by impulses. The earlier impulse (297-293 Ma): small amounts of enriched sub-alkaline gabbros and basalts, which indicates low degrees of melting. Following this, the formation of complex gabbro-granite intrusions was noted, which indicates the beginning of the active mantle-crust interaction. At this time, mantle magmas heat crust sedimentary-metamorphic substrates, causing the appearance of granites. The largest volume of granitoids in Eastern Kazakhstan corresponds precisely to 290-285 Ma. The final impulse of mantle magmatism began in ~ 280 million years ago. The most primitive mantle melts (MgO, on average, 14.5 wt.%) appeared, as a result of the greatest degree of melting of the non-depleted mantle. The latest impulse of mantle magmatism was the dikes of dolerite and lamprophyres of the Mirolyubovka complex. They appeared at the level of the middle-upper crust after cooling, solidification and cracking of the lithosphere.Table. Text, text, text … Text, text, text …

Conclusions

The analysis of geochemical and geochronological data allows us to determine the geodynamic evolution of the region according to the following scheme: Accretion → Collision → Collapse of orogen → Large Igneous Province at post-orogenic settings. The formation of the latter corresponds to the activity of the Tarim mantle plume (Ernst, 2014; Yarmolyuk et al., 2014; Xu et al., 2014). The sequence of development of mafic and granitoid magmatism as a whole corresponds to the process of interaction of the mantle plume with the lithosphere (Dobretsov et al., 2010).

Acknowledgements

This study was conducted according to the state assignment of IGM SB RAS. It was also supported by the Ministry of Science and Higher Education of the Russian Federation (Projects no. 5.1688.2017/4.6 and 14.Y26.31.0018) and the Russian Foundation for Basic Research (Project no. 17-05-00825).

References

1. Dobretsov N.L., Borisenko A.S., Izokh A.E., Zhmodik S.M. (2010) A thermochemical model of Eurasian Permo-Triassic mantle plumes as a basis for prediction and exploration for Cu-Ni-PGE and rare-metal ore deposits. Russian Geology and Geophysics 51(9): 903–924
2. Ernst R.E. (2014) Large Igneous Provinces. Cambridge University Press 653 p.
3. Khromykh S.V., Kotler P.D., Izokh A.E., Kruk N.N. (2019) A review of Early Permian (300–270 Ma) magmatism in Eastern Kazakhstan and implications for plate tectonics and plume interplay. Geodynamics & Tectonophysics 10(1): 79-99
4. Khromykh S.V., Tsygankov A.A., Burmakina G.N., Kotler P.D., Sokolova E.N (2018) Mantle-crust interaction in petrogenesis of gabbro-granite association in Preobrazhenka intrusion, Eastern Kazakhstan. Petrology 26(4): 368–388
5. Khromykh S.V., Vladimirov A.G., Izokh A.E., Travin A.V., Prokop'ev I.R., Azimbaev E., Lobanov S.S. (2013) Petrology and geochemistry of gabbro and picrites from the Altai collisional system of Hercynides: Evidence for the activity of the Tarim plume. Russian Geology and Geophysics 54(10): 1288-1304
6. Windley B.F., Alexeiev D., Xiao W., Kröner A., Badarch G. (2007) Tectonic models for accretion of the Central Asian Orogenic Belt. Journal of the Geological Society, London 164: 31-47
7. Xiao W.J., Huang B., Han Ch., Sun Sh., Li J. (2010) A review of the western part of the Altaids: A key to understanding the architecture of accretionary orogens. Gondwana Research 18(2-3): 253-273
8. Xu Y-G., Wei X., Luo Z-Y., Liu H-Q., Cao J. (2014) The Early Permian Tarim Large Igneous Province: Main characteristics and a plume incubation model. Lithos 204: 20-35
9. Yarmolyuk V.V., Kuzmin M.I., Ernst R.E. 2014. Intraplate geodynamics and magmatism in the evolution of the Central Asian Orogenic Belt. Journal of Asian Earth Sciences 93: 158-179

LATE PALEOZOIC WESTERN TRANSBAIKALIAN GRANITOID PROVINCE (ANGARO-VITIM BATHOLITE): FORMATION STAGES AND GEODYNAMIC ENVIRONMENT

Khubanov V. B.[1,2], Tsygankov A. A.[1,2], Burmakina G. N.[1]

[1]*Geologic Institute SB RAS, Ulan-Ude, Russia*
[2]*Buryat State University, Ulan-Ude, Russia*

Keywords: *SLIP, granitoids, Western Transbaikalian, U-Pb, LA-ICP-MS*

Introduction

The Western Transbaikalian granitoid province (Angaro-Vitim batholite, AVB) with a total area of more than 200 thousand km^2 hosts hundreds or thousands of granitoid plutons (Salop, 1967; Litvinovsky et al., 1993; Yarmoluk et al., 1997). AVB is comparable to the Silicic Large Igneous Province (SLIP) (Bryan, 2007; Bryan, Ernst, 2008) by magnitude of the manifestation of magmatism. Five intrusive suites composed by different geochemical types of granitoids were emplaced throughout the Western Transbaikalian region. In order of formation it is: 1) the Barguzin suite include calc-alkaline auto- and allochthonous biotite granites (330-280 Ma); 2) the Chivyrkui suite - high-potassium quartz monzonites, quartz syenites and gabbroids (305-280 Ma); 3) the Zaza suite comprising transitional from calc-alkaline to alkaline granite and quartz syenite (305-280 Ma); 4) the shoshonitic Low Selenga suite made up of monzonite, syenite and alkali rich microgabbro (285-278 Ma); 5) the Early Kunalei suite of alkaline (alkali feldspar) and peralkaline syenite and granite (281-275 Ma) (Litvinovsky et al., 2011; Tsygankov et al., 2017). More than two-thirds of the province is represented by calc-alkaline granites of the Barguzin suite.

The geodynamic environment of Late Paleozoic magmatism in western Transbaikalia is a matter of long-lasting and hot discussions, which are mostly centered around the following models: a plume model, a model of an active continental margin, a postcollisional model, and a model of delamination of the crust of a collisional orogeny (review in Tsygankov et al., 2017). The diversity of views is due to the fact that there is no complete clarity in understanding the total duration and chronology of the formation of different types of granitoids.

This paper presents the results of geochronological studies of magmatic zircons from the granites of the Barguzin suite and detrital zircons from modern sediments Angarakan river.

Materials and Methods

The Angarakan river basin in the Northern Muya Range in the northern part of Western Transbaikalia is one of the territories composed mainly of calc-alkaline granites of the Barguzin suite. In this area, among the calc-alkaline allochthonous and autochthonous granites, there are rare occurrences of only Precambrian metamorphosed rocks, which form the roof pendants for granite massifs. Magamatic zircons were derived from granites and granosyenites of Burgusin suite from the upper and average reaches of the Angarakan river. Detrital zircons were derived from the gray heavy concentrate from river medium-grained arkose sand of the Middle Angarakan region.

U-Pb isotopic dating for zircons was carried out using Laser Ablation Inductively Coupled Plasma Mass Spectrometry (LA-ICP-MS) (Khubanov et al., 2016; Buyantuev et al., 2017).

Results, Discussion and Conclusion

On the example of dating of magmatic and detrital zircons from the Angarakan river area revealed two stages of the formation of granitoids of the Barguzin suite: 320–305 Ma and 300–280 Ma, with the total duration of the formation of the batholith at least 40–50 Ma. It seems that extensive granite formation took place in consequence of the plume-lithospheric interaction. Moreover, at the early (first) stage, this interaction took place against the background of tectonic compression of the lithosphere of Western Transbaikalia. At this time, the calc-alkaline Barguzin granites, derivatives of continental crust, were formed predominantly. The absence and/or rarity of Late Carbon mafic rocks is explained by the difficulty of penetration of mantle and hybrid lower crust melts in the granitogenesis overlying area of in the middle part of the thickened continental lithosphere. Impermeability middle crust to mafic magmas is due to its compression conditions, relatively lower density and ductility due to heating during shear-thrust deformations, accumulation of radiogenic heat, and heat input from lower-lying magmatic mafic melts. At the last (second) stage the Barguzin granites, mixed mantle-crustal granitoids (Chivyrkui, Zaza, Low Selenga, Early Kunalei suites), gabbroids and basites were developed, which was due to the change of tectonic compression to tension and the possibility of intrusion of mantle and lower crustal hybrid magmas to higher middle and upper crust.

Acknowledgements

The U-Pb zircon dating was performed in the Center for "Analytical center of mineralogical, geochemical and isotope Studies" at the Geological Institute, SB RAS Ulan-Ude, Russia.

This work was conducted as a government task project No IX.129.1.2 (AAAA-A16-116122110027-2) and financially supported by Grant 17-05-00275 from the Russian Scientific Foundation (principal investigator A.A. Tsugankov) and project II.1.39 (The complex program of basic scientific research of the SB RAS).

References

1. Bryan S.E. (2007) Silicic Large Igneous Provinces. Episodes 30(1):20-31.
2. Bryan S.E., Ernst R.E. (2008) Revised definition of Large Igneous Provinces (LIPs). Earth. Sci. Rev. 86:175-202.
3. Buyantuev MD, Khubanov VB, Vrublevskaya TT. (2017) UPb LAICPMS dating of zircons from subvolcanics of the bimodal dyke series of the Western Transbaikalia: Technique, and evidence of the Late Paleozoic extension of the crust. Geodynamics & Tectonophysics 8:369-384.

4. Khubanov VB, Buyantuev MD, Tsygankov AA. (2016) U–Pb dating of zircons from PZ3 –MZ igneous complexes of Transbaikalia by sector-field mass spectrometry with laser sampling: technique and comparison with SHRIMP. Russian Geology and Geophysics 57:190-205.
5. Litvinovsky B.A., Zanvilevich A.N., Alakshin A.M., Podladchikov Yu.Yu. (1993) The Angara–Vitim Batholith, the Largest Granitoid Pluton. Izdatelstvo OIGGM SO RAN, Novosibirsk:143 (in Russian).
6. Litvinovsky BA, Tsygankov AA, Jahn BM, Katzir Y, Be'eri-Shlevin Y. (2011) Origin and evolution of overlapping calc-alkaline and alkaline magmas: The Late Palaeozoic post-collisional igneous province of Transbaikalia (Russia). Lithos 125:845-874
7. Salop L.I. (1967) Geologiya Baikal'skoi gornoi oblasti (Geology of the Baikal Mountain Area). Moscow: Nedra. V 2:700 p. (in Russian).
8. Tsygankov AA, Burmakina GN, Khubanov VB, Buyantuev MD. (2017) Geodynamics of Late Paleozoic Batholith-Forming Processes in Western Transbaikalia. Petrology 25:396-418.
9. Yarmolyuk V.V., Budnikov S.V., Kovalenko V.I., Antipin V.S., Goreglyad A.V., Sal'nikova E.B., Kotov A.B., Kozakov I.A., Kovach V.P., Yakovleva Z.S., Berezhnaya N.G. (1997) Geochronology and geodynamic setting of the Angara-Vitim batholith. Petrology 5(5):401-414.

AN IDENTITY CRISIS SOLVED BY U-PB DATING: THE CASE OF THE CEDERBERG DYKE SWARM, WESTERN AND NORTHERN CAPES, SOUTH AFRICA

Kingsbury C. G.[1], Altermann W. [2], Ernst R. E.[3,4], Söderlund U. [5]

[1]*University of Pretoria, Pretoria, South Africa*
[2]*University of Johannesburg, Johannesburg, South Africa*
[3]*Carleton University, Ottawa, Canada*
[4]*Tomsk State University, Tomsk, Russia*
[5]*University of Lund, Lund, Sweden*

Keywords: *large igneous province, U-Pb baddeleyite, Karoo-Ferrar, Parana-Etendeka.*

Introduction

The geologic evolution of South Africa during the Mesozoic was heavily imprinted with dyke swarms and sill networks representing the plumbing systems of the 183 Ma Karoo-Ferrar Large Igneous Province ("Karoo LIP") and the c. 50 Myr younger Parana-Etendeka LIP (134 Ma). These LIPs are thought to be the products of mantle plume heads that were, at the time of their formation, under present-day extreme NE South Africa (Karoo) and the central Namibian coast (Parana-Etendeka). Each of these two magmatic provinces are associated in time with the breakup of the supercontinent Pangaea (White and McKenzie, 1989).

The Cederberg dyke swarm predominantly consists of two parallel, NW-striking mafic dykes in western South Africa that are separated by ~50 km (Figs. 1 & 2). The NW-trend of these dykes extends towards the plume centre of the 134 Ma Parana-Etendeka LIP and therefore could represent the plumbing system of the Parana-Etendeka LIP (Fig. 2). However, the eastern extent of the Cederberg dykes extends into the Karoo Basin, thereby clouding certainty over their origin; they could alternatively represent a western extent of the 183 Ma Karoo LIP in the Namaqualand and Cederberg region. The purpose of this study is to test our hypothesis that the Cederberg dykes represent the plumbing system of the 134 Ma Parana-Etendeka LIP and to do so by applying high-precision U-Pb age determinations on baddeleyite.

Results

Sample 18CK003 was collected from a dolerite dyke that measures ~90 m in width and strikes 305° (towards the NW). The dyke is exposed as a roadcut along R363, 26 km southwest from Nuwerus in the Western Cape (coordinates 31.356°S, 18.235°E; Figure 1). Baddeleyite extraction of sample 18CK003 was successful. U-Pb TIMS dating gave a $^{206}Pb/^{238}U$ age of 131.4±4.5 Ma MSWD of 0.1; Fig. 3), based on two concordant fractions.

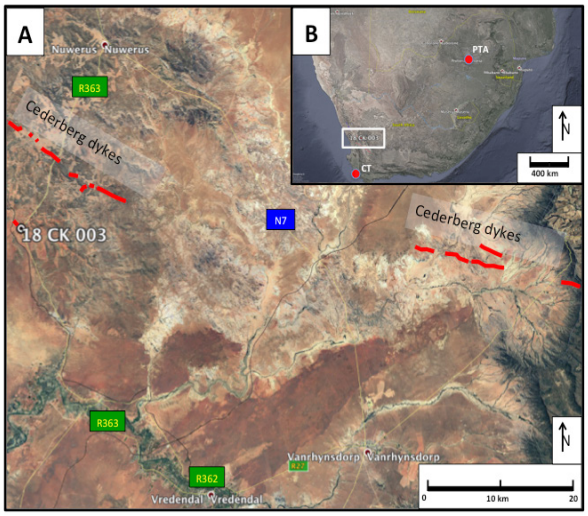


Figure 1. Google Earth® map showing (A) the location of where sample 18CK003 was collected. Thin red, NW-trending lines represent mapped dykes of the Cederberg dyke swarm in the vicinity of the sample collection site. (B) Inset map showing the location of sample 18CK003 (white box) relative to South Africa. Key to abbreviations: CT = Cape Town and PTA = Pretoria.

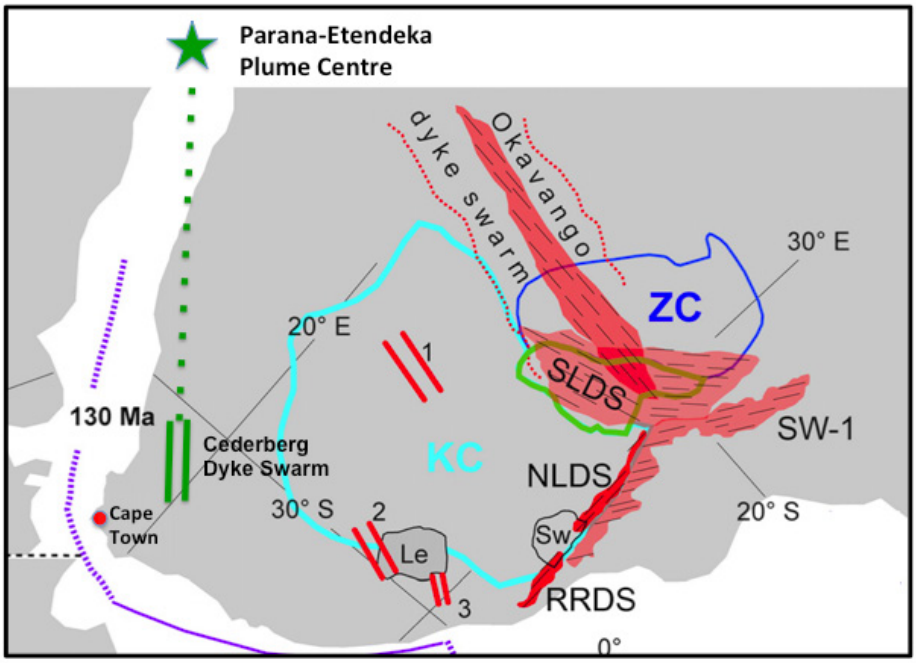


Figure 2: Distribution of dykes (in red) of the 183 Karoo LIP (after Hastie et al. 2014) and the Cederberg dyke swarm (in green after Figs. 7 and 8 in Ernst and Buchan 1997). Note that based on their trend, the Cederberg dyke swarm is proposed to be linked to the 134 Ma Parana-Etendeka LIP. Key to select abbreviations and designations: NLDS = Northern Lebombo dyke swarm; RRDS = Rooi Rand dyke swarm; SLDS = Save-Limpopo dyke swarm; KC = Kaapvaal Craton; ZC = Zimbabwe Craton; 1 = Southern Botswana dyke swarm; 2 = Southern Lesotho dyke swarm.

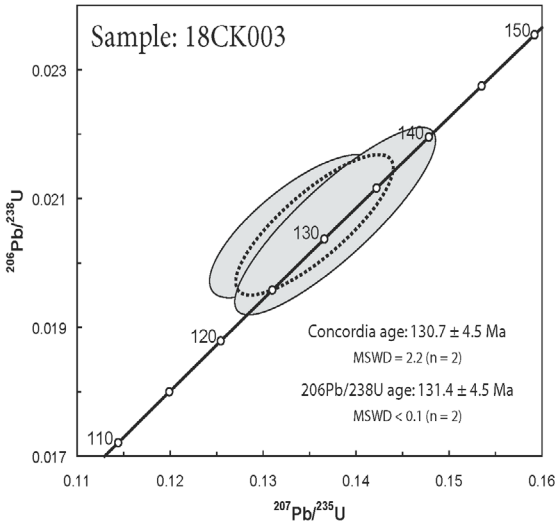


Figure 3: U-Pb concordia diagram of Sample 18CK003

Acknowledgements

The first author acknowledges the financial support of the DST-NRF Centre of Excellence for Integrated Mineral and Energy Resource Analyses (DST-NRF CIMERA) through a postdoctoral research grant. Opinions expressed and conclusions arrived at, are those of the author and are not necessarily to be attributed to the CoE. Additional funding for this study is provided through a NSERC-CRD research grant to R. Ernst # CRDPJ 523131-17.

References

1. Almeida, V. V, V.A. Janasi, L.M. Heaman, B.J. Shaulis, M.H. Hollanda & P.R. Renne. 2017. Contemporaneous alkaline and tholeiitic magmatism in the Ponta Grossa Arch, Paraná-Etendeka Magmatic Province: Constraints from U–Pb zircon/baddeleyite and 40Ar/ 39Ar phlogopite dating of the José Fernandes Gabbro and mafic dykes. J. Volcanol. Geotherm. Res.
2. Ernst, R.E. & K.L. Buchan. 1997. Giant radiating dyke swarms: their use in identifying pre-Mesozoic large igneous provinces and mantle plumes. AGU Geophysical Monograph, 100: 297–333
3. Florisbal, L.M., L.M. Heaman, V.A. Janasi & M.F. Bitencourt. 2014. Tectonic significance of the Florianópolis Dyke Swarm, Paraná- Etendeka Magmatic Province: A reappraisal based on precise U – Pb dating. J. Volcanol. Geotherm. Res. 289: 140–150.
4. Hastie, W.W., M.K. Watkeys & C. Aubourg. 2014. Magma flow in dyke swarms of the Karoo LIP: Implications for the mantle plume hypothesis. Gondwana Res. 25: 736–755.
5. Janasi, V.A., V.A. Freitas & L.H. Heaman. 2011. The onset of flood basalt volcanism, Northern Paraná Basin, Brazil: A precise U – Pb baddeleyite/zircon age for a Chapecó-type dacite. Earth Planet. Sci. Lett. 302: 147–153.
6. Pinto, V.M., L.A. Hartmann, J.O.S. Santos, N.J. McNaughton & W. Wildner. 2011. Zircon U – Pb geochronology from the Paraná bimodal volcanic province support a brief eruptive cycle at ~135 Ma. Chem. Geol. 281: 93–102.
7. White, R. & D. McKenzie. 1989. Magmatism at Rift Zones : The Generation of Volcanic Continental Margins. J. Geophys. Res. 94: 7685–7729.

YOKO-DOVYREN MASSIF, IRKUTSK LIP: GENESIS OF CHROMITITES

Kislov E. V. [1, 2], Kamenetsky V. S. [3, 4], Vanteev V. V. [1, 2]

[1] *Geological institute, Siberian Branch, Russian Science Academy, Ulan-Ude, Russia, evg-kislov@ya.ru*
[2] *Buryat state university, Ulan-Ude, Russia*
[3] *University of Tasmania, Hobart, Australia, dima.kamenetsky@utas.edu.au*
[4] *Institute of Experimental Mineralogy, RAS, Chernogolovka, Russia*

Keywords: *layered intrusion, chromitite, metasomatic paragenesis, skarns*

Introduction

Yoko-Dovyren dunite-troctolite-gabbro intrusion is located at 60 km to the northeast of the North bank of the Lake Baikal (North Baikal region, Russia). The massif represents a lens like body of 26×3.5 km in size. It is a part of the Synnyr-Dovyren volcano-plutonic complex. Yoko-Dovyren age is 728 million years (Ariskin et al., 2013). It is surrounded by carbonate and terrigenous rocks (mainly black shales) of the Synnyr rift (Kislov, 1998; Rytsk et al., 2002). Yoko-Dovyren intrusion belongs to Irkutsk LIP (Ernst et al., 2016; Mekhonoshin et al., 2016).

The massif feature is a large number of xenoliths after terrigenous and carbonate rocks. Xenoliths consist of magnesian, calcic-magnesian skarns and hornfels now. The xenoliths sizes vary from n cm up to 100-150 m. The most part the apocarbonate magnesian skarn lies at the dunite horizon top part, forming the layer subconcordant with the general structure of the massif (Pertsev, Shabynin, 1978; Kislov, 1998; Wenzel et al., 2002; Pertsev et al., 2003). Skarns are low-deep and high-temperature rocks.

Wehrlites, diopsidites and chromitites are related to the zone of magnesian skarns at the left board of upper part of Bol'shoy (Big) stream. Endocontact wehrlites and vein diopsidites differ from other massif rocks by wide variations of structures and mineral structure. Clinopyroxene (diopside to fassaite, f=8-10 %) forms the large euhedral crystals including isometric resorpted olivine grains, isometric crystals of black and green spinel. Olivine and more rare pyroxenes are serpentinizated on cracks. Nests and calcite streaks are characteristic this rocks. The nests of calcite and amesite surround the large sulfides at the coarse-crystalline taxitic wehrlite sometime (Kislov, 1998).

Chromitites are schlieren like segregation of chromespinels most often (Fig. 1). Its size is up to 0.5-1 m in length and 10-20 cm width. Chromitites consist from 40-60% of euhedral chromespinel (Fig. 1). Veins of massive chromitite with width up to 2 cm are less often. The olivine, grassy-green clinopyroxene, chlorite, green or greenish-brown garnet are typical for chromitites. The clinopyroxene and chlorite surround the chromespinel grains often.

The silicate inclusions in chromespinels were described as single (seldom 2-3), consisting of pargasite and phlogopite with the increased Ti, Cr, Na content, chlorite and carbonate also earlier. The hopper growth of chromespinel caused by magma enrichment by water and alkalis as a result of interaction with xenoliths or postcumulus recrystallization of chromespinel were offered as mechanisms of inclusions formation (Kislov, 1998, 2000).



Fig. 1. Sample B1b: two chromespinel layers are parallel to magnesian skarn.

Chromespinel at chromitites are a picotite and a chromepikotite with prevalence of Al over Cr. Olivine from chromitites is characterized by higher magneziant (Mg#=0.97-0.89) in comparison with olivine of the no contaminated dunnites (Mg#=0.87-0.85) and several times higher CaO content (up to 1.2%, on average 1%). Clinopyroxene of bright grass-green color is characterized by the high content of Al_2O_3 (6-8%), Cr_2O_3 (1%) and TiO_2 (0.5-0.7%) in comparison with clinopyroxene of the no contaminated dunnites (Pushkarev et al., 2003; Pushkarev, Kislov, 2005).

The Mössbauer researches of chromespinel and quantum chemical calculations were made for definition of chromitites genesis conditions at the Yoko-Dovyrensky massif (Pushkarev et al., 2003, 2004). The temperatures of olivine-chromite equilibrium vary from 1000 to 1130 °C at oxygen fugacity approximately on one unit of a logarithm above the FMQ buffer. Formation of chromitite is attributed to decomposition reaction of the dolomite taken in the form of xenoliths by picrobasalt magma (Wenzel et al., 2002) and release of large CO_2 volume - strong oxidizer. Significant increase in oxygen fugacity in around skarn space led to strengthening of crystallization of oxidic minerals (Pushkarev, etc., 2003, 2004).

Results

Mineral composition of chromitite was studied in detail during this research. Rock-forming minerals are olivine, diopside and chromespinel. Olivine is greenish-brown on a fresh chip and yellow on a weathered crust. It is presented by isomeric euhedral grains from 0.2 mm to 4-5 mm in size.

It has crystallographic outlines mainly in the bulk. The inclusions of olivine roundish grains in larger grains of olivine, diopside and chromespinel are observed also. The pronounced parting reminding the perfect cleavage is characteristic. It is determined by the microscopic lamels of the monticellite created by exsolution of a high-Ca olivine (Bailau et al., 2008). The serpentine, chlorite, calcite, magnetite are developed on numerous cracks. Variations on composition in one grain are characteristic for olivine. Spotty distribution of different compositions is more often. The zoning with increase of Fe content to the periphery is rare. The inclusions of chromespinel, magnetite (sometime with diopside inclusions), the monticellite (roundish, facetted or lath-shaped), diopside (roundish or lath-shaped), chlorapatite, pyrrhotine, halitet, problematic chlorides of calcium, magnesium, iron, barium and potassium are noted at the olivine.

Bright green diopside forms fringes of chromespinel crystals and the poikilokrists including and, perhaps, corroding the roundish grains of olivine. Grossular inclusions (both separate grains, and streaks), magnetite, chrommagnetite, chromespinel, chlorite, chlorapatite are noted at the diopside. Then melilite surround the diopside sometimes.

Black color chromespinel forms the large isometric grains from 1 to 3 mm in size. It has isotropic black color with a reddish shade at one nikol. The majority of grains are broken by the cracks filled with serpentine, chlorite, calcite, magnetite.

The sites of different composition are peculiar for grains of chromespinel. It's are high aluminous and low aluminous up to spinel with Zn and without Cr on the one hand and pure chromite with another. The chrommagnetite fringes, veins, chains of grains are typical too. Chromespinel grain is met which one corner is titanomagnetite, separated by the crack filled with chlorite (fig. 2). The hopper grain of chromespinel by composition, in %: 0.7 TiO_2, 11.05 Al_2O_3, 32.83 Cr_2O_3, 47.3 FeO, 7.4 MgO, 0.54 V_2O_3 is noted in phlogopite.

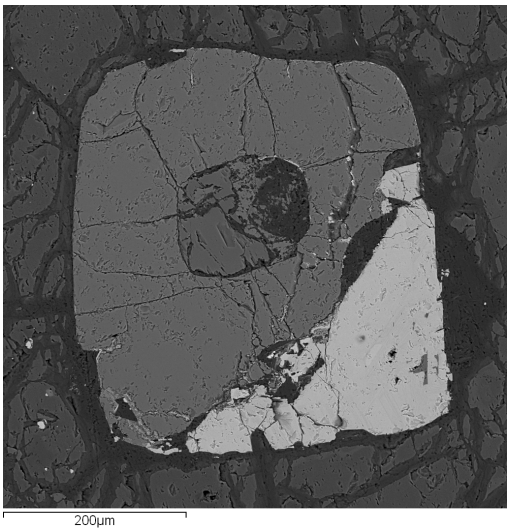


Fig. 2. Chromespinel grain at the olivene (sample 16-3-16): inclusion from left to right consist of diopside, grossular, chlorite, the left bottom corner is titanomagnetit.

The chlorite, diopside, olivine, magnetite, titanomagnetite, chromemagnetite, low-aluminous chromespinel, grossular, pargasite, phlogopite, apatite, chlorapatite, fluorapatit, vesuvianite (zoning sometimes), nepheline, cuspidine, halite, pentlandite, calcite (iron and magnesium content rare), serpentine, melilite, perovskite, chalcopyrite, djerfisherite, galena form inclusions in chromspinels. The nepheline grains are noted in roundish inclusion of diopside. Diopside acquires grossular and is chlorite consistently in inclusions sometimes (fig. 2). The chromemagnetite develops on border with inclusion directly sometimes, the chromite is more rare.

The chlorite, grossular (with hydrogrossular or chromemagnetite at the core of crystals sometimes), phlogopite, chlorapatite, fluorapatit, calcite, magnetite, pentlandite, chalcopyrite, pyrrhotine, galena, magnesian siderite are noted at the bulk of chromitite also. The streak consisting of diopside, grossular, apatite, chromemagnetite, chlorite among larger olivine grains is noted.

Calcic mica clintonite $CaAlMg_2(SiAl_3)O_{10}(OH)_2$ characteristic of skarn is met also. It forms the inclusion in chlorapatite in one case (sample B1b). It was found on contact of chromespinel and diopside in other case (sample 15-15).

Grains of sulfides sometimes contain inclusions of olivine or magnetite. The chlorite laths penetrating the anhedral grains of sulfides in all directions are noted. Pentlandite grain contains the inclusion of galena. Zoning crystals with chromemagnetite at core and with magnetite at external zone is met. The pentlandite-calcite-magnetite aggregate in joint of chromespinel crystals is noted.

Sulfides are replaced by magnetite or chrommagnetite, and those, in turn, by goethite are often. The bornite; cuprite; Fe oxides, hydroxides, carbonates with Cu; Fe oxides with Si and Mg develop on primary sulfides.

Serpentine, calcite, chlorite fill the cracks in the olivene, chromespinel, diopside. The magnetite is usual in such streaks. The galena and cubanite meet a less often. Streaks of white calcite are larger - about 2-2.5 mm long with a width of 0.1-0.2 mm. Calcite and chlorite fill interstices between grains of olivine, compose euhedral grains also. The pyrrhotine-pentlandite, pentlandite-magnetite grains meet in the euhedral grains of calcite.

Conclusions

Thus, composite heterogeneity of olivine and chromespinel is characteristic for chromitite of the Yoko-Dovyren massif. This two minerals are counterequlibrated in magmatic situation quickly usually.

Olivin is more magnesian, contains more Ca, diopside contains more Al, Cr, Ti, chromespinel is aluminous unlike intrusive rocks of the massif.

The metasomatic paragenesis of minerals is characteristic: grossular, monticellite, vesuvianite, cuspidine, calcite, siderite, melilite, perovskite, clintonite, djerfisherite. The nepheline, halite, other chlorides are unusual to such association also.

It confirms made earlier (Pushkarev, Kislov, 2005) conclusions that chromitites at the contaminated dunites of the Yoko-Dovyren massif represent high-chromium skarn of a magmatic stage. Its formation is connected with reaction of picrobasalt melt with CO_2 fluid and excess calcium extracted at a decarbonatization of dolomitic xenoliths.

Acknowledgements

The study was made within the Geological Institute state task on the IX.130.3.3. project, No. state registration AAAA-A17-117011650012-7 and funded by RFBR according to the

research project № 19-05-00337. Study of the Yoko-Dovyren massif, field research and chromitite sampling were carried out with financial support of RNF, grant No. 16-17-10129 partially. The study was conducted using facilities of Analytical center of mineralogical, geochemical and isotope studies at the Geological Institute, SB RAS, Ulan-Ude, Russia.

References

1. Ariskin A.A., Kostitsyn Yu.A., Konnikov E.G., Danyushevsky L.V., Meffre S., Nikolaev G.S., McNeill A., Kislov E.V., Orsoev D.A. (2013) Geochronology of the Dovyren intrusive complex, northwestern Baikal area, Russia, in the Neoproterozoic. Geochemistry International. 51: 859-875.
2. Bailau R., Pertsev N.N., Kislov E.V., Galuskin E.V. (2008) Olivine with perfect cleavage from Yoko-Dovyren massif, Russia. Mineralogia – Special Papers. 32: 41.
3. Ernst R.E., Hamilton M.A., Söderlund U., Hanes J.A., Gladkochub D.P., Okrugin A.V., Kolotilina T., Mekhonoshin A.S., Bleeker W., Buchan K.L., LeCheminant A.N., Chamberlain K.R., Didenko A.N. (2016) Long-lived connection between Southern Siberia and Northern Laurentia in the Proteozoic. Nature Geoscience. 9: 464-469.
4. Kislov E.V. (1990) Silicate inclusions in chrome-spinels of marginal dunites of the Ioko-Dovyren massif // Soviet Geology and Geophysics (10): 47-50.
5. Kislov E.V. (1998) Ioko-Dovyren layered massif. Ulan-Ude: RAS SD Buryat Scientific Centre Publishing House. 265 p. (In Russian with English abstract).
6. Mekhonoshin A.S., Kolotilina T.B., Ernst R., Soderlund U., Hamilton M.A., Izokh A.E., Polyakov G.V., Tolstykh N.D. (2016) Relationship between platinum-bearing ultramafic-mafic intrusions and large igneous provinces (exemplified by the Siberian craton). Russian Geology and Geophysics 57: 822-833.
7. Pertsev N.N., Shabynin L.I. (1978) Skarn, carbonate and brucite xenoliths of the Yoko-Dovyren massif. Contact processes and mineralization in a gabbro-peridotite intrusions. Moscow: Nauka (Science). P. 85-96. (In Russian).
8. Pertsev N.N., Konnikov E.G., Nekrasov A.N., Kislov E.V., Orsoev D.A. (2003) Merwinite-facies magnesian skarns in xenoliths from dunite of the Dovyren layered intrusion. Petrology. 11: 464-475.
9. Pushkarev E.V., Kislov E.V. (2005) Chromitites of Ioko-Dovyren massif, Northern Transbaikalia, as endoskarns at the contaminated dunites. Ultramafic-mafic complexes of Precambrian fold regions. Proceedings of the International Conference. September 6-9 2005. Enkhaluk on the Baikal. Ulan-Ude: RAS SD Buryat Scientific Centre Publishing House. P. 89-93. (In Russian with English abstract).
10. Pushkarev E.V., Votyakov S.L., Chashukhin I.S., Kislov E.V., Shapova Yu.V., Galakhova O.L. (2003) Ore chromshpinels of the Yoko-Dovyren layered massif (North Baikal region): structure, features of structure and condition of education. Year book 2002. Institute of geology and geochemistry UrO RAS. P. 215-223. (In Russian).
11. Pushkarev E.V., Votyakov S.L., Chashchukhin I.S., Kislov E.V. (2004) Olivine-chromespinel oxythermobarometry of ultramafic rocks of the Ioko-Dovyren layered massif. Doklady Earth Sciences. 395: 266-270.
12. Rytsk E.Yu., Shalaev V.S., Rizvanova N.G., Krymskiy R.Sh., Makeev A.F., Rile G.V. (2002) Olokit zone of the Baikal folded region: new isotope geochronological and petrochemical data. Geotektonika. (1): P. 29-41. (In Russian with English abstract).
13. Wenzel T., Baumgartner L.P., Brügmann G.E., Konnikov E.G., Kislov E.V. (2002) Partial melting and assimilation of dolomitic xenoliths by mafic magma: the Ioko-Dovyren Intrusion (North Baikal Region, Russia). Journal of Petrology. 43: 2049-2074.

RARE METAL PEGMATITE MINERALIZATION OF THE KALBA RIDGE, EASTERN KAZAKHSTAN – CONNECTION WITH THE TARIM LIP

Kotler P. D.[1,2], Khromykh S. V.[1,2], Oitseva T. A.[3], D'yachkov B. A.[3], Smirnov S. Z.[1,2]

[1] V.S. Sobolev Institute of Geology and Mineralogy SB RAS, Novosibirsk, Russia
[2] Novosibirsk State University, Novosibirsk, Russia
[3] D. Serikbayev East Kazakhstan State Technical University, Ust-Kamenogorsk, Kazakhstan

Keywords: *Rare metal pegmatite, granite batholith*

Kalba-Narym granite batholith in East Kazakhstan is one of the largest intrusions on the territory of the Central Asian Orogenic Belt (CAOB). With Kalba-Narym batholith granite are associated large rare metal deposits (Ta-Nb, Li-Rb-Cs, Sn-W). The most important of them are represented by large veins of rare-metal pegmatites with rich lithium, cesium, tin and tantalum-niobium mineralization (Belogorskoe, Yubileynoye and other fields). Based on the close spatial location, the formation of rare metal deposits are associated with granitoids of Kalba complex I phase, which compose main volume of the Kalba-Narym batholith intrusive rocks (Pushko, Navozov, 2010; D'yachkov, 2012). According to the latest U-Pb isotopic-geochronological studies (Kotler et al, 2014; Khromykh et al., 2016), the formation age of porphyritic biotite granites, which are injected by ore-bearing veins of rare metal pegmatites of Krasnyy Kordon field, is 296-286 Ma.

Krasnyy Kordon and Yubileynoye deposits are considered as part of the Asubulak ore field, related to large roof deflection of Tastyube and Priirtysh massifs of Kalba-Narym batholith. Host rocks for rare-metal pegmatites are coarse-grained porphyritic biotite granites of Kalba complex. Deposits are presented by the system of sublatitudinal pegmatite veins in length from 150 to 1000 m. with an average thickness of 2-6 m. On the Yubileynoye field from pegmatites with Li-Cs-Ta-

Nb mineralization were selected two monofractions of lepidolite and one muscovite monofraction for 40Ar/39Ar isotopic dating from albite-lepidolite complex with spodumene and colored tourmaline, which yielded the following ages: 295 ± 4 Ma (Ms), 292 ± 4 Ma (Lpd), 288 ± 3 Ma (Lpd).

Within the Krasnyy Kordon field were studied two pegmatite body, one of which is characterized by a Li-Cs-Ta-Nb specialization and this body is most representative pegmatite of the field, and the other body is a quartz-muscovite-feldspar body with schorl, garnet, and large crystals of beryl. We received five isotopic ages by pegmatites of Krasnyy Kordon fields: from block part of the pegmatite without signs of Li mineralization by muscovite - 288 ± 2 Ma; from ore-bearing albite-lepidolite complex with color tourmaline and petalite by lepidolite - 289 ± 3 Ma, 281 ± 2 Ma and muscovite - 282 ± 2 Ma.; from beryl-bearing quartz-muscovite-feldspar pegmatite by muscovite - 282 ± 2 Ma.

The Belogorskoye deposit is located in the endocontact of Belogorsky massif, represented in the area of ore-bodies by medium-grained biotite granite. Deposit formed by suite of submeridional veins a few meters of thickness and with length of 200 to 2700 m. Pegmatites are presented by quartz-muscovite-feldspar composition veins without Li-mineralization and by veins with albite-lepidolite complexes containing spodumene, petalite, pollucite, tantalite-columbite and cassiterite. On pegmatites of Belogorskoe deposit were obtained two ages: from block of quartz-feldspar-muscovite pegmatite by muscovite - 290 ± 2 Ma; from muscovite-quartz-albite complex with lepidolite, spodumene and petalite by muscovite - 286 ± 2 Ma.

Crystals of muscovite selected for geochronological studies form close intergrowths with primary pegmatite minerals: quartz, albite and/or K-feldspar and show no connection with mineralized fractures and paragenesis, resulting from hydrothermal replacement of primary minerals. This allows us to consider them as a result of pegmatite magma crystallization, and their age - is the age of pegmatites formation. Lepidolite forms massive aggregates with quartz and albite (cleavelandite) and develops through cracks in the pegmatite. Thus, lepidolite, apparently, formed after muscovite by alteration of quartz-muscovite-feldspar paragenesis in the later stages of pegmatite process.

All received $^{40}Ar/^{39}Ar$ ages from rare-metal pegmatites of Kalba-Narym batholith are presented in figure 1. Based on these data, we can assume that the formation of rare metal pegmatite deposits in Eastern Kazakhstan was evidenced in the range of about 12 million years, from 295 to 283 Ma. This interval is coeval to the existing $^{40}Ar/^{39}Ar$ ages of Kalba complex granitoids (Kotler et al, 2014), which confirms their genetic relationship.

For the studied objects two stages of pegmatite formation can be identified: 1) 295-285 million years - the most massive formation of nonmetallic and rare metal pegmatites; 2) 285-282 million years - forming of beryl-containing pegmatites and possibly the second stage of pegmatite formation with rich Ta-Nb and Li-Rb-Cs mineralization.

However, an insufficient number of geochronological data on beryl-containing pegmatites can also assume that specialization is not associated with multi-temporal influence of different sources of the substance. Sources of pegmatite magma, corresponding to one-time step, may greatly vary in composition, which in turn, allows to attract the model of heterogeneous magma sources, where the area, saturated with volatile components, complete crystallisation at low temperatures and pass pegmatite stage.

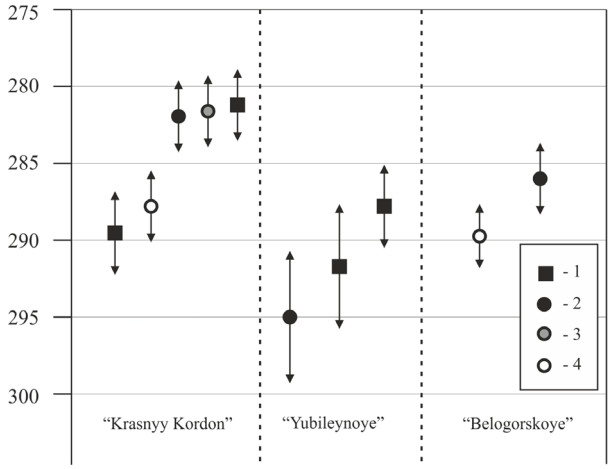


Figure 1. Results of Ar-Ar isotopic dating of pegmatites. 1 - lepidolite from lithium pegmatites; 2 - muscovite from lithium pegmatites; 3 - muscovite from beryl-containing pegmatite; 4 - muscovite from nonmetallic pegmatites.

Based on the fact that the age interval of pegmatite formation corresponds to the time of Kalba-Narym granitoid batholith formation, we can assume that the appearance of rare metal magmatism associated with large-scale processes of granite formation (the formation of Kalba complex granites). However, granitoids of Kalba complex show no signs of rare metal (average content in granites Ta - 1,2 pp

Acknowledgements

The work is done on state assignment of IGM SB RAS (Novosibirsk) and supported by the Ministry of Science and Higher Education of the Russian Federation (Projects no. 5.1688.2017/4.6 and 14.Y26.31.0018).

References

1. D'yachkov B.A. Genetic types of rare metal deposits of Kalba-Narym belt. – Ust-Kamenogorsk, 2012.-130c.
2. Khromykh, S.V., Tsygankov, A.A., Kotler, P.D., et al., 2016. Late Paleozoic granitoid magmatism of Eastern Kazakhstan and Western Transbaikalia: Plume model test. Russian Geology and Geophysics 57 (5), 773-789.
3. Khromykh S.V., Vladimirov A.G., Izokh A.E., et al., Petrology and geochemistry of gabbros and picritoids of Hercyn Altai collisional system: evidence of Tarim plume activity // Russian Geology and Geophysics, 2013. - Vol. 54. - № 10. - pp. 1648-1667
4. Kotler, P.D., Khromykh, S.V., Vladimirov, A.G.,et al., N.G. 2015. New data on the age and geodynamic interpretation of the Kalba-Narym granitic batholith, Eastern Kazakhstan. Doklady Earth Sciences 462 (2), 565-569.
5. Pushko Ye.P., Navozov O.V. Metallogenic aspects of Kalba Narymsky ore belt rare-metal pegmatites and rare-metal granites formation // Geology and protection of natural resources. Almaty, 2010. № 7, pp. 28-38.

ORIGIN OF ULTRAMAFIC XENOLITHS FROM CANARY ISLANDS

Krylova V. A.[1], Gertner I. F.[1] , Gutierrez-Alonso G.[2]

[1]*National Research Tomsk State University, 36 Lenin Avenue, Tomsk, 634050, Russia. E-mail: labspm@ggf.tsu.ru*
[2]*Salamanca University, Spain*

Keywords: *Ultramafic xenoliths, mantle xenoliths, Canary islands.*

Introduction

The Canaries are an age progressive volcanic island chain located ~100 km off the coast of northwest Africa. The Canaries span a lateral distance of ~500 km, trending roughly east–west and are comprised of seven main islands: Lanzarote, Fuerteventura, Gran Canaria, Tenerife, La Gomera, La Palma, and El Hierro. The entire island chain has sub-aerial lavas dated from 20.6 million years old to recent historical eruptions (Abdel-Monem et al., 1972; Guillou et al., 1996; 1998; Paris et al., 2005). The westward trending age progression of the Canary Islands has been interpreted as a symptom of a slow-moving mantle 'hotspot' with a low buoyancy flux (Abdel-Monen et al., 1972; Carracedo et al., 2001, 2002).

Results

An important aspect in interpreting nature of ultramafic xenoliths is their mineralogical composition. Presence of plagioclase (Traver & Caitlin Mary, 2013) does not let us consider these inclusions as real mantle xenoliths, as products of sub asthenosphere mantle. Our mineralogy analyses of ultramafic xenoliths from La Palma Island suggest capturing of ultramafic crystallization fragments in an intermediate deep magma chamber at a border between lithospheric mantle and lower crust (Krylova et al., 2018). Compositions of rock-forming minerals confirm this interpretation. In particular, presence of endiopside and basic plagioclase, as well as orientation of olivine grains (that corresponds to the olivine analogue of dunites from Yoko-Dovyren layered Massif in Northern Trans Baikal) indicates potential crust nature for these xenoliths. This orientation shows reflects cumulative nature of olivine, which does not suggest the mineral deformation in restite ultrabasites.

We have chosen cumulative dunites from Yoko-Dovyren layered pluton and "restite" peridotites from Kuznetsk Alatau (dunites from chromite mineralization zone of Barkhatny Massif) as standards. Analysis of olivine grain orientations from studied xenolith by EBSD method shows obvious axis maximum [001], which means Nm that corresponds to maximum extension of olivine crystal and shows/reflects orientation of its earlier crystals in magmatic melts.

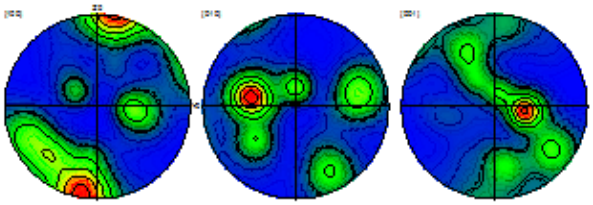


Figure 1. Diagram of olivine optical orientation from dunites of Yoko-Dovyren massif.

One of the signs of olivine's cumulative nature is an obvious axis maximum [001] and belted/ dissipation/scattering of two other crystallographic axes, which is observed in dunites from Yoko-Dovyren massif and xenoliths from Canary basalts.

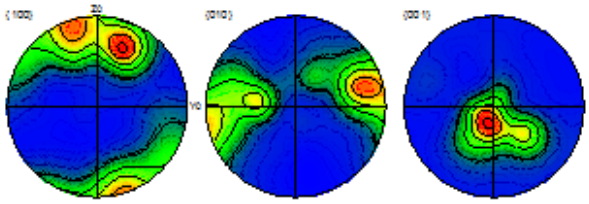


Figure 2. Diagram of olivine optical orientation of xenoliths from Canary Islands.

Such petro fabric pattern is caused by quite chaotic olivine grain orientations in magmatic melt. In addition, introducing magma flow suggests orientation of early olivine crystals to be parallel the flow itself, i.e. orientation of maximum grain extension in this direction. Other axes while having crystal lattice-like parameters are characterized by "blurred" zones/ belts, which possibly indicate grain rotations along two flat surfaces.

Conclusions

Considering specifics of mineral composition of studied xenoliths, namely presence of plagioclase and quite ferruginous olivine (same level as in chrysotile), we can assume a cumulative nature of xenoliths from ultrabasic rocks, which was caused by early crystallization in an intermediate magmatic chamber at a significant depth. The results of our petro fabric study confirm this assumption.

Acknowledgements

This work was conducted as a government task of the Ministry of Education and Science of the Russian Federation, Project Number 5.2352.2017.

References

1. Abdel-Monem, A., Watkins, N.D., Gast, P.W. Potassium-argon ages, volcanic stratigraphy, and geomagnetic polarity history of the Canary Islands: Tenerife, La Palma and El Hierro. American Journal of Science, 272. – 1972. P. – 805-825.
2. Carracedo, J.C., Rodríguez Badiola, E., Guillou, H., De La Nuez, J. & Perez Torrado, F.J. (2001) Geology and volcanology of La Palma and El Hierro (Canary Islands). Estudios Geologicos, 57, 175-273.

3. Carracedo, J.C., Pérez-Torrado, F. J., Ancochea, E., Meco, J., Hernán, F., Cubas, C. R., Casillas, R., Badiola, E. R. & Ahijado A. (2002) Cenozoic volcanism II: the Canary Islands. In: Gibbons, W. & Moreno, T. (Eds.) The Geology of Spain. Geological Society, London, pp. 439-471.
4. Gertner I.F. Petrology of Yoko-Dovyren layered ultramafic-mafic complex (Norther Baikalia). PhD Thesis. Tomsk: TSU, 1994, p. 309. Ultramafic massifs of Severnaya, Zelenaya and Barkhatnaya Mountains. PhD Thesis abstract, 2005.
5. Krasnova T.S. Goncharenko A.I. Petrology of deformation and petrofabric evolution of Alp-type hyperbasites. Tomsk: TSU publishing house, 1989, p. 404.
6. Sheinmann Y.M. Sketches of deep geology / -M.: Nedra, 1986 – p. 232.
7. Simkin T., Smith G. Minor element distribution of olivine // J. Geol., 1970. V. 78 №3. P. 304-325.

PALEOMAGNETISM OF THE PERMIAN-TRIASSIC INTRUSIONS OF THE NORILSK REGION: IMPLICATIONS OF THE SIBERIAN TRAPS EMPLACEMENT AND THE CU-NI-PGE DEPOSITS ORIGIN

Latyshev A. V.[1,2], Veselovskiy R. V.[1,2], Fetisova A. M.[1,2], Krivolutskaya N. A.[3], Ulyakhina P. S.[2], Pasenko A. M[2], Pavlov V. E.[2]

[1]Lomonosov Moscow State University, Faculty of Geology, Moscow, Russia, anton.latyshev@gmail.com
[2]Schmidt Institute of the Physics of the Earth, Russian Academy of Sciences, Russia
[3]Vernadsky Institute of Geochemistry and Analytical Chemistry, Russian Academy of Sciences, Moscow Russia

The Norilsk region of the Siberian platform is an area of the great scientific interest due to the unique Cu-Ni-PGE sulfide deposits. These deposits are related to the layered mafic-ultramafic intrusions which are associated with the Permian-Triassic Siberian Traps Large Igneous Province. The Norilsk region is located in the northwestern part of the platform and contains the thickest tuff-lava section of the Siberian Traps (up to 3500 m). According to the current schedule, trap intrusions of the Norilsk region are subdivided into seven complexes. One of them, namely Norilsk complex, contains four intrusive types. Ore deposits of economic importance are found only in the Norilsk-type intrusions of the Norilsk complex.

Despite the continuous and extensive investigation of the Norilsk intrusions, many aspects of the ore genesis and relationship of ore-bearing intrusions with the volcanic sequence of the Norilsk region are still debated. Most of the ore genesis models predict the different versions of correlation of ore-bearing Norilsk-type intrusions with the Siberian Traps volcanic sequence of the Norilsk region. According to various models, Norilsk-type intrusions are considered to be coeval with the lavas of Mokulaevsky (Rad'ko, 1991), Nadezhdinsky – Lower Morongovsky (Naldrett et al., 1992), or high-Mg picrites of Gudchikhinsky and Tuklonsky formations (Zolotukhin et al., 1986). Furthermore, some researchers assume that since Norilsk-type intrusions are the products of the specific magma type, not related to any volcanic formation, they could not be directly correlated with the tuff-lava sequence of the Norilsk region (Czamanske et al., 1994; Latypov, 2002). Thus, different models demonstrate a wide variety of correlation between lavas and ore-bearing intrusions.

Recently, we obtained the detailed flow-to-flow record of geomagnetic secular variations in the tuff-lava section of Norilsk as well as the preliminary paleomagnetic results on the Norilsk-2 intrusion, which is attributed to the Norilsk type (Pavlov et al., 2019). Here we present the results of detailed paleomagnetic investigation of the intrusions of Norilsk region, including economically important intrusive bodies of the Norilsk type. Based on the geomagnetic secular variations analysis, we obtained the new constraints on the timing of ore-bearing intrusions emplacement and suggested the correlation scheme of the intrusions with the volcanic sequence of the Norilsk region. Our method is based on the suggestion that if two magmatic bodies are formed simultaneously, their paleomagnetic directions have to be statistically indistinguishable, and, on the contrary, products of different magmatic events would likely have different directions. Using this approach, we compared the mean paleomagnetic directions for the studied intrusions with the directions of different stratigraphic levels from the tuff-lava sequence of Norilsk.

Our comparison demonstrated that all studied ore-bearing intrusions of the Norilsk region (including economically important Norilsk-1, Kharaelakh and Talnakh intrusions) and their satellites have paleomagnetic directions which are statistically indistinguishable from some volcanic units (volcanic pulses or individual flows) within the Morongovsky and Mokulaevsky formations in the middle part of the Norilsk tuff-lava sequence. It is the strong argument that the emplacement of all ore-bearing intrusions occurred during the same stage of the Siberian Traps magmatic activity. Within this stage, we were able to distinguish discrete magmatic events corresponding to the emplacement of three main ore-bearing intrusions, namely Norilsk-1, Kharaelakh and Talnakh, and some bodies spatially related to them. According to our paleomagnetic results, weakly differentiated Kruglogorsky-type intrusions and barren sills of the Oganer complex were at the same stage too. Finally, we obtained very close paleomagnetic directions from thin inclined dikes of the southern slope of the Kharaelakh plateau and Arylakh intrusion (the Norilsk type), and attributed them to the same phase, corresponding to the Morongovsky-Mokulaevsky level of the volcanic sequence.

The emplacement duration of the ore-bearing intrusions is another vital question of the Norilsk region geology. Since the mean virtual geomagnetic poles for the most intrusions differ statistically from the Permian-Triassic "Siberian Traps" paleomagnetic pole of the Siberian craton NMK (Pavlov et al., 2019), we suggest that geomagnetic secular variations re-

corded within these intrusions are not averaged. According to the modern estimations of time, sufficient for the variations averaging, we can assume that each single intrusion was cooling and acquiring remanent magnetization during not more than 1-10 kyr. The tight clustering of site-mean paleomagnetic directions within each of ore-bearing intrusions (Norilsk-1, Talnakh, Chernogorsky, Kharaelakh, Arylakh) is an additional argument in favor of this suggestion.

We also obtained the detailed paleomagnetic data from the sills of the Yergalakhsky complex. The studied intrusions demonstrated the paleomagnetic record of both normal and reverse polarities, sometimes within the same intrusion. According to our correlation, the emplacement of Yergalakhsky complex occurred at the very Permian-Triassic boundary, during and around the geomagnetic reversal. Thus, the Yergalakhsky intrusions are coeval to the uppermost part of the Ivakinsky Formation, corresponding to the initial stage of the Siberian Traps magmatic activity.

Besides, we studied some dikes of the Daldykan and Avamsky complexes. All these intrusions demonstrate the reverse polarity and therefore are younger than the whole tuff-lava sequence of the Norilsk region. Thus, the dikes of the Avamsky and Daldykan complexes probably represent the last stage of the magmatic activity in the northwestern Siberian platform.

Finally, we believe that paleomagnetic analysis is the promising tool of the magmatic provinces investigation, and our approach can be used for the distinction of magmatic events, correlation of intrusions and lava sections, and estimation of the emplacement time of intrusions in other large igneous provinces and ore regions.

This work was supported by the Limited Liability Company "Norilskgeologiya" (project No. NG-172/17), and Russian Foundation for Basic Research (grants No. 18-35-20058, 18-05-70094).

References

1. Czamanske, G. K., Wooden, J. L., Zientek, M.L., Fedorenko, V.A., Zen'ko, T.E., Kent, J., King, B-SW, Knight, R. J., and Siems, D. F., 1994, Geochemical and isotopic constraints on the petrogenesis of the Norilsk-Talnakh ore-forming system: Proceedings of the Sudbury-Norilsk symposium, Ontario Geological Survey Special Publication, v. 5, p. 313-342.
2. Latypov, R.M., 2002, Phase equilibria constraints on relations of ore-bearing intrusions with flood basalts in the Norilsk region, Russia: Contrib. Mineral Petrol., v. 143, p. 438–449.
3. Naldrett, A.J., 1992, A model for the Ni-Cu-PGE ores of the Noril'sk region and its application to other areas of flood basalt: Economic Geology, v.87, p. 1945-1962.
4. Pavlov, V., Fluteau, F., Latyshev, A., Fetisova, A., Elkins-Tanton, L.T., Black, B., Burgess, S., Veselovskiy, R., 2019, Geomagnetic Secular Variations at the Permian-Triassic Boundary and Pulsed Magmatism During Eruption of the Siberian Traps: Geochemistry, Geophysics, Geosystems, v. 20 (2), p. 773-791, doi: 10.1029/2018GC007950.
5. Rad'ko, V.A., 1991, Model of the Dynamic Differentiation of Intrusive Traps from the Northwestern Siberian Platform: Geology and Geophysics, v. 11, p. 19–27. (in Russian)
6. Zolotukhin, V.V., Vilenskii, A.M., and Dyuzhikov, O.A., 1986, Basalts of Siberian platform: Novosibirsk, Nauka (in Russian), 344 p.

CHEMICAL WEATHERING OF LARGE IGNEOUS PROVINCES: AGE AND TEMPERATURE DEPENDENCE

Li G-J.[1], Börker J.[2], Chen Y.[1], Hedding D. W.[3], Hartmann J.[2], Li X-M.[1], Romero-Mujalli G.[2], Wu W-H.[1]

[1]MOE Key Laboratory of Surficial Geochemistry, Department of Earth and Planetary Sciences, Nanjing University, Nanjing 210023, China
[2] Institute for Geology, CEN (Center for Earth System Research and Sustainability), Universität Hamburg, Bundesstraße 55, 20146 Hamburg, Germany.
[3]Department of Geography, University of South Africa, Pioneer Avenue, Florida 1710, South Africa
E-mail: ligaojun@nju.edu.cn (G. Li.)

Chemical weathering is arguably the most crucial and fundamental phenomenon on the Earth's surface. Most notably, the negative feedbacks between pCO_2 (climate) and weathering consumption rate of atmospheric CO_2 may have helped to maintain balance of the carbon cycle and the habitability of the Earth over timescales of millions of years (Walker et al., 1981). Basaltic fields have been the focus of recent studies of weathering processes due to its disproportional share (~30%, Dessert et al., 2003; Gaillardet et al., 1999) of the global weathering flux relative to its small areal coverage (~3.5%, Hartmann and Moosdorf, 2012). Deciphering the factors that control basalt weathering is of great importance for understanding the impact(s) of Large Igneous Provinces (LIPs) on climate change. Age and temperature seem to be the major controls on the weathering of basaltic fields. Newly erupted volcanic fields generally show a much higher weathering flux compared to the older volcanic fields under the same climate conditions. Our recent work shows that the higher weathering reactivity of the volcanically active region correlates well with the areal coverage of Holocene volcanic rock (Börker et al., 2018). The contribution of fresh volcanic ash and processes related to volcanic activity may explain the higher weathering reactivity of the volcanically active region. In the volcanically inactive fields, where the complexities associated with reactive volcanic ash can be avoided, we have shown that the rate of basalt weathering, as approximated by the consump-

tion rate of atmospheric CO_2 correlates well with temperature (Li et al., 2016). The large weathering flux, strong climate sensitivity, and the ongoing renewing of volcanic rocks on the Earth's surface make basalt the most likely candidate to have helped maintain the balance of the carbon cycle and the habitability of the Earth (Li and Elderfield, 2013).

The observed climate dependence of basalt weathering in volcanically inactive fields would favor a 'kinetically-limited' weathering regime. A 'kinetically-limited' weathering regime is generally associated with high erosion rates so that the residence time of regolith is short and the weathering intensity of the eroding materials is relatively low (West et al., 2005). Thus, weathering flux is not limited by the supply of bedrock but rather by environmental factors (West et al., 2005). However, detailed investigation shows that LIPs on stable cratons with extremely low erosion rates, such as the Deccan Traps, the Siberia Traps, the Parana Traps, and the Karoo in South Africa, retain a weathering rate that is consistent with the temperature dependence identified mainly on rugged inactive volcanic islands. Rock detachment and thus denudation, controlled by chemical weathering is suggested to reconcile the paradox between the observed temperature dependence of chemical weathering rate and the low denudation rate of the LIPs.

Our findings suggest that the influence of LIP eruptions on climate depends on the considered time-scale. Episodic cooling may prevail on an annual timescale, associated with volcanic events, because of short-lived sulfate aerosols. Periods of intensive eruptions and concomitant CO_2 degassing may cause global warming due to the relatively extended lifetime of CO_2 in the atmosphere. Decreasing volcanic activities after the main eruption period may introduce cooling due to the rapid consumption of atmospheric CO_2 by the fresh volcanic ash. On the timescale of a million years, LIPs may act as a buffering system that helps to maintain the balance of carbon cycle and the long-term habitability of the Earth.

References

1. Börker, J., Hartmann, J., Romero-Mujalli, G., Li, G., 2018. Short Communication: Aging of basalt volcanic systems and decreasing CO2 consumption by weathering. Earth Surf. Dynam. Discuss. 2018, 1-9.
2. Dessert, C., Dupré, B., Gaillardet, J., François, L.M., Allègre, C.J., 2003. Basalt weathering laws and the impact of basalt weathering on the global carbon cycle. Chem. Geol. 202, 257-273.
3. Gaillardet, J., Dupré, B., Louvat, P., Allègre, C.J., 1999. Global silicate weathering and CO_2 consumption rates deduced from the chemistry of large rivers. Chem. Geol. 159, 3-30.
4. Hartmann, J., Moosdorf, N., 2012. The new global lithological map database GLiM: A representation of rock properties at the Earth surface. Geochem., Geophys., Geosys. 13, Q12004.
5. Li, G., Elderfield, H., 2013. Evolution of carbon cycle over the past 100 million years. Geochim. Cosmochim. Acta 103, 11-25.
6. Li, G., Hartmann, J., Derry, L.A., West, A.J., You, C.-F., Long, X., Zhan, T., Li, L., Li, G., Qiu, W., Li, T., Liu, L., Chen, Y., Ji, J., Zhao, L., Chen, J., 2016. Temperature dependence of basalt weathering. Earth Planet. Sci. Lett. 443, 59-69.
7. Walker, J.C.G., Hays, P.B., Kasting, J.F., 1981. A negative feedback mechanism for the long-term stabilization of Earths surface temperature. J. Geophys. Res. 86, 9776-9782.
8. West, A.J., Galy, A., Bickle, M., 2005. Tectonic and climatic controls on silicate weathering. Earth Planet. Sci. Lett. 235, 211-228.

METALLOGENY OF LIPS FROM SIBERIAN OF RUSSIA AND EMEISHAN OF CHINA

Liu J-M.[1], Zhang S-H.[1], Zhao Y.[1], Li J-B.[2]

[1]*Institute of Geomechanics,Chinese Academy of Geological Sciences*
[2]*University of Chang'an,China*

Keywords: *Metallogeny, LIPs, Siberian, Emeishan*

Introduction

One of the most important concerns about LIPs is their economic interest, because some related mafic to ultramafic intrusive rocks host voluminous copper, nickel, and platinum-group element (PGE) deposits and vanadium, titanium, and magnetite deposits as those in the Siberian LIPs of Russia and Emeishan LIPs of China, respectively. A great number of studies and works have been made for the origin and magmatic nature of the deposits and their relation to the large igneous provinces (Czamanske et al.,1994; Fedorenko et al.,1994b; Zhou et al., 2008). However, what on earth caused the differences of metallogenic specialization and mechanism between different LIPs is unclear.

This paper makes a comprehensive study on the variations of geochemical compositions of volcanic lavas and associated ore-bearing mafic to ultramafic intrusive rocks from the two LIPs of Siberian of Russia and Emeishan of China. Also, the varying of ore-types in the ore-bearing mafic to ultramafic intrusive rocks suggests that crystal fractionation due to density differences may play the key role for the differences of metallogenic specialization and mechanism between different LIPs.

Results

Variations in rocks and geochemical compositions

The information of the two LIPs of Siberian of Russia and Emeishan of China shows the presence of two distinct series in petrography and geochemistry, either for the volcanic or the intrusive rocks. Although the volcanic sequences from the two LIPs are predominantly composed of basalts, the basalts

from the Siberian Flood Basalt Province are kind of tholeiitic, porphyritic, and taxitic and slightly high SiO_2 wt%. The rocks from the Emeishan Large Igneous Province are characterized by high amount of TiO_2 wt%. For the ore-bearing intrusive rocks, the Siberian mainly consists of large sills, well-differentiated from picritic gabbrodolerite to magnetite gabbro and leucogabbro. The Emeishan is mainly composed of gabbro and leucogabbro with well-defined layered and rhythmic structures. In the variation diagram of SiO_2-(Na_2O+K_2O), the Cu, Ni, PGE-bearing intrusions generally have a slightly higher SiO2 wt% and lower Na_2O+K_2O wt% than those of the V, Ti, Magnetite-bearing intrusions.

Variations in metallogenic specializations and mechanisms

The ore-bearing intrusions of the Noril'sk and Talnakh district associated with the SFBP are characterized by enormous amounts of Cu, Ni, and PGE mineralization. Whereas those intrusions from the Emeishan LIPs present voluminous V, Ti, and Magnetite mineralization, with a little amount of Cu, Ni, and PGE mineralization. We noticed that the three distinct ore-bearing intrusions of the Noril'sk and Talnakh district occupy successively higher positions in sedimentary strata within 650 m of the contact with highly varying in mineralization. Walker et al. (1994) made a detailed description about the ore-types in the Noril'sk Cu-Ni-PGE deposits, which displayed the intimate relationships among the ore structures and intrusive positions in the strata columns. For example, the Noril'sk 1 intrusion lies in the Middle Carboniferous-Upper Permian strata with disseminated and droplet Cu-Ni-PGE ore. The Talnakh and Kharaelakh intrusions lie in Middle Carboniferous to Lower Permian sedimentary rocks and the Lower to Middle Devonian marine sedimentary rocks, respectively. They are characterized by extremely large massive-sulfide orebodies situated along the base of these intrusions or in footwall hornfels. Similarly, the ore-bearing ultramafic intrusions in the Emeishan LIPs predominantly intrude into the Middle Proterozoic metamorphic basement rocks. These intrusions and related Cu-Ni-PGE ores are generally small as stock or veins.

Similarly, the ore-bearing mafic banded gabbro intrusions in the Emeishan LIPs lie mainly in the Proterozoic Sinian sedimentary limestone strata. Those intrusions are generally batholitic with more than 19 km long and 2 km wide and 1.2-1.8 km in depth. These intrusions are characterized by the world class vanadium, titanium, and magnetite deposits.

Combined with many other evidences such as the layered structures and the variations in mineral and geochemical compositions, we suggests that crystal fractionation due to density differences may play the key role for the differences of metallogenic specializations and mechanisms between different LIPs.

Conclusions

(1) The rocks from the LIPs of Siberian of Russia and Emeishan of China belong to the two distinct series in petrography and geochemistry, either for the volcanic or the intrusive rocks.

(2) The mafic to ultramafic intrusions associated the LIPs show some kind of metallogenic specializations. The variations of ore-types in the ore-bearing mafic to ultramafic intrusive rocks suggests that crystal fractionation due to density differences may play the key role for the differences of metallogenic specializations and mechanism between different LIPs.

Acknowledgements

This work was funded by grants from the Ministry of Science and Technology of China (2014DFR21270). Dr. Oleg Petrov and his colleagues from the A. P. Karpinsky Russian Geological Research Institute are deeply appreciated for cooperation on the study on the Siberian Flood Basalt Province.

References

1. Czamanske G. K., Wooden J. L., Zientek M. L., Fedorenko V. A., Zen'ko T. E., King Bi-S. W., Knight R. J. and Siems D. F. (1994) Geochemical, Pb, and Sr-isotopic constraints on the petrogenesis of the Noril'sk-Talnakh ore-forming system. In Proceedings of the Sudbury-Noril'sk Symposium (P. C. Lightfoot and A. J. Naldrett, eds.). Ontario Geol. Surv. Spec. 5: 313-342.
2. Walker R. J., Morgan J. W., Horan M. F., Czamansk G. K., Krogstad E. J., Fedorenko V. A., and Kunilov V. E.(1994) Re-Os isotopic evidence for an enriched-mantle source for the Noril'sk-type, ore-bearing intrusions, Siberian. Geochimica et Cosmochimica Acta 58(19):. 4179-4197.
3. Fedorenko V. A. (1994b) Model of genetic relationships between flood basalts, ore-bearing intrusions, and Cu-Ni-Pt ores in the Noril'sk region, NW Siberian platform, Russia. VII International Platinum Symposium, Moscow, Abstr., p. 26.
4. Zhou M., Arndt N.T., Malpas J., Wang C.Y. and Kennedy A.K. (2008). Two magma series and associated ore deposit types in the Permian Emeishan large igneous province, SW China. LITHOS, 103(3): 352 - 368.

PETROGENESIS OF PALEO-MESOPROTEROZOIC MAFIC ROCKS IN THE SOUTHWESTERN YANGTZE BLOCK OF SOUTH CHINA: IMPLICATIONS FOR TECTONIC EVOLUTION AND PALEOGEOGRAPHIC RECONSTRUCTION

Lu G-M.[1,2], Wang W.[1,], Ernst R. E.[2,3], Söderlund U.[4]

[1] State Key Laboratory of Geological Processes and Mineral Resources, School of Earth Sciences, China University of Geosciences, Wuhan 430074, China
[2] Department of Earth Sciences, Carleton University, Ottawa, Ontario K1S 5B6 Canada
[3] Faculty of Geology and Geography, Tomsk State University, 36 Lenin Ave, Tomsk, 634050, Russia
[4] Department of Geology, Lund University, Sölvegatan 12, SE 223 62 Lund, Sweden
Emails: luguimei@cug.edu.cn, wwz@cug.edu.cn, Richard.Ernst@ErnstGeosciences.com, ulf.soderlund@geol.lu.se.

The Archean and Paleoproterozoic rock units in the Yangtze Block are tentatively incorporated within Nuna Supercontinent (Yin et al., 2013) (Furlanetto et al., 2016) (Wang et al., 2016) (Cawood et al., 2018), while the absence of precise paleomagnetic data has resulted in a number of contrasting and in some cases mutually exclusive models (Zhou et al., 2014) (Wang et al., 2014). During supercontinent breakup, extensive mafic magmatism can occur within and between previously connected crustal blocks (Ernst et al., 2008). These mafic magmatism can thus provide invaluable information on supercontinent reconstruction through the technique of magmatic barcodes comparison between different crustal blocks (Ernst et al., 2016).

In this study, three episodes of mafic magmatism are identified by zircon and baddeleyite U-Pb dating at 2299 ± 17 Ma, 1703 ± 8 Ma and 1511 ± 14 Ma in the southwestern Yangtze Block. These mafic rocks have tholeiitic compositions with enrichment of LILE but an absence of Nb, Ta, Zr, Hf anomalies, features similar to E-MORB. They have La/Ta (<22) and La/Nb (<1.5) ratios similar to asthenosphere- derived mafic melts. The ca. 2.3 Ga, ca.1.7 Ga and ca. 1.5 Ga mafic rocks have $\varepsilon_{Nd}(t)$ values of +0.2 to +4.3, −2.8 to +2.8 and +0.7 to +5.8, respectively. Furthermore, the ca. 2.3 Ga and ca. 1.7 Ga mafic rocks have $\varepsilon_{Hf}(t)$ values varying from −3.6 to +0.8 and +0.1 to +9.2. All these geochemical and isotopic data indicate that the studied mafic rocks may be dominantly sourced from asthenospheric mantle.

Thermodynamic modeling indicates that the mantle potential temperatures for the studied ca. 2.3 Ga and ca. 1.7 Ga dolerites are 1447 °C−1568 °C, 1511 °C −1529 °C, suggesting relatively hot mantle below the southwestern Yangtze Block at ca. 2.3 Ga and ca. 1.7 Ga. REE modeling indicates the ca. 2.3 Ga and ca. 1.5 Ga dolerites were generated by low degree melting (3–15%) of mantle source, while the ca. 1.7 Ga gabbros were derived from variable degree melting (5–20%) of mantle source. Fractionation of olivine, pyroxene and plagioclase contributes to changing the chemical compositions of the primary magma, while crustal contamination was relatively insignificant. These three episodes of mafic magmatism were generated in extensional setting. The ca. 2.3 Ga dolerite represents the oldest mafic magmatism identified in the southwestern Yangtze Block by far, documenting the dispersion of the Yangtze Block from the Nunavutia supercraton. Comparing the younger magmatic barcode records for various crustal blocks shows that the mafic magmatism at ca. 1.75–1.65 Ga in the Yangtze Block, has matches in northwestern Laurentia and southern Siberia. This period of extensive magmatism was presumably linked to the early attempted breakup of the Nuna supercontinent, indicating tight linkage among these continents in that supercontinent.

References

1. Cawood, P.A., Zhao, G., Yao, J., Wang, W., Xu, Y., Wang, Y., 2018. Reconstructing South China in Phanerozoic and Precambrian supercontinents. Earth-Science Reviews 186, 173-194.
2. Ernst, R.E., Hamilton, M.A., Söderlund, U., Hanes, J.A., Gladkochub, D.P., Okrugin, A.V., Kolotilina, T., Mekhonoshin, A.S., Bleeker, W., Lecheminant, A.N., 2016. Long-lived connection between southern Siberia and northern Laurentia in the Proterozoic. Nature Geoscience 9, 464-469.
3. Ernst, R.E., Wingate, M.T.D., Buchan, K.L., Li, Z.X., 2008. Global record of 1600–700 Ma Large Igneous Provinces (LIPs): Implications for the reconstruction of the proposed Nuna (Columbia) and Rodinia supercontinents. Precambrian Research 160, 159-178.
4. Furlanetto, F., Thorkelson, D.J., Rainbird, R.H., Davis, W.J., Gibson, H.D., Marshall, D.D., 2016. The Paleoproterozoic Wernecke Supergroup of Yukon, Canada: Relationships to orogeny in northwestern Laurentia and basins in North America, East Australia, and China. Gondwana Research 39, 14-40.
5. Wang, W., Cawood, P.A., Zhou, M.F., Zhao, J.H., 2016. Paleoproterozoic magmatic and metamorphic events link Yangtze to northwest Laurentia in the Nuna supercontinent. Earth & Planetary Science Letters 433, 269-279.
6. Wang, W., Zhou, M.F., Zhao, X.F., Chen, W.T., Yan, D.P., 2014. Late Paleoproterozoic to Mesoproterozoic rift successions in SW China: Implication for the Yangtze Block–North Australia–Northwest Laurentia connection in the Columbia supercontinent. Sedimentary Geology 309, 33-47.
7. Yin, C.Q., Lin, S.F., Davis, D.W., Zhao, G.C., Xiao, W.J., Li, L.M., He, Y.H., 2013. 2.1–1.85 Ga tectonic events in the Yangtze Block, South China: Petrological and geochronological evidence from the Kongling Complex and implications for the reconstruction of supercontinent Columbia. Lithos s 182–183, 200-210.
8. Zhou, M.F., Zhao, X.F., Chen, W.T., Li, X.C., Wang, W., Yan, D.P., Qiu, H.N., 2014. Proterozoic Fe–Cu metallogeny and supercontinental cycles of the southwestern Yangtze Block, southern China and northern Vietnam. Earth-Science Reviews 139, 59-82.

EARLY PALEOPROTEROZOIC LARGE IGNEOUS PROVINCE OF THE KARELIAN PROTOCRATON: PALEOMAGNETIC ASPECT

Lubnina N., Tarasov N.

M.V. Lomonosov Moscow State University, Moscow, Russia

Keywords: *LIP, Karelia protocraton, Paleoproterozoic, paleomagnetism, geodynamic reconstructions*

Introduction

Early Paleoproterozoic – time of the first break-up of the Neoarchean supercontinent Kenorland. It is generally assumed that mantle and crust melting at ca. 2.50–2.45 Ga was caused by the ascent of a mantle plume.

Within the Karelian protocraton, the Early Paleoproteorozoic event of 2.45 Ga most clearly appeared in the Vodlozero and northern part of the Central Karelian terranes.

The Vodlozero terrane is located in the southern part of the Karelian protoraton. The 3.30–2.95 Ga granite-greenstone rocks of the Voldozero terrane compose a basement of the Onega Paleoproterozoic structure (Slabunov et al., 2006, Glushanin et al., 2011), or Onega Basin (Melezhik et al., 2013). The Onega structure is filled by Paleoproterozoic supracrustal rocks of Sumian (2.50−2.40 Ga), Sariolian (2.40–2.30 Ga), Jatulian (2.30−2.10 Ga), Ludicovian (2.10−1.92 Ga), Kalevian (1.92−1.80 Ga), and Vepsian (1.80−1.65 Ga) Super-Horizons, with a cumulative thickness of up to 10 km (Glushanin et al., 2011 and references therein).

At least two pulses of mafic magmatism occurred in this area: at 2.50–2.45 Ga (Amelin et al., 1995; Puchtel et al., 1997) and at ca. 1.98–1.96 Ga (Puchtel et al., 1998; Stepanova et al., 2014). The older event is presented by komatiitic, basaltic, and felsic volcanic rocks and siliciclastic sediments formed in rift-related volcano-sedimentary belts synchronous with layered mafic intrusions, granite massifs, and gabbronorite dyke swarms (Stepanova et al., 2015 and references therein). The younger event comprise diverse, possibly plume-related mafic complexes that include picrites, high- and low-Ti tholeiites, subalkaline basalts, syenites, carbonatites, and kimberlites (Puchtel et al., 1998, Stepanova et al., 2015 and references therein).

Paanajarvi structure is located at the northern part of the Central Karelian terrane and represented a narrow compressed synclinal structure northeastern stretch. Basement rocks constituted by Neoarchean granitoids Pyaozero sanukitoid batholith. Mafic intrusions and dykes are widespread in the basement rocks of the Paanajarvi structure. Paleoproterozoic mafic rocks presented here by intracratonic volcanic rocks, layered intrusions and mafic dykes swarms of 2.5–2.0 Ga. Based on geological and isotopic data several age groups have been divided: (1) Sumian (2.5–2.4 Ga), Sariolian (2.4–2.3 Ga), Jatulian (2.3–2.06 Ga) and Ludikovian (2.06–1.96 Ga).

According to available data, Sumian–Sariolian and Jatulian–Ludikovian mafic rocks are contrasting differ in composition: the first one correspond to the siliceous high-Mg series (Sharkov et al., 1997), the second one – to the Fe-Ti toleiites.

We present a new paleomagnetic data from the Early Paleoproterozoic layered gabbronorite intrusions and mafic dykes and Archean host rocks within two terranes of the Karelian protoraton, eastern Fennoscandian Shield. Early Paleorproterozoic Burakovka and Kivakka layered gabbronorite intrusions have been collected at Vodlozero and Central Karelian terranes respectively. Three groups of dykes have been collected within Pyaozero area of Central Karelian terrane: NE-trending ca. 2.45 Ga gabbronorite and diorite dykes, NW-trending ca. 2.4 Ga dolerite dykes (Stepanova et al., 2014). We also sampled Sariolian (ca 2.3 Ga) conglomerates containing pebbles both Early Paleozoic gabbronorites and NeoArchean granites at Vodlozero and Central Karelian terranes.

Results

All studied samples from the Early Paleoprotrozoic layered intrusions and mafic dykes carried two stable components. Most typical is component of intermediate down to the NNW, corresponds to the Svecofennian remagnetisation (Mertanen et al., 1999).

Component of SE intermediate down direction yielding a paleomagnetic pole 2.45 Ga based on a positive baked contact test is interpreted to represent the primary magnetization. It's correlate with D-component obtained early for Burakovka intrusion and Pjaozero Sumian dykes (Mertanen et al., 1999: Meratnen et al., 2006).

In the Sariolian conglomerates, two remanence components were isolated in both in the gabbronorite and granite pebbles. Stable mid-temperature components were removed in fields up to 20-40mT, and in temperatures up to 540°C, after which scattered component were disclosed in high fields/temperatures. Mid temperature component demonstrate northwestern directions with moderate downward inclinations, close to the mid-temperature/coercivity components in mafic dykes and correspond to the Svecofennian age remagnetization (negative conglomerate test). The high-temperature component isolated in both gabbronorites and granites has a chaotic distribution on the sphere. The high-temperature/coercivity component isolated in both gabbronorites and granites has a chaotic distribution on the sphere (positive conglomerate test). This only shows the partial remagnetization of rocks in Svecofennian time (ca 1.8 Ga), while the high temperature component has a primary origin.

Conclusions

The new paleomagnetic data from the Karelia protocraton compared to similar-aged paleomagnetic data from the Superior protocraton does not support the recently proposed Superia configuration, based upon dyke swarm trajectories (Bleeker, Ernst, 2006).

We propose a new Early Paleoproterozoic paleogeography at 2.5–2.45 Ga for Karelian and Superia protocratons.

Acknowledgements

This is a contribution to the RFBR project 17-05-01270.

References

1. Amelin Y.V., Heaman L.M., Semenov V.S. (1995) U-Pb geochronology of layered mafic intrusions in the eastern Baltic Shield: implications for the timing and duration of Paleoproterozoic continental rifting. Precambrian Research 75 (1–2): 31–46
2. Bleeker, W. & Ernst, R. (2006) Short-lived mantle generated magmatic events and their dyke swarms: The key unlocking Earth's paleogeographic record back to 2. 6 Ga. In: Hanski, E. et al. (eds.): Dyke Swarms - Time Markers of Crustal Evolution. Taylor and Francis/Balkema, London: 3–26
3. Glushanin, L.V., Sharov, N.V., Shiptsov, V.V. (eds.), (2011) Paleoproterozoic Onega structure (Geology, tectonics, deep structure and mineralogeny). Karelian Sci. Center RAS, Petrozavodsk: 431 p
4. Melezhik, V.A., Medvedev, P.V., Svetov, S.A. (2013) The Onega basin. In: Melezhik, V.A., Prave, A.R., A.E. Fallick, A.E., Kump, L.R., Strauss, H., Lepland, A., Hanski, E.J. (Eds.), Reading the Archive of Earth's Oxygenation, Volume 1: The Palaeoproterozoic of Fennoscandia as Context for the Fennoscandian Arctic Russia – Drilling Early Earth Project. Frontiers in Earth Sciences, Springer, Berlin, Heidelberg: 387–490.
5. Mertanen S., Halls H.C., Vuollo J.I, Pesonen L.J., Stepanov V.S. (1999) Paleomagnetism of 2.44 Ga mafic dykes in Russian Karelia, eastern Fennoscandian Shield –implications for continental reconstructions. Precambrian Research 98: 197–221
6. Mertanen, S., Vuollo, J.I., Huhma, H., Arestova, N.A., Kovalenko, A. (2006) Early Paleoproterozoic-Archean dykes and gneisses in Russian Karelia of the Fennoscandian Shield - New paleomagnetic, isotope age and geochemical investigations. Precambrian Research 144: 239–260
7. Puchtel, I.S., Arndt, N.T., Hofmann, A.W., Haase, K.M., Kröner, A., Kulikov, V.S., Kulikova, V.V., Garbe-Schönberg, C-D., Nemchin, A.A. (1998) Petrology of mafic lavas within the Onega plateau, central Karelia: evidence for 2.0 Ga plume-related continental crustal growth in the Baltic Shield. Contributions to Mineralogy and Petrology 130: 134-153
8. Puchtel I. S., Haase K. N., Hofman A. W. et al. (1997) Petrology and geochemistry of crustally contaminated komatiitic basalts from Vetreny Belt, southeastern Baltic Shield: evidence for an early Proterosoic mantle plume beneath rifted Archean continental lithosphere. Geochimica et Cosmochimica Acta 61: 1205–1222
9. Samsonov A. V, Stepanova A. V, Salnikova E.B., O L.Y., Egorova S. V, Larionov A.N. (2016) Mafic Dyke Records of Paleoproterozoic Mantle Plume Activity in the Karelian Craton : U-Pb Baddeleyite / Zircon Geochronology and Sr-Nd Isotopic Data. Acta Geological Sinica (English Edition) 90: 118–119
10. Sharkov E. V., Smol'kin V. F., and Krasivskaya I. S. (1997) Early Proterozoic Igneous Province of Siliceous High-Mg Boninite-Like Rocks in the Eastern Baltic Shield. Petrology 5: 448–465
11. Slabunov, A.I., Lobach-Zhuchenko, S.B., Bibikova, E.V., Sorjonen-Ward, P., Balagansky, V.V., Volodichev, O.I., Shchipansky, A.A., Svetov, S.A., Chekulaev, V.P., Arestova, N.A., Stepanov, V.S. (2006) The Archaean nucleus of the Fennoscandian (Baltic) Shield. In: Gee, D.G., Stephenson, R.A. (Eds.), European Lithosphere Dynamics, Geological Society, London Memoirs 32: 627–644
12. Stepanova, A.V., Samsonov, A.V., Salnikova, E.B., Puchtel, I.S., Larionova, Y.O., Larionov, A.N., Stepanov, V.S., Shapovalov, Y.B., Egorova, S.V. (2014) Palaeoproterozoic continental MORB-type tholeiites in the Karelian Craton: petrology, geochronology, and tectonic setting. Journal of Petrology 55: 1719–1751
13. Stepanova A. V., Salnikova E.B., Samsonov A. V., Larionova Y.O., Stepanov V.S. (2015) Composition and duration of Paleoproterozoic plume events: A case study of 2.45 Ga mafic dyke swarms in the Karelian Craton. Goldschmidt 2015 Abstracts: 2988

A RISE IN GLOBAL OXYGEN AT CA. 800 MA: TECTONIC CAUSES AND BIOLOGICAL CONSEQUENCES

Lyons T. W., Diamond C. W.

Department of Earth and Planetary Sciences and the Alternative Earths Astrobiology Center, University of California, Riverside, CA 92521 USA (timothy.lyons@ucr.edu)

A near absence of biospheric oxygen (O_2) dominated the first two billion years of Earth history, yet biological O_2 production, local enrichments in the surface ocean, and transient build-up in the atmosphere appeared long before the first persistent accumulation of appreciable atmospheric O_2. Wide-ranging data point to the first major step in oxygenation—the Great Oxidation Event—at 2.3 to 2.4 Ga. Despite this rise, oxygen in the oceans and atmosphere remained mostly low for another billion and a half years, although a growing body of data defines intervals of increased oxygenation in the oceans and atmosphere with possible mechanistic relationships to LIPs activity. Multiple geochemical proxies point to the second major increase in ocean-atmosphere O_2 around 800 million years ago (Ma), coincident with a time of rapid eukaryotic innovation and the earliest evidence for appreciable primary production by algae. Diverse geochemical and paleontological records argue for a major biogeochemical transition at that time, but whether and how rising biospheric O_2 triggered innovation in eukaryotic life and specifically the emergence of animals is debated. This talk will focus on the transition at roughly 800 Ma from the preceding 'boring billion' to a world with higher but still dynamic levels of O_2. We will emphasize evidence for concurrent biological and environmental change. This comparison reveals temporal and perhaps mechanistic relationships between dynamic biospheric oxygenation and coevolving life, including the early rise of animals. We will speculate on possible relationships between ca. 800 oxygenation and breakup of Rodina and related LIPs activity.

THE DERCETO-KALLISTOS LIP EVENT, LADA TERRA, VENUS

MacLellan L. M.[1], Ernst R. E.[1,2]

[1]*Department of Earth Sciences, Carleton University, Ottawa, ON, Canada*
[2]*Faculty of Geology and Geography, Tomsk State University, Tomsk, Russia*

Keywords: *Venus, planetary geology, flood basalt, Derceto Corona, Kallistos Vallis*

Introduction

Derceto Corona, previously known as Ammavaru Caldera (Lancaster et al, 1995) is an elliptical-shaped corona occupying northern Lada Terra on Venus. It is centred at

-46.8°N latitude and 20.2°E longitude, with a maximum diameter of 200 km along a north-west to south-east axis. We propose that this corona is a part of a regional volcanic event herein termed the Decerto-Kallistos large igneous province (LIPs) event (Fig. 1). This event includes: 1) two stages of flows on the eastern flank of a broad uplift spatially associated with Derceto Corona, 2) the Kallistos Vallis system which begins as a collapsed magma chamber 100 km south-west of Derceto Corona, and which feeds the Ubastet Fluctus (flow field) and 3) a separate flow system that extends from the Corona to the west (outside of the map area shown in Fig. 1).

The two eastern stages of flows and the Kallistos Vallis system are blocked on the eastern side by the pre-existing Vaidilute Rupes (a 2000 km long ridge system), but locally breach it and spread to the east of the ridge.

The order of discussion will reflect the suggested emplacement order of the volcanism, as determined by cross-cutting relationships and morphological characteristics (cf. López, 2011).

Although some of the above-mentioned features have formerly been mapped, they have not previously been considered collectively as an integrated magmatic event. Kallistos Vallis was mapped and determined to be a compound channel by Baker et al (1992), and both eastern stages were mapped by Lancaster et al (1995).

The purpose of this project is to develop a preliminary geological history of the Derceto-Kallistos LIP, and compare it with terrestrial LIPs (Ernst et al. 2019). As the first stage of this research, we provide a detailed map of the important elements of this magmatic system (Fig. 1). Mapping utilizes SAR images from the Magellan mission with a resolution of 100 m/pixel

Stages of Flow Emplacement

Eastern Stage 1

The eastern flank of the Decerto Corona regional uplift is covered by a fan-shaped distribution of lava flows. These flows head downslope toward Vaidilute Rupes and locally breach the ridge from the west side and continued to the east for another 200 km. The overall length of this flow stage is at least 550 km. The flow terrain is characterized as being radar-dark, meaning that it likely pahoehoe basaltic lava, rather than a'a (e.g. Keresztur et al, 2014).

Eastern Stage 1 is also locally overprinted by Eastern Stage 2, particularly on the lower slopes of the uplift. As well, the termination of the radar-dark Stage 1 flows to the east of Vaidilute Rupes is difficult to determine given that the regional plains volcanism is also radar-dark.

Eastern Stage 2

At a lower elevation of the eastern flank of the uplift, there is a stage of radar-bright lobate flows. They appear to be fed from multiple NW to NNW trending grabens that likely represent an underlying regional dyke swarm. Looking at all the individual flows together, a radial trend outward from Derceto Corona is observed.

These Eastern Stage 2 flows are radar-bright and have clear lobate boundaries, so they are easily discernable as a separate unit. Some of these flows breach the Vaidilute Rupes and continue to the east for another 300 km. Throughout their extent the Eastern Stage 2 radar-bright flows are superimposed onto the Eastern Stage 1 radar-dark flows.

Western Stage

A separate stage of radar-bright lava flows extend to the west of the uplift and seem to be fed from individual circumferential grabens (of Derceto Corona)

Kallistos Vallis-Ubastet Fluctus Stage

Kallistos Vallis begins as a collapsed magma chamber 100 km south-west of Derceto Corona. It continues as an anastomosing channel system for 900 km by first progressing south and then east until it reaches Vaidilute Rupes, where it travels north alongside the ridge. It then breaches Vaidilute Rupes (at the same place as both eastern stages) and continues to the east supplying the lava flow field known asof Ubastet Fluctus. This stage also includes channel overflows that are associated with the portion of Kallistos Vallis on the west side of Vaidilute Rupes. In Kargel et al (1994) it is stated that the Kallistos Vallis channel system begins at a topographic high and experiences an elevation drop from 1300 m to 800-900 m. On the steeper slopes, Kallistos Vallis exhibits a series of braids and meandering paths, many terminating or rejoining the main path. After this drop, the terrain flattens into a delta-like feature; this flatter portion of the channel system is associated with the lava overflow outside the channel.

Discussion

Major volcanic features in this northern region of Lada Terra are combined into a single event consisting of the elliptical Derceto Corona, two volcanic stages on the eastern flank of the uplift associated with the corona, one on the western flank and another stage (Kallistos Vallis) emanating from a collapsed magma chamber on the southern flank about 100 km from the corona's centre, and feeding Ubastet Fluctus. This combined magmatic event is inferred to be similar to LIP events on Earth and hence is labelled as the Derceto-Kallistos LIP event. On Earth the plume centre regions are typically deformed and the volcanic material removed by erosion. On Venus, the volcanic features are typically not eroded and so the recognition and characterization of Venusian LIP analogues

provides an opportunity to better understand the primary volcanic patterns in the plume centre region of terrestrial LIPs.

We infer a provisional magmatic history beginning with Derceto Corona (and its associated circumferential graben system) then the three flank eruption stages: two on the east side and one on the west side, and finally Kallistos Vallis and its links with over bank flows and with Ubastet Fluctus.

The setting of Kallistos Vallis is interesting because its source area is the collapsed magma chamber on the flanks of the uplift associated with Derceto Corona, and it can be inferred to be associated with a magma chamber offset from the mantle plume that would be centred under the Corona (cf. plume-related LIP plumbing system model of Ernst et al. 2019).

As noted above, Vaidilute Rupes is a pre-existing ridge system that blocks and deflects lavas of this LIP event and is breached in only one place by Eastern Stage 1, Eastern Stage 2 and the Kallistos Vallis-Ubastet Fluctus flows. The location of this breach is where the Vaidilute Rupes ridge seems offset. This offset and resulting breach may be explained by an approximately 30 km left lateral strike slip fault that predates the Derceto-Kallistos LIP event .

Acknowledgements

LM appreciates the time and helpfulness of Jennifer Lee during the learning curve of using ArcMap for the first time.

References

1. Baker, V.R. et al. 1992. Channels and valleys on Venus: Preliminary analysis of Magellan data. Journal of Geophysical Research 97, 13,421- 13,444.
2. Ernst et al. 2019. A New Plumbing System Framework for Mantle Plume-Related Continental Large Igneous Provinces and Their Mafic-Ultramafic Intrusions. Journal of Volcanology and Geothermal Research (in review)
3. Kargel, J.S. et al. 1994. Carbonate-sulfate volcanism on Venus? Icarus 112, 219-252.
4. Kereszturi, A. et al. 2014. Lava flow. Encyclopedia of Planetary Landforms. 1171-1181.
5. Lancaster, M.G., et al. 1995. Great lava flow fields on Venus. Icarus 118, 69-86.
6. López, I. 2011. Embayed intermediate volcanoes on Venus: Implications for the evolution of the volcanic plains. Icarus 213, 73-85.

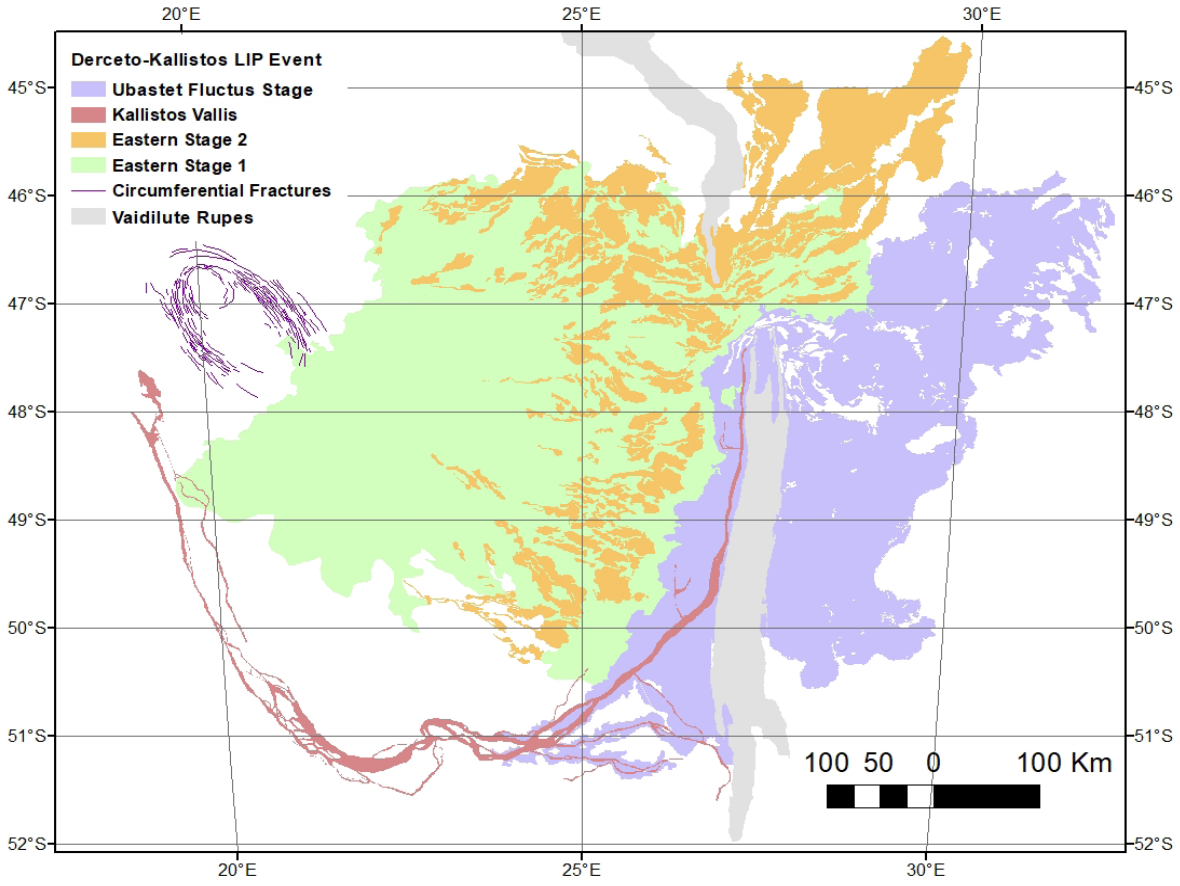


Fig. 1. Preliminary geological map of the Decerto-Kallistos LIP event.

FEATURES OF COMPOSITION AND PLASTICITY OF TWO ASTENOSPHERES OF PLANET EARTH

Manankov A.V.
Tomsk University of Architecture and Civil Engineering, National Research Tomsk State University
E-mail: mav.39@mail.ru

Since ancient times, facts are known about the rapid movement of rock blocks and changes in their properties. The great thinker and politician B. Franklin wrote in 1782 "In my opinion, such changes in the near-surface parts of the Earth could not have happened if the Earth was solid inside. There may be a fluid, denser and heavier than any solid body we know, which could therefore float inside or on top of that fluid. Then the surface of the Earth should be something like a shell, which can be pierced and broken by powerful movements of the fluid on which this shell rests. "

O. Fisher in 1889 in his work "Physics of the Earth's Crust" led the first scientifically based mobilistic ideas in the form of the concept of compression and stretching of the crust. The actual material was the discovery of two global active zones. One of them is the young mountain systems with their corresponding deep-sea depressions and island arcs that surround the Pacific Ocean and stretch across the Himalayas to the Alps and the Mediterranean. The other is the system of mid-ocean ridges (MOR) over land in East Africa, Iceland and in the West of North America. In the first system, the forces of compression and contraction of the cortex predominate, in the second, signs of its stretching and expansion. Both systems have not only global scale, but also cyclic activity and, probably, positive feedback between each other.

The first fairly reasonable ideas about the continental drift are associated with the names of A. Snyder, (1858) and A. Wegener (1912), whose views were developed (G. Baker, J. Darwin, F.B. Taylor, etc.). In 1925, an extended mountain range was discovered in the middle of the Atlantic Ocean. In 1953, physicists M. Ewing and B. Chizen discovered that along the submarine ridges the troughs extend - deep faults in the earth's crust. Somewhat later, G. Hess suggested that the MOR system is an area where a new oceanic crust is constantly being born.

So formed the main manifestation of plate tectonics. The methods were improved, a lot of hypotheses accumulated (about the age of the ocean floor, drift velocity, plate motion parameters, types of boundaries between the plates, on ore deposits above the subsurface zones, etc.), but the mechanism controlling the generation of the Earth's internal heat and plate drift one remained - convection-plume currents in the "subcrustal substrate".

In Russia, for a number of reasons, in the 60-70 s the "continental" thinking continued, therefore a new theory was born here "in spite of". The direction "Underground Thunderstorm" under the direction of physicist A.A. Vorobyov. It was born on the ideas of the Frenchman Georges Dari, expressed in 1885, and academicians V.A. Obrucheva and M.A. Usov (1936-1940). This direction was developed in the works of Professor TPU V.N. Salnikov. We have worked together for many years, obtained new experimental data on the geometry of constructive interference, the effect of which is similar to the effect of proton or impurity or defective superlattices. From a position of quantum-mechanical principles, A.A. Friedman pointed out the possible proton-like structure of the Universe.

Since the end of the 70-/s, E.A. Kozlovsky, A.V. Peive, S.A. Ushakov, V.E. Khain, O.G. Sorokhtin, L.P. Zonenshain, E.G. Mirlin, M.I. Kuzmin, V.M. Moralev, N.L. Dobretsov, L.M. Natapov and others publish results on global tectonics and its connection with mineral resources, mineralogical and petrogenesis. Concerning the reasons for convection, it appeared that it was thermal, according to the principle of V.J. Pfan, or caused by radioactivity. O.G. Sorokhtin and his colleagues developed a mechanism for the chemical- density gravitational differentiation of terrestrial matter in the framework of the first law of thermodynamics.

For more than half a century of the space age, man learned about the structure of the Earth much more than in the entire previous history. A need and opportunity has emerged to develop on a modern scientific basis a conceptual theory of the geodynamics of the Earth. In recent years, progress has been made in the synthesis of Euclidean and non-Euclidean representations of space. We are engaged in the theory of geodynamics of the Earth since the early 70-s of the twentieth century based on the concepts of spatially closed dynamic structures (CDS), which are a function of the autointerference of wave perturbations of space. The space is structured by areas of constructive and destructive interference. Areas of constructive interference exhibit signs of matter. By themselves, areas of constructive interference are coherent, but differing in phase and field sources. This "secondary" field creates its own interference grid both within the system and in its immediate environment, identical to those that arise in the fractal theory. The interaction of areas of constructive interference ultimately generates the interference structuring of the following hierarchical levels of space and defines a single mechanism for the formation of real dynamic systems of any scale. In this sense, the most striking manifestations are visible in the periodic structures of metals. But the internal structure of the planet, its relief and the location of planets and even galaxies are the result of resonating interference patterns of various hierarchical levels.

So, the geoid of the Earth and the surrounding air sphere (ionosphere) is a giant spherical resonator. The first to discover the low and ultra-low electromagnetic pulsations of the Earth's atmosphere, Nikola Tesla, then the physicist V.O. Schumann and doctor G. Koenig. They proved that in the Earth's atmosphere there are standing electromagnetic waves called "Schumann waves". These waves are the natural electromagnetic frequencies of the Earth. One of them, the main one, is on average 7.8 Hz. And yet, with these resonances in a new way, we need to approach the concept of "self-organization" and the knowledge of the limits of self-organization.

The principles of CDS have found application in crystallography of real crystals, in technical mineralogy and materials science in the management of material properties.

When applied to a geoid, firstly, the system under study

is complicated; it includes, in addition to the lithosphere and the mantle, all internal and external geospheres. Secondly, all CDS are the functions of the autointerference of the wave disturbances of space. The condition for the occurrence of autointerference is the Poynting vector closure. The most adequate mathematical apparatus for describing closed dynamic structures is the torus geometry, which interprets the Clifford surface. Thirdly, the transfer of matter in the torus space occurs along closed trajectories, when the torus rotates the inversion from the outside to the inside and from the inside to the outside. This transfer causes the birth and growth of all internal coordinated closed spaces (geospheres) and allows (taking into account the change in the size of the geoid) to simulate the dynamics of continental drift.

Modern resonant field theory of geodynamics. Near the center of the torus, the speeds of motion of the substance are maximum, and to the periphery they fall to a minimum, like the structure of a tornado. Therefore, intensive movement here under the action of both longitudinal and transverse vibrations unambiguously leads to the formation of gaps and the dismemberment of the shells. The wave (holographic) nature of tectonic activity, geodynamics is reflected in the structuring of the earth's crust and other geospheres. With the addition of vibrations, the method is used by A. A. Lissajous.

Based on the behavior of the geoid's own long-period oscillations, a rheological model of the Earth was created, in which two asthenospheric intervals were identified:

1) at depths of 10 – 225 km (belt B ");

2) 2700 - 2885 km - boundary layer D "between the lower mantle and the outer core, which should be reflected in the fundamental features of geodynamics, starting with the mechanisms for generating the internal heat of the planet.

Basalts are presumably in the molten state in the upper mosaic-discontinuous asthenosphere B", since their melting points are lower than those of peridotites, which are here in the solid state. Basaltic magma smelting takes place in the process of partial melting of typical mantle rocks, harzburgites, verlites, etc. The smelting composition is determined by the chemical and mineral composition of the protolith by physical and chemical melting conditions, the degree of melting and the melting mechanism. According to experimental data, the melting points of silicates in the presence of water have a minimum in the pressure range of 500–1000 MPa.

In the lower asthenosphere belt D", the melt is represented by iron in low spin states (at temperatures below 2200 K) in a silicate matrix of ferripericlase (Mg, Fe) O and (Mg, Fe) SiO_3 with a perovskite structure. The asthenosphere behaves as an overheated and extremely viscous fluid, where an increase in electrical conductivity and a decrease in the velocity of seismic waves, indicating the manifestation of its plasticity.

For a long time (before Maxwell's theory), the plasticity of the asthenosphere was largely hypothetically explained by the fact that the substance is either in an amorphous state or in a semi-molten state. In geological sections, the manifestation of the plastic properties of rocks, starting with the micro level in the form of flow patterns in olivine crystals and up to various folds, diapirs is a confirmation of this. The theory of electromagnetism of Maxwell received full experimental confirmation and became the generally accepted classical basis of modern physics and should be used by geodynamics. The role of this theory was vividly characterized by A. Einstein: "... there was a great turning point, which is forever associated with the names of Faraday, Maxwell, Hertz. The lion's share in this revolution belongs to Maxwell. After Maxwell, physical reality was conceived in the form of continuous fields that could not be mechanically explained ... This change in the concept of reality is the most profound and fruitful of those that physics has experienced since Newton. " Therefore, from the position of the Maxwell relaxation time τ (reaching equilibrium of the system), the effect of plasticity becomes possible under the condition that the time of action of forces t exceeds many times τ:

$$t >> \tau.$$

With dynamic compression over a geological time in excess of about 30,000 years, under the effect of all-round pressure at depths where the pressure is weaker than temperature (close to the liquidus), any hard part of the lithosphere is able to experience a flow like a viscous fluid.

Potential mechanisms for the generation of internal heat on the new model. The proposed theory allows the problem of energy sources to be solved at the modern level due to a whole range of new mechanisms instead of convection and plumes: 1) Subastospheric hot spots; 2) Electron-gas; 3) Comet-asteroid; 4) Friction heat of liquant in the outer core during the rotation of the Earth; 5) The heat of gravitons and nucleons based on analogies between electromagnetic and gravitational fields, generating proton purge.

TRIGGER EFFECTS OF GEODYNAMICS AND GLOBAL TOXICATION OF THE ATMOSPHERE

Manankov A. V.

National Research Tomsk State University,
Tomsk University of Architecture and Civil Engineering,
E-mail: mav.39@mail.ru

The concepts of trigger effects developed in studies of the formation and development of the geodynamics of the lithosphere encompass a wide range of phenomena considered by tectonophysics, geomechanics, geodynamics, planetology, petrology, geochemistry and other sciences. But such approaches are not yet properly implemented. The empirical connections of magmatism and mineralization in most cases have exhausted their capabilities and do not help to isolate metallogenic taxa of various ranks, therefore, under the influence of mobilistic hypotheses, models of magmatic and ore formation are actively developed in connection with plume tectonics. The lack of ideas is due to the fact that the place and mechanism of energy generation for plumes has not changed for a long time. These were convection-plume foci in the "subcrustal substrate". For more than half a century of the space age, man learned about the structure of the Earth much more than in the entire previous history. A need and opportunity has emerged to develop on a modern scientific basis a conceptual theory of the geodynamics of the Earth, an alternative to convection-plume.

The end of the twentieth century coincided with an awareness of the physical limitations of Euclidean space, a serious transformation of science from discrete-atomic (traditional) Platonic to a holistic resonant-field Aristotle, where the shape of the systems is of fundamental importance. But the Earth sciences and its methods, including mineralogy under high T-P conditions, astromineralogy, deep geoelectrics, seismic tomography, are developing, resulting in a complicated geosphere structure for continental, island arc and oceanic conditions. The effects of phase transitions in the main pyrolyte minerals have been established:

1) the transformation of orthopyroxene (the elastic limit is 6, 7 ± 1 GPa) into a high-density garnet polymorph - majorite at 13.5 ± 1 GPa,

2) phase transition of g-olivine to perovskite – magnesioviustite at 23.3 GPa,

3) the process of melting clinopyroxene at 75-80 GPa (~ 2000 km).

On this basis, many models have been built, in which two fault zones in the already three-layer mantle are identified, the possibility of separation of currents with separation of convection in the upper and lower mantles, as well as changes in the convection speed at a depth of 410 km and at a depth of 660 km, the selection of single-layer and two-layer convection.

In search of a new paradigm, we turned to elliptical ideas about space, based on the ideas of B. Riemann›s geometry, which was used to create the general theory of relativity (GTR). As a result, a holographic model of matter (SMW) was formed, where a torus acts as a space with a curvature. The shape of the torus in the Euclidean space is represented by the convolution of the right circular Clifford cylinder in the Riemannian space. It is significant here that the Clifford cylinder is interpreted as a Euclidean plane, therefore the geometry of the torus is the most adequate mathematical apparatus for describing the closed dynamic structures (DPS) of various hierarchical levels. Our model does not deny the essence of the approaches from the perspective of Euclidean Principles, it turns them into special cases, as it happened in general with I. Newton mechanics in the framework of A. Einstein's quantum mechanics. In this article, from this point of view, the capabilities of the geodynamics of the Earth, whose geoid as a complex megasystem, includes all the geospheres of the planet, as well as its application for the geochemical evolution of the atmosphere, are shown.

The transfer of matter in the torus space occurs along closed trajectories, when the torus rotates the inversion from the outside to the inside and from the inside to the outside. Such a transfer causes the nucleation and growth of the internal coordinated closed spaces (geospheres) and allows (taking into account the change in the size of the geoid) to simulate the dynamics of continental drift. As a result, a central, relatively compact, but most difficult core core of the planet due to the vortex separation of matter was formed during the first 500-600 Ma. The core of the planet, which in the limiting case of symmetry, can have a close to spherical shape and heterogeneous composition. The structure of the central part (in any case) and the gravitational-kinetic interaction in the system determine its unambiguous correspondence with the structure of the upper shells of the planet, as well as the ongoing and ongoing emergent transfer of matter and energy, capturing both internal regions and surface arrays (subduction, spreading, continental drift) as well as upper geospheres.

From the position of elliptical geometry, the traditional theories of the Earth's formation are not quite correct, because they do not take into account the kinetic features. The nature of the motion of matter at the initial stages of accretion must correspond to the structure of the closed space formed by the parallel transfer of torus surfaces, as a result of which the condensed body is formed in the form of a polar or Equatorial torus. Equatorial Thor protoplanetary substances evolyutsioniruet, forming topolcianky Central (the Sun) polar tor. In accordance with this, the formation of planets in the closed toroidal space of the Solar system, according to this concept, is separated from the appearance of the Sun for a significant time period. The set of real flows of protozemals in the form of an Equatorial torus retains its helical character in the formation of a compact polar torus, the product of the evolution of which at a certain stage is the planet Earth.

Structuring of spatially closed objects, i.e. having quite definite boundaries, is connected with interference of wave oscillations of different nature. Thus, in a body with a shape close to spherical, which is a planet, elastic waves of arbitrary direction as a result of multiple reflections from the surface turn into tangential, propagating in opposite directions. The presence of two traveling waves predetermines the formation of standing waves with areas of compression and stretching. The position of these areas is determined mainly by the geometry of the sphere and is manifested in two global structures:

1) stretching of the ocean floor and the formation of the basalt oceanic lithosphere (COX),

2) lineaments under the action of compression forces.

The addition of oscillation used in the method of W A. Lissajous. The earth's crust, like other geospheres, being bounded on both sides by a substance with sharply different dispersion properties, is a waveguide for tangential seismic oscillations. The presence of six continents and four oceans on the planet Earth now is the result of a quark-like three-loop self-interference of the main mode of transverse oscillations of the earth's crust. The directions of movement of its plates correspond to at least two successive turns on the surface of the polar torus, manifested in the Cenozoic in the form of continental groups and two systems of oceanic faults.

Trigger effects, set and projected for the first hundred years of studying the drift of the plates.

1) Seismotomographic models made it possible to clarify the deep Petrology of the geoid at depths up to 310 km. At a depth of 100 km, the upper mantle is heated under the boundaries of the plates, and especially under the COX (where seismic velocities are low). On the contrary, under the continents the upper mantle is cold. At a depth of 310 km there is no correlation with surface tectonics. The amplitude of anomalies below 300 km is significantly reduced. In subduction zones, seismic velocities are increased (cold plates are immersed in the mantle). Only SOH is still a slower speed.

2) In the process of spreading through the rift zones of the geoid, basitic magma rushes to the surface, creating mid-ocean ridges (COX) and there is a pushing of the young seabed sections lying on both sides of the trench (divergence).

(3) Along island arcs and continental margins, linear signs of compression and subduction (subduction) of oceanic plates of the lithosphere to depths of at least 700 km (convergence) are assumed.

4) Within the active structures of the lithosphere occur

earthquakes, volcanic eruptions and juvenile removal of fluids with ore (black, gray smokers) and hydrocarbon (white smokers) components.

5) When high-speed tectonomagmatic phenomena, followed by a release of huge masses of seismic energy ("underground storm"), as a result of the dispersion and phase transitions in minerals, the rocks are generated by electric radiation and anomalies: (lightning, Catatumbo), electromagnetic (plasma sprites, St. Elmo's fire) and low frequency (below 25 Hz) acoustic (sound of Whistler, triboluminescence, sonoluminescence).

6) the influence of wave processes excited by strong catastrophes on the state of the surface atmosphere was Found: before the earthquake in the form of anomalous aerosol fields, resulting in heating of the atmosphere and a sharp change in its parameters. And after disasters – necessarily concomitant cold snap with progressive growth, which develops the law F. Omori 1984

7) Lowering the temperature of the atmosphere can be determined by the amount of oxygen, and the decrease in its energy is due to the removal of energy from the tectonosphere. It is estimated that this effect is not small, especially in conjunction with the effect of emanation from the active zones of the planet impressively huge masses of dusty plasma, carbon oxides, nitrogen and sulfur. Their number should be taken into account in the Geology of sedimentary facies and the atmosphere, as well as in the assessment of these pollutants in the formation of the greenhouse effect and global warming.

In recent years, a deep study of dust and gas clouds in the atmosphere, the properties and processes occurring in it from the point of view of nanoscale physics. A model describing the processes of motion of fine dust particles in the plasma of dusty atmosphere from the position of the wave theory is created and the possibility of the existence of dusty sound solitons in it is shown. Registered pollutants are dielectrics capable of long-term polarization to become a source of electric field, called electret. The theoretical prediction of electret in nature was made by the English physicist O. Havisaid in 1896, and their experimental discovery was made by the Japanese physicist M. Eguchi in 1920, he also proved their relevance to the new technology. Among the electrets established the following genetic types: mechanoelectrets, termoelectrects, electroelectrets, photoelectrets, radioelectets, triboelectrets and plasmoelectrets. According to the structural characteristics of the electret belong to different molecular groups of dielectrics: 1 group – N_2, H_2, O_2, CO_2, CH_4...; the second group – CO, SO_2, H_2O, NH_3; the third group – inorganic dust. According to these groups, there are three types of polarization. The measure of polarity is a physical quantity called the electric moment. This parameter is an important parameter of electrets, it is also responsible for the geometric structure of molecules. Thus, the CO_2 molecule is nonpolar, and the SO_2 molecule has the electric moment of the dipole. This means that the CO_2 molecule has a linear structure, and the electrets of SO_2 molecules have angular structure.

The investigated number of substances has been studied for a long time, and not by chance. It began with the discovery of explosives and smoky (black) gunpowder. The latter consists of a fine mixture of three substances: coal, sulfur and potassium nitrate (nitric acid salt), Under the action of a spark in a closed volume, this mixture explodes, and this is a model of an underground thunderstorm. Nitric acid is formed by reaction of nitrogen dioxide with nanocapillary water squeezed from the compacting of the rocks. This process is studied experimentally.

From the theoretical sphere of the main electrets rapidly moving into a new technique. Thus, CO_2 lasers are among the most powerful lasers. Now in their family already seven types of. Sulfur as photoelectret widely used in Electrophotography. The emergence of, for example, seismotomography determined the transition of Geophysics and geodynamics to a new level. In the mid-80s deep geodynamics was born, which became the youngest and most promising direction in Geoecology and in General in the earth Sciences.

TWO GENETIC TYPES OF METALLOGENIC ZONES IN WAVE GEODYNAMICS

Manankov A. V.

National Research Tomsk State University, Tomsk University of Architecture and Civil Engineering,
E-mail: mav.39@mail.ru

There are not many publications in which the achievements of the theory of tectonics of lithospheric plates would be sufficiently fully used in analyzing the metallogeny of the well-known mining provinces of the World and clarifying the genesis of many types and known mineral deposits. Among foreign publications are the books of A. Mitchell and M. Garson [1984], R. Sillitoe [1974], F. Saukins, P. Lazniski. In Russian literature, these are the works of P. Zonenshayn [1976], N.L. Dobretsov [1980, ets.], O.G. Sorokhtin [1985, 2010], A, A. Kovalev [1978, 1994], A.A. Kovalev, E.I. Leonenko [1992, 1993] et al. An obvious systematic flaw is the presence of two metallogenies, i.e. endogenous and exogenous. Until recently, there is a perception that endogenous minerageny is very far behind the level of exogenous minerageny. It seems to me the situation is different. Mineralogs and petrologists led by Acad. D.S. Korzhinsky created a scientific foundation of acid-base interaction, mosaic equilibrium for open systems, which has not yet been assimilated, including by hypergenic tectonists. And the desire of petrologists, beginning with Baddington, Groot, to link the features of mineralization with the petrography of magmatites turns out to be unpromising. It is necessary to know the features of all objects, including the composition of magmatites, the degree of their contamination, the role of host rocks, their composition, age, tectonics, and their dynamics in the geotectonics of the territory.

For more than half a century of the space age and the achievements of experimental mineralogy, man learned about the structure of the Earth much more than in the entire previous history. A need and opportunity has emerged to develop on a modern scientific basis a conceptual theory of the geodynamics of the Earth, an alternative to convection-plume. In this report, within the framework of the modern theory of resonant field geodynamics, the wave-particle duality is analyzed and features of the distribution of ore and hydrocarbon metallogenic belts, their types and deposits in spatially closed dynamic structures are established.

Our distant ancestors did not even guess what the planet looked like. In ancient philosophy, there are several "first" who have declared that the earth is spherical and that its place is in the middle (of the whole). According to various sources, this is Anaximander of Milles or Pythagoras, or Parmenides, or Hesiod. Representations of the ancient Greeks from the VI. BC. about the universe with a spherical Earth in the center summarized in the II century Alexandrian astronomer Claudius Ptolemy. Isaac Newton concluded that the Earth rotates and is under the influence of inertia. This force is great at the equator, but absent at the poles, so the Earth, according to Newton, was not a sphere, but a compressed ellipsoid. Scientists are divided into two camps - the British were for the "flattened" Earth, the French - for the elongated.

The earth is a sphere and it spins - these are two fundamental facts from the establishment of which the science of the Earth began. In 1872, the German mathematician I. Listing called the shape of the Earth "geoid", which means "earth-like." The name is very capacious: no matter how the ideas about the shape of the planet change, the "geoid" will always be. In 2011, scientists built a very accurate geoid model using the GOCE probe information; according to new data, it was updated already in 2014.

From the position of resonance field geodynamics developed by us for a geoid, the most adequate mathematical apparatus for describing closed dynamic structures (CDS) is the torus geometry (Fig. 1).



Figure 1. The surface of the planet Earth in the shape of a torus

Peculiarities of substance transfer in torus space makes it possible to expand the system, study all subordinate geospheres, including the core, simulate the drift dynamics of plates in space – time, and also understand the mechanism of geoid elongation to the north pole.

Geoid oscillations are described by spherical harmonics. The latter can always be expanded in a natural orthogonal basis and, in some approximation, for ease of analysis, consider separately one or another type of oscillation. The natural basis for a geoid is the directions of radial and tangential oscillations, which can also be decomposed into orthogonal, within a separate shell. It is important to emphasize that the role of radial oscillations in the formation of the shell structure may be decisive.

The above consideration reveals in general terms the mechanism of the formation of the inner shells of celestial bodies, but it cannot, of course, be exhaustive. The fact is that the approximation of radial oscillations is essentially one-dimensional and does not cover the essential details of the phenomenon. The radial oscillations themselves can be described by a combination of (in principle, infinite) Cartesian orthogonal components.

Each inner layer and the crust of the planet, being bounded on both sides by a substance with sharply different dispersive properties, constitute a waveguide for tangential seismic vibrations. The structure of stresses for the lowest mode of tangential oscillations of a spherical shell is in many respects similar to the structure of an electromagnetic field, if we consider oscillations of the transverse type. Longitudinal waves, of course, complicate the overall picture. Nevertheless, the presence of six continents and four oceans on our planet corresponds just to the quark-like three-loop self-interference of the main mode of transverse oscillations of the earth's crust (Fig. 2).

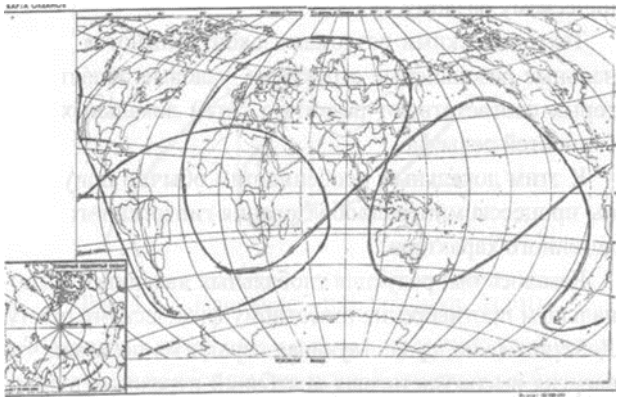


Figure 2. Three-loop self-interference of the main mode of transverse oscillations of the earth's crust

The earth's crust as a whole and its individual parts within their borders are waveguides for tangential vibrations. For the first time M.V. Lomonosov identified four forms of deformation of the earth's crust and saw in each wave nature. At the same time, long-period excitations have low attenuation and are able to accumulate in the form of antinodes, mechanical stresses and deformations. In the global zones of spreading, against the background of compression forces, powerful protonation is accompanied, accompanied by white and gray sulphate smokers, and the maturation of metallogenic zones of hydrocarbon raw materials, including gas hydrate (MZ of the UVS) (Fig. 3).

The map must be supplemented with metallogenic zones (MZ) of the second-type UVS formed on the continents. For example, on the territory of the Western Siberian platform, the MZ of the UVS is confined to the S-shaped nodal line, decorated by the valley of the Ob River, where there is a second harmonic node near Surgut and the hydrocarbon mega-deposit.

Two types of ore metallogenic zones (RMZ) are also distinguished. The first is confined to the global mid-ocean ridges (MOR), in the form of linear, grandiose submarine ridges created by the spreading of the ocean floor, where tensile and expansion forces prevail with a speed of up to 16 cm / year. This type is represented by the following formations: copper-zinc-pyrite, pyrite-polymetallic, ferric oxide, manganese oxide. They first discovered in black smokers. Genetically, this form of RMZ is a product of fluid processing (with the participation of micro-

organisms, of which 8 are still unknown) at E = 300-400 ° C, iron-rich depression basites of MOR.

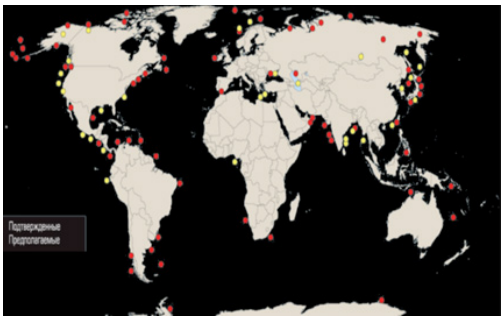


Figure 3. Circles - deposits of hydrocarbons and gas hydrates located within the global active subduction zones and nodal lines delineating the continents (shelf deposits of the Arctic)

The second type of RMZ is manifested as if in parallel, according to another vector of bifurcation with respect to the second-type MZ. The process begins with the regional supergene kaolinization within the continent, followed by large-scale diffusion and infiltration differentiation, and results in the formation of deposits oolite goethite-leptohlorit ore (the largest in the world Bakcharsky pool), zircon, ilmenite deposits (Tarskoe, Tuganskoe, Georgievskoe) deposits kaolinite not until the end of the studied manifestations of gold, rare-earth, radioactive elements, etc. At the same time, in the nodal zones such sedimentary deposits, being affected by physicochemical barriers formed metamorphic (glandular quartzite) and contact- metasomatic iron-gold ore and other deposits. Here, in contrast to the submarine MZ, the spatial and temporal timing of the formation of the MZ of the UVS and RMZ turns out to be completely natural.

SULFIDES OF IVAKINSKY FORMATION BASALTS, NORIL'SK ORE DISTRICT: REVISITED

Marfin A. E.[1,2], Yakich T. Yu.[3], Abersteiner A.[4], Ivanov A. V.[1], Kamenetsky V. S.[2,4]

[1]*Institute of the Earth's Crust, Siberian Branch of the Russian Academy of Sciences, Irkutsk, Russia*
[2]*Institute of Experimental Mineralogy, Russian Academy of Sciences, Chernogolovka, Russia*
[3]*Tomsk Polytechnic University, Tomsk, Russia*
[4]*School of Natural Sciences, University of Tasmania, Hobart, Australia*

Keywords: *sulfide Cu-Ni-PGE ore, Noril'sk, Siberian Traps, Ivakinsky trachybasalt, liquide immiscibility, metasomatism*

Introduction

The study of Cu-Ni-PGE deposits in northwestern Siberia is important due to the presence of large economic reserves and their spatial-genetic association with The Siberian Traps. This paper examines sulfide mineralization, which sometimes occurs in volcanic rocks of the Ivakinsky formation, which are located beneath the Norilsk-1 intrusion.

Geology. The Ivakinsky formation lies above the Tunguska series. It consists of two basalt packages which are separated by a layer of tuffs. Subalkaline basalts, trachybasalts, and tuffs represent the formation (Rudakova and Krivolutskaya, 2009). A part of the Norilsk-1 intrusion emplaced into the Ivakinsky formation basalts.

Geomagnetic data. The Ivakinsky formation has reverse polarity, and the differences in polarity in the upper parts of the formation are usually used as a marker of the Permian-Triassic boundary (Lind et al., 1994). The transitional zone, during which the polarity reversed, covers an interval ranging from the Syverminsky to the middle of the Nadezhdensky formations and is several thousand years in duration (Pavlov et al., 2019). Paleomagnetic characteristics of the Norilsk-1 intrusion correspond to those obtained for the rocks from the boundary between the Morongovsky and Mokulaevsky formations (Pavlov et al., 2019). Thus, the period between the Ivakinsky formation volcanism and the emplacement of the Norilsk-1 intrusion was tens, and possibly the hundred thousands of years.

U-Pb data. The age of the Norilsk-1 intrusion was determined with great accuracy by the U-Pb method on zircon and baddeleyite and, according to the latest data, is estimated to be 251.64±0.10 – 251.907±0.067 Ma (Burgess and Bowring, 2015).

Results

Samples. During study of the Norilsk-1 deposit, samples of the Ivakinsky formation were obtained. A few samples contain sulfide mineralization (Fig. 1). According to major and trace element data, the studied samples correspond to those described earlier (Lightfoot et al., 1993; Wooden et al., 1993). The only significant difference is the high contents of copper and nickel in sulfide-bearing samples.

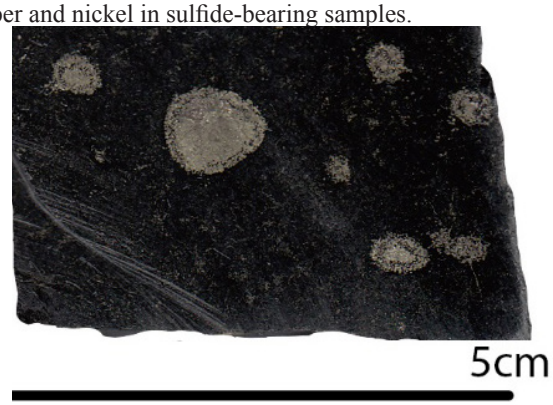


Figure 1. Sulfide globules in the Ivakinsky trachybasalt.

The sample is composed of plagioclase (35%), biotite-chlorite aggregates (50%), sulfide, Fe- and Ti-oxide ore minerals (15%). In thin section, pyroxene is observed in sulfide globules and in groundmass. The structure is patchy. Volcanic glass has been completely altered to chlorite (Fig. 2).

Sulfide globules contain large amount of inclusions; namely, pyroxene (Fig. 2), amphibole, ilvaite, ilmenite, apa-

tite, calcite, magnetite, pseudobrookite, PGE minerals, SiO_2 etc. (Fig. 3 a,b,c). SiO_2 associates with ilvaite and probably is due to decomposition of this mineral. Noble metal minerals are menshikovite, sobolevskite, sperrylite and native gold with admixture of silver.

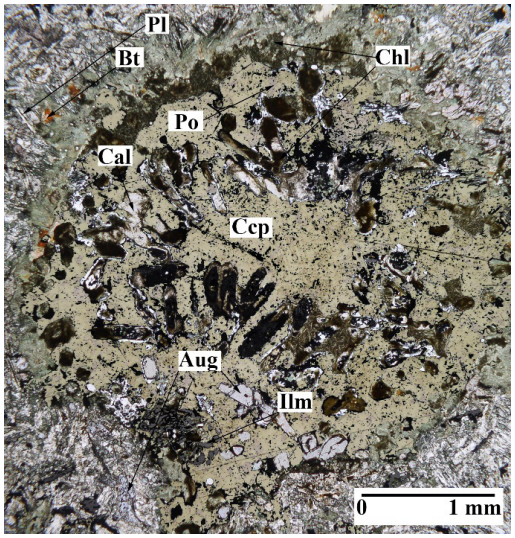


Figure 2. An example of sulfide globule in a thin-section under a polarized microscope. The image is a combination of transmitted and reflected light. Ccp – chalcopyrite, Po – pyrrhotite, Ilm – ilmenite, Aug – augite, Pl – plagioclase, Chl – chlorite, Cal – calcite.

The genesis of these sulfide globules was discussed in detail by (Spiridonov et al., 2015), who suggested that sulfide melt infiltrated from the overlying intrusion into the vesicular trachybasalts of the Ivakinsky formation (see Fig. 2., p. 406 in Spiridonov et al., 2015). However, our data does not support this hypothesis because network of sulfide veins infilling vesicles is not observed. We suggest that these sulfide globules were rather formed from Ivakinsky trachybasalt melt itself.

Conclusions

The timing between effusive and intrusive magmatism was tens, and possibly hundred thousands of years apart. The shape of sulfide globules in the Ivakinsky trachybasalt, composition of sulfides and their mineral inclusions indicate in-situ sulfide-silicate liquid immiscibility. The idea of the sulfide liquid supply from Norilsk-1 requires re-evaluation.

Acknowledgements

The study has been conducted under RSF grants №16-17-10068 and 16-17-10145.

References

1. Burgess, S.D., Bowring, S.A., 2015. High-precision geochronology confirms voluminous magmatism before, during, and after Earth's most severe extinction. Science Advances 1, e1500470.
2. Lightfoot, P., Hawkesworth, C., Hergt, J., Naldrett, A., Gorbachev, N., Fedorenko, V., Doherty, W., 1993. Remobilisation of the continental lithosphere by a mantle plume: major-, trace-element, and Sr-, Nd-, and Pb-isotope evidence from picritic and tholeiitic lavas of the Noril'sk District, Siberian Trap, Russia. Contributions to Mineralogy and Petrology 114, 171-188.
3. Lind, E.N., Kropotov, S.V., Czamanske, G.K., Gromme, S.C., Fedorenko, V.A., 1994. Paleomagnetism of the Siberian flood basalts of the Noril'sk area: a constraint on eruption duration. International Geology Review 36, 1139-1150.
4. Pavlov, V.E., Fluteau, F., Latyshev, A.V., Fetisova, A.M., Elkins Tanton, L.T., Black, B.A., Burgess, S.D., Veselovskiy, R.V., 2019. Geomagnetic secular variations at the Permian Triassic boundary and pulsed magmatism during eruption of the Siberian Traps. Geochemistry, Geophysics, Geosystems.
5. Rudakova, A., Krivolutskaya, N., 2009. Structural and textural specific features of rocks of Trap Rock Association in the Norilsk Trough (NW of Siberian platform). Moscow University Geology Bulletin 64, 364.
6. Spiridonov, E., Kulagov, E., Serova, A., Kulikova, I., Korotaeva, N., Sereda, E., Tushentsova, I., Belyakov, S., Zhukov, N., 2015. Genetic Pd, Pt, Au, Ag, and Rh mineralogy in Noril'sk sulfide ores. Geology of Ore Deposits 57, 402-432.
7. Wooden, J.L., Czamanske, G.K., Fedorenko, V.A., Arndt, N.T., Chauvel, C., Bouse, R.M., King, B.-S.W., Knight, R.J., Siems, D.F., 1993. Isotopic and trace-element constraints on mantle and crustal contributions to Siberian continental flood basalts, Noril'sk area, Siberia. Geochimica et Cosmochimica Acta 57, 3677-3704.

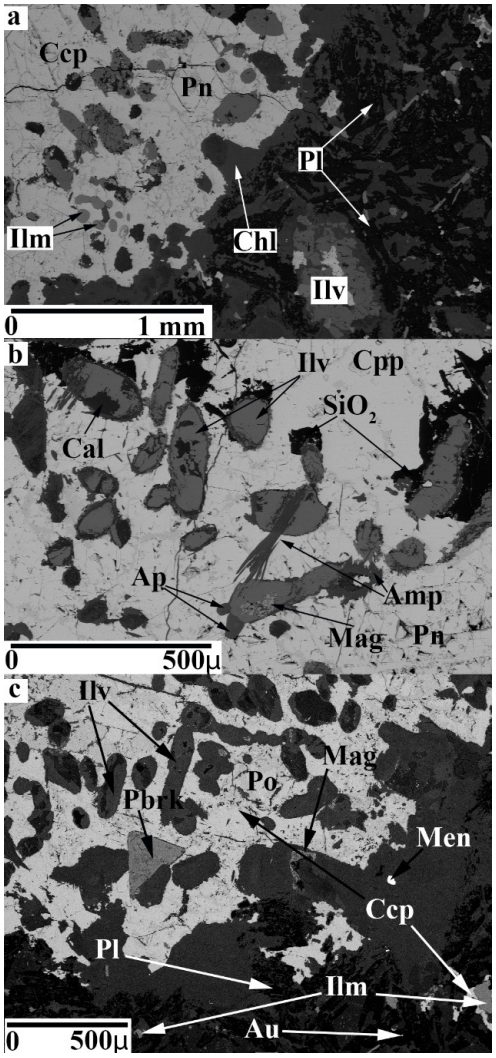


Figure 3. Back-scattered electron (BSE) images of a typical sulfide globule. Ccp – chalcopyrite, Pl – plagioclase, Chl – chlorite, Ap – F-apatite, Amp – amphibole, Cal – calcite, Pn – pentlandite, Ilv – ilvaite, Men – menshikovite, Pbrk – pseudobrookite, Au – gold, Mag – magnetite, Ilm – ilmenite

HIGH-FERROUS OLIVINE IN ECLOGITE FROM KIMBERLITE PIPE UDACHNAYA: METASOMATIC TRANSFORMATION OF ECLOGITE TO PYROXENITE-PERIDOTITE

Mikhailenko D.[1], Korsakov A.[1], Golovin A.[1], Rezvukhin D.[1], Aulbach S.[2]

[1]*Sobolev Institute of Geology and Mineralogy, Russian Academy of Sciences, Novosibirsk, Koptyuga aven. 3, 630090, Russia*
[2]*Institut für Geowissenschaften, Goethe-Universität, Frankfurt am Main, Germany*

Keywords: *Olivine; Eclogite; Kimberlite.*

Introduction

Diamond-bearing mantle eclogites present best examples of deepest metamorphic rocks with typical Ultra High Pressure minerals - diamond and coesite. Mixed paragenesis mineral inclusions in diamond were described in many kimberlite pipes (Wang 1998; Ragozin et al 2006). The coexistence of a SiO_2-phase and harzburgitic garnet or olivine within one diamond could indicate repeated stages of diamond growth, connected with a strong change in chemical environment (Stachel et al., 1998). Herein we present results of our ongoing research investigation of diamondiferous eclogite with coesite and olivine.

Results

In hand specimen Uv-09-537, eclogite are coarse-grained, consisting of 40% garnet, 50% clinopyroxene and 10% coesite. Accessory minerals include diamond, diopside, sodalite, phlogopite, plagioclase, coesite/quartz, olivine and potassium feldspar. Garnet grain show distinct chemical zonation. Chemically homogeneous core is surrounded by the rim with significantly different composition. MgO content increases from 19.2 wt% to 13.3 wt. % and FeO decreases from core to rim from 16.1 wt. % to 10.5 wt. %. Clinopyroxene is omphacite with admixture of K_2O up to 0.3 wt%. Olivine occurs as rare grains up to 60 μm along grain boundaries between garnet and omphacite, and it was never found in direct contact with coesite. The chemical composition of olivine is significantly differs from olivine of lherzolite paragenesis. Forsterite content is very low (#69-76). It contains the no admixture of NiO, but that of MnO (0.7 wt%), CaO (0.3) and P_2O_5 (0.7 wt%). Core part of garnet show typical Rare-Earth Elements (REE) patterns with decrease from medium REE (MREE) toward the light REE (LREE). In the same time, rim part of garnet shown REE patterns with progressive decrease from HREE to LREE. Concentrations of MREE elements in rim part are significant low that in core part of garnet. According to Jerde et al. (1993), these REE patterns can be result of partial melting of eclogite.

Conclusions

The presence of olivine in association with coesite, two generations of clinopyroxene, diamonds located in the interstitial space and zoned garnet testify for the complex history of the formation of the sample. Reactions of olivine formation and replacement primary of eclogite mineral assemblages can be summarize is follow: (i) Coe +1/6K2O +1/12Prp + 1/12Grs = 1/3Kfs + 1/4Di; (ii) Coe + 2/9K2O + 2/9Prp = 4/9Kfs + 1/3Fo (Safonov and Butvina, 2016).

The formation of Mg-rich olivine core, sodalite and phlogopite is likely related with partial melting of garnet/omphacite due to interaction with primary kimberlite melt enriched in alkaline-chloride components (K-Na and Cl). This metasomatic interaction may transform primary eclogite to pyroxenite-peridotite. The formation of Fe-rich olivine is not connected with Siberian flood basalts as was suggested Sobolev et al. (2015). Crystallization of Fe-rich olivine is likely occur during transporting of eclogite xenolith by kimberlite melt.

Acknowledgements

The study was supported by grant of RFBR (№18-35-00219, 18-05-00643 and 18-35-20072).

References

1. Wang, W. (1998) Formation of diamond with mineral inclusions of “mixed” eclogite and peridotite paragenesis. Earth and Planetary Science Letters. 160:831-843.
2. Ragozin, A., Shatsky, V., Zetgenizov, D., Mityukhin, S. (2006) Evidence for evolution of diamond crystallization medium in eclogite xenolith from the Udachnaya kimberlite pipe, Yakutia. Doklady Earth Sciences. 407:465-468.
3. Stachel, T., Harris, J., Brey, G. (1998). Rare and unusual mineral inclusions in diamonds from Mwadui, Tanzania. Contributions to Mineralogy and Petrology, 132:34-47.
4. Safonov, O., Butvina, V. (2016) Indicator reactions of K and Na activities in the upper mantle: natural mineral assemblages, experimental data, and thermodynamic modeling. Geochemistry International, 54:858-872.
5. Sobolev, N. V., Sobolev, A. V., Tomilenko, A. A., Batanova, V. G., Tolstov, A. V., Logvinova, A. M., Kuz’min, D. V. (2015) Unique compositional peculiarities of olivine phenocrysts from the post flood basalt diamondiferous Malokuonapskaya kimberlite pipe, Yakutia //Doklady Earth Sciences. V. 463. №. 2. P. 828.

SURFACE AND SUBSURFACE DESCRIPTIONS OF THE EARLY JURASSIC KAROO DOLERITES: TOWARD A COMPREHENSIVE UNDERSTANDING OF THE EMPLACEMENT MECHANISM AND POSSIBLE GAS MIGRATION

Muedi T.[1], de Wit M. J.[2], Linol B. [2], Nengovhela V.[2], Dhansay T.[1],

[1] *Thomas Muedi, Council For Geoscience, 280 Pretorius Street, Pretoria, 0184*
tmuedi@geoscience.org.za\thomas.muedi@nmmu.ac.za
[2] *Nelson Mandela Nelson Mandela University, P.O Box 77000, Port Elizabeth, South Africa.*

Keywords: *Geochemistry, Geochronology, Groundwater; Shale Gas, black shale; dolerites and volcanics.*

This research focuses on the Karoo (182 Ma) dolerites and the possible impact related to their intrusion on the gas shale and groundwater. Fieldwork was conducted for mapping natural fractures and outcropping dolerite dyke and sill complexes in the eastern Karoo Basin that was compared with the Karoo Large Igneous Province (KLIP). This was followed by re-logging dolerites in the old SOEKOR boreholes drilled in the Karoo basin.

The goal is to analyze (geochemistry and geochronology) these intrusive rocks from different levels of emplacements from sea-level to the Lesotho foothill circa 1580 masl. The number and percentage thicknesses of the dolerites in each borehole are calculated: OL1/69=23 %; AB1/65 = 24 %; QU1/65 = 20.40 %; G39856 = 30.50 %; G39980 = 35.10 %; G39974 = 25.5 %; LA1/68 = 33 %; SP1/69 = 4.5 %. The dolerites thickness ranges from >5 m to 280 m thick from one borehole to another. In OL1/69 (westernmost studied borehole), thick sills emplaced into the Permian Ecca Group close to the surface, whilst in borehole SP1/69 (south easternmost studied borehole) the thin dolerite dyke/sill intruded the same sequences at greater depth (4000 m).

The new host-rock fracture data, geochemistry and geochronology from the Karoo dolerites and basalt samples yielded comparable results from previous investigation in the study area. The silica dioxides (SiO2 wt %) and Magnesium oxides (Mg wt %) from the dolerites and Drakensberg basalts content varies. Their significant variations may indicate that the Karoo dolerites and basalts are likely from different magmatic sources. However, the higher content of both elements (SiO2 and Mg) are prominent on the Drakensberg basalt and lesser in the Karoo dolerites.

AGE-VARIATIONS OF DOLERITES INTRUDED AT DIFFERENT ELEVATIONS ACROSS THE KAROO LIP

Muedi T.[1,2], MacLennan S.[3], Schoene B.[3], Linol B.[1], de Wit M.J.[1]

[1] *Africa Earth Observatory Network (AEON), Nelson Mandela University, South Africa*
[2] *Council for Geosciences (CGS), Pretoria, South Africa*
[3] *Department of Geosciences, Princeton University, Princeton, NJ, USA*

Dolerite sills and dykes in southern Africa are the major preserved igneous rocks across more than 1000km^2 of the Karoo Large Igneous Province (KLIP) that record the initial separation between Africa and Antarctica. While the relative ages of these intrusions are well constrained based on pioneering mapping of Alex du Toit in the early 1900s, precise ages from modern high-resolution isotope analyses are rare. Additionally, no emplacement dates have been determined from cores drilled up to 4km below surface. We report new dates of dolerites from the Eastern Cape (EC), flanking the Drakensberg escarpment with Karoo lavas at ca.1750m above sealevel (masl), to test for possible age variations at different depths using ID-TIMS U-Pb data from zircons in dolerites. Samples were collected at sealevel (Mazeppa Bay) and at 1350masl (Engcobo), and correlated with a previously dated dolerite at 1580masl (New Amalfi; Burgess et al., 2015). We also dated a dolerite at 220masl from core (Kransfontein) drilled 400km inland (Fig. 1). The data in the EC show the youngest intrusions (183.001 and 183.069Ma) occur at sealevel, and the oldest (183.246Ma) just below 1600masl, with a sill at 1350masl slightly younger at 183.080Ma (Fig. 2), suggesting here dolerite emplacement progressed downward (Fig. 3). It is likely that the sills presently at sealevel were originally emplaced 2250-2300mbsl, since Drakensberg pillow lavas, presently at 1750masl, formed at least 500mbsl (Figure 3; see Abstract 1 for details). In addition, drilling near the coast has encountered dolerite sills at depths of 4000mbsl. Thus, dolerite intrusions cover a minimal vertical depth of 6km, with the oldest apparent emplaced at the highest levels.

Clearly much more HR geochronology is required now to refine the emplacement history and mechanisms of the Karoo dolerites, their link to the Drakensburg volcanics, and those in Antarctica (FLIP); and their potential influence on enduring global Pliensbachian-Toarcian climate fluctuations during the onset of continental separation and uplift history of Gondwana.

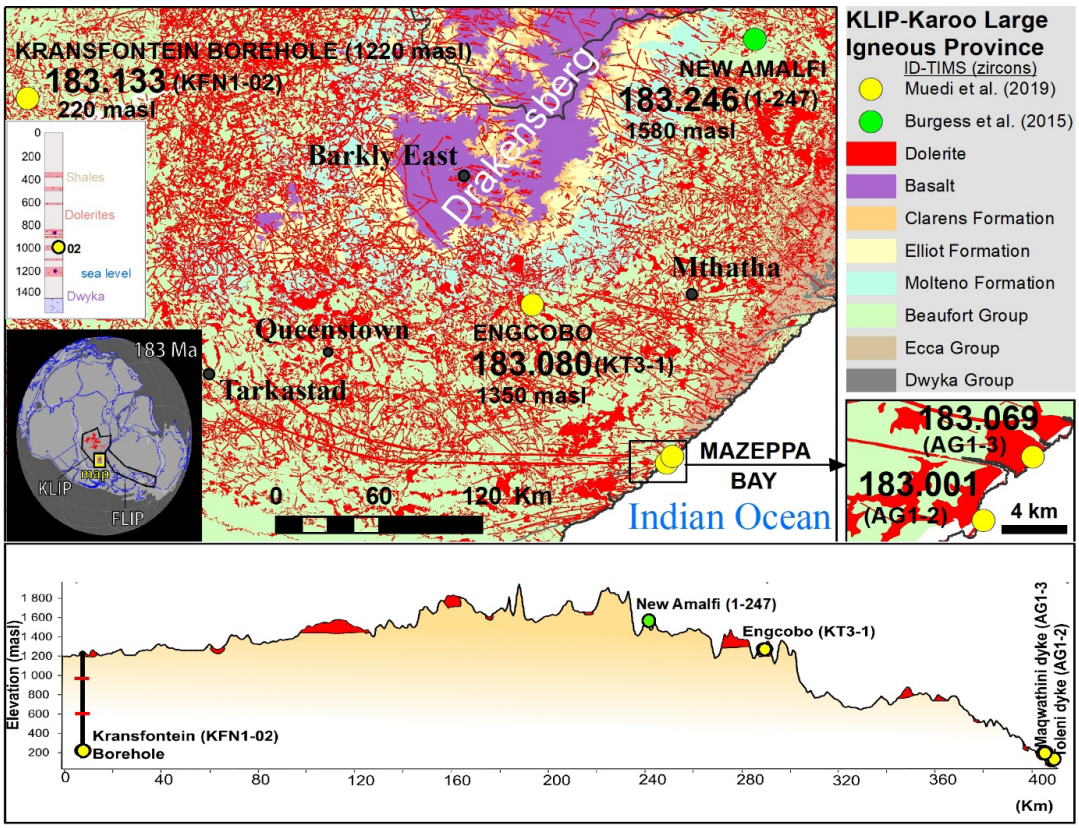


Figure 1. Geologic map and section the Karoo Basin, showing sample localities of dolerites in the Eastern Cape at sealevel, 1350 and 1650masl, and at 220masl from a drill core in the Western Cape. Zircons were dated using high resolution ID-TIMS U-Pb at Massachusetts Institute of Technology (AG1-3 and KT3-1) and Princeton University (AG1-2 and KFN) using similar tracer solutions ^{202}Pb-^{205}Pb-^{233}U-^{235}U (ET2535). Host rocks are predominantly Triassic-Jurassic shales and sandstones.

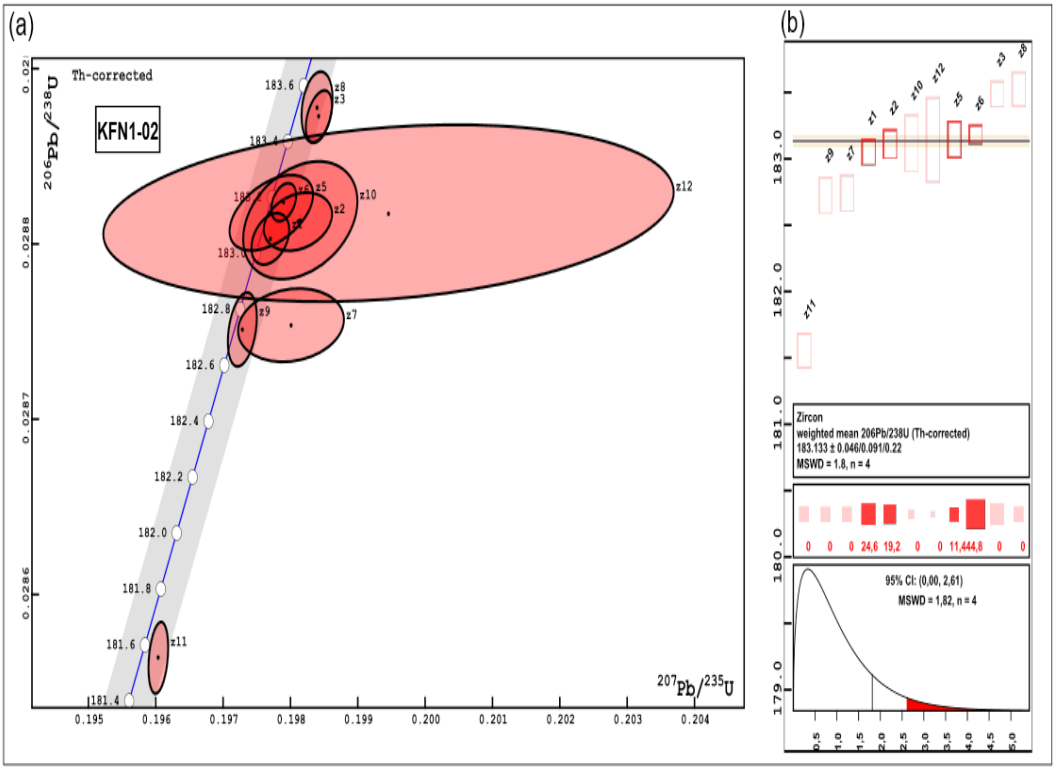


Figure 2. Example of Concordia plots (a) and weighted mean 206Pb/238U (b) of dolerite KNF1-02 drilled at a depth of 220masl. Individual zircons from were chemically abraded and annealed for 60 hours at 900°C, and placed in capsules. Samples were then leached at 190°C for 12 hours in HF and HCl, rinsed in acetone and water, and dissolved in HF for 48 hours at 210°C, placed at 110°C on a hotplate, dried and re-dissolved in 6NHCl. Samples were then spiked with EARTHTIME 202Pb-205Pb-233U-235U (ET2535) tracer solution. (Schoene 2013, for details)

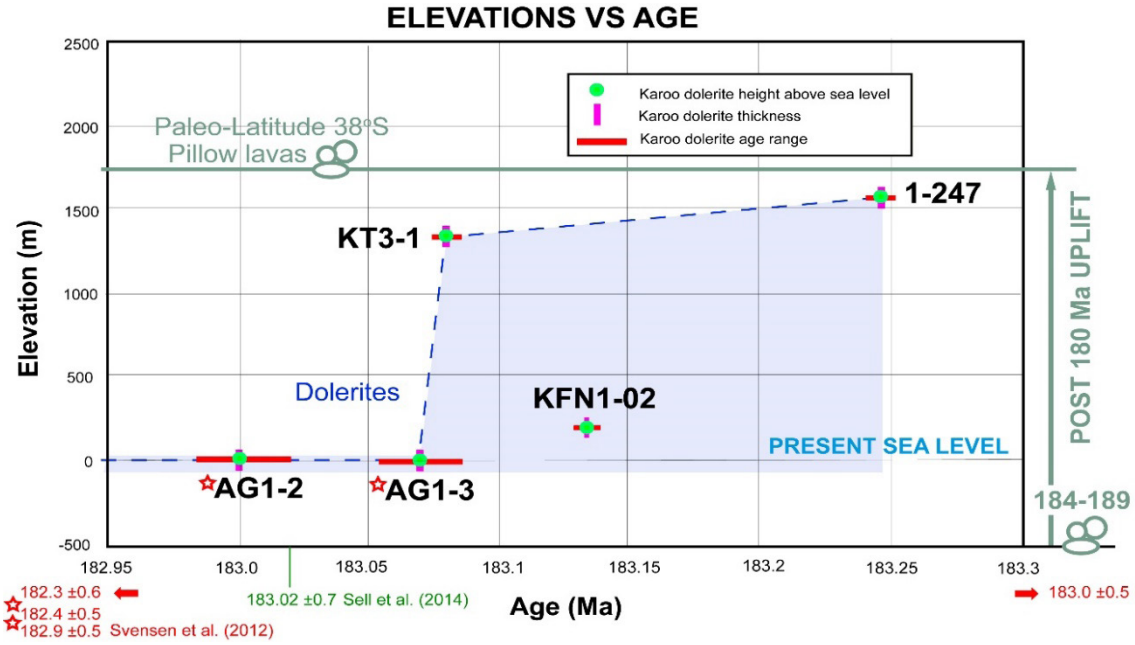


Figure 3. Summary of the zircon dates from this study, and (1-247) by Burgess et al. (2015), imply that dolerites at highest elevation are about 113-166Ka older than those at sealevel. Zircon ages of dolerites at present sealevel AG1-2&3 (183.001 and 183.069Ma) are older by ca. 0.6-1.0Ma compared those of Svensen et al. (2012) from the same dolerites at the same two locations. In general, the range of earlier zircon dates across the Karoo is greater by nearly an order of magnitude compared to the new dates. The date of Sell et al. (2014) is within the range of those at sealevel from this study. Note that Ar/Ar dates of the lowest volcanic rocks (184-189Ma; Moulin et al., 2017) that overly the highest dated dolerite imply they are older. Since these volcanics are intruded by many large, albeit as yet, undated dolerites sills and dykes (see Figure 1), the intrusions may cut a minimal vertical crust of more than 6-8km.

References:

1. Svenson, H., et al., 2012. Rapid magma emplacement in the Karoo Large Igneous province. EPSL 235-326, 1-9, doi.org/10.1016/j.epsl.2012.01.015.
2. Burgess, S.D. et al., 2015, High-precision geochronology links the Ferrar large igneous province with early-Jurassic ocean anoxia and biotic crisis, EPSL 415, 90–99, doi:10.1016/j.epsl.2015.01.037.
3. Moulin, M., et al., 2017. Eruptive history of the Karoo lava flows and their impact on early Jurassic environmental change. J. Geophys. Res. Solid Earth, 122, doi:10.1002/2016JB013354.
4. Sell, B., et al., 2014.Evaluating the temporal link between the Karoo LIP and climatic-biologic events of the Toarcian Stage with high-precision U-Pb geochronology, EPSL 408, 48–56, doi:10.1016/j.epsl.2014.10.008.
5. Schoene, B. 2013. U-Th-Pb Geochronology. Treatise on Geochemistry, v 4, 2nd edition.

NEW SM-ND ISOTOPIC DATA ON THE UNIVERSITY ALKALINE-GABBRO MASSIF (NE KUZNETSK ALATAU)

Mustafayev A. A.[1], Gertner I. F.[1], Serov P. A.[2]

[1]National research Tomsk State University, 36 Lenin Avenue, Tomsk, 634050, Russia
E-mail: labspm@ggf.tsu.ru
[2]Kola scientific center of the Russian Academy of sciences, 14 Fersman Street, Apatity, 184209, Russia

Keywords: *Ultrabasic, basic foydolites, sub-alkaline gabbro, Sm-Nd dating*

Introduction

Features of the geological structure University massif assume its localization on the boundary of two contrasting associations carbonate and volcanic ensembles, which indicates a weak erosive slice located close analogue Kiya-Shaltyr deposit nepheline ores and allows estimating the structure of the upper portion of the front alkaline intrusive magmatic gabbro in a particular segment Kuznetsk Alatau region. The wide development of dike varieties of ultrabasic and basic foidoliths confirms the presence of a probable body of potential nepheline ores at the boundary of the carbonate and volcanogenic strata. The geochemical parameters of the studied rocks of the University massif suggest the formation of this alkaline-basic association in the conditions of a complex marginal-continental geodynamic setting due to a combination of subduction and plume processes (Mustafayev et al., 2018).

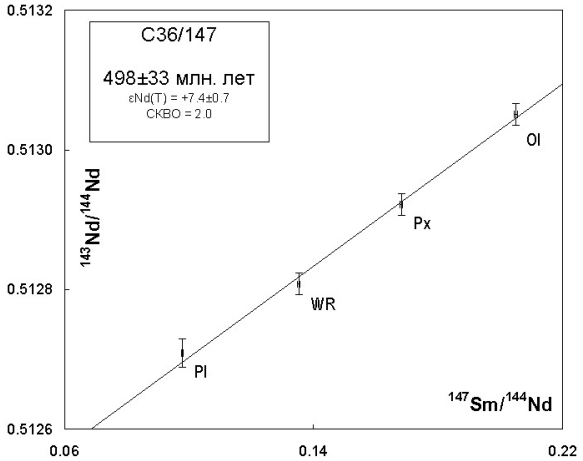
Results

Sm-Nd Isotope dating.

Neodymium isotope composition and Sm and Nd concentrations were measured on a Finnigan-MAT 262 7-channel solid-phase mass spectrometer (RPQ) in a statistical two-filament mode using rhenium and tantalum filaments (Serov et al., 2014).

Melanogabbro, leucogabbro. The average ^{143}Nd / ^{144}Nd value in La Jolla standard was 0.512081 ± 13 (N = 11) during the measurement period. The error of the (2σ) $^{147}Sm/^{144}Nd$ values does not exceed 0.5 wt.%, and 0.005 wt.% for $^{143}Nd/^{144}Nd$. When we were calculating primary isotope ratios, ε_{Nd}, ε_{Sr}, T_{Nd} (DM) values, we referenced present-day values of CHUR model reservoirs ($^{143}Nd/^{144}Nd$ = 0.512638, $^{147}Sm/^{144}Nd$ = 0.1967) and depleted mantle (DM) ($^{143}Nd/^{144}Nd$ = 0.51315, $^{147}Sm/^{144}$ Nd = 0.2137) (Faure, 1989). The isochrones were plotted by D. York method (York, 1966) using Isoplot/Ex software (Ludwig, 1999). The most accurate Sm-Nd isochrones were obtained from mineral phases and whole-rock composition of two sub-alkaline gabbroid samples. (Figure 1, samples C36/147 and c41/87,6).

Ijolite, analcime syenite (globul). The average $^{143}Nd/^{144}Nd$ value in JNdi-1 standard was 0.512090 ± 13 (N = 9) during the measurement period. The (2σ) error of the $^{147}Sm/^{144}Nd$ value is 0.4%– this is the average error between 7 measurements taken in the BCR-2 standard (Raczek et al., 2003). The analytical error for Nd isotope composition in an individual analysis did not exceed 0.005%. When calculating isochrones, we used real analytical errors for Nd isotopic composition, but never below the reproducibility level of the measurement of Nd isotopic composition (0.004%). Accuracy of Sm and Nd measurements is ±0.5%, and up to ±10% for minerals with low concentrations (ppm). Isotopic ratios were normalized to $^{146}Nd/^{144}Nd$ = 0.7219, and then recalculated to the ratio $^{143}Nd/^{144}Nd$ = 0.512115 in JNdi-1 standard (Tanaka et al., 2000). When calculating values $\varepsilon_{Nd}(T)$ and model ages T (DM), we referenced present-day CHUR values (^{143}Nd / ^{144}Nd = 0.512630, ^{147}Sm / ^{144}Nd = 0.1960) by (Bouvier et al., 2008) and DM (^{143}Nd / ^{144}Nd = 0.513151, ^{147}Sm / ^{144}Nd = 0.2136) by (Goldstein, Jacobsen, 1988). The most accurate Sm-Nd isochrones were obtained from mineral phases and whole-rock composition of plagioclase-bearing ijolite (sample 6A) and analcime syenite presented as a globul inclusion in this rock (sample 7A) (Figure 1).



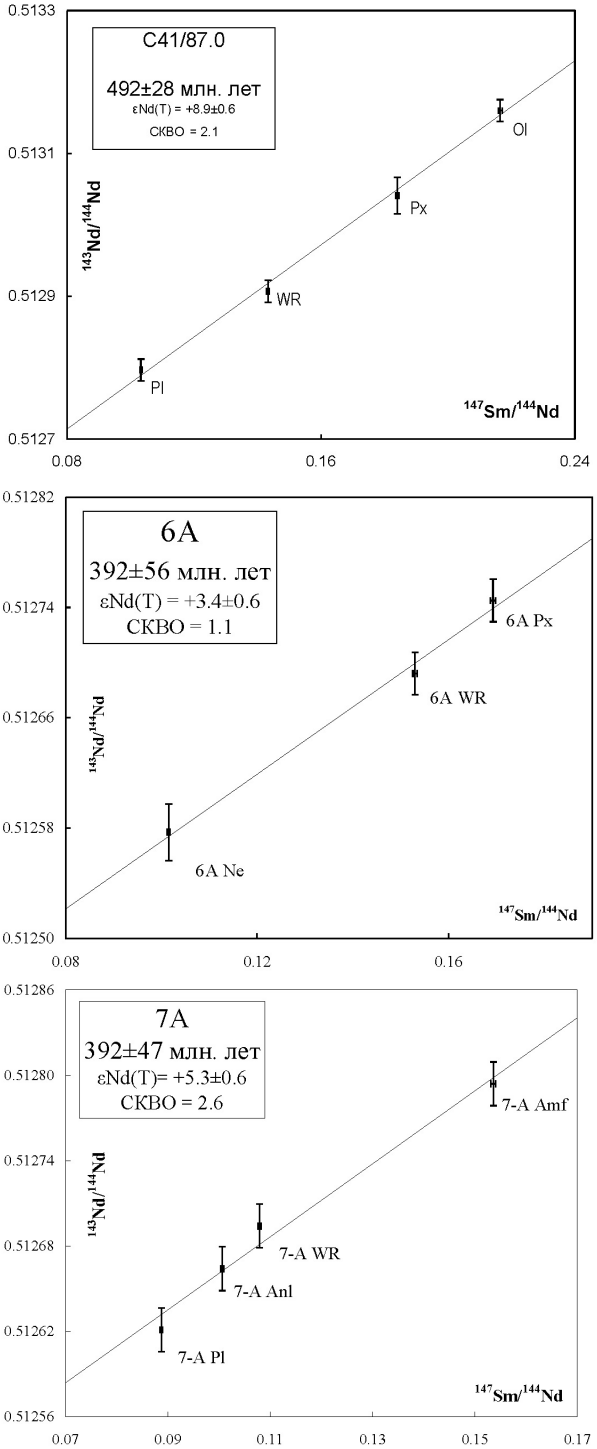


Figure 1. Sm-Nd mineral isochrones for different kinds of studied rocks.

Samples: C36/147 - melanogabbro, C41/87.0 - leukogabbro, 6A - ijolite, 7A - analcime syenite (globul).

Conclusions

One of the main surprises during this study was the age of gabbroids studied, which corresponds to the upper interval $Є_{2-3}$ 498-492 Ma with an error of about 33-28 Ma. Such alkaline magmatism manifestation in this region related exclusively to the western sector of Mariinsk Taiga and was recorded in the alkaline-gabbroid association of the Upper Petropavlovsk Massif (Vrublevskii et al., 2016).

The results of Sm-Nd dating of alkaline rocks correspond to the Eifelian tier D_2 392 Ma with an error of about 56-47 million years. We can suggest Devonian for formation age (380–430 Ma), which corresponds to the main phase of foydolite manifestation in this part of the region. An important element of the University Massif study is its intermediate structural position between the western and eastern sectors of high-alkalinity magmatism on the northern slope of the Kuznetsk Alatau, which according to the latest geochronological studies were formed in a wide time range (507-265 Ma) (Vrublevskii et al., 2014)). We accept a possibility of combining several ages of high-alkalinity magmatism manifestations within this geological object. A more detailed study will contribute to the development of a geodynamic model of high-alumina alkaline magmas formation under conditions of mantle plume activity in the folded structures in ancient continent margins.

Acknowledgements

This work was conducted as a government task of the Ministry of Education and Science of the Russian Federation, Project Number 5.2352.2017. Isotope analysis Sm-Nd were funded by Russian Science Fund (project No. 18-17-00240).

References

1. Bouvier A., Vervoort J.D., Patchett P.J. The Lu–Hf and Sm–Nd isotopic composition of CHUR: Constraints from unequilibrated chondrites and implications for the bulk composition of terrestrial planets // Earth Planet. Sci. Lett. 2008. V. 273 (1–2). P. 48–57.
2. Faure G. Fundamentals of isotope geology. – M.: World, 1989. – 590 p.
3. Goldstein S.J., Jacobsen S.B. Nd and Sr isotopic systematics of river water suspended material implications for crystal evolution // Earth Plan. Sci. Letters. 1988. V. 87. P. 249-265.
4. Ludwig K.R. ISOPLOT/Ex - A geochronological toolkit for Microsoft Excel, Version 3.6 // Berkeley Geochronology Center Special Publication. No. 4. 2008. 76 p.
5. Mustafayev A.A., Gertner I.F., Serov P.A. Features of geology and composition of rocks from the alkaline-gabbroic University massif (N-E Kuznetsky Alatau ridge, Siberia) / IOP Conference Series: Earth and Environmental Science 9, Petrology of Magmatic and Metamorphic Complexes. - 2018. Vol 110. – P. 012016.
6. Raczek I., K. P. Jochum, A. W. Hofmann. Neodymium and strontium isotope data for USGS reference materials BCR-1, BCR-2, BHVO-1, BHVO-2, AGV-1, AGV-2, GSP-1, GSP-2 and eight MPI-DING reference glasses // Geostandards and Geoanalytical Research. 2003. V. 27. p. 173–79.
7. Serov P.A., Ekimova N.A., Bayanova T. B., Mitrofanov F. P. Sulphidic minerals – new geochronometers at Sm-Nd dating of a rudogenez of the intrusions of Baltic Shield stratified the mafit-ultramafitovykh // The Litosphere. 2014. No. 4. Page 11-21.
8. Tanaka T., Togashi S., Kamioka H., Amakawa H.,. Kagami, Hamamoto T., Yuhara M, Orihashi Y., S. Yoneda S., Shimizu H., Kunimaru T., Takahashi T., Yanagi T., Nakano T., Fujimaki H., Shinjo R., Asahara Y., Tanimizu M., Dragusanu C. JNdi-1: a neodymium isotopic reference in consistency with LaJolla neodymium// Chemical Geology. 2000. V. 168. p. 279-281.
9. VrublevskiiV. V., Grinev O. M., Izokh A. E., Travin A. V. Geochemistry, isotope triad (Nd-Sr-O), and 40Ar-39Ar age of Paleozoic alkaline mafic intrusions of the Kuznetsk Alatau (by the example of the Beloya Gora pluton) // Russian Geology and Geophysics. 2016. Vol. 57, № 3. P. 464-472.
10. Vrublevskii V. V., Gertner I. F., Gutierrez-Alonso G. et al. Isotope (U-Pb, Sm-Nd, Rb-Sr) geochronology of alkaline basic plutons of the Kuznetsk Alatau. Russian geology and Geophysics (Geologiya I Geofizika) 55. 2014. P. 1264-1277.
11. York D. Least squares fitting of straight line // Can. J. Phys. V. 44. – 1966. – P. 1079-1086.

THERMAL EVOLUTION OF THE NORTHERN SIBERIAN TRAPS LIP AS INFERRED FROM APATITE FISSION TRACK DATING OF THE GULI PLUTON

Myshenkova M. S.[1], Veselovskiy R. V.[1,2], Zaitsev V. A.[3], Thomson S.[4], Latyshev A. V.[1,2], Zakharov V. S.[1,5]

[1] *Lomonosov Moscow State University, Moscow, Russia*
[2] *Schmidt Institute of Physics of the Earth RAS, Moscow, Russia*
[3] *Vernadsky Institute of Geochemistry and Analytical Chemistry RAS, Moscow, Russia*
[4] *University of Arizona, Tucson, United States*
[5] *Dubna University, Dubna, Moscow region, Russia*

Keywords: *The Siberian traps LIP, Guli pluton, thermal history, apatite fission-track dating, low-temperature thermochronology*

Models of thermal evolution of ancient platforms (cratons) are the results of geochronological studies and are mostly based on the reconstruction of the tectonothermal history of individual geological objects. The thermal history of the Siberian platform is still practically unexplored because the thermochronological studies within its area are extremely rare (Rosen et al., 2009). The formation of the Permian-Triassic Siberian Traps – the largest surviving continental large igneous provinces – is currently considered as one of the key manifestations of endogenous processes on the Earth. According to the modern point of view (Ernst, 2014), eruption of the Siberian Permian-Triassic basalts and emplacement of numerous coeval magmatic bodies (dikes, sills, etc.) occurred during the plume-lithospheric interaction, which thermal effect on the lithosphere and crust (in particular, the sedimentary cover) of the Siberian platform has not been sufficiently studied. This issue is of great importance for understanding of the formation and subsequent evolution of LIPs, but also for clarifying of the pattern of the mineral deposits locations, which is mostly determined by the tectonothermal evolution of the upper crust.

The time of the main phase of magmatic activity within the Siberian Traps LIP is estimated ~252.0-251.3 Ma (Kamo et al., 1996, 2003; Burgess and Bowring, 2015). At the same time, the question about the total duration of the Siberian traps formation remains controversial. In particular, a significant number of Ar/Ar ages are represented by values of ~240 Ma (Ivanov et al., 2005; 2009; 2013); at the same time, few fission track ages of apatite, corresponding to the cooling of the uppermost part of the crystalline basement of the Siberian platform below 110°C, are 222-185 Ma (Rosen at el., 2009). Obviously, the thermochronological data is extremely insufficient to create of reliable tectonothermal model of the Siberian platform in Phanerozoic.

In this study we performed fission track dating of apatite from the Guli pluton on the northern part of the Siberian LIP, as well as computer modeling of the process of its post-emplacement cooling. Obtained results allowed us to create two alternative models of the tectonothermal evolution of the Guli pluton. According to the first model, the emplacement and cooling of the present-day surface rocks of the pluton took place at depths less than 1.5 km. Alternative model suggests that after its emplacement ~250 Ma in hypabyssal conditions, the Guli pluton undergone burial under sedimentary/volcanic cover of 2-3 km thick, which resulted in the secondary heating of the Guli pluton to temperatures above 110°C, followed by its exhumation and cooling below 110°C ~218 Ma. Additional low-temperature thermochronological data need to test and develop these models.

Acknowledgements

This work was supported by the Russian Foundation for Basic Research (grants 18-35-20058 and 18-05-00590). Computer modelling was carried out using the equipment of the shared research facilities of HPC computing resources at Lomonosov Moscow State University.

References

1. Burgess S.D. and Bowring S.A., 2015. High-precision geochronology confirms voluminous magmatism before, during, and after Earth's most severe extinction. Science Advances 1 (7), e1500470–e1500470. https://doi.org/10.1126/sciadv.1500470.
2. Ernst R.E. Large Igneous Provinces. Cambridge University Press. 2014. 653 p.
3. Ivanov A.V., He H., Yan L., Ryabov V.V., Shevko A.Y., Palesskii S.V., Nikolaeva I.V., 2013. Siberian Traps large igneous province: evidence for two flood basalt pulses around the Permo-Triassic boundary and in the Middle Triassic, and contemporaneous granitic magmatism. Earth-Science Reviews 122, 58–76. https://doi.org/10.1016/j.earscirev.2013.04.001.
4. Ivanov A.V., He H., Yang L., Nikolaeva I.V., Palesskii S.V., 2009. 40Ar/39Ar dating of intrusive magmatism in the Angara-Taseevskaya syncline and its implication for duration of magmatism of the Siberian Traps. Journal of Asian Earth Sciences 35 (1), 1–12. https://doi.org/10.1016/j.jseaes.2008.11.006.
5. Ivanov A.V., Rasskazov S.V., Feoktistov G.D., He H., Boven A., 2005. 40Ar/39Ar dating of Usol'skii sill in the southeastern Siberian Traps Large Igneous Province: evidence for long-lived magmatism. Terra Nova 17 (3), 203–208. https://doi.org/10.1111/j.1365-3121.2004.00588.x.
6. Kamo S.L., Czamanske G.K., Amelin Y., Fedorenko V.A., Davis D.W., Trofimov V.R., 2003. Rapid eruption of Siberian flood-volcanic rocks and evidence for coincidence with the Permian–Triassic boundary and mass extinction at 251 Ma. Earth and Planetary Science Letters 214 (1-2), 75–91. https://doi.org/10.1016/S0012-821X(03)00347-9.
7. Kamo S.L., Czamanske G.K., Krogh T.E., 1996. A minimum U-Pb age for Siberian flood-basalt volcanism. Geochimica et Cosmochimica Acta 60 (18), 3505–3511. https://doi.org/10.1016/0016-7037(96)00173-1.
8. Rosen O.M., Soloviev A.V., and Zhuravlev D.Z., 2009. Thermal Evolution of the Northeastern Siberian Platform in the Light of Apatite Fission-Track Dating of the Deep Drill Core. Izvestiya, Physics of the Solid Earth 45 (10), 912–929. https://doi.org/10.1134/S1069351309100085.

LATE PRECAMBRIAN MAFIC DYKE SWARMS OF THE ALDAN SHIELD AND THEIR IMPORTANCE IN ORE-MAGMATIC PROCESSES

Okrugin A. V.[1], Ernst R. E.[2,3], Beryozkin V. I.[1], Popov N. V.[4]

[1] *Diamond and Precious Metal Geology Institute (DPMGI), SB RAS, Yakutsk, Russia*
[2] *Carleton University, Ottawa, Canada*
[3] *Tomsk State University, Tomsk, Russia*
[4] *Trofimuk Institute of Petroleum Geology and Geophysics, SB RAS, Novosibirsk, Russia*

Keywords: *Dyke swarm, basite, mafic magmatism, mantle plume, Aldan Shield*

Introduction

Integrated petrological-geochemical, geochronological, and ore-mineralogical studies of mafic magmatism are of prime importance in reconstructing the formation history and metallogeny of ancient platforms (Gladkochub et al., 2012; Guryanov et al., 2013; Okrugin et al., 2018; Ernst et al., 2016). This paper presents geochemical and age data for the swarms of Late Precambrian unmetamorphosed mafic dykes of the Aldan shield, which formed in course of a long evolution of the Siberian platform following consolidation of the ancient basement of the Siberian (North Asian) craton, but are overlain by the Phanerozoic sedimentary cover.

Results

Mafic dykes are widespread within the Aldan shield that represents the northern Chara-Aldan domain of the Aldan-Stanovoy superterrane including the West Aldan, Nimnyr, Sutam, Uchur, and Batomga terranes separated by tectonic mélange zones (Fig.1). The dykes dip steeply (70-90°) showing clear intrusive contacts with the enclosing rocks. Their traceable length varies from a few to 15 km and the thickness – from several to 200-300 m. The dykes form 200-500 km long and 20-60 km wide swarms crosscutting different terranes. The ENE dyke swarms occur mainly in the western part of the Aldan shield where the Nirekta (NR), Olondo (OL), Udokan-Tommot (UT), and Kalar-Nimnyr (KN) swarms are identified (Mironyuk et al., 1971). In the middle part of the Aldan shield, apart from the Timpton-Gynym (TG) swarm there are recognized the Timpton-Algama (TA) and the El'kon-Gonam (EG) belts of NW strike (Okrugin et al., 2000). In the east of the shield, the dykes of the Maimakan Complex are grouped into the Uchur-Uyan (UU), South-Uchur (SU), and Ukikan (UK) fields of dyke swarms (Guryanov et al., 2013).

The Precambrian age of the dykes was earlier supported by K-Ar dating (1050-1650 Ma) of the rocks (Okrugin et al., 2000). More well-constrained ages were obtained recently from U-Pb dating of zircon and baddeleyite (Ernst et al., 2016), which are shown in Fig.1 with a star (*).

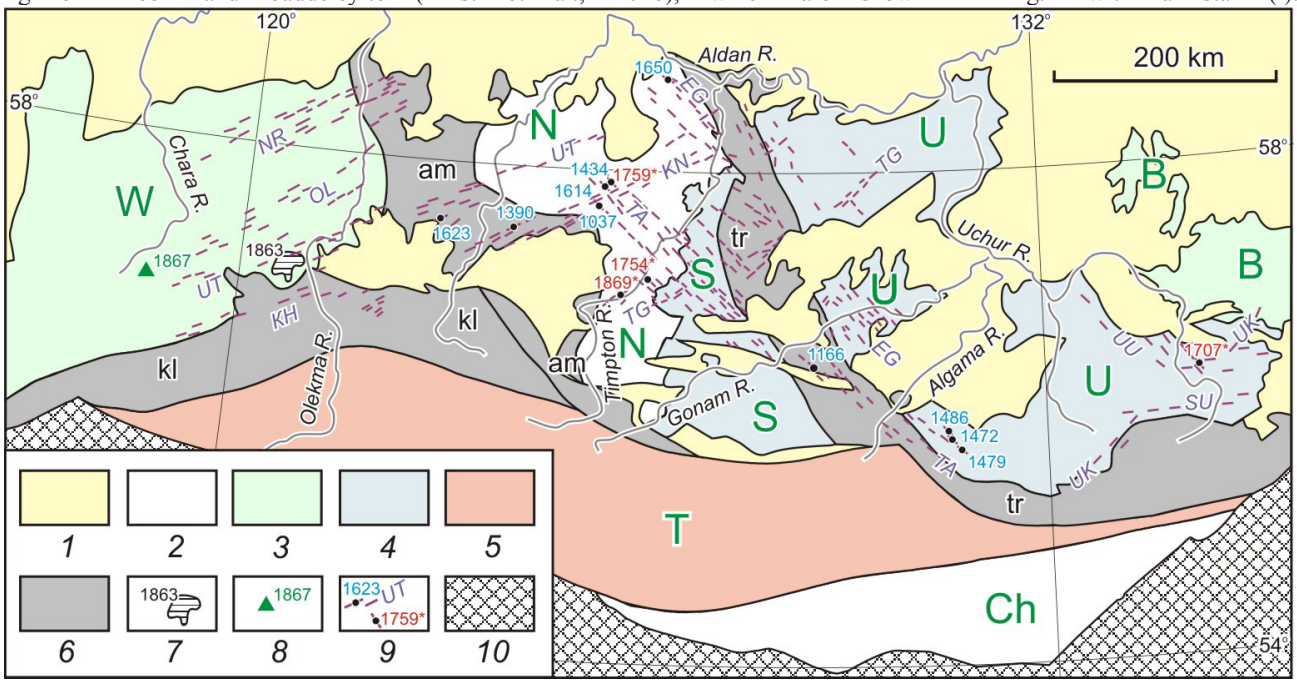


Figure 1. Sketch map of Late Precambrian dyke swarms in the Aldan shield

1 – Siberian platform cover; 2-5 – terranes of the Aldan-Stanovoy shield (after Smelov et al., 2009): 2 – Nimnyr (N) and Chogar (Ch) granite-orthogneiss; 3 – West Aldan (W) and Batomga (B) granite-greenstone; 4 – Sutam (S) and Uchur (U) granite-paragneiss; 5 – Tynda (T) tonalite-trondhjemite-gneiss; 6 – tectonic mélange zones (am - Amga, kl - Kalar, tr - Tyrkanda; 7 – Lower Khani graben-syncline with metagabbro-diabase dykes and sills (Popov et al, 2012); 8 – Chiney layered gabbroic massif; 9 – dyke swarms; 10 – folded complexes of South Siberia.

The age of the NE Kalar-Nimnyr belt (1869 Ma) obtained from dating of a dyke of the TG swarm is close to that (1844 Ma) of the NE dyke swarm in northern Cisbaikalia, which suggests they had a similar origin (Gladkochub et al., 2012). The dates (1754-1759 Ma) of the NW dykes from the TA belt coincide with the ages of the SE dyke swarms in the Anabar uplift and the NE Chay swarm in the Baikal uplift. The swarms are proposed to intersect in the lower Vilyui river area where the center of the Timpton plume aged at 1758-1752 Ma was located (Gladkochub et al. 2012; Ernst et al., 2016).

The dykes under consideration were not subjected to metamorphism. According to the Russian Petrographic Code (2008) they belong to basalts (B) and andesite basalts (BA), more rarely to trachybasalts (TB) and andesites (A) (Fig.2).

In terms of mineral and chemical compositions, the dyke rocks are divided into two groups. The first group consists of the rocks of the differentiated dolerite-diorite series, and the second one includes dolerites with transition to trachydolerites. The dolerite-diorite rocks are characterized by a high SiO_2 content (49-59%), the presence of interstitial quartz-feldspar micropegmatite (up to 10%), and by the appearance of hypersthene. This series exhibits significant variation (0.52-0.86) in the fractionation ratio F = $FeO_{tot}/(FeO_{tot}+MgO)$. SiO_2, K_2O, Na_2O, P_2O_5, and TiO_2 increase and CaO decreases with the growing fractionation ratio. That behavior of petrogenic elements suggests the formation of homogeneous dykes in course of multiple injections of tholeiite-basalt melts and their differentiates from deep-seated intermediate magma chambers. The rocks of the second group are marked by a lower SiO_2 content and by higher values of TiO_2 (1.5-3.1%), P_2O_5 (0.2-0.7%), and alkalis, mainly K_2O, thus corresponding to dolerites and subalkaline dolerites. Unlike the rocks of the first group, the subalkaline dolerites exhibit no clear relationship between the distribution of petrogenic elements and the fractionation ratio.

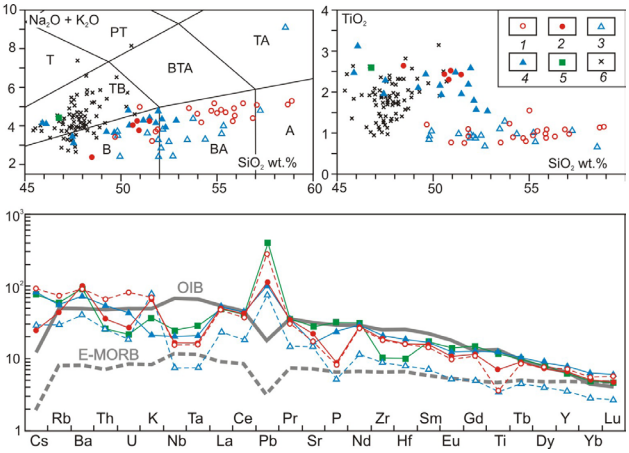


Figure 2. Compositions of Late Precambrian dykes in the Aldan shield

1 – NE dykes, low-Ti; 2 – same, high-Ti; 3 – NW dykes, low-Ti; 4 – same, high-Ti; 5 – dykes of the Uchur-Uyan swarm, high-Ti (Guryanov et al., 2013); 6 – metagabbro- diabases of the Kuranakh Complex (Smelov et al., 2009); spidergram, normalized by primitive mantle (Sun, McDonough, 1989).

In the distribution of elements on a spidergram, the high-Ti mafic dykes are very close to intraplate basalts of oceanic islands, but differ from them by the presence of well-defined negative Th-U and Nb-Ta anomalies and a positive Pb peak. The low-Ti rocks of the differentiated dolerite-diorite series (open symbols connected by dotted lines) are characterized by a lower P_2O_5 content and a deeper Nb-Ta minimum.

The age of metagabbro-diabase dykes and sills of the Kuranakh Complex (1863±9 Ma) in the Lower Khani graben-syncline is identical to that of basic rocks (1867±3 Ma) in the Chiney layered massif (Popov et al, 2012).

Conclusions

The source of magma for the Late Precambrian dyke swarms in the Siberian (North Asian) craton were undepleted intraplate plume-type mafic melts. Magma retardation in deep chambers could have resulted in contamination of the melts by crustal material, and could also be responsible for a dual behavior of Ti during fractionation of various Ti-bearing minerals.

Intrusion of significant volumes of mafic material in the form of plumes leads to the formation of large igneous provinces with mafic-ultramafic complexes that can host high-grade deposits of platinum-group metals (PGM), Ni, Cu, Cr, rare elements, etc. Within the limits of the Aldan-Stanovoy shield there are present numerous Au-Pt placers with various PGM associations for which the bedrock sources are as yet unknown.

Acknowledgements

This work was carried out as part of the scientific research of the DPMGI SB RAS, No. 0381-2016-0003 and supported by the RFBR project No. 17-05-00390.

References

1. Gladkochub D.P., Donskaya T.V., Ernst R. et al. (2012) Proterozoic basic magmatism of the Siberian Craton: Main stages and their geodynamic interpretation. Geotectonics 46: 273-284
2. Guryanov V.A., Perestoronin A.N., Didenko A.N., Peskov A. Yu., Kosynkin A. V. (2013) Late Paleoproterozoic Basic Dykes in the Ulkan-Uchur District, Aldan-Stanovoy Shield. Geotectonics 47: 279–290
3. Mironyuk, E.P., Lyubimov, V.K. and Magnushevsky, E.L. 1971. Geology of the western part of the Aldan shield. Moscow. Nedra, 236. (in Russian).
4. Okrugin, A.V., Koroleva, O.V. and Beryozkin, V.I. 2000. Distribution and specific composition of Riphean basites of the Aldan shield //Petrography on border of centuries. Syktyvkar, pp. 150-153 (in Russian).
5. Okrugin A.V., Yakubovich O.V., Ernst R., Druzhinina Zh.Yu. (2018) Platinum-bearing placers of Siberian platform: mineral associations and their age characteristics as indicators of large igneous provinces manifested. Artic and Subartic natural resources 3: 36-52
6. Popov N.V., Postnikov A.A., Kotov A.B. et al. (2012) Kuranakh complex diabases in the western part of the Aldan-Stanovoi shield: age and tectonic setting // Doklady Earth Sciences. 2012. V. 442. 1. p. 45-48.
7. Smelov A.P., Beryozkin V.I., Timofeev V.F. et al. (2009) Geology of the western part of the Aldan-Stanovoy shield and chemical composition of the Early Cambrian rocks. Yakutsk. 168 pp. (in Russian).
8. Ernst R.E. Hamilton M.A., Söderlund U. et al. (2016) Long-lived connection between southern Siberia and northern Laurentia in the Proterozoic. Nature Geoscience 6: 464-469
9. Sun S.S., McDonough W.F. (1989) Chemical and isotopic systematic of oceanic basalts. Magmatism in the Ocean Basins 42: 313-345

PLATINUM-BEARING PLACERS OF THE SIBERIAN PLATFORM AND THEIR POTENTIAL LINKS WITH LARGE IGNEOUS PROVINCES

Okrugin A. V.[1], Yakubovich O. V.[2,3], Ernst R. E.[4,5], Druzhinina Zh.Y.[3]

[1] *Diamond and Precious Metal Geology Institute (DPMGI) SB RAS, Yakutsk, Russia.*
[2] *Institute of Precambrian Geology and Geochronology (IPGG) RAS, St. Petersburg, Russia.*
[3] *Saint Petersburg State University, Russia.*
[4] *Carleton University, Ottawa, Canada;*
[5] *Tomsk State University, Tomsk, Russia*

Keywords: *platinum-group minerals, ^{190}Pt-^{4}He dating, Siberian craton*

Introduction

Placer deposits in the Siberian platform are closely associated with well-known platiniferous intrusions (Kondyor, Inagli, Noril'sk, Chiney, and Guli) (Genkin, 1968; Krivenko et al., 1996; Lichachev et al., 1987 etc) but there are also numerous PGM placers of large areal extent in the river basins of Siberia (Vilyui, Lena, Aldan, Anabar, and Olenek) for which the primary sources are still unknown. Comparison of the Pt-bearing placers and correlation between the Re-Os and ^{190}Pt-^{4}He isotope ages of the PGM and with ages of major magmatic events in the Siberian craton showed that the potential sources for some of the placers are buried Precambrian mafic-ultramafic intrusions of Large Igneous Provinces (LIP). The approach of this paper can be applied to other cratonic areas with alluvial PGM of unknown origin.

Results

PGM placers in the Vilyui, Lena, Aldan, Anabar, and Olenek river basins belong to following mineralogical-geochemical types: rich-Rh ferroan platinum (Vilyui type); Rh-Ir-ferroanplatinum (Anabar type); Ir-ferroan platinum (mid-Lena type); and platinum-sperrylite association in placers of the Aldan shield. In the northeastern part of the platform (Anabar, and Olenek river basins) there are also compound gold-platinum-diamond placers from which not only diamonds and noble metals are recovered, but also rare-metal minerals (Okrugin, 1998; Okrugin et al., 2019; Shpunt, 1970); in these cases also, the sources are unknown.

Extensive Pt-bearing placers are likely eroded from buried mafic-ultramafic massifs. PGM as well as gold were supplied into recent placers from buried intermediate depth reservoirs as a result of repeated recycling of Proterozoic and Phanerozoic basal conglomerates. The fine fraction (less than 0.5-1 mm) of thin-platy "floating" PGM and gold migrated over great distances forming extensive dispersion haloes, potentially far from the primary sources.

In an attempt to establish potential source rocks for the placer platinum we compared mineralogical and geochemical characteristics of PGM with known ultramafic complexes and also correlated the ages of PGM (Okrugin et al. 2006, 2019; Yakubovich et al., 2018) dated by the Re-Os and ^{190}Pt-^{4}He methods with ages of major intraplate magmatic events (including some thought to belong to LIPs) that occurred in the Siberian craton (Ernst et al., 2016). In addition to the earlier determined Re-Os model ages (Okrugin et al., 2006) of Ru-Ir-Os minerals, we dated Fe-Pt alloys and sperrylite from some placers using a ^{190}Pt-^{4}He isotope method (Shukolyukov et al., 2012). The high stability of radiogenic He in the naturally occurring metallic (isoferroplatinum, ferroan platinum) and a non-metallic platinum compound (sperrylite) permits their use as a ^{190}Pt-^{4}He geochronometer (Yakubovich et al., 2015).

U-Pb dating of dolerite dykes and sills in South Siberia and North Laurentia revealed nine Proterozoic LIPs (Ernst et al., 2016), and 3 Phanerozoic LIPs, the 252 Ma Siberian Traps LIP, the 370-360 Ma Yakutsk-Vilyui LIP, and the 135 Ma High Arctic LIP (HALIP) (Ernst, 2014), and their ages in part match (within uncertainties) the alluvial PGM ages, which is suggestive of their genetic association in the period 1.9-0.15 Ga (Figure). These correlations allow us to make a step forward to identify specific (likely buried) bedrock intrusive sources for extensive platinum placers of the Siberian platform.

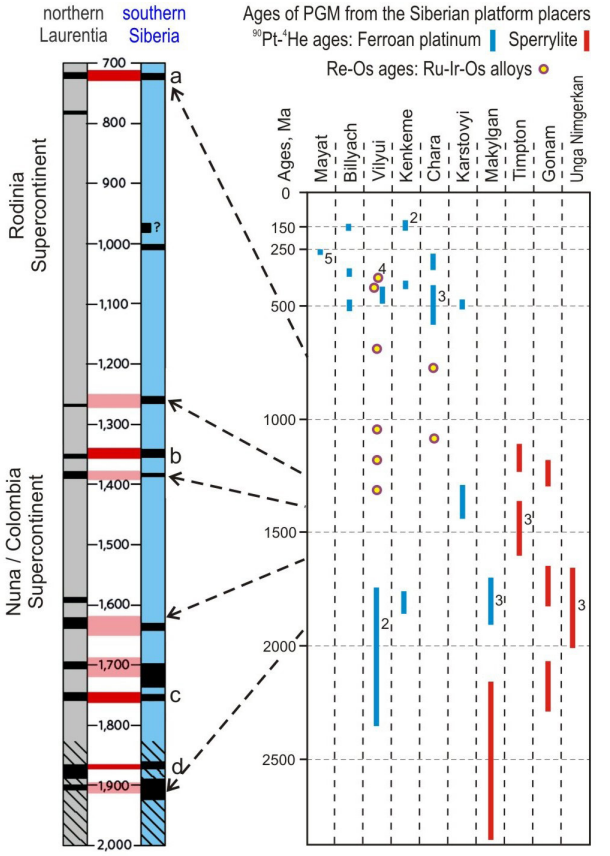


Figure. Correlation between the time of LIPs in the southern Siberian and the northern Canadian (Laurentia) cratons [Ernst et al. 2016] and the ages of Pt-group minerals from the Siberian platform placers

Thus, the variety of mineralogical-geochemical types of PGM assemblages in the Siberian platform placers may be explained by the presence of source rocks of several distinct types: from highly refractory cumulates of ultramafic rocks with chromite ores (Ru-Ir-Os minerals) to late-magmatic derivatives of differentiated intrusions of mafic rocks with sulfide ores containing Pt-Pd-rich phases.

Paleomagnetic, isotope-chronological, and geochemical studies of mafic rocks in the Siberian and North American (Laurentia) cratons (Ernst et al., 2016) revealed nine LIP events in the period 1.9-0.7 Ga (see left column of Figure). This indicates that the cratons were in close contact for more than 1.2 Ga. They jointly survived all tectonic/magmatic events during the formation and breakup of two supercontinents: Nuna (1.7-1.3 Ga) and Rodinia (1.1-0.7 Ga). The right side of the Figure presents Re-Os and ^{190}Pt-^{4}He isotope ages of PGM from the studied placers of the Siberian platform (Okrugin et al., 2006, 2019; Yakubovich et al., 2018). If the age was determined by the isochron method, then next to the lines of ranges is the number corresponding to the number of samples on which the isochron was obtained.

Next we consider whether the source of the Siberian platform PGM could be mafic-ultramafic intrusions belonging to large intraplate magmatic events (i.e. LIPs); We test these correlations on the basis of Re-Os and ^{190}Pt-^{4}He dating of the PGM in comparison with well-dated LIPs of the Siberian platform. For comparison we have a record of nine Proterozoic LIPs present in the Siberian craton (Figure) and two large Phanerozoic LIPs. However, given many regional mafic dyke swarms and other intrusive units that have not been dated, it is expected that additional LIPs remain to be discovered, of both Phanerozoic and Proterozoic age.

Conclusions

The data presented here on the chemical compositions and ages of PGM from Pt-bearing placers of the Siberian platform indicate a relationship between the placers and repeated episodes of Precambrian mafic-ultramafic magmatism within the platform. Ophiolites are not likely to be the potential source PGM given the geology and river flow patterns of the Siberian platform, leaving intraplate magmatism as a more likely source. Many of the PGM deposits were formed as a result of the basic and alkali-ultramafic intrusions associated with the Siberian Traps LIP at 252 Ma. We can link some placers of Anabar and Vilyui rivers to the 370-360 Ma Yakutsk-Vilyui LIP. There is also a PGM age match to the c. 500 Ma Kharaulakh LIP. We also see c. 1700-1800 Ma ages of ferroan platinum PGM that could be linked to either the 1750 Ma Timpton LIP or the 1870 Ma Kalar-Nimnur LIP.

Tectonic activation in the southern margin of the Siberian platform caused by Mesozoic subduction forming the Mongol-Okhotsk belt (Parfenov et al., 1999) was accompanied by subalkaline and alkaline magmatism including the Aldanian-type Pt-bearing concentrically-zoned massifs – Kondyor, Inagli, Chad, and others. So, some of the PGM could also be from these sources.

Acknowledgements

This work was carried out as part of the scientific research of the DPMGI, Nos. 0381-2016-0003; 0381-2016-0004 and supported by the RFBR project No. 17-05-00390.

References

1. Ernst R.E. (2014) Large Igneous Provinces. Cambridge University Press. 653 p.
2. Ernst R.E. Hamilton M.A., Söderlund U. et al. (2016) Long-lived connection between southern Siberia and northern Laurentia in the Proterozoic. Nature Geoscience 6: 464-469
3. Genkin A.D. (1968) Platinum-group minerals and theirassociations in copper-nickel ores of the Nord'sk deposit. Moscow. Nauka. 106 p. (in Russian).
4. Krivenko A.P., Izokh A.E., Tolstykh N.D., Gongal'skiy B.I. (1996) Stability of platinum and palladium minerals during the breakdown of sulfide ores. Transactions (Doklady) of the Russian Academy of Sciences. Earth Science Sections. 345: (8) 214-219
5. Likhachev A.P., Kirichenko V.T., Lopatin G.G. et al. (1987) Distinctive features of platinum occurrences in the massifs of alkaliullrabasic formations: Zap. Vses. Mineral. Obshch. 1: 122-125 (in Russian).
6. Okrugin A.V. (1998) Mineralogy, types, and origin of platinum-bearing placer deposits of the Siberian platform. International Geology Review. 8: 677–687
7. Okrugin A.V., Kostoyanov A.I., Shevchenko S.S., Lazarenkov V.G. (2006) The model Re–Os age of platinum group minerals from Vilyui placers in the eastern Siberian Craton. Dokl. Earth Sci. 410: 1044-1047
8. Okrugin A.V., Yakubovich O.V., Gedz A.M., Zemnukhov A.L., Ivanov P.O. (2019) Mineralogical–geochemical types and 190Pt–4He Age of ferroan platinum of placers of the Anabar river basin, Northeastern of the Siberian Platform. Doklady Earth Sciences. 484: 134–137
9. Parfenov L.M., Popeko L.I., Tomurtogoo O. (1999) Problems of the tectonics of the Mongol–Okhotsk orogenic belt. Tikhookeanskaya Geologiya. 5: 24–43
10. Shpunt B. R. (1970) Platinum minerals in Quaternary deposits of the Anabar-Olenek Uplift. Geologiya rudnykh mestorozhdeniy. 2: 123-126 (in Russian).
11. Shukolyukov Yu.A., Yakubovich O.V., Mochalov A.G., et al. (2012) New geochronometer for the direct isotopic dating of native platinum minerals (190Pt-4He method). Petrology. 20: (6) 491-505.
12. Yakubovich O.V., Mochalov A.G., Sluzhenikin S.F. (2015) Sperrylite (PtAs2) as a 190Pt-4He geochronometer. Dokl. Earth Sci. 462: 472-474.
13. Yakubovich O.V., Okrugin A.V., Druzhinina Zh.Yu., Gedz A.M., Ernst R. (2018) 190Pt-4He ages of platinum metals from placers of the Siberian platform and their possible connection with large igneous provinces. 13th International Platinum Symposium. Abstracts. Polokwane. South Africa. p. 213-214.

ANOROGENIC MAGMATISM OF NIGERIA: CHARACTERISTICS, AGE TRENDS AND TECTONO STRUCTURAL CONSTRAINS

Okunlola O.

Department of Geology University of Ibadan, Nigeria

Anorogenic magmatism in West Africa transcends lower Paleozoic (Air), Upper Paleozoic (Zinder) upper Triassic to Jurassic (Jos Plateau) and Tertiary (Cameroon). Clusters of ring complexes emplaced into the Pan African basement bordering Mesozoic sedimentary basins occur in these well-defined areas, all clearly showing a strong southward progression of ages. An N-S trending belt aligned in the northward projection of the western Coastline of South Africa defines the first three which are about 1500km long.

Over 40 individual granitoid ring complexes recognized in Nigeria as the Younger Granites shows similar petrologic and geochemical variations ranging in size from <2km to 1500km^2, though mostly concentrating in a 200km^2 wide North - south zone centered around Jos plateau . Occurrence of basic intermediate and rhyolitic rocks together with granitic equivalents suggest a basic parent with evolution through plagioclase, fayalite, clinopyroxene , K-feldspar and quartz fractionation .The 'S' shaped distribution pattern of the Ring complex province resembles a N-S spreading ridge truncated by E-NE trending transform faults. An interpretation of high resolution aeromagnetic data reveals a prominent shear zone in Wase area interpreted as an eastward continuation of a southern transform fault. Rb –Sr isotopic measurements on minerals and whole rock have revealed southerly decreasing age trend from Dutse complex, the most northerly -late Triassic (Rhaetian,203Ma), to the most southerly Ma Upper Jurassic, (Tithonian , 147Ma). Three age cluster trend seems obvious viz the Tithonian- Aalenian (147 174 Ma; the Toarcian -Hattergia 174-199Ma and the Rhaetian (208 Ma) which may be concordant with the Air complex in Niger Republic. The possible linkages of these trends with drifting motion of the African continent and or the continental breakup of the equatorial Atlantic as evidenced from other dyke swarms intruding the Boborrema province of NE Brazil are considered in the Paper

APPLICATION OF PALEOMAGNETIC RECORD OF GEOMAGNETIC SECULAR VARIATIONS FOR CONSTRAINING THE RATE AND DURATION OF VOLCANISM IN LARGE IGNEOUS PROVINCES

Pavlov V. E.[1], Veselovskiy R. V. [1,2], Latyshev A. V.[1,2], Fetisova A. M. [1,2]

[1]*Institute of Physics of the Earth, Russian Academy of Science, Moscow, Russia*
[2] *Moscow State University? Moscow, Russia*

Keywords: *Geomagnetic secular variations, time constraints, rate and duration of volcanic activity, Large igneous provinces.*

Study of geomagnetic paleosecular variations recorded in volcanic flows and in subvolcanic intrusions can be considered as a quite powerful tool to constrain the rate and duration of their emplacement, to correlate them and to subdivide volcanic piles into packets corresponding to volcanic pulses.

In our report we consider the principle of the method, which allows to solve such tasks and demonstrate several examples of its successful application to volcanic piles of the Siberian P-T large igneous province.

When studying the volcanic sections of the Norilsk and Maymecha-Kotuy regions we have shown that volcanic activity in these regions occurred during a limited number of volcanic pulses and individual eruptions and that the total duration of eruption did not exceed a time of the order of 10,000 years (the lulls between volcanic events are not included). Our studies confirm the occurrence of the thick interval in the lower part of the Norilsk trap sections, which contains record of geomagnetic reversal and excursion. This interval, which has been found earlier by Heunemann et al. (2004) and Gurevitch et al. (2004) indicate that up to 1 km thick lava pile (~20 000 km3 of basalts) of the Kharaelakh, Norilsk and Imangda troughs was formed during a brief, voluminous eruptive period of only several thousand years or less.

Our data suggest that the ore-bearing Norilsk-type intrusions are coeval or nearly coeval with the boundary of the Morongovsky and Mokulaevsky Fms, and therefore the ages obtained for Norilsk-1 intrusion (251.907±0.067 Ma (Burgess and Bowring, 2015) and 251.2±0.3 Ma (Kamo et al., 1996)), can also be attributed to this boundary.

Acknowledgements

This work was supported by grant of RSF # 19-47-04110

References

1. Burgess S.D., Bowring S. A. High-precision geochronology confirms voluminous magmatism before, during, and after Earth's most severe extinction // Science

PROSPECTS OF PALEOMAGNETIC RESEARCHES OF THE OKHOTSK-CHUKOTKA VOLCANIC BELT FOR DECIPHERING THE TECTONIC HISTORY OF NORTHEASTERN ASIA AND FOR STUDYING THE EVOLUTION OF THE EARTH MAGNETIC FIELD.

Pavlov V. E.[1], Tikhomirov P. L.[2] ,Pasenko A. M[1], Gavryushkin D. A.[1], Lebedev I. E.[1]

[1]*Institute of Physics of the Earth, Russian Academy of Science, Moscow, Russia*
[2]*Moscow State University, Moscow, Russia*

Keywords: *Ochotsk-Chukotka volcanic belt, silicic LIPs, paleomagnetism, geomagnetic superchron*

The Cretaceous Okhotsk–Chukotka volcanic belt (OCVB) is a subduction-related magmatic province with estimated total extrusive volume ranges between 5.5×10^5 km^3 (the most conservative estimate) and over 10^6 km^3. The belt extends over than 3000 kms along the Pacific margin of Asia and its main volumetric, temporal and compositional parameters are similar to those of silicic LIPs. In spite of the OCVB represents a geological structure of the planetary scale, its paleomagnetic study is limited only by several works, only two of which correspond to currently accepted quality requirements. Especial interest in studying of the OCVB is stipulated by the fact that the majority of its volcanic series has been formed during the Cretaceous Normal Polarity superchron (CNPS) which makes it promising object for reconstruction of the geomagnetic field evolution.

This year in the Chukotka region we have undertaken large-scale field studies of the volcanic series's of the OCVB aimed to obtain paleomagnetic constraints both on the tectonic history of North-Eastern Eurasia and on the behavior of the geomagnetic field parameters during the CNPS. In our report we present the objects of the region, which currently seems to be the most promising for paleomagnetic studies, discuss the preliminary results and the tasks of further investigations.

Acknowledgements

This work was supported by grant of RSF # 19-47-04110

LIP PRINTING: A GEOCHEMICAL PROXY APPROACH TO THE CHARACTERIZATION OF LARGE IGNEOUS PROVINCES

Pearce J. A.[1], Ernst R. E.[2], Rogers C.[2] , Peate D. W. [3]

[1]*Cardiff University, Cardiff, UK*
[2] *Carleton University, Ottawa, Canada*
[3] *University of Iowa, Iowa City, USA*

Keywords: *Large Igneous Provinces, (LIPs) trace elements, geochemical fingerprinting*

Introduction

One effective way to compare and contrast large igneous provinces is by using geochemical proxies for parameters such as mantle temperature, mantle composition, nature and degree of partial melting, crustal composition, and assimilation-fractional crystallization. In the ideal world, each geochemical proxy would highlight just one petrogenetic variable. Here, we focus on two immobile element proxies in basic rocks: Th/Nb as a proxy for crustal input (via subduction and/or assimilation); and Ti/Yb as a proxy for depth and degree of mantle melting. The methodology is a further development of the use of Th/Nb and Ti/Yb for geochemical fingerprinting of oceanic basalts (Pearce, 2008). Here we use the Th/Nb-Ti/Yb projection (which we term the 'LIP printing diagram') to distinguish different types of LIP basalt

Results

The LIP printing diagram is made up of two main fields. The first is an island arc basalt field which (as a result of high degree of shallow melting accompanied by influx of a subduction component) has low Th/Yb and high and variable Th/Nb. For LIPs, this field represents basalts derived from sub-continental lithospheric mantle (SCLM) containing an inherited subduction zone (SZ) component and so is termed the 'SZ-SCLM' field. The second is an oceanic basalt field which (because of an absence of crustal input) has low Th/Nb and (and because of variable degrees and depths of melting) has variable Ti/Yb. For LIPs, this field represents basalts derived from the asthenosphere mantle and so is termed the 'mantle plume' field. It divides into low Ti/Yb (MORB-like) and high Ti/Yb (OIB-like) segments. For any two LIP basalts to have identical LIP prints, they would require similar plume temperatures, similar lithospheric thicknesses, similar contributions and compositions of plume mantle and mantle lithosphere, and similar degrees of interaction with continental crust. Thus, most LIP prints are distinctive. Nonetheless, our LIP database provides evidence that LIP basalts can usefully be grouped on the basis of their LIP prints into four types.

Type I LIP basalts plot almost entirely within the 'mantle plume' field. Oceanic LIPs (e.g. Shatsky, Ontong-Java Nui), some continental break-up LIPs (e.g. NAIP basalts in Green-

land), some dyke swarm LIPs (e.g. the 1880Ma Circum-Superior LIP) and some of the oldest LIPs (e.g. 3450Ma Onverwacht) are dominated by this basalt type. They can be explained by plume melting beneath lithosphere of variable thickness where the lithosphere has no history of subduction-related metasomatism.

Type II LIP basalts plot almost entirely within the 'SZ-SCLM' field. Some continental break-up LIPs (e.g. CAMP, Parana and Karroo-Ferrar), some economically-important LIPs (e.g. Siberia and Bushveld) and some dyke swarm LIPs (e.g. Gunbarrel and Matachewan) contain abundant basic rocks of this type. They can best be explained by derivation from a SZ-SCLM source with the underlying plume providing heat but no, or little, magma.

Type III LIP basalts form trends between the 'SZ-SCLM' field and the MORB-like segment of the 'mantle plume' field. The Siberian Traps, Columbia River, Wrangellia and Belingwe are all LIPs containing basalt sequences of this type. They can be generally explained by plume-lithosphere interaction, where the plume contribution is the product of significant degrees of melting and the lithosphere contribution could be subduction-modified mantle or continental crust.

Type IV LIP basalts form trends between the 'SZ-SCLM' and the OIB-like segment of the 'mantle plume' field.. Examples include parts of the Deccan, Karroo and Parana LIPs, and the Mistassini and Franklin dyke swarms. This type of LIP also requires plume-lithosphere interaction but the plume contribution comprises small degree melts, and assimilation of continental crust has little effect.

LIP printing has a number of applications, which include: matching dyke swarms within and between continents; documenting the evolution of individual LIPs in space and time; investigating mantle sources in the early Earth; and identifying volcanic units with ore prospecting potential.

Conclusions

Like lip prints used in forensic science, the LIP prints defined here provide an effective means of fingerprinting. Our study shows that, globally, LIP basalts exhibit a very wide range of LIP prints, reflecting the similarly wide range of petrogenetic histories experienced by LIPs throughout the geological record.

Acknowledgements

Canadian NSERC CRDPJ 523131-17 provided partial support. Ernst is additionally supported by Russian Mega-Grant 14.Y26.31.0012

References

1. Pearce J.A. (2008). Geochemical Fingerprinting of oceanic basalts with implications for the classification of ophiolites and search for Archean oceanic crust. Lithos 100: 14-48.

LIPS AND SUPERCONTINENT RECONSTRUCTIONS

Pisarevsky S. A.

Institute of the Earth's Crust, Irkutsk, Russia
Curtin University, Perth, Australia

Keywords: *Precambrian, paleogeography, LIPs, paleomagnetism, supercontinent*

Introduction

The supercontinental cycle hypothesis and its relationship with global geodynamic processes attracts a lot of attention from the Earth science community. Most of the workers accept this hypothesis as plausible, but its details are still debated for several reasons. First of all, there is no consensus about the definition of a supercontinent. For example – is Gondwana a supercontinent? Depending on the answer, various estimations of the longevity of supercontinent cycle(s) arise. Another concern regards the methodological approach to paleogeographic reconstructions. For instance, some workers consider that the Precambrian supercontinent Nuna (aka Columbia) was assembled as a result of the widespread 2.0-1.8 Ga orogeny. However, careful consideration of geological, geochronological and paleomagnetic evidence instead suggests that only building blocks of this supercontinent were assembled during this 2.0-1.8 Ga time interval, and the assembly of these building blocks into a supercontinent occurred about 200 Myr later (Fig.1).

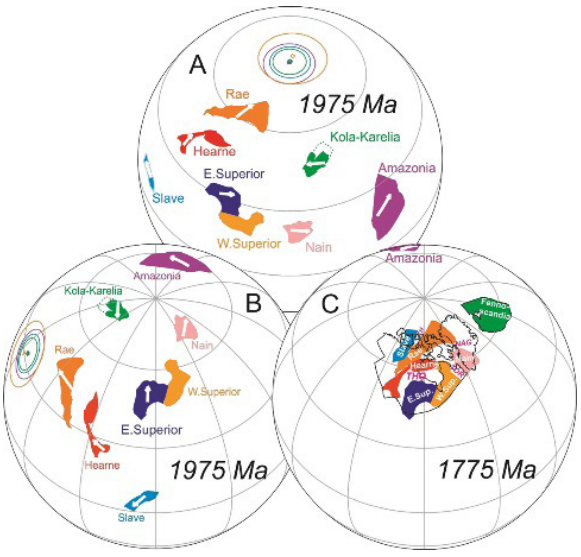


Figure 1. 2000-1775 Ma assemblies of the Nunan building blocks (after Lubnina et al., 2017)

Discussion

There are only two quantitative tools for Precambrian paleogeographic reconstructions – paleomagnetic data and LIPs and regional mafic dyke swarms geometries. The abundance of Meso-Cenozoic and Late-Middle Paleozoic paleomagnetic data permit producing robust global paleogeographic reconstructions for the Gondwana-Pangea time and provide a sufficient knowledge for the history of assembly and breakup of these supercontinents. Unfortunately, there are not yet enough high quality Precambrian paleomagnetic data to produce Apparent Polar Wander Paths (APWPs) for most Precambrian continents and to reconstruct their relative position with respect to each other, as was done for Phanerozoic paleogeography. Consequently all published reconstructions of Precambrian supercontinents are suggestive but not definitive. The only way to build a plausible Precambrian paleogeographic reconstruction is to combine paleomagnetic data with geological, geochemical and geochronological evidence. The combination of paleomagnetic data with matching coeval Large Igneous Provinces (LIPs) and their regional dyke swarms, is especially helpful (Fig. 2). Moreover, there are only few highly reliable Early Paleoproterozoic and Archean paleomagnetic data, so the LIPs barcode matching becomes a leading method for such ancient reconstruction. A detailed studies of LIPs also contribute to the modelling of processes of the breakup of supercontinents. One example is shown in Fig. 3.

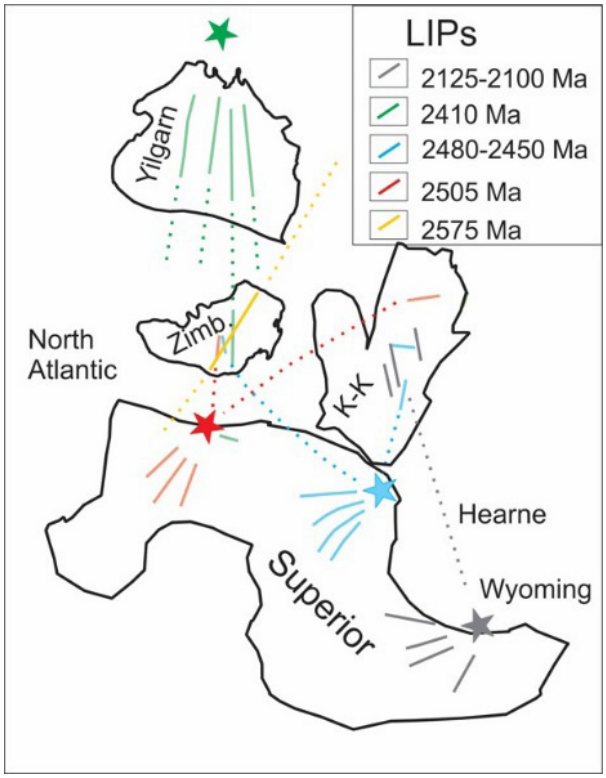


Figure 2. Example of the ~2400 Ma paleogeographic reconstruction made by paleomagnetic data and LIPs matching (after Pisarevsky et al., 2015)

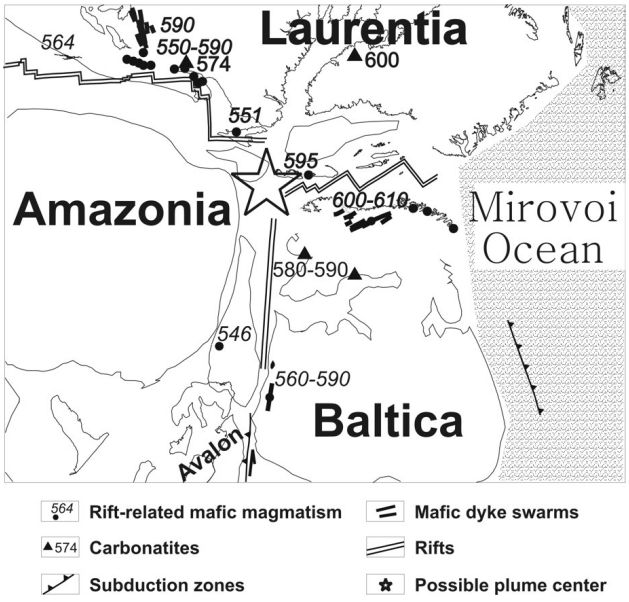


Figure 3. The final breakup of Rodinia and opening of Iapetus Ocean and Tornquist Sea (after Pisarevsky et al., 2008)

Acknowledgements

This research was supported by Russian Science Foundation (grant # 18-17-00101).

References

1. Lubnina, N.V., Pisarevsky, S.A., Stepanova, A.V., Bogdanova, S.V., Sokolov, S.J., 2017. Fennoscandia before Nuna/Columbia: Paleomagnetism of 1.98–1.96 Ga mafic rocks of the Karelian craton and paleogeographic implications. Precambrian Research 292, 1-12.
2. Pisarevsky, S.A., De Waele, B., Jones, S., Söderlund, U., Ernst, R.E., 2015. Paleomagnetism and U–Pb age of the 2.4 Ga Erayinia mafic dykes in the south-western Yilgarn, Western Australia: Paleogeographic andgeodynamic implications. Precambrian Research 259, 222-231.
3. Pisarevsky, S.A., Murphy, J.B., Cawood, P.A., Collins, A.S., 2008. Late Neoproterozoic and Early Cambrian palaeogeography: models and problems. In: Pankhurst, R.J., Trouw, R.A.J., Brito Neves, B.B. & de Wit, M.J. (eds) West Gondwana: Pre-Cenozoic Correlations Across the South Atlantic Region. Geological Society of London, Special Publications, 294, 9-31.

THE MIDDLE PALAEOZOIC STAGE OF MAFIC MAGMATISM AND EVOLUTION VILYUI PALEORIFT BASIN (EASTERN SIBERIAN PLATFORM): PLUME- OR EXTENSION-RELATED?

Polyansky O. P.[1], Prokopiev A. V.[2], Koroleva O. V.[2], Babichev A. V.[1]

[1]*Sobolev Institute of Geology and Mineralogy, Siberian Branch, Russian Academy of Sciences, Ak. Koptyug Prospect 3, Novosibirsk 630090, Russia*
[2]*Diamond and Precious Metal Geology Institute, Siberian Branch, Russian Academy of Sciences, Lenin Prospect 39, Yakutsk 677980, Russia*

Keywords: *Siberian craton; dykes, Vilyui rift basin; backstripping analysis; numerical modelling*

Introduction

It has been known that many of the large igneous provinces (LIPs) are spatially associated with intracontinental sedimentary basins, particularly with rift-related ones (Bryan and Ernst, 2008). The periods of basic magmatism coincide with synrift and postrift stages of the basin development. In relation to the problem of the Vilyui basin origin (Polyansky et al., 2013) and the associated Yakutsk-Vilyui LIP (Ernst, 2014), it is vital to establish time correlation between the dyke intrusion and the stages of extension and rapid subsidence in different parts of the basin. Dyke swarms extending for hundreds of kilometers with a cumulative thickness of hundreds of meters to kilometers are a specific feature of continental rifting, and are widely used in tectonic plate reconstructions.

In this study we discuss 40Ar/39Ar ages of plagioclase and pyroxene grains from dolerites and quartz monzonites of the dyke swarms framing the Vilyui rift basin. Seventeen previously published 40Ar/39Ar and U-Pb dates of dykes of these swarms were used in statistical analysis (Fig.1).

To estimate the degree of extension, we have modified 1D model for "instant" crustal extension of D.McKenzie. The model involved the lithospheric rifting due to the extension and emplacement of mafic dikes. We have considered the model for nonuniform stretching (over depth) of two-layered lithosphere consisting of the crust and the lithospheric mantle. Total subsidence is achieved by plotting the depth at the base of the studied section restored through time; this method is termed backstripping (Polyansky et al., 2013).

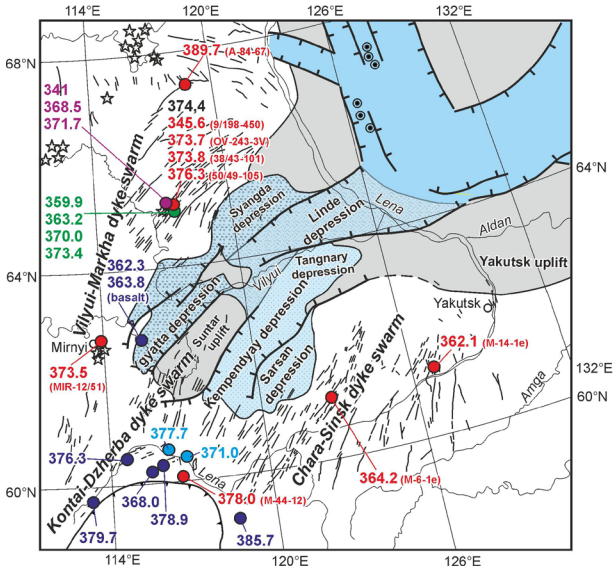


Figure 1. Structure of the Vilyui basin and available 40Ar/39Ar and U/Pb ages of Middle Paleozoic dykes, sills and basalt (color circles and numbers – see (Polyansky et al., 2017).

Results

Backstripping method has been used to analyze data on 14 boreholes, within an area of 400x250 km along the longitudinal and transverse axes of the Vilyui basin (Prokopiev et al., 2001). Two stages of rapid subsidence are recognized. The first rifting stage happened in the Middle-Late Devonian at 400-375 Ma. The second, foreland stage was recorded in the Middle-Late Jurassic at 190-140 Ma.

The reconstructions show that the lithosphere thinning is nonuniform over depth. The mantle lithosphere usually stretches more than the crust: by a factor of 1.2-2.0 against the 1.1-1.4-fold in the crust. The expansion due to intrusion of dykes varies from 1 to 12 % in different basin parts. The greatest extension is predicted for the deepest (up to 14 km) central part of the Linde depression (by a factor of 1.43-1.83) and for the neighboring Tangnary depression (by a factor of 1.39-1.77). The degree of extension decreases toward the periphery of the Vilyui basin to 1.18 in the Kempendyay depression and 1.178-1.25 times in the Sarsan depression. Considerable extension due to intrusion of dykes is expected both in the central, closer to the rift axis of the basin and on its flanks (Sarsan depression).

40Ar/39Ar isotope ages are obtained for nine Middle Paleozoic mafic dykes of Yakutsk-Vilyui LIP and all recently published dates are summarized. Statistical analysis of the dyke ages revealed a repeated character of magmatism in the study area. Two major pulses of mafic magmatism are identified: one at the Frasnian-Famennian boundary time, with a main peak at about 374.1 Ma, and the other in the Late Devonian with a peak at about 363.4 Ma. Maximum intensity of dyke intrusions coincides (within the limits of dispersion) with the rapid subsidence phase of the Vilyui rift basin (Fig. 2).

The data independently obtained by isotope-geochronological and backstripping analysis suggest two models for the development of the Vilyui rift and LIP.

The first model is based on observations in spreading sedimentary basins (Halls, 1978). Old feeder channels normally occupied marginal positions, which were consistent with crustal spreading away from the axial zone of dyke intrusion. According to this model, the marginal dykes of Vilyui-Markha and Chara-Sinsk swarms must have been separated

by ~ 600 km. With the initial basin width of 250-300 km, the degree of crustal extension will be over 2, which is higher than the value obtained by the backstripping method. The spatial age distribution analysis of the dykes did not reveal their younging in the direction from the marginal zones to the central axis of the rift basin (see Fig. 1). The second scenario has been based on the model of a magmatic or "active" rifting. Active rift models in which the driving forces providing for extension are generated by mantle plume impingement on the base of the lithosphere (Fig. 3). Isotope ages of the dykes vary from 373-374 Ma to 364-362 Ma (Fig. 2b). This sequence of dyke intrusion may be due to the area expansion during basaltic magma underplating beneath the crust.

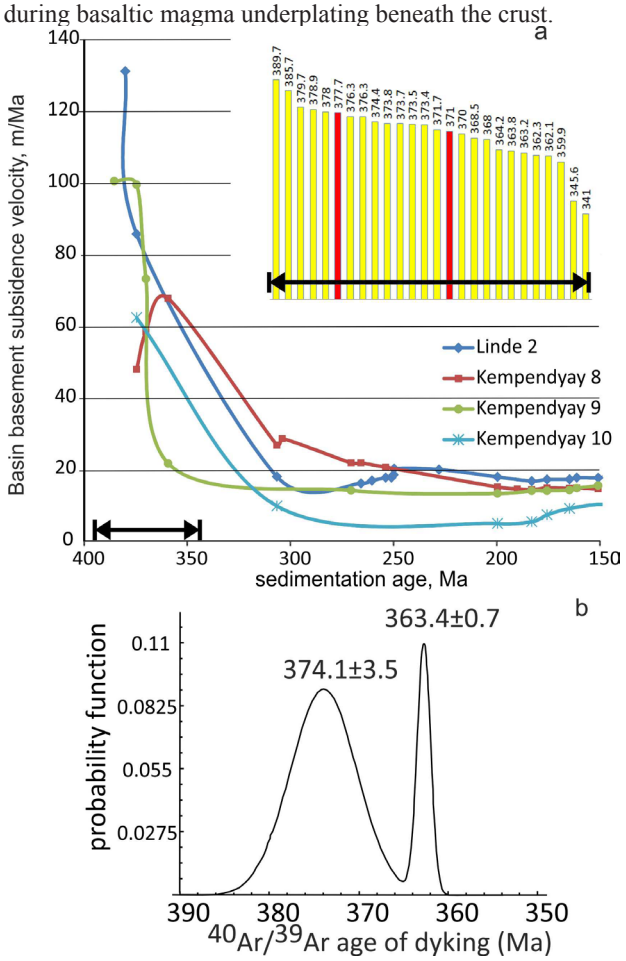


Figure 2. A) Backstripping data of subsidence rate of the Vilyui rift basement for the axial zone and compilation of the dykes isotope ages, in Ma, shown in a histogram, based on the data from (Polyansky et al., 2017). 40Ar/39Ar data are shown by yellow bars and U/Pb data by red bars; B) Results of statistical analysis of 22 isotope ages of the Vilyui dykes showing binormal distribution with twin peaks at 374±3.5 and 363±0.7 Ma.

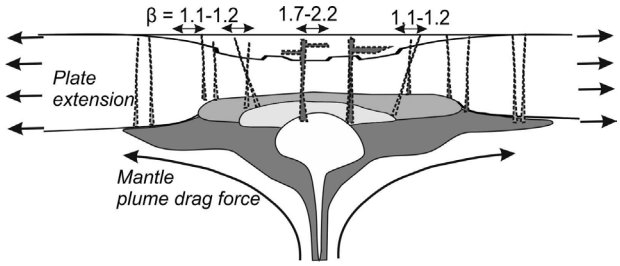


Figure 3. Generalized best-fit model for the Vilyui rift/LIP formation based on geochronological ages of dike swarms and numerical modeling. The areas of magma underplating are shown in gray shades, the lines with arrows depict the inferred trajectories of material flows.

Conclusions

Middle Palaeozoic mafic magmatism in the Yakutsk- Vilyui LIP was extended in time in contrast to the Siberian traps.

Isotope ages of the dykes vary from 374 Ma at the time of the main peak of dyke intrusion, to 362 Ma at the second peak.

We estimated a minimum volume of mafic magmatism of 100–215 K km3 in the Vilyui paleorift.

Best-fit model offered for the Vilyui rift/LIP formation is a combined active/passive rifting.

References

1. Bryan S.E., Ernst R.E. (2008) Revised definition of Large Igneous Provinces (LIPs). Earth-Science Reviews 86: 175–202.
2. Ernst R.E. (2014) Large igneous provinces. Cambridge University Press. 653 p.
3. Polyansky O.P., Prokopiev A.V., Babichev A.V., Korobeinikov S.N., Reverdatto V.V.(2013) The rift origin of the Vilyui basin (East Siberia) from reconstructions of sedimentation and mechanical mathematical modeling. Russ. Geol. Geophys. 54 (2): 121–137
4. Polyansky O.P., Prokopiev A.V., Koroleva O.V., Tomshin M.D., Reverdatto V.V., Selyatitsky A.Yu., Travin A.V., Vasiliev D.A. (2017) Temporal correlation between dyke swarms and crustal extension in the middle Palaeozoic Vilyui rift basin, Siberia platform. Lithos. 282-283: 45-64 Prokopiev A.V., Parfenov L.M., Tomshin M.D., Kolodeznikov I.I. (2001). The Cover of the Siberian Platform and adjacent fold-thrust belts, in: Parfenov, L.M., Kuz'min, M.I. (Eds.), Tectonics, Geodynamics, and Metallogeny of the Sakha Republic (Yakutia) (in Russian). Nauka/Interperiodika, Moscow, pp. 113–146.

GEOLOGY, MATERIAL COMPOSITION OF BREEDS AND ISSUES OF GEODYNAMICS OF MATYSKEN BASIT-HYPERBASITE MASSIF (KORYAKIA)

Popov Yu. V., Grinev O. M.

National Research Tomsk State University, Tomsk, Russia

***Keywords**: Matysken array, Ural-Alaskan type*

Concentrically zonal gabbro-clinopyroxenite-dunite massifs of Kamchatka and Koryakia in the region form an extended belt and are confined to the Achayvayam-Valaginsky terrain. The belt stretches in the North-Eastern direction from the sources of the river Lake Kamchatka to the bay of Natalia for 1400 km with a width of 30-50 km. (Sidorov et al., 2012). The Matysken array is located in the northeastern part of the platinum-bearing belt and is included in Vyvensky dunite-clinopyroxenite-gabbro complex of late cretaceous-paleocene age.

These Intrusive complexes have a high potential in the formation of platinum placers. For several typomorphic characteristics Matysken and similar arrays Vyvensky complex of identical concentrically zoned plutons of the Urals, which has been associated with large alluvial deposits of platinum. Within Koryakia, a similar example is also known – the Galmoenan array. Therefore, it is important to study the geological and material features of the root source (Matysken massif), which will allow us to answer a number of questions that interest us, which were raised a long time ago, by other researchers, but have not yet found a definite answer. One of the fundamental issues is the problem of determining the source of the substance of intrusives. It is believed that the formation of plutons is directly related to the evolution of the lithosphere in the zones of transition from ocean to continent (Lazarenkov, 2002). There is also an opinion that during the formation of the geostructures of Kamchatka, alternation of collisional and rift regimes took place (Filatova, 2008), which affected the composition of magmatites.

The Matysken array is located in the headwaters (ridge zone) of the river. Matysken and Snow. It is represented by the main body with an area of about 7 km2, and a number of its satellites. The internal structure of the body of the massif is concentric zonal. Most of the area of the massif is composed of dunite bodies (4.5 km^2). Each of the zones of the massif is separated from each other by a system of faults, tectonic contacts are observed along their entire length.

According to the latest state geological survey of 1: 50,000 scale (Reasonable et al., 2000), the Vyvensky complex was formed in two phases of implementation, each of which is represented by several subphases: the first phase (campan-maastricht of the late cretaceous): the first subphase is dunites; the second subphase - clinopyroxenite, verlite; the third subphase is represented by eucrites and gabbropegmatites; second subphase (paleocene early paleogene). The rocks of the phase are distributed sporadically in the form of dikes, lived mainly in connection with the main body of the massif, but they are also found at a distance from it. Composition: the first subphase is represented by the bodies of olivinite dikes; the second subphase is represented by gabbro, gabbro-dolerite, diorite, monzodiorite.

Petrochemical characteristic

The most characteristic petrochemical features of the rocks of the massif are in the bimodal distribution of figurative points in the diagrams. At the same time, the main continuous

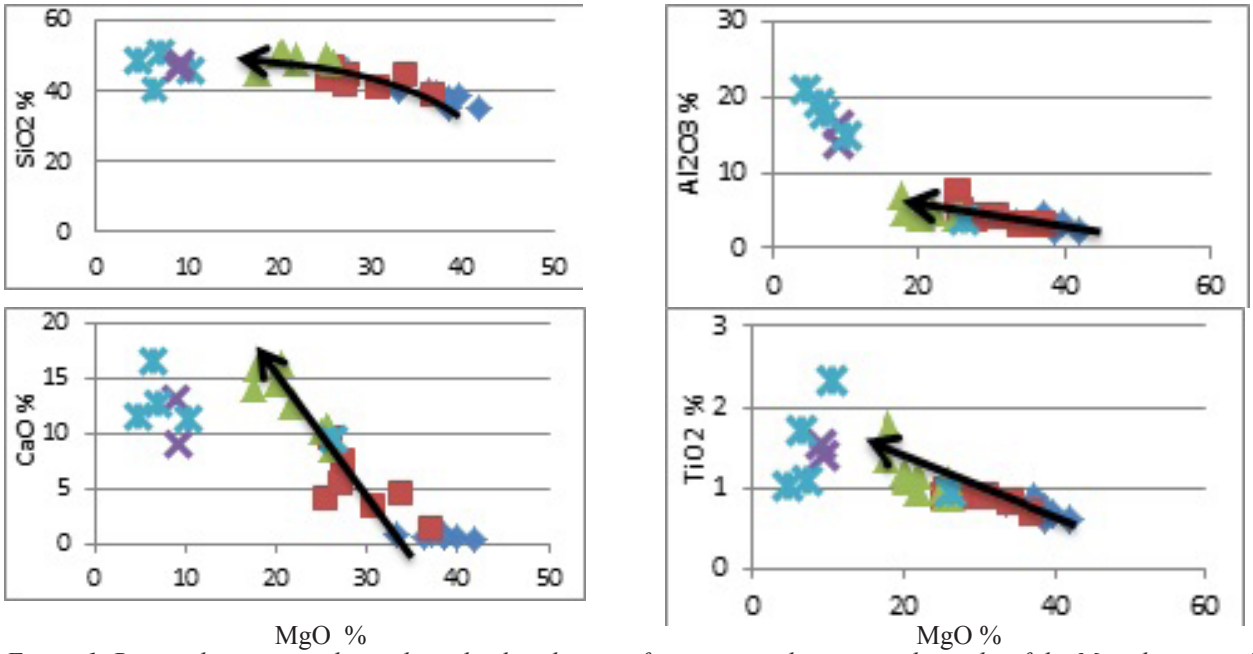


Figure 1. Binary diagrams with trends in the distribution of petrogenic elements in the rocks of the Matysken massif

dunites; verlite; clinopyroxenite; gabbro; veins

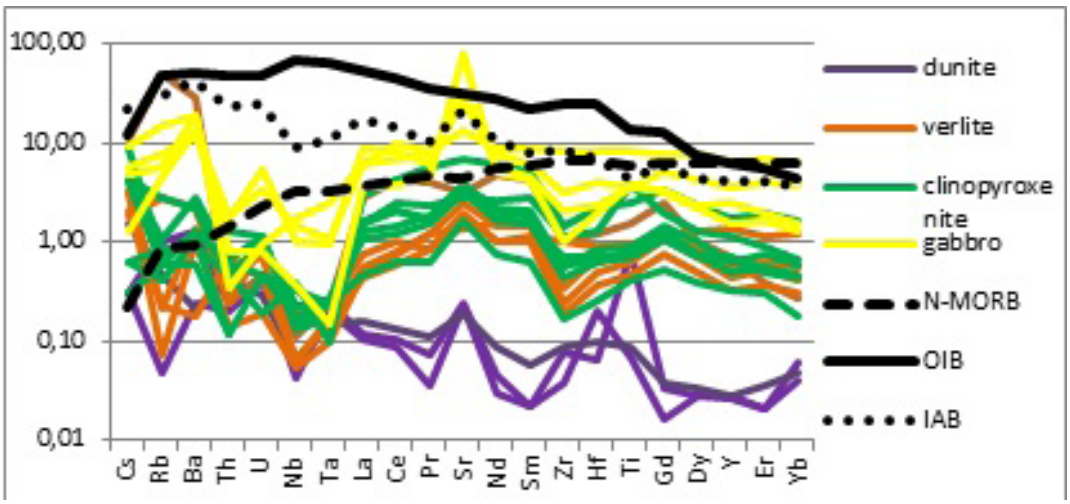


Figure 2. Multi-element spider diagram of distribution of trace elements in the rocks of the Matysken massif

trend is formed by the rocks of the phase (dunites => verlites => clinopyroxenites). They are characterized by a gradual accumulation of titanium dioxide, total iron and calcium from dunites to clinopyroxenes with a corresponding decrease in the magnesium content (olivine control, close to Fenner differentiation).

The gabbros and related vein formations with them form a separate group of contiguous figurative points. The tendencies of their material differentiation are either close (for SiO_2, CaO) or differ markedly from the rocks of the first phase (for TiO_2, $Al2O_3$), which indicates a certain originality of their origin relative to the rocks of the first phase.

The geochemical characteristic

Breeds are considered in accordance with the sequence of introduction established for them: 1) dunites (first subphase) => verlites, clinopyroxenites (second subphase) => eucrites (third subphase).

On the multi-element diagram, geochemical spectra of rocks are located along the ordinate axis in the sequence of their formation. In the lowest part (at the level of 0.1 and lower), dunites, above with a gap from Ta to Yb and verlites pyroxenites and the upper position are occupied by gabbroids. According to the configuration of the geochemical spectra, the rocks are related to each other, but significantly differ in the levels of trace element concentrations — low in dunites and maximum in gabbroids. For the rocks, positive peaks of Ba, U, Sr, Ti, and negative for Rb, Nb-Ta, Zr, and Hf are well pronounced.

With respect to geochemical benchmarks, the rocks most closely correspond to the N-MORB benchmark, gabbroids approach the IAB benchmark.

The geodynamic assessment of rocks was determined using well-known discriminant diagrams (Wood, 1980; Meshede, 1986; Cabanis, Lecolle, 1989). On the Th-Hf-Nb diagram, the figurative points of the dunites are located in the field B and near the field C (enriched with MORB COX and tholeiite intraplate basalts); pyroxenites and part of gabbroids formed in the center of the field D (basalts of the destructive margins and their differentials) and in the extreme upper part of the field D and A (normal MORB COX).

In the Zr-Nb-Y diagram, dunites are scattered in the A1, C, and D fields (intraplate tholeites, volcanic arc basalts, and normal MORB COX), while the remaining rocks are concentrated in field D and partially in the adjacent C field (volcanic arc basalts and MORB).

The diagram of La-Y-Nb shows that dunites are located in field 2 - continental basalts, and the rest in field 1B, 1C - island-arc tholeiites.

Conclusion

The Matysken array belongs to the concentric-zonal bodies of the Ural-Alaskan formation type. Among the many arrays of the Vyvensky complex, it is the most representative of the composition of the rocks, which determines its status as a petrotypic array. The next stage of the study of this massif is associated with the characteristic of its ore-bearing nature, the identification of patterns in the manifestation of indigenous platinum metal mineralization.

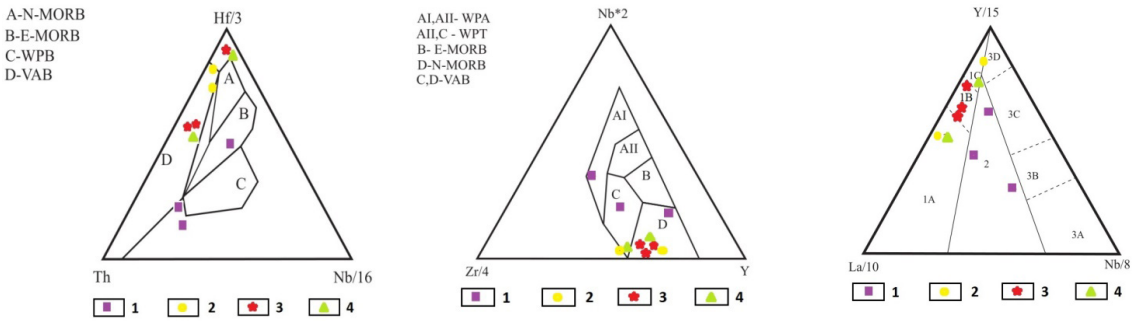


Figure 3. The position of rocks in the triple charts: 1- dunites, 2- verlites, 3- clinopyroxenites, 4-gabbro

References

1. Lazarenkov V.G., Petrov S.V., Talovina I.V. Deposits of platinum metals. SPb .: Nedra, 2002. 298 p.
2. Razumny AV, Sheludchenko SD, Mazur MI, and others. Report on a group geological survey of 1: 50,000 scale with a general search on the territory of sheet P-59. The works were performed by the Vatynsky party in 1995-2000. Compiled by the KoryakGeolDobycha Closed Joint-Stock Company in December 2000.
3. Filatova N.I. The specificity of magmatism in the marginal continental and marginal-marine basins of the synshear nature, the western periphery of the Pacific Ocean // Petrology, 2008, vol. 16, No.5, p. 480-500.

LIP RECORD OF THE URALS: RECOGNIZING PLUMES IN A FOLD BELT

Puchkov V. N.

Institute of Geology and Geochemistry, Uralian branch of Russian Academy of Sciences, Ekaterinburg, Russia.
Institute of Geology, Ufimian Research Centre RAS.

As it is widely accepted (e.g.Ernst, 2014), we regard LIPS (Large Igneous Provinces) as srong manifestations of plumes. Recognizing ancient plumes in history of fold belts such as Urals meets serious problems. Their plumes have cooled a long time ago, and therefore it is impossible to apply seismic tomography to unravel them. The magmatic complexes, as main manifestations of plumes, are partly eroded and partly concealed under younger sediments and thrusts; very often they are subjected to strong deformations. Such classical features of individual plumes as time-progressive volcanic chains are as a rule not revealed in orogens. Although the bulk of magmatic rocks of plumes is represented by flood basalts and dolerite dykes, plume magmatism is variable and may include trachybasalts, picrite-basalts, A- granites, layered mafic-ultramafic intrusions and also alkaline, carbonatite and kimberlite magmatic complexes. Fortunately, the properties of plume complexes distinguish them from spreading and subduction types, while many epicontinental rifts of active, volcanic type, may be plume-dependent. LIPs occupy wide areas and are characterized by short periods of activity (10−15 Ma). These features help to reveal ancient plumes even in foldbelts. The problem of a repeated plume activity in the Urals was raised only recently (Puchkov, 2010). A considerable progress was achieved recently in the study of geochemistry of magmatic rocks of the western slope of the Urals, and their isotopic ages became more accurate owing to the application of modern methods. The new data permit to correlate them with simultaneous magmatic events in some other regions. In addition, the identified even-aged magmatic complexes can be placed on reconstructions of ancient supercontinents, demonstrating their relatively compact primary positions above hypothetical superswells. Ten complexes can be established provisionally as material witnesses of plume episodes in the history of the western slope of the Urals (Puchkov, 2018).

1. Navysh episode. In the Southern Urals near the base of the Lower Riphean (Uppermost Paleoproterozoic and Lower Mesoproterozoic), covering the crystalline Taratash complex dated as Archean and Lower Paleoproterozoic, there are volcanic deposits of the Navysh Subformation, represented mostly by trachybasalts. The яшксог age of the unit was determined as 1752±11Ma. It is shown that volcanic rocks of the age range of 1750−1780 Ma are developed in some other places of Baltica, and also in the Northern Africa, Siberia, Laurentia, parts of the Nuna supercontinent at that time. Therefore, they may belong to a LIP.

2. Mashak episode. Higher up the section of the Riphean, at the Middle Riphean base, rhyolites of the Mashak Formation were dated in three isotopic laboratories ща the world as 1380−1385 Ma. The same ages have also basalts, rapakivi granites, layered gabbro (Kusa−Kopan Intrusion), carbonatites (Sibirka) and dolerite dykes and sills that widely eveloped in the Southern Urals and are encountered in boreholes of East European platform; magmatic rocks of the same age are traced to Greenland, Laurentia and Siberian cratons and represent the beginning of the Nuna supercontinent break-up.

3. Igonino episode. Recently, the stratigraphy of the upper part of the Riphean was reconsidered. A new straton, the Terminal (Uppermost) Riphean was established instead of the presumably Vendian Arshinian Series.The series was subdivided into four formations, mostly terrigenous in composition, but with a volcanic Igonino Formation among them. The study of zircons from this formation gave two peaks: 707.0±2.3 Ma and 732.1±1.7 Ma. Comparable ages have nearby granite massifs Barangulovo and Mazara, layered gabbro-ultramafic Sarana intrusion in the Middle Urals, and also Misaelga ferrogabbrodiabase-picrite differentiated intrusions in the Taratash uplift (726 ± 13Ma, Rb-Sr method). In the 1-Kipchak borehole, on the East European platform, lava flows are dated as 730 Ma (R−Sr method). All these magmatic rocks may belong to a hypothetical LIP with a median age 720 Ma, developed on a fragment of breaking-up Rodinia supercontinent.

4. Kiryabinka episode. Somewhat younger is the Proterozoic Kiryabinka layered peridotite-pyroxenite-gabbro intrusion, situated at the North-Eastern margin of the Bashkirian meganticlinorium (680±3.4 Ma, zircons, U−Pb method).The even-aged magmatic rocks are found toward North, in the Middle Urals − Schegrovitsk trachybasalt, Zhuravlik wehrlite-gabbro-granodiorite and Troitsk granitoid formations. In the East European platform, comparable ages belong to basites of the Onega graben. They may be the parts of a concealed LIP.

5. Mankhambo episode. In the North of the Urals, within the Central Uralian zone, A-type granites are widely developed, with a predominance of leucocratic rocks, associated with gabbro, making a contrast association; comagmatic volcanics belong to a basalt-rhyolite association. Petrochemical features are char-

actericticof divergent intraplate situation. The age is between 564–487 Ma, and mostly Cambrian. The geodynamic character indicates to a beginning of formation of Paleouralian ocean.

6. Kidryas episode. It is represented by subalkaline volcanics connected with a rift process that started at ca. 490 Ma, and led to oceanic spreading and formation of the Paleouralian ocean. This accompanied the formation of the Baltica passive margin and can be attributed to a plume-dependend volcanogenic type. The comparable and contemporaneous rifting events, accompanied by volcanism, took place in the Lower-Middle Ordovician along the eastern (in modern coordinates) margin of the Siberian continent. As it is shown by paleomagnetic data (Paverman, 2016), the "upside-down" position of the Siberia, and sub-longitudinal strike of the Uralian margin could suggest close, vis-a-vis positions of the margins, and their volcanism may belong to the same superplume episode, occurring above the same superswell.

7. Ushat episode. It was marked by an eruption of trachytes in the Bashkirian meganticlinorium, and was dated (SHRIMP, zircons) between 435 and 455 Ma. It can be correlated with the early, principal stage of development of the Vishnevogorsk plume-related carbonatite complex (Puchkov, 2018).According to data of Paverman (2016), in the Late Ordovician-Early Silurian the Uralian passive margin of Baltica could still be very close to the eastern margin of Siberia and therefore the Kidryas and Ushat complexes could be correlated with Indigiro-Kolymsk and Sourdakh events (Bulgakova, 1991, Chamberlain et al., 2018).

8. Timaiz episode. Probably it is one of several Devonian episodes. The Devonian dolerite and basalt magmatism is traced along the western slope of the Urals to Pay-Khoy and Novaya Zemlya. The rocks match excellently with the Middle–Upper Devonian volcano-intrusive complexes of the East European platform, including flood basalts, dolerite dykes, alkaline and carbonatite intrusions and kimberlites, and belong to the marginal part of the LIP called Kola-Dnieper. The late, reliably dated stage of the Devonian magmatism of the East European platform and Urals-Novozemelian belt is Frasnianin in age. They are well correlated with the Yakutsk-Vilui plume episode in the Siberian Craton and demonstrate an influence of a superswell called Tuzo.

9. Stepninsky episode. Four massives in the Middle Urals belong to the Stepninsky monzogabbro-granosyenite-granite complex (Snachev et al., 2018). They form a chain, crossing the fold and thrust structures of the orogenic Urals and are dated as 281-286 Ma. It is shown that the intrusions of the complex belong to the intraplate type. At the early stage, the basic-intermediate rocks of a deep-mantle genesis were formed, which can be regarded as a derivative of an individual plume; at the later stage they were changed by granites and leucogranites of the calc-alkaline type, formed as a result of anatexis of the lower crust.

10. Uralo–Siberian LIP and superplume. Last, but not least, are the Triassic (250-230 Ma) flood basalts, dolerite and rhyolite dikes traced from the easternmost parts of the Southern and Middle Urals to the western margin of the Polar Urals. It became evident that they belong to enormous Uralo-Siberian LIP, developed above Tuzo superswell (Reichow et al., 2009).

References

1. Bulgakova M.D., 1991. The Early Paleozoic of the Northeast of the USSR (sedimentological analysis). Yakutsk, 102 p. (in Russian).
2. Chamberlaim K.R.,Khudoley A.,Ernst R., 2018. Improved U-Pb dating of the ca. 450 Ma Suordakh mafic event in eastern Siberia will test whether this is the missing LIP related to end-Ordovician mass extinction. Petrology of magmatic and metamorphic complexes, 10. Tomsk. P.9-12.
3. Ernst, R.E. (2014). Large Igneous Provinces. Cambridge University Press. 653 p.
4. Paverman V.I., 2016. Paleomagnetism of the Middle Paleozoic of the South of the Siberan platform: geodynamic conclusions. Candidate of Sciences Thesis. Moscow, 26 p. (in Russian).
5. Puchkov V.N., 2010. Geology of the Urals and Cis-Urals (actual problems of stratigraphy, tectonics, geodynamics and metallogeny). – Ufa: Design Poligraph Service, 280 p. (In Russian).
6. Puchkov, V., Ernst, R.E., Hamilton, M.A., Söderlund, U., Sergeeva, N. ,2016. A Devonian >2000-km long dolerite swarm-belt and associated basalts along the Urals-Novozemelian fold-belt: part of an East-European (Baltica) LIP tracing the Tuzo Superswell. GFF, v. 138, p. 6-16.).
7. Puchkov, V., 2018.The Plumes – a new word in Geology of the Urals. Lithosphere, ,v.18, 4, 483–499 (in Russian).
8. Reichow M.K., Saunders A.D., Pringle M.S .et al., 2009. The timing and extent of the eruption of the Siberian Traps large igneous province: Implications for the End-Permian environmental crisis, Earth and Planetary Sci. Letters, 277, 1–2: 9–20.
9. Snachev A.V.,Puchkov V.N., Snachev V.I.,Romanovskaya M.A.,2018. Geodynamic and physicochemical conditions of formation of the Stepninsk monzogabbro-granosyenite-granite complex .Vestnik of Moscow State University, 4, geology, 6, 82-92.

POTENTIAL LINK BETWEEN UPPER CRETACEOUS LIPS AND FORMATION OF OOIDAL IRONSTONE DEPOSIT

Rudmin M., Mazurov A.

Tomsk Polytechnic University, Tomsk, Russia

Keywords: *ooidal ironstone, pyrite framboids, geochemistry, Western Siberia, Bakchar deposit, redox conditions.*

Introduction

The origin of ooidal ironstone remains controversial as there is no unanimity amongst researchers regarding the source of iron. Several workers considered that iron is available by weathering of continents and it is delivered into the ocean by river or ground water. Others suggested submarine hydrothermal exhalative source of iron.

Recent investigations explore the relationship between periods of intense volcanism (Large Igneous Provinces, LIPs), global ocean anoxic events and the formation of ooidal ironstone deposits (Ernst and Youbi, 2017). Although (Van Houten and Arthur, 1989) indicated a relationship between ooidal ironstones and anoxic events, this is yet to be investigated thoroughly. Although the origin of the giant ironstone in Meso-Cenozoic Bakchar deposit has been debated, no study attempts to relate hypoxia, global volcanism and ironstone deposits, because of lack integration of data related to mineralogical and chemical composition of ironstones with proxies for redox and volcanism. An integrated study involving pyrite framboids, trace element concentrations and mercury anomaly of the Bakchar ironstone deposit is likely to provide a detailed perspective for establishing the relationship between hypoxia, global volcanism, rifting and the origin of ooidal ironstone.

The Bakchar ironstone deposit occurs in the south-eastern part of the Western Siberia (52°01’45’’N; 82°07’20’’E) situated 200 km northwest of Tomsk. This Upper Cretaceous to Palaeogene iron ore deposit occurs in subsurface at a depth ranging from 165 to 230 m. Ooidal ores occur at three stratigraphic levels in this deposit viz. Narym, Kolpashevo and Bakchar (Rudmin et al., 2019).

Eighty seven core samples were collected from the Bakchar ironstone deposit with an interval from 0.5 to 2 m from two wells, viz. 570 and 803 at eastern and western sectors respectively. Sixty-eight thin sections were investigated for pyrite framboids by scanning electron microscope (SEM). Major element concentrations of the powdered samples were estimated by HORIBA XGT 7200 X-ray fluorescence microscope (XRF). Concentrations of trace elements (TEs), including rare earth elements (REEs), were estimated using inductively coupled plasma-mass spectroscopy (ICP-MS). Pyrolysis was performed on samples using a model 6 turbo ROCK-EVAL analyzer (Vinci Technologies). Mercury concentrations were measured using 50 mg of powdered sample with a Lumex RA-915 Portable Mercury Analyzer fitted to the PYRO-915 Pyrolyzer.

Results

Size of pyrite framboids as well as trace element enrichment factors distinguishes three hypoxic intervals within the Meso-Cenozoic Bakchar deposit. Absence of pyrite framboids as well as the mineralogical assemblage dominated by goethite ooid with illite-smectite and lepidocrocite cement indicates oxic depositional conditions for the Maastrichtian and Palaeocene intervals. High values of Mo EF (above 11.3), U EF (above 2) and V EF (above 16.2) as well as occurrence of tiny pyrite framboids indicate hypoxic shelf waters during the Coniacian. The Coniacian deposits encompass the time interval corresponding to OAE-2 (Jenkyns, 2010). Widespread anoxic depositional condition during the Santonian results in the formation of tiny pyrite framboids at the water column and/or on the sea floor. This interval is marked by high values (from 11 to 28) of Mo EF, U EF, and V EF. The hypoxic interval in Santonian include the OAE-3, which is known for the accumulation of organic-rich marine sediments. The TOC content of sediments remained low notwithstanding the isolation of West Siberian Sea. Dysoxic bottom seawater promoted the formation of large framboids (mean diameter from 6.2 to 12.0 μm) and macro-framboids (diameter 20 to 46.4 μm) as well as large number of micro-aggregates of pyrite below the sediment water interface during the early Coniacian and late Campanian.

Bottoms of Kolpashevo and Bakchar ironstones in well 803 are marked by sharp swing in Mo EF, U EF and V EF. Similar sharp swing in Mo EF and V EF (34.9 and 30.4 respectively) marks the Santonian hypoxic interval underlying the Kolpashevo ironstone. The Narym ironstone (Coniacian) exhibits a sharp increase in U EF from 2.1 to 2.6 mark in well 570. While the accumulation of chamosite-goethite ooids and different cement reflect a change in the geochemical environment from oxic to anoxic conditions during formation of ironstones (Rudmin et al., 2019). It is characterized by sequential formation of goethite-chamosite ooids, glauconite, berthierine or chamosite, pyrite and/or siderite. Narym and Kolpashevo ironstones encompassing hypoxic intervals consist of different mineral assemblages such as chamosite/glauconite-berthierine-goethite-siderite-occassional large pyrite and chamosite-glauconite-siderite -tiny pyrite, respectively.

Enhanced hydrothermal activity possibly led to the extensive emission of iron and methane saturated fluids and induced hypoxia on shelf of the West Siberian Sea. Redox sensitive proxies, pyrite framboids as well as chamosite-pyrite-siderite mineral assemblages of ironstones indicate hypoxic bottom water. Hypoxic bands in Narym and Kolpashevo ironstones correspond to global geological events such as OAE-2 and OAE-3, respectively. Therefore, the formation of ooidal ironstones is closely associated with periods of oceanic hypoxia.

Several intervals in Turonian, Early Santonian, Santonian-Campanian boundary, Early Maastrichtian and Maastrichtian-Palaeocene boundary in the section of the western and eastern parts of the deposit are marked by high contents of mercury (both Hg and Hg/TOC). Peaks of Hg and Hg/TOC patterns precede or coincide with hypoxic intervals in Coniacian and

Santonian. Higher values of Hg and Hg/TOC patterns in well 703 than in well 507 relates to closeness of the exhalation site in case of former. Ore bodies in the western sector (well 703) occur close to the tectonic uplift and therefore remain close to the exhalation site. Mercury anomalies in Meso-Cenozoic sediments of the West Siberian Sea correlates with LIP volcanisms such as Greater Ontong-Java Plateau, Karoo-Ferrar Province, High Arctic Province and Deccan Traps) in Cenomanian-Turonian, Campanian, Maastrichtian-Palaeocene (Ernst and Youbi, 2017). The close correspondence between mercury anomalies and hypoxic intervals within the Meso-Cenozoic ironstone deposits in West Siberian sea establishes the relationship between LIPs and OAEs (Ernst and Youbi, 2017; Percival et al., 2018). These large volcanic events possibly contributed to the formation of extensive ironstone ore deposits on ocean floor.

Intense accumulation of ooidal ironstone may take place soon after an oceanic hypoxia (Bekker et al., 2014; Van Houten and Arthur, 1989). Underwater exhalations of iron-saturated fluids intensifies during global volcanic events. Increase in bioproductivity and related marine hypoxia results in abundant ferrous iron in shelf waters. The immobilization of this iron as silicates causes accumulation of chamosite/glauconite-siderite-pyrite ironstones, as in Kolpashevo and Narym deposits. While the exhalation of fluids in oxic condition leads to the rapid precipitation of iron as oxyhydroxides (goethite, lepidocrocite) as in case of Bakchar ironstone (Rudmin et al., 2019). Global volcanic events possibly triggered hydrothermal convection in the continental rift systems of the West Siberian Plate (Surkov, 2002). Metal-saturated, aqueous fluids moved into the near-bottom waters by convection, similar to the continental rift system of the Dead Sea or by underwater exhalations similar to Panarea area, Mahengetang Island, the Hawaiian Islands and Trinidad Island. The methane fluid degassing possibly accompanied intensive removal of iron and formation of ironstones in the geological past (Rudmin et al., 2018).

Conclusions

Pyrite of different sizes occurs in various morphological forms such as framboids, irregular and subhedral masses, and euhedral crystals. Variation in diameter of pyrite framboids reveals three hypoxic intervals within the Meso-Cenozoic shelf sequence in Western Siberia. Occurrence of ooidal ironstone correspond to three hypoxic intervals in middle Coniacian, Santonian and early Campanian. Trace element enrichment factors exhibit sharp swings in these intervals. Narym and Kolpashevo ironstones encompassing and the hypoxic layers, which reflect to different mineral assemblages and geochemistry. Therefore the formation ooidal ironstone is closely linked to the hypoxic shelf water.Enhanced hydrothermal activity resulted in low-temperature fluid emissions and induced oceanic hypoxia during the formation of ironstones in Bakchar. Redox sensitive geochemical proxies, pyrite framboids and ore mineral assemblages record the hydrothermal activation. Mercury anomalies characterize hypoxic intervals, which are contemporaneous with global volcanic events. Thus, a potential geological connection is established between LIPs, OAEs and ooidal ironstone deposits. Hydrothermal exhalation associated with rifting contributed iron for the ooidal ironstone deposits.

Acknowledgements

This work was funded by Russian Foundation for Basic Research (18-35-00022).

References

1. Bekker A., Planavsky N.J., Krapež B., Rasmussen B., Hofmann A., Slack J.F., Rouxel O.J., Konhauser K.O. (2014) 9.18 – Iron Formations: Their Origins and Implications for Ancient Seawater Chemistry, in: Treatise on Geochemistry: 561–628 pp.
2. Ernst R.E., Youbi N. (2017) How Large Igneous Provinces affect global climate, sometimes cause mass extinctions, and represent natural markers in the geological record. Palaeogeography, Palaeoclimatology, Palaeoecology 478: 30–52.
3. Jenkyns H.C. (2010) Geochemistry of oceanic anoxic events. Geochemistry, Geophysics, Geosystems 11: 1–30.
4. Percival L.M.E., Jenkyns H.C., Mather T.A., Dickson A.J., Batenburg S.J., Ruhl M., Hesselbo S.P., Barclay R., Jarvis I., Robinson S.A., Woelders L. (2018) Does large igneous province volcanism always perturb the mercury cycle? Comparing the records of Oceanic Anoxic Event 2 and the end-Cretaceous to other Mesozoic events. American Journal of Science 318: 799–860.
5. Rudmin M., Mazurov A., Banerjee S. (2019) Origin of ooidal ironstones in relation to warming events: Cretaceous-Eocene Bakchar deposit, south-east Western Siberia. Marine and Petroleum Geology 100: 309–325. https://doi.org/10.1016/j.marpetgeo.2018.11.023
6. Rudmin M., Roberts A.P., Horng C.-S., Mazurov A., Savinova O., Ruban A., Kashapov R., Veklich M. (2018) Ferrimagnetic Iron Sulfide Formation and Methane Venting Across the Paleocene-Eocene Thermal Maximum in Shallow Marine Sediments, Ancient West Siberian Sea. Geochemistry, Geophysics, Geosystems 19: 1–22.
7. Surkov V.S. (2002) Neogean evolution of the young ural-Siberian platform. Geologiya i Geofizika 43: 754–761.
8. Van Houten F.B., Arthur M.A. (1989) Temporal patterns among Phanerozoic oolitic ironstones and oceanic anoxia. Geological Society Special Publication 46: 33–49.

PACIFIC-TYPE CONVERGENT MARGINS AND MANTLE PLUMES

Safonova I.[1,2], Maruyama S.[1], Perfilova A.[1,2]

[1] *Novosibirsk State University, Pirogova St. 1, Novosibirsk, 630090, Russia*
[2] *Sobolev Institute of Geology and Mineralogy SB RAS, Koptyuga ave. 3, Novosibirsk, 630090, Russia*

Pacific-type convergent margins (ocean - continent) and their related orogenic belts exist/form over subduction zones, which are the only ways to deliver surface materials to the deep mantle. Pacific-type orogens keep records of the evolution of paleo-oceans, formation and transformation of continental crust at their active margins, and generation of hydrous-carbonated plumes in the mantle transition zone (MTZ) and its related intra-plate magmatism. We propose a new approach for linking paleo-oceans, active margins and plume magmatism for Central and East Asia. The approach "stands" on three "whales": the model of Ocean Plate Stratigraphy (OPS), the parameters of active convergent margins and the model of hydrous-carbonated plumes. The OPS model was created by many detailed studies of western Pacific (Japan) accretionary complexes; it allows recognizing different oceanic plates within one paleo-ocean and evaluating their sizes and ages.

A geology-based model of Ocean Plate Stratigraphy (OPS) was proposed by Japanese scientists (Isozaki et al., 1990) and later developed by other researchers (e.g., Kusky et al., 2013). OPS is a regular succession of igneous (MORB, mid-ocean ridge basalt; OIB, oceanic island basalt; gabbro-peridotite) and sedimentary (pelagic chert, hemipelagic siliceous sediments, trench turbidite, seamount carbonate "cap", slope and foothill facies) rocks of the oceanic lithosphere, that were, respectively, erupted and deposited on the sea floor as the underlying oceanic basement traveled from the mid-oceanic ridge to the subduction zone (Fig. 1). During subduction OPS units get accreted to active margins to be later incorporated into accretionary complexes or subducted to the deep mantle. The OPS model can be used as a basis for the reconstruction of paleo-oceans and processes of accretion and subduction at their active margins. The fragments of oceanic crust or OPS units are important constituents of Pacific-type orogenic belts. The subdivision and mapping of accretionary complexes have been always very problematic due to their extremely complicated structure. Although most of the oceanic crust is subducted into the mantle, fragments of OPS may remain on the surface and appear accessible to our study.

An important issue for reconstructing the history of paleo-oceans is to estimate major parameters of the Pacific-type convergent margins (geometrical length, life endurance, character: accreting vs. eroding, etc.). Tectonic erosion and subduction carry oceanic and continental materials to the deep mantle and evaluation a possibility of their accumulation in the mantle transition zone (MTZ) and generation of hydrous-carbonated plumes. Our study is aimed to develop a holistic model linking the evolution of paleo-oceans, the erosion and subduction of oceanic and continental crust materials at Pacific-type convergent margins, their accumulations in the MTZ, mantle metasomatism and intra-plate magmatism.

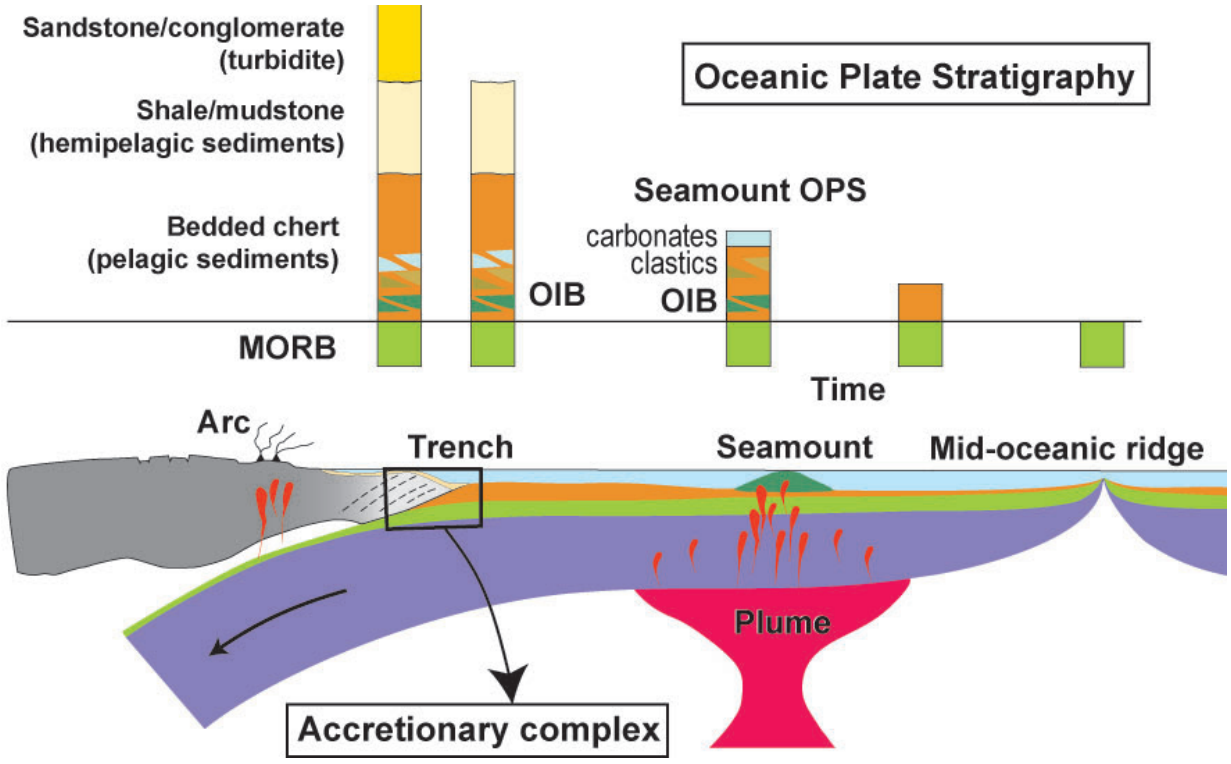


Fig. 1. A principal scheme of Ocean Plate Stratigraphy or OPS (Maruyama et al., 2010).

Pacific-type convergent margins are places of major continental growth by island-arc juvenile magmatism and accretion, but they are also places of strong plate interactions and crust destruction. Recent studies of those margins have recognized two contrast types of those margins: accreting ones accompanied by the formation of accretionary complexes, and eroding ones accompanied by the tectonic and subduction erosion of accretionary wedge, fore-arc prism and volcanic arc and even by direct subduction of intra-oceanic arcs. The major materials, which can be eroded and further subducted to the deep mantle, are water, carbonates, serpentinite, basalts and sediments of oceanic slab and rocks of volcanic arcs (Yamamoto et al., 2009; Safonova et al., 2015). The subducting slabs can deliver water and carbon dioxide to the mantle and metasomatise it. The data from seismic tomography (Huang and Zhao, 2006) show that the fragments of dehydrated oceanic slabs, which melting temperature is 200 K lower than that of the ambient mantle, can be accumulated in the MTZ. Recently it has been proved that granitic material possessing a lower density compared to mafic and ultramafic rocks also can be subducted by a mechanism of viscous dragging acting in the subduction channel (Ichikawa et al., 2015). The physical process of granite subduction is still unclear and requires comprehensive and novel, both numerical ad experimental, petrological studies. However, a recent comparative study of the densities and seismic wave velocities of major mantle lithologies has shown that the accumulation of granitic materials containing much higher concentrations of radioactive elements (K, Th, U) and consequently representing an addition source of heating in the mantle is possible in the MTZ only (Kawai et al., 2013). Thus, the materials, which are eroded at Pacific-type convergent margins, can accumulate in the MTZ and induce mantle metasomatism. All those processes, the subduction of hydrated and carbonated oceanic crust, the destruction of continental crust at eroding margins, and the accumulation of mafic and sialic materials in the MTZ can synergistically trigger the generation of hydrous-carbonated mantle plumes in the MTZ, slab and mantle melting at a depth of approximately 410 km, mantle upwelling, surface rifting and intra-plate magmatism (Fig. 2).

The accretionary complexes of Central Asia host OPS units/terranes formed during four major age intervals: late Neoproterozoic-early Paleozoic (Tuva, Transbaikalia, Altai), Middle Paleozoic-early Carboniferous (Tienshan, East Kazakhstan, Mongolia); late Carboniferous-Permian (Sikhote-Alin), Triassic-Neogene (Sikhote-Alin, Sakhalin, and Kamchatka). The most promising areas of tectonic, subduction and other types of erosions in Central Asia are Russian Altai, East Kazakhstan, South Tienshan and Transbaikalia (Safonova, 2017). To prove tectonic erosion we must (1) discriminate intra-oceanic (Mariana-type) and continental (Andean-type) arcs by petrological, geochemical and isotope data; (2) identify related fore-arc prism and trench units; (3) determine the age of igneous and sedimentary rocks; (4) estimate the distance between coeval arc and fore-arc prism or trench.

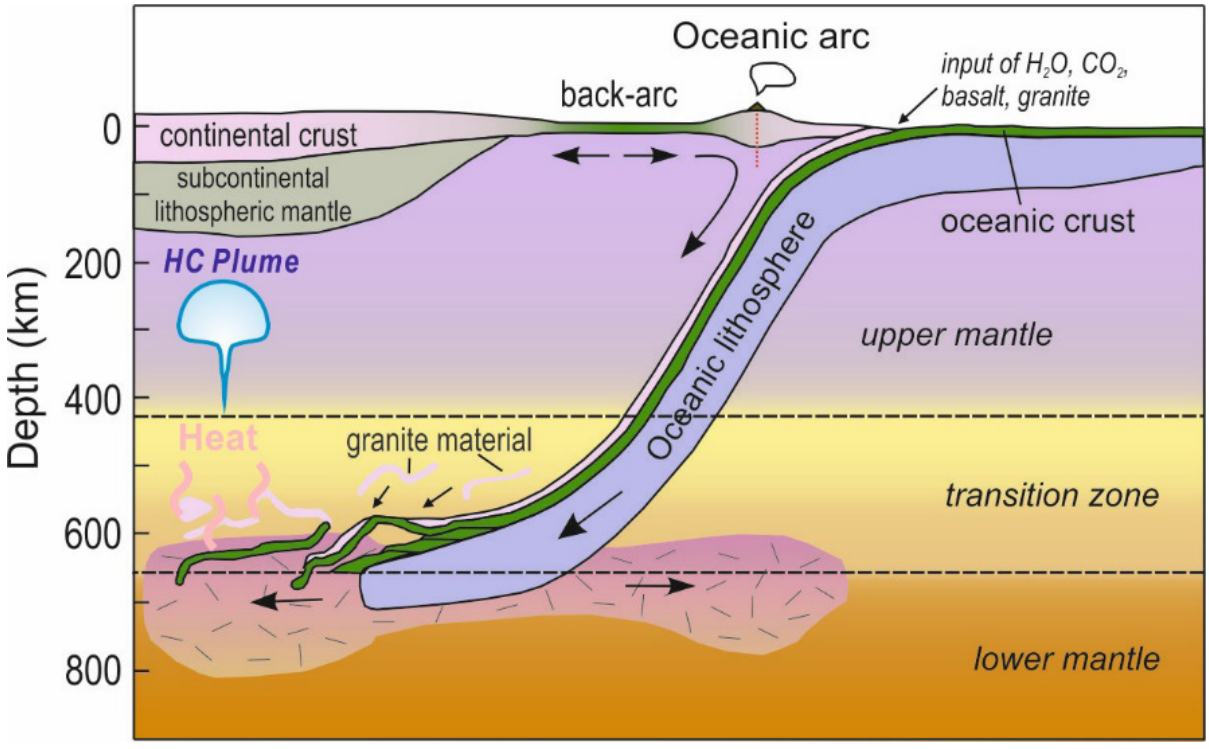


Fig. 2. A model of the subduction of different materials to the deep mantle, their accumulation in the MTZ and generation of hydrous-carbonated plumes (modified from Kawai et al., 2013).

The longer are the periods of tectonic erosion and subduction, the larger will be the volume of the material arriving to the mantle and metasomatising it. According to rough evaluations, the age of metasomatism in the upper mantle can be 50-100 Ma younger than that of the maximal subduction and erosion. Since the Miocene, the already amalgamated Eurasian continent has been surrounded by double-sided subduction zones of India-Sumatra and western Pacific, which have been permanently delivering volatiles and other oceanic and continental crust materials to the deep mantle. Consequently, the Quaternary to modern intra-plate volcanism manifested in Transbaikalia, Mongolia and East China could be triggered by the volatiles and oceanic and continental crust materials supplied by those two giant subduction zones (Safonova et al., 2015). To explore a possibility of the generation of hydrous-carbonated plumes in the MTZ as a result of synergetic interaction of subduction and continental and oceanic crust materials accumulated therein we must correlate the periods of mantle metasomatism, eroding convergent margins and continuous subduction with the periods of intra-plate magmatism and rifting in Central and East Asia from the late Paleozoic to the Cenozoic.

The presence of volatiles coming from hydrated and carbonated subducting oceanic crust and the presence of subducted MORB-dominated dehydrated slabs both can reduce melting temperature. The presence of subducted continental crust material, which may serve an additional radiogenic heater, can synergistically trigger the generation of hydrous-carbonated plumes (HCP) in the MTZ (Kawai et al., 2013; Safonova et al., 2015). Those HCPs can induce mantle upwelling, melting of the metasomatized mantle and subducted slabs and formation of mafic and bimodal intra-plate magmatic complexes on the Earth's surface. On the surface, the peaks of plume-related magmatism can be constrained through identification of bi-modal igneous series and OIB-type mafic rocks in the intra-continental areas of Central and East Asia and investigation of their age and composition. A new holistic model thus should link (1) Ocean Plate Stratigraphy, its subduction and accretion to Pacific-type convergent margins; (2) accreting and eroding convergent margins and the processes of tectonic and subduction erosion; (3) mantle metasomatism; (4) generation of hydrous-carbonated plumes in the MTZ under the influence of water, CO_2 and subducted granitic materials and oceanic slabs, and (5) intra-plate magmatism in Central and East Asia. Such a novel model, when fully developed and proved, would account the whole spectra of data from different fields of Earth Sciences and link the geological objectives and processes on the Earth's surface, which are accessible to our study, and those in the deep mantle, which are much less accessible. Finally, the model will contribute to our knowledge about the global material circulation between the crust and the mantle, deep mantle material cycles and global geodynamics.

The parameters of ancient oceans, size and age, the periods of continuous subduction and the peaks of juvenile crustal growth can be evaluated by studying OPS rocks at key accretionary complexes of Central and East Asia. This huge region encompasses oceanic, active margin and plume-related rock formed during four major periods: late Neoproterozoic - early Paleozoic, middle Paleozoic – early Carboniferous, late Carboniferous - Permian, Triassic - Paleogene. Of special importance is to define the type of convergent margin, accreting or eroding, in ancient Pacific-type orogenic belts by evaluating the distance between coeval supra-subduction igneous rocks (arc) and accretionary units (fore-arc). It is necessary to outline the main periods of tectonic and subduction erosion at the active margins of Central and East Asia paleo-oceans from the late Neoproterozoic to the Cenozoic and consequently to recognize the major stages of the supply of volatiles and oceanic and continental crust materials to the deep mantle. The holistic model of the evolution of oceans, convergent margins and "shallow-rooted" or "hydrous-carbonate" plume magmatism can be developed by the correlation of the periods of eroding convergent margins, mantle metasomatism and intra-plate continental magmatism.

The study was supported by the Ministry of Education and Science of the Russian Federation (project no. 14.Y26.31.0018). Additional support came from the Russian Foundation for Basic Research (grant # 16-05-00313).

References

1. Huang, J., Zhao, D., 2006. High resolution mantle tomography of China and surrounding regions. Journal of Geophysical Research: Solid Earth 111(B9).
2. Ichikawa, H., Kawai, K., Yamamoto, S., Kameyama, M., 2013. Supply rate of continental materials to the deep mantle through subduction channels. Tectonophysics 592, 46-52.
3. Isozaki, Y., Maruyama, Sh., Fukuoka, F., 1990. Accreted oceanic materials in Japan. Tectonophysics 181, 179-205.
4. Kawai, K., Yamamoto, S., Tsuchiya, T., Maruyama, S., 2013. The second continent: existence of granitic continental materials around the bottom of the mantle transition zone. Geoscience Frontiers 4, 1–6.
5. Kusky, T., Windley, B., Safonova, I., Wakita, K., Wakabayashi, J., Polat, A., Santosh., M., 2013. Recognition of Ocean Plate Stratigraphy in accretionary orogens through Earth history: A record of 3.8 billion years of sea floor spreading, subduction, and accretion. Gondwana Research 24, 501-547.
6. Maruyama, S., Kawai, T., Windley, B.F., 2010. Ocean plate stratigraphy and its imbrication in an accretionary orogen: the Mona complex, Anglesey-Lleyn, Wales, UK. Geological Society, London, Special Publications 338, 55-75.
7. Safonova I., 2017. Juvenile versus recycled crust in the Central Asian Orogenic Belt: Implications from ocean plate stratigraphy, blueschist belts and intra-oceanic arcs. Gondwana Research 47, 6–27. Gondwana Research 47, 6–27.
8. Safonova, I., Maruyama, S., Litasov, K., 2015. Generation of hydrous-carbonate plumes in the mantle transition zone linked to tectonic erosion and subduction. Tectonophysics 662, 454–471.
9. Yamamoto, S., Senshu, H., Rino, S., Omori, S., Maruyama, S., 2009. Granite subduction: arc subduction, tectonic erosion and sediment subduction. Gondwana Research 15, 443–453.

LIP'S TIMING – WHAT'S NEW

Salnikova E. B., Stifeeva M. V., Kotov A. B.

Institute of Precambrian Geology and Geochronology, Saint-Petersburg, Russia

Keywords: *U-Pb ID-TIMS, zircon, calcic garnets*

Introduction

Timing of the magmatic events is a crucial point in the LIPS study. High precision age data have been published for the numerous mafic LIPS components however the provinces consisting of alkaline and alkaline-ultramafic rock with carbonatites are still deficient of precise duration.

Zircon, the best precise U-Pb geochronometer, is absent in the most of agpaitic and ultrabasic alkaline rocks or susceptible to Pb loss, leading to low precision of isotopic measurements. High content of common, often inherited Pb in zircon from alkaline granitoids whose crystalline structure remains thereby well preserved, and a relatively low U concentration, as well caused significant errors and uncertainties in the U–Pb zircon dates. Our new results demonstrate the annealing and leaching (chemical abrasion) eliminates phases affected by both Pb loss and inheritance in the zircons from high alkaline granites.

Alkaline igneous silicate and carbonate rocks often contain calcic garnets of the andradite-schorlomite-morimotoite-grossular-kimzeyite composition which until recently were not considered as U-Pb geochronometers. We have demonstrated based on the high precision U-Pb ID-TIMS data for numerous alkaline and carbonatitic intrusive rocks that calcic garnets are ideal multi-system geochronological tools. On the example of garnet ages of five massifs from the Kola Alkaline Province we constrained time interval of the main phase of magmatic activity during 1-7 Ma (373±2 Ma to 377±1 Ma) which much less that previously assumed.

Acknowledgements

This work was supported by the RFBR (№ 17-05-00912).

AN UPDATED OVERVIEW ON THE LARGE IGNEOUS PROVINCE (LIP) RECORD OF THE INDIAN SHIELD

Samal A. K.[1], Srivastava R. K.[1], Ernst R. E.[2,3], Söderlund U. [4]

[1]Centre of Advanced Study in Geology, Institute of Science, Banaras Hindu University, Varanasi 221005, India
[2]Department of Earth Sciences, Carleton University, Ottawa, ON K1S5B6, Canada
[3]Faculty of Geology and Geography, Tomsk State University, 36 Lenin Ave, Tomsk 634050, Russia
[4]Department of Geology, Lund University, Sölvegatan 12, SE-223 62 Lund, Sweden
corresponding author's e-mail: amiyasamal007@gmail.com

Keywords: *Large Igneous Provinces, Mafic Dyke Swarms, Indian Shield, Precambrian, Phanerozoic*

Large Igneous Provinces (LIPs) are significant source of information for constraining paleocontinental reconstructions and providing considerable opportunity to understand the nature, composition and evolution of the underlying subcontinental lithospheric mantle. LIPs (both continental and oceanic) may comprise flood basalts, and a plumbing system of mafic dyke swarms (MDSs), sill complexes, layered intrusions, and crustal magmatic underplating. Most of the Phanerozoic LIPs are usually represented by CFBs (continental flood basalts), however, during the Precambrian, the flood basalts are typically eroded exposing the LIP plumbing system of MDSs which provides a robust record of the rhythm of intraplate mantle melting events (cf. Ernst, 2014).

The different Archean Cratons of the Indian Shield have an extensive record of large magmatic events (i.e. LIPs) throughout Earth's evolution, which range in age from Precambrian to Paleogene, and are an integral part of ancient supercontinents (cf. Ernst, 2014; Samal et al., 2019a,b; Söderlund et al., 2019; Srivastava et al., 2019). Based on available precise geochronological data and the grouping of mafic dykes into swarms (based on their age, trend and chemistry), twelve Precambrian and four Phanerozoic LIP events have been identified in the Indian Shield (see Fig.1).

The 12 Precambrian LIP events comprise 24 dyke swarms, 10 other intrusions and 15 mafic magmatic events bracketed between 2.8 Ga and 0.76 Ga. These are ~2.75-2.80 Ga, ~2.36-2.50 Ga, ~2.25-2.26 Ga, ~2.21-2.22 Ga, ~ 2.18 Ga, ~2.08, ~1.98 Ga, ~1.85-1.90 Ga, ~1.77-1.79 Ga, ~1.42-1.46 Ga, ~1.05-1.12 Ga and ~0.76-0.77 Ga LIP. The four prominent Phanerozoic LIPs are (i) ~290–270 Ma, (ii) ~100-135 Ma, (iii) ~84-94 Ma, and (iv) ~64-69 Ma, which are supposed to be associated with the Crozet, Kerguelen, Marion and Réunion hot spots. These LIP records of the Indian Shield have been correlated with the matching LIPs on other crustal blocks of the globe, which suggest that the Indian Shield was an integral part of almost all the known supercontinents during Earth's history. The improving characterization of the LIP record of the Indian Shield (both their dyke swarms, flows and associated intrusions) is helping to constrain the timing and pattern of the assembly of the various Indian Cratons and any post-assembly rotations between the various Cratons.

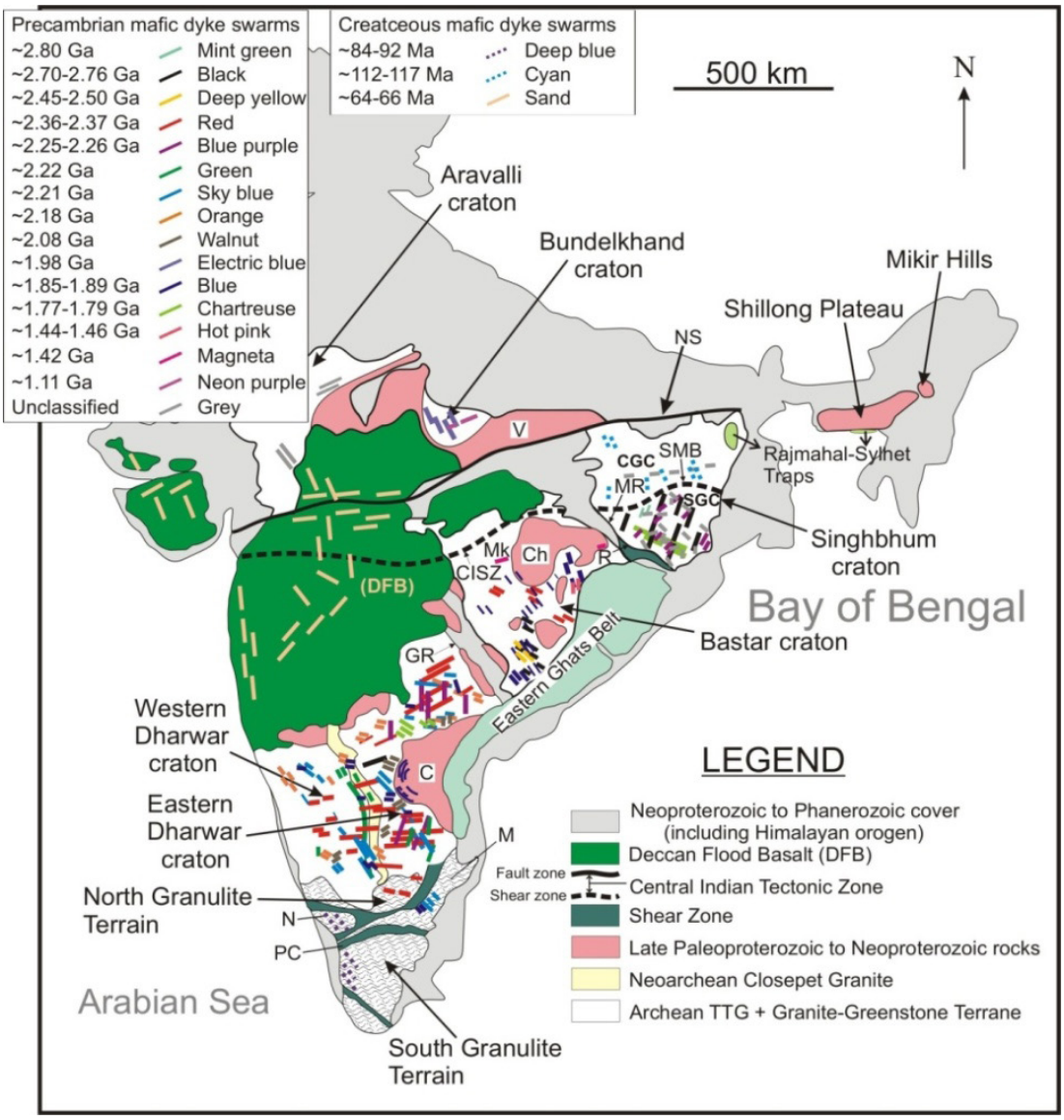


Figure 1: Map showing distinct Precambrian and Cretaceous mafic dyke swarms (MDSs) and Cretaceous continental flood basalts (CFBs) in different Cratons of the Indian Shield (after Samal et al., 2019b; Srivastava et al., 2020).

References

1. Ernst R E (2014) Large Igneous Provinces. Cambridge University Press, Cambridge
2. Samal A K, Srivastava R K, Ernst R E and Söderlund U (2019a) Neoarchean-Mesoproterozoic Mafic Dyke Swarms of the Indian Shield Mapped Using Google Earth™ Images and ArcGIS™, and Links with Large Igneous Provinces In: Dyke Swarms of the World: A Modern Perspective (Eds: Srivastava R K, Ernst R E, Peng P), Springer Nature Singapore Pte Ltd 335–390
3. Samal A K, Srivastava R K, Ernst R E and Söderlund U (2019b) Precambrian large igneous province record of the Indian Shield: an update based on extensive U-Pb dating of mafic dyke swarms. In: LIP of the Month March 2019; URL:http://wwwlargeigneousprovincesorg/19mar
4. Söderlund U, Bleeker W, Demirer K, Srivastava R K, Hamilton M A, Nilsson M, Pesonen L, Samal A K, Jayananda M, Ernst R E and Srinivas M (2019) Emplacement ages of Paleoproterozoic mafic dyke swarms in eastern Dharwar Craton, India: implications for paleoreconstructions and evidence for a ~30° internal block rotation. Precamb Res 329:26–43
5. Srivastava R K, Söderlund U, Ernst R E, Mondal S K and Samal A K (2019) Precambrian mafic dyke swarms in the Singhbhum Craton (eastern India) and their links with dyke swarms of the eastern Dharwar Craton (southern India). Precamb Res 329:5–17
6. Srivastava R K, Samal A K, Ernst R E, Söderlund U and Shankar, R (2020) Spatial and Temporal Distribution of Large Igneous Provinces in the Indian Shield – Highlights of Recent Investigations. Proc Indian Nat Sci Acad (accepted)

NEOARCHEAN MAFIC DYKE SWARMS IN THE MURMANSK CRATON: PETROLOGY, TECTONIC SETTING, AND PALEOCONTINENTAL SIGNIFICANCE

Samsonov A. V.[1], Stepanova A. V.[2], Salnikova E. B.[3], Larionova Y. O.[1], Arzamastsev A. A.[3], Egorova S. V.[2], Veselovskiy R. V.[4,5], Erofeeva K. G.[1], Stifeeva M. V.[3]

[1]*Institute of Geology of Ore Deposits, Petrography, Mineralogy and Geochemistry RAS, Moscow, Russia*
[2]*Institute of Geology Karelian Science Centre RAS, Petrozavodsk, Russia*
[3]*Institute of Precambrian Geology and Geochronology RAS, Saint-Petersburg, Russia*
[4]*LomonosovMoscow State University, Moscow, Russia*
[5]*Schmidt Institute of Physics of the Earth RAS, Moscow, Russia*

Keywords: *Neoarchean doleritic and ferropicritic dykes, Murmansk craton*

Early Precambrian mafic dykes are important objects for petrological, geodynamic and paleocontinental reconstructions of early stages of the Earth's history (Ernst et al., 2013). We present geochronological, geochemical and isotopic data for Neoarchean mafic dykes in the Murmansk Craton, Fennoscandian Shield.

Two geochemical types of ca. 2680 Ma Neoarchean mafic dykes were recently recognized in the northern part of the Murmansk craton. The dykes cross-cut Neoarchean basement comprising of ca 2860 Ma TTG gneisses, variably deformed ca. 2732 Ma granites and trondhjemites and ca. 2724 Ma sanukitoid series dioritic dykes (unpublished data).

The Group I includes dolerite dykes that outcrop along Barents Sea coast from Dalnie Zelentsy to Savikha Bay. Most dykes have porphyritic texture with a large (up to 12 cm) plagioclase phenocrysts in a fine-grained Cpx-Pl dolerite matrix. The dykes vary in thickness from 1 to 30 m and form ca. 150 km width radial swarm. The proposed focal point of this swarm could be projected in the Keivy terrain. This tectonic unit is characterized by a wide occurrence of ca. 2680 Ma alkaline granite, syenite and gabbro-anorthosite intrusions (Zozulya et al., 2005; Vetrin, Rodionov, 2009). Three U-Pb (ID-TIMS) analyses of baddeleyite from dyke in the Dalnie Zelentsy area define a Discordia with an upper intercept age of 2692 ± 10 Ma (MSWD = 1.4). Baddeleyite from the high-Al tholeiitic aphyric dolerite dyke in the Tryaschina Bay area has a similar age of 2680 ± 5 Ma. All studied dykes have a tholeiitic affinity. The available data suggest that primary magma of studied tholeiitic dykes could be generated via partial melting of depleted mantle at the level of the spinel stability field. The subsequent fractional crystallization and crustal contamination define low concentrations of MgO, Fe_2O_3, TiO_2, Cr, Ni, SiO_2 with enrichment in Al_2O_3, relatively flat HREE and enrichment in LREE, strong negative Nb anomalies and εNd_T ranging from -0.5 to +0.4 in studied dykes.

The Group II includes mafic dykes with ferropicritic chemical affinity. These olivine melanogabbro dykes form NNE-trending ca 70 km width swarm that outcrops along Barents Sea coast between the Litsky Cape and Savikha Bay. The dykes within this swarm vary in thickness from 0.5 to 20 m. The chilled margin of the most well-preserved 20 m thick dyke in the Litsky cape area is composed of olivine-phyric rock, whereas the internal part comprises medium-grained massive kaersutite-bearing olivine melagabbronorite. The most of other dykes of this swarm are strongly metamorphosed in amphibolite facies. The U-Pb (ID-TIMS) baddeleyite concordant age of 2680 ± 2 Ma from the Litsky cape dyke define the crystallization age of ferropicritic dykes. All dykes are strongly enriched in MgO, Fe_2O_3, TiO_2, Cr, Ni, HFSE, have highly fractionated light and heavy REE patterns and positive εNd_T values varying from +0.6 to +1.5. Geochemical characteristics of the 2680 Ma olivine melanogabbro dykes have resemblance to those of Paleoproterozoic (1.98 Ga) ferropicrites of the Pechenga basin (Hanski, Smolkin, 1989, 1995). However, distinctive features of the Neoarchean ferropicrites such as higher concentrations of SiO_2 (up to 50 wt.%), Al_2O_3 (up to 10 wt.%), lower concentrations of Fe_2O_3 and negative Nb anomalies which could be explained by crustal contamination are not typical of the Pechenga rocks. Available data indicate that primary melts of Neoarchean ferropicrites were generated in the garnet stability field via partial melting of the mantle source that was probably enriched in Fe.

The analysis of available data and comparison of studied dyke episode with other magmatic events in the Fennoscandia and another Archean crustal provinces allow to conclude that:

1. The studied Neoarchean tholeiitic and ferropicritic dykes in the Murmansk craton together with alkaline granite, syenite and gabbro-anorthosite intrusions of the adjacent Keivy terrane, Kola province (Zozulya et al., 2005; Vetrin, Rodionov, 2009; Vetrin, 2018) were formed synchronously at ca. 2680 Ma and could be considered as a components of a single magmatic event. Variations in the rock geochemistry suggest that their primary melts originated from the mantle sources that differ in depth and composition. This phenomena could be explained by interaction of a deep-seated mantle plume with metasomatized lithosphere in the frame of the model of plume-triggered delamination (Camp and Hanan, 2008) or lithospheric drip magmatism (Furman et al., 2016).

2. Neoarchean ferropicritic dykes of the Murmansk craton are similar in composition and age with Neoarchean (2720-2690) ferropicrites in the Superior Province, Canadian Shield (Goldstein, Francis, 2008; Milidragovic et al., 2014). These coeval igneous rocks could be considered as components of a single Neoarchean LIP that should be taken into account in paleocontinental reconstructions.

3. Similarity of 2680 Ma Neoarchean and 1980 Ma Paleoproterozoic of tholeiitic and ferropicritic igneous rocks in the northeastern Fennoscandia probably provide evidence for the repetition of tectonic setting that had operated during these two magmatic events in the Fennoscandian Shield. Specific petrology of ferropicritic magmatism (Gibson, 2002; Goldstein, Francis, 2008; Zhang et al., 2017) could be related with post-subduction stages of the Neoarchean and Paleoproterozoic supercontinental cycles, when preceding subduction

caused an intensive metasomatic reworking of the continental lithospheric mantle and provided storage of subducted plates in the deep mantle that gave rise to the enrichment in Fe and deep-seated melting.

Acknowledgements

This work was supported by the Russian Science Foundation (Grant 16-17-10260).

References

1. Camp V.E., Hanan B.B. (2008) A plume-triggered delamination origin for the Columbia River Basalt Group. Geosphere 4: 480–495
2. Ernst R.E., Bleeker W., Söderlund U., Kerr A.C. (2013) Large Igneous Provinces and supercontinents: Toward completing the plate tectonic revolution. Lithos 174: 1–14
3. Furman T., Nelson W.R., Elkins-Tanton L.T. (2016) Evolution of the East African rift: Drip magmatism, lithospheric thinning and mafic volcanism. Geochimica et Cosmochimica Acta 185: 418–434
4. Gibson S.A. (2002) Major element heterogeneity in Archean to Recent mantle plume starting-heads // Earth Planet. Sci. Lett. 195: 59–74
5. Goldstein S. B. and Francis D. (2008) The petrogenesis and mantle source of Archaean ferropicrites from the western Superior Province, Ontario, Canada. J. Petrology 49: 1729–1753
6. Hanski E.J., Smolkin V.F. (1989) Pechenga ferropicrites and other early Proterozoic picrites in the eastern part of the Baltic Shield. Precambrian Research 45: 63-82
7. Hanski E.J., Smolkin V.F. (1995) Iron- and LREE-enriched mantle source for early Proterozoic intraplate magmatism as exemplified by the Pechenga ferropicrites, Kola Peninsula, Russia. Lithos 34: 107-125
8. Milidragovic D., Francis D., Weis D. and Constantin M. (2014) Neoarchean (c. 2.7 Ga) plutons of the Ungava Craton, Querbec, Canada: parental magma compositions and implications for Fe-rich mantle source regions. J. Petrology 55: 2481–2511
9. Vetrin V. R.,Rodionov N. V. (2009) Geology and geochronology of Neoarchean anorogenic magmatism of the Keivy structure, Kola Peninsula. Petrology 17: 537-557
10. Vetrin V. R. (2018) Isotope-geochemical systematics (Sm-Nd, Lu-Hf) of Neoarchean subalkaline and alkaline rocks of the Keivy structure (Kola Peninsula): their age and genetic relations. Zapiski RMO Pt. CXLVII. N 4: 1-13
11. Zhang J.B., Liu Y.S., Ling W.L., et al. (2017) Pressure-dependent compatibility of iron in garnet: Insights into the origin of ferropicritic melt. Geochim.Cosmochim. Acta 197: 356–377
12. Zozulya D.R.,Bayanova T.B., Eby N.G. (2005) Geology and age of the late ArchaeanKeivy alkaline province, NE Baltic Shield. The Journal of Geology 113: 601–608

THE ORDOVICIAN MAGMATIC EVENTS IN THE SIBERIAN PLATFORM AND MONGOLIAN TERRAINS – ARE THEY RELATED?

Savelev A. D.[1,2], Khudoley A. K.[1,2]

[1]Saint Petersburg State University, St. Petersburg, 199034, Universitetskaya nab., 7–9, Russian Federation
[2]Tomsk State University, Tomsk, 634050, pr. Lenina, 36, Russian Federation
aleksandr.d.savelev@gmail.com

The Ordovician mafic magmatic event, commonly known as the Suordakh event, based on U-Pb baddeleite dating was first reported 20 years ago and, after that, it age and distribution was supported by more recent SIMS study (Khudoley et al., 2013). However, tectonic setting of the Ordovician intrusions are still under question, and two possible scenarios have been discussed:

1) Suordakh event mafic intrusions are almost synchronous with a granite intrusion in the area between the Siberian craton and Okhotsk cratonal terrane: 445.7±1.5 and 444.1±1.5 Ma (Kuzmin et al., 2003), suggesting that rather than being orogenic related, this silicic magmatism may have resulted from partial melting of lower crust by magmatic underplating associated with the Suordakh event (Khudoley et al., 2013).

2) The assumption of the location of granitoids and mafic intrusions in a single LIP is unlikely due to the fact that the granite intrusions belong to I-type. Ordovician magmatism was most likely associated with the mantle plume, but not with intense rifting. The synchronous existence of passive and active margin is possible as well (Khudoley & Prokopiev, 2018).

However, new isotopic and paleomagnetic data on the Ordovician magmatism allow to propose another scenario for the formation of the Suordakh complex. Kilian et al. (2016) introduced U-Pb zircon age of 446.03 ± 0.21 Ma of a rhyolite in the Teel Formation on the Zavkhan terrane of Mongolia (Kilian et al., 2016). In study area within the Zavkhan terrane Ordovician to Silurian transtension resulted in narrow rift basins that accommodated volcanic and minor sedimentary rocks of the Teel Formation. The Teel Formation is composed of bimodal series of rhyolite and basalt, which intercalated with siliciclastic sedimentary rocks (Togtokh et al., 1995).

The paleolatitude of the Zavkhan terrane at ca. 446 Ma was 19±5°N, which is consistent with it being associated with the Siberia craton in the Late Ordovician (near the present-day southern Siberia margin). A similar geologic history potentially links the Zavkhan terrane with the southern Siberian margin from ca. 510 to 450 Ma, when the southwestern margin of the Zavkhan and Lake terranes may have accreted to southern Siberia (Bold et al., 2016). At the beginning of Ordovician, both southern Siberia and the Zavkhan and Lake terranes hosted rift-related extensional magmatism (Yarmolyuk et al., 2011; Bold et al., 2016), including the volcanics of the Teel Formation. Due to this constraint, Kilian et al. (2016) prefers a model whether Zavkhan terrane rifted off of a landmass, likely Siberia, during or soon after ca. 446 Ma eruption of the Teel Formation basalts in extensional basins (Kilian et al., 2016).

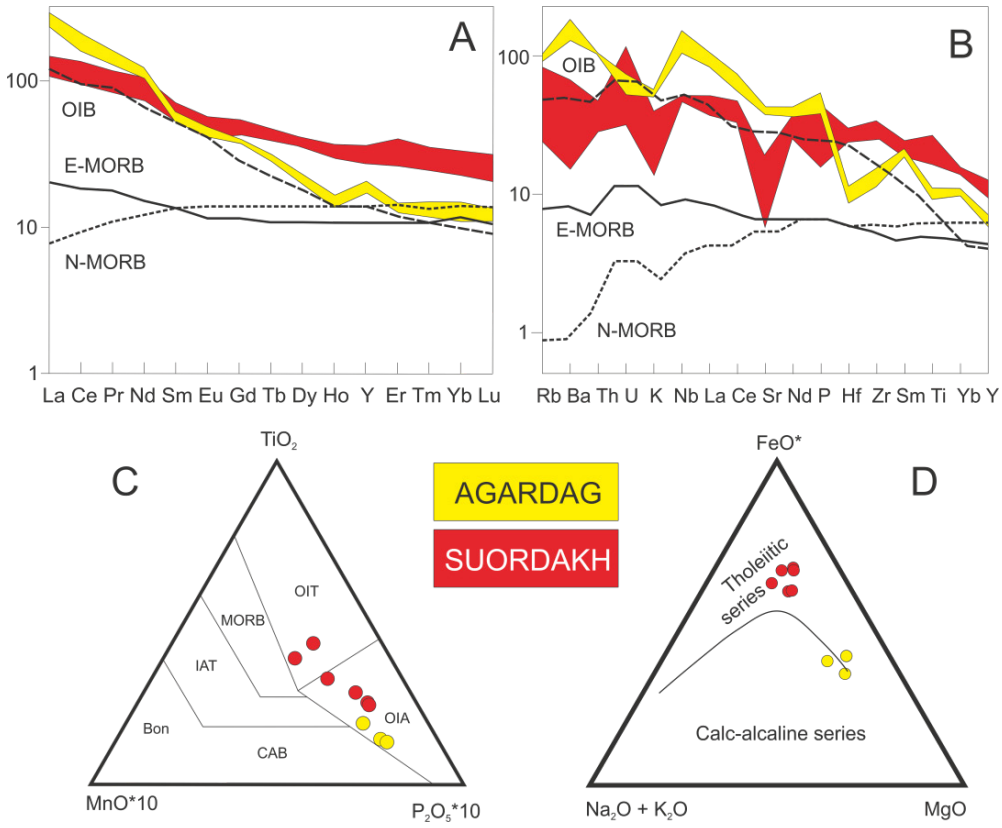


Fig. 1. Agardag - a field of igneous rocks of the Agardag complex. Suordakh - a field of igneous rocks of the Suordakh complex; A, B - elements spidergrammes, normalized (A) - to chondrite, (B) - to the primitive mantle (according to Sun & McDonough, 1989); C, D - tertiary discrimination diagrams (Rollinson, 1993), OIT – ocean island tholeiite, OIA – ocean island alkalic, MORB - mid-ocean ridges basalt, IAT - island-arc tholeiite, CAB - island-arc calc-alkaline basalt.

However, earlier Ordovician isotopic datings for the region are also known. The dikes of the Agardag complex, manifested to the north-western margin of the Sangilen block (southeast of the Tyva-Mongolian microcontinent), also showed Late Ordovician age (Izokh et al, 2001). The Sangilen and Zavkhan blocks have a common border, divided by the Bulnai fault (Bold et al., 2016) and are considered as parts of associated continent (Kilian et al., 2016). This allows usage of data from the Sangilen block for comparison with the Suordakh complex.

Samples of both complexes (fig. 1) follow OIB distribution on the spidergrams, however, Suordakh is enriched with heavy REEs, and Agardag is enriched with light REEs. Agardag complex are characterized by enrichment with large-ion lithophilic elements (Cs, Rb, Ba) and depletion of U and Th relative to Nb and Ta, whose contents on the distribution spectrum form a positive anomaly. Two large negative anomalies are fixed on K and Sr for Siberian magmatic rocks. In the discriminatory diagrams, both complexes occupied fields of intra-plate basalts, but Agardag samples fall into the zone of calc-alkaline series, while Suordakh rocks turned up in tholeiitic series fields (Shelepaev et al., 2018).

The study was supported by the RSF grant 18-17-00240

References

1. Bold, U., Crowley, J., Smith, E., Sambuu, O., and Macdonald, F., 2016, Neoproterozoic to early Paleozoic tectonic evolution of the Zavkhan terrane of Mongolia: Implications for crustal growth in the Central Asian orogenic belt: Lithosphere, doi: 10 .1130 /L549 .1
2. Izokh, A.E., Polyakov, G.V., Malkovets, V.G., Shelenaev, R.A., Travin, A.V., Litasov, Yu.D., Gibsher ,A.A., 2001. The Late Ordovician age of the Agardag complex of the South-Eastern Tuva is evidence of plume magmatism in collisional processes, Reports of the Academy of Sciences, 379, 5, p. 511-514.
3. Khudoley, A K, Prokopiev, A V, Chamberlain, K R, Ernst, R E, Jowitt, S M, Malyshev, S V, Zaitsev, A I, Kropachev, A P, Koroleva, O V, 2013. Early Paleozoic mafic magmatic events on the eastern edge of the Siberian Craton Lithos 174, 45–56
4. Khudoley, A K, Prokopiev, A V. 2018. Magmatic and tectonic evolution of the southeast margin of the Siberian Craton in Ordovician. Petrology of magmatic and metamorphic complexes. Issue 10. Pceeding of science meeting. – Tomsk: Tomsk CSTI Publishing house. p. 409-415
5. Kilian, T.M., Swanson-Hysell, N.L., Bold, U., Crowley, J., and Macdonald, F.A., 2016, Paleomagnetism of the Teel basalts from the Zavkhan terrane: Implications for Paleozoic paleogeography in Mongolia and the growth of continental crust: Lithosphere, doi: 10 .1130 /L522 .1.
6. Kuzmin, V.K., Belyatskiy, B.V., Naumov, M.V., 2003. New isotopic-geochemical data on the Late Ordovician age of granitoids from the western part of the Okhotsk massif (Upper Maya uplift). Regional Geology and Metallogeny 19, 101–105 (in Russian).
7. Rollinson, H. 1993. Using geochemical data: Evaluation,

presentation, interpretation. Logman Group, London,
8. Shelepaev, R.A., Egorova, V.V., Izokh, A.E., Zeltmann, R., 2018. Collisional mafic magmatism of the fold–thrust belts framing southern Siberia (Western Sangilen, southeastern Tuva), Geology and Geophysics, 59, 5, p. 653–672
9. Sun, S.-S., McDonough, W.F. Chemical and isotopic systematics of oceanic basalts: implications for mantle composition and processes. In: Saunders, A.D., Norry, M.J. (eds.) Magmatism in the Ocean Basins, Geol. Soc. Lond. Spec. Publ. 42, 1989, p. 313-345
10. Togtokh, D., Baatarkhuyag, A., and Bayardalai, S., 1995, The Report of Result of the Geological Grouped Mapping: Ulaanbaatar, Mongolia, Mineral Resources Authority of Mongolia, scale 1:200,000.
11. Yarmolyuk, V.V., Kovach, V.P., Kovalenko, V.I., Salnikova, E.B., Kozlovskii, A.M., Kotov, A.B., Yakovleva, S.Z., and Fedoseenko, A.M., 2011, Composition, sources, and mechanism of continental crust growth in the Lake zone of the Central Asian Caledonides: I. Geological and geochronological data: Petrology, 19, 1, p. 55–78.

GLOBAL STRATALEVEL OF INCREASED AND INTENSIVE ORE-, OIL-, GAS- AND SHALE FORMATION AS A CONSEQUENCE OF THE MANIFESTATION OF GALACTIC, TECTONOMAGMATIC AND BIOTIC EVENTS AT THE TURN OF DEVONIAN AND CARBONIFERIOUS PERIODS

Sedaeva K. M.

Lomonosov Moscow State University, Geological faculty, Moscow, Russia, E-mail: sedaeva-mgu@mail.ru

The Tectonomagmatic processes at the turn of Devonian – Carboniferous periods ($D_3 - C_1$) are large-scale and relatively short-term geological processes that took place synchronously on different paleocontinents and in paleoseas. They caused a sharp increase in the number of ore and oil and gas formations due to enrichment of the Earth's crust by organic matter (OM) and chalcophyllic, noble and rare-earth elements. This predetermined the formation of evenaged large deposits, ore and oil and gas provinces and belts, defining endogenous mineralization in orogenic areas and exogenic mineralization - on ancient platforms. They were caused by the Early-Hercynian phase of tectogenesis, the nature and extent of crustal



Figure 1. Nicaragua, volcano awakens.



Figure 2. Klyuchevskaya Sopka, ash discharge

and mantle magmatism, which were due in general to galactic processes in the Universe due to the intense formation of supernova stars [4]. At this stage of the tectogenesis there was a revival of the Riphean rifts on the periphery of the ancient platforms (East European, Siberian, North American, South China and Australian) and the laying of new rifts almost all over the area of the West-Arctic Continental margin and within the median massifs (Omolonskiy, Kazakhstano-Tianshan), which were formed at the Caledonian stage of Tectogenesis [3-4]. Riftogenesis was accompanied by basalt-mantle magmatism, formation of depression structures, destabilization of geomagnetic field of the Earth, and fluid-hydrothermal activity. This led to the formation of various types of ore formations and deposits by genesis and composition with different associations of valuable components (diamond-bearing, gold-silver, platinum, rare-earth and rare-metal, sulphide-polymetallic, etc.) that was associated with the possibility of generating a wide range of melts from the original mantle substrate. Endogenous ores were formed in Paleozoic orogenic areas. At The turn of the D_3-C_1 is the largest in the history of the planet peak of sulphide-volcanogenic formation (about 43% of total reserves of the world's sulphide ores) and establishing of the largest sulphide-bearing provinces of the World (Iberian, Ural, Rudnoaltasky and a number of large fields in Alaska (Ambler region) and the North Caucasus, Australia, British Columbia, Yukon, Appalachia and the region of West Shasta. Within the ancient platforms, there were numerous fields of diamond-bearing kimberlites within a single strip stretching from Spitsbergen to southeast Australia (the Strait of Carpentaria). This strip has contoured the area of the exit of profound energy, as evidenced by the numerous diamond-bearing diatremes on the Eastern European, Siberian, Chinese and Australian platforms. This outbreak of sulphide-volcanogenic ore and Kimberlite formation coincides with the relative peak of mantle plumes activity due to the manifestation of major galactic events – the intensity of the formation of supernova stars [1.4].

On the background of the main phase of riftogenesis and basalt-mantle magmatism was further: 1) The formation of the system of uplifts and depressions on the periphery of the ancient platforms; 2) The raising and lowering of significant blocks of the Earth's crust and 3) the deepening of the small oceanic basins that existed from the late Devon – Angayuchan, Oymykon, Seventimil, Gudnews, Slide Mountain and others. Tectono-magmatic processes have caused: a) The inflow into the atmosphere and hydrosphere of a significant amount of ash, CO2, H2S, SO2 and other Gases, SiO2, sulfur and associated minor, rare, non-earth elements (which led to a decrease in the level of oxygen in these geospheres); b) abrupt eustatic fluctuations of sea level; c) paleoclimatic changes (in connection with Gondwanian glaciation in the Southern hemisphere), d) Change of sedimentation regime and e) appearance of anoxic conditions in sea basins. This resulted in a change in the paleo-landscape environments and paleoecological conditions and caused, on the one hand, the mass extinction among eukaryotes and blossom of prokaryotes, and the restructuring of the biosphere, and on the other - the formation of large masses (100-500, rarely 800 m) micrograined limestone of the microbiological nature in the sedimentary cover of the ancient platforms of the Northern hemisphere [3]. Carbonate accumulation occurred against the background of intense compensated subsidence, with the appearance in the sea basins stagnant pitted environments with disrupted gas and salt regime, in which the accumulation of siliceous-

pelitic sediments with elevated content of the organic matter, enriched with rare-earth, minor and scattered ore elements. Thanks to the high sedimentation rates, they were immersed in the depths required for the generation of liquid and gaseous carbonaceous matters. As a result, synchronized with ore genesis, the formation of oil source complexes, with which the largest deposits of combustible and black shale, oil and gas in many regions of the Northern hemisphere – USA, Canada, Russia, China, North Africa are associated [2.4].

The magmatic and metallogenic specificity of the D_3-C_1 boundary is characterized by a planetary manifestation of ore-generating and ore-localizing processes, which have led to the formation of a global metallogenic stratalevel with high metallogenic productivity. Its formation took place during specific geodynamic regime, when oceanic processes in some segments of the Earth's crust were completed, others did not come; orogenic continental processes of some segments of the Earth's crust were completed, and others did not begin. As a result, the formation of contrasting ore formations and deposits occurred during the transitional period between two geodynamic cycles (oceanic and subsequent continental), against the background of the manifestation of a mantle plume-type magmatism. Their formation was not accompanied by oceanic and granite-continental metallogeny, indicating that "geodynamics of paleo-oceans, continents and intermediate continental-oceanic structures acquire one type of pattern, plate tectonics fades and ultra-deep structures and subvertical fault tectonics got activated that cause local focal plume-mantle magmatism of different basicity-alkalinity "[1, p. 259].

Thus, the D_3-C_1 global stratalevel of increased and intensive ore, oil, gas and shale formation reflects the close connection of galactic processes, tectonics, magmatism, petro- and sedimentogenesis with endogenous and exogenous world genesis of industrial metallic, non-metallic ore and oil and gas deposits.

References

1. Abdrakhmanov K. A. Global metallogenic stratalevels and their ore-generating plume mantle sources. Fundamental problems of mineral deposits and metallogeny: XXI Int. Scientific. Konf., Dedi. 100-the anniversary of academician V.I. Smirnov-M.: MAX Press, 2010. P. 254-261.
2. Perrodon A. Formation and placement of oil and gas deposits-Moscow: Science. 1991.391.
3. Sedaeva K. M, Ryabinkina N.N., Kulyashov V.N., Valyaev O.V. Reflection of the Hangenberg global geological event of the Devonian and Carboniferous border in the sections of the western slope of the Subpolar (r. Kojim) and the Southern (r. Sikaza) Urals//Litosphere. 2010. № 6. P. 25-37.
4. Starostin V.I. Metallogeny. Moscow: KDU. 2012.560 p.

ISOTOPIC ND-SR HETEROGENEITY NEAR THE ORE-BEARING ZONES OF "TERRASA" DEPOSIT (MONCHEGORSK PGE-CR-CU-NI ORE REGION, KOLA PENINSULA)

Serov P. A., Bayanova T. B., Kunakkuzin E. L., Steshenko E. N.

Geological Institute of the Kola Science Centre of the Russian Academy of Sciences, Apatity, Russia

Keywords: *Monchegorsk ore region, Sm-Nd, Rb-Sr, mafic-ultramafic intrusions, ore genesis, isotopic heterogeneity.*

Introduction

In the north-eastern part of the Fennoscandinavian shield (Kola Peninsula) there are two large Palaeoproterozoic layered intrusions: Monchegorsk mafic-ultramafic pluton of 55 km^2 and Monchetundra massif of 120 km^2. They are combined into the Monchegorsk complex of layered intrusions and are a part of the Monchegorsk PGE-Cr-Cu-Ni ore region (Sharkov, 2006; Chashchin et al., 2016). The ore potential of the Monchegorsk ore district is mainly determined by the deposits associated with Monchegorsk pluton.

Our geochronological studies by the U-Pb and Sm-Nd methods confirm the time interval for the formation of the main varieties of intrusive rocks - 2480-2506 Ma [Bayanova et al., 2009, 2014, 2019; Rundkvist et al., 2014; Serov et al., 2015, Chashchin et al., 2016]. A change in the rock composition in the vertical section is disturbed by the presence of the ore dunite-harzburgite bed among the orthopyroxenites of Mt Sopcha (ore bed "330") and the "critical" horizon with olivine-containing rocks on Mt Nyud [Sharkov, 2006]. The age of the harzburgite ore bed "330" of Mt Sopcha is 2442±59 Ma (the Sm-Nd method), which agrees with the idea of its formation due to the introduction of an additional portion of high-temperature ultrabasic magma that experienced significant crustal contamination (Sharkov, Chistyakov, 2014; Chashchin et al., 2016;).

Results

The "critical horizon" of Mt Nyud in the deposit "Terrasa" area was studied over two sections during field work. The initial isotopic composition of strontium for most of the studied samples varies in a narrow range – 0.702–0.704; however, for metamorphized differences and rocks with sulphide mineralization lower values of the initial isotopic composition are observed - about 0.702. At the same time, the Sm-Nd data for the same samples show an extreme scatter of εNd(T) values, which range from small negative (-1.25) to strongly positive values (fig. 1).

Such variations are probably caused by several factors, including: increased analytical errors in measuring samples with low, fractions of ppm, element concentrations, possible mixing of several sources with different isotopic characteristics, varying degrees of change due to metamorphic or metasomatic processes and fluids, a possible rearrangement

of the isotopic systems during the introduction of additional portions of magma and heating of the contacting rocks as well as the diffusion processes of REE.

To check up our hypothesis about a possible mixing of sources with different isotopic characteristics, test diagrams were constructed in the coordinates "inverse concentration vs isotopic composition" (fig. 2).

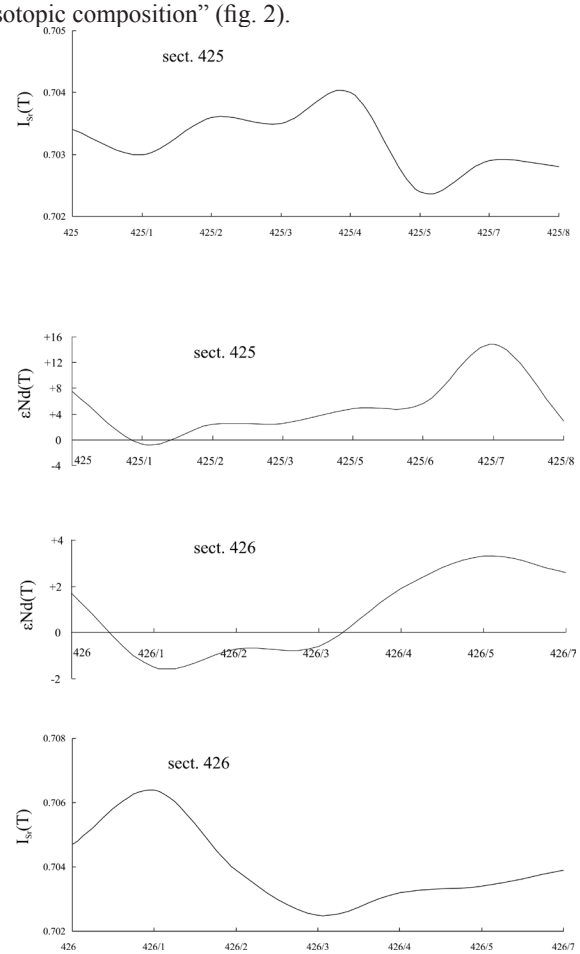
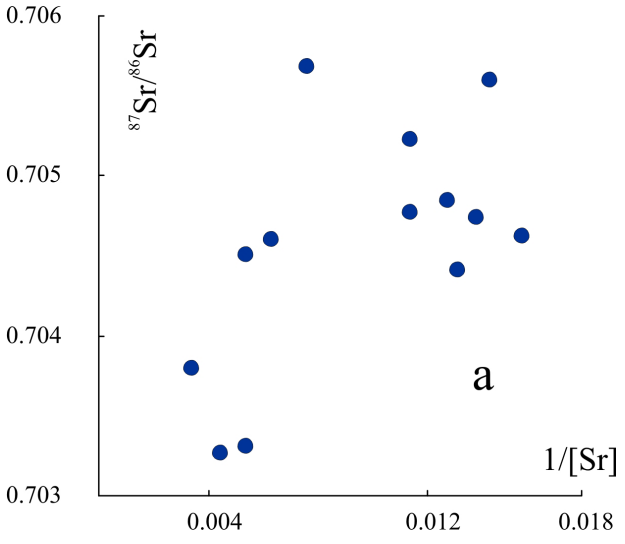


Fig. 1. Variations of $I_{Sr}(T)$ and εNd(T) for olivine norites near the ore layer of "Terrace" deposit.



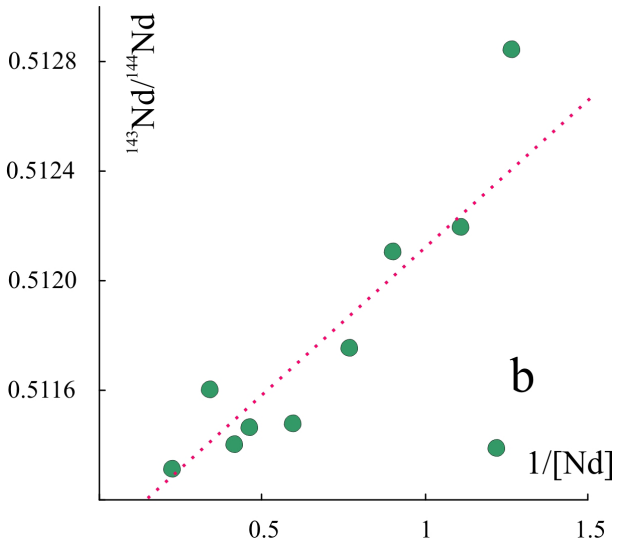


Fig. 2. Mixing diagrams in the coordinates "1/[Sr] vs ^{87}Sr-^{86}Sr" (a) and "1/[Nd] vs $^{143}Nd/^{144}Nd$" (b) for olivine norites.

In the diagram with Rb-Sr data (fig. 3a), the points of the analyzed samples form a cloud without correlation, which indicates the absence of dependencies between the isotopic composition and concentration. In this case, one can say that the Rb-Sr systems of the studied samples are not the result of mixing sources with different isotopic parameters. In the case of the Sm-Nd system, most of the points form a linear trend in the diagram (fig. 3b), which may indicate a mixed source or contamination processes.

Conclusions

Thus, it has been found that:

the results of the Rb-Sr and Sm-Nd analyzes suggest that the Rb-Sr system is better preserved than the Sm-Nd system, for which the signs of isotopic rearrangement when mixed or contaminated are observed;

the sites with industrial concentrations of Pt+Pd are often characterized by sharp variations in the isotopic composition of neodymium, which is probably due to increased fluid saturation and diffusion of REE.

Acknowledgements

All investigations were supported by the RFBR 18-05-70082, 18-35-00246, Presidium RAS Program №48 and are in frame of the theme of scientific research № 0226-2019-0053.

References

1. Bayanova T., Korchagin A., Mitrofanov A., Serov P., Ekimova N., Nitkina E., Kamensky I., Elizarov D., Huber M. Long-lived mantle plume and polyphase evolution of Palaeoproterozoic PGE intrusions in the Fennoscandian Shield // Minerals. 2019. № 9 (1). V. 59 doi:10.3390/min9010059
2. Bayanova, T. B, Ludden, J., & Mitrofanov, F. P. Timing and duration of Palaeoproterozoic events producing orebearing layered intrusions of the Baltic Shield: metallogenic, petrological and geodynamic implications. In S.M. Reddy, R. Mazumder, D.A.D. Evans, & A.S. Col-

lins (ed.), Palaeoproterozoic Supercontinents and Global Evolution. Geological Society, London. Special Publications. 2009. V. 323. P. 165–198.
3. Bayanova T., Mitrofanov F., Serov P., Nerovich L., Yekimova N., Nitkina E. and Kamensky I. Layered PGE Paleoproterozoic (LIP) Intrusions in the N-E Part of the Fennoscandian Shield – Isotope Nd-Sr and 3He/4He Data, Summarizing U-Pb Ages (on Baddeleyite and Zircon), Sm-Nd Data (on Rock-Forming and Sulphide Minerals), Duration and Mineralization / Geochronology – Methods and Case Studies / Edited by Nils-Axel Mörner // INTECH, 2014. P. 143-193. (http://dx.doi.org/10.5772/58835).
4. Chashchin, V. V., Bayanova, T. B., Mitrofanov, F. P., & Serov, P. A. (2016). Low sulfide PGE ores in Palaeoproterozoic Monchegorsk Pluton and massifs of its southern framing, Kola Peninsula, Russia: geological characteristic and isotope geochronological evidence of polychronous ore magmatic systems. Geology of Ore Deposits, 58 (1), 37–57.
5. Rundkvist, T. V., et al. (2014). The Palaeoproterozoic Vurechuayvench layered Pt bearing pluton, Kola Peninsula: new results of the U Pb (ID TIMS, SHRIMP) dating of baddeleytte and zircon. Dokl. Earth Sci., 454, (1), 1–6.
6. Serov P., Bayanova T., Steshenko E., Ekimova N. Ore genesis dating: implication of Sm-Nd method using sulfide minerals for mafic-ultramafic layered intrusions of Fennoscandian Shield // EGU General Assembly 2015. Geophysical Research Abstracts. Vol. 17. EGU2015-501.
7. Sharkov, E. V. (2006). Formation of Layered Intrusions and Related Mineralization. Moscow: Scientific World, 364.
8. Sharkov E.V., Chistyakov A.V. Geological and petrological aspects of Ni Cu PGE mineralization in the Early Palaeoproterozoic Monchegorsk Layered Mafic Ultramafic Complex, Kola Peninsula // Geol. Ore Deposits. 2014. V. 56 (3). P. 147–168.

THE JURASSIC GLOBAL VOLCANIC EVENTS RECORDED IN SEDIMENTARY BLACK SHALE DEPOSITS (BAZHENOV FORMATION, WEST SIBERIA)

Shaldybin M.V., Kondrashova E.S.

TomskNIPIneft JSC, RF, Tomsk, [2] Tomsk Polytechnic University, RF, Tomsk

Keywords: *Luminescent layers, Bazhenov Formation, Volcanic events*

Argillites with luminesce under UV radiation were detected in some layers in the Bazhenov Shale Formation of the West Siberian Basin (Figure 1). Their distribution was found to be persistent over an area of more than 500 km wide (Shaldybin et al, 2019). The Bazhenov Formation was sedimented during the Late Jurassic time and represents the main source rock in the West Siberia petroliferous basin.

The mineralogy and fabric of these luminescent layers were studied by optical and fluorescence microscopy, SEM, XRD, ICP-MS, INAA and IR methods. Optical microscopy in thin sections and mineralogy showed that the luminescent layers are clayey rocks but with significant degree of secondary alteration of clastic debris. The layers are clay-rich and XRD showed that two principal clay minerals are present, namely a well-crystallized kaolinite and a felted network of mixed-layer illite/smectite (I/S) stacked in a regular arrangement. View and appearance of these “debris” under microscope showed a large extent of their deriving from volcanic ash falls and could be described as meta-tuffites (Figure 2).

Total organic matter content in the luminescent layers is much lower than that in the enclosing Bazhenov Formation clayey-silty siliceous sediments above and below luminescent layers. Studied luminescent argillites can be compared with tonsteins in coal beds (derived from volcanic ash falls with high content of) kaolinite or with benthonic clays in volcanic beds. However, tonsteins originate at or near land surface (Spears 2012), whereas the studied argillites as we consider could form in a deep marine basin of West Siberia. But just as tonsteins can be used for detailed stratigraphic studies in coal basins, so may the luminescent argillites prove to be significant as stratigraphic markers for West Siberia basin.

Thus, Jurassic time in the West Siberia area was characterised global volcanic events. It is not possible to fixed the similar volcanoclastic material in casual terrigenous deposits as it has the same chemical and mineral composition, while they can be recorded in contrasted beds saturated by organic substance like coals or anomalous black shales layers (in case of Bazhenov Formation). Obviously, sources for Jurassic magmatism should be looking for on the margins of basin depression.

Geochemical data for luminescent layers was characterised by complex of microelements (ICP-MS, INAA) identification and revealed the specialisation of intermediate rock corresponds to it andesite-rhyodacite chemical composition (Figure 3).

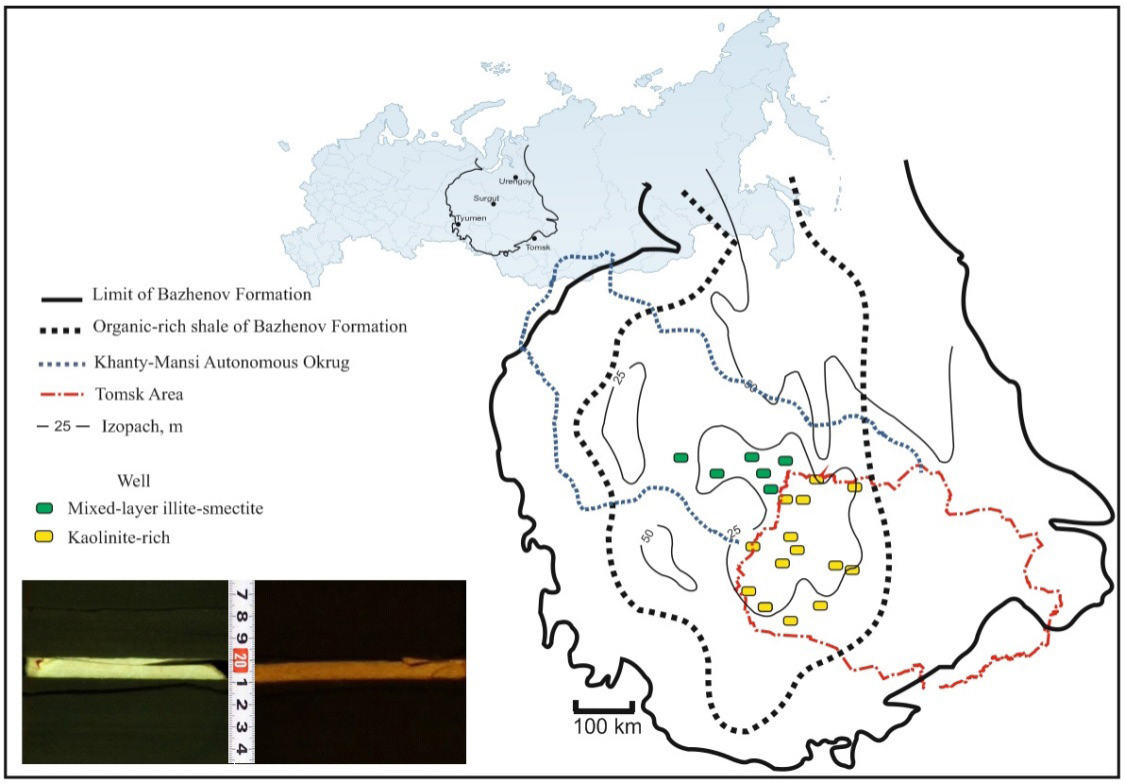


Figure 1. Map of distribution Bazhenov Formation and studied well locations in limit of West Siberia basin.

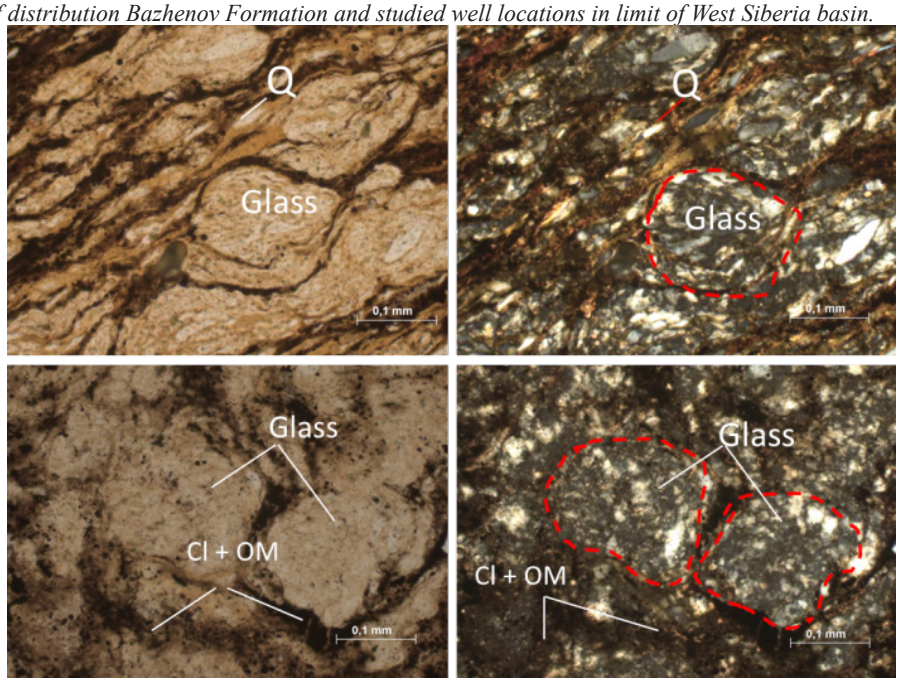


Figure 2. Optical micrographs showing the fabric of the luminescent layers in core. Plane polarized light (left) and crossed polars (right). Notes: red circles - volcanic "debris"(or Glass); Q - quartz; OM – organic matter; Cl - clay.

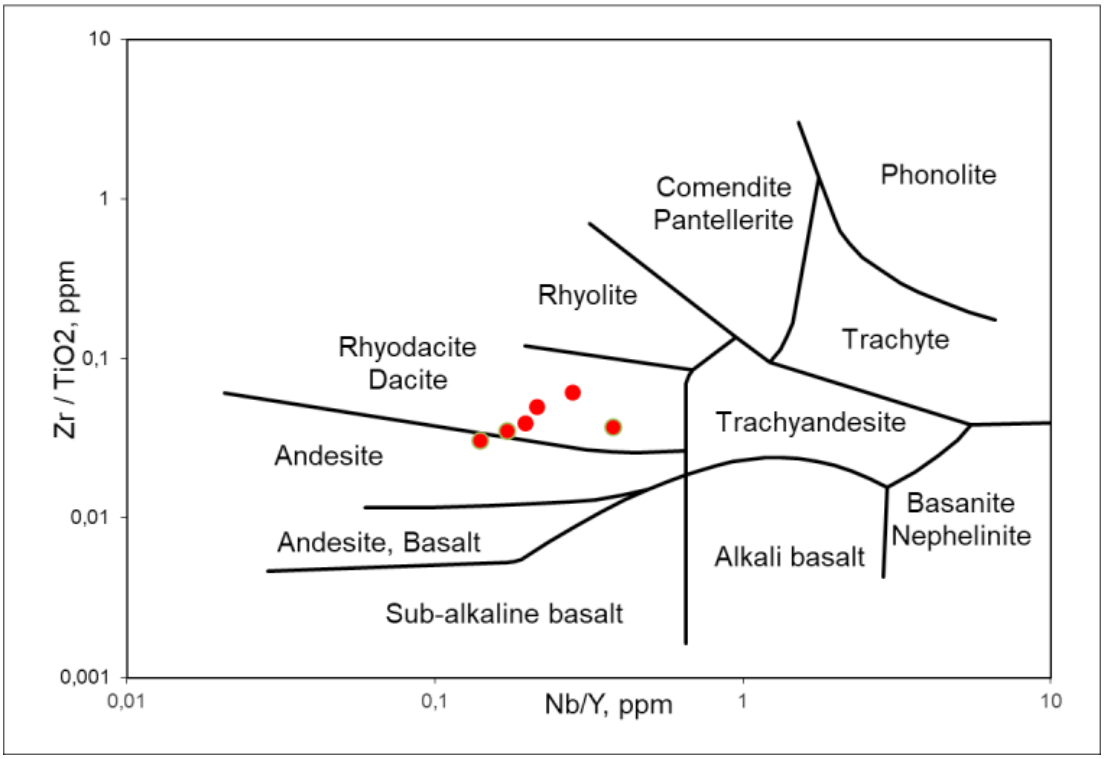


Fig. 3. Plot of luminescent layer samples on the magmatic discriminant diagram (Winchester and Floyd, 1977)

References:

1. Shaldybin, M.V., Wilson, M.J., Wilson, L., Lopushnyak, Yu.M., Brydson, R., Krupskaya, V.V., Kondrashova(Deeva), E.S., Glotov, A.V., Goncharov, I.V., Samoilenko, V.V., Arbuzov, S.I., Bether, O.V., Fraser, A.R., Bowen, L., White, D., Dorofeeva, N.V., 2019. The nature, origin and significance of luminescent layers in the Bazhenov Shale Formation of West Siberia, Russia. Mar. and Petr. Geol. 100, 358-375.
2. Spears, D.A., 2012. The origin of tonsteins, an overview and links with seatearths, fireclays and fragmental clay rocks. Int. J. Coal Geol. 94, 22–31.
3. Winchester, J.A., Floyd, P.A., 1977. Geochemical discrimination of different magma series and their differentiation products using immobile elements. Chem. Geol. 20, 325–343.

CU-NI-PGE MINERALIZATION OF MAFIC-ULTRAMAFIC INTRUSIONS OF THE KHANGAY UPLAND (MONGOLIA)

Shapovalova M.[1,2], Tolstykh N.[1,2], Shelepaev R.[1,2]

[1]VS Sobolev Institute of Geology and Mineralogy SB RAS, Novosibirsk, Russia
[2]Novosibirsk State University, Novosibirsk, Russia

Keywords: *Large igneous provinces, mafic-ultramafic intrusions, Cu-Ni-PGE mineralization*

Introduction

Based on the results of investigations performed in the Permian structures of the Khangay upland (Izokh et al. 1998; Shelepaev et al. 2015; Shapovalova et al. 2018), the Khangay large igneous province (LIP) has been expected and it is actively studied today by us. It hosts the various PGE-Cu-Ni ore occurrences localized in Permian mafic-ultramafic massifs: Oortsog, Dulaan, Mankhan, Yamat and Nomgon. The new geochronological, mineralogical, and geochemical data obtained by now permit correlation between ore-bearing massifs each other and to discover the similarities between them, including the PGE-Cu-Ni mineralization.

The samples under study have been collected from outcrops at the intrusions of Khangay upland during the field trips 2014-2017 years. The concentrations of PGE (Os, Ir, Ru, Pt, Pd and Rh) and Au were determined by an Element 2 Finnigan MAT (ICP-MS); the contents of Cu, Ni, Zn, Cr, S were determined by a Perkin-Elmer atomic absorption spectrophotometers (AAS) at the institute of geochemistry SB RAS (Irkutsk, Russia). The chemical compositions of the minerals were examined at the analytical center for multielemental and isotope research of the VS Sobolev Institute of Geology and Mineralogy SB RAS (IGM SB RAS) using a LEO-413VP scanning electron microscope (SEM) with INCA Energy 350 microanalysis system equipped with EDS (analysts Dr. N. Karmanov and M. Khlestov).

Results

The Oortsog, Dulaan, Mankhan, Yamat and Nomgon mafic-ultramafic massifs are located in the Khangay upland of Mongolia (Fig. 1). The Khangay upland belongs to the Central Asian Orogenic Belt. The mafic-ultramafic massifs intruded in the earliest stages of the formation of the Khangay batholite (Izokh et al. 2011) with the most of them in the southern part of the batholite being Permian in age. It is believed that the massifs were a thermal source for formation of granitoids (Izokh et al. 2011; Shelepaev et al. 2015). All massifs have the same characteristics: composition (from peridotites to monzogabbro), REE contents (positive Cs, Ba, Sr anomalies and negative Ta, Nb and Zr, Hf anomalies), age (determined as Perm for some of them) and geodynamic conditions of formation. The similar characteristics are observed in the Nomgon massif (Izokh et al. 1998). In early study (Shapovalova et al. 2018) we suggested that mafic-ultramafic massifs of the Khangay upland (Oortsog, Dulaan, Mankhan and Yamat) with dual geochemical characteristics were formed as a result of the interaction of plume and a lithospheric mantle; and the massifs are the parts of LIP (250-278 Ma).

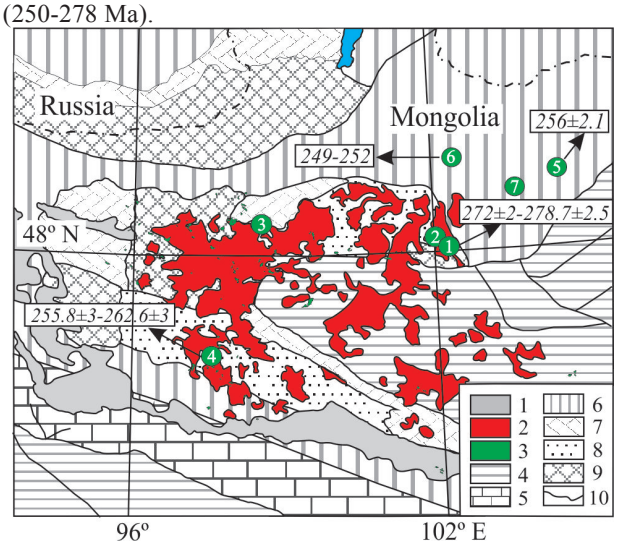


Figure. 1. Geological map of the mafic-ultramafic massif of Khangay upland in CAOB (modified after Sal'nikova et al. 2014); 1 – Mesozoic-Cainozoic troughs; 2 – Late Paleozoic granitoid of Hangay batholite; 3 – Permian gabbroids of Khangay uplands; 4-7 – orogens: 4 Middle –Late Paleozoic (gercynides), 5 – Early-Middle Paleozoic (late caledonides), 6 – Vendian-Early Paleozoic (early caledonides), 7 – Neoproterozoic; 8,9 – Tectonic blocks with the Early Precambrian basement (8) and the Pre-Vendian orogenic basement (9); 11 – tectonic boundaries. The numbers in circles are the mafic-ultramafic massifs: 1 – Oortsog; 2 – Dulaan; 3 – Mankhan; 4 – Yamat; 5 – Nomgon; 6 – Nariyntolburiyngol; 7 – Erdenet.

The Oortsog, Yamat, Dulaan, and Mankhan host base metal sulfide mineralization as well as pyrrhotite, pentlandite and chalcopyrite, while the sulfide mineralization of Nomgon massif represented by the chalcopyrite-bornite association with cubanite. The sulfide of Dulaan and Mankhan represented by the disseminated mineralization. The Oortsog and Yamat massifs include the disseminated sulfide. The main sulfide of Oortsog massif is pentlandite therefore, sulfide melt was enriched in Ni. Whereas chalcopyrite-bornite association is characteristic of Nomgon massif (sulfide melt was enriched in Cu). The disseminated mineralization of the Nomgon massif is a rare copper type of deposits associated with layered mafic-ultramafic intrusions (Krivenko et al. 1990). Sulfides are in the interstitium of silicates but not included in rock-forming minerals (olivine, plagioclase) therefore their formation took place at the final stage of crystallization of the mafic melt.

The Nomgon and Oortsog layered intrusions host the PGE mineralization (Izokh et al. 1991, Shapovalova et al. 2015). PGE concentrations in 100% sulfide phase of the Nomgon disseminated ore are higher than the Oortsog ores (Fig. 2). The PGE patterns of Nomgon (Fig. 2b) is characterized by a steeper positive slope than the PGE patterns of Oortsog (Fig. 2a) that indicates a greater degree of sulfide melt fractionation and as a result, a greater potential for platinoids in this massif.

The Ni/Cu ratios in rocks of the Ortsog massif are 1.25-2.31 are similar to that (1.4) of the Jinchuan Cu-Ni deposit, western China (Chai and Naldrett 1992). Whereas Ni/Cu (0.38-0.06) ratios in rocks of the Nomgon massif close to disseminated ores of Noril'sk deposit (Ni/Cu = 0.66) (Naldrett 2004).

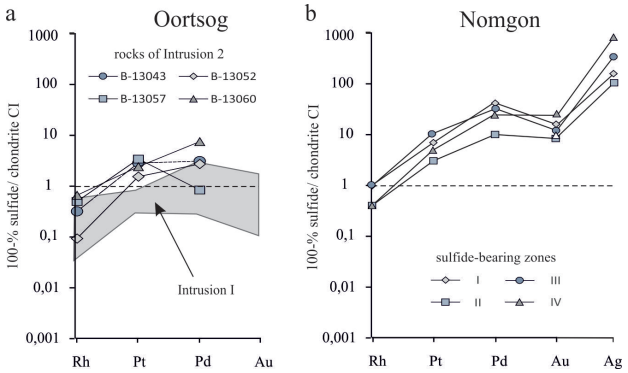


Figure. 2. Chondrite-normalized PGE, Au and Ag patterns (Anders and Grevesse 1989) of rocks from the Oortsog (a) and the Nomgon (Izokh et al. 1991) massifs (b).

Platinum group minerals (PGM) in studied samples of the Oortsog massif (Intrusion 2) are sperrylite $PtAs_2$, braggite (Pt,Pd,Ni)S, isoferroplatinum PtFe and Au-Ag alloys. A large number of PGM in the Nomgon massif represented by sperrylite, mertieite $Pd_8(Sb,As)_3$, majakite PdNiAs, kotulskite Pd(Bi,Te), keithconnite Pd_3Te, merenskyite $Pd(Bi,Te)_2$, michenerite PdBiTe (Izokh et al. 1991).

Conclusions

1) All studied massifs including Nomgon are part of a Khangay large igneous province (250-278 Ma) with PGE-Cu-Ni metallogeny;

2) The Nomgon massif is enriched in Cu and Pd compared with the Oortsog massif, that indicates a more high degree of fractionation of his sulfide melt;

3) The Oortsog ore on Ni/Cu ratios is comparable with the Jinchuan Cu-Ni deposit, while the Nomgon massif is similar to Noril'sk deposit;

4) Pt compounds characterize the Oortsog massif, whereas Pd compounds are more characteristic for the Nomgon massif.

Acknowledgements

The studies were carried out in IGM SB RAS, projects no.

0330-2016-0003 and №14.Y26.31.0018 financed by Ministry of Science and Higher Education of the Russian Federation. This work was supported by the RFBR integration project of SB RAS "Carbon-Permian-Triassic granitoid batholites and mafic-ultramafic complexes of the southern border of the North Asian craton: age boundaries, numerical models of formation, metallogeny".

References

1. Anders E., Grevesse N. (1989) Abundances of the elements: meteoric and solar. Geochimica et Cosmochimica Acta 53: 197-214
2. Chai G., Naldrett A.J. (1992) PGE mineralization of the Jinchuan Ni-Cu sulfide deposit, N.W. China. Economic Geology 87: 1475-1495
3. Izokh A.E., Polyakov G.V., Anoshin G.N., Golovanova N.P. (1991) Geochemistry of platinum metals, gold and silver in the Nomgon troctolite-anorthosite-gabbro massif (MNR). Geochemistry 10:114-117
4. Izokh A.E., Polyakov G.V., Gibsher A.S., Balykin P.A., Zhuravlev D.Z., Parkhomenko V.A. (1998) The high-aluminous layered gabbroids of the Central Asian orogenic belt: geochemical features, Sm-Nd age and geodynamic conditions of formation. J Geol Geophys 39(11): 1565-1577
5. Izokh A.E., Vishnevsky A.V., Polyakov G.V., Shelepaev R.A. (2011) Age marks of picritic and picrodolerite magmatism in Western Mongolia. Geology and Geophysics 52(1): 10-31
6. Krivenko A.P., Lopukhov A.S., Glotov A.I. (1990) Geochemical associations of rare and radioactive elements in ore igneous complexes. Novosibirsk: Science : 55 p.
7. Naldrett A.J. (2004) Magmatic sulfide deposits: geology, geochemistry and exploration. Springer, New York: 727 p.
8. Sal'nikova E.B., Yakovleva S.Z., Kotov A.B., Tolmacheva E.V., Plotkina Y.V., Fedoseenko A.M., Kozlovskii A.M., Yarmolyuk V.V. (2014) Crystallogenesis of zircon in alkaline granites and specifics of zircon U-Pb dating: A case study of the Khangai magmatic area. Petrology 22(5): 450-461
9. Shapovalova M., Shelepaev R., Tolstykh N., Kalugin V., Safonova I. (2015) Petrology of the Ortsog-Uul Gabbro-Petidotite PGE-Bearing complex, Western Mongolia. Conf materials: 13th SGA Biennial Meeting 3: 983–985
10. Shapovalova M., Shelepaev R., Tolstykh N., Izokh A. (2018) Gabbroid massifs of Khangay upland as a result of interactions of the mantle plum with the lithospheric mantel. Proceeding of science meeting. Tomsk: 428-432
11. Shelepaev R.A., Polyakov G.V., Izokh A.E., Vishnevsky A.V., Egorova V.V., Shelepov Ya.Yu. (2016) The Perm intraplate mafic-ultramafic associations of Asia. Materials of conf. Correlation of Altaides and Uralides: magmatism, metamorphism, stratigraphy, geochronology, geodynamics and metallogeny. Novosibirsk: 214-216

THREE MAJOR TYPES OF THE LIPS IN THE EARLY PRECAMBRIAN: EVDENCE FROM THE EASTERN FENNOSCANDIAN SHIELD

Sharkov E., Bogina M., Chistyakov A.

Institute of Geology of ore deposits, Petrography, Mineralogy and Geochemistry RAS, Moscow, Russia

Keywords: *komatiites, siliceous high-Mg series. Fe-Ti picrites and basalts, irreversible change of composition*

Introduction

The most researchers believe that large igneous provinces (LIPs) are formed owing to the ascent of mantle plumes via adiabatic melting of their heads. Because the LIPs have existed throughout the geological history of the Earth (Ernst, 2014), their rocks can be used to probe the composition of the plumes and thereby to decipher the evolution of deep-seated processes in the Earth's interior.

We discuss the problem of the early stages of the LIPs evolution by the example of the eastern Fennoscandian Shield, where three major types of the LIPs successively changed each other during the early Precambrian: (1) Archean LIPs composed mainly of komatiite-basaltic series, (2) Early Paleoproterozoic LIPs made up mainly of siliceous high-Mg series, and (3) Mid Paleoproterozoic LIPs composed of picrites and basalts similar to the Phanerozoic LIPs (Sharkov, Bogina, 2009). If the first two types of LIPs practically were extinct after the Mid Paleoproterozoic, the last type is survived till now without essential change.

Evolution of the LIPs throughout the Earth's history

As Archean structures around the world, major Archean tectonic structures of the Eastern Fennoscandian Shield were represented by granite-greenstone terranes (GGTs) and intervening granulite belts. Greenstone belts consist of irregular network of greenstone belts (< 10-15% of area) among a plagiogranite-gneiss matrix. They look like specific protorift structures filled up by predominated volcanics of high-Mg komatiite-basaltic series derived from a depleted mantle source.

The early Paleoproterozoic (2.5-2.4 Ga) Sumian-Sariolian LIP is widely developed at the eastern Fennoscandian. By this time, already rigid crust was rifted and penetrated by dike swarms and large platiniferous mafic-ultramafic layered intrusions. Magmatism was dominated by siliceous high-Mg (boninite-like) series (SHMS), which formed large igneous provinces. SHMS are close in composition to the Phanerozoic subduction-related magmas, however, in contrast, were formed in an intracratonic setting. Like magmas of the Archean

komatiite-basaltic series, SHMS melts were also derived from depleted ultramafic mantle sources, however, they are enriched in incompatible elements, for example, LREE, etc. The LIPs of this composition and age or their fragments are found on practically all Precambrian shields. This means that the appearance of the SHMS magmas was an important global event and these LIPs mark the next stage of the Earth's mantle evolution.

This LIP, in turn, was replaced by the Mid Paleoproterozoic (2.35-1.95 Ga) Jatulian-Ludikovian LIP, which built on structures made up of the previous LIP. However, the composition of magmas that composed this LIP was cardinally changed: new melts were characterized by the elevated and high contents of Fe, Ti, Cu, P, Mn, alkalis, LREE, and other incompatible elements (Zr, Ba, Sr, U, Th, F, etc.), which are typical of the Phanerozoic LIPs and indicate geochemically enriched mantle sources. Syenite-gabbros and ultramafic-alkali-carbonatite intrusive complexes typical of the Phanerozoic LIPs also occur among intrusive analogs of the volcanics. So, Jatulian-Ludikovian LIP in the Fennoscandian Shield can be considered as the oldest manifestation of the Phanerozoic LIPs. This cardinal change in the character of magmatism occurred in the Mid Paleoproterozoic on a global scale. Since this time, the composition of LIPs has practically not changed till now.

Thus, based on the LIPs composition, the irreversible change of deep-seated processes in the Earth'e interior occurred in the Mid Paleoproterozoic.

DISCUSSION

The cardinal change in the LIPs composition occurred within period from 2.35 to 2.0 Ga: the early Precambrian high-Mg magmas derived from depleted mantle sources gave way to the geochemically-enriched Fe-Ti picrites and basalts, which are similar to the Phanerozoic within-plate magmas. This type of magmatism is survived till now without essential changes (Sharkov, Bogina, 2009). Hence, data available on the Phanerozoic LIPs can be used for understanding deep-seated processes in the Mid Paleoproterozoic.

According to modern paradigm (Maruyama, 1994; Dobretsov et al., 2001, 2010; French, Romanowicz, 2015, etc.), formation of the LIPs is explained by ascent of the thermochemical mantle plumes, which are generated at the liquid outer core-mantle boundary (CMB) due to the percolation of core's fluids in overlying mantle. So, mantle plumes consist of two kinds of material, mantle silicates and core's fluids, which in different proportions could be involved in melting of plume heads (Sharkov et al., 2017).

Very important information on mantle plume composition can be obtained from mantle xenoliths in within-plate (plume-related) basalts, which are fragments of the upper cooled margin of the plume head above zone of adiabatic melting. This study confirms the existence of two types of plume material: (i) green spinel peridotites (mainly lherzolites) representing silicate mantle matrix, and (ii) veined rocks of the "black series" , which are composed of Al-Ti augite, kaersutite, phlogopite, etc. and were derived from melt/fluids. Two major types of mantle fluids contributed in the fluid-assisted melting: (1) easy mobile carbonate fluid enriched in LREE, Na, Th, U, and depleted in Si, Ti, Zr and Hf; and (2) silica-hydrous melt/fluid enriched in Ti, Fe, Ba, P, K, Zr, Nb, etc. (Downes et al., 2001; Ma et al., 2015; Ryabchikov et al., 2010, etc.).

Geochemical data showed that incompatible elements are mainly accumulated in the "black-series" rocks. This indicates that the mantle matrix of the plumes' matter was composed of depleted ultramafics, while peculiar enriched features of the newly formed basalts were provided by the core's fluids. Hence, in the early Precambrian mantle plumes, especially, in Archean's ones, core's material (fluids) was minor or absent. From this follows that the early Precambrian LIPs (Archean and Early Paleoproterozoic) were derived from thermal plumes, based on weak enrichment of SHMS melts in LREE. Thermochemical plumes appeared only in the Mid Paleoproterozoic and caused an irreversible changes in LIPs composition.

Conclusions

We think that the Earth's core in the early Precambrian (up to the Mid Paleoproterozoic) did not participate in formation of the mantle plumes, and they were represented by simple thermal variety. However, situation cardinally changed only in the Mid Paleoproterozoic, when fluids from the outer liquid core became to percolate in the mantle bottom and generated thermochemical plumes that operate till now. We suggest that in that time geochemically-enriched material of the primordial core became to be involved in tectonomagmatic processes

References

1. Dobretsov, N.L., Kirdyashkin, A.G., Kirdyashkin, A.A. (2001). Deep Geodynamics. 2nd Ed. Nauka--Geo, Novosibirsk, 409 p. (in Russian).
2. Downes, H. (2001). Formation and modification of the shallow sub-continental lithospheric mantle: a review of geochemical evidence from ultramafic xenolith suites and tectonically emplaced ultramafic massifs of Western and Central Europe. Journal of Petrology, 41, 233--250.
3. Ernst, R.E. (2014). Large Igneous Provinces. Cambridge Univ. Press, Cambridge, 653 p.
4. French, S.W., Romanowicz, B., 2015. Broad plumes rooted at the base of the Earth's mantle beneath major hotspots. Nature 525, 95-99.
5. Ma, G. S.-K., Wang, K.-L., Malpas. J. et al. (2015). Melt-pockets and spongy clinopyroxenes in mantle xenoliths. In: Khan, A., Deschamps, F. (Ed.). The Earth's Heterogeneous Mantle. Springer International Publishing, Cham, pp. 205-257.
6. Maruyama, S. (1994). Plume tectonics. Journal of Geological Society of Japan, 100, 24--49.
7. Ryabchikov, I.D., Sharkov, E.V., and Kogarko, L.N., 2011. Rhönite from mantle peridotites in Syria. Bulletin of the Tethys Geological Society, Cairo, 6, pp. 120--126.
8. Sharkov, E.V., Bogina, M.M. (2009). Mafic-ultramafic magmatism of the Early Precambrian (from the Archean to Paleoproterozoic) Stratigraphy and Geolological Correlation, 17, 117-136.
9. Sharkov,E., Bogina, M., Chistyakov, A. (2017). Magmatic systems of large continental igneous provinces. Geoscience Frontiers 8(4), 621-640.

MERCURY CHEMICAL SPECIATION IN SEDIMENTS AND THEIR APPLICATIONS

Shen J.
State Key Laboratory of Geological Processes and Mineral Resources, China University of Geosciences, Wuhan, Hubei, 430074, P.R. China
shenjun@cug.edu.cn

Volcanisms (e.g., Large Igneous Province, LIP) were assumed as the ultimate trigger for numerous oceanic perturbations (e.g., Oceanic Anoxia Event, OAE) as well as biotic crisis (e.g., mass extinctions) in Earth history. Mercury (Hg), a novel proxy in sediments were widely used as ancient volcanic records during the Paleozoic Era. However, it`s still poor know about the Hg speciation (host for Hg) in both modern and ancient sediments, although most of the studies had assumed organic matter associated Hg as the dominantly speciation in sediments. Here, we present Hg concentrations from four modern anoxic settings (Black Sea, Saanich Inlet, Japanese Sea, and Peru Upwelling area), as well as seven black shales units (two sites from the Lower Cambrian, one sites from the Upper Carboniferous, one unit from the Middle Permian, two units from the Upper Permian, as well as one site from the Lower Jurassic) from the Phanerozoic, as well as Hg speciation from subset samples from four units (two units from lower Cambrian, and two units from Late Permian). Our data show organic-matter associated mercury is the dominated fractionation in modern anoxic sediments present here, as well as some black shales in earth history. However, Hg could also be dominated host by other minerals (e.g., sulfides) in sediments under more reducing conditions. Our work document that it is essential to explore the speciation of Hg in sediments when using Hg as proxy of paleo-volcanisms.

NEOGENE WITHINPLATE MAGMATISM OF DE LONG ISLANDS: FOOTPRINT OF YOUNG MANTLE PLUME OF THE EASTERN ARCTIC BASIN

Silantyev S.

Vernadsky Institute of Russian Academy of Sciences

The geochemical and petrological data obtained for samples of volcanic and plutonic rocks collected on the islands of the De Long archipelago make it possible to reconstruct the geodynamic nature of the magmatic complexes of this region of the Eastern Arctic. The established magmatic evolution at De Long Islands implies its close relations with the activity of a mantle plume that occurred beneath the continental shelf on the boundary between Laptev and East Siberian Seas and was responsible for magmatic events in this area of the eastern sector of the Arctic over the past 5 m.y. The origin of the volcanic complexes widespread in area examined reflects magmatism related to at least two geochemically distinct mantle sources. One of them gave rise to reservoir parental for Cretaceous volcanic complexes belonging to HALIP (High Arctic LIP) - Bennett Island. Other one produced young plume-type melts (Ol-basalts and Limburgites of Zhokhov and Vilkitsky Islands).

Young lavas of the central part of the De Long archipelago are brought to the surface on the Zhokhov and Vilkitsky Islands xenoliths of crustal and mantle origin which make it possible to imagine the possible construction of lithosphere below studied islands (Fig. 1). The estimated conditions of formation characteristic mineral paragenesis in studied mantle xenoliths allow to delineate the possible P − T trajectory corresponding to the ascent of the magmatic melt in which fragments of mantle rocks were entrapped at different depth levels. These depths likely corresponded to the following upper mantle levels beneath Zhokhov and Vilkitsky islands: 60 km (_21 kbar); 50 km (_16 kbar); and 45 km (_15 kbar) (Silantyev et al., 2004). Xenoliths belonging to older continental crust are present by granites as well as quartzites and siliciclastic rocks (Silantyev et al., 2004; Akinin et al., 2015). Data obtained for dolerite xenolith sampled at Zhokhov Island demonstrate that its geochemical characteristics allow consider this rock as a fragment of the early Cretaceous crustal material of the East Siberian shelf which belongs to HALIP.

Rough sketch presented on Fig. 1 demonstrates sequential trapping of mantle and crustal xenoliths by olivine basalts and limburgites in the central part of the De Long archipelago. The hypothetical cross-section of the lithosphere below the central part of the De long archipelago is made according to the data given in (Franke et al., 2004; Silantyev et al., 2004; Franke, Hinz, 2009; Thorarinsson et al., 2011; Gaina et al., 2014; Akinin et al., 2015). The presented data testify in favor of the existence of a young mantle plume in the considered region of the Eastern Arctic. The first manifestation of plume related magmatism in the central part of De Long archipelago (Zhokhov Island) correspond to the age of 5.62 Ma, and the youngest - 0.4 Ma (Vilkitsky Island).

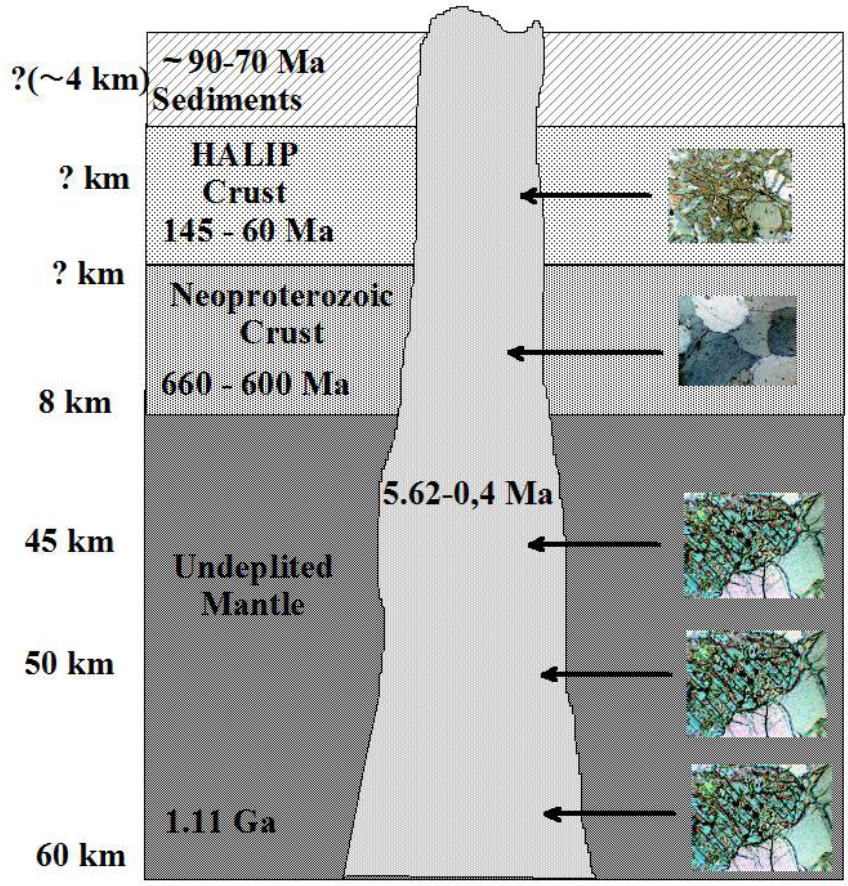


Fig. 1. Idealized scheme of the interaction of a rising plume with mantle and crustal substratum's below Zhokhov and Vilkitsky Islands. Were used data borrowed from (Franke et al., 2004; Silantyev et al, 2004; Franke, Hinz, 2009; Thorarinsson et al., 2011; Gaina et al., 2014; Akinin et al., 2015)..

Reference

1. Akinin V.V., Gottlieb E.S., Miller E.I., Polzunenkov G.O., Stolbov N.M., Sobolev N.N. Age and composition of basement beneath the De Long archipelago, Arctic Russia, based on zircon U–Pb geochronology and O–Hf isotopic systematics from crustal xenoliths in basalts of Zhokhov Island // Arktos. 2015. V. 1. N 9. DOI 10.1007/s41063-015-0016-6.
2. Franke D., Hinz K., Reichert C. Geology of the East Siberian Sea, Russian Arctic, from seismic images: Structures, evolution, and implications for the evolution of the Arctic Ocean Basin // J. of Geophys.Res. 2004. V.109.N B07106, doi:10.1029/2003JB002687.
3. Franke D., Hinz K. Geology of the Shelves surrounding the New Siberian Islands, Russian Arctic //Stephan Mueller Spec. Publ. Ser. 4. 2009. PP. 35–44. www.stephan-mueller-spec-publ-ser.net/4/35/2009/
4. Gaina C., Medvedev S., Torsvik T.H., Koulakov I., Werner S.C. 4D Arctic: A Glimpse into the Structure and Evolution of the Arctic in the Light of New Geophysical Maps, Plate Tectonics and Tomographic Models //Surv Geophys.2014. V. 35. PP.1095–1122. DOI 10.1007/s10712-013-9254-y
5. Silantyev S.A., Bogdanovskii O.G., Fedorov P.I., Karpenko S.F., Kostitsyn Yu.A. Intraplate magmatism of the De Long Islands: A response to the propagation of the ultraslow-spreading Gakkel Ridge into the passive continental margin in the Laptev Sea // Russian Journal of Erath Sciences. 2004. V.6. N3. PP. 1-31.
6. Thorarinsson S.B., Holm P.M., Tappe S., et al. Late Cretaceous–Palaeocene continental rifting in the High Arctic: U–Pb geochronology of the Kap Washington Group volcanic sequence, North Greenland //J. of Geol. Soc. London. 2011. V.168. PP. 1093–1106. doi: 10.1144/0016-76492011-018.

ULTRABASIC IGNEOUS PROVINCE OF THE SIBERIAN PLATFORM: PHYSICAL AND CHEMICAL CONDITIONS OF INTRUSIVE COMPLEXES FORMATION

Simonov V. A.[1], Vasiliev Y. R.[1], Kotlyarov A. V. [1], Prihodko V. S.[2]

[1]*Sobolev Institute of Geology and Mineralogy, SB RAS, Novosibirsk, Russian Federation*
[2]*Kosygin Institute of Tectonics and Geophysics FEB RAS, Khabarovsk, Russian Federation*

Keywords: *ultrabasic igneous province, Siberian Platform, melt inclusions in Cr-spinels, computational modelling*

The ultrabasic massifs have a sufficiently wide distribution on the Siberian Platform and draw attention of many researchers as a representatives of deep mantle magmatic systems. Also, ultramafic rocks of this region have a great significance in connection with their platinum concentrations (Malich, 1991; Kogarko et al., 1994; Nekrasov, et al., 1994). As a whole, on the Siberian platform it is possible to allocate perfectly large-scale ultrabasic igneous province. Thus until recent time the representative information on conditions of crystallization of the most high-temperature minerals of ultramafic rocks (olivine, Cr-spinel) has been received mainly for meimechite effusive complexes of northern part of the Siberian Platform (Sobolev et al., 2009). At the same time many questions, connected with physical and chemical conditions of formation of ultrabasic intrusive complexes of the Siberian Platform remained unsettled.

Researches during last years (Simonov et al., 2011, 2014, 2016) have allowed to receive considerable volume of information on conditions of formation of the ultrabasic intrusive complexes on the Siberian Platform (Fig. A). On the basis of results of study of melt inclusions in Cr-spinels from dunites (Fig. B - inclusions with «spinifex» structures before high-temperature experiments: Ol - olivine, Cpx - clinopyroxene; Fig. C - inclusions after high temperature experiments and quenching: Fl - fluid bubble, Gl - glass) physical and chemical parameters of ultrabasic rocks crystallization from such well-known platinum bearing massifs as Konder, Inagli and Chad, settling down in the structures of the Southeast of the Siberian Platform have been established. The representative data on melt inclusions in Cr-spinels of Guly massif (the North of the Siberian Platform) is obtained also.

The special technique (Simonov et al., 2011) of melt inclusions study, taking into account that Cr-spinels practically are not transparent, was applied. During experiments the grains of Cr-spinels were heated up to 1330-1340°C at the graphite microcontainers. Further training in water for glass reception was spent. Phases in inclusions were analyzed in the Sobolev Institute of Geology and Mineralogy, Siberian Branch of Russian Academy of Science (Novosibirsk) on the electronic scanning microscope MIRA 3 LMU. Contents of rare, rare-earth elements and water in glasses of the heated-up and quenched inclusions are defined on ionic microanalyzer IMS-4f at the Institute of microelectronics and computer science of the Russian Academy of Sciences (Yaroslavl) by the published technique (Sobolev, 1996). For finding-out of a temperature mode of crystallization of rocks, and also for the purpose of establishment of features of evolution of the magmatic systems which were taking part in formation of ultrabasic intrusive complexes of the Siberian platform calculated modelling with use of programs PETROLOG (Danyushevsky, Plechov, 2011) and PLUTON (Lavrenchuk, 2004) has been spent. For a basis of calculations compositions of melt inclusions are taken.

As a result of research of melt inclusions in Cr-spinels the considerable volume of the original information on formation of rocks of the ultrabasic massifs of the Siberian Platform is accumulated. Melt inclusions show the general regularities of behavior of magmatic systems during formation of the ultrabasic massifs of the Siberian Platform, tracing the cardinal evolutionary trend of falling magnesia against growth SiO_2 in melts with consecutive transition from picrites through picrite basalts to basalts. Compositions of melt inclusions testify to difference of conditions of crystallization of rocks of concentric zone massifs (Konder, Inagli, Chad) from peculiarities of formation of the Guly massif. As a result of computational modelling by means of two programs (PETROLOG and PLUTON) on the basis of the data on composition of melt inclusions in Cr-spinels the maximum temperatures of crystallization of olivines from dunites of Konder (1545-1430°C), Inagly (1530-1430°C), Chad (1460-1420°C) and Guly (1520-1420°C) massifs, and also Cr-spinels from the same complexes were determined: Konder (1420-1380°C), Inagly (to 1430°C), Chad (1430-1330°C) and Guly (1410-1370°C). For the Guly massif calculations under program PLUTON on the basis of melt inclusions have shown possibility of formation of alkaline rocks at a final reversive stage of evolution of picritic magmas (with reduction SiO_2 and accumulation of alkalis) after finalization of olivine crystallization at decrease in temperatures from 1240-1230°C to 1200-1090°C. Computational modelling by means of program PLUTON has shown that during formation of dunites from the Guly massif were existed high ferriferous (with the average content of the titan) melts, which crystallization (since 1210°C) led to formation of pyroxenes between cumulative olivine crystals. At further temperature decrease (since 1125°C), from melts with falling contents of FeO and TiO_2, clinopyroxenes of pyroxenites were formed. In the case of the Konder massif computational modelling under program PLUTON testifies to possibility of kosvite formation from picrite-basaltc magmas (since 1350°C) and crystallization of clinopyroxenites and olivine-diopside rocks from melts of olivine-basalt composition (since 1250°C).

The analysis by means of an ionic microprobe of values of volatile components in glasses of heated-up melt inclusions in Cr-spinels shows affinity of the maximum contents of water in the magmatic systems forming ultrabasic intrusive complexes on the Siberian platform (Konder - till 0.53 wt. %, Inagly - till 0.63 wt. % and Guly - till 0.76 wt. %) and in the paleoceanic structures (Karashat massif at the South Tuva - till 0.58 wt. %).

For the Guly massif it was possible to spend modelling of processes of crystallization of initial magma, for which basis

the composition of parental melts for meimechites (Sobolev et al., 2009) was taken.Calculations with use of the program PETROLOG (Danyushevsky, Plechov, 2011) have shown that temperatures of liqiudus crystallization of olivine from this melt at the presence of water (0.5 wt. %) depending on pressure could be the following: 20 kbar - 1600°C, 14 kbar - 1570°C and 10 kbar - 1550°C. Considering established by us liqiudus crystallization temperatures of olivine from dunites of the Guly massif (1520-1420°C), for calculations with program COMAGMAT (Ariskin, Barmina, 2004) were taken values of pressure 10 kbar, suitable to the intermediate magmatic chamber on the depth of 30 km at the basis of Earth crust.

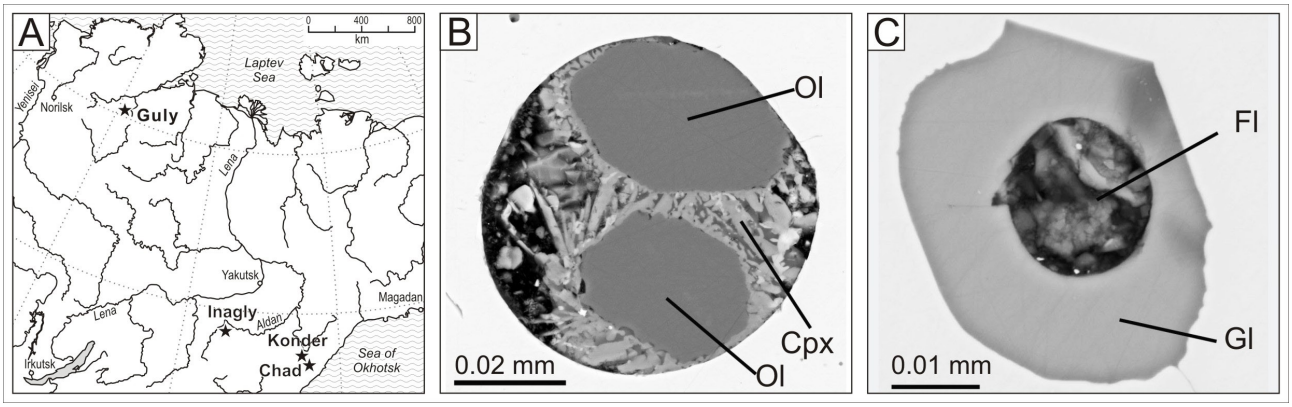
Computational modelling has shown that results of decompressional (from 10 to 2 kbar) equilibrium and fractional crystallization of the meimechite parental melt (at the presence of water - it is primary 0.1 wt. %, with accumulation to 0.3 wt. %) are similar to each other. It has been found out that olivines (with values of forsterite component up to 90-91 %), corresponding with compositions of minerals from dunites of the Guly massif (in accessory Cr-spinals from which melt inclusions have been studied) and also of olivines from inclusions, were formed basically at pressure 6-7 kbar. At the same time clinopyroxenes, corresponding with compositions of pyroxenes (to 49 % En) from inclusions with «spinifex» structures and of pyroxenes (to 46 % En) from inclusions with gabbro structure crystallized at lower pressure: to 5.4 kbar and 3.9 kbar accordingly.

Comparison of the received calculating data of fractional crystallization of meimechite parental melt and picrite magma with the compositions of melt inclusions in Cr-spinals has shown similarity of magmatic systems of meimechites and the Guly massif. Thus, experimental data on inclusions show reliability of actually calculating trends fractionating of meimechite parental melt and picrite magma, that as a whole testifies to formation of the Guly massif dunites with the assistance of the initial magma similar on the composition to parental meimechite melts.

Work is executed under the state task of the Sobolev Institute of Geology and Mineralogy, Siberian Branch of Russian Academy of Science, with support of the Ministry of Science and Higher Education of the Russian Federation and the contract № 14.Y26.31.0029.

Reference

1. Ariskin A.A., Barmina G.S. COMAGMAT: Development of a magma crystallization model and its petrologic applications // Geochemistry International, 2004, v. 42 (Supp. 1), p. S1–S157.
2. Danyushevsky L.V., Plechov P.Yu. Petrolog 3: Integrated software for modeling crystallization processes // Geochemistry, Geophysics, Geosystems, 29 July 2011, 2011, v. 12, № 7. Q07021, doi: 10.1029/2011GC003516.
3. Kogarko L.N., Uhanov A.V., Nikolsky N.E. New data on contents of elements of platinum group in rocks ijolit-karbonatit formation (Guly and Kugda massifs, the Maimecha-Kotui province, Polar Siberia) // Geochemistry, 1994, № 11, p. 1568-1576 (in Russian).
4. Lavrenchuk A.V. «PLUTON» program for calculation of intrachamber differentiation of the basic magma // The second Siberian international conference of young scientists on Earth Sciences. Novosibirsk, 2004, p. 105-106 (in Russian).
5. Malich K.N. About formation of accessories of platinum bearing ultrabasic concentric-zone massifs of the Siberian platform // Dokl. AH USSR. 1991, v. 318, № 6, p. 1452-1457 (in Russian).
6. Nekrasov I.Y., Lennikov A.M., Octyabrsky R.A., et al. Petrologiya and platinum concentrations in the ring alkaly-ulrabasic complexes // M: Science, 1994, 381 p. (in Russian).
7. Simonov V.A, Vasiliev Y.R., Stupakov S.I., Kotlyarov A.V., Karmanov N.S. Petrogenezis of dunites of the Guly ultrabasic massif (the north of the Siberian Platform) // Geology and Geophysics, 2016, v. 57, № 12, p. 2153-2177 (in Russian).
8. Simonov V.A, Prihodko V.S, Kovyazin S.V. Conditions of formation of platinum bearing ultrabasic massifs of the Southeast of the Siberian Platform // Petrologiya, 2011, v. 19, № 6, p. 579-598 (in Russian).
9. Simonov V.A, Prihodko V.S, Stupakov S.I., Kotlyarov A.V. Petrogenezis of dunites of the Chad massif, the Siberian Platform (data on melt inclusions in Cr-spinels) // Materials of XVI All-Russia conference on thermobarogeochemistry. Irkutsk: Publishing house of Institute of Geography of the Siberian Branch of the Russian Academy of Science, 2014, p. 102-103 (in Russian).
10. Sobolev A.V. Inclusion of melts in minerals as a source of basic petrological information // Petrologiya, 1996, v. 4, p. 228-239 (in Russian).
11. Sobolev A.V., Sobolev S.V., Kuzmin D.V., Malich K.N., Petrunin A.G. Mechanism of formation of Siberian meimechites and the nature of their communication with trapps and kimberlites // Geology and Geophysics, 2009, v. 50, № 12, p. 1293-1334 (in Russian).



PRECAMBRIAN MAFIC DYKE SWARMS IN KOLA-MURMANSK AND KARELIAN PROVINCES, EASTERN FENNOSCANDIA: BAR-CODE CORRELATIONS AND IMPLICATIONS FOR TECTONIC RECONSTRUCTIONS

Stepanova A. V.[1], Samsonov A. V.[2], Salnikova E. B.[3], Arzamastsev A. A.[3], Egorova S. V.[1], Larionova Y. O.[2], Veselovskiy R. V.[4,5], Erofeeva, K. G.[2], Stifeeva M. V.[3]

[1] *Institute of Geology KarRC RAS, Petrozavodsk, Russia*
[2]*IGEM RAS, Moscow, Russia*
[3]*IPGG RAS, Saint-Petersburg, Russia*
[4]*IFZ RAS, Moscow, Russia*
[5]*LomonosovMoscow State University, Moscow, Russia*

Keywords: *Paleoproterozoic, Fennoscandia, mafic dykes, baddeleyite U-Pb dating, supercontinents*

The eastern Fennoscandian Shield comprise the Archean Kola-Murmansk and Karelia-Belomorian lithospheric segments are separated by the Paleoproterozoic Lapland-Kola orogen. The Archean crustal segments of Fennoscandia usually considered as a whole crustal block during the Archean and Paleoproterozoic excluding the short time of Lapland-Kola ocean opening (Melezhik, Hanski, 2013 and references therein). These reconstructions were based on similarities in volcanic and sedimentary sequences (Melezhik, Hanski, 2013), and in a lesser degree in similarities in age and composition of mafic dyke swarms (Vuollo, Huhma, 2005, Fedotov et al., 2012). New baddeleyite U-Pb (ID TIMS) and zircon (SIMS) ages, and geochemical and isotopic data for 2.68-1.86 Ga mafic dyke swarms and sills in the Karelian and Kola-Murmansk provinces allow us to draw and compare bar-codes for these crustal blocks.

Karelian province. The Archean continental lithosphere of the Karelian province preserved a lot of mafic dykes and sills of age 2.51-1.96 Ga (Vuollo and Huhma, 2005). In contrast to ca. 2505 Ma event that is recognized only in the south-eastern part of the Karelian province (Bleeker et al., 2008), mafic rocks of age 2.45 Ga are wide spread. They form mafic dyke swarms, layered intrusions and mafic volcanics and show wide variations in trace element and Sr-Nd isotopic composition. The obtained data suggests that 2.45 Ga mafic magmatic rocks were originated via simultaneously melting of mantle at various degrees and different depths.

2405 and 2310 Ma events in the central part of the Karelian province comprise mafic dyke swarms composed of low-Mg dolerites (Stepanova et al., 2015, 2017). They probably represent strongly evolved liquids of primary plume-derived melts. High-Mg mafic volcanics of age ca. 2.4 Ga are recognized in the Vetreny belt in the south-eastern part of the Karelian province (Puchtel et al., 2016).

Voluminous 2220 Ma event comprise differentiated mafic sills that are now recognized not only in Finnish but also in Russian (Stepanova et al., 2018 and references therein) side of the Karelian province. 2130 Ma event includes high-Ti enriched and MORB-type tholeiitic dykes which are widespread on the Karelian Craton, show strong similarity with Phanerozoic syn-breakup basalts of Afar and NAIP in trace-element geochemistry and Nd isotopic composition, and probably indicate a stage of continental breakup of Archean lithosphere (Stepanova et al., 2014). 2.06 Ga event is recognized in the north-west of Karelian province and comprise layered intrusions and high-Mg mafic volcanics (Vuollo, Huhma, 2005). The 1.96-1.98 Ga event includes small amount of high-Mg rocks and volumetrically prevail low-Mg, high-Fe-Ti mafic rocks (Lubnina et al., 2016 and references therein).

Kola-Murmansk province. According to the available age data and compositional similarities, mafic dykes and sills in the Kola-Murmansk province have been considered as an analogues of mafic dyke swarms in the Karelian province (Fedotov et al., 2012). Recent U-Pb baddeleyite and zircon age data allow to recognize previously unknown events and get a detailed bar-code for mafic dyke swarms in the Kola and Murmansk Provinces.

The earliest 2680 Ma event comprise abundant Pl-porphyritic dykes (2692 ± 10 Ma) that form radial swarm and well-preserved olivine gabbro (2680 ± 2 Ma) of Fe-picritic chemical affinity. The age of dykes is determined by U-Pb (ID TIMS) dating of baddeleyite. Mafic intrusions of similar age have been previously recognized in the Keivy terrane but not recognized in the other parts of the Shield (see details in Samsonov et al., this volume).

Huge 2505 Ma event is well-known and have been previously dated within the Kola province (Bayanova et al., 2009). Baddeleyite dating results for the mafic dykes in Li-inakhamary area (2508±6 Ma), Kola Bay (2523±48 Ma), Varzina Bay (2505±6 Ma) and Olenegorsk area indicate the existence of several large NNE and N-oriented swarms both in Kola and Murmansk crustal segments (see details in Egorova et al., this volume).

Newly recognized 2400 Ma event in the NW Kola province includes differentiated S-type mafic sills of age 2399±2 Ma and coeval 2401±5 Ma gabbronorite and dolerite mafic dykes. The age of dykes and sills is determined by single grain U-Pb ID TIMS dating of baddeleyite. The detailed description and petrology of this event is given in Erofeeva et al. (2019).

The event of age 2060 Ma is newly recognized in the NW Kola province (Sor-Waranger, Norway) on the basis of zircon U-Pb SIMS dating. Two greenschist facies altered mafic dykes within the NW-oriented swarm give the ages of 2060 ±7 и 2063 ±6 Ma. The voluminous event of age 1940-1980 Ma have been previously well-dated and studied in detail in the Pechenga area (Skuf'in, Bayanova, 2006). It includes Fe-picritic mafic volcanics and dykes and gabbro-wehrlite intrusions. New U-Pb baddeleyite dating results for gabbronorite dyke in the Kola Bay (1983 ±5 Ma) indicate a wide distribution of ca. 1980 Ma dykes both if Kola and Murmansk provinces.

1860 Ma event comprise I-type mafic sills located in the northern part of the Murmansk province. Baddeleyite extracted from two thick sills gives similar age for Dalnie Zelentsy (1860 ± 4 Ma) and Dvorovaya (1863± 7 Ma) localities (Veselovskiy et al., 2019 and this volume).

The comparison of dyke bar-codes for Karelian and Kola-Murmansk provinces indicates the presence of several important differences in the succession of magmatic events in various segments of the Fennoscandian Shield. Both the Karelian and Kola-Murmansk provinces most likely belonged to the Superia supercraton as suggested by Bleeker and Ernst (2010). This is supported by the similarity in the succession of events from 2505 to 2400 Ma. Recognized differences in volume of ca. 2505 – 2400 Ma mafic rocks suggest that at this period Karelian and Kola-Murmansk provinces were probably not in neighboring position within this supercraton.

Noteworthy differences occur within the period 2400-2060 Ma. Several voluminous events of ca. 2310, 2220 and 2130 Ma age occur in the Karelian province. In contrast, mafic dykes of such age have not yet been recognized in the Kola-Murmansk province. Since 2060 Ma up to 1860 Ma the Karelian and Kola-Murmansk provinces have a similar succession of events and compositions of mafic rocks. The available data suggest that the Lapland-Kola Ocean could opened between 2400 and 2310 Ma. A wide occurrence of 1980 Ma mafic rocks both in Kola-Murmansk and Karelian provinces indicates that the Lapland-Kola Ocean was already closed at 1980 Ma. Ca. 2060 Ma event that is now recognized in the northern Karelia and western Kola provinces could be considered as a possible indicator of the Lapland-Kola Ocean closure. Later intraplate events occur within single Fennoscandian continent and indicate variations in crustal architecture related with Lapland-Kola and Svecofennian orogens.

Acknowledgements

This work was supported by the Russian Science Foundation (Grant 16-17-10260).

References

1. Bayanova T, Ludden J, Mitrofanov F (2009) Timing and duration of Palaeoproterozoic events producing ore-bearing layered intrusions of the Baltic Shield: metallogenic, petrological and geodynamic implications. Geol Soc London, Spec Publ 323:165–198.
2. Bleeker W., Hamilton M.A., Ernst R.E. et al. (2008) The search for Archean-Paleoproterozoic supercratons: New constraints on Superior-Karelia-Kola correlations within supercraton Superia, including the first ca. 2504 Ma (Mistassini) ages from Karelia. Abstract for IGC33 Meeting, Oslo, Norway.
3. Ernst R, Bleeker W (2010) Large igneous provinces (LIPs), giant dyke swarms, and mantle plumes : significance for breakup events within Canada and adjacent regions from 2.5 Ga to the Present. Can J Earth Sci 47:695–739.
4. Ernst, R.E. (2014) Large Igneous Provinces. Cambridge University Press, Cambridge. 653 p.
5. Erofeeva KG, Stepanova A V, Samsonov A V, et al (2019) 2.4 Ga Mafic dikes and sills of Northern Fennoscandia: petrology and crustal evolution. Petrology 27:17–42.
6. Fedotov Zh.A., Bayanova T.B., Serov P.A. (2012) Spatiotemporal relationships of dike magmatism in the Kola region, the Fennoscandian Shield. Geotectonics: 412-426
7. Hanski EJ, Huhma H, Vuollo JI (2010) SIMS zircon ages and Nd isotope systematics of the 2.2 Ga mafic intrusions in northern and eastern Finland. Bullentin Geol Soc Finl 82:31–62
8. Lubnina N V., Stepanova A V., Ernst RE, et al (2016) New U–Pb baddeleyite age, and AMS and paleomagnetic data for dolerites in the Lake Onega region belonging to the 1.98–1.95 Ga regional Pechenga–Onega Large Igneous Province. GFF 138:54–78.
9. Melezhik VA, Hanski EJ (2013) The Early Palaeoproterozoic of Fennoscandia: Geological and Tectonic Settings. pp 111–178
10. Puchtel IS, Touboul M, Blichert-Toft J, et al (2016) Lithophile and siderophile element systematics of Earth's mantle at the Archean-Proterozoic boundary: Evidence from 2.4 Ga komatiites. Geochemica Cosmochim Acta 180:227–255.
11. Skuf'in P. K., Bayanova T. B. (2006) Early Proterozoic central-type volcano in the Pechenga structure and its relation to the ore-bearing gabbro-wehrlite complex of the Kola Peninsula. Petrology 14: 609-626
12. Söderlund, U., Johansson, L., (2002) A simple way to extract baddeleyite (ZrO2). Geoch., Geoph., Geosys.. 3.
13. Stepanova A V, Samsonov A V, Salnikova EB, et al (2014) Palaeoproterozoic continental MORB-type tholeiites in the Karelian Craton: petrology, geochronology, and tectonic Setting. J Petrol 55:1719–1751.
14. Stepanova A V., Salnikova E B, Samsonov A V., et al (2015) The 2.31Ga mafic dykes in the Karelian Craton, eastern Fennoscandian shield: U–Pb age, source characteristics and implications for continental break-up processes. Precambrian Res 259:43–57.
15. Stepanova A V., Salnikova E B, Samsonov A V., et al (2017) The 2405 Ma doleritic dykes in the Karelian Craton: A fragment of a Paleoproterozoic large igneous province. Dokl Earth Sci 472:72–77.
16. Stepanova AV., Larionov AN, Larionova YO (2018) 2.2 Ga mafic sills in the central part of the Karelian Craton: U-Pb dating of zircons and geochemistry of gabbro-dolerites in the lake Bolshozero area. Proc Karelian Res Cent Russ Acad Sci 3–16
17. Veselovskiy R V, Samsonov A V, Stepanova A V, et al (2019) 1.86 Ga key paleomagnetic pole from the Murmansk craton intrusions – Eastern Murman Sill Province, NE Fennoscandia: Multidisciplinary approach and paleotectonic applications. Precambrian Res 324:126–145.
18. Vuollo J, Huhma H (2005) Paleoproterozoic mafic dikes in NE Finland. In: Precambrian Geology of Finland - Key to the Evolution of the Fennoscandian Shield. pp 195–236

PETROGENESIS OF TWO GENERATIONS OF SILLS IN THE XUHUAI RIFT: IMPLICATIONS FOR THE EVOLUTION OF THE ~925-890 MA LARGE IGNEOUS PROVINCE IN SE MARGIN OF THE NORTH CHINA CRATON

SU Xiangdong[1, 2], PENG Peng[1, 2], WANG Chong[1], SUN Fengbo[1, 2], ZHANG Zhiyue[1, 2], ZHOU Xiaotong[1, 2]

[1]*State Key Laboratory of Lithospheric Evolution, Institute of Geology and Geophysics, Chinese Academy of Sciences, P.O. Box 9825, Beijing 100029, China*
[2]*University of Chinese Academy of Sciences, Beijing 100049, China*

Keywords: *Neoproterozoic; North China Craton; Large igneous province; Xuhuai rift; Fe-Ti-rich gabbro; Sill complex; Wilson cycles*

Introduction

Recently, several Early Neoproterozoic mafic dyke swarms and sill complexes have been identified in the North China Craton, Sao Francisco Craton, Congo Craton, etc. (Tack et al., 2001; Peng et al., 2011a, b; Wang et al., 2012; Zhang et al., 2016; Su et al., 2018a; Zhu et al., 2019; Chaves et al., in Press). The geochemical features of these suites are similar to global continental flood basalts (CFBs) which show negative Nb-Ta anomalies and moderately depleted to slightly enriched Sr-Nd isotope ratios (e.g., Peng et al., 2011a, b; Su et al., 2018a; Zhu et al., 2019). The comparably chemical data and palaeomagnetism studies suggested that these cratons were probably connected (Tack et al., 2001; Peng et al., 2011a; Evans et al., 2016; XiXi Zhao, Personal communication) before ~930 Ma leading to the propose of a large igneous province (Peng et al., 2011a). However, whether these extensive Neoproterozoic magmas are associated with the opening of a new oceanic crust and how the magmatic process led to the formation of the large igneous province are poorly understood. The Chulan sill complex (CSC), a series of coeval sheet-like concordant magmatic body emplaced horizontal into the contemporary Huaibei Group (Xuhuai basin) around Xuzhou area at SE margin of the North China craton, belongs to the Dashigou LIP (Peng et al., 2011a; Ernst, 2014). Its genesis will help in understanding the tectonic background of the event.

Results

Over the past three years, we examine the field relationships and petrography of these sills. Whole-rock major (XRF) and trace elements (ICP-MS), baddeleyite age dating (SIMS) as well as Sr-Nd isotopic compositions (TIMS) were analyzed, combining with morphology and crystal size distribution (CSD) of plagioclase crystals to decipher their magmatic evolution and explore the magmatic rift zone.

As a result, two type sills are identified according to their different occurrence in the stratigraphy: A slightly older generation (G1) emplaced at lower-level strata, and a slightly younger generation (G2), intruding into relatively higher-level strata. The G1 is typically represented by the Niutishan sill. The Niutishan sill, exhibiting a C-shaped profile that is revealed by their whole-rock MgO, CaO, Ni, Cr contents (Fig. 1a), An in plagioclase and En in clinopyroxene (not show), was formed by the combined processes of fractionation, accumulation and compaction under water-unsaturated and low-fO_2 conditions. In terms of petrography and whole-rock chemistry, unlike the Niutishan sill, the Pingshan sill (G2) can be subdivided into an upper and a lower sequence that meet at a Sandwich Horizon. Two significant En (in clinopyroxene) reversal in the upper sequence and one in the lower sequence are accompanied with the variation of CaO and Cr (Fig. 1b). Clinopyroxene shows broad compositional variations (En values of ~10 and Mg# values of ~20). The variations in compostion of intercumulus and cumulus clinopyroxene crystals present an almost M-shaped profile, which is different from a C-shaped profile in the Niutishan sill. This inconsistent cannot be explained by a closed-system crystal fractionation.

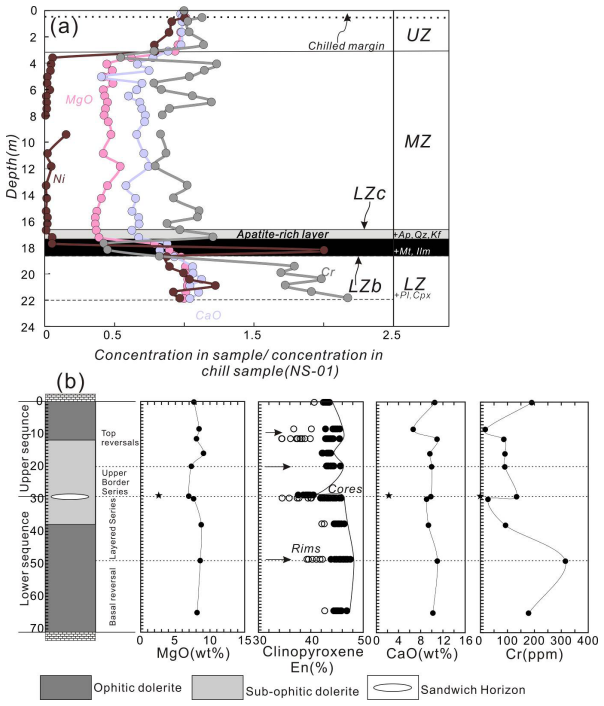


Figure 1. (a) Chill sample-normalized MgO, CaO, Ni and Cr in the Niutishan sill (Su et al., 2018a, b). (b) Simplified section through the drill core 15ZK14 (sampled by RZ Zhu in 2015) from the Pingshan sill showing its stratigraphic subdivision and M-shaped profiles particularly in clinopyroxene composition.

Isotopic compositions indicate that the G1 had a relatively weak continental signature ($87Sr/86Sr_i$=0.7040-0.7048, initial εNd=-0.84 to 1.91, Nb/La=0.8-1.2), while some of the G2 show continental effect during the maturation of the magmatic system ($87Sr/86Sr_i$=0.7060-0.7079, initial εNd=-1.34 to -0.23, Nb/La=0.6-0.7). Isotopic modelling suggest that the two type sills were both contaminated by the enriched sub-continental lithospheric mantle (<10 %) under the North China craton. An increasing continental influence from the G1

to G2 may suggest that they have their own magma plumbing systems from deep mantle to shallow crust and represent different batches of mantle melting magmas.

Conclusions

Combined with the previous published data, we consider the magmatic activities of the Niutishan sill and the coeval Dashigou dyke swarm (c. 925 Ma) (with high REE and LILE contents) may represent the initiation of the Xuhuai rifting event that is dominated by a radiating mafic dyke swarm. However, the Pingshan sill and associated coeval doleritic sills (916-890 Ma) occurred in Liaodong peninsular (Dalian sills) and North Korea (Sariwon sills) are related the subsequent development of the Xuhuai rift and are represented by the multiple magmas injected into the sedimentary basins. MORB-type feature of these numerous mafic sills may be generated in the transition from continental rifting to lithospheric rupture in the divergent of the Wilson cycles. The thermal structure and thickness of the lithopheric crust during rifting may influence the occurrence of the rising magmas in this case. The extensional strain field of the North China plate shows progressive, time-transgressive model in the form from radial to linear patterns during the Early Neoproterozoic era, implying that asthenospheric plume-matrial upwelling, instead of plate boundary processes, governed the initial and early evolution of this intracontinental rift.

Acknowledgements

This study was financially supported by the NFSC Project (41890833, 41772192) and the Key Research Project of CAS Frontier Research Project Scientific (QYZDB-SSW-DQC04281712250). We are grateful to D. Zhang, D. Xue, W. Li, B. Gao, J. Li, X. Ling and R. Li for their help during analyses.

References

1. Chaves, A.d.O., Ernst, R.E., Söderlund, U., Wang, X., Naera, T., in Press. The 920–900Ma Bahia-Gangila LIP of the São Francisco and Congo cratons and link with Dashigou-Chulan LIP of North China craton: New insights from U-Pb geochronology and geochemistry. Precambrian Research
2. Evans, D.A.D., Trindade, R.I.F., Catelani, E.L., D'Agrella-Filho, M.S., Heaman, L.M., Oliveira, E.P., Söderlund, U., Ernst, R.E., Smirnov, A.V., Salminen, J.M., 2016. Return to Rodinia? Moderate to high palaeolatitude of the São Francisco/Congo craton at 920 Ma. Geological Society, London, Special Publications 424, 167-190.
3. Ernst, R.E., 2014. Large Igneous Provinces. Cambridge University Press.
4. Liu, Y., Gao, L., Liu, Y., Song, B., Wang, Z., 2006. Zircon U-Pb dating for the earliest Neoproterozoic mafic magmatism in the southern margin of the North China Block. Chinese Science Bulletin 51, 2375-2382.
5. Peng, P., Bleeker, W., Ernst, R.E., Söderlund, U., McNicoll, V., 2011a. U–Pb baddeleyite ages, distribution and geochemistry of 925Ma mafic dykes and 900Ma sills in the North China craton: Evidence for a Neoproterozoic mantle plume. Lithos 127, 210-221.
6. Peng, P., Zhai, M.-G., Li, Q., Wu, F., Hou, Q., Li, Z., Li, T., Zhang, Y., 2011b. Neoproterozoic (~900Ma) Sariwon sills in North Korea: Geochronology, geochemistry and implications for the evolution of the south-eastern margin of the North China Craton. Gondwana Research 20, 243-254.
7. Su, X., Peng, P., Wang, C., Sun, F., Zhang, Z., Zhou, X., 2018a. Petrogenesis of a ~900 Ma mafic sill from Xuzhou, North China: Implications for the genesis of Fe-Ti-rich rocks. Lithos 318-319, 357-375.
8. Su, X., Peng, P., Wang, C., Sun, F., Zhang, Z., Zhou, X., 2018b. Whole-rock and mineral chemical data from a profile of the ~900 Ma Niutishan Fe-Ti-rich sill in Xu-Zhou, North China. Data in Brief 21, 727-735.
9. Tack, L., Wingate, M.T.D., Liégeois, J.P., Fernandez-Alonso, M., Deblond, A., 2001. Early Neoproterozoic magmatism (1000-910 Ma) of the Zadinian and Mayumbian Groups(Bas-Congo): onset of Rodinia rifting at the western edge of the Congo craton. Precambrian Research 110, 277-306.
10. Wang, Q., Yang, D., Xu, W., 2012. Neoproterozoic basic magmatism in the southeast margin of North China Craton: Evidence from whole-rock geochemistry, U-Pb and Hf isotopic study of zircons from diabase swarms in the Xuzhou-Huaibei area of China. Science China Earth Sciences 55, 1461-1479.
11. Zhang, S.-H., Zhao, Y., Ye, H., Hu, G.-H., 2016. Early Neoproterozoic emplacement of the diabase sill swarms in the Liaodong Peninsula and pre-magmatic uplift of the southeastern North China Craton. Precambrian Research 272, 203-225.
12. Zhu, R.-Z., Ni, P., Wang, G.-G., Ding, J.-Y., Fan, M.-S., Ma, Y.-G., 2019. Geochronology, geochemistry and petrogenesis of the Laozhaishan dolerite sills in the southeastern margin of the North China Craton and their geological implication. Gondwana Research 67, 131-146.

GEOCHEMICAL CHARACTERIZATION OF THE SOL HAMED NEOPROTEROZOIC OPHIOLITIC SERPENTINITES, SOUTHERN EASTERN DESERT, EGYPT

Sedki T., Ali S., Mohamed H. A.

Geology Department, Faculty of Science, Minia University, El–Minia, 61519, Egypt

Keywords: *Sol Hamed; Ophiolitic complex; Serpentinites; Serpentinization; harzburgite; peridotite*

Introduction

The Sol Hamed (SH) area is a part of the Arabian-Nubian Shield (ANS) ophiolites occurred within Onib-Sol Hamed suture zone in the southern Eastern Desert of Egypt (Shackleton 1994 Abdelsalam and Stern, 1996). The ophiolitic assemblages in this area are represented by serpentinite, metagabbro and arc assemblages represented by metavolcanics. They later intruded by gabbroes and granites.

Results and discussion

Geochemistry

SH serpentinites display affinity to the typical metamorphic peridotites on the AFM diagram (Coleman, 1977; Fig. 1a). The bulk-rock Al_2O_3 content is relatively unaffected by serpentinization and therefore retains its original primary signature (Bonatti and Michael 1989). The studied serpentinites have Al_2O_3 contents (0.05–1.02 wt. %) comparable to oceanic and active margin peridotites and fore-arc and Pan-African serpentinites (Fig. 1b; Abdel-Karim et al., 2018). Like other Eastern Desert ultramafites, the SH serpentinites have SiO_2/MgO ratios and Al_2O_3 contents analogous to ophiolitic peridotite (Abdel-Karim et al. 2018) (Fig. 1c). The serpentinites the nature of peridotitic komatiite by using of Jensen's cation plot (after Jensen, 1976) (Fig. 1d). The Al_2O_3 and CaO depletion is typical of fore-arc peridotites (Fig. 2a; Ishii et al., 1992) and characterizes ED ophiolitic ultramafites. In terms of Al_2O_3/SiO_2 and MgO/SiO_2 ratios, they are like Arabian–Nubian shield and fore-arc peridotites (Fig. 2b; Pearce et al. 2000; Abdel-Karim et al. 2018). The studied serpentinites have enriched compatible trace elements (Cr=2426–2709 ppm, Ni=1657–2377 ppm and Co=117–167 ppm) suggesting derivation from a depleted mantle peridotite source.

Alteration and serpentinization

Metamorphism ranging from low-grade greenschist to medium-grade amphibolite facies usually influenced the ophiolitic ultramafites of the Egyptian ED forming serpentinite and/or mixtures of serpentine, talc, chlorite, carbonates and magnetite (e.g., Abdel-Karim et al. 2018). The time and source of carbonate metasomatism that commonly affected the Egyptian ultramafites still debated. Stern and Gwinn (1990) adopted mixing between mantle-derived CO_2-rich fluids and remobilized sedimentary carbonate.

Therefore, the low CaO contents (0.05–0.75 wt. %) in the serpentinites indicate restricted effect of Ca–metasomatism. The CaO contents are not correlated with LOI further confirming this implication. Moreover, the trace element compositions (except U and Sr) are not significantly modified during serpentinization (e.g., Deschamps et al. 2013). Accordingly, the major and trace element data reflect the primary signature of the serpentinites protolith in subduction zones (Deschamps et al. 2013). LOI reach up to 10.34-13.92 wt. %, which supports the role of hydrothermal alteration

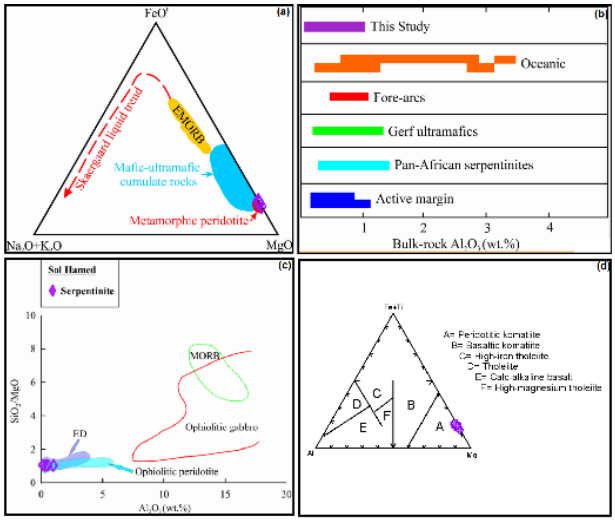


Fig. 1. a) AFM diagram for SH serpentinites (after Coleman, 1977), b) Bulk-rock Al_2O_3 (wt. %) contents of SH compared with those from other tectonic settings and the Pan-African serpentinites, c) SiO_2/MgO ratios vs. Al_2O_3 diagram. Ophiolitic peridotite, ophiolitic gabbro and. Data from (ED) are shown for comparison and d) Jensen's cation plot (after Jensen, 1976).

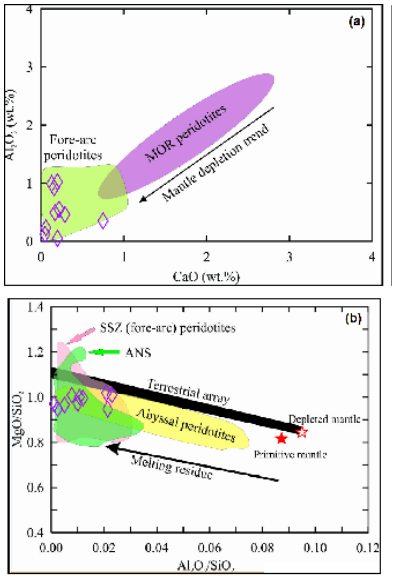


Fig. 2. a) CaO vs. Al_2O_3 diagram showing SH serpentinites compared with fore-arc and MOR peridotites (after Ishii et al., 1992), b) MgO/SiO_2 vs. Al_2O_3/SiO_2 diagram. Primitive and depleted mantle values are after McDonough and Sun (1995, respectively. The "terrestrial array" represents the bulk silicate Earth evolution. Abyssal and fore-arc peridotite fields are after Pearce et al. (2000). ANS ophiolitic peridotite field is after Abdel-Karim et al., 2018.

Tectonic implications

The MgO/SiO_2 and Al_2O_3/SiO_2 ratios of serpentinites agree with SSZ peridotites from fore-arc setting (Fig. 2b; Pearce et al. 2000). Generally, the Al_2O_3 and CaO depletion characterizes fore-arc peridotites (Fig. 2a) (Ishii et al. 1992). The Cr vs. TiO_2 diagram also supports the SSZ setting for the SH serpentinites (Fig. 3a; Pearce et al., 1984).

The studied rocks show low Al_2O_3 content reflecting depleted upper mantle source (Bonatti and Michael 1989). Their high Mg#, Cr and Ni are consistent with a depleted mantle peridotite source (e.g., Khalil 2007). The MgO/SiO_2 and Al_2O_3/SiO_2 ratios (Fig. 2b) accord with peridotites generated from subduction-related magma source.

Numerous geochemical studies demonstrated restricted mobility of major elements during serpentinization and protolith primary signature were retained (Deschamps et al. 2013). The SH serpentinites have low CaO contents comparable to ophiolitic peridotites. Moreover, their low Al_2O_3/SiO_2 ratios (mostly < 0.03) are similar to fore-arc mantle wedge serpentinites suggesting that their protoliths had experienced partial melting before serpentinization which has no effect on this ratio (e.g., Deschamps et al. 2013). Also, their low MgO/SiO_2 ratios (< 1.1) resemble serpentinised lherzolites and harzburgite (Deschamps et al. 2013). They have low TiO_2 contents (0.01–0.06 wt. %) compared to depleted mantle composition but like subduction zone serpentinites (Deschamps et al. 2013). Their major element data consistent with harzburgitic source (Fig. 3b).

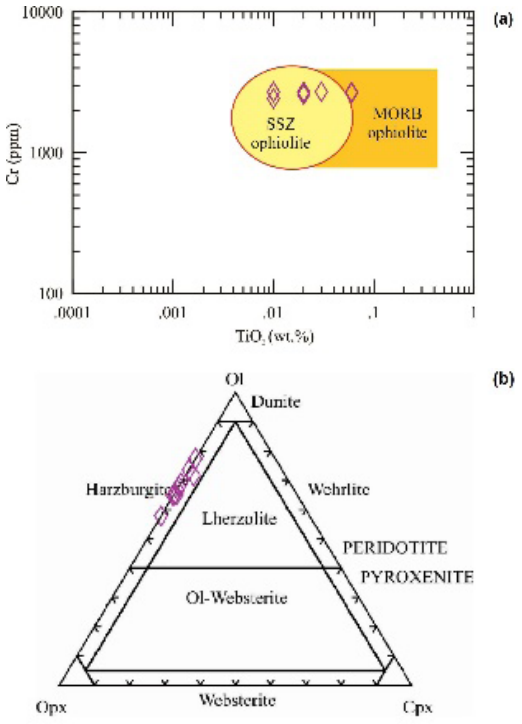


Figure 3. a) Cr vs. TiO_2 plot to discriminate SSZ and MORB ophiolites (after Pearce et al., 1984) and b) Ol–Cpx–Opx diagram (Streckeisen, 1976).

Conclusion

The compatible trace elements (Cr-Ni-Co) enrichment in SH serpentinites indicate derivation from a depleted mantle peridotite source. They show affinity to the typical metamorphic peridotites with peridotitic komatiite nature. The normative compositions reflect harzburgitic mantle source. Their Al_2O_3 contents (0.05–1.02 wt. %) are akin to oceanic and active margin peridotites and Pan-African serpentinites. The Cr and TiO_2 contents indicate SSZ environment with tectonic character destructive plate margins and depleted mantle sources. Their Al_2O_3/SiO_2 and MgO/SiO_2 ratios support the SSZ affinity and are similar to ANS peridotites with fore-arc setting. Low value of Al_2O_3/SiO_2 (fore-arc field), suggesting that these rocks were derived from a mantle source with high degrees of partial melting. Moreover, their Al_2O_3 and CaO depletion is typical of fore-arc peridotites. The normative compositions replicate harzburgitic mantle source.

Acknowledgments

The first author is grateful to Shalateen Mineral Resource Company for helping during geologic field work. He also, thanked his wife for continuous support.

References

1. Abdel-Salam, M., and Stern, R., 1996, Sutures and shear zones in the Arabian-Nubian Shield: Journal of African Earth Sciences, v. 23, no. 3, p. 289-310.
2. Abdel-Karim AM, Ali S, El-Shafei SA (2018) Mineral chemistry and geochemistry of ophiolitic metaultramafics from Um Halham and Fawakhir, Central Eastern Desert, Egypt International Journal of Earth Sciences, 107:2337–2355. тhttps://doi.org/10.1007/s00531-018-1601-2
3. Coleman, R.G. 1978. Ophiolites. "Mir", 261 p.
4. Deschamps F, Godar M, Guillot S, Hattori K (2013) Geochemistry of subduction zone serpentinites: a review. Lithos 178:96–127.
5. Ishii T, Robinson PT, Maekawa H, Fiske R (1992) Petrological studies of peridotites from diapiric Serpentinite Seamounts in the Izu- Ogasawara-Mariana forearc, leg 125. In: Pearce J, Stokking LB, et al (eds), Proceedings of the Ocean Drilling Project, Leg 125, Scientific Results (College Station), pp 445–485.
6. Jensen, L.S., 1976. A new cation plot for classifying subalkaline volcanic rocks. Ontario Division Mines Miscellaneous Paper No. 66.
7. Khalil KI (2007) Chromite mineralization in ultramafic rocks of the Wadi Ghadir area, Eastern Desert, Egypt: mineralogical, microchemical and genetic study. Neues Jb Mineral Abh 183:283–296.
8. Pearce JA, Barker PF, Edwards SJ, Parkinson IJ, Leat PT (2000) Geochemistry and tectonic significance of peridotites from the south sandwich arc-basin system, South Atlantic. Contrib Miner Petrol 139:36–53.
9. Pearce, J.A., Lippard, S.J., Roberts, S., 1984. Characteristics and tectonic significance of supra-subduction ophiolites. In: Kokelaar, B.P., Howells, M.F. (Eds.), Geological Society of London, Special Publication 16, 777–794.
10. Shackleton R.M. (1994) Review of late proterozoic sutures, ophiolitic mélanges and tectonics of eastern Egypt and northeast Sudan. Geol Rundsch 83:537–546
11. Stern RJ, Gwinn CJ (1990) Origin of late Precambrian intrusive carbonates, Eastern Desert of Egypt and Sudan: C, O, and Sr isotopic evidence. Precambr Res 46:259–272.

INTERNATIONAL LITHOSPHERE PROGRAM (ILP)

Thybo H.

Eurasia Institute of Earth Sciences, Istanbul Technical University, Turkey
School of Earth Sciences, China University of Geosciences, Wuhan, China
Centre for Earth Evolution and Dynamics (CEED), University of Oslo, Norway

The Lithosphere is the connection between the deep Earth and the surface, and it forms the basis for society's exploitation of natural resources. The lithosphere is the topic of focused research in geology, geophysics, geochemistry and geotechnology. Experience shows that breakthroughs in the study of the Lithosphere can only be achieved through integration of imaging, monitoring, reconstruction and process modelling.

The International Lithosphere Program (ILP) has since 1980 supported research on the nature, dynamics, origin and evolution of the lithosphere. ILP promotes and directs research on first-order problems in modern integrated Solid Earth Science with focus on the lithosphere by organising international, multidisciplinary geoscience research projects and coordinating committees.

The program seeks to achieve a balance between: "addressing societal needs", e.g. providing information for improved resource exploration and environmental protection, as well as understanding natural catastrophes and other Solid Earth processes that affect the biosphere, and "satisfying scientific curiosity", e.g through studying the basic processes at the Earth's surface and in the crust and mantle that affect Lithosphere evolution. The projects address topics within the key topics of Geoscience of Global Change, Contemporary Dynamics and Deep Processes, Continental Lithosphere, and Oceanic Lithosphere. The multidisciplinary task forces address their subjects through integrated interpretation of the lithosphere, modelling mantle dynamics, identification of links between the lithosphere and surface processes, and addressing the influence of paleoclimate changes.

I will provide an overview of the development of ILP, some of the major achievements by the programme, and an introduction to the on-going interdisciplinary projects in terms of task forces and regional coordinating committees.

MAGMATIC UNDERPLATING IN CONTINENTAL LITHOSPHERE

Thybo H.[1,2,3], Artemieva I. M.[4]

[1]*Eurasia Institute of Earth Sciences, Istanbul Technical University, Maslak, Istanbul, Turkey*
[2]*School of Earth Sciences, China University of Geosciences, Wuhan, China*
[3]*Centre for Earth Evolution and Dynamics (CEED), University of Oslo, Oslo, Norway*
[4]*Geology Section, IGN, Copenhagen K, Denmark.*

Underplating was originally proposed as the process of magma ponding at the base of the crust and was inferred from petrologic consideration, often thought to be associated with extensional regions. The process may have main importance for the formation of continental crust with its characteristic low average density, and may have been mainly active during the early evolution of the Earth. However, despite the assumed importance of underplating processes and associated fractionation, the available geophysical images of underplated material remain relatively sparse and confined to specific tectonic environments. Direct ponding of magma at the Moho is only observed in very few locations, probably because the magma interacts with the surrounding crustal rocks. There is no direct discriminator between traditionally underplated material and lower crust magmatic intrusions in the form of batholiths and sill-like features, and in the current review of new results on underplating we include both these phenomena. Underplating in this sense is observed in a variety of tectonic settings, including island arcs, wide extensional continental areas, rift zones, and continental margins. Recent new data show that magmatic processes around Moho level may take the form of sill intrusions in the lower crust (at continental rift zones and slopes) as well as in the vicinity of major crustal intrusions, and that underplating may even take the form of massive magmatic intrusion into the crust in giant magma chambers. We review the structural styles observed by geophysical imaging and discuss these first order observations in relation to the Moho.

EVOLUTION OF SULPHIDE MELT IN THE LOW-SULPHIDE HORIZON OF THE NORIL'SK-1 DEPOSIT

Tolstykh N.[1,2], Zhitova L.[1,2], Shapovalova M.[1,2], Chayka I.[1,2]

[1]*V.S. Sobolev Institute of Geology and Mineralogy of SB RAS, Novosibirsk, Russia*
[2]*Novosibirsk State University, Novosibirsk, Russia*

Keywords: *Noril'sk 1 intrusion, low-sulphide horizon, PGE-minerals, sulphide inclusion in PGM, reducing conditions*

Introduction

The new mineralogical data on the chromite segregations in the PGE-rich low-sulphide horizon that locate in taxitic gabbro-dolerite of the upper endocontact zone of the Noril'sk 1 intrusion have been received. Numerous droplet-shaped inclusions of sulfides in the chromian spinel, and in minerals of the platinum group elements (PGM) have been found. The changes of mineral parageneses in trapped sulfide droplets and changes in the compositions of sulfides included in successively crystallizing host minerals make it possible to follow the evolution of the sulfide melt in the ore-forming systems.

The chemical compositions of the minerals were examined at the analytical centre for multi-elemental and isotope research of the VS Sobolev Institute of Geology and mineralogy SB RAS using a LEO-413VP scanning electron microscope with INCA Energy 350 microanalysis system equipped with EDS (analyst M. Khlestov).

Results

Sulphides

Sulphides occur in two textural settings: as interstitial segregations (Fig. 1) and as droplet-shaped inclusions in sperrylite (10 pieces), Pt-Fe alloys (19) and mertieite I (1) (Fig. 2). The sulphide interstitial segregations contain the pyrrhotite (Po), pentlandite (Pn), chalcopyrite (Ccp), pyrite (Py), and millerite (Ml) but Po is the most common mineral. PGM include the one-phase, two-phase (Po+Pn) (Fig. 2), and three-phase (Po+Pn+Ccp) droplets (Fig. 2d). But the mono Ccp inclusions are found only in Pt-Fe.

The composition of pyrrhotite varies from troilite $Fe_{0.99}S_{1.01}$ (inclusions in sperrylite) to pyrrhotite of intermediate composition $(Fe_{0.95}Ni_{0.01})_{0.96}S_{1.04}$ (inclusions in Pt-Fe alloys) and to monoclinic pyrrhotite $Me_{0.91}S_{1.09}$ in the sulphide segregations (Fig. 3 a).

The Ni/(Ni+Fe) ratios (k) in different grains of pentlandite increases from 0.46 to 0.66. The Ni content increases from Pn hosted in sperrylite (k is 0.46-0.47) to Pn included in Pt-Fe alloys (k is 0.51-0.53) and to the sulphide segregations (k is 0.53-0.54 in Pn lamellas and 0.55-0.65 in granular Pn), and reaching 0.66 in Pn included in mertieite I (Fig. 3 b).

Pyrite grains are surrounded by chlorite and cobaltite in sulphide segregations. It is associated with millerite in sample where Ml is as lamellae in chalcopyrite matrix. In this case pyrite contains up to 5.33 wt.% Ni. Chalcopyrite occurs in subordinate amounts.

PGM minerals

Twenty four PGE mineral species were diagnosed based on the analyses of their compositions. The most common PGM are Pt-Fe alloys and sperrylite. Cooperite, moncheite, rustenburgite, tetraferroplatinum, hongshiite, hollingworthite, zvyagintsevite, atokite, palarstanide, paolovite, palladoarsenide, vincentite, naldrettite, stibiopalladinite, isomertieite, mertieite I and II, kotulskite, michenerite, keithconnite, moncheite, vysotskite and menshikovite have been found among which a series of unnamed phases there are.

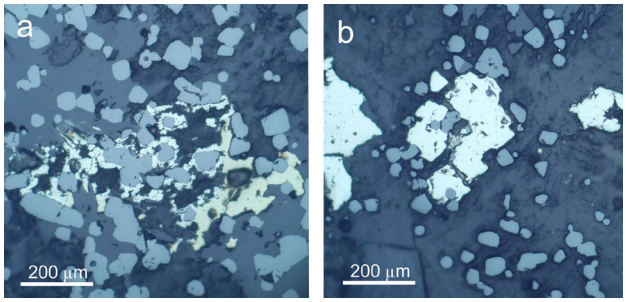


Figure 1. Sulphide segregations and inclusions of chromian spinel in the rocks of low-sulphide horizon (reflected light).

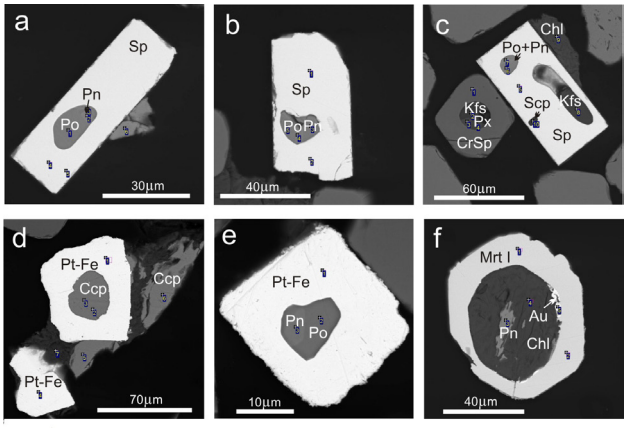


Figure 2. The droplet-shaped inclusions of sulphides and silicate in PGM (BSE images). Pt-Fe – ferroan platinum and isoferroplatinum, Sp – sperrylite, Mrt I – mertieite I, Po – pyrrhotite, Pn – pentlandite, Ccp – chalcopyrite, Chl – chlorite, CrSp – chromian spinel, Scp – scapolite, Px – pyroxene.

Discussion and conclusions

The captured sulphide droplets are fragments of a sulphide melt fractionated to varying degrees that existed at the moment of crystallization of host Pt-Fe alloys and sperrylite (Sp). Therefore, these two PGM are high-temperature and crystallize from the silicate melt until the solidify of the sulphide bulk. It has been shown that direct crystallization of Sp from an S-undersaturated basalt melt is possible (Maier et al. 2015) in the reducing conditions of FMQ-2 (Canali et al. 2017). In other conditions, Pt and As will concentrate in the sulfide liquid, and sperrylite will crystallizes from it at a late

stage as pneumolitic mineral (Spiridonov 2010) or metacrystals (Genkin and Evstigneeva 1986).

The ferrous platinum with Fe/(Fe+Pt) in range of 0.26-0.37 crystallized also under reducing conditions (below FMQ buffer) according to (Roeder and Jamieson 1992). The source of reducing fluids may be a sedimentary rocks of the Siberian platform cover (Ryabov et al. 2014).

The concentrations of Ni in pentlandite and S in pyrrhotite increase with an increasing of sulfur fugacity (fS_2) in ore-forming system in the field of pentlandite stability (600 to 400°C) (Ehlers 1972; Vaughan and Craig 1978; Barton and Skinner 1967; Kolonin et al. 2000; Kosyakov et al. 2003). The Ni-poor pentlandite and S-poor pyrrhotite (paragenesis I) found in sulphide droplets in sperrylite, exclusively. The higher concentrations of Ni in pentlandite and S in pyrrhotite are characteristics of sulphide droplets in Pt-Fe alloys (paragenesis II). S-richer Po, Ni- richer Pn±pyrite, millerite (paragenesis III and IV) are typical for interstitial sulfide segregations.

Therefore, sperrylite of the studied association forming in reducing conditions is the first mineral among PGMs, which captured the droplets of the least fractionated sulphide liquid in comparison with the liquid, which has been captured by the later Pt-Fe alloys. The most fractionated sulphide liquid was captured by mertieite I, which indicates its crystallization at the later stages of the evolution of the ore-forming system.

1) The sulphide liquid was captured during progressive crystallization of the PGM: sperrylite crystallized at > 800°C and reducing conditions (fO_2 about FMQ-2); Pt-Fe alloys crystallized the next (fO_2 < FMQ up to FMQ) before the bulk of the sulfides.

2) The compositions of the captured sulphide liquid was evolved with increasing of sulfur fugacity: fS_2 in sulphide droplets in sperrylite is < -10.5, at Pt-Fe alloys ≈ - (9-10). Sulphides from the sulphide segregations in taxitic gabbro of the low-sulphide horizon have a more evolved compositions with respect to those trapped as the inclusions in sperrylite and Pt-Fe alloys.

Acknowledgements

The studies were carried out within the framework of the state assignment of the IGM SBRAS, project No 0330-2016-0003 financed by Ministry of Science and Higher Education of the Russian Federation.

References

1. Barton P.B., Skinner B.J. (1967) Sulfide stabilities. In Geochemistry of hydrothermal ore deposits (Ed. H.L. Barnes), New York: 278-403
2. Canali A.C., Brenan J.M., Sullivan, N.A. (2017) Solubility of Pt-As melt and sperrylite in synthetic basalt at 0.1 MPa and 1200oC with implications for arsenic sreciation and platinum sequestration in mafic igneous systems. Geochimica et Cocmochimica Asta 216: 153-168
3. Ehlers E.R. (1972) The interpretation of geological phase diagrams. San Francisco
4. Genkin A.D., Evstigneeva T.L. (1986) Associations of platinum-group minerals of the Noril'sk Copper-Nickel sulphide ores. Economic Geology 81:1203-1212
5. Kolonin G.R., Orsoev D.A., Sinyakova E.F., Kislov E.V. (2000) Using the ratio Ni:Fe in pentlandite to assess the volatility in the formation of sulphur-containing PGE sulphide mineralization of the Yoko-Dovyren massif. Doklady RAN 370(1): 87-91 (in Russian)
6. Kosyakov V.I., Sinyakova, E.F., Shestakov V.A. (2003) The dependence of fugacity of sulphur from the composition of phase associations of Fe-FeS-NiS-Ni at 873oK Geochemistry 7: 730-740 (in Russian)
7. Maier W., Rasmussen B., Fletcher I., Godel B., Barnes S.J., Fisher L., and Yang S. (2015) Petrogenesis of the ~2.77 Ga Monts de Cristal complex, Gabon: Evidence for direct precipitation of Pt-arsenides from basaltic magma Journal of Petrology 56: 1285-1308
8. Roeder P.L., Jamieson H.E. (1992) Composition of chromite and co-existing Pt–Fe alloy at magmatic temperatures. Austr. Journ. Earth Sciences 39: 419-426
9. Ryabov V.V., Shevko A.Ya., Gora M.P. (2014) Trap Magmatism and Ore Formation in the Siberian Noril'sk Region. Springer, Trap Petrology 1
10. Spiridonov E.M. (2010) Ore-magmatic systems of the Noril'sk ore field. Russian Geology and Geophysics. 51(9): 1059-1077
11. Vaughan D.J. and Craig J.R. (1978) Mineral chemistry of metal sulphides. Cambridge University Press. Cambridge London-New York-Melbourn

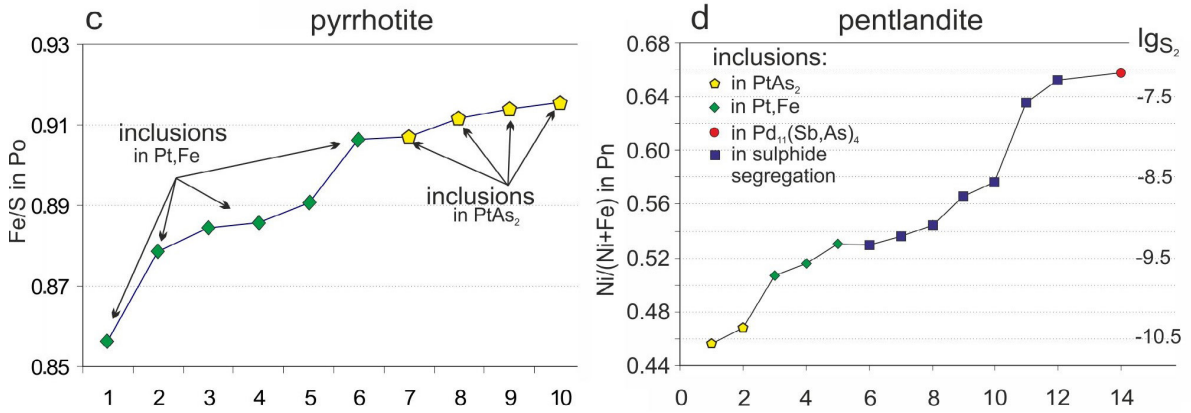


Figure 3. The ratios of Fe/S in pyrrhotite (a) and Ni/(Ni+Fe) in pentlandite (b) showing the change in sulfur fugacity (lgS_2) at 550°C in the studied sulphide parageneses on the base of dependence of lgS_2-T°C and Fe/Ni ratio in pentlandite (Barton and Skinner 1967; Vaughan and Craig 1981; Kolonin et al. 2000 and other).

PETRO-GEOCHEMICAL COMPARISON OF TRAPS FROM THE NORTHEASTERN TUNGUSKA SYNECLISE AND THE SOUTHWESTERN OLENEK UPLIFT

Tomshin M. D., Kopylova A. G., Vasilyeva A. E.

Diamond and Precious Metal Geology Institute, Siberian Branch, Russian Academy of Sciences

Keywords: *traps, basites, magmatism, Siberian platform*

The plume-induced magmatism that occurred beneath the Siberian platform in Mid-Paleozoic time caused its significant reworking. Separation of the craton into large geoblocks moving vertically relative to one another was accompanied by the formation of trap syneclises. The largest of them is the Tunguska syneclise. Trap exposures are also traced along the northeastern slope of the Anabar anteclise and in the Olenek uplift area. The extent of trap magmatism in the Tunguska syneclise and the Olenek uplift differs. In the Tunguska syneclise, the tectonomagmatic activity was accompanied by a supply of huge volumes of tholeiitic-basaltic magmas that formed a series of thick multilayered sills and lava flows. The Olenek syneclise that previously existed at the site of the Olenek uplift (Oleynikov and Shpunt, 1988) was supplied with much less magma that produced thin (up to 50 m) subsurface sills, thin basalt flows, and tuffs. The aim of this study is making comparison between the traps of the Tunguska syneclise and the Olenek uplift in an attempt to find evidence in support of the once existing independent Olenek trap syneclise of which the fragments are found now within the limits of the Olenek uplift.

In the northeastern margin of the Tunguska syneclise, a band of trap sills is localized in its zone of junction with the Anabar anteclise. The band extends southeastward from the upper Olenek R. to the Morkoka-Markharata R. valley over a distance of more than 400 km. On the basis of active contacts with the sedimentary rocks the traps are estimated to be Upper Permian in age. The papers published by the authors show that traps of the Tunguska syneclise were formed in three independent phases, each with a specific petrochemistry (Tomshin et al., 2001; Tomshin et al., 2005; Tomshin et al., 2014). Most of the intrusions in the region are composed of basites of the first petrochemical type (I), represented by monotonous poikilophitic dolerites. The identified petrochemical types of the traps differ in chemical and trace element compositions (Table, Fig.1). I-type dolerites are characterized by a moderate TiO_2 content (1.40-1.80%), $FeO_{tot.}$ up to 13%, and Mg#=48-47. The melts that produced intrusions of the second petrochemical type (II) bear evidence of a pre-chamber crystallization. The dolerites have a porphyritic habit due to the presence of glomeroporphyritic aggregates and individual porphyritic crystals of early plagioclase. They contain invariably early-formed magnesian olivine and low-Fe clinopyroxene. The texture of the rocks is mainly ophitic, which distinguishes them from the I-type dolerites. The content of major oxides in the II-type dolerites varies within a narrow range. They are low-titaniferous (0.8-1.25% TiO_2), often with high SiO_2, moderately ferruginous (8.9-11.3% $FeO_{tot.}$), and somewhat rich in MgO (Mg#=56 and 58). The III-type intrusions are less abundant. They are made of middle- and coarse-grained rock varieties. The dominant texture of the rocks is ophitic in combination with gabbro-ophitic one. Dolerites of these intrusions have a trachytoid habit. A characteristic feature of the III-type dolerites is invariable presence of both glassy and partly crystalline mesostasis (up to 10%). In terms of chemical and trace element composition, the III-type gabbro-dolerites differ radically from other rocks. They are high in Ti and Fe, low in Mg (Mg#=38), and have a minimum Al content. The petrochemical types of traps also differ in rare element composition. Maximum concentrations of LILE, REE, and Ti-group elements (V, Nb, Zr, Y) are established in the highly titaniferous III-type dolerites, and minimum values are recorded in the II-type dolerites. The amount of transient elements (Ni, Co, Cr) in the I-type dolerites is somewhat lower than in the II-type magmatites. Minimal values of these elements are found in the III-type gabbro-dolerites characterized by low Mg content. Direct geological observations revealed that the II-type intrusions cut the I-type intrusions and, in turn, are cut by those of the III-type. All data available support conclusions about independent intrusion of each of the recognized phases and a long formation of traps.

A band of trap sills of the Olenek uplift extends for more than 400 km from the upper Udzha R. in the west to the Upper Molodo R. in the east. Individual sills have a length of 100-120 km and a thickness varying from 15-50 to 110 m. From the relations with the sedimentary rocks it can be said with confidence that the intrusive bodies have Lower Triassic age. The subsurface location of the intrusions predetermined rapid crystallization of magma and development of breccias at the top of the sills. The intrusions are made of glass-bearing poikilophitic and taxitophytic dolerites and olivine-bearing gabbro-dolerites. Two mineral associations are clearly defined, which correspond to a pre-chamber and an intra-chamber stages in fractionation of basaltic melts. Petrographically, the traps of the Olenek uplift differ from those of the eastern Tunguska syneclise. They are close to the I-type dolerites in their dominantly poikilophitic texture and are identical to the III-type dolerites in the presence of glassy mesostasis. With regard to the major element composition, they are comparable to the II-type dolerites. A well-defined pre-chamber stage of melt crystallization in the dolerites of the Olenek uplift is characteristic only of the II-type traps of the Tunguska syneclise.

Major oxide and trace element composition of the traps of the Olenek uplift is transitional between the I- and II-type traps, approaching the values close to II-type dolerites, but differing from them in higher Ti, Fe, and Ti-group elements (V, Nb, Zr) contents. Their high Fe and Mg amounts promoted maximum concentrations of elements entering into the composition of Fe-Mg minerals such as Cr, Ni and Co. The REE distribution patterns for the traps of the Olenek uplift are steeper (La/Yb_n=2.4-2.8) as compared with the Tunguska syneclise traps. The total amount of REE (g/t) in them is within 58-63, which is higher than that of the II-type dolerites. A

well-defined Sr maximum promoted by the presence of the early-formed basic plagioclase is characteristic of the II-type magmatites and traps of the Olenek uplift (Figure). Contrastingly, the I-type traps display a Sr minimum.

In the Nb/Th-Zr/Nb and Nb/Y-Zr/Y diagrams, dolerites of the Olenek uplift form composition fields isolated from those of the Tunguska syneclise traps, thus showing their specific nature. The conducted comparative analysis of traps in the Olenek uplift and in the eastern Tunguska syneclise showed they differ sharply in age and in structural-mineralogical, petrochemical and geochemical parameters. This suggests two different sources for the traps of the Tunguska syneclise and the Olenek uplift. They resulted from independent plume-induced magmatic events. Thus there are no grounds to consider the traps of the Olenek uplift as parts of the Tunguska syneclise.

The study was carried out under the State Assignment project of DPMGI, SB RAS and was financially supported by grant 18-45-140043 p_ a from the Russian Foundation for Basic Research.

References

1. Oleinikov B.V. and Shpunt B.R. Genetic types and geodynamic settings of magmatism manifestation in the Siberian platform//Composition and processes of deep zones of continental lithosphere. Novosibirsk, 1988, pp.57-60 (in Russian).
2. Sun S., and McDonough W.F. Chemical and isotopic systematics of oceanic basalts: implications for mantle composition and processes // Geol. Soc.Amer. Spec. Publ. 1989. V.42. P. 313–345.
3. Tomshin M.D., Lelyukh M.I., Mishenin S.G., Soontsova S.P., Kopylova A.G., and Ubinin S.G. Schematic representation of trap magmatism on the eastern side of the Tunguska syneclise//Otechestvennaya Geologiya, 2001, no. 5, pp. 19-24 (in Russian).
4. Tomshin M.D, Kopylova A.G., and Tyan O.A. Petrochemical diversity of traps on eastern periphery of the Tunguska syneclise //Geology and geophysics 2005. V. 46. P. 72-82
5. Tomshin M.D., Kopylova A.G., Vasilyeva A.E., and Zaitsev A.I. Geochemical and isotope characteristics of intrusive traps in the eastern Siberian Platform // 14th GeoConferences on Science and Technologies in Geology, Exploration and Mining. Conference Proceedings. 2014. Albena, Bulgaria. STEF92 Technology Ltd., Volume I. P. 113-120.

Table. Chemical composition of traps , wt.%, g/t.

	Tunguska syneclise					Olenek uplift				
Type	I	II	III	I	II					
SiO_2	48,81	49,30	47,14	49,23	48,84	49,17	48,95	48,54	49,59	48,97
TiO_2	1,50	1,09	3,22	1,59	1,06	1,31	1,27	1,35	1,20	1,25
Al_2O_3	15,80	15,35	11,50	14,68	15,81	15,51	15,36	15,43	14,51	15,21
FeO_{tot}	12,22	11,03	16,50	12,54	10,95	11,62	11,59	11,75	11,97	11,62
MnO	0,19	0,20	0,28	0,20	0,17	0,20	0,21	0,19	0,12	0,26
MgO	6,95	7,85	5,74	6,23	8,41	7,28	7,54	6,65	7,41	7,45
CaO	10,50	11,38	10,55	10,83	11,06	11,12	11,39	11,49	10,77	11,99
Na_2O	2,33	1,90	2,33	2,16	1,91	2,15	2,19	2,16	2,27	2,15
K_2O	0,44	0,41	0,54	0,48	0,38	0,30	0,30	0,27	0,48	0,32
P_2O_5	0,23	0,13	0,24	0,16	0,10	0,13	0,13	0,14	0,25	0,15
Mg#	48	56	38	47	58	55	56	52	52	53
∑REE	67,05	53,6	102,3	85	64,5	60,1	59,0	61,2	62,6	61,0
(La/Yb)n	2,06	2,13	2,02	3,21	2,67	2,37	2,44	2,31	2,79	2,48
Eu/Eu*	1,01	0,96	0,96	0,82	0,87	0,95	0,94	0,90	0,95	0,94
Nb/Nb*	0,61	0,78	0,58	0,32	0,3	0,38	0,41	0,47	0,56	0,46

Note: Chemical composition of traps was determined by classical wet chemistry analysis (DPMGI, SB RAS) and trace elements were analyzed by ICP-MS (IMGRE).

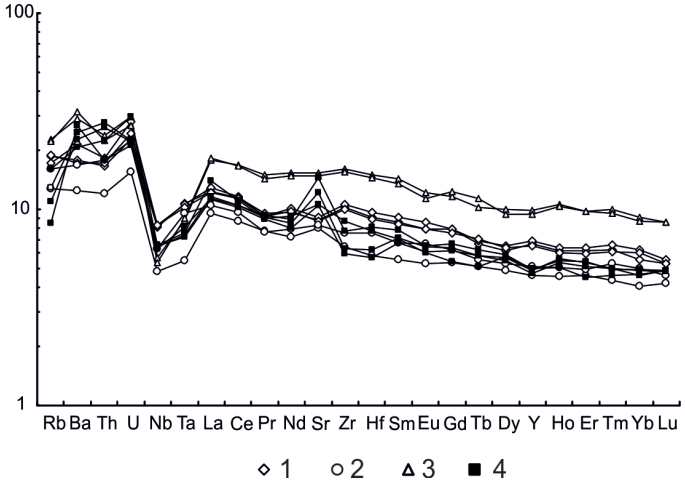


Figure. Distribution of incompatible elements in the primitive mantle-normalized traps (Sun and McDonough, 1989). 1-3 – traps of the Tunguska syneclise: 1 – I-type, 2 – II-type, 3 – III-type; 4 – traps of the Olenek uplift.

THERMOCHRONOLOGY OF THE ANGARA-VITIM GRANITOID BATHOLITH AS A PROXY INDICATOR OF PLUME EVENTS?

Travin A. V.[1,2,3], Vladimirov A. G.[1,2,3], Tsygankov A. A.[4,5], Khanchuk A. I.[6], Ernst R. E.[3,7], Murzintsev N. G.[2], Mikheev E. I.[1,2], Khubanov V. B.[4,5]

[1]*Novosibirsk State University, Novosibirsk, Russia*
[2]*V.S. Sobolev Institute of Geology and Mineralogy SB RUS, Novosibirsk, Russia*
[3]*Tomsk State University, Tomsk, Russia*
[4]*Geological Institute, SB RUS, Ulan-Ude, Russia*
[5]*Buryat State University, Ulan-Ude, Russia*
[6]*Far Eart Geological Institute FEB RAS, Vladivostok, Russia*
[7]*Department of Earth Science, Carleton University, Ottawa, Canada*

Keywords: *granitoid batholithes, thermochronology, $^{40}Ar/^{39}Ar$ dating, U/Pb dating*

Introduction

In comparison with others the Phanerozoic granitoids of the Angara-Vitim batholith (AVB) are characterized by the formation of huge volumes ($S \geq 150\ 000\ km^2$, $V \sim 10^6\ km^3$) of granite magma in a short period of time - 30 Ma (U/Pb, zircon) (Tsygankov et al. 2017). Magmatism in Transbaikalia has been explained by several models which invoke (i) suprasubduction magma generation (Donskaya et al. 2013; Jahn et al. 2009), (ii) slab detachment or crust delamination in the collision zone and asthenospheric diapirism (Khain et al. 1986), (iii) activity of an independent mantle superplume (a mantle hot field) (Yarmolyuk et al. 1997), water rich mantle plume at the final stage of Hercynian orogeny (Tsygankov et al. 2017).

Detailed field mapping, geochronology, thermochronology, and thermal modeling can be used to test competing hypotheses for batholith formation processes and the link with the geodynamic settings.

On the basis of the gravity data obtained (Turutanov, 2011), most of large plutons and some small bodies of AVB coalesce at depth into a single sheet, the area of which exceeds 100 000 km^2. Its average thickness is 5-7 km, reaching locally 10-30 km. The deep geometry of the AVB can be comparable with the giant plate is constructed with an uneven base and a flat eroded top.

We have carried out thermochronological reconstruction for samples of the Barguzin (S-type granites) and Chivyrkui (I/H-type granites) complexes of AVB using U/Pb and $^{40}Ar/^{39}Ar$ dating on primary magmatic minerals.

$^{40}Ar/^{39}Ar$ dates obtained by step heating (Travin, 2016), on the basis of a Plateau. U/Pb Dating on zircon obtained by LA-ICPMC (Tsygankov et al. 2017).

Results

The U/Pb zircon dates, which is an estimate of consolidation of granite melt, fall in a range of 320-290 Ma (Figure), with two prominent peaks at 318±1 Ma and 293±1 Ma. The thermal history of the AVB included three events at 245±1, 212±1, 156±1 Ma marked by clusters of U/Pb and $^{40}Ar/^{39}Ar$ Ages for samples from different parts of the batholith (Figure). They could be accompanied by a short-term, local increase in temperature and, then, rapid cooling. The explanation of these pulses may be related to the pulsating nature of the manifestation of intraplate mantle magmatism within the Siberian platform and its folded frame. Thus, pulses with the age of 245±1, 212±1 Ma are correlated, respectively, with the formation of the Khangai (255±10 Ma), Khentei (220±15) zonal magmatic areas with homonymous batholith nuclei (Kuzmin et al. 2010). Tectono-thermal activity could be transferred to the geological time scale almost instantly (several Ma) on the mechanism of the structural deformation of solid lithoplates. Probably, the impulse with the age of 245±1 Ma was a response to the formation of a large igneous province under the influence of the Siberian superplume, the maximum activity time of which is T=250±1 Ma (Al'mukhamedov et al. 2004, Reichow et al. 2009).

Such a long history of closure of isotope systems for samples corresponding to the modern erosion level imposes strict restrictions on the history of consolidation and cooling for granites corresponding to the deep (> 20 km) levels of the magmatic chamber. It was modelled using a mathematical algorithm describing the dynamics of heat and mass transfer in a magmatic chamber (Murzintsev et al. 2019) corresponding to the size of the AVB. The results of numerical calculations show (Figure) that after the formation of the magma chamber consolidation with the formation of the solid crust begins at the roof of the batholith. Gradually, the volume of the chamber is consolidated from top to bottom, and the lifetime of the residual melt at the deep levels of the chamber can reach 100 Ma or more.

After a period of relative calm in Central Asia 150-160 Ma ago there was a resumption of magmatic activity, expressed in the formation of the West Trans-Baikal, South-Khangai, East Mongolian rift zones (Kuzmin et al. 2010). Apparently, these events are associated with the activation of the processes of the collapse of the Hercynian orogen in Transbaikalia, recorded by isotopic systems of AVB granites, and dating Intrusive rocks associated with the metamorphic core complexes of Western Transbaikalia (Figure, Donskaya et al. 2016).

Thus, thermochronological approach to the study of the Angara-Vitim batholith allows us to record the responses of the isotopic systems of granitoids on the pulse of the manifestations of intraplate mantle magmatism within the Siberian platform and its folded framing in the age range from early Triassic to early Cretaceous, inclusive.

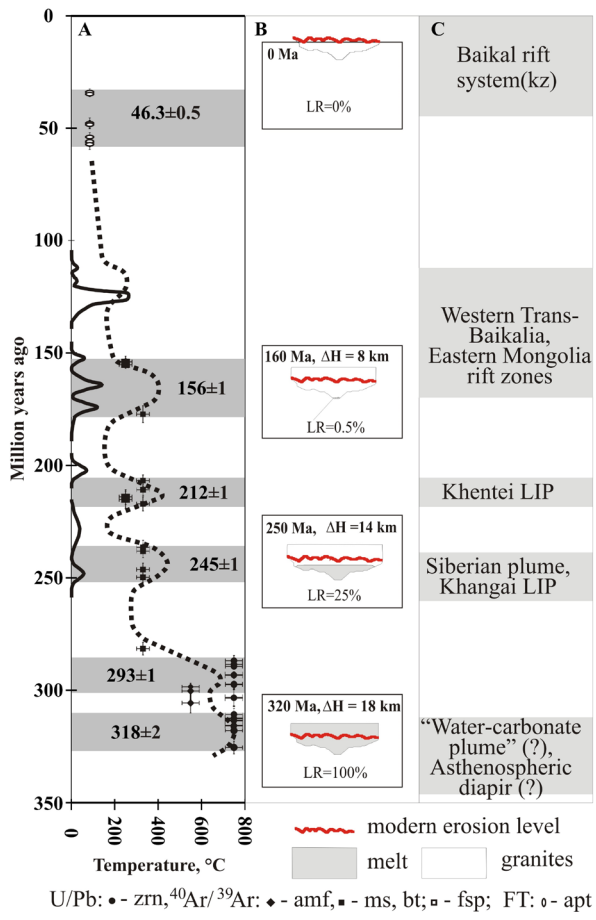


Figure. Termochronology of AVB.

A. History of closing of isotope systems of minerals of AVB granitoids. The solid line shows the probability density based on the dating of the dating of the metamorphic core complexes of Transbaikalia (Donskaya et al. 2016).

B. Results of numerical modelling of cooling and consolidation of granite magma chamber. LR(%) is the percentage of melt remaining in the magma chamber.

C. Main events of intraplate magmatism in the Siberian platform and surrounding areas (Kuzmin et al. 2010).

Conclusions

320-290 Ma ago in the section of the Earth's crust of Transbaikalia was the formation of molten granitic layer (the underlying granitoid batholith), and the existence and evolution of the melt continued for another 100 Ma.

Tectonic-thermal events with age 245 ± 1, 212 ± 1, 156 ± 1, 125 ± 2 Ma reflect the gradual transformation of the "semi-frozen granite layer" and the discrete nature of its tectonic exposure to the upper level of the earth's crust as part of the Trans-Baikal terrain under the influence of tangential elastic deformations caused by the pulsating manifestation of intra-plate mantle magmatism within the Siberian platform and its folded frame.

Acknowledgements

The study was carried out under support of the Ministry of Science and Education of the Russian Federation, project 5.1688.2017/PC (expedition work and 40Ar/39Ar isotope dating), projects 14.Y26.31.0012, 14.Y26.31.0018 (geodynamic analysis), and supported by the Russian Foundation for Basic Research № 17-05-00936 (thermochronological reconstructions and mathematical modeling), № 17-05-00275 (regional Geology, U/Pb dating).

References

1. Al'mukhamedov, A.I., Medvedev, A.Ya., Zolotukhin, V.V. (2004) Petrology. 12:297–311
2. Donskaya T.V., Gladkochub D.P., Mazukabzov A.M., et al. (2013) Journal of Asian Earth Sciences. 62:79-97
3. Donskaya, T.V., Gladkochub, D.P., Mazukabzov, A.M. et al. (2016) Russian Geology and Geophysics. 57:1591-1605
4. Jahn B.M., Litvinovsky B.A., Zanvilevich A.N., Reichow M.K. (2009) Lithos. 113:521–539
5. Khin, V.E., Tychkov, S.A. & Vladimirov, A.G. (1986) Geologiya i Geofizika (Russian Geology and Geophysics). 37:3–13
6. Murzintsev N.G., Annikova I.Yu., Travin A.V., Vladimirov A.G., Dyachkov B.A., Maslov V.I., Oitseva T.A., Gavryushkina O.A., (2019) Geodynamics & Tectonophysics 10(2)
7. Kuzmin M.I., Yarmolyuk V.V., Kravchinsky V.A. (2010) Earth-Science Reviews. 102:29-59
8. Reichow M. K., Pringle M. S., Al'Mukhamedov A. I., et al. (2009) Earth Planet. Sci. Lett. 277:9–20
9. Travin, A.V. (2016) Russian Geology and Geophysics. 57:434-450
10. Tsygankov, A.A., Burmakina, G.N., Khubanov, V.B., Buyantuev, M.D. (2017) Russian Petrology. 25(4):395-418
11. Turutanov, E.Kh. (2011) Dokl. Earth Sci. 440:1464–1466
12. Yarmolyuk, V.V., Budnikov, S.V., Kovalenko, V.I., Antipin, V.S., Goreglyad, A.V., Salnikova, E.B., Kotov, A.B., Kozakov, I.K., Kovach, V.P., Yakovleva, S.Z. & Berezhnaya, N.G. (1997) Petrology. 5:401-414

GIANT GRANITOID BATHOLITES OF CENTRAL AND NORTHEASTERN ASIA – A NEW TYPE OF SILICEOUS LARGE IGNEOUS PROVINCE (SLIP)?

Tsygankov A. A., Khubanov V. B., Burmakina G. N.

Geological Institute, SB RAS, Ulan-Ude, Russia

Introduction

Large igneous provinces, as a special type of magmatic formations, were identified in the early 1990s. Nearly three decades of intensive and diverse research have significantly expanded our understanding of this geological phenomenon. In particular, it has been recognized that the siliceous rock suites are not only a part of the majority of mafic LIPs, but can also be predominant and make up a siliceous type of large igneous provinces (SLIPs) (Bryan, 2007; Bryan & Ernst, 2008; Ernst, 2014).

According to modern concepts (Bryan & Ernst, 2008; Ernst, 2014), siliceous large igneous provinces are characterized by (1) Areal extents > 0.1 M km^2, which is the minimum areal extent for LIPs; extrusive volumes are > 0.25 M km^3. (2) Prevailing volume of dacites–rhyolites(> 80%), with transitional calc-alkaline I-type to A-type granites and presence of S-type granites; (3) Rhyolitic ignimbrite as a most typical volcanic lithology. (4) The overall duration of igneous activity is for up to 40 Ma, whereby most of magmas erupted during shorter intervals or pulses (3–10 Ma). The relatively long life span of some SLIPs is likely due to the presence of multiple magmatic pulses, both pre-rifting and syn-rifting. (5) In terms of geodynamic setting, SLIPs are exclusively continental and sited along paleo- and active continental margins as they are produced by a large-scale crustal anatexis, caused by thermal anomalies of non-subduction origin. Some examples were clearly emplaced into intraplate settings, far removed from active plate boundaries whereas others have been emplaced in closer proximity to a subducting plate margin, where igneous activity was extensive (up to 1000 km) inboard of the plate margin.

Only a few SLIPs that fully meet these requirements are known (Ernst, 2014). It is important to emphasize that volcanic and subvolcanic formations dominate in all large eruptive provinces, while the extent and role of plutonic suites, with some rare exceptions (e.g. Bushveld), is underestimated. The bulk of SLIPs is composed of rhyolite and rhyolite-dacite ignimbrites. However, it is well known that among the most common rocks on the Earth's surface granites and basalts dominate. Therefore, the largest accumulations of siliceous rocks, especially at the scale of LIPs, should be represented by a plutonic facies (granites), but not their volcanic counterparts.

In this context, giant granitoid batholiths of central and northeast Asia, such as the Angara-Vitimsky (Transbaikalia), the Khangai and the Hentiya-Daursky (Mongolia), the Kalba-Narymsky (NE Kazakhstan), the Tannuolsky (eastern Tuva) and the Ozernaya Zone (western Mongolia), the Kolyma batholithic belt (NE Asia) are of great interest. According to preliminary data, the volume of each batholith estimated from several hundred thousand to a million km^3 or more, and the formation time does not exceed the first tens of Ma.

The aim of this study is to demonstrate that the studied batholiths have SLIP provenance.

Results

The area of the Angara-Vitim Batholith (AVB) (Transbaikalia) covers more than 200,000 km^2, including the unroofed part (geophysical data); average thickness according to various estimates is 5–7 km (Turutanov, 2011), or 10–12 km (Litvinovsky et al., 1993). The volume of the AVB can range from 1.0 to 2.0 million km^3. The level of the erosion cut can vary from 1 to 3 km, but with such rough estimates it can be neglected. The Batholith is composed of granitoids of autochthonous (20%) (Litvinovsky et al., 1993) and allochthonous facies, among which calc-alkaline granites and granodiorites predominate. Subalkaline leucogranites, quartz syenites and quartz monzonites are subordinate. High-alkali granitoids, accompanied by syn-plutonic basic intrusions and mingling dykes, often contain the mafic microgranular enclaves (MME, Tsygankov et al., 2016; Burmakina et al., 2018). Gabbro-monzonite and gabbro-syenitic intrusions coeval with the granitoids are relatively uncommon. The total amount of mafic rocks in the AVB does not exceed 1 - 2%.

The existing geological and geochemical data are used to define 1) "crustal" granites within the AVB, which represent the melting products of the predominantly Neoproterozoic terrigeneous protoliths, and 2) "mantle-crustal" granites in which a proportion of the "mantle component" (magma mixing and / or melting of metabasic protoliths) can be as high as 30% (Tsygankov, 2014). The total period of the AVB formation is approximately 45 Ma (325 - 280 Ma). The intensity of magmatism during this time was different. According to the U-Pb dating of detrital zircon from recent sediments there are two peaks of igneous activity at 314 and 285 Ma, which represent the age of > 65% of the studied grains. It is important that these data correlate well with the results of U-Pb dating of in-situ zircon from the protolith (Tsygankov et al., 2017 and references in this work). This is in agreement with several cycles of magmatic activity.

The formation of the AVB began after the Late Hercene orogenesis, the nature of which is not fully understood. Moreover, the igneous formations that can be synchronous with this tectonic event so far remain unknown in Transbaikalia. The mantle plume (Yarmolyuk et al., 2014), "superimposed" over young, relatively hot and plastic crust may have triggered the wholesale melting, metamorphism and granite formation (Tsygankov et al., 2017). Thus, the Angara-Vitim batholith meets almost all criteria for belonging to SLIPs, except for presence of volcanic suites. However, the latter can be assumed to be initially present but completely destroyed by erosion, although this assumption cannot be confidently supported.

The Khangai and Khentey-Daur granitoid batholiths of Mongolia have very similar occurence. These batoliths are dominated by granodiorite-granite-leucogranite series, accompanied by synplutonic mafic intrusions and alkaline A-type granites. The

area of the batholiths is 100 and 150 thousand km^2, respectively, and the volume is estimated at 0.65 - 1.5 million km^3. Their formation time is estimated as ~ 30 Ma (273 - 238 and 229 - 195) (Yarmolyuk et al., 2019). Batoliths formation, including the AVB, was completed with rifting of different degrees. Alkaline granitoids A-type magmatism was controlled by rifting.

The formation of giant batholiths of the eastern part of the Central Asian fold belt is considered to result from the mantle plume impact on the lithosphere of a young folded region formed in the marginal zone of the Siberian paleocontinent in a series of accretion-collision events, before granite formation (Yarmolyuk et al., 2019). Probably, these batholiths should be considered as one large siliceous igneous province, with a pulsatory development of more than 120 Ma.

The classification of other large batholiths and granitoid belts as intrinsic members of SLIP is a subject of discussions. The main support is provided by large areal extent of the granite rocks and, probably, their significant volumes (no data) with a duration of magmatism from ≈ 20 Ma (Kolyma batholith belt), up to 30 - 40 Ma (Kalba-Narym batholith). At the same time the geodynamic conditions for the formation of these batholiths are not completely clear.

Conclusions

Therefore, the Late Paleozoic and Early Mesozoic giant granitoid batholiths of Transbaikalia and Mongolia (Angara-Vitimsky, Khangaysky, Khentey-Daursky) meet almost all the criteria for belonging to the siliceous large igneous provinces, but the lack of associated volcanic rocks is an obvious mismatch. In this regard, it may be necessary to introduce a subtype of SLIPs (Sheth, 2007) or extend the existing criteria. The question whether large batholiths of East Kazakhstan, Tuva and Kolyma correspond to the category of SLIPs requires additional study.

Acknowledgements

The work was supported by the Basic Research Program of Geological Institute SB RAS (project IX.129.1.2., registration number AAAA-A16-116122110027-2); the Complex Program of Basic Scientific Research of the SB RAS (project II.1.39); Russian Foundation for Basic Research (grants № 17-05-00275).

References

1. Bryan S.E. (2007) Silicic Large Igneous Provinces. Episodes 30: 20-31.
2. Bryan S.E., Ernst R.E. (2008) Revised definition of Large Igneous Provinces (LIPs). Earth-Science Reviews 86: 175-202.
3. Burmakina, G.N. and Tsygankov, A.A., Khubanov V.B., 2018. Petrogenesis of composite dikes in granitoids of western Transbaikalia. Russian Geology and Geophysics 59: 23-48.
4. Ernst R.E. (2014) Large Igneous Provinces. 8 - Silicic LIPs. Cambridge University Press pp 214-244.
5. Litvinovsky B.A., Zanvilevich A.N., Alakshin A.M., Podladchikov Yu.Yu. (1993) The Angara-Vitim Batholith, the Largest Granitoid Pluton. Izdatelstvo OIGGM SO RAN, Novosibirsk, 143 p. (in Russian).
6. Sheth H.C. (2007) Large Igneous Provinces (LIPs): Definition, recommended terminology, and a hierarchical classification . Earth-Science Reviews 85: 117-124.
7. Tsygankov A.A. (2014) Late Paleozoic granitoids in western Transbaikalia: sequence of formation, sources of magmas, and geodynamics. Russian Geology and Geophysics 55: 153-176.
8. Tsygankov A.A., Burmakina G.N., Khubanov V.B., Buyantuev M.D. (2017) Geodynamics of Late Paleozoic Batholith-Forming Processes in Western Transbaikalia. Petrology 25: 396-418.
9. Tsygankov, A.A., Khubanov, V.B., Travin, A.V. et al., (2016) Late Paleozoic gabbroids of Western Transbaikalia: U–Pb and Ar–Ar isotopic ages, composition, and petrogenesis. Russian Geology and Geophysics 57: 1005–1027.
10. Turutanov E.Kh. (2011) The Angara-Vitim batholith: Data on morphology and sizes based on gravimetric data. Dokl. Earth Sc. 440: 1464–1466.
11. Yarmolyuk V.V., Kozlovsky A.M., Travin A.V. et al., (2019) Duration and geodynamic nature of Giant Central Asian Batholiths: geological and geochronological stadies of the Khangai batholith. Stratigraphy and Geological Correlation 27: 79-102.
12. Yarmolyuk V.V., Kuzmin M.I., Ernst R.E. (2014) Intraplate geodynamics and magmatism in the evolution of the Central Asian Orogenic Belt. Journal of Asian Earth Sciences 93: 158-179.

MESOARCHEAN BIMODAL VOLCANICS OF SOUTHWESTERN SIBERIAN CRATON, ARE THEY RELATED TO MANTLE PLUME ACTIVITY?

Turkina O. M.

V.S. Sobolev Institute of Geology and Mineralogy SB RAS, Novosibirsk, Russia

Keywords: *Mesoarchean, extension/rifting volcanism, geochemistry, Hf-in-Zr isotope composition*

Introduction

Many geological and geochemical changes are recorded on Earth between 3 and 2 Ga that allows to consider this time span as a transitional period (Condie, 2018). Progressive cooling of the Earth and associated changes in the mantle temperature and rheology probably led to the formation of a stable rheologically rigid continental lithosphere. Synthesis of available data on mantle peridotites, as well as inclusions of sulphides and alloys, reveals a sharp increase in the number of model Re-Os ages (T_{RD}) from 3 Ga and a distinct peak in the range of 2.5-2.9 Ga (Griffin et al., 2014), which indicates the formation of a stable subcontinental lithosphere separated from convective mantle in the Meso-Neoarchean. At the upper crust level indicators of the formation of rheologically

rigid lithospheric plates are the processes of stretching and rifting, which are marked by the emplacement of mafic dike swarms and sills and the formation of intra-plate volcanic associations including bimodal, basalt-rhyolite ones. The oldest manifestations of such processes occurred in the earliest Mesoarchean. To highlight the Mesoarchean evolution of the southwestern Siberian craton and clarify the tectonic setting of greenstone volcanism, this work focuses on the bulk rock composition, the U-Pb age and Lu-Hf isotope composition of zircon, and the genesis of the felsic metavolcanic rocks of the Onot greenstone belt (GB).

Results

The Sharyzhalgay uplift in the southwestern margin of the Siberian craton consists of four tectonic units, namely the Bulun and Onot granite-greenstone terranes in the northwest and the Kitoy and Irkut granulite-gneiss terranes in the southeast. The Onot granite-greenstone terrane, with a length of more than 80 km, is composed of a package of tectonic sheets, composed of rocks of metasedimentary-volcanogenic sequence and Paleoarchean (3.4 Ga) basement of the tonalite-trondhjemite-granodiorite (TTG) complex, which are thrusted to southwest onto the high-grade rocks of the Kitoy terrane. The greenstone sequence consists of lower bimodal metavolcanic unit and overlapping metavolcanic-sedimentary units. The lower unit consists of fine-grained biotite-amphibole and rare biotite microgneisses, as well as boudin-like bodies and rare thin layers of amphibolites. Zircons of microgneiss yielded a concordant U-Pb age of 2886±8 Ma. Microgneisses were metamorphosed at 660-690°C and about 6 kbar in the Late Paleoproterozoic, ca. 1.88 Ga and intruded by post-tectonic granites at 1.86 Ga.

The Onot microgneisses are high ferroan metarhyolites, enriched in REE and HFSE, and compositionally similar to A-type granitoids. The multi-element spectra of high- and low-Ti metabasalts (amphibolites) show weak LILE enrichment and a weak to distinct Nb minimum, which are signatures of both subduction-related and continental flood basalts contaminated by crustal material. Metabasalts in the lower and upper units of the Onot GB define an oblique trend from the mantle array in Th/Yb versus Nb/Yb diagram of Pearce (2008) indicating crustal contamination (Fig. 1). Metarhyolites are similar to melts from tonalite and granodiorite sources in its high Fe-index (Patiño Douce, 1997; Bogaerts et al., 2006), but differs markedly in higher contents of FeO, MgO and TiO_2 that indicate melting of a heterogeneous source, probably composed by quartz-feldspathic and mafic rocks. Whole-rock ε_{Nd} values of metarhyolites are negative (from -3.8 to -0.8), and zircons from felsic rocks show a wide range of slightly positive to mostly negative ε_{Hf} values (from +1.1 to -8.5) partially overlapping with the isotopic evolution area of Paleoarchean TTG crust of the Onot terrane with shift to higher ε_{Hf} values (Fig. 1). Thus, the isotope data is consistent with melting of a heterogeneous crust of the Paleoarchean TTG basement and a more juvenile mafic source. The contribution of a mafic source is responsible for FeO, MgO and TiO_2 enrichment of metarhyolites and variable to high concentrations of Cr and Ni. Experimental data (Bogaerts et al., 2006) allow us to infer that crust melted at shallow depth, near 2-4 kbar and high (> 900°C) temperature, which agree with the zirconium saturation temperatures of metarhyolites reaching 890°C. The geochemical signatures of the Onot metarhyolite (high Fe-index, low $(La/Yb)_n$ of 2.8-9.6; Zr/Y of 5.7-12.4, high concentrations of HFSE) correspond to types FIIIa and FIIIb felsic volcanics of Archean greenstone belts. These felsic volcanics may result from melting of mafic to sialic sources at low pressures in extensional or rifting settings (Hart et al., 2004). Taken together, the geochemical and isotope characteristics of the Onot felsic and associated mafic volcanic rocks indicate that the greenstone belt is a Mesoarchean continental rift formed on a Paleoarchean basement. The coeval formation of high- and low-Ti basalts and the generation of felsic melts at low P and high T were probably associated with decompression mantle upwelling in a setting of continental extension and lithospheric thinning.

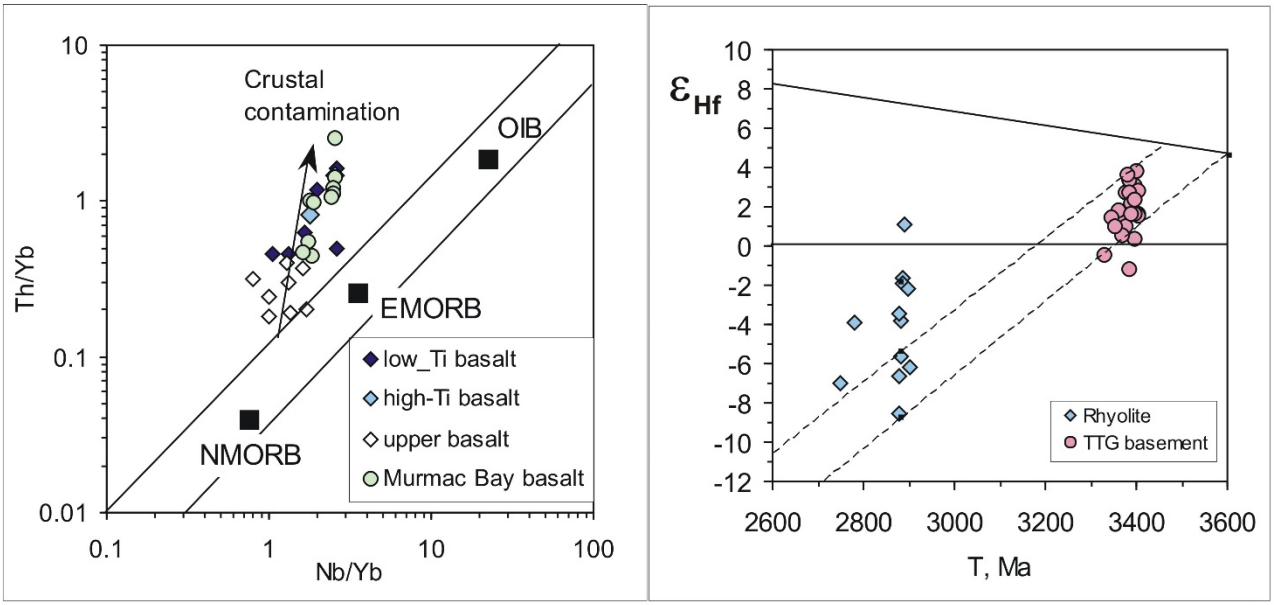


Figure 1. Diagrams of Nb/Yb vs. Th/Yb and T (Ma) - ε_{Hf} for the Onot GB rocks. Rift basalts of Murmac Bay Group, Rae Province, Canada are after (Hartlaub et al., 2004).

The emplacement of mafic dike swarms and sills and intraplate/rift magmatic associations serve as indicators of the formation of rheologically rigid lithospheric plates. The earliest traces of such processes in the Kaapvaal and Pilbara Cratons relate to the earliest Mesoarchean (3.2 Ga) (Saumitra et al., 2010; Van Kranendok et al., 2010). There is numerous evidence of Mesoarchean and early Neoarchean extension/rifting events: ca. 2.97–2.98 Ga dike swarms and coeval volcanics in the Kaapvaal craton (Olson et al., 2010); a bimodal association of flood basalts and felsic tuffs (ca. 2.77-2.72 Ga) in the eastern Pilbara Craton (Blake et al., 2004); rift tholeiitic basalts (2.77-2.63 Ga) in Rae Province (Canadian shield) (Hartlaub et al., 2004) and many other. The Meso-Neoarchean intraplate/rifting events were coeval with the formation of the subcontinental lithospheric mantle.

Conclusions

The Onot terrane is composed of a package of tectonic sheets composed of a greenstone metasedimentary-volcanic sequence and a TTG complex. Bimodal felsic and mafic volcanic rocks of the Onot greenstone belt formed through rifting of the Paleoarchean continental crust. Evidence of the Meso-Neoarchean extension/rifting events, such as mafic dike swarms and intra-plate volcanic associations including bimodal, basalt-rhyolite ones, indicate the formation of rheologically rigid continental plates. Since Meso-Neoarchean time the intraplate magmatic series probably became similar in geochemical characteristics and formation conditions to modern mantle plume-related associations.

Acknowledgements

This work was conducted as a government task of IGM SB RAS.

References

1. Blake, T.S., Buick, R., Brown, S.J.A., Barley, M.E. (2004) Geochronology of a Late Archaean flood basalt province in the Pilbara Craton, Australia: constraints on basin evolution, volcanic and sedimentary accumulation, and continental drift rates // Precambrian Research 133: 143-173.
2. Bogaerts M., Scaillet, B., Vander Auwera, J. (2006) Phase equilibria of the Lyngdal granodiorite (Norway): implications for origin of metaluminous ferroan granotoids. J. Petrology 47: 2405-2431.
3. Condie, K.C. (2018) A planet in transition: the onset of plate tectonics on Earth between 3 and 2 Ga? Geoscience Frontiers 9: 51-60.
4. Griffin W.L., Belousova E.A., O'Neil C., O'Reilly Y., Malkovets V., Pearson N.J., Spetsius S., Wilde S.A. (2014). The world turns over: Hadean-Archean crust-mantle evolution. Lithos 189: 2-15.
5. Hart, T.R., Gibson, H.L., and Lesher, C.M. (2004) Trace element geochemistry and petrogenesis of felsic volcanic rocks associated with volcanogenic massive Cu–Zn–Pb sulfide deposits. Economic Geology 99: 1003–1013.
6. Hartlaub R.P, Heaman L.M, Ashton K.E, Chacko T. (2004) The Archean Murmac Bay Group: evidence for a giant Archean rift in the Rae Province, Canada. Precambrian Research 131: 345-372.
7. Olsson J.R., Söderlund U., Klausen M.B., Ernst R.E. (2010) U–Pb baddeleyite ages linking major Archean dyke swarms to volcanic-rift forming events in the Kaapvaal craton (South Africa), and a precise age for the Bushveld Complex. Precambrian Research 183: 490–500.
8. Pearce, J.A. (2008) Geochemical fingerprinting of oceanic basalts with implications for the classification of ophiolites and search for Archean oceanic crust. Lithos 100: 14-48.
9. Saumitra M., Reinhardt J., Wilson A. H. (2017) Petrochemical evolution of the White Mfolozi Granite pluton: Evidence for a late Palaeoarchaean A-type granite from the SE Kaapvaal Craton, South Africa. Lithos, 286: 480-501.
10. Van Kranendonk M.J., Smithies R.H., Hickman A.H., Wingate M.T.D., Bodorkos S. (2010) Evidence for Mesoarchean (3.2 Ga) rifting of the Pilbara Craton: the missing link in an early Precambrian Wilson cycle. Precambrian Research 177: 145-161.

GEOCHEMISTRY OF BASALTS OF THE MOKULAEVSKY FORMATION (SIBERIAN TRAP): MANTLE SOURCES AND MAGMA EVOLUTION IN INTERMEDIATE MAGMA CHAMBER

Turkina O. M., Kalugin V. M., Shevko A. Y., Gora M. P.

V.S. Sobolev Institute of Geology and Mineralogy SB RAS, Novosibirsk, Russia

Keywords: *Mokulaevsky Formation, Siberian plume, subcontinental lithosphere, asthenosphere*

Introduction

Flood basalt sequence of the Siberian traps of the Norilsk region is subdivided into two series (Lightfoot et al., 1994). The Lower Series (from Ivakinsky to Gudchikhinsky Formation) show significant variations in Mg# and consists of high-Ti basalts and picrites relatively enriched in incompatible elements. On the contrary, the Upper Series (from the Tuklonsky to the Samoedsky Formation) is an exceptionally low-titanium basalts, rarely picrites with wide range of trace element composition. Variable concentrations of incompatible elements and isotopic features in Upper Series rocks were suggest to result from crustal contamination (Lightfoot et al., 1994). Upper Series basalts of the Mokulaevsky Formation show mostly uniform major and trace element composition that implies the negligible influence of crustal contamination. Consequently, these rocks suitable to estimate their mantle sources and analyze an impact of fractionation on the volcanic composition. In this work, we focused on detailed study

of the geochemistry and isotopic composition of the basalts of the Mokulaevsky Formation to highlight the contribution of the mantle plume, asthenospheric and lithospheric mantle to their genesis and clarify evolution of parental magmas in intermediate chambers.

Results

The Mokulaevsky Formation is divided into lower and upper sub-suite (T_1mk_1 и T_1mk_2). Each sub-suit has the two units: $T_1mk_1^1$, $T_1mk_1^2$, and $T_1mk_2^1$, $T_1mk_2^2$ respectively. The three lower units are composed of plagioporphiric basalts. The second unit is enriched in plagioclase phenocrysts. The fourth unit consists of aphyric and poikilophitic basalts without porphyritic phenocrysts. Major and trace element composition was determined for each lava flow. All rocks are subalkalic low-Mg (MgO ≤8%, Mg# = 0.49–0.56) and low-Ti (TiO_2 ≤1.45 wt%) basalts and are similar to the volcanic rocks of the underlying Morongovsky Formation (Mg# = 54-56, TiO_2 = 1.1-1.17 wt%). All basalts have slightly varying La/Sm (2.1-2.8) and Gd/Yb (1.4-1.8) ratios corresponding to the values for low-Ti basalts of the Upper Series (La/Sm <3, Gd/Yb <2) (Lightfoot et al., 1993). The basalts show uniform weakly fractionated REE patterns with LREE enrichment, which are similar to REE spectra of the Morongovsky basalts. Multi-element spectra of basalts demonstrate an enrichment of Ba and Th, distinct Nb minimum and weak positive anomalies of Sr and Zr. Despite the narrow range of major and trace elements, there are distinct trends of their concentrations up the section (Fig. 1). The contents of TiO_2 and Fe_2O_3 are inverse correlated with Mg# value. Concentrations of TiO_2 and Fe_2O_3 slightly increase from $T_1mk_1^1$ to $T_1mk_1^2$ unit. Subsequent significant growth of TiO_2 and Fe_2O_3 through $T_1mk_2^1$ is changing by a sharp decrease in the top of $T_1mk_2^1$, or at the bottom of the $T_1mk_2^2$, unit.

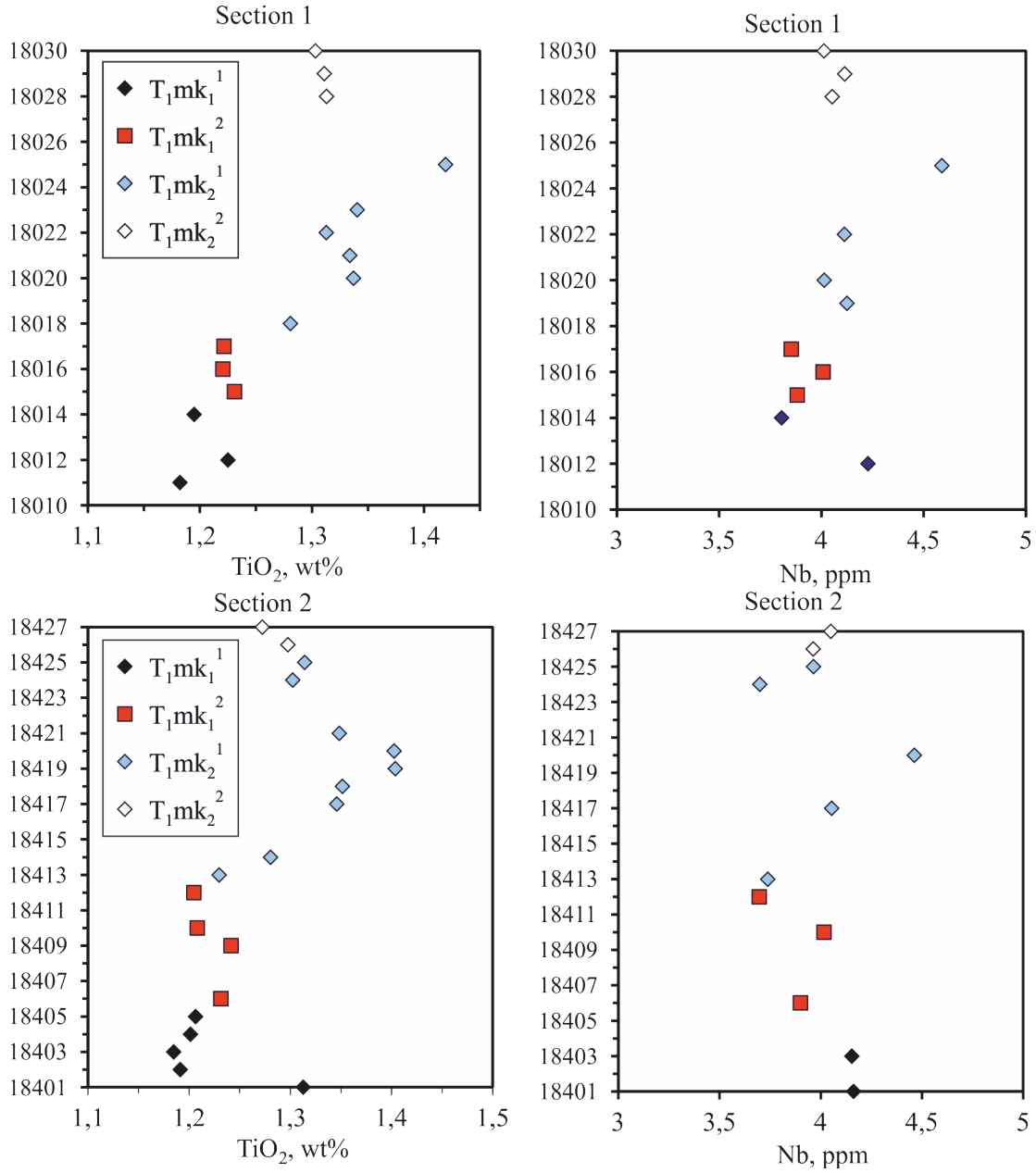


Fig. 1. Variations of TiO_2 and Nb concentrations in the vertical sections of the Mokulaevsky basalt sequence.

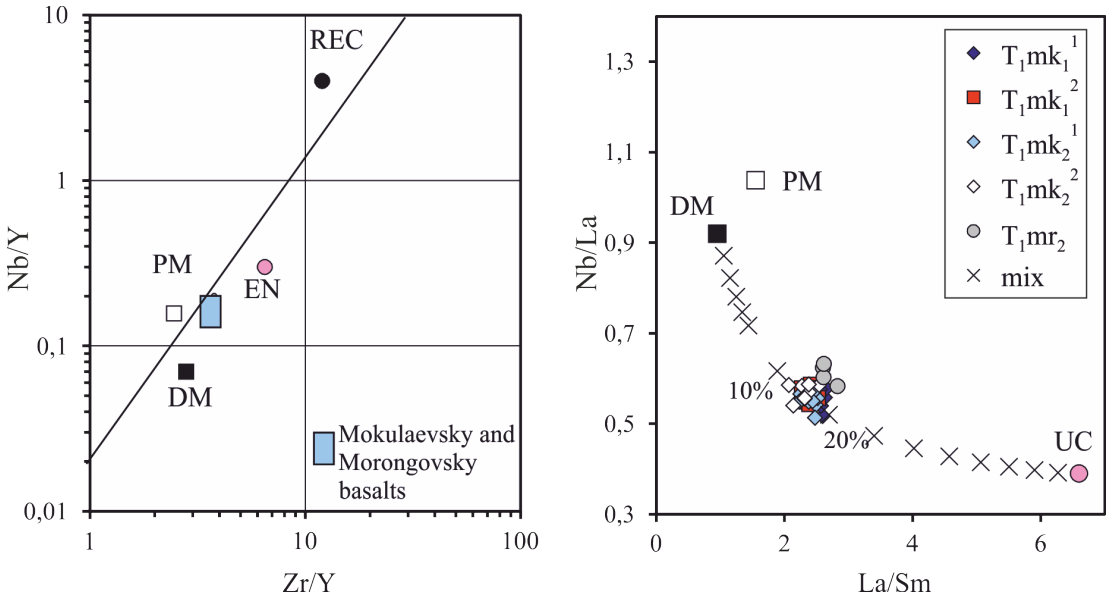


Fig.2. Diagrams of Nb/Y vs Zr/Y and Nb/La vs La/Sm for the Mokulaevsky basalt.

PM – primitive mantle, DM – depleted mantle, EN – enriched mantle component, REC – recycled slab component, UC – upper crust. Number on mixing line (mix) are percentage of component.

These variations, along with a change in Mg# value, indicate the differentiation of magma in the intermediate chamber and the periodic replenishment of the new magma portion. Synchronously with TiO_2 concentrations of Nb, Zr, LREE and Th slightly increase from $T_1mk_1^1$ to $T_1mk_1^2$ unit, and their significant growth through $T_1mk_2^1$ is changing by a sharp fall in the top of $T_1mk_2^1$ or at the bottom of the $T_1mk_2^2$ unit. Thus, the fractionation of the parent melt in the intermediate chamber led to an increase in REE, Zr, Nb, Y, Th, and TiO_2, and the replenishment with new portions of the parent magma led to decrease in their concentrations.

All basalts of the Mokulaevsky Formation have a narrow range of Nd and Sr isotopic composition (e_{Nd} of +0.6 to -0.7; e_{Sr} of +12 to +18) similar to the isotope composition of other basalts of the Upper Series with the exception of the Nadezhinsky Formation. The uniform Nd-Sr isotopic composition of these basalts as well as narrow range of trace element content suggests a uniform magma source and the negligible influence of crustal contamination. In geochemical features, primarily a clear Nb minimum in multi-element spectra the studied basalts are similar to low-Ti continental flood basalts (CFB) and distinct from the oceanic island basalts. CFB genesis is argued to involve four sources: 1. deep mantle plume, 2. asthenospheric mantle, 3. subcontinental lithospheric mantle, 4. continental crust (Hawkesworth et al., 1995, Lightfoot et al., 1993; 1994; Farmer, 2003). In the diagram of Nb/Yb vs Th/Yb, studied basalts plot in a triangle between points of PM, DM and EN indicating contribution primitive, enriched subcontinental lithospheric (enriched) and asthenospheric (depleted) mantle. The composition of the basalts in the diagram of La/Sm vs Nb/La corresponds to the mixing line between the enriched component and the depleted rather than primitive mantle suggesting involvement only two main sources, i.e. depleted asthenosphere mantle and enriched subcontinental lithospheric mantle contaminated by crustal-derived subducted sediments. Although melting of the lithosphere may have been triggered by conductive heating from the Siberian mantle plume as suggested by Lightfood and co-authors (1994), but geochemical contribution of the mantle plume was probably negligible.

Conclusions

All basalts of the Mokulaevsky Formation have uniform major and trace element, and isotope composition similar to low-Ti continental flood basalts. The intermediate chamber for basalts was an open system, replenish by new portions of the parental magma result in depletion of TiO_2, REE, Zr, Nb, Y and Th. According geochemical features, these basalts have been derived from mainly two sources, namely depleted asthenospheric mantle and subcontinental lithospheric mantle enriched by subducted sediments. A geochemical fingerprint of the deep mantle plume was probably negligible.

Acknowledgements

The study was conducted with the support of Norilskgeology LLC and in the framework of the government assignment of the IGM SB RAS.

References

1. Farmer G.L. (2003) Continental Basaltic Rocks. In Treasure of geochemistry (Eds. Turekian K.K., Holland H.D.). Oxsford: Elsevier Ltd. Vol. 3: 85-121.
2. Hawkesworth C.J., Lightfoot P.C., Fedorenko V.A., Blake D., Naldrett A.J., Doherty W., Gorbachev N.S. (1995) Magma differentiation and mineralization in the Siberian continental flood basalts. Lithos 34: 61-88.
3. Lightfoot P.C., Naldrett A.J., Gorbachev N.S., Fedorenko V.A., Hawkesworth C.J., Hergt J., Doherty W. (1994) Chemostratigraphy of Siberian trap lavas, Noril'sk District: implications for the sources of flood basalt magmas and their associated Ni-Cu mineralization. In Proceedings of the Sudbury – Noril'sk Symposium. Special Volume 5: 283-312.

NEW 1.86 GA EASTERN MURMAN SILL PROVINCE, THE KOLA PENINSULA: PALEOMAGNETISM, GEOCHRONOLOGY AND PETROLOGY

Veselovskiy R. V.[1,2], Samsonov A. V.[3], Stepanova A. V.[4], Salnikova E. B.[5], Larionova Y. O.[3], Travin A. V.[6], Arzamastsev A. A.[5,7], Egorova S. V.[4], Erofeeva K. G.[3], Stifeeva M. V.[5], Shcherbakova V. V.[8], Shcherbakov V. P.[8,9], Zhidkov G. V.[8], Zakharov V. S.[1,10]

[1]*Lomonosov Moscow State University, Geological Dept., Moscow, Russia*
[2]*Schmidt Institute of Physics of the Earth RAS, Moscow, Russia*
[3]*Institute of Geology of Ore Deposits, Petrography, Mineralogy, and Geochemistry RAS, Moscow, Russia*
[4]*Institute of Geology, Karelian Research Centre RAS, Petrozavodsk, Russia*
[5]*Institute of Precambrian Geology and Geochronology RAS, Saint Petersburg, Russia*
[6]*Sobolev Institute of Geology and Mineralogy Siberian Branch Russian Academy of Sciences, Novosibirsk, Russia*
[7]*Institute of Earth Sciences, Saint Petersburg State University, Saint Petersburg, Russia*
[8]*Geophysical Observatory "Borok" IPE RAS, Russia*
[9]*Institute of Geology and Petroleum Technologies, Kazan Federal University, Kazan, Russia*
[10]*Dubna University, Dubna, Moscow region, Russia*

Keywords: *Paleoproterozoic LIP, mafic sills, the Kola Peninsula, paleomagnetism, geochronology.*

The validity and reliability of paleocontinental reconstructions depend on using multiple methods, but among these approaches the paleomagnetic method is particularly important. However, the potential of paleomagnetism for the Early Precambrian rocks is often dramatically restricted, primarily due to the partial or complete loss of the primary magnetic record during the rocks' life, as well as because of difficulties with dating the characteristic magnetization. We present the first 1.86 Ga paleomagnetic key pole of Fennoscandia obtained for the dolerite sills of the Murmansk craton – Eastern Murman Sill Province (Veselovskiy et al., 2019; Stepanova et al., 2020), that outcrop in the northern part of the Kola Peninsula along the Barents Sea coast for a distance of 200 km (Slat = 68.5°; Slong = 37.9°; N = 16 sites; Plat = 54.7°; Plong = 234.7°; dp/dm = 4.3°/6.3°). The age of the sills and their characteristic remanent magnetization (ChRM) was determined by four independent geochronometers: U-Pb – 1860 ± 4 and 1863 ± 7 Ma (ID-TIMS, baddeleyite), Sm-Nd – 1889 ± 57 Ma, Rb-Sr ~ 1850 Ma, Ar/Ar – 1865 ± 8 and 1857 ± 20 Ma (biotite). The primary nature of the ChRM is confirmed by the results of petrographic, geochemical, paleo- and rock magnetic studies, as well as by thermochronological data. The similarity of the petrographic and geochemical characteristics of sills from different localities indicates that these dolerite sills were formed during a single magmatic event and their cooling down to 580°C occurred at depths of about 10±2 km and lasted ~2800 years or even faster. Paleogeographic reconstruction of Fennoscandia on the basis of the obtained paleomagnetic pole is in general agreement with the previously suggested configuration of core of the Nuna/Columbia supercontinent (Evans and Mitchell, 2011; Meert and Santosh, 2017). A new reliable Thellier-Coe paleointensity determination for this time reveals a rather low mean VDM = 1.8 (± 0.1) × 10^{22} Am^2 that supports the Proterozoic dipole low hypothesis (Biggin et al., 2009).

Acknowledgements

This work was supported by Russian Science Foundation, grant #16-17-10260. Paleointensity studies were supported by the Ministry of Education and Science (grant MD-1116.2018.5) and by the state assignment of GO "Borok" IPE RAS; rock magnetic measurements were supported by the Russian Foundation for Basic Research (grant 17-05-01121). Computer modelling was carried out using the equipment of the shared research facilities of HPC computing resources at Lomonosov Moscow State University.

References

1. Biggin, A.J., Strik, G.H.M.A., Langereis, C.G., 2009. The intensity of the geomagnetic field in the late-Archaean: New measurements and an analysis of the updated IAGA palaeointensity database. Earth, Planets Sp. https://doi.org/10.1186/BF03352881
2. Evans, D.A.D., Mitchell, R.N., 2011. Assembly and breakup of the core of Paleoproterozoic-Mesoproterozoic supercontinent Nuna. Geology 39, 443–446. https://doi.org/10.1130/G31654.1
3. Meert, J.G., Santosh, M., 2017. The Columbia supercontinent revisited. Gondwana Res. https://doi.org/10.1016/j.gr.2017.04.011
4. Stepanova A.V., Samsonov A.V., Larionova Yu.O., Egorova S.V., Arzamastsev A.A., Salnikova E.B., Veselovskiy R.V., Erofeeva K.G., Stifeeva M.V. 1860 Ma I-type mafic sills in the Murmansk Craton, Eastern Fennoscandia: petrology and implications for tectonic setting of intraplate mafic melts during Nuna assembly // Petrology, 2020, N 2 (in press).
5. Veselovskiy Roman, Alexander Samsonov, Alexandra Stepanova, Ekaterina Salnikova, Yulia Larionova, Alexey Travin, Andrey Arzamastsev, Svetlana Egorova, Kseniya Erofeeva, Maria Stifeeva, Valentina Shcherbakova, Valeriy Shcherbakov, Grigoriy Zhidkov, Vladimir Zakharov. 1.86 Ga Key Paleomagnetic Pole from the Murmansk craton intrusions – Eastern Murman Sill Province, NE Fennoscandia: multidisciplinary approach and paleotectonic applications // Precambrian Research. 2019. 324. P. 126-145. DOI: https://doi.org/10.1016/j.precamres.2019.01.017

THERMOCHRONOLOGY AND EXHUMATION HISTORY OF THE NORTHEASTERN FENNOSCANDIAN SHIELD BEFORE AND AFTER THE KOLA DEVONIAN ALKALINE LIP FORMATION: EVIDENCE FROM ^{40}AR/^{39}AR AND APATITE FISSION TRACK DATA

Veselovskiy R. V.[1,2], Thomson S. N.[3], Arzamastsev A. A.[4,5], Botsyun S. B.[6], Travin A. V.[7,8], Yudin D. S.[7,8], Samsonov A. V.[9], Stepanova A. V.[10], Myshenkova M. S.[1]

[1]*Geological Faculty, Lomonosov Moscow State University, Moscow, Russia*
[2]*Institute of Physics of the Earth, Moscow, Russia*
[3]*Department of Geosciences, University of Arizona, Tucson, AZ, USA*
[4]*Institute of Precambrian Geology and Geochronology, Saint Petersburg, Russia*
[5]*Institute of Earth Sciences, Saint Petersburg State University, Saint Petersburg, Russia*
[6]*Department of Geosciences, University of Tuebingen, Germany*
[7]*Sobolev Institute of Geology and Mineralogy Siberian Branch Russian Academy of Sciences, Novosibirsk, Russia*
[8]*Novosibirsk State University, Novosibirsk, Russia*
[9]*Institute of Geology of Ore Deposits Petrography Mineralogy and Geochemistry, Moscow, Russia*
[10]*Institute of Geology, Karelian Research Centre, Petrozavodsk, Russia*

Keywords: *Kola Devonian Alkaline LIP, low-temperature geochronology, fission track dating, Kola Peninsula, tectonothermal history.*

Northeastern Fennoscandia, especially the Kola Peninsula, is very poorly characterized by currently published thermochronological data. For this reason, the thermal evolution of this part of the Fennoscandian Shield remains poorly known. This problem becomes particularly acute when compared to southwestern and central Fennoscandia, the areas of Finland, Norway and Sweden, which have been extensively studied using modern thermochronological methods, such as ^{40}Ar/^{39}Ar dating (Soderlund et al., 2008; Sandstrom et al., 2009) and detailed zircon, titanite and apatite fission track analysis (Hendriks et al., 2007; Ksienzyk et al., 2014; Fossen et al., 2017). Available estimates of the Phanerozoic denudation from the Kola part of the Fennoscandian Shield and the corresponding amplitudes of its vertical movements are largely ambiguous. Semi-quantitative estimates of the Phanerozoic erosion of sedimentary cover and Devonian intrusive bodies and diatremes, show significant differences in the amplitude of the denudation of the area – from 0 km on the periphery of the Kola Peninsula up to 6 km in its central part (Hall, 2015). Reliable models of the Precambrian thermal history and quantitative estimates of the denudation volume of the Kola Peninsula are absent. Published thermochronological data, obtained by fission track analysis of apatite, titanite and zircon from the Kola Superdeep Borehole (SG3) (Hendriks et al., 2007; Kohn & Gleadow, 2019), are very local, and thus likely do not reflect processes operating at the scale of the whole Kola Peninsula.

Recently, to test the hypothesis of a Mesozoic regional remagnetization event within the Fennoscandian Shield (Veselovskiy et al., 2013, 2016), we obtained apatite fission track (AFT) ages from samples taken from various depths of the Devonian Khibina pluton (Veselovskiy et al., 2015). These AFT data, together with computer modeling of the post emplacement cooling of the Khibina massif, allowed us to model its tectono-thermal evolution during the last 360 Myr. The results of this modeling showed post-Devonian denudation of the Khibina massif of around 5-6 km, and that the mean geothermal gradient remained ~20°C/km for at least the last 250 Myr. But this conclusion contradicts independent post-Devonian erosion estimates for the central part of the Kola Peninsula of ~1-2 km proposed in (Hall, 2015).

The main goal of this study is to produce quantitative model of the tectonothermal evolution of northeastern Fennoscandia before and after the Kola Devonian LIP emplacement. We use both new and previously published multimineral ^{40}Ar/^{39}Ar data (amphibole, mica and feldspar) on the various Precambrian magmatic and metamorphic complexes to reconstruct the thermal history of NE Fennoscandia within the Kola Peninsula area in the interval 1900-360 Ma. Using the apatite fission track method as well as a numerical model of the heating-cooling process of northeastern Fennoscandia's upper crust, we have reconstructed its thermal evolution for the interval 360-0 Ma. According to our model (Veselovskiy et al., 2019), since Lapland-Kola orogenesis (1930-1905 Ma) northeastern Fennoscandia experienced a quasi-monotonous cooling with the average rate of ~0.15°C/Myr, which is equal to an exhumation rate of ~1-2 m/Myr. New apatite fission track data and time-temperature modeling reveal a "hidden" endogenous thermal event in the NE Fennoscandia that took place between 360-300 Ma. This we attribute to an elevated geothermal gradient due to Baltica's drift over the African Large Low Shear-wave Velocity Province in the lowest mantle and/or thermal blanketing by insulating Devonian-Carboniferous sedimentary/volcanic cover. Our model is further supported by evidence of Late Devonian-Carboniferous rifting in the East and South-Western Barents Basin, as well as various 360-300 Ma magmatic events within SW Fennoscandia and the Baltic countries.

Acknowledgements

This work was funded by the grant of Russian Science Foundation #16-17-10260, the grant of the Russian Government (#220, project #14.Z50.31.0017), the grant of President of Russian Federation MD1116.2018.5 and partly supported by the State scientific program of IPGG and IPE RAS, and by the state assignment project of Sobolev Institute of Geology and Mineralogy, Siberian Branch of Russian Academy of Sciences no 0330-2016-0013. Computer modelling was carried out using the equipment of the shared research facilities of HPC computing resources at Lomonosov Moscow State University.

References

1. Fossen, H., Ksienzyk, A. K., Jacobs, J. (2017). Correspondence: Challenges with dating weathering products to unravel ancient landscapes. Nature Communications, 8(1), 1502.
2. Hall, A.M. (2015). Phanerozoic denudation across the Kola Peninsula, Northwest Russia: implications for long-term stability of Precambrian shield margins. Norwegian Journal of Geology, 95, 153–169.
3. Hendriks, B., Andriessen, P., Huigen, Y., Leighton, C., Redfield, T., Murrell, G., Gallagher, K., Nielsen, S.B. (2007). A fission track data compilation for Fennoscandia. Norwegian Journal of Geology, 87, 143-155.
4. Kohn, B. & Gleadow, A. (2019). Application of low-temperature thermochronology to craton evolution. Chapter 21 in Malusa, M.G. and Fitzgerald, P.G. (eds.), Fission track thermochronology and its Application to Geology, 373-393, Springer. https://doi.org/10.1007/978-3-319-89421-8_21
5. Ksienzyk, A.K., Dunkl, I., Jacobs, J., Fossen, H., Kohlmann, F. (2014). From orogen to passive margin: constraints from fission track and (U-Th)/He analyses on Mesozoic uplift and fault reactivation in SW Norway. Geological Society, London, Special Publications, 390, 679–702.
6. Sandström, B., Tullborg, E.L., Larson, S.Å., Page, L. (2009). Brittle tectonothermal evolution in the Forsmark area, central Fennoscandian Shield, recorded by paragenesis, orientation and 40Ar/39Ar geochronology of fracture minerals. Tectonophysics, 478(3–4), 158–174.
7. Söderlund, P., Page, L.M., Söderlund, U. (2008). 40Ar-39Ar biotite and hornblende geochronology from the Oskarshamn area, SE Sweden: Discerning multiple Proterozoic tectonothermal events. Geological Magazine, 145(6), 790–799.
8. Veselovskiy, R., Thomson, S.N., Arzamastsev, A.A., Zakharov, V.S. (2015). Apatite Fission Track Thermochronology of Khibina Massif (Kola Peninsula, Russia): Implications for post-Devonian Tectonics of the NE Fennoscandia. Tectonophysics, 665, 157-163.
9. Veselovskiy, R.V., Arzamastsev, A.A., Demina, L.I., Travin, A.V., Botsyun S.B. (2013). Paleomagnetism, Geochronology, and Magnetic Mineralogy of Devonian Dikes from the Kola Alkaline Province (NE Fennoscandian Shield). Izvestiya, Physics of the Solid Earth, 49(4), 526–547.
10. Veselovskiy, R.V., Bazhenov, M.L., Arzamastsev,A.A. (2016). Paleomagnetism of Devonian dykes in the northern Kola Peninsula and its bearing on the apparent polar wander path of Baltica in the Precambrian. Tectonophysics, 675, 91–102.
11. Veselovskiy Roman, Stuart N. Thomson, Andrey A. Arzamastsev, Svetlana B. Botsyun, Aleksey V. Travin, Denis S. Yudin, Alexander V. Samsonov, Alexandra V. Stepanova. Thermochronology and exhumation history of the northeastern Fennoscandian Shield since 1.9 Ga: evidence from Ar/Ar and apatite fission track data from the Kola Peninsula // Tectonics. DOI: 10.1029/2018TC005250

ORDOVICIAN AND DEVONIAN STAGES OF VOLCANISM IN THE SW TUVA: SYNTHESIS OF GEOCHEMICAL, GEOCHRONOLOGICAL AND ISOTOPE-GEOCHEMICAL DATA

Vetrov E. V. [1,2], Uvarov A. N.[1], Vishnevskaya I. A.[3], Vetrova N. I.[2], Zhimulev F. I.[2], Chervyakovskaya M. V.[4]

[1]*Siberian Research Institute of Geology, Geophysics and Mineral Resources, Novosibirsk, Russia*
[2]*Sobolev Institute of Geology and Mineralogy Siberian Branch Russian Academy of Sciences, Novosibirsk, Russia*
[3]*Vernadsky Institute of Geochemistry and Analytical Chemistry of Russian Academy of Sciences, Moscow, Russia*
[4]*Zavaritsky Institute of Geology and Geochemistry Ural Branch of the Russian Academy of Sciences, Ekaterinburg, Russia*

Keywords*: geochronology, isotope geochemistry, zircon, volcanism, Tuva*

Introduction

In Tuva, as in many other areas of the Altai-Sayan folded region, the formation of rift volcanic strata is usually associated with the Early Devonian tectonic-magmatic activation cycle (Berzin and Kungurtsev, 1996; Babin et al., 2006). The works of the last decades (Rublev et al., 1999, Kruk et al., 2002, Vorontsov et al., 2018, etc.) made it possible to pick out the Ordovician (or Ordovician-Silurian) stage of volcanism, the products of which previously belonged to the early Devonian formations. We studied sections of the volcanic rocks of the SW Tuva, a priori considered as Early Devonian (Kenday Formation). The purpose of this work is studying and comparing the material composition, geochemical and isotope-geochemical characteristics of felsic volcanic rocks of the SW Tuva, clarify the age of their formation and estimate Sm/Nd model age.

Results

In general, the results of geochemical studies showed similar characteristics of both Ordovician and Devonian felsic volcanic rocks. The rocks are characterized by slightly elevated potassium (K_2O = 2.5–4.5%) and sodium (Na_2O = 3-5%) and, accordingly, high total alkalinity. The contents of magnesium and iron allow attributing the rocks to a ferrous type, in accordance with the contents of alkalis and calcium they occupy an intermediate position between the calcareous and alkaline types. The Devonian felsic volcanic rocks are characterized by differentiated spectra of the REE distribution (La/Ybn = 1.2–3), the presence of a weak "europium minimum" or its absence (Eu/Eu*= 0.72–1.11) (Fig a). On the multi-element spectra, negative anomalies in Ta, Nb, P, Ti are expressed (Fig. b). The Ordovician felsic volcanic rocks show similar spectra and are distinguished by a higher degree of

fractionation (La/Ybn = 4.05–9.24) and a more distinct "europium minimum" (Eu/Eu* = 0.39–0.76) (Fig a). The ratios Y-Nb, Y + Nb-Rb according to (Pierce et al., 1984) and Rb-Hf-Ta according to (Harris et al., 1986) classify the studied Ordovician and Devonian rocks as island-arc formations. In other words, these rocks possess the geochemical properties of island-island rocks.

The one definition of age for the Devonian volcanic rocks is obtained by the U/Pb zircon dating using LA-ICP-MS system (Perth University, Australia). Fifteen grains of rhyolite (sample 2039-2) was analyzed and concordant age of 397 Ma was obtained. This result is consistent with the geological data, since the underlying late Silurian and overlying Middle Devonian sediments have a reliable justification of age for the remnants of flora and fauna. Two age determinations for Ordovician volcanic rocks were obtained (samples 2251-1 and 17002-4) the U/Pb zircon dating rhyodacites using SHRIMP II method (A.P. Karpinsky Russian Geological Research Institute, St. Petersburg, Russia). Ten idiomorphic prismatic zircon crystals were analyzed for each of these samples and Ordovician ages of 453 and 460 Ma were obtained, respectively. The resulting ages correspond to the Ordovician age of granitoids (453 Ma according to Vetrov et al., 2019) intruded these volcanic rocks.

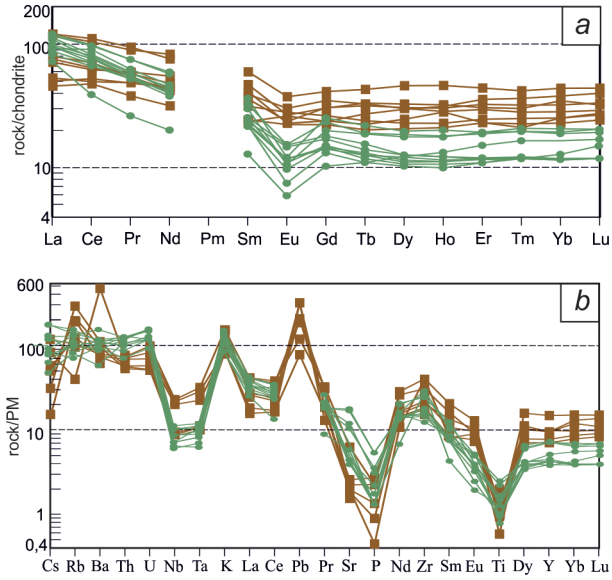


Figure. REE (a) and multi-element (b) diagrams for Ordovician (green) and Devonian (brown) volcanic rocks according to (Sun and McDonough, 1989).

Sm/Nd isotope studies of felsic Devonian volcanic rocks show these rocks are characterized by a high primary ratio of $^{143}Nd/^{144}Nd$, and εNd (T) values vary in a fairly wide range from +0.4 to + 7.0. The model age for the minimum value of εNd (T) = +0.4 is estimated as Mesoproterozoic ((TNd(DM-2st) = 1.17 Ga) and for the maximum value of εNd (T) = +7 is estimated as early-middle Cambrian ((TNd(DM-2st) = 0.52 Ga). The Sm/Nd isotope studies carried out for felsic Ordovician volcanic rocks indicate εNd (T) = + 3.1…+ 5.5 is close to those obtained for Ordovician granitoids εNd (T) = + 5.5 and +4.7 (Vetrov et al., 2019). The model age of the source of the Ordovician felsic rocks, as well as the Ordovician granitoids intruded volcanic rocks, corresponds to the Neoproterozoic (TNd (DM-2st) from 0.71 to 0.94 Ga). In general, such isotope-geochemical parameters indicate the predominance of the mantle substrate during the formation of melts for both Ordovician and Devonian magmas.

Conclusions

This study allowed identifying the stage of Ordovician volcanism in Tuva and comparing it with the most studied stage of Devonian volcanism. Ordovician felsic volcanic rocks have a higher degree of REE fractionation and a relatively homogeneous source of melts with Neoproterozoic model age. At the same time, Devonian felsic volcanic rocks show not so high enrichment of the REE melt and apparently have a heterogeneous composition of the melt source (model ages from Mesoproterozoic to Cambrian). Geochemical and isotope-geochemical data indicate a special role of the mantle in the formation of Ordovician and Devonian magmas. The Devonian volcanism is usually associated with the development of the rear zones of the active continental margin, but the geodynamic conditions of Ordovician volcanic rocks remain unobvious. Probably, their formation is associated with local processes of post-collisional stretching and relaxation of the thickened Early Caledonian crust.

Discovery of Ordovician volcanism products among Devonian volcanic formations in the Altai-Sayan region is repeated and known on the eastern slope of the Kuznetsk Alatau (Perfilova et al., 1999; Babin et al., 2006), in Minusa depressions (Rublev et al., 1999; Vorontsov et al., 2018), in East Sayan (Kruk et al., 2002; Shkol'nik et al., 2017) and in East Tuva. It is possible that further study of similar rift formations using geochronological methods will significantly overestimate the Devonian and Ordovician volcanism stages in the Altai-Sayan region.

Acknowledgements

The reported study was funded by RFBR according to the research projects (№18-35-20025, № 19-05-00145) and the state assignment of IGM SB RAS

References

1. Babin, G.A., Zeyfert, L.L., Shchigrev, A.F. (2006). The legend for the Altai-Sayan map series of the Russian Federation State geological map in scale 1: 1 000 000 (third edition) (In Russian)
2. Berzin, N.A., Kungurtsev, L.V. (1996). Geodynamic interpretation of Altai-Sayan Geological complexes. Russian Geology and Geophysics 37 (1): 56-73
3. Harris N.B.W., Peaece J.A., Tindle A.G. (1986). Geochemical characteristics of collision zone magmatism / Coward M.P., Ries A.C. (Eds.) Collision tectonics. Geol. Soc. Spec. Pub. 19: 67-81
4. Kruk N.N., Babin G.A., Vladimirov A.G., Rudnev S.N., Gibsher, A.S, Sovetov Y.K., Sergeev S.A, Kotov A.B., Salnikova E.B., Levchenkov O.A., Makhlayev M.L., Derban A.G. (2002). "Devonotypic" magmatism of the East Sayan (according to U-Pb isotope research data). Petrology of magmatic and metamorphic complexes: 189-193 (In Russian)
5. Pearce J.A., Harris N.B.W., Tindle A.G. (1984). Trace element discrimination diagrams for the tectonic inter-

pretation of granitic rocks // J. Petrol. 25: 956-983
6. Perfilova O.Yu., Mikhaylenko V.V., Koptev I.I., Sidoras S.D. (1999). Koshkulak standard of the Ordovician volcano-plutonic association (Kuznetsk Alatau). Krasnoyarsk: RIC KNIIGiMS: 159 (In Russian)
7. Rublev A.G., Shergina Yu.P., Berzon E.I. (1999). The isotopic age of Paleozoic volcanoes of the Krasnoyarsk Rise and the problem of the stratigraphy of the Byskarian series. Domestic Geology 3: 47-54
8. Shkol'nik S.I., Ivanov A.I., Reznitsky L.Z., Letnikova E.F., Hyaiyu He, Zhiglang Y., Youjueen Li., Vishnevskaya I.A., Barash I.G. (2017) Middle ordovician effusive rocks of the Khamsara terrane (Tyva) as an indicator complex. Russian Geology and Geophysics 58 (9): 1032-1044
9. Sun S.-s., McDonough W. F. (1989). Chemical and isotopic systematics of oceanic basalts: implications for mantle composition and processes. Geological Society. London, Special Publications, 42: 313-345
10. Vetrov, E.V., Chernykh, A.I., Babin, G.A. (2019). Early Paleozoic granitoid magmatism in the East Tannu-Ola sector of the Tuvinian magmatic belt: geodynamic position, age, and metallogeny. Russian Geology and Geophysics 60 (5): 492-513
11. Vorontsov A.A., Perfilova O.Yu., Kruk N.N. (2018). Geodynamic setting, structure, and composition of continuous trachybasalt-trachyandesite-rhyolite series in the north of Altai-Sayan area: the role of crust-mantle interaction in continental magma formation. Russian Geology and Geophysics 59(12):1640-1659

ORDOVICIAN–DEVONIAN VOLCANISM IN THE NORTH OF THE ALTAI–SAYAN FOLDED AREA (GEOLOGY, GEOCHEMISTRY, GEODYNAMICS)

Vorontsov A. A.[1,2], Perfilova O. Y. [3], Grinev O. M. [4], Ernst R. E. [4,5]

[1] *Vinogradov Institute of Geochemistry, Siberian Branch, Russian Academy of Sciences, Irkutsk, Russia*
[2] *Irkutsk State University, Irkutsk, Russia*
[3] *Siberian Federal University, Krasnoyarsk, Russia*
[4] *National Research Tomsk State University, Tomsk, Russia*
[5] *Carleton University, Ottawa, Canada*

Keywords: *volcanic series, geochemistry, Ordovician, Devonian, Minusa basin*

Introduction

A volcanic series is widespread in the north of the Altai–Sayan folded area (ASFA) comprising the Minusa basin and its mountainous surroundings. Two magmatic stages are recognized from geologic and geochronological (Rb–Sr, K–Ar, Ar–Ar and U–Pb) studies: 480–430 Ma (Ordovician–early Silurian) and 410–390 Ma (Early–Middle Devonian). The volcanic rocks of these two stages are concentrated within the Minusinsk depression and share a similar rock association, petrographic characteristics and total alkalinity (Perfilova, 2004; Vorontsov et al., 2015). However, geochemical appraisal of basaltoids in both series (Vorontsov et al., 2017) indicates different contents of HFSE (High Field Strength Elements), LILE (Large Ion Lithophile Elements) and Sr and Nd isotopes reflecting differences in the sources, as well as the paths for primary magma evolution, and possibly indicating differences in geodynamic settings for magma generation. Herein, we provide a comprehensive comparison of geochemical and isotope characteristics of both the Ordovician–early Silurian and Early–Middle Devonian suites.

Results

Geology

Volcanic rocks of the Ordovician–early Silurian stage include trachybasalts, basaltic trachyandesites, trachyandesites, trachytes and trachyrhyodacites. There also associated volcano-plutonic units that include numerous syenite–granite plutons in the basement to the Minusa basin (e.g., East Sayan, West Sayan, and Kuznetsk Alatau mountains). The volcanic series of the Early–Middle Devonian stage include trachybasalts, basaltic trachyandesites, trachyandesites, trachytes, trachydacites, trachyrhyolites, and rhyolites. Their formation is linked with the development of the Minusa basin. The rocks of the series comprise part of sedimentary-volcanic sequences lying with structural unconformity over the pre-Devonian folded basement. Approximate values show that the volume of Ordovician–early Silurian volcanics is less than half the size of the Early–Middle Devonian volcanics (about 20,000 km^3) of the Minusa-basin.

Geochemistry

Three geochemical subgroups are distinguished that each include units of both stages (Ordovician–early Silurian and Early–Middle Devonian).

Subgroup 1 (trachybasalts and basaltic trachyandesites, SiO2 47–55 wt.%). Normalized to primitive mantle, the shape of multi-element spectra of all volcanics of this subgroup (irrespective of which stage they belong to) seem close to that for island arc basalts (IAB) with typical minima in Th, Nb, Ta, Ti and maxima in Ba and Sr. However, the absolute values of all incompatible elements exceed their contents in IAB. Such excess is most distinct for LILE, as well as REE (Rare Earth Elements), their contents reaching the values observed in within-plate basalts (OIB). The Ordovician–early Silurian basaltoids (belonging to this subgroup) are distinguished by a high degree of REE fractionation basically due to LREE enrichment ((La/Yb)n which varies from 11.6 to 32.8). In the Early–Middle Devonian volcanics the (La/Yb)n value varies

from 7.6 to 13.0. In all rocks of the Ordovician–early Silurian series, in contrast to the Early–Middle Devonian series, there is direct correlation between TiO2 and La/Yb value.

Subgroup 2 (trachyandesites, SiO2 55–63 wt.%). These rocks retain a high degree of REE fractionation. The $(La/Yb)_n$ value varies from 10.2 to 23.8 in trachyandesites of the Ordovician–early Silurian and from 9.6 to 14.1 in trachyandesite of the Early–Middle Devonian. The rocks of both age groups retain Th, Nb, Ta minima, Ba maximum; dispersion arises in Sr. Subgroup 2 has the poorer Ti and Eu, but the higher Rb.

Subgroup 3 (trachytes, trachydacites, trachyrhyodacites, trachyrhyolites, and rhyolites, SiO2 63–77 wt.%). In this subgroup, volcanics of the two different age stages differ in geochemical specifics. Thus, in the Ordovician–early Silurian volcanics with increasing SiO2 the concentrations of many incompatible elements increase as well, except for P (fractionation of apatite), Ti (fractionation of titanium-magnetite) and Ba decreasing to 57 ppm, Sr decreasing to 7 ppm and Eu (fractionation of feldspars). In subgroup 3 the selective depletion in Nb and Ta is not intensive as in the rocks of basic and intermediate compositions; however, the (La/Yb)n varies from 7.4 to 18.2. In contrast, in the Early–Middle Devonian volcanics there are two types of rocks with different distributions of rare elements. The first type is close to the Ordovician–early Silurian volcanics, differing from them by the absence of rocks with anomalously low contents of Ba and Sr, weak Eu minimum, and narrow range in total REE and LREE to HREE ratios ((La/Yb)n varies from 6.6 to 10.5). In the rhyolites ($74.0 < SiO2 < 76.6$ wt.%) with respect to trachyrhyolites ($72.0 < SiO2 < 74.0$ wt.%) HSFE, REE, and Y concentrations decrease, violating the tendency of accumulating incompatible elements during fractionation. Their composition is close to that of upper crustal values, and island arc and accretionary–collisional granites of the Central-Asian fold belt.

Isotope composition of Sr and Nd in basaltoids

In the εSr(T)– εNd(T) diagram data from the two age stages plot in the first quadrant, and concentrate in two isolated fields. One field characterizes the substrates giving rise to melting of Ordovician–early Silurian (εNd(476) 0.4–1.0 and εSr(476) 11.3–12.8). The other field is for Early–Middle Devonian (εNd(391) 3.5–4.7 and εSr(391) 5.7–7.9) basaltoids. Both fields are displaced from the line of mantle correlation towards substrates enriched in radiogenic strontium. Such a deviation points to assimilation of melts of moderately depleted mantle (with intermediate characteristics between PREMA and EMII) with an additional component having high Sr, increased $^{87}Sr/^{86}Sr$ and low REE values. The compositions of this additional component is most likely common for carbonate rocks, which could be involved in the Vendian–Cambrian subduction processes and magma formation, enriching the substance of mantle wedge with radiogenic strontium and forming the metasomatic mantle substratum-giving rise to fusion of primary magmas of the volcanic series.

Conclusions

The Ordovician–early Silurian and Early–Middle Devonian volcanic series which occur in the northern part of the Altai–Sayan region are composed of rocks of primarily moderately–alkaline series, with SiO2 varying from 45 to 77 wt.%. The Ordovician–early Silurian series is distinguished from the Minusa trough volcanics by low TiO2 content (less than 1.7 wt.%), Fe2O3tot and increased Al2O3 concentrations in all rock varieties, and a more fractionated pattern of REE distribution in trachybasalts. Both series are governed by the two contemporaneous mechanisms of magma evolution. The major process—the fractional crystallization is responsible for origination of the rock spectrum ranging from trachybasalts to trachyrhyodacites. The secondary mechanism is contamination of fractionated melts with crustal components, anatectic crustal melting and mixing of deep-seated magmas with crustal melts. Specifics of these processes are common for both age stages; they are controlled by the composition of parent melt sources. Their geochemical characteristics are typical of the Central Asian Foldbelt areas, in which a mantle plume interact with lithospheric mantle metasomatically modified during the preceding Vendian–early Cambrian subduction processes related to the development of the Kuznetsk Alatau and Altai–North Sayan island arc systems. The composition of the products of magmatism was determined by the processes of mantle metasomatism and crustal contamination.

Acknowledgements

This work was conducted as a task of RFBR, project No. 19-05-00300.

References

1. Perfilova O.Yu., Makhlaev M.L., Sidoras S.D. (2004). Ordovician volcanic-plutonic association in structures of the folded surrounding of the Minusa depression. Russ. Lithosphere 3: 137–152.
2. Vorontsov A.A., Gazizova T.F., Yarmolyuk V.V., Fedoseev G.S., Travin A.V., Perfilova O.Y., Posokhov V.F. (2015). Differentiated volcanic association of the Minusa trough: mechanisms of formation and sources of melts, as examplified by Batenevo rise. Petrology 23 (4): 353–375.
3. Vorontsov A.A., Perfilova O.Yu., Buslov M.M., Travin A.V., Makhlaev M.L., Dril S.I., Katraevskaya Ya.I. (2017). Plume magmatism in the northeast of Altay-Sayan area: stages, composition of sources, geodynamics (exemplified by the Minusa basin). Dokl. Earth Sci. 472 (4): 449–455.

MAIN STAGES OF THE PALEOZOIC ALKALINE MAGMATISM IN THE WESTERN CAOB: ISOTOPE AGE AND GEOCHEMISTRY OF PLUTONIC ROCKS ACCORDING THE PERIODIC MANTLE PLUMES ACTIVITY

Vrublevskii V. V.[1], Doroshkevich A. G.[1,2,3], Izokh A. E.[1,2,4]

[1]*Tomsk State University, Tomsk, Russia*
[2]*Institute of Geology and Mineralogy SB RAS, Novosibirsk, Russia*
[3]*Geological Institute SB RAS, Ulan-Ude, Russia*
[4]*Novosibirsk State University, Novosibirsk, Russia*

Keywords: *alkaline magmatism, isotope geochemistry, Paleozoic, mantle plume, Central Asian orogenic belt*

Introduction

Alkaline magmatic activity in the continents and the oceans usually is related to periods of mantle plume activity (Ernst, 2014; Yarmolyuk et al., 2014). Geochemical and isotopic characteristics of formed volcanic-plutonic associations can be attributed to participations of distinct mantle components (Bell et al., 1998; Gwalani et al., 2010). Contamination by material of accretionary-collisional complexes of primary alkaline magmas from orogenic belts complicates their mantle characteristics (Doroshkevich et al., 2012; Vrublevskii, 2015; Vrublevskii et al., 2012, 2014, 2016, 2018, 2019a, b).

Results

With minor exceptions, the alkaline magmatism in the Western Central Asian orogenic belt (CAOB) is Paleozoic. There are alkaline plutonic complexes of the NE Kuznetsk Alatau, SE Russian Altai (Edel'veis complex), SE Tuva (Sangilen plateau), Western Transbaikalia (Vitim plateau) and Baikal region, Northern Mongolia (Hovsgol region) and East Sayan. The complexes form differentiated series of rocks and include subalkaline and alkaline gabbro, foidolites, nepheline and alkaline syenites. According to U–Pb, Sm–Nd, Rb–Sr, and Ar–Ar data, the 520–470, 405–385, 310–250 Ma intervals of alkaline rock emplacement are distinctly determined (Figure 1).

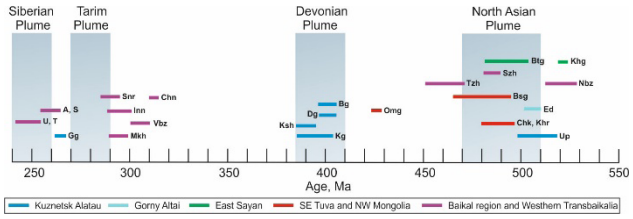


Figure 1. Correlation between plume activity events and pluton ages: plutons of the alkaline provinces are shown according to published data. Igneous provinces are shown by different colors.

Massifs of subalkaline gabbro and foidic igneous rocks of all age events (Late Cambrian (~ 500 Ma), Early Devonian (~ 400 Ma) and Late Permian (~ 265 Ma)) occur in the NE Kuznetsk Alatau (Vrublevskii et al., 2014, 2016; Mustafayev et al., 2017). Alkaline complexes in the Vitim plateau and Baikal region were emplaced at Early Paleozoic and Late Carbon-Early Triassic (Sklyarov et al., 2009; Doroshkevich et al., 2012, 2018). Some massifs in the SE Russian Altai, SE Tuva, East Sayan and Hovsgol region (NW Mongolia) can be formed in relatively wide age interval from Cambrian through Silurian (Vrublevskii et al., 2012, 2019a,b; Sal'nikova et al., 2018).

Independent of ages, these alkaline igneous rock associations exhibit geochemical convergence that suggests a participation in magma generation of mantle plume material and continental lithospheric material. Such mixing of heterogeneous material is evidenced by the features of both trace element composition and radiogenic isotope relationship. Wide variations of initial Nd–Sr isotope ratios ($\varepsilon_{Nd}(t) \approx$ from –1 to +8; $^{87}Sr/^{86}Sr(t)$ from 0.7032 to 0.7076) can testify the interaction of depleted (PREMA-type) and enriched (EM-type) mantle components in the sources and/or contamination of primary melts at crustal levels. Furthermore, Nd–Sr isotopic compositions of alkaline rocks correlate to trend of isotopic evolution of the mantle plumes that are responsible for Paleozoic mafic magmatic activity in the CAOB (Figure 2).

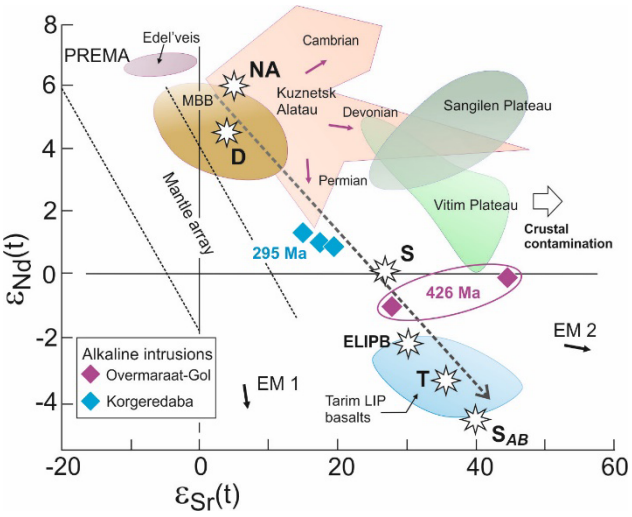


Figure 2. $\varepsilon_{Nd}(t)$ vs. $\varepsilon_{Sr}(t)$ plot for alkaline complexes from the Western CAOB (our published data). MBB=Devonian Minusa basin basalts in the Altai–Sayan area, after Vorontsov et al., 2013. Nepheline syenites of the Korgeredaba (~ 295 Ma, SE Tuva) and Overmaraat-Gol (~426 Ma, NW Mongolia) plutons, after Nikiforov et al., 2018; Vrublevskii et al., 2019a. White stars are average basalt compositions of the North Asian (NA), Devonian (D), Siberian (S, AB = alkali basalts) and Tarim (T) mantle plumes, after Yarmolyuk and Kovalenko, 2003; Vorontsov et al., 2013; Lightfoot et al., 1993; Zhang et al., 2010; Li et al., 2012; Wei et al., 2014. Dash line shows composition trend of the

plume component. ELIPB=the average basalt composition of the Emeishan large igneous province (Li et al., 2015). Predominant basalt compositions from the Tarim LIP given by (Zhang et al., 2010; Li et al., 2012; Wei et al., 2014). "Mantle array" domain and PREMA, EM 1 and EM 2 modern mantle reservoirs are according to (Zindler and Hart, 1986; Stracke et al., 2005).

Predomination of EM component in the primary source is a typical at the Late Paleozoic plume activity. However, initial Pb isotope ratios in rocks and minerals confirm the presence of enriched components in Cambrian and Devonian alkaline intrusions ($^{208}Pb/^{204}Pb$ 37.21–38.02; $^{207}Pb/^{204}Pb$ 15.40–15.71; $^{206}Pb/^{204}Pb$ 17.28–19.67). Direct correlation between $^{87}Sr/^{86}Sr(t)$ and high $\delta^{18}O$ (to ~ 8–14 ‰) values in rocks is an evidence of crustal contamination signatures; these features are typical for magmatic complexes in orogenic belts. $\delta^{34}S$ values (to 4.6 ‰) in sulfides from alkaline rocks are higher than those of the mantle values. Isotopic heterogeneity is observed within individual massifs and can be caused by different degree of mixing of heterogeneous material in intermediate chambers.

Conclusions

The primary melts for Paleozoic alkaline rocks of the Western CAOB were formed from heterogeneous mantle sources. The main mixing components are PREMA and EM mantle sources. High $^{87}Sr/^{86}Sr(t)$ and $\delta^{18}O$ values in rocks is an evidence of crustal contamination signatures of magmas. It can be a result of interaction between mantle plume components and materials of accretionary-collisional complexes.

Acknowledgements

This study was financially supported by grants of Russian Government (no. 14.Y26.31.0012), the Russian Foundation for Basic Research (no. 17–05–00309–a) and Russian Ministry of Science and Higher Education (no. 5.8988.2017/6.7).

References

1. Bell K., Kjarsgaard B.A., Simonetti A., 1998. Journal of Petrology 39:1839–1845.
2. Doroshkevich A.G., Ripp G.S., Izbrodin I.A., Savatenkov V.M., 2012. Lithos 152:157–172.
3. Doroshkevich A.G., Izbrodin I.A., Rampilov M.O., Ripp G.S., Lastochkin E.I., Khubanov V.B., 2018. Russian Geology and Geophysics 59:1061–1077.
4. Ernst R.E., 2014. Large igneous provinces. Cambridge University Press, Cambridge.
5. Gwalani L.G., Moore K., Simonetti A., 2010. Mineralogy and Petrology 98:5–10.
6. Li Z., Li Y., Chen H., Santosh M., Yang S., Xu Y., Langmuir C.H., Chen Z., Yu X., Zou S., 2012. Journal of Asian Earth Sciences 49:191–202.
7. Li H., Zhang Z., Ernst R., Lu L., Santosh M., Zhang D., Cheng Z., 2015. Terra Nova 27:247–257.
8. Lightfoot P.C., Hawkesworth C.J., Hergt J., Naldrett A.J., Gorbachev N.S., Fedorenko V.A., DohertyW., 1993. Contributions to Mineralogy and Petrology 114:171–188.
9. Mustafayev A.A., Gertner I.F., Serov P.A., 2017. IOP Conference Series: Earth and Environmental Science 110, 012016.
10. Nikiforov A.V., Yarmolyuk V.V., 2007. Doklady Earth Sciences 412:6–10.
11. Nikiforov A.V., Sal'nikova E.B., Sugorakova A.M., Polyakov N.A., Khertek A.K., 2018. Proceedings of Geology, Magmatism and Metallogeny of Central Asia. TuvIENR SB RAS, Kyzyl, Russia, 84–88.
12. Sal'nikova E.B., Stifeeva M.V., Nikiforov A.V., Yarmolyuk V.V., Kotov A.B., Anisimova I.V., Sugorakova A.M., Vrublevskii V.V., 2018. Doklady Earth Sciences 480(2):778–782.
13. Sklyarov E.V., Fedorovsky V.S., Kotov A.B., Lavrenchuk A.V., Mazukabzov A.M., Levitsky V.I., Sal'nikova E.B., Starikova A.E., Yakovleva S.Z., Anisimova I.V., Fedoseenko A.M., 2009. Russian Geology and Geophysics 50:1091–1106.
14. Stracke A., Hofmann A.W., Hart S.R., 2005. Geochemistry, Geophysics, Geosystems 6(5), Q05007.
15. Vorontsov A.A., Fedoseev G.S., Andryushchenko S.V., 2013. Russian Geology and Geophysics 54:1001–1025.
16. Vrublevskii V.V., 2015. Russian Geology and Geophysics 56:379–401.
17. Vrublevskii V.V., Krupchatnikov V.I., Izokh A.E., Gertner I.F., 2012. Russian Geology and Geophysics 53:721–735.
18. Vrublevskii V.V., Gertner I.F., Gutiérrez-Alonso G., Hofmann M., Grinev O.M., Tishin P.A., 2014. Russian Geology and Geophysics 55:1264–1277.
19. Vrublevskii V.V., Grinev O.M., Izokh A.E., Travin A.V., 2016. Russian Geology and Geophysics 57:592–602.
20. Vrublevskii V.V., Morova A.A., Bukharova O.V., Konovalenko S.I., 2018. Journal of Asian Earth Sciences 153:252–281.
21. Vrublevskii V.V., Gertner I.F., Ernst R.E., Izokh A.E., Vishnevskii A.V., 2019a. Minerals 9(3), article 170.
22. Vrublevskii V.V., Nikiforov A.V., Sugorakova A.M., Kozulina T.V., 2019b. Russian Geology and Geophysics 60:436–445.
23. Wei X., Xu Y.-G., Feng Y.-X., Zhao J.-X., 2014. American Journal of Science 314:314–356.
24. Yarmolyuk V.V., Kovalenko V.I., 2003. Petrology 11:504–531.
25. Yarmolyuk V.V., Kuzmin M.I., Ernst R.E., 2014. Journal of Asian Earth Sciences 93:158–179.
26. Zhang Y., Liu J., Guo Z., 2010. Gondwana Research 18:596–610.
27. Zindler A., Hart S.R., 1986. Annual Review of Earth and Planetary Sciences 14:493–571.

PALEOMAGNETIC CONSTRAINTS ON DURATION OF THE BUSHVELD LARGE IGNEOUS PROVINCE

Wabo H., de Kock M., Belyanin G.

University of Johannesburg, Johannesburg, South Africa

Keywords: *Kaapvaal Craton, Bushveld magmatism, age, paleomagnetism*

Introduction

The Bushveld Large Igneous Province (LIP) in the Kaapvaal Craton is associated with considerable amounts of platinum group elements, nickel, chromium, copper, apatite, uranium, zircon, vermiculite and vanadium (e.g. Cawthorn et al., 2006). It consists of the main Bushveld Complex (with the famous Rustenburg Layered Suite) surrounded by numerous satellite intrusions and a suite of ultramafic to mafic marginal sills. The Bushveld LIP involved three parental liquids namely the more primitive B1 magma, and the younger and more evolved B2 and B3 magmas. The marginal sills, which are genetically related to the RLS, are believed to share these parental affinities (e.g. Sharpe, 1982).

Reliable paleomagnetic poles exist for B2 and B3 related Bushveld rocks (Letts et al., 2009), while the B1 Bushveld rocks have received less paleomagnetic attention. A reliable B1-Bushveld paleopole can contribute to provide new constraints on the timing of Bushveld emplacement.

Results

For this study, 18 Bushveld marginal sills (13 dolerites and 5 gabbronorites) were collected in the eastern and western limbs of the Rustenburg Layered Suite (RLS) for paleomagnetic study. The studied sills were previously postulated to derive from B2 and B3 Bushveld magmas solely based on petrography (e.g. Sharpe, 1982). However, trace element compositions reported here clearly demonstrate that all samples represent compositional equivalents of B1-type magma of RLS. The slight enrichment in trace elements of samples compared to known primitive (pyroxenite) B1 sills can be explained as reflecting the crystallization of a progressively evolved B1 Bushveld magma over a relatively short period of time. This observation concurs with the $^{40}Ar/^{39}Ar$ age of 2058 ± 7.8 Ma of this study which is near identical to baddeleyite U-Pb ages 2058.4 ± 1.3 Ma and 2058 ± 6 Ma (Wabo et al., 2016) previously reported from more primitive B1 Bushveld sills.

Stepwise demagnetization allowed to identify a high-stability (up to 575°C) magnetization carried by Ti-magnetite. The dual-polarity nature and improved grouping of site means upon tilt-correction suggests a primary remanence in combination with existing data from B1 Bushveld rocks. A new mean 2058 Ma paleopole is statistically indistinguishable to the existing 2061 Ma Phalaborwa Complex pole (Letts et al., 2010). It, however, only partially overlaps with the very well-defined 2055 Ma pole from Critical, Main and Upper zones of RLS (B2 type and B3 type parentage) (Letts et al., 2009), indicating a small apparent polar wander path between the early stages of Bushveld magmatism and the bulk of this LIP.

Conclusions

The data sets reported here provide evidence to further strengthen previous radiometric findings in suggesting that the RLS represents two episodes of magma emplacement separated in time by at least 3 million years (i.e. B1-type magma pulse around 2058 Ma and the B2 and B3- type magma pulses following closely on each other around 2055 Ma).

Acknowledgements

HW received financial support from the South African National Research Foundation (NRF) and also acknowledges research funding from CIMERA as well as the PPM Research Group of the Department of Geology at the University of Johannesburg. Many thoughts in the manuscript were developed while HW was visiting the Harvard University and Yale University. D. Evans is thanked for fruitful discussions about the paleomagnetism of the Kaapvaal craton.

References

1. Cawthorn R.G., Eales H.V., Walraven F., Uken R., Watkeys M.K. (2006) The Bushveld Complex, in Johnston, M. R., Anhaeusser, C. R., and Thomas, R. J., eds., The Geology of South Africa.: Pretoria, South Africa, The Geological Society of South Africa and Council for Geosciences, p. 261-281.
2. Letts S., Torsvik T.H., Webb S.J., Ashwal L.D. (2009) Palaeomagnetism of the 2054 Ma Bushveld Complex (South Africa): implications for emplacement and cooling: Geophysical Journal International 179: 850-872.
3. Letts S., Torsvik T.H., Webb S.J., Ashwal L.D. (2010) New Palaeoproterozoic palaeomagnetic data from the Kaapvaal Craton, South Africa: Geological Society, London, Special Publications, 357: 9-26.
4. Sharpe (1982) Petrology, classification and chronology of the intrusion of mafic sills beneath the eastern Bushveld Complex., Institute for the geological research on the Bushveld Complex, Pretoria, 51 p.
5. Wabo H., de Kock M.O., Klausen M., Soderlund U., Beukes N.J. (2016) Paleomagnetism and chronology of B-1 marginal sills of the Bushveld Complex from the eastern Kaapvaal craton. South Africa, GFF 138: 133-151.

SEISMIC PROPERTIES OF THE LOWER CRUST BENEATH LARGE IGNEOUS PROVINCES

Wang Q.

Nanjing University, Nanjing, China

Keywords *Seismic velocity, Large igneous provinces, Siberian Traps, magma underplating, crustal growth, metamorphism, Moho*

Introduction

Our knowledge about the lower crust beneath large igneous provinces (LIPs) is mainly from petrology and geochemistry of kimberlite- or basalt-brought xenoliths, and from seismic and electrical structures of the crust. Because LIPs were produced by a high-degree melting in the lithospheric mantle, magmatism-related processes such as lithospheric thinning by thermal erosion and crustal growth by magma underplating, should play an important role in the composition and structure of the lower crust beneath LIPs.

LIPs in cratons can be traced back to the Archean, whereas oceanic plateaus present increased oceanic crust production in the Mesozoic to Cenozoic (Bryan and Ferrari, 2013). Although high velocity anomaly is often observed in the lowermost crust of LIPs in cratons or rifted continental margins (e.g., Cherepanova et al., 2013; Becker et al., 2014; Xu et al., 2015), the lack of systematic petrological interpretation hampers our evaluation of the crustal growth by mantle plumes through the Earth's history.

Results

In this study, we summarized seismic structures of several typical LIPs from previous seismic investigation, including the Siberian Craton with the Siberian Traps erupted at ~250 Ma, the Yangtze Craton with the Emeishan Flood Basalt Province erupted at ~260 Ma, the Kaapvaal Craton with the Bushveld Complex at ~2055-2060 Ma and the Karoo LIP at ~183 Ma, the Fennoscandian Shield with the Sumian LIP at 2.5–2.4 Ga, and the Ontong Java Plateau at ~122 Ma. Based on laboratory-derived seismic properties of rocks at high pressure and high temperature in the past five decades (Ji et al., 2004; Wang et al., 2013) and P-T conditions of rocks, we interpreted the composition of the lower crust beneath these LIPs. The results indicate that the lower crust beneath LIPs in cratons is mainly composed of mafic granulites but could be very heterogenous in composition. The very high P-wave velocity (> 7.2 km/s) in the lowermost crust can be fit by a mixture of garnet granulites, two-pyroxene granulites, and garnet gabbros due to magma underplating. Depending on the fluid activity, the ultrahigh-pressure metamorphism of basaltic rocks could result in eclogites in the upper mantle, which may appear as high velocity anomaly in the upper mantle. The variations in the Moho reflectivity and mantle velocity could be used to trace the fossil magma chamber in the lithospheric mantle.

Conclusions

The widespread high velocity anomaly in the lower crust beneath the LPIs indicate the crustal growth by mantle plumes. Magmatism-induced compositional change and dehydration will increase viscosity of the lithospheric mantle, and finally trigger lithospheric thickening after mantle plume activity. The strong lower crust would weld the crust and upper mantle together and make the lithosphere of a LIP deform as a rigid block.

Acknowledgements

This work was funded by Natural Science Foundation of China, project No. 41825006.

References

1. Becker K., Franke D., Trumbull R., et al. (2014) Asymmetry of high-velocity lower crust on the South Atlantic rifted margins and implications for the interplay of magmatism and tectonics in continental breakup.
2. Bryan S.C., Ferrari L. (2013) Large igneous provinces and silicic large igneous provinces: Progress in our understanding over the last 25 years. GSA Bulletin 125: 1053–1078
3. Cherepanova Y., Artemieva I., Thybo H., Chemia Z. (2013) Crustal structure of the Siberian craton and the West Siberian basin: An appraisal of existing seismic data. Tectonophysics 209: 154-183
4. Ji S.C., Wang Q., Xia B. (2002) Handbook of Seismic Properties of Minerals, Rocks and Ores. Polytechnic International Press, Montreal, Canada, 630 pp.
5. Wang Q., Bagdassarov N., Ji S. (2013) The Moho as a transition zone: A revisit from seismic and electrical properties of minerals and rocks. Tectonophysics 609: 395-422.
6. Xu T., Zhang Z.J, Liu B.F. (2015) Crustal velocity structure in the Emeishan large igneous province and evidence of the Permian mantle plume activity. Science China-Earth Sciences 58: 1133-1147.

LATE PALEO- TO EARLY MESOPROTEROZOIC MAFIC MAGMATISMIN SW YANGTZE BLOCK: A MANTLE PLUME ASSOCIATED WITH NUNA BREAKUP?

Wang W.[1,2], Lu G_M.[1], Cawood P.[2], Ernst R. E.[3], Huang S-F.[1], Xue E-K.[1]

[1] *China University of Geosciences, Wuhan 430074, China*
[2] *Monash University, Melbourne, VIC 3800, Australia*
[3] *Carleton University, Ottawa, Ontario K1S 5B6, Canada*

Keywords: *Yangtze Block; Late Paleoproterozoic to early Mesoproterozoic; Mafic magmatism; Mantle plume; Supercontinent breakup, Nuna*

Introduction

Proterozoic supercontinental reconstruction is crucial for understanding the long- term evolution history of the Earth, including continental crust growth, mantle evolution geodynamics, climatic change, global scale mineralization and the explosion of life. Two Proterozoic supercontinents been proposed: Nuna (also termed as Columbia) and Rodinia. During supercontinent breakup, extensive mafic magmatism can occur within and between previously connected crustal blocks. The chemical compositions of these mafic rocks can thus provide important clues for understanding the geodynamic setting of the magmatism (e.g., subduction or mantle plume) and hence the process of supercontinent breakup.

The Paleoproterozoic rock units in the Yangtze Block are tentatively incorporated within Nuna, while the absence of precise paleomagnetic data has resulted in a number of contrasting and in some cases mutually exclusive models. Voluminous late Paleoproterozoic and minor early Mesoproterozoic mafic igneous rocks, which were deemed to be produced in intracontinental rift environment, are exposed in the SW Yangtze Block and correspond to the early breakup of the Nuna supercontinent.

Results

This paper focuses on the setting of this mafic magmatism in the Dongchuan area, providing an integrated petrological, geochemical and geochronological study. This data, in combination with previously published work, suggests generation associated with a mantle plume and potentially links the Yangtze Block to contemporaneous magmatism in Siberia and Laurentia within the Nuna supercontinent.

The geochronological data reveal three episodes of mafic magmatism at ~1740 Ma, 1700 Ma and 1500 Ma. The two older generations have MORB-like Nb/Ta ratios and superchondritic Nd-Hf isotopes. In contrast, the ~1500 Ma mafic rocks possess OIB-like Nb/Ta (16.7–19.1) and Zr/Hf (41.0–45.1) ratios, εNd (t) values (-0.8 to +0.1) and εHf (t) values (-3.3 to +8.4). These three pulses of mafic magmatic activity in the Yangtze Block have geochemical features (such as high TiO2, Nb/Y and La/Yb ratios), similar to coeval mafic rocks in Siberia and Laurentia.

Conclusions

Three major episodes of mafic magmatism occurred at ca. 1740 Ma, 1700 Ma, and 1500 Ma in the southwestern Yangtze Block of South China. The 1740 Ma mafic rocks were most likely derived from asthenospheric mantle sources, with AFC process involving minor contamination of TTG-like components and fractionation of olivine, clinopyroxene and plagioclase. The 1700 Ma mafic rocks were derived from a similar mantle source, with minor contamination of SCLM and fractionation of olivine and clinopyroxene. The 1500 Ma mafic rocks originated from a deep mantle plume with negligible crustal contamination and experienced crystal fractionation of olivine, clinopyroxene and plagioclase during magma evolution.

Comparison of geochronological and geochemical data from the Yangtze with other continental blocks in Nuna suggest that two separate ~1.75 Ga mantle plumes beneath southern Siberia and northern Laurentia produced extensive mafic magmatism radiating into the Yangtze Block. Far field extensional setting under the Yangtze Block was induced by these two mantle plume activities. The ~1.5 Ga mafic magmatism in the Yangtze Block is likely linked to a shared, single mantle plume that also impacted the São Francisco–Congo Craton. The Yangtze Block was possibly the nearest neighbor to western Siberia at ~1.5 Ga and finally drifted from the Nuna supercontinent, induced by the 1.5 Ga Kuonamka mantle plume, followed by magmatic and tectonic quiescence throughout the Mesoproterozoic.

Acknowledgements

This study was supported by the, Fundamental Research Funds for the Central Universities (CUGCJ1709), MOST Special Fund from the SKLGPMR (MSFGMR 01-1). Cawood acknowledges support from Australian Research Council grant FL160100168. R. Ernst was partially supported from Mega-Grant 14.Y26.31.0012 of the government of the Russian Federation.

A POSSIBLE PLUME HEAD LOCATION OF THE PERMIAN LARGE IGNEOUS PROVINCE: CONSTRAINTS FROM MAFIC SILL PROVINCE AND DOMING STRUCTURE IN NW TARIM BLOCK

Wu H-X.[1, 2], Zhang F-Q.[1, 2], Dilek Y.[1,3], Li P.[1, 2], Chen X-X.[1, 2],
Lin X-B.[1, 2], Cheng X-G.[1, 2], Chen H-L.[1, 2]

[1] *School of Earth Sciences, Zhejiang University, Hangzhou 310027, China*
[2] *Structural Research Center of Oil & Gas Bearing Basin of Ministry of Education, Hangzhou 310027, China*
[3] *Department of Geology & Environmental Earth Science, Miami University, Oxford, OH 45056, USA*
Corresponding author: zhangfq78@zju.edu.cn

Keywords: *Tarim Large Igneous Province; earliest Permian; Mafic sill province; Doming structure; Mantle plume.*

One hypothesis suggested that the early Permian Tarim Large Igneous Province (TLIP) in Northwest China was attributed to a mantle plume. The observations that large volumes of flood basalts erupted in western half part of the Tarim block and several kimberlitic intrusions exposed in the Wajilitag area led many geologists to suggest that the plume head was probably near the NW Tarim block, while others suggested that its head was located in the northern margin. In addition, intense Mesozoic tectonism and Cenozoic overprint have significantly remolded much of the crust of the block edge.

In this work, we propose a possible plume head location of the Permian TLIP in Aksu-Wushi area, northwestern margin of the Tarim block. Extensive basic rocks over an equant area about 1800 km^2 are exposed around the Precambrian outcrops in this area. At least two layer-concordant diabase sills are redefined which used to be known as Ediacaran basaltic interlayers. Field observation shows that these layered diabase sills intruded in the lower Ediacaran reddish sandstones and mudstones. For example, the beds of Ediacaran strata are truncated by some sills locally. In addition, diabase is composed of its granular pyroxene and amphibole, and plagioclase microcrystals with automorphic lath clusters. It is a typical diabase structure in intrusive environment. The magmatic zircons separated from one of diabase sills obtained a concordia U-Pb mean age of 292±5 Ma. Our new age data shows that the diabase sills were emplaced in the earliest Permian epoch. We recommend these Permian widespread diabase sills in Ediacaran could regard as a mafic sill province as another subsurface part of TLIP. Besides, an oval doming structure also has been identified in the Aksu-Wushi area. The Aksu blue schist, as the oldest exposed basement of NW Tarim block was just in the doming center, and Cryogenian to Paleozoic sedimentary strata embraced the doming trap from inner to outside. Field mapping and seismic reflection profiles indicate that this doming structure was formed in the latest Carboniferous before the large volumes of mafic magma intrusion and eruption. We attribute this rapid and significant surface uplift, doming structure, subsequent mafic sill province emplacement and continental flood basalts eruptions during earliest Permian to the rising and giant melting above a plume head.

Acknowledgements

This study was supported by the National Natural Science Foundation of China (grant No. 41772205, 41330207; 41720104003), the National Key Research and Development Program of China (2016YFC0601004) and the National Science and Technology Major Project Fund of China (grant No. 2017ZX05008-001, 2017ZX05009-001).

A COMPARATIVE STUDY OF TWO LARGE IGNEOUS PROVINCES (SIBERIA, EMEI MOUNTAIN) IN RUSSIA AND CHINA

Yong P.

Tomsk State University, Geology and Geography Faculty, Tomsk

Keywords: *Large igntous provinces; Continental flood basalt; Mantle plume; Siberian large igneous province; Emei Mountain large igneous province.*

Introduction

A large igneous province (LIP) is an extremely large accumulation of igneous rocks, including intrusive (sills, dikes) and extrusive (lava flows, tephra deposits), arising when magma travels through the crust towards the surface. The formation of LIPs is variously attributed to mantle plumes or to processes associated with divergent plate tectonics(Bryan et al. 2008). Since the Late Permian, there have been four large igneous provinces on the Asian continent. Among them, Emei Mountain (~260 Ma) and Siberia (~250 Ma) large igneous provinces have the highest degree of research. This paper will summarize the main geological and rock geochemical characteristics of the two large igneous provinces, and highlight the activities of large igneous provinces and regional lithospheric uplifts, continental rift and stratification, bio-extinction events and large the linkages between scale mineralization events are assessed.

Results

The Siberian flood basalts and the Emei Mountain flood basalts are composed of basalt and picrite. According to Ti/Y values, they can be classified into two types of magma, high Ti/Y (HT, Ti/Y>500) and low Ti/Y (LT, Ti/Y>500). According to the Nb/La value, HT and LT lavas can be further divided into HT1 (Nb/La<1), HT2 (Nb/La≥1) and LT1 (Nb/La<1), LT2 (Nb/La≥1) 4 lava subclasses.

It is clear from Figure 2 that all the LT2 basalts that are not contaminated by the earth's crust (or lithosphere) in the Emeishan and Siberian large igneous provinces all fall

within the mantle plume defined by DEP and PM above the ΔNb line. The composition points of most of the contaminated HT1 and LTI lavas fall within the area defined by the enrichment component (EN), which represents the mantle plume source basalt contaminated by the continental crust or (and) submarine lithosphere. This suggests that LT2 basalts that are not contaminated by the earth's crust (or lithosphere) may be derived from the front of the mantle plume, while HT2 basalts (including picrites) that are not contaminated by the crust (or lithosphere) may be derived from the end of mantle plume.

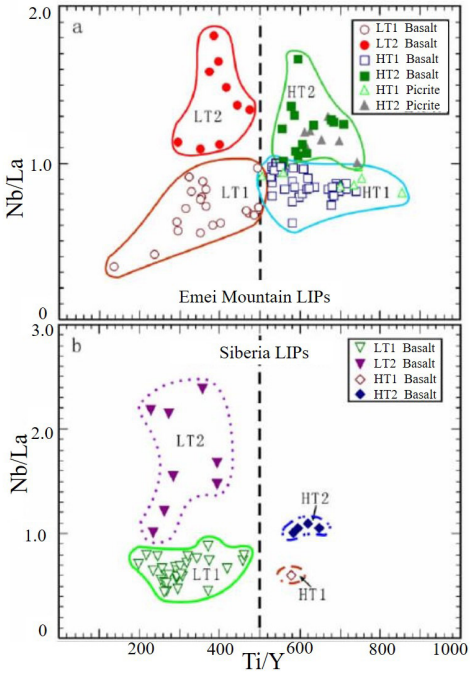


Fig 1. Classification of (a) the Emei Mountain basalts and (b) the Siberian basalts in terms of Ti/Y versus Nb/La. Data Sources: Emei Mountain: Chung and Jahn, 1995; Xu et al., 2001; Xiao et al., 2004; Wang et al., 2007; Zhang et al. 2008; Zhou et al. 2008. Siberian: Lightfoot et al., 1993; Wooden et al., 1993.

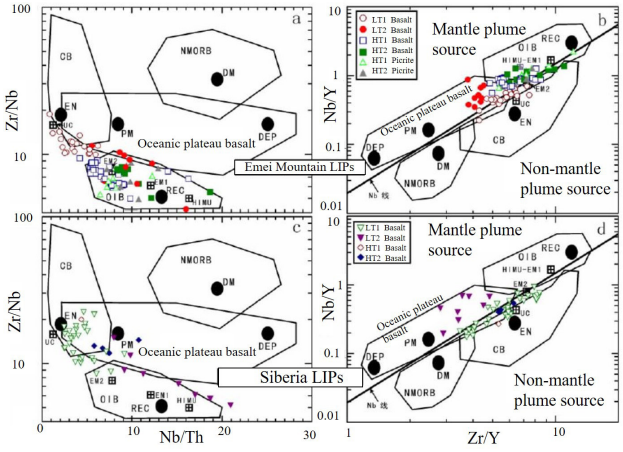


Fig 2. Distribution of (a,b) the Emei Mountain basalts and (c,d) the Siberian basalts on Nb/Th- Zr/Y , and Zr/Nb-Nb/Y disgrams (disgrams after Condie,2005). Abbreviations: UC-upper continental crust; CB-contaminated(by continental crust or/and subcontinental lithosphere) basalts; PM-primitive mantle; DM-shallow depleted mantle; HIMU-high-μ(U/Pb) source; EM1 and EM2-enriched mantle sources; OIB-oceanic island basalt; DEP-deep depleted mantle; EN-enriched component.

Conclusions

(1) These two large igneous provinces are composed of continental overflow basalts, dominated by basalt, followed by acidic rocks, and a small amount of picrite and picrite basalt, and symbiotic intrusion.

(2) Emei Mountain and Siberian Large Igneous Province contain world-class magma deposits. The existence of ore-bearing continental overflow basalts is a favorable condition for large-scale metallogenesis.

Acknowledgements

This article is based on previous research. This work needs to thank the experts who studied the Emei Mountain LIPS and the Siberian LIPS.

References

1. Bryan, S.E., Ernst, R.E.. (2008) Revised definition of large igneous provinces(LIPS). Earth-Science Reviews, 86: 175-202.
2. Chung, S.L., Jahn, B.M.. (1995) Plume-lithosphere interaction in generation of the Emeishan flood basalts at the Permian-Triassic boundary. Geology, 23: 889-892.
3. Condie, K.C.. (2005) High field strength element ratios in Archean basalts: a window to evolving sources of mantle plumes. Lithos, 79: 491-504.
4. Lightfoot, P.C., Hawkesworth, C.J., Nardrett, A.J., et al.. (1993) Remobilisation of the continental lithosphere by a mantle plume: major-, trace-element, and Sr-, Nd-, and Pb-isotope evidence from picritic and tholeiitic lavas of the Noril'k district, Siberian Trap, Russia. Contributions to Mineralogy and Petrology, 114: 171-188.
5. Wang, C.Y., Zhou, M.F., Qi, L.. (2007) Permian flood basalts and mafic intrusions in the Jinping(SW China)-Song Da(northern Vietnam) district: mantle sources, crustal contamination and sulfide segregation . Chemical Geology, 243: 317-343.
6. Wooden, J.L., Czamanske, G.K., Fedorenko, V.A., et al.. (1993) Isotopic and trace element constraints on mantle and crustal contribution to Siberian continental flood basalts, Noril'k area, Siberia. Geochim et Cosmochim Acta, 57: 3677-3704.
7. Xiao, L., Xu, Y.G., Mei, H.J., et al.. (2004) Distinct mantle sources of low-Ti and high-Ti basalts from the western Emeishan large igneous province, SW China: implications for plume-lithosphere interaction. Earth and planetary letters, 228: 525-546.
8. Xu, Y.G., Chung, S.L., Jahn, B.M.,Wu G.Y.. (2001) Petrologic and geochemical constraints on the petrogenesis of Permian-Triassic Emeishan flood basalts in southwestern China. Lithos, 58: 145-168.
9. Zhang M., O'Reilly S.Y., Wang K.L., Hronsky J., Griffin W.L., (2008) Flood basalts and metallogeny: the lithospheric mantle connection. Earth Science Review, 86: 145-174.
10. Zhou M.F., Arndt N.T., Malpas J., Wang C.Y., Kennedy A.K.. (2008) Two magma series and associated ore deposit types in the Permian Emeishan large igneous province, SW China. Lithos, 103: 352-368.

U-PB BADDELEYITE AGE OF A NE TRENDING DOLERITIC DYKE SWARM IN THE TAGRAGRA OF AKKA INLIER: ADDITIONAL CONSTRAINTS ON THE CA. 1416-1360 MA MESOPROTEROZOIC MAGMATIC EVENT(S) IN THE ANTI-ATLAS OF MOROCCO (WEST AFRICAN CRATON).

Youbi N.[1,2], Söderlund U.[3,4], Ernst R. E.[5,6], Ait Lahna A.[1],
Gong Z.[7], Evans D.[7], Wen B.[7], Jing X-Q.[7], Ait Malek M.[1],
Palassia M.[1], Boumehdi M. A.[1,2], Bensalah M. K.[1,2], Admou H.[1],
Ikenne M.[8], Cousens B.[5], El Bahat A.[9]

[1]*Department of Geology., Faculty of Sciences-Semlalia, Cadi Ayyad University, P.O. Box 2390, Marrakech, Morocco*
[2]*Instituto Dom Luiz, Faculdade de Ciências, Universidade de Lisboa, 1749-016 Lisboa, Portugal*
[3]*Department of Geology, Lund University, Sölvegatan 12, SE-223 62 Lund, Sweden*
[4]*Department of Geosciences, Swedish Museum of Natural History, SE-114 05 Stockholm, Sweden*
[5]*Department of Earth Sciences, Carleton University, 1125 Colonel By Drive, Ottawa, Canada K1S 5B6*
[6]*Faculty of Geology and Geography, Tomsk State University, 36 Lenin Ave, Tomsk 634050, Russia*
[7]*Department of Geology and Geophysics, Yale University, New Haven, Connecticut 06520, USA*
[8]*Department of Geology, Faculty of Sciences, Ibnou Zohr University, P.O. Box 28/S, Agadir, Morocco*
[9]*Managem-ONA Group, Twin Center, Tour A, Angle Bd Zerktouni & Massira Khadra, Casablanca, Morocco*

Keywords: *West African craton, Anti-Atlas, Morocco, U-Pb baddeleyite, Mesoproterozoic, Ca. 1415-1360 Ma LIP*

In the Tagragra of Akka Inlier (Anti-Atlas, West African craton, Morocco), the Paleoproterozoic basement is crosscut by numerous dykes with various trends, and mostly of uncertain age. Four baddeleyite fractions from a NE trending doleritic dyke were analyzed using the ID-TIMS U-Pb method and indicate an emplacement age of 1359 ± 6 Ma (upper intercept age, MSWD = 1.8). This age is ca. 50 Myr younger than a N40°E trending dyke in the Bas Draa inlier, dated at 1416 ± 7 Ma using the LA-ICPMS U-Pb method (Söderlund et al., 2013). This ca. 1416 Ma age replaces the previously obtained U-Pb TIMS age of 1384 ± 6 Ma (El Bahat et al., 2013), which also casts some age uncertainties for a N135°E trending dyke in the Bas Draa inlier that yielded a U-Pb ID-TIMS age of ca. 1381 ± 8 Ma (El Bahat eta l., 2013). The cause of these seemingly conflicting results between dissolution and in-situ techniques presumably relate to a complex geological history involving zircon overgrowths, as discussed by Söderlund et al. (2013). Despite these age complications, the U-Pb baddeleyites dates represent further geochronological evidence for a ca. 1416-1360 Ma Mesoproterozoic magmatic event(s) in the Anti-Atlas. The poorly dated Taghdout and Taarotihate Groups of the Anti-Atlas could represent ca. 1.4-1.3 Ga rift magmatism and associated sedimentation (Youbi et al., 2013). The Atar Group in the Taoudeni basin (Mauritania) is also a good candidate for rift-related sedimentation although it postdates the 1416-1360 Ma mafic intrusions by ca. 270 Myr. The dated ca. 1415-1360 Ma dykes have a distinct negative Nb anomaly (a common feature in many Large Igneous Provinces, LIPs), and this suggests interaction with the lithosphere, which may have occurred at the level of the lithospheric mantle or the crust. The 1416-1359 Ma dykes may converge to the north of the Bas Draa inlier, suggesting a magmatic center (mantle plume?) along the northern margin, linked to rifting and possible breakup along that margin. Contemporaneous 1380-1390 Ma LIP magmatism in northeastern Laurentia (northern Greenland), in northern Siberia (Anabar shield), and in Baltica (southern Urals) can be reconstructed with that of the Tagragra of Akka and Bas Drâa Inliers (Anti Atlas region of the West African Craton, WAC) into a single LIP extending over an area of > 1 million km^2, and associated with the final fragmentation of the Columbia (Nuna) supercontinent.

Acknowledgements

R. E. Ernst was partially supported from Mega-Grant 14.Y26.31.0012 of the government of the Russian Federation. Funding was also provided by the Hassan II Academy of Science and Technology of the Kingdom of Morocco Acad-HIIST/SDU/2016-02 (grant to Abderrazzak El Albani and Nasrrddine Youbi and others), the Swedish Research Council (2015-05875) (grant to Ulf Söderlund, Nasrrddine Youbi and Richard E. Ernst) and Yale University (grant to David Evans, Zheng Gong and others).

References

1. El Bahat A., Ikenne M., Söderlund U, Youbi, N., Ernst R. E., Soulaimani A., El Janati M., Hafid A. (2013) U-Pb ages of dolerite dykes in the Bas Drâa Inlier of the Anti-Atlas of Morocco: newly identified 1380 Ma event in the West African Craton. Lithos 174: 85-98
2. Söderlund U., Ibanez-Mejia M., El Bahat A., Ernst R. E., Ikenne M. Soulaimani A., Youbi N., Cousens B. , El Janati M, Hafid A. (2013) Reply to Comment on "U–Pb baddeleyite ages and geochemistry of dolerite dykes in the Bas-Drâa inlier of the Anti-Atlas of Morocco: Newly identified 1380 Ma event in the West African Craton" by André Michard and Dominique Gasquet Lithos 174: 101-108
3. Youbi N., Kouyaté D., Söderlund U., Ernst R. E., Soulaimani A., Hafid , A. , Ikenne M. , El Bahat A. , Bertrand H. , Rkha Chaham K., Ben Abbou M., Mortaji A., El Ghorfi M., Zouhair M. & El Janati M. (2013) The 1750 Ma Magmatic Event of the West African Craton (Anti-Atlas, Morocco). Precambrian Research Volume 236: 106–123.

CA. 1.65 GA MAFIC SILLS EMPLACED INTO THE QUARTZITE OF JBEL LKEST FROM KERDOUS INLIER, ANTI-ATLAS, WEST AFRICAN CRATON, MOROCCO: ADDITIONAL EVIDENCE THAT THE BASAL PART OF TAGHDOUT GROUP IS NEARLY 1 GA OLDER THAN PREVIOUSLY THOUGHT.

Youbi N.[1,2], Söderlund U.[3,4], Ernst R. E.[5,6], Ait Malek M.[1], Barzouk A.[1], Ait Lahna A.[1], Palassia M.[1], Gong Z.[7], Evans D.[7], Wen B.[7], Jing X-Q.[7], Boumehdi M. A.[1,2], Ikenne M.[8], Bensalah M. K.[1,2], Admou H.[1], Bajddi A.[9], Maacha L.[9]

[1]*Department of Geology., Faculty of Sciences-Semlalia, Cadi Ayyad University, P.O. Box 2390, Marrakech, Morocco*
[2]*Instituto Dom Luiz, Faculdade de Ciências, Universidade de Lisboa, 1749-016 Lisboa, Portugal*
[3]*Department of Geology, Lund University, Sölvegatan 12, SE-223 62 Lund, Sweden*
[4]*Department of Geosciences, Swedish Museum of Natural History, SE-114 05 Stockholm, Sweden*
[5]*Department of Earth Sciences, Carleton University, 1125 Colonel By Drive, Ottawa, Canada K1S 5B6*
[6]*Faculty of Geology and Geography, Tomsk State University, 36 Lenin Ave, Tomsk 634050, Russia*
[7]*Department of Geology and Geophysics, Yale University, New Haven, Connecticut 06520, USA*
[8]*Department of Geology, Faculty of Sciences, Ibnou Zohr University, P.O. Box 28/S, Agadir, Morocco*
[9]*Managem-ONA Group, Twin Center, Tour A, Angle Bd Zerktouni & Massira Khadra, Casablanca, Morocco*

Keywords: *West African craton, Anti-Atlas, Morocco, U-Pb baddeleyite, Taghdout Group, Ca. 1.65 LIP*

The Taghdout Group is a passive margin sequence deposited during rifting and break-up of the northern margin of the West African craton (WAC), culminating with the creation of an oceanic basin between the northern edge of the WAC and an unknown terrane. However, the age of this passive margin has been poorly constrained. It was previously thought to be ca. 1000-800 Ma on the basis of the age of contact metamorphism in host rocks to mafic dykes (Rb/Sr, 789 ± 10 Ma). However, new attempts to date dykes in the Anti-Atlas Inliers using U-Pb geochronology on baddeleyite have yielded ages that mostly are significantly older i.e. ca. 885, 1416-1380, 1640, 1750, and 2040 Ma (El Bahat et al., 2013; Kouyaté et al., 2013; Söderlund et al., 2013; Youbi et al., 2013). Youbi et al. (2013) proposed that the Taghdout Group could be Mesoproterozoic in age, with a suggestion for rifting at ca. 1750 Ma. In order to test this idea, two mafic sills within the basal part of the Taghdout Group were chosen for U-Pb ID-TIMS and LA-ICPMS dating on baddeleyite. One of the sills (sample 17YN47) yielded an upper intercept date of ca. 1640 Ma, constrained from ID-TIMS of three fractions. LA-ICPMS of the same sample yields a weighted mean $^{207}Pb/^{206}Pb$ date of ca. 1650 Ma, identical within analytical uncertainties to the ID-TIMS age. Only a single fraction of baddeleyite has been analyzed from the second sill, indicating a similar crystallization age of ca. 1650 Ma. These results confirm that the Taghdout Group is much older than previously thought. Further geochronology work is required to determine whether this ca. 1650 Ma age, some 50 Myr younger than the ca. 1706 ± 7 Ma obtained for mafic intrusions cross-cutting basal quartzites in the neighboring Ighrem inlier (Ikenne et al., 2017) and about 10 Myr older than the age 1639 ± 34 Ma of a thick sill intruding the basal part of the Taghdout Group in the Zenaga inlier (Ait Lahna et al., 2016), represents a new intraplate event in the WAC or belong to a long-lived 1.7-1.64 Ga LIP event across the WAC. With these results, we propose a new lithostratigraphic framework for the Proterorozoic in the Anti-Atlas.

Acknowledgements

R. E. Ernst was partially supported from Mega-Grant 14.Y26.31.0012 of the government of the Russian Federation. Funding was also provided by the Hassan II Academy of Science and Technology of the Kingdom of Morocco Acad-HIIST/SDU/2016-02 (grant to Abderrazzak El Albani and Nasrrddine Youbi and others), the Swedish Research Council (2015-05875) (grant to Ulf Söderlund, Nasrrddine Youbi and Richard E. Ernst) and Yale University (grant to David Evans, Zheng Gong and others).

References

1. Ait Lahna A, Tassinari C.C.G, Youbi N, Admou H, Mata J, Bouougri E.B, Chaib L; Ernst E.R., Söderlund U., Boumehdi M.A., Bensalah M.K, Aarab E.M. (2016) Refining the stratigraphy of the Taghdout Group by using the U-Pb Geochronology of the Taghdout Sill (Zenaga inlier, Anti-Atlas, Morocco). Special Issue: The Seventh International Dyke Conference: Dyke Swarms: Keys to Paleogeographic Reconstruction IDC7, 18–20 August, Beijing. Acta Geologica Sinica 90: 1-1
2. El Bahat A., Ikenne M., Söderlund U, Youbi, N., Ernst R. E., Soulaimani A., El Janati M., Hafid A. (2013) U-Pb ages of dolerite dykes in the Bas Drâa Inlier of the Anti-Atlas of Morocco: newly identified 1380 Ma event in the West African Craton. Lithos 174: 85-98.
3. Ikenne M., Söderlund U., Ernst R. E., Pin C., Youbi N., El Aouli E. H., Hafid A. (2017) A c. 1710 Ma mafic sill emplaced into a quartzite and calcareous series from Ighrem, Anti-Atlas-Morocco: Evidence that the Taghdout passive margin sedimentary group is nearly 1 Ga older than previously thought. Journal of African Earth Sciences 127:62-76.
4. Kouyaté, D., Söderlund, U, Youbi, N., Ernst, R., Hafid, A., Ikenne, M., Soulaimani, A., Bertrand, H., El Janati, M., Rkha Chaham, K. (2013) U-Pb baddeleyite ages of 2040

Ma, 1650 Ma and 885 Ma on dolerites in the West African Craton (Anti-Atlas inliers): possible links to break-ups of Precambrian supercontinents. Lithos 174: 71-84.
5. Söderlund U., Ibanez-Mejia M., El Bahat A., Ernst R. E., Ikenne M. Soulaimani A., Youbi N., Cousens B. , El Janati M, Hafid A. (2013) Reply to Comment on "U–Pb baddeleyite ages and geochemistry of dolerite dykes in the Bas-Drâa inlier of the Anti-Atlas of Morocco: Newly identified 1380 Ma event in the West African Craton" by André Michard and Dominique Gasquet Lithos 174: 101-108
6. Youbi N., Kouyaté D., Söderlund U., Ernst R. E., Soulaimani A., Hafid , A. , Ikenne M. , El Bahat A. , Bertrand H. , Rkha Chaham K., Ben Abbou M., Mortaji A., El Ghorfi M., Zouhair M. & El Janati M. (2013) The 1750 Ma Magmatic Event of the West African Craton (Anti-Atlas, Morocco). Precambrian Research Volume 236: 106–123.

WESTERN SIBERIA – THE LAND OF NATURAL GAS, RIFTS AND VOLCANOES SINCE TRIASSIC TO THIS DAY

Zagorovsky Y.[1,2], Galinsky K.[2], Kobylinsky D.[2], Ufelman Z.[2]

[1]*Gazprom geologorazvedka LLC, Tyumen, Russia*
[2]*Industrial University of Tyumen, Tyumen, Russia*

Keywords: *West Siberian basin, natural gas, rift, Urengoy, overpressure, gas chimneys, seismic*

Introduction

Western Siberia is known as a seismically quiet region. It is a large wetland, the surface of this huge plain is covered with terrigenous sediments. Therefore, this region is rarely considered by volcanologists as an interesting object of study. In our opinion, the subsurface volcanoes of Western Siberia worth a great deal of attention.

All the geological information (ultra-deep wells like SG-6, SG-7 and others, gravity gradiometry, magnetic survey, seismic exploration, wide angle reflection and refraction seismic data) shows that there is a system of rifts filled with basalt, tuff and other effusive rocks at the base of Western Siberia (Surkov, Zhero 1981; Khain 2001; Ulmishek 2003). Western Siberia probably was an ocean with a system of mid-ocean rifts in Triassic (Reichow et al. 2002; Cherepanova et al. 2013).

Results

If we look at the world map of the geothermal gradient, we can see that the thermal regime of the area between the Eastern European and Siberian platforms is similar to the areas of modern volcanism and seismically active regions (Smyslov et al. 1995). It is warmed up as much as the Kamchatka Peninsula and Kuril Islands, the Caucasus, the Baikal rift. So the rifts and buried volcanoes of Western Siberia are probably active, not extinct.

West Siberian sedimentary basin is one of the richest in the world by natural gas reserves. «Gazprom» company products here about 12% of world natural gas (Gazprom Annual Report 2017; BP Statistical Review 2017). Some of the largest deposits of natural gas in the world are here: Urengoy, Yamburg, Zapolyarnoye, Bovanenkovo and others. The relationship between natural gas fields and the rift system of the basin is demonstrated in picture (Figure 1). Gas-bearing uplifts are stretched folds with big amplitude and meridional orientation as the Triassic rifts (Rudkevich 1974). According to the thickness analyses they were formed in Neogene (Naumov et al. 1983).

The gas chimney seismic anomalies, push down in seismic sections across the Urengoy, Yamburg, Zapolarnoye, Kharasavey, Yurkharovskoye, Khalmerpayutinskoye and other fields (Figure 2) show the relationship between the overpressure and vertical migration of hydrocarbons, methane from the pre-Jurassic basement of West-Siberian basin (Gataulin 2003; Zagorovskiy 2015, 2017).

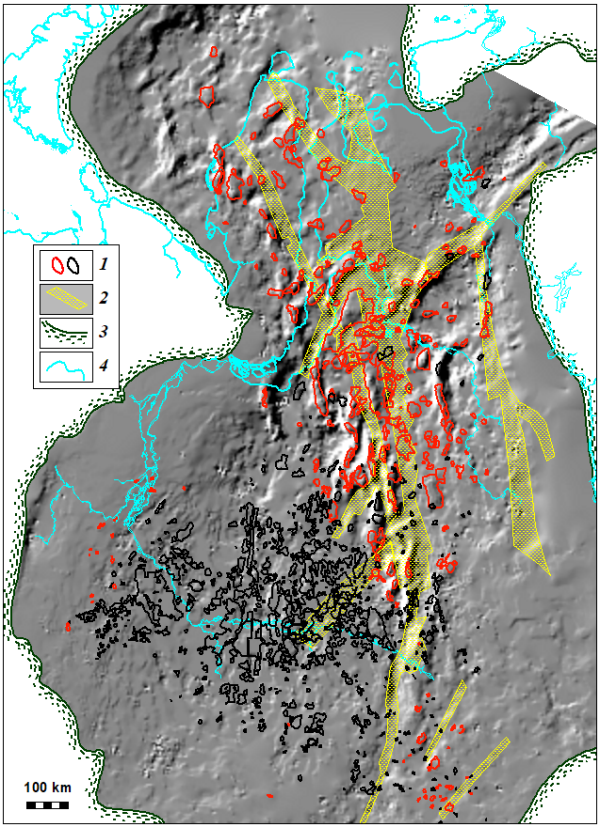


Figure 1. The surface of Cenomanian formation of West-Siberian basin (1-gas (red) and oil (black) fields; 2-big Triassic rifts (Surkov, Zhero 1981); 3-boudary of West-Siberian basin; 4-hydrography elements)

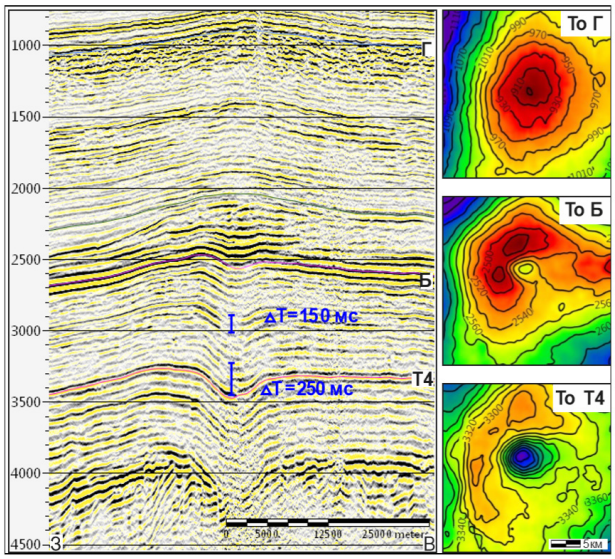


Figure 2. «Gas chimney» at seismic time section across the Yamburg gas field (Zagorovsky 2017)

Sedimentary cover is detector of these gas flows, where they create overpressure (Zagorovsky 2016). So faults along rifts could pass the vertical flows of hot water, methane and other hydrocarbon gases to form the deposits across the basin (Gold 1999; Nezhdanov et al. 2000; Zagorovsky 2017).

There are some strange seismic anomalies in the periphery of basin (Figure 3) that look like volcanic pipes (Bembel 2016, Zagorovsky 2018). According to the relationship between hydrocarbons and carbon (Gold 1999) it is possible that here we can find not only methane deposits, but also diamonds like in the nearest Krasnovishersk area of the Urals.

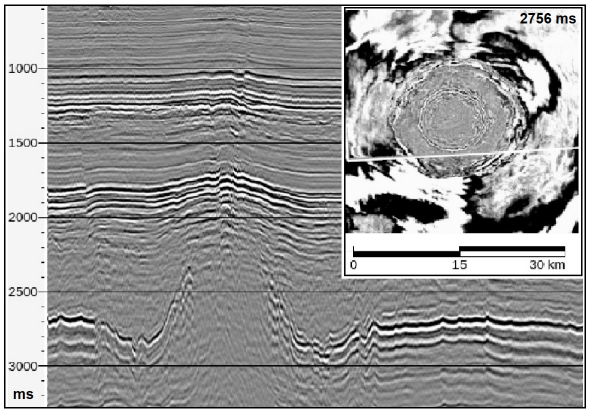


Figure 3. Seismic anomaly looks like volcanic pipe at seismic time sections in Kara Sea (Zagorovsky 2018)

Conclusions

Western Siberia is the main source of gas for Gazprom and one of the largest gas-bearing basins in the world. From the Triassic to the present day Western Siberia is a land of rifts and volcanoes, of methane seeps, creating large gas fields, as well as other natural resources.

References

1. Bembel S.R. (2016) Geology and exploring of structural features of oil and gas fields in Western Siberia. Industrial University of Tyumen, Tyumen.
2. BP Statistical Review of World Energy 2017.
3. Cherepanova Y., Artemieva I.M., Thybo H., Chemia Z. (2013) Crustal structure of the Siberian Craton and the West Siberian Basin: An appraisal of existing seismic data. Tectonophysics 609, 154-183. DOI: 10.1016/ j.tecto.2013. 05.004
4. Gataulin R.M. (2003) Seismic isometric inverse structures of West Siberia - A Nadym-Taz syneclise case study, SEG Technical Program Extended Abstracts. doi. org/10.1190/ 1.1817779
5. Gold T. (1999) The Deep Hot Biosphere / The Myth of Fossil Fuels, Springer-Verlag Inc., New York.
6. Khain V.E. (2001) Tectonics of Continents and Oceans (year 2000), Nauchnyi Mir, Moscow.
7. Naumov A.L., Onishchuk, T.M., Dyadyuk N.P. Ivaschenko A.E., Kirgintseva G.A., Romanenkov V.A. (1983) Regional tectonic restructuring and gas fields in Western Siberia. Geotectonics, 5. 67-73.
8. Nezhdanov A.A., Gorbunov S.A., Ponomarev V.A., Turenkov N.A. (2000) Geology and oil and gas potential of the Achimov formation of Western Siberia. Academy of mining Sciences, Moscow.
9. PJSC Gazprom Annual Report 2017.
10. Reichow M.K., Saunders A.D., White R.V., Pringle M.S., Al'mukhamedov A.I., Medvedev A.I., Kirda N.P. (2002) 40Ar/39Ar Dates from the West Siberian Basin: Siberian Flood Basalt Province doubled. Science 296, 1846–1849. DOI: 10.1126/science.1071671
11. Rudkevich M.Ya. (1974) Paleotectonic criteria of petroleum potential, Nedra, Moscow.
12. Smyslov A.A., Boguslavsky E.I., Boisova G.P., Vainblat A.B., Gasheva I.M., Surikov S.N. (1995) Geothermal map of Russia in 1:10000000 scale, VSEGEI, St.Petersburg.
13. Surkov V.S., Zhero O.G. (1981) Basement and Development of the Platform Cover of the West Siberian Platform, Nedra, Moscow.
14. Ulmishek G. F. (2003) Petroleum Geology and Resources of the West Siberian Basin, Russia. U.S. Geological Survey Bulletin 2201-G.
15. Zagorovskiy Y.A. (2015) Fluid-dynamic anomalies of seismic data in the fields of Western and Eastern Siberia. EAGE Geomodel 2015 - 17th science and applied research conference on oil and gas geological exploration and development, Extended Abstracts, Tu 00 11. DOI: 10.3997 /2214-4609.201413900.
16. Zagorovsky Yu.A. (2016) The correlation between fluid-dynamic process and petroleum potential of deep horizons in the North of Western Siberia. Exposition Oil & Gas magazine, 6 (52), 48-51.
17. Zagorovsky Yu.A. (2017) The role of fluid dynamic processes in the formation and location of hydrocarbon deposits in the north part of Western Siberia. Extended Abstract of Candidate (Geol.-Min.) Dissertation, Tyumen.
18. Zagorovsky Yu.A. (2018) The results of a study of Leningrad gas field and nearest areas in Kara sea by 3D seismic data and drilling of well № 3 in 2017, V Conference Earth science/Current state in Shira, Extended Abstracts, 83-85.

CA.890 MA LIP FRAGMENT IN SOUTHERN TARIM, NW CHINA

Zhang C-L.[1], Li H-K.[2], Ernst R. E.[3]

[1]*Hohai University, Nanjing, China*
[2]*University, City, Country*
[3]*Dept. of Earth Sciences, Carleton U., 1125 Colonel By Drive, Ottawa, Canada K1S 5B6*

Keywords: *ca.890 Ma LIP, Tarim, plume, Rodinia configuration.*

Introduction

The IGCP 440 Rodinia configuration in Li et al. (2008) positioned the combined São Francisco (SF)—Congo cratons (i.e., SF/Congo craton) and the North China craton at the southwestern side and northeastern side of the Laurentia, respectively. However, rifting at 920-900 Ma is recognized for the Araçuaí (Brazil), West Congo (Africa) regions and North China (Chaves et al. 2019 and references therein), which led to linking the São Francisco craton, West Congo (Africa) and North China in a Rodina configuration (Peng et al., 2015).

In this contribution we present a newly identified dismembered c. 890 Ma large igneous province (LIP) fragment in STT, NW China (herein we term it as the Sailajiazitage LIP fragment), and discuss the linkages with c. 920-890 Ma LIP magmatism of SF/Congo and North China cratons, and setting within the Rodinia supercontinent.

Results

The thickness of the volcanic sequence of the Sailajiazitage LIP fragment, mainly composed of basalts (ca. 4600 meters) and minor rhyolites (ca. 800 meters), is up to ca.5300 meters. Four zircon samples from the three layers of rhyolite at the top, middle and lower parts of the lava sequence yield consistent and concordant SHRIMP/LA-ICPMS U-Pb ages of 895.8±3.7 /892.0±4.1 Ma, 891.8±3.5/894.5±5.8 Ma, 899.0±4.6/893.0±5.9 Ma and 884.5±4.9/ 894.2±4.8 Ma, respectively, indicating the short duration of the thick volcanic sequence. Systematic geochemical data revealed that the basalts were derived from partial melting of a depleted asthenospheric mantle source coupled with variable degrees of AFC effect. The rhyolites show typical A-type (or A_1-type) granite geochemical features as demonstrated by their high HFSE contents (e.g., Zr=400-900 ppm, Nb=70-140 ppm). Both elemental and Nd-Hf-O isotope compositions argue that the silicic magma was daughter product of the intensive fractionation of the coeval basalts and their zirconium saturation temperature was up to 900ºC, significantly higher than those of A-type granites emplaced in a post-orogenic setting but consistent with those A-type granites genetically related to a mantle plume. Its huge thickness (more than 5300 meters), short duration (ca. 890 Ma) and typical continental flood basalt (CFB) geochemical features unambiguously argue for this being a fragment of an early Neoproterozoic LIP and proximal to its plume centre.

Conclusions

The c. 890 Ma age suggests a link with the previously proposed reconstruction of North China, São Francisco and Congo cratons, based on their shared 920-890 Ma LIP fragments. This study supplies further evidence for a ca. 920-890 Ma plume or superplume inducing the initial breakup of Rodinia.

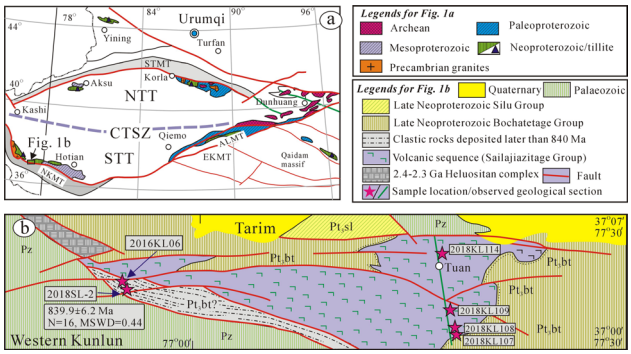


Figure. 1 (a) Tectonic framework of the Tarim Block and adjacent areas showing the Precambrian terranes along its margin, i.e., the NTT (north Tarim terrane) and STT (south Tarim terrane), of distinct Precambrian igneous rock packages may have amalgamated along the central Tarim suture zone (CTSZ) in middle Neoproterozoic (Xu et al., 2013; Zhang et al., 2016b). (b) Sketch geological map of the Sailajiazitage Group (SG) (modified after Yin et al., 2014). Note: two members are shown here, i.e., the clastic member and the volcanic member. Previous work had grouped them and collectively termed them the Sailajiazitage Group (SG). In this study, in line with their distinct rock associations and ages, the clastic member is redefined as part of the Bochatetage Formation (Pt_3bt) and is excluded from the SG group. NTT-north Tarim terrane, STT-south Tarim terrane, CTSZ-central Tarim suture zone (820-800 Ma, Xu et al., 2013; Zhang et al., 2016b).

Acknowledgements

This project is funded by the National 305 Project of China (2018A03004-1) and the Fundamental Research Fund for Central Universities (B16020127)

References

1. Chaves, A.O., Ernst, R.E., Söderlund, U.,et al., 2019. The 920-900 Ma Bahia-Gangila LIP of the Sao Francisco and Congo cratons and link with Dashigou-Chulan LIP of North China craton: new insights from U-Pb geochronology and geochemistry. Precambrian Res. In press
2. Peng, P., 2015. Precambrian mafic dyke swarms in the North China Craton and their geological implications. Sci. China Earth Sci. 58 (5), 649–675.
3. Zhang, C.L., Ye, X.T., Ernst, R.E.,et al., 2019. Revisiting the Precambrian evolution of the Southwestern Tarim Terrane: implication for its role in Precambrian supercontinents. Precambrian Res. 324, 18-31.

PETROLOGY OF CALC-ALKALINE LAMPROPHYRES IN THE EAST KUNLUN OROGENIC BELT, NORTHERN TIBET PLATEAU AND ITS IMPLICATIONS FOR MAGMA HISTORY

Zhang N., Ma C-Q.

School of Earth Sciences, China University of Geosciences, Wuhan 430074, China

***Keywords**: calc-alkaline lamprophyre; mineralogy; magma process; Tibetan Plateau*

The East Kunlun orogenic belt (EKOB) located in the northern margin of the Tibetan Plateau, is a composite orogenic belt resulted from the subduction of the Proto- and Paleo-Tethys, and terrance collision from early Plaeozoic to early Mesozoic. The orogenic history of EKOB during early Mesozoic is of considerable importance for the reconstruction of eastern Paleo-tethys because it occupies a central place in the boundary between the Gondwana and Eurasia domains. Yang et al. (2009) and Jiang et al. (1992) have distinguished Mid-Ocean Ridge Basalt (308 Ma) and island arc volcanic rocks (260 Ma) in EKOB, respectively, which may constrain the time of ocean opening and subduction. Recently, Xiong et al. (2013) have identified the syn-collisional granits (240-231 Ma) and post-collisional granitoid rocks (226-208 Ma) in EKOB, which could constrain the time of continents collision and accompanied extension in the deep lithosphere. However, mantle chemistry and magmatic evolution during orogenic processes are less well constrained.

Recently, we have identified a series lamprophyre dyke swarms in EKOB, which have zircon U-Pb geochronology of 253.0 ± 2.5 Ma. These dykes are enriched in large-ion lithophile elements (e.g., K, Rb, Sr, Ba) and light rare-earth elements, but depleted in high-field-strength elements (e.g., Ta, Nb, P and Ti), and have enriched Sr-Nd-Hf isotopic compositions ($(^{87}Sr/^{86}Sr)_i$ = 0.70883 ~ 0.71045, $\varepsilon_{Nd}(t)$ = -5.51 ~ -5.72, εHf(t) = -4.42 ~ -0.38). Geochemical studies show that the dykes were derived from enriched lithospheric mantle that has been metasomatized by subduction-related fluid. The lamprophyre is thus regarded as a useful probe to metasomatic lithospheric mantle.

According to the classification scheme of Rock (1987), the studied lamprophyres are spessartite with euhedral amphibole phenocrysts. Plagioclase is essentially confined to the groundmass. Minerals respond texturally and compositionally to changing magmatic environments, so they can, in their crystal growth stratigraphy preserve a wealth of information regarding their past history of magmatic processes (e.g., Streck, 2008). Therefore, investigations of mineral textures, compositional zoning and linked thermobarometer from core to rim of the crystals provide a window into the magmatic evolution.

Amphiboles are present as phenocrysts and groundmass. The core of phenocrysts has much higher contents of MgO, CaO and Na_2O and lower contents of FeO than the rim. Most of the cores can be classified as magnesiohastingsite with Mg# [(Mg# = atomic ratios Mg/(Mg+Fe)] varies from 62 to 68 (Leake et al. 1997), while most rims of phenocrysts are ferropargasite with Mg#<50. This change is recorded as the chemical zoning, which indicates that a Fe-rich, Si-rich, Mg-poor and Ca-poor magma appeared later. The amphiboles in groundmass have compositions similar to those in the rims of phenocrysts, with varing Mg# from 29 to 69. Two types of plagioclase are identified, i.e., zoned plagioclase and unzoned plagioclase. The cores of zoned plagioclase are compositionally identical to the unzoned plagioclase (~An_{68-83} and An_{66-89}, respectively), which is in equilibrium with their parental magma, indicating their mantle origin. However, the composition of the rim in zoned plagioclase varies from An_{43} to An_{65}, which is much lower than that in the core. Furthermore, because the crystal composition in a magma mainly depends on crystallization conditions, such crystals provide us with a record of the magma conditions (pressure and temperature) in the magma chamber. “Normal” zoning in plagioclase is a monotonous change from a high-temperature Ca-rich composition in the core to a lower-temperature Na-rich composition at the rim (decreasing from 1150 to 950). This compositional change suggests cooling and chemical differentiation of the lamprophye magma. The Al content in hornblende is a useful geobarometer for appropriate plutonic and volcanic rocks, since a positive correlation exists between total pressure and the Al content of hornblende in certain assemblages o f minerals and silicate melt. The “Normal” zoning of amphibole phenocrysts show decreasing in aluminum from core to rim, indicating that decompression during magma ascending further promoted the crystallization of phenocrysts, with pressure decreasing from 9.2~11.4 kbar to 7.8~8.2 kbar. This study shows that porphyritic rocks can actually contain two type minerals with phenocryst cores in chemical equilibrium with their primary magma, and the matrix and phenocryst rims just reflecting an evolved magmatic system.

IDENTIFICATION OF AN EARLY NEOPROTEROZOIC GABBRO SILL FROM THE GUYANG AREA IN THE NORTHWESTERN NORTH CHINA CRATON: IMPLICATIONS FOR BREAKUP OF THE NCC IN THE RODINIA SUPERCONTINENT

Zhang Q-Q.[1], Zhang S-H.[1,2], Zhao Y.[1,2]

[1] *Institute of Geomechanics, Chinese Academy of Geological Sciences, Beijing, China*
[2] *Key Laboratory of Paleomagnetism and Tectonic Reconstruction, Ministry of Natural Resources, Beijing, China*

Keywords: *Neoproterozoic; Mafic sill; North China Craton (NCC); Rodinia supercontinent*

Introduction

Since the conception of Rodinia supercontinent was proposed during 1990s, many different reconstructions have been proposed (Dalziel, 1991; Hoffman, 1991; Condie, 2001; Li et al., 2008). As one of the oldest cratons in the world, whether or how the North China Craton (NCC, or Sino-Korean Craton) was involved in the amalgamation and breakup of the Rodinia supercontinent and its position within the Rodinia supercontinent remains unclear or controversial due to limited exposures of late Mesoproterozoic-early Neoproterozoic tectonism and magmatism in the NCC (Zhai et al., 2003; Lu et al., 2008). In recent years, numerous early Neoproterozoic mafic magmatism in the central and southeastern North China Craton have been identified (Fig. 1), including: (1) Xu-Huai mafic sills in the southeastern NCC (Liu et al., 2006; Wang et al., 2012); (2) Dalian mafic sills in the Liaodong Peninsula (Zhang et al., 2016); (3) Sariwon mafic sills in the Korean Peninsula (Peng et al., 2011a); (4) Dashigou mafic dykes in the central NCC (Peng et al., 2011b). These mafic sills and mafic dykes constitute an early Neoproterozoic large igneous province in the North China Craton (Peng et al., 2011b; Zhang et al., 2016).

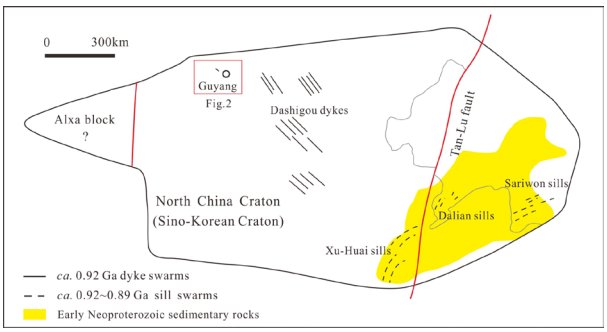


Figure. 1. A reconstruction map showing distribution of the early Neoproterozoic mafic sills and mafic dykes in the North China Craton (Sino-Korean Craton) during the early Neoproterozoic period (modified after Peng et al., 2011b; Zhang et al., 2016)

In this presentation, we present new zircon U-Pb ages, major and trace element dates for a newly identified early Neoproterozoic gabbro sill from the Guyang area in the northwestern NCC. The gabbro sill emplaced into the Agulougou Formation within the Zhaertai Group in the Guyang area, show plank or wedge-shaped with a thickness about 6 meters (Fig. 2a and 2c), and the length of it over 130 meters. The gabbro was suffered from greenschist-facies metamorphism and the hosting rocks have experienced intensive marbleization (Fig. 2b).

Results

Zircon U-Pb ages

Two gabbro sample (16148-1 and 16148-1R) were collected and the results of their LA-ICP-MS zircon U-Pb analyses are plotted on concordia diagrams in Fig. 3. Twice LA-ICP-MS U-Pb dating of the sample 16148-1 at the State Key Laboratory of Geological Processes and Mineral Resources, China University of Geosciences, Wuhan (Fig. 3a and 3b) and the Wuhan Sample Solution Analytical Technology Company Limited (Fig. 3c and 3d), respectively. LA-ICP-MS U-Pb dating of the sample 16148-1R at the Wuhan Sample Solution Analytical Technology Company Limited (Fig. 3e and 3f). Zircon LA-ICP-MS U-Pb dating on two gabbro samples yields emplacement ages of 940~900 Ma.

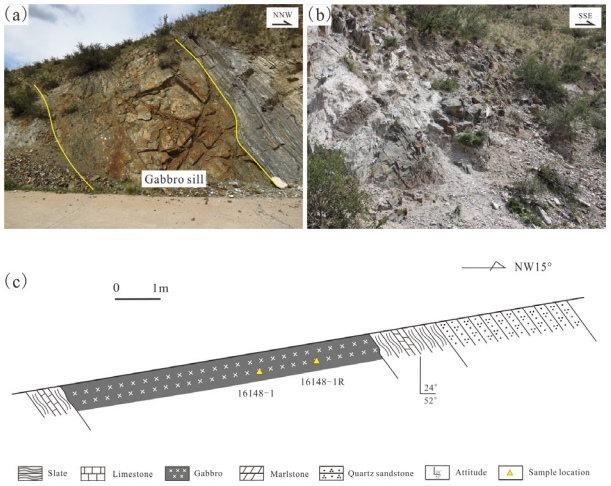


Figure. 2. Representative outcrop photographs (a, b) and geological sections (c) of the gabbro sill emplaced into the Agulugou Formation in the Guyang area.

Major and trace element compositions

The gabbros are characterized by low SiO_2 (45.8–47.9 wt.%), high TiO_2 (2.79–3.14 wt.%), TFe_2O_3 (12.60–14.97 wt.%), MgO (3.61–6.33 wt.%). They display weak enrichment in LREE (La_N/Yb_N=3.62–4.02) and weak negative Eu anomalies (Eu_N/Eu_N*=0.75–0.92) and enrichment in Rb, Th, U, La and Ce and depletion in Ba, Nb, Ta and Sr. They belong to subalkaline and tholeiitic series.

The early Neoproterozoic gabbro sill in the Guyang area exhibits similar geochemical compositions to those of the early Neoproterozoic Dashigou mafic dykes in the central NCC and the mafic sill swarms (Xu-Huai-Dalian-Sariwon diabase sills) in the southeastern NCC.

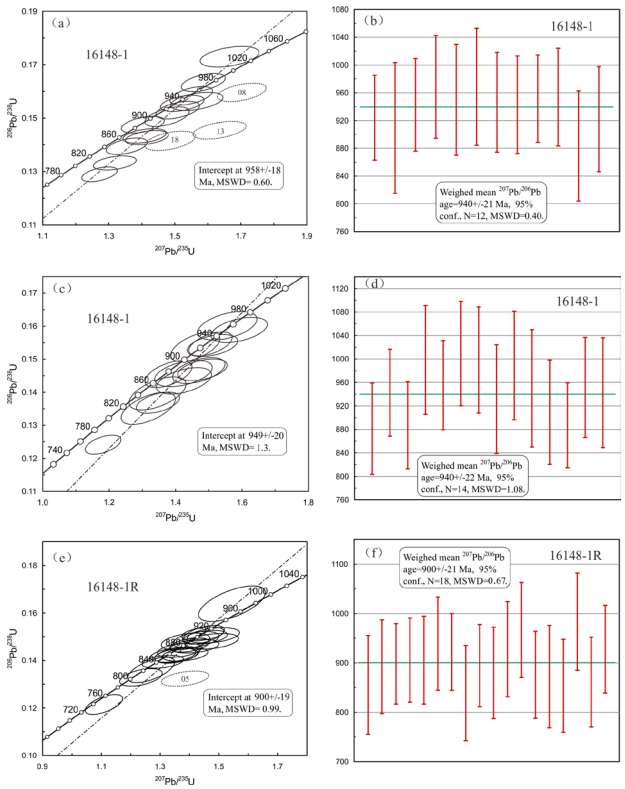


Figure. 3. LA-ICP-MS U-Pb concordia diagrams of the zircons from the gabbro samples.

Conclusions

The 940~900 Ma gabbro sill from the Guyang area in the northwestern NCC is most likely the northwestern extension of the contemporary mafic magmatism in the central and southeastern NCC, and it is part of the early Neoproterozoic large igneous province in the NCC. Formation of the rifting and large igneous province is usually associated with breakup of the supercontinent (Ernst et al., 2008; Li et al., 2008). In spite of Li et al. (2008) suggested that the breakup of the main continents of the Rodinia supercontinent at Mid-Neoproterozoic, we inferred that the early Neoproterozoic large igneous province in the NCC may represent the earliest mafic magmatism record of the breakup of the Rodinia supercontinent.

Acknowledgements

This research was financially supported by the National Natural Science Foundation of China (41725011).

References

1. Condie, K.C. (2001) Continental growth during formation of Rodinia at 1.35–0.9 Ga. Gondwana Research 4 (1): 5-16
2. Dalziel, I.W.D. (1991) Pacific margins of Laurentia and East Antarctica-Australia as aconjugate rift pair: evidence and implications for an Eocambrian supercontinent. Geology 19: 598-601
3. Hoffman, P.F. (1991) Did the breakout of Laurentia turn Gondwanaland inside-out? Science 252: 1409-1412
4. Ernst. R.E., Wingate, M.T.D., Buchan, K.L., Li, Z.X. (2008) Global record of 1600–700 Ma Large Igneous Provinces (LIPs): implications for the reconstruction of the proposed Nuna (Columbia) and Rodinia supercontinents. Precambrian Research 160: 159-178
5. Li, Z.X., Bogdanova, S.V., Collins, A.S., Davidson, A., De Waele, B., Ernst, R.E., Fitzsi-mons, I.C.W., Fuck, R.A., Gladkochub, D.P., Jacobs, J., Karlstrom, K.E., Lu, S., Natapov, L.M. Pease, V., Pisarevsky, S.A., Thrane, K., Vernikovsky, V. (2008) Assembly, configuration, and break-up history of Rodinia: a synthesis. Precambrian Research 160: 179-210
6. Liu, Y.Q., Gao, L.Z., Liu, Y.X., Song, B., Wang, Z.X. (2006) Zircon U-Pb dating for the earliest Neoproterozoic mafic magmatism in the southern margin of the North China Block. Chinese Science Bulletin 51: 2375-2382
7. Lu, S.N., Zhao, G.C., Wang, H.C., Hao, G.J. (2008) Precambrian metamorphic basement and sedimentary cover of the North China Craton: a review. Precambrian Research 160: 77-93
8. Peng, P., Zhai, M.G., Li, Q.L., Wu, F.Y., Hou, Q.L., Li, Z., Li, T.S., Zhang, Y.B. (2011a) Neoproterozoic (~900 Ma) Sariwon sills in North Korea: Geochronology, geochemistry and implications for the evolution of the south-eastern margin of the North China Craton. Gondwana Research 20: 243-254
9. Peng, P., Bleeker, W., Ernst, R.E., Söderlund, U., McNicoll, V. (2011b) U-Pb baddeleyite age distribution and geochemistry of 925 Ma mafic dykes and 900 Ma sills in the North China craton: Evidence for a Neoproterozoic mantle plume. Lithos 127: 210-221
10. Wang, Q.H., Yang, D.B., Xu, W.L. (2012) Neoproterozoic basic magmatism in the southeast margin of North China Craton: Evidence from whole-rock geochemistry, U-Pb and Hf isotopic study of zircons from diabase swarms in the Xuzhou-Huaibei area of China. Science China-Earth Sciences 55 (9): 1461-1479
11. Zhai, M.G., Shao, J.A., Hao, J., Peng, P. (2003) Geological signature and possible position of the North China Block in the supercontinent Rodinia. Gondwana Research 6 (2): 171-183
12. Zhang, S.H., Zhao, Y., Ye, H., Hu, G.H. (2016) Early Neoproterozoic emplacement of the diabase sill swarms in the Liaodong Peninsula and pre-magmatic uplift of the southeastern North China Craton. Precambrian Research 272: 203-225

POTENTIAL ENVIRONMENTAL EFFECT OF LARGE-SCALE CA. 1.32 GA MAFIC SILL EMPLACEMENT IN THE NORTH CHINA AND NORTHERN AUSTRALIAN CRATONS

Zhang S-H., Shui G-H., Hu G-H., Zhang Q-Q., Zhao Y., Pei J-L.

Institute of Geomechanics, Chinese Academy of Geological Sciences, MNR Key Laboratory of Paleomagnetism and Tectonic Reconstruction, China

Keywords: *Black shales, dolerite sills, contact metamorphism, environmental effect, Xiamaling Formation, North China Craton*

Introduction

Recent results show that emplacement of large-scale Phanerozoic mafic sills into carbonate, evaporate, coal or organic-rich black shales can generate large quantities of greenhouse and toxic gases (CO_2, CH_4, SO_2), which resulted in global warming and mass extinctions (e.g., Ganino and Arndt, 2009; Heimdal et al., 2018, 2019; Svensen et al., 2018). For Phanerozoic large igneous provinces (LIPs) coinciding with mass extinctions, it seems that release of sediment-derived gases had a far greater impact on the environment and mass extinctions than the emission of magmatic gases (Ganino and Arndt, 2009).

The 1.33–1.30 Ga Yanliao large igneous province in the North China Craton (NCC) consists mainly of dolerite sills intruded into the black shales of the Xiamaling Formation and dolomite of the Wumishan and Gaoyuangzhuang Formations (Zhang et al., 2017). The sills are distributed over a region that is >600 km long and >200 km wide, with areal extent >1.2´10^5 km^2 and cumulative thickness of the sills in any one area ranging from 50 m to >1800 m. Paleomagnetic and geological evidences indicate that the Yanliao LIP in the NCC and the Derim Derim–Galiwinku LIP in the McArthur Basin in the Northern Australian Craton (NAC) represent separated fragments of the same LIP (Zhang et al., 2012, 2017). The ca. 1.32 Ga Derim Derim–Galiwinku LIP in the NAC is composed of dolerite Derim Derim sills and Galiwinku dykes that are distributed over an area that is >600 km long and >400 km wide, with areal extent >2.4´10^5 km^2. The Derim Derim sills are very common within the black shales of the Velkerri Formation. Both the middle part of the Xiamaling Formation in the NCC and the Velkerri Formation in the NAC are organic-rich black shales with total organic carbon (TOC) concentrations of 2 to 20 wt.% (Zhang et al., 2016; Wang et al., 2017) and 0.08 to 29.93 wt.% with an average value of 3.76 wt.% (Revie, 2017), respectively.

Results

Our field investigation results show that hornfelsing and decarbonation zones between the ca. 1.32 Ga dolerite sill and Xiamaling black shales in Wulongji and Renjiazhuang sections near Chengde are 4 to 6 meters in thickness (Figures 1 and 2). The contact metamorphism and marble zones due to emplacement of dolerite sills into dolomites of the Wumishan and Gaoyuzhuang formations are around 50 meters thick (Figure 3). Since the magmatic and plume centre of the Yanliao LIP is located in the northeastern part (Zhang et al., 2017), the thickness of the hornfelsing and decarbonation zones between dolerite sill and Xiamaling black shales decreases from northeast (4 to 6 meters) to southwest (10 to 20 centimeters), due to decrease of magma temperatures from magmatic centre to its margins.



Figure 1. Hornfelsing and decarbonation zone between the ca. 1.32 Ga dolerite sill and Xiamaling black shales in Wulongji, Chengde.



Figure 2. Hornfelsing and decarbonation zone between the ca. 1.32 Ga dolerite sill and Xiamaling black shales in Renjiazhuang, Chengde.

Conclusions

Emplacement of large volume of ca. 1.32 Ga dolerite sills in the Yanliao LIP into the black shales of the Xiamaling Formation and dolomite of the Wumishan and Gaoyuangzhuang Formations in the NCC most likely generated huge amounts of greenhouse and toxic gases (CO_2, CH_4, SO_2), which may have significant effects on atmosphere and oceans. If the ca. 1.32 Ga Derim Derim–Galiwinku LIP in the NAC is considered together, emplacement of the large-scale ca. 1.32 Ga dolerite sills in the NCC and NAC may have great impact on global atmosphere and ocean environment.



Figure 3. Contact metamorphism and marble zone due to emplacement of dolerite sills into dolomite of the Wumishan Formation near Chaoyang.



Figure 4. Marbles near the intrusive contact between dolerite sills and dolomite of the Wumishan Formation near Chaoyang.

Acknowledgements

This research was financially supported by the National Natural Science Foundation of China (41725011) and the Chinese Academy of Geological Sciences fundamental research fund (YYWF201718).

References

1. Ganino C., Arndt N.T. (2009). Climate changes caused by degassing of sediments during the emplacement of large igneous provinces. Geology 37: 323–326.
2. Heimdal T.H., Svensen H.H., Ramezani J., Iyer K., Pereira E., Rodrigues R., Jones M.T., Callegaro S. (2018). Large-scale sill emplacement in Brazil as a trigger for the end-Triassic crisis. Scientific Reports, 8: 141.
3. Heimdal T.H., Callegaro S., Svensen H.H., Jones M.T., Pereira E., Planke, S. (2019). Evidence for magma–evaporite interactions during the emplacement of the Central Atlantic Magmatic Province (CAMP) in Brazil. Earth and Planetary Science Letters 506: 476–492.
4. Revie D. (2017). Unconventional petroleum resources of the Roper Group, McArthur Basin: Northern Territory Geological Survey, Record 2017-002, 64 p.
5. Svensen H.H., Frolov S., Akhmanov G.G., Polozov A.G., Jerram D.A., Shiganova O.V., Melnikov N.V., Iyer K., Planke S. (2018). Sills and gas generation in the Siberian Traps. Phil. Trans. R. Soc. A 376: 20170080.
6. Wang X., Zhang S., Wang H., Bjerrum C.J., Hammarlund E.U., Haxen E.R., Su J., Wang Y., Canfield D.E. (2017). Oxygen, climate and the chemical evolution of a 1400 million year old tropical marine setting. American Journal of Science 317: 861–900.
7. Zhang S.C., Wang X.M., Wang H.J., Bjerrum C.J., Hammarlund E.U., Costa M.M., Connelly J.N., Zhang B.M., Su J., Canfield D.E. (2016). Sufficient oxygen for animal respiration 1,400 million years ago. Proceedings of the National Academy of Sciences of the United States of America 113: 1731–1736.
8. Zhang S., Li Z., Evans D.A.D., Wu H., Li H., Dong J. (2012). Pre-Rodinia supercontinent Nuna shaping up: A global synthesis with new paleomagnetic results from North China. Earth and Planetary Science Letters 353–354: 145–155.
9. Zhang S.H., Zhao Y., Li X.H., Ernst R.E., Yang Z.Y. (2017). The 1.33–1.30 Ga Yanliao large igneous province in the North China Craton: Implications for reconstruction of the Nuna (Columbia) supercontinent, and specifically with the North Australian Craton. Earth and Planetary Science Letters 465: 112–125.

NORTH CHINA CRATON IN NUNA/COLUMBIA SUPERCONTINENT DURING THE LATE PALEOPROTEROZOIC: IMPLICATIONS FROM THE LARGE IGNEOUS PROVINCE

Zhao Y.[1,2], Wang W.[1,2], Pei J-L.[1,2], Cai Y-H.[1,2], Zhang S-H.[1,2]

[1] *Institute of Geomechanics, Chinese Academy of Geological Sciences, Beijing, China*
[2] *Key Laboratory of Paleomagnetism and Tectonic Reconstruction, Ministry of Natural Resources, Beijing, China*

Keywords: *Late Paleoproterozoic; Large igneous province; North China Craton (NCC); Nuna/Columbia supercontinent*

Introduction

In this presentation we review the recent progress on the evolution of the North China Craton during the late Paleoproterozoic period, base on the new investigation on the 1.75–1.68 Ga igneous suite, ca. 1.78 Ga large igneous province and the basement of the Ordos Basin.

The basement of the Ordos Basin was basically Paleoproterozoic in age, with minor Archean component (Hu et al., 2013; Wan et al., 2013; Wang et al., 2014; Zhang et al., 2015). The Paleoproterozoic basement documented a complete cycle from prograde burial-heating to retrograde exhumation-cooling and shed new light on the evolution of the North China Craton (Wang et al., 2019). The new paleomagnetic poles at

1.63 Ga and 1.68 Ga were obtained from the extensive late Paleoproterozoic mafic dyke swarms in western Shandong Province in Eastern block of the North China Craton and were suggested as a key pole and a reference pole, at 20.8° N, 182.5° E (k=28.3, A95=8.3°, N=9) and at 17.8° N, 184.9° E (k=29.6, A95=14.3°, N=5) respectively (Cai et al., 2019, under review), which were selected to depict a more detailed apparent polar wander path (APWP) for comparison of the North China Craton with other main Paleo-Mesoproterozoic cratons. Combined with other coeval paleomagnetic poles of Laurentia, Baltica, Siberia, North Australian and India cratons as well as geological evidence, our scenario supports the potentially temporal and spatial connections between North China, North Australian, Siberia and Baltica Cratons. The 1.75–1.68 Ga igneous suite and ca. 1.78 Ga large igneous province in the North China Craton were most likely post-assembled large igneous provinces related to rifting.

Acknowledgements

This research was financially supported by the National Natural Science Foundation of China (41725011) and the Chinese Academy of Geological Sciences fundamental research fund (YYWF201718).

References

1. Cai, Y.-H., Pei, J.-L., Zhang, S.-H., Tong, Y.-B., Yang, Z.-Y., Zhao, Y. (2019) New paleomagnetic results from the ca. 1.68–1.63 Ga mafic dyke swarms in Western Shandong Province, Eastern North China Craton: Implications for the reconstruction of the Columbia Supercontinent. Precambrian Research, under review.
2. Hu, J.M., Liu X.S., Li, Z. H., Zhao, Y., Zhang, S. H., Liu, X. C., Qu, H. J., Chen, H., 2013. SHRIMP U-Pb zircon dating of the Ordos Basin basement and its tectonic significance. Chinese Science Bulletin 58(1): 118–127.
3. Wan, Y.S., Xie, H.Q., Yang, H., Wang, Z.J., Liu, D.Y., Kröner, A., Wilde, S.A., Geng, Y.S., Sun, L.Y., Ma, M.Z., Liu, S.J., Dong, C.Y., Du, L.L. (2013) Is the Ordos Block Archean or Paleoproterozoic in age? Implications for the Precambrian evolution of the North China Carton. American Journal of Science 313: 683–711.
4. Wang, W., Liu, X.S., Hu, J.M., Li, Z.H., Zhao, Y., Zhai, M.G., Liu, X.C., Clarke, G., Zhang, S.H., Qu, H.J. (2014) Late Palaeoproterozoic medium-P high grade metamorphismof basement rocks beneath the northern margin of the Ordos Basin, NW China: petrology, phase equilibrium modeling and U–Pb geochronology. Precambrian Research 251: 181–196.
5. Wang, W.-(RZ), Zhao, Y., Liu, X.-C., Hu, J.-M., Wei, C.-J., Xiao, W.-J., Du, J.-X., Wang, S.-L., Zhan, L.-Q. (2019) Metamorphism of diverse basement gneisses of the Ordos Basin: Record of multistage Paleoproterozoic orogenesis and constraints on the evolution of the western North China Craton. Precambrian Research 328: 48–63.
6. Zhang, C.L., Diwu, C.R., Kröner, A., Sun, Y., Luo, J., Li, Q., Gou, L.L., Lin, H, Wei, X. Zhao, J. (2015) Archean-Paleoproterozoic crustal evolution of the Ordos Block in the North China Craton: constraints from zircon U–Pb geochronology and Hf isotopes for gneissic granitoids of the basement. Precambrian Research 267, 121–136.

TEMPORAL EVOLUTION OF THE PANXI-HANNAN ARC IN SOUTH CHINA

Zhao J-H.

State Key Laboratory of Geological Processes and Mineral Resources, School of Earth Sciences, China University of Geosciences, Wuhan 430074, China. Email address: jhzhao@cug.edu.cn

Keywords: *Gabbro, Hf-O-Nd isotopes, Neoproterozoic, South China, Rodinia*

Fluids and melts derived from subducted oceanic slabs will chemically modify mantle wedges, but how mantle sources are temporally evolved is difficult to be constrained. We carried out in situ zircon U-Pb age and Hf-O isotope analyses for the Neoproterozoic mafic intrusions from the Panxi-Hannan arc in western margin of the Yangtze Block to examine a coupled evolution of magmas and mantle sources above a subduction zone. The results show that the mantle wedge was progressively modified by slab fluids, sediment melts and altered oceanic crust (AOC) melts. The 870-Ma gabbros have normal δ18O (4.79‰ to 6.07‰), high εHf (+10.4 to +15.0) and εNd (+4.0 and +6.4), and were derived from a mantle wedge enriched by slab fluids. The 860-840-Ma gabbros have overall relatively high δ18O (5.61‰ to 7.42‰), variable εHf (-3.5 to +15.0) that are decoupled from εNd (+1.85 to +3.87), and were sourced from a mantle wedge modified by sediment melts. However, the 820-780-Ma gabbros have relatively low δ18O (4.22 ‰ to 5.49‰), and constant εHf (+4.7 to +9.6) that are decoupled from εNd (-0.52 to +1.92), which could be explained by a mantle source contaminated by 18O-depleted AOC melts.

Similar Neoproterozoic magmatism also occurred in Greater India and Madagascar, suggesting a giant Andean-type arc system existed along the western margin of Rodinia. In this arc system, mantle-derived magmas were dominated by an arc-affinity in the earlier stage before 820 Ma and became rift-related after that, reflecting regional slab tearing and breakoff.

Our study also provides evidence for the linkage between the marginal subduction and the internal rifting in Rodinia, and suggest that slab breakoff probably triggered its breakup. These findings are inconsistent with the mantle plume model which proposed that a giant mantle plume induced the Neoproterozoic magmatism in South China and breakup of the supercontinent.

PARTIAL MELTING OF AN ANCIENT SUB-CONTINENTAL LITHOSPHERIC MANTLE IN THE EARLY PALEOZOIC INTRACONTINENTAL REGIME AND ITS CONTRIBUTION TO PETROGENESIS OF THE COEVAL PERALUMINOUS GRANITES IN SOUTH CHINA

Zhong Y-F., Wang L-X., Zhao J-H.

School of Earth Sciences, China University of Geosciences, Wuhan, 430074, China

Introduction

The appinite–granite association has been found in various tectonic regimes related to recent subduction, arc-continent or continent–continent collision and post-collision (orogen), and appinites generally originate from recently subduction-modified lithospheric mantle. Weconducted a study on a rarely reported appinite–granite association formed in an intracontinental regime, the Zhangjiafang–Qinglongshan complex (ZQC), in which the appinites were derived from an ancient sub-continental lithospheric mantle (SCLM).

Results

The ZQC is located in the western Wugongshan domain, and consists of basaltic to intermediate appinites and granitoids(Fig.1-2).

Ten dated samples (including massive and gneissoid granitoids, hornblende gabbro, and diorite) give zircon $^{206}Pb/^{238}U$ ages ranging from444±3 Ma to 452±4 Ma, indicating that these various lithologies were emplaced synchronously.

The basaltic appinites show radiogenic $^{87}Sr/^{86}Sr_i$ (0.71016–0.71431) and negative εNd(t) (−6.1 to−8.9) and zircon εHf(t) (−4.2 to −7.5) values. Combined with regional geological background, an origin from the Neoproterozoic metasomatised SCLM can be inferred for the appinites in the Wugongshan domain. The granitoids are peraluminous and almost high-K calc–alkaline to shoshonitic. They exhibit a wide range of isotopic compositions ($^{87}Sr/^{86}Sri$=0.70828–0.71857, εNd(t)=−6.2 to−10.5, zircon εHf(t)=−9.5 to−26.6). Some of the granitoids display the most evolved Sr–Nd isotopic signatures among all the studied lithologies, which are consistent with those of the middle to upper crust, suggesting a pure crustal origin. Other granitoids show relatively mafic composition and less evolved isotopic signature. The intermediate appinites have intermediate chemical compositions between those of the basaltic appinites and granitoids, and similar Sr–Nd isotopic compositions to those of the basaltic appinites that have relatively evolved composition and isotopic signature.

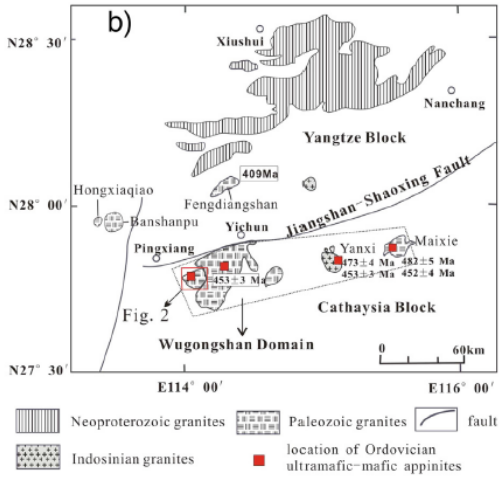


Fig.1 Distribution of the early Paleozoic magmatisms in the middle part of the suture zone between the Yangtze and Cathaysia blocks.

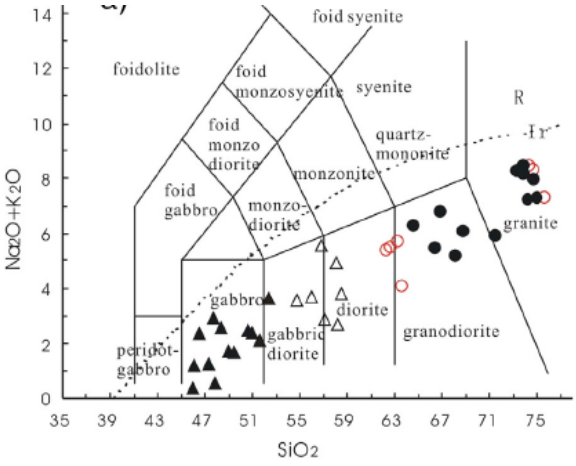


Fig.2 Lithological nomenclature for samples from the Zhangjiafang–Qinglongshan complex on the basis of the plutonic TAS diagram of Middlemost (1994).

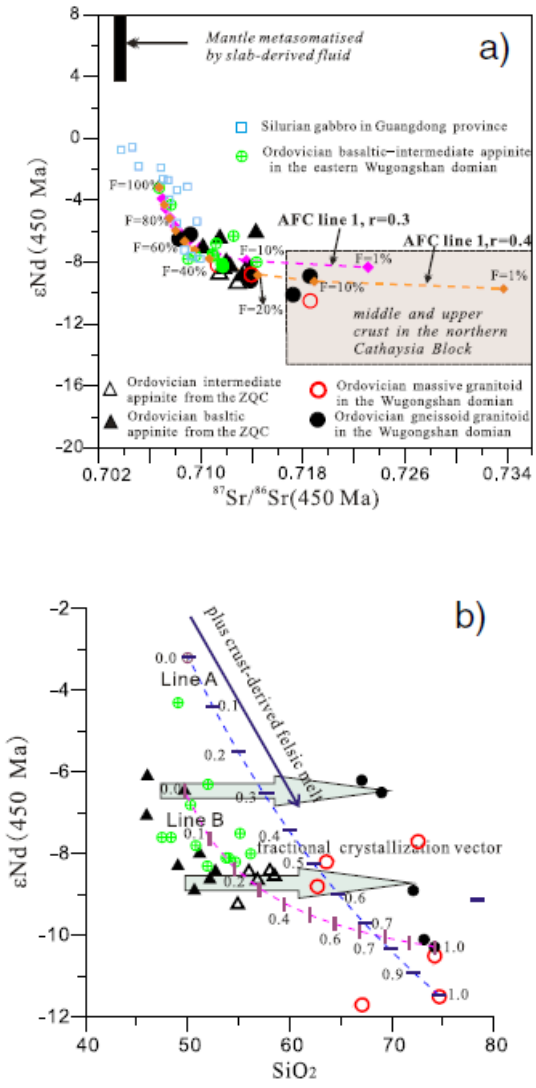


Fig.3 (a) Initial Sr–Nd isotopic compositions of the appinites and granitoids from the ZQC. (b) A plot of εNd (t) vs. SiO_2, showing trends of fractional crystallization and magma mixing and mingling.

For line A, the mafic magma is represented by sample 9JH54-2 (which has the least evolved Sr and Nd isotope among all the basaltic appinites in the Wugongshan domain) and the felsic magma by 9JH49 (SiO_2 = 74.52%, εNd(t) = −10.1), respectively. For line B, the mafic magma is represented by sample 11JX33 (which has the least evolved Sr and Nd isotope among all the basaltic appinites from the ZQC) and the felsic melt by sample WG41(SiO2=74.66%, εNd(t) = −11.5).

Conclusions

The petrographical and the geochemical studies, as well as magma mixing and mingling between mafic magma and felsic magma observed in fieldwork, indicate that the ZQC was formed by several complex magmatic processes including assimilation and fractional crystallization (AFC) of a basaltic magma derived from an enriched mantle, magma mixing and mingling, fractional crystallization of a crust-derived felsic magma. The contribution of the Neopreoterozoic subduction-modified lithospheric mantle to the early Paleozoic granitoids in South China has been poorly constrained due to its evolved isotopic signatures (such as negative εNd(t) and εHf(t) values, high initial ratio of $^{87}Sr/^{86}Sr$) and few studies on the early Paleozoic basaltic–felsic rock association. Our work here suggests that the Wugongshan appinite–granite association was formed in an intracontinental orogen, and the ancient enriched mantle may have had a significant chemical contribution to the formation of some of the Paleozoic peraluminous granites in South China.

Acknowledgements

We greatly appreciate the assistance of Dr. Zhaochu Hu, Keqing Zong and Haihong Chen in zircon U-Pb, Hf isotope, and whole-rock trace element analyses; Dr. Lian Zhou in Sr-Nd isotope analysis and Dr. Shu Zheng in mineral chemistry analysis and zircon CL images. This study was financially supported by the National Natural Science Foundation of China (40872053, 41272081).

ВУЛКАНОГЕННАЯ ПИРОКЛАСТИКА КАК ФАКТОР ФОРМИРОВАНИЯ NB(TA)-ZR(HF)-REE-GA ОРУДЕНЕНИЯ В УГЛЯХ (НА ПРИМЕРЕ СИБИРИ)

Арбузов С. И., Вергунов А. В.

Национальный исследовательский Томский политехнический университет

Уголь, как и его прекурсор торф, является контрастным геохимическим барьером, обуславливающим накопления различных химических элементов и, как следствие, благоприятен для формирования в угольных пластах геохимических аномалий, проявлений и месторождений многих металлов. Уже более 100 лет с переменным успехом решается вопрос извлечения из угля и отходов его использования попутных элементов-примесей. В настоящее время известна большая группа разнообразных типов месторождений редких, благородных и цветных металлов в углях и углистых породах (Seredin, Finkelman, 2008; Seredin, Dai, 2013; Seredin et al., 2013; Арбузов и др., 2014; Dai et al., 2016, Dai et al., 2018). В промышленных масштабах из угля добывается только германий, а с недавнего времени – литий и галлий (Seredin, 2012; Lin et al., 2013). Общие тенденции возрастания спроса на редкие металлы, появление новых технологий переработки сырья позволяют с оптимизмом смотреть на перспективы освоения традиционных и новых типов редкометалльно-угольных месторождений. Попытки выявления новых месторождений не прекращаются. Помимо группы германий-угольных месторождений в Китае в последние годы выявлено несколько месторождений комплексных REY–Zr(Hf)–Nb(Ta)–Ga руд (Dai et al., 2010; 2012). Аналогичные по составу редкометалльно- угольные месторождения с прошлого века известны в Кузбассе и в Минусинском бассейне (Середин, 1994; Арбузов и др., 2000, 2003; Арбузов, Ершов, 2007). Особый интерес представляет оруденение в пласте XI в Кузнецком бассейне в связи с его высокой контрастностью и значительными масштабами. Природа такого типа комплексного оруденения трактуется по-разному: от сингенетичного гидрогенного (Середин, 1994) до вулканогенного (Арбузов и др., 2003; Арбузов, Ершов, 2007; Seredin, Finkelman, 2008; Dai et al., 2012) и вулканогенно-гидротермального (Середин, 1994; Dai et al. 2016; 2016a; Zhao, 2017, 2017a). Понимание механизмов образования таких руд, создание моделей формирования месторождений подобного типа, позволит эффективно прогнозировать и выявлять аналогичное оруденение на ранее не опоискованных территориях.

В данной работе исследованы основные минералого-геохимические особенности комплексного Nb-Ta-Zr-Hf-Y-REE-Ga-оруденения в пласте XI на юге Кузбасса, выбранного в качестве эталонного объекта, и рассмотрена возможная природа его формирования. Оруденение было выявлено в 1989 году В.В. Ершовым и кратко описано В.В. Серединым (Середин, 1994, 2004). Предварительно были оценены ресурсы этих руд (Арбузов и др., 2000, Арбузов, Ершов 2007), однако детального комплексного исследования их не проводилось в связи с ограниченными техническими возможностями того периода.

Исследуемый пласт находится в южной части Кузнецкого бассейна в непосредственной близости к области питания древнего бассейна угленакопления. Кузнецкий бассейн представляет собой межгорную впадину, сформировавшуюся в С-Р время на палеозойском фундаменте.

Стратиграфически пласт XI находится в составе отложений кемеровской свиты верхнебалахонской подсерии раннепермского возраста (Угольная база., 2003).

Пласт имеет достаточно невыдержанную мощность, но протягивается на значительные расстояния при колебаниях мощности от 0,3 до 5,0 м. Средняя мощность уменьшается с востока на запад. На западе бассейна пласт XI выклинивается и промышленного значения не имеет.

Как следует из проведенных исследований, природа формирования породного прослоя является ключом к пониманию условий образования металлоносных углей пласта XI. По своим геохимическим характеристикам рассматриваемый породный горизонт значительно отличается от других углевмещающих пород юга Кузбасса. Прослой аномально обогащен Ta, Nb, Zr, Hf, Y, REE, Ga, Sn, Th и другими литофильными элементами. На первом этапе исследований этот горизонт рассматривался как специфическая терригенная осадочная порода. Геохимическая специфика самой породы и контактирующих с ней углей, с образованием аномальных концентраций Ta, Nb, Zr, Hf, Ga, REE, Th и U, связывалась с особенностями состава пород области питания бассейна угленакопления (Середин, 1994; Арбузов и др., 2000). Во многом такая интерпретация была логична в связи с широким распространением в обрамлении Кузбасса массивов геохимически специализированных щелочных гранитоидов, щелочных эффузивов и даже массивов карбонатитов.

Однако, как показывает анализ полученной минералого-геохимической информации, этот сравнительно маломощный горизонт (6-15 см) в угольном пласте существенно отличается по своим характеристикам от подстилающих и перекрывающих отложений. Прослой аномально обогащен Ta, Nb, Zr, Hf, Ga, REE, Th и U. При этом породы кровли и подошвы пласта XI характеризуются рядовыми содержаниями этих элементов.

Такое аномальное накопление данного спектра элементов-гидролизатов в осадочном процессе возможно только в процессе россыпеобразования. Однако формирование россыпей для углеобразовательного процесса не характерно (Юдович, Кетрис, 2002). К тому же, при достаточно малой мощности металлоносный горизонт имеет значительную площадную распространенность. В настоящее время он прослежен более чем на 20 км в субширотном направлении и более чем на 5,8 км в субмеридиональном. Общая протяженность горизонта с востока на запад превышает 50 км, а площадь распространения – 290 км^2. Формирование такого контрастного по составу горизонта малой мощности на большой площади при отсутствии ясно выраженной стратификации возможно только в результате катастрофического явления. Единст-

венным возможным механизмом такого одновременного поступления резко отличающегося по составу от углевмещающих пород материала может быть достаточно мощное катастрофическое извержение вулкана.

Другая важная особенность – значительное обогащение угля Ta, Nb, Zr, Hf, Ga, REE, Th и U на контакте с неугольным прослоем. Это указывает на перераспределение элементов в процессе углеобразования. Определить время перераспределения: торфонакопление, диагенез, катагенез, не представляется возможным, но характер обогащения угля позволяет предполагать, что первичным источником были именно породы прослоя. При этом перерасчет содержания этих элементов в породах прослоя с учетом выщелоченного вещества показывает, что первоначальный состав пород, сформировавших прослой, соответствовал комендитам-пантеллеритам. Это породы кислого, иногда ультракислого состава, но при этом высокой щелочности.

Таким образом, полученный в результате исследований массив данных позволяет уверенно заключить, что породный прослой (партинг) в пласте XI, являющийся источником для накопления группы редких элементов в углях, представлен геохимически специализированными измененными пеплами пантеллеритового состава. Отсутствие первичной, до поступления в торфяную залежь, переработки вулканогенного материала в зоне гипергенеза обеспечило сохранность его редкометалльного потенциала и дальнейшее перераспределение в угольном пласте с формированием промышленного Nb-Ta-Zr-Hf-Y-REE-Ga оруденения.

Исследование выполнено за счет гранта Российского научного фонда (проект № 18–17–00004).

Список литературы

1. Арбузов С.И., Ершов В.В., Поцелуев Л.Л., Рихванов Л.П. Редкие элементы в углях Кузнецкого бассейна. – Кемерово, 2000. - 248 с
2. Арбузов С.И., Ершов В.В., Рихванов Л.П., Усова Т.Ю., Кяргин В.В., Булатов А.А., Дубовик Н.Е. Редкометалльный потенциал углей Минусинского бассейна. –Новосибирск: Изд-во СО РАН, филиал “Гео”, 2003. – 347 с.
3. Арбузов С.И., Ершов В.В. Геохимия редких элементов в углях Сибири. – Томск: Изд. дом «Д-Принт”, 2007. –468 с
4. Арбузов С.И., Машенькин В.С., Рыбалко В.И., Судыко А.Ф. Редкометалльный потенциал углей Северной Азии (Сибирь, Российский Дальний Восток, Монголия) // Геология и минерально-сырьевые ресурсы Сибири. – 2014. - №3с. – Ч.2. – С.41-44
5. Середин В.В. Первые данные об аномальных концентрациях ниобия в углях России. // Доклады академии наук, 1994. – Т.335. - №5. – С. 634-636.
6. Середин В.В. Металлоносность углей: условия формирования и перспективы освоения. //Угольная база России. ТомVI (сводный, заключительный). Основные закономерности углеобразования и размещения угленосности на территории России. – М.:ООО «Геоинформмарк», 2004. - С.453-509.
7. Угольная база России. Том II. Угольные бассейны и месторождения Западной Сибири (Кузнецкий, Горловский, Западно-Сибирский бассейны; месторождения Алтайского края и Республики Алтай. – М.:ООО «Геоинформмарк», 2003. – 604 с.
8. Юдович Я.Э., Кутрис М.П. Неорганическое вещество углей.- Екатеринбург: УрО РАН, 2002. – 423 с.
9. Dai, S., Ren, D., Chou, C.-L., Finkelman, R.B., Seredin, V.V., Zhou, Y. 2012. Geochemistry of trace elements in Chinese coals: a review of abundances, genetic types, impacts on human health, and industrial utilization. Int. J. of Coal Geol., 94, 3–21.
10. Dai, S., Chekryzhov, I., Seredin, V., Nechaev, V., Graham, I., Hower, J., Ward, C., Ren, D., Wang, X., 2016. Metalliferous coal deposits in East Asia (Primorye of Russia and South China): a review of geodynamic controls and styles of mineralization.// Gondwana Res., 2016a. V. 29(1). P. 60-82 http://dx.doi.org/10.1016/j.gr.2015.07.001.
11. Dai, S, Yan, X, Ward, C R., Hower, J.C., Zhao, L., Wang, X., Zhao, L., Ren, D., Finkelman, R.B., 2016a. Valuable elements in Chinese coals: a review, Int. Geology Review, doi.:10.1080/00206814.2016.1197802.
12. Dai, S., Finkelman R.B. Coal as a promising source of critical elements: Progress and future Prospects // Int. J. of Coal Geol., 2018. -V. 186. - P. 155-164
13. Lin M., Bai G., Duan P., Xü J., Duan D., Li Z. Perspective of comprehensive exploitation of the valuable elements of Chinese coal. // Energy exploration & exploitation, 2013. - V. 31. – N. 4. – P. 623–627
14. Seredin, V.V., 2012. From coal science to metal production and environmental protection: A new story of success. Int. J. Coal Geol. 90-91, 1–3.
15. Seredin, V., Dai, S., Sun, Y., Chekryzhov, I., 2013. Coal deposits as promising sources of rare metals for alternative power and energy-efficient technologies. Appl. Geochem. 31, 1–11.
16. Seredin, V., Finkelman, R., 2008. Metalliferous coals: a review of the main genetic and geochemical types. Int. J. Coal Geol. 76, 253–289.
17. Zhao, L., Dai, S., Graham, I.T., Li, X., Liu, H., Song, X., Hower, J.C., Zhou, Y., 2017. Cryptic sediment-hosted critical element mineralization from eastern Yunnan Province, southwestern China: mineralogy, geochemistry, relationship to Emeishan alkaline magmatism and possible origin. Ore Geol. Rev. 80, 116–140.
18. Zhao, L., Zhu, Q., Jia, S., Zou, J., Nechaev, V., Dai, S., 2017a. Origin of minerals and critical metals in an argillized tuff from the Huayingshan Coalfield, southwestern China. Minerals 7, 92. http://dx.doi.org/10.3390/min7060092.

ПОЗДНЕДОКЕБРИЙСКО-ДЕВОНСКИЙ ПЛЮМОВАЫЙ МАГМАТИЗМ АЛТАЕ-САЯНСКОЙ СКЛАДЧАТОЙ ОБЛАСТИ: ЭВОЛЮЦИЯ ГОРЯЧЕЙ ТОЧКИ

Буслов М. М [1,2], Куликова А. В. [1,2], Рубанова Е. С. [1,2], Семенова Д. В. [1,2]

[1].Новосибирск, Институт геологии и минералогии СО РАН, buslov@igm.nsc.ru
[2].Казань, Казанский (Приволжский) федеральный университет
[3].Новосибирск, Институт нефтегазовой геологии и геофизики

К числу важных геолого-геодинамических закономерностей, выявленных в Алтае-Саянской складчатой области, относятся : 1) широкое развитие в аккреционных клиньях Кузнецко-Алтайской зрелой островодужной системы Сибирского континента фрагментов неопротерозойской примитивной островной дуги и разновозрастных палеосимаунтов с возрастами от венда до раннего ордовика (Симонов и др., 1994; Буслов, Ватанабе , 1996; Буслов, 2011, Буслов и др.. 2013; Добрецов и др., 1992; 2004, 2005, 2017; Dobretsov et al., 2004; Safonova et al., 2004; Kulikova et al.,2017), 2) смена геодинамического режима активной окраины на пассивную окраину в раннем ордовике (Буслов, 2011, Буслов и др.. 2013; Добрецов и др.,2017), 3) проявление в позднем ордовике-раннем девоне в тыловой части Кузнецко-Алтайской островной дуги на Батеневском кряже и Хакасии внутриплитного плюмового магматизма (Перфилова и др., 2004; Берзина и др., 2011; Воронцов и др., 2010, 2017). Для объяснения перечисленных закономерностей хорошо подходит модель погружения в зону субдукции срединно-океанического хребта и мантийной струи (горячей точки), что позволяет реконструировать детали палеогеодинамических процессов формирования позднепротерозойско-девонской окраины Сибирского континента, которая развивалась в различные периоды времени по аналогии с окраинами Тихоокеанской плиты. В позднем докембрии –раннем ордовике горячая точка формировал цепочку палеосимаунтов в пределах плиты Палеопацифики, которые сохранились в аккреционных клиньях Кузнецко-Алтайской островной дуги. Начиная с среднего кембрия происходило погружение срединно-океанического хребта в зону субдукции с формированием рассеянного комплекса параллельных даек и вулканических построек усть- семинской свиты, проявленных на севере Горного Алтае. Затем , в ордовике в зону субдукции погрузилась мантийная струя, которая проявилась с формирование плюмового внутриплитного магматизма в тыловой части островной дуги.

U-Pb датирование детритовых цирконов (Буслов и др., 2013; Добрецов и др., 2017; Cai et al., 2016, Chen et al., 2014a,b, 2015 a,b) из кембрийских турбидитов глубоководного желоба, среднекембрийско-раннеордовикского преддугового прогиба и ордовикско-раннедевонской пассивной окраины показало удивительную сходимость возрастов , отвечающую диапазону 530-470 млн лет. Этот период времени характерен для формирования магматических пород зрелой стадии Кузнецко-Алтайской островной дуги. В силурийско-раннедевонских отложениях встречаются цирконы с возрастами 470-430 млн.лет. Их источником сноса могли быть плюмовые магматические породы Батеневского кряжа и Хакасии. На раннедевонском уровне появляется не многочисленная популяция палеопротерозойских (2431-1879 млн лет) цирконов, источником сноса которых могли являться породы Сибирского кратона. В неопротерозойско- раннедевонских окраино-континентальных образованиях не встречены магматические цирконы с гренвильскими возрастами (0. 9 - 1.4 млрд. лет).

Характерно, что все перечисленные выше геодинамические комплексы ограничены с юга среднепалеозойской Чарышско-Теректинско-Улаганско-Саянской сутурно-сдвиговой зоны.

В южной части Алтае-Саянской складчатой области, Туве, Монголиии, Китае , южнее сутурно-сдвиговой зоны, широко развиты геодинамические комплексы пород Казахстанско-Байкальского составного континента, характерные для окраино-континентальных образований Индо-Австралийской плиты. Их отличительной особенностью , наряду с проявлением фрагменов океанической коры (офиолитов и палеосимаунтов) , является наличие докембрийских блоков континентальной коры (Тувино-Монгольский, Дзабханский, Центрально Тянь-Шаньский, Илийский, Кокчетавский и др. микроконтиненты) с характерным гренвильским возрастом магматических пород (Буслов, Добрецов, 2007; Буслов и др., 2013; Добрецов и др., 2017; Rojas Agramonte et al. 2011).

Таким образом, в Алтае-Саянской складчатой области широко распространены разновозрастные плюмовые образования, пространственно-временные закономерности проявления которых объясняются сложной эволюцией единой горячей точки.

Работа выполнена в рамках государственных заданий ИГМ СО РАН и ИНГГ СО РАН, при поддержке гранта Министерства образования РФ № 14.Y26.31.0029 .

Список литературы

1. Берзина А.П., Берзина А.Н., Гимон В.О. Сорское Cu-Mo-порфировое месторождение (Кузнецкий Алатау): магматизм, влияние мантийного плюма на развитие рудно-магматической системы // Геология и геофизика, 2011, т. 52 (12), с. 1974-1986.
2. Буслов М.М. Тектоника и геодинамика Центрально-Азиатского складчатого пояса: роль позднепа-леозойских крупноамплитудных сдвигов // Геология и геофизика, 2011, т. 52 (1), с. 66-90.
3. Буслов М.М., Ватанабе Т. Внутрисубдукционная коллизия и ее роль в эволюции аккреционного клина (на примере Курайской зоны Горного Алтая, Центральная Азия) // Геология и геофизика, 1996, т. 37 (1), с. 82-93.

4. Буслов М.М., Джен Х., Травин А.В., Отгонбаатар Д., Куликова А.В., Чен Минг, Глори С.,Семаков Н.Н., Рубанова Е.С., Абилдаева М.А., Войтишек Е.Э., Трофимова Д.А. Тектоника и геодинамика Горного Алтая и сопредельных структур Алтае-Саянской складчатой области // Геология и геофизика, 2013, т. 54 (10), с. 1600-1628.
5. Воронцов А.А., Ярмолюк В.В., Федосеев Г.С., Никифоров А.В., Сандимирова Г.П. Изотопно-геохимическая зональность девонского магматизма Алтае-Саянской рифтовой области: состав и геодинамическая природа мантийных источников // Петрология, 2010, т. 18, № 6, с. 621-634.
6. Воронцов А.А., Перфилова О.Ю., Буслов М.М., Травин А.В., Махлаев М.Л., Дриль С.И., Катраевская Я.И. Плюмовый магматизм северо-восточной части Алтае-Саянской области: этапы, состав источников, геодинамика (на примере Минусинского прогиба) // ДАН, 2017, т. 472(4), с. 449-455.
7. Добрецов Н.Л., Буслов М.М., Сафонова И.Ю., Кох Д.А. Фрагменты океанических островов в структуре Курайского и Катунского аккреционных клиньев Горного Алтая // Геология и геофизика, 2004, т. 45 (12), с. 1381-1403.
8. Добрецов Н.Л., Симонов В.А., Буслов М.М., Котляров А.В. Магматизм и геодинамика Палеоазиатского океана на венд-кембрийском этапе его развития // Геология и геофизика, 2005, т. 46 (9), с.952-967.
9. Добрецов Н.Л., Симонов В.А., Буслов М.М., Куренков С.А. Океанические и островодужные офиолиты юго-восточной части Горного Алтая// Геология и геофизика, 1992, т. 12, с. 3-14.
10. Добрецов Н.Л., Буслов М.М., Рубанова Е.С., Василевский А.Н., Куликова А.В., Баталева Е.А. Среднепозднепалеозойские геодинамические комплексы и структура Горного Алтая и ее отображение в гравитационных данных. Геология и геофизика, 2017, т. 58, с.1277-1283.
11. Перфилова О.Ю.,Махлаев М.Л., Сидорас С.Д. Ордовикская вулкано-плутоническая ассоциация в структурах горного обрамления Минусинских впадин // Литосфера, 2004, № 3, с. 137-152.
12. Симонов В.А., Добрецов Н.Л., Буслов М.М. Бонинитовые серии в структурах Палеоазиатского океана // Геология и геофизика, 1994, т. 35 (7-8), с. 182-199.
13. Cai Keda , Min Sun, M.M. Buslov, Bor-ming Jahn, Wenjiao Xiao, Xiaoping Long, Huayong Chen, BoWan, Ming Chen, E.S. Rubanova, A.V. Kulikova, E.E. Voytishek . Crustal nature and origin of the Russian Altai: Implications for the continental evolution and growth of the Central Asian Orogenic Belt (CAOB)// Tectonophysics , 2016, v.674 , pp. 182–194.
14. Chen, M., Sun, M., Cai, K., Buslov, M.M., Zhao, G., Rubanova, E.S. Geochemical study of the Cambrian-Ordovician meta-sedimentary rocks from the northern Altai-Mongolian terrane, northwestern Central Asian Orogenic Belt: Implications on the provenance and tectonic setting//Journal of Asian Earth Sciences, 2014a, v.96,pp. 69-83.
15. Chen, M., Sun, M., Cai, K., Buslov, M.M., Zhao, G., Rubanova, E.S., Voytishek, E.E. Detrital zircon record of the early Paleozoic meta-sedimentary rocks in Russian Altai: Implications on their provenance and the tectonic nature of the Altai-Mongolian terrane //Lithos, 2014b, v.233, pp.209-222.
16. Chen Ming, Sun Min, Buslov Mikhail M., Cai Keda, Zhao Guochun, Zheng Jianping, Rubanova Elena S., Voytishek Elena E. Neoproterozoic–middle Paleozoic tectono-magmatic evolution of the Gorny Altai terrane, northwest of the Central Asian Orogenic Belt: Constraints from detrital zircon U–Pb and Hf-isotope studies. Lithos, 2015 a, v. 233, pp. 223–236.
17. Chen Ming, Sun Min, Cai Keda , Buslov Mikhail M., Zhao Guochun, Rubanova Elena S., Voytishek Elena E..Detrital zircon record of the early Paleozoic meta-sedimentary rocks in Russian Altai: Implications on their provenance and the tectonic nature of the Altai–Mongolian terrane . Lithos, 2015b, v.233, pp. 209–222.
18. Dobretsov N.L., Buslov M.M., Uchio Y. Fragments of oceanic islands in accretion-collision areas of Gorny Altai and Salair, southern Siberia, Russia: early stages of continental crustal growth of the Siberian continent in Vendian-Early Cambrian time // Journal of Asian Earth Sciences,2004,v.23(5),pp. 673-690.
19. Kulikova A.V., Buslov M.M., Travin A.V. Geochronology of the metamorphic rocks in the Kurai accretionary prism (South-Eastern Gorny Altai) // Geodynamics & Tectonophysics, 2017, v. 8(4), pp. 1049–1063.
20. Rojas Agramonte, Y., Kröner, A., Demoux, A., Xia, Wang W., Donskaya, T.,Liu, D., Sun, M., 2011. Detrital and xenocrystic zircon ages from Neoproterozoic to Palaeozoic arc terranes of Mongolia: Significance forthe origin of crustal fragments in the Central Asian Orogenic Belt. Gondwana Res. 19 (3), pp.751–763.
21. Safonova I.Y., Buslov M.M., Iwata K., Kokh D.A. Fragments of Vendian-early Carboniferous oceanic crust of the Paleo-Asian Ocean in foldbelts of the Altai-Sayan region of Central Asia: Geochemistry,biostratigraphy and structural setting // Gondwana Res., 2004, v. 7 (3), pp. 771-790.

U/PB ВОЗРАСТ СФЕНОВ, ПЕТРОХИМИЧЕСКИЕ, МИНЕРАЛОГИЧЕСКИЕ И ГЕОХИМИЧЕСКИЕ ОСОБЕННОСТИ ЩЕЛОЧНЫХ ПОРОД МАССИВА БОГДО (АРКТИЧЕСКАЯ СИБИРЬ)

Добрецов Н. Л.[1], Жмодик С. М.[1,2], Лазарева Е. В.[1], Толстов А. В.[1,3], Белянин Д. К. [1,2], Сурков О. Н.[1], Добрецов Н. Н.[1], Родионов Н. В.[4]

[1]Институт геологии и минералогии им. Соболева, Новосибирск, Россия
[2]Новосибирский государственный университет Соболева, Новосибирск, Россия
[3]LLC «Arctic Capital», Якутск, Россия
[4]ВСЕГЕИ, Санкт-Петербург, Россия

Keywords. *Щелочные породы, сфен, U/Pb возраст, Богдо, Арктика*

Введение

На севере Сибирской платформы, восточнее Анабарского щита известно несколько массивов щелочных пород с карбонатитами: Томторский, Богдо, Промежуточный, Буолкалах, Чюэмпэ, Уэле. Массивы располагаются среди известняков, доломитов, терригенных метаморфизованных пород NP_1-NP_3 возраста и перекрываются континентальными (P), морскими (J) и рыхлыми (Q) отложениями. Положение массивов контролируется меридиональной рифтогенной структурой - «Уджинским сводом» и пересекающими её трансформными разломами. На теневых моделях рельефа и спектрозональных космических снимках положение Томторского и Богдинского массивов подчеркивается кольцевыми структурами, осложненными разломными зонами субширотного (Томторский массив) и СВ направления (массив Богдо). Центральная часть массива Богдо примерно совпадает с геологическим центром крупной кольцевой структуры. В магнитном и гравитационном полях массивы выделяется положительными округлыми аномалиями.

Массив Богдо расположен примерно в 20-40 км на С от наиболее крупного Томторского массива. Сведения о массиве Богдо крайне фрагментарны. Возраст определен K-Ar методом для нефелиновых сиенитов, ювита, мельтейгита, биотита и калишпата - от 338 до 421 Ма. Скорректированное на возраст значение $^{87}Sr/^{86}Sr$ равно 0,7043 и сопоставляется с фоидолитами Томторского массива (Зайцев и др., 1992; Толстов, Тян, 1999). Данные о минералого-геохимических особенностях и возрасте щелочных массивов представляют значительный интерес с точки зрения обоснования масштабов распространения щелочного магматизма и оруденения томторского типа.

В плане массив Богдо имеет форму овала, размерами около 7 х 8 км и характеризуется концентрически-зональным, слабо ассиметричным строением. Массив Богдо может быть отнесен к формации ультраосновных щелочных пород и карбонатитов. Согласно геологического картирования, периферическая часть массива выполнена скарнированными, фенитизированными и мраморизованными известняками. В центральной части массива выделяется блок, сложенный кальцитовыми карбонатитами. Основная площадь массива представлена нефелиновыми сиенитами и ювитами, среди которых в виде полукольцевых участков распространены породы якупирангит-ийолитовой серии и блоки «поздних» карбонатитов.

Результаты

Нами был детально изучен керн скважины № 3257.5, вскрывающей на глубине 32-42 м в разной степени измененные щелочные породы массива. В зависимости от количеств калиевого полевого шпата, нефелина, лейцита, эгирина, биотита и изменений, породы имеют различные текстурные и структурные особенности: представлены как мелкозернистыми, так и крупнозернистыми разновидностями. Макро- и микроскопически породы могут быть разделены на четыре типа: 1 – крупнозернистые лейкократовые светло-серой или зеленовато-серой окраски полевошпат-нефелиновые сиениты (рисчорриты) пойкилитовой структуры с пироксеном, биотитом, амфиболом, сфеном; 2 – средне- и 3 - мелко-зернистые темно-серые с красно-коричневыми идиоморфными зернами либенерита (псевдоморфозы серицита по нефелину, представленные микрозернистым серицит-нефелиновым агрегатом), K-Ba-полевым шпатом, меланитом биотит-эгириновые либенеритовые сиениты; 4 – светло-серые пятнистые пойкилитовой структуры карбонатизированные с симплектитами и нефелин-полевошпатовыми агрегатами псевдо-лейцитовые нефелиновые сиениты (ПЛНС). Породы массива Богдо содержат Zr-Nb-рутилы, сложные оксиды, карбонаты и силикаты Ti, Zr, Nb, REE, реже фосфаты – апатит и монацит.

Уровень содержания SiO_2 в породах соответствует группе основных пород (49.0 - 52.6 мас.%), но с высокими концентрациями Al_2O_3 (20.5 - 23.6 мас.%) и Na_2O+K_2O (12.3 - 17.4 мас.%), с преобладанием K_2O (8.16-11.4 мас.% и Na_2O/K_2O 0.11 - 0.84), а также низкими содержаниями CaO (1.08 - 3.5 мас.%), MgO (0.27 - 0.78 мас.%) и FeO_{tot} (2.52 - 4.2 мас.%). Коэффициент агпаитности [(Na+K)/Al] пород первого типа превышает 1 (1.0 - 1.13; среднее – 1.10); второго и третьего типа меняется от 0.83 до 1.01 (среднее – 0.9); четвертого – от 0.89 до 0.96 (среднее – 0.93).

На диаграмме SiO_2 – Na_2O+K_2O точки составов соответствуют нефелиновым сиенитам (основным фоидолитам и основным фоидитам по (Магматические породы …, 1983)) и нефелин-содалитовым кумулатам. На диаграмме Na-Al-K точки составов щелочных пород массива Богдо ложатся на продолжение линий трендов, выявленных для магматических серий массива Nechalacho Layered Suite, возникновение которых объясняется фракционированием расплава (Moller, Williams-Jones, 2016).

Из 4 проб пород массива Богдо были выделены сфены ($CaTi[SiO_4]$), для определения U/Pb возраста с помощью

вторично-ионного микрозонда SHRIMP-II (Rodionov et al., 2018). В сфенах из 2 проб либенеритовых сиенитов содержания урана оказались очень низкими (0.1 - 1 ppm U). В сфенах из 2 проб (рисчоррит и ПЛНС) содержания урана варьируют от 3-4 до 13 ppm U. Рассчитанный для 4 проб сфенов (63 зерна) U/Pb возраст соответствует 394.4±3.2 Ma (рис.).

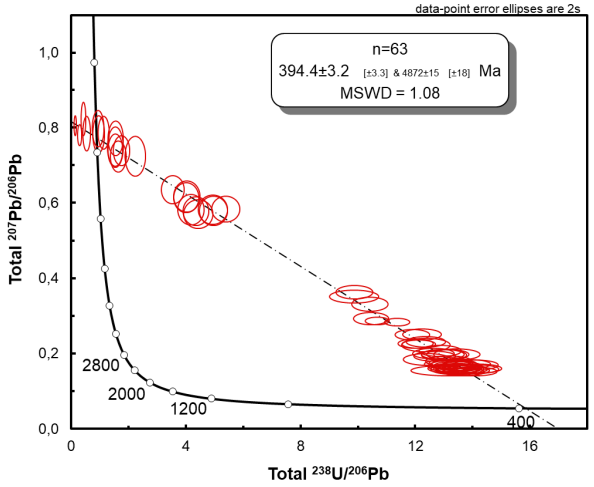


Рисунок. Результаты U-Pb датирования сфенов из четырех проб щелочных пород массива Богдо.

Обсуждение результатов и заключение

По структурным особенностям (пойкилитовая структура, симплектиты), петрохимическим и минералого-геохимическим данным породы массива Богдо соответствуют рисчорритам, либенеритовым сиенитам и ПЛНС (Заварицкий, 1961; Магматические породы, 1983). Эти данные свидетельствует в пользу представлений о формировании пород на магматической стадии. Проявление карбонатизации щелочных пород, со значительным возрастанием содержаний TiO_2 (2.88 мас.%), REE и редких элементов, с мультиэлементным спектром, близким к томторским карбонатитам, позволяют предположить распространение карбонатитов с редкометалльной и REE минерализацией в массиве Богдо.

Полученные данные свидетельствуют о среднедевонском времени формирования щелочных магматических пород массива Богдо – 394.4±3.2 Ma. Выделенный возрастной рубеж не уникален для истории Сибирского кратона и в полной мере согласуются с эпохой крупнейших проявлений внутриплитного магматизма. На основании U-Pb и Ar-Ar датирования пород массива Томтор сделан вывод о двух этапах его формирования: 701–675 и 414–387 Ma. Девонский период формирования массива Томтор связывается с воздействием Вилюйского плюма на восточный край Сибирского кратона, что привело к разрывам литосферы и образованию Вилюйской крупной изверженной провинции с радиальной системой рифтов, разломов, дайковых поясов (Vladykin et al., 2014, Kiselev et al., 2012). Известно, что возраст Кольской щелочной провинции соответствует 410-362 Ma (Kramm, Sindern, 2004) и этот факт требует поисков более общих причин регионального проявления плюмового магматизма девонского возраста. Одной из таких причин может быть влияние периферических зон (в максимальной мере контролирующих положение LIP и кимберлитов) Africa Large Low Shear Velocity Province (“Tuzo”) в девонскую эпоху на Балтику и Сибирь (Torsvik et al., 2010). Подобную полихронность формирования можно ожидать и для массива Богдо. Глобальное проявление Сибирского суперплюма должно быть также подтверждено минеральными ассоциациями и изотопными характеристиками пород массива Богдо.

Благодарности

Работа поддержана РФФИ (грант 05-18-70109_Арктика) и Министерством Образования и Науки РФ.

Литература

1. Заварицкий А.Н. (1961) Изверженные горные породы. М.: Изд-во АН СССР. 479 с
2. Зайцев А.И., Энтин А.Р., Ненашев Н.И. и др. Геохронология и изотопная геология Якутии. Якутск: ЯНЦ СО РАН. 1992. 248 с
3. Магматические горные породы (1983) Классификация, номенклатура, петрография. Ч. 2. Гл. ред. О.А. Богатиков. М.: Наука. 767 с
4. Толстов А.В., Тян О.А. (1999) Геология и рудоносность массива Томтор. Якутск: ЯНЦ СО РАН. 164 с
5. Kiselev A. I., Ernst R. E., Yarmolyuk V. V., Egorov K. N. (2012) Radiating rifts and dyke swarms of the middle Paleozoic Yakutsk plume of eastern Siberian craton J. Asian Earth Sci. 45:1–16
6. Kramm U., Sindern, S. (2004) Timing of Kola ultrabasic, alkaline and phoscorite-carbonatite magmatism. In: Phoscorites and carbonatites from mantle to mine: the key example of the Kola Alkaline Province. Eds F. Wall, A.N. Zaitsev. Mineralogical Society Series 10:75–97
7. Rodionov N.V., Lepekhina E.N., Antonov A.V. et al. (2018) U–Pb SHRIMP-II ages of titanite and timing constraints on apatite–nepheline mineralization in the Khibiny and Lovozero alkaline massifs (Kola Peninsula). Russian Geology and Geophysics 59:962–974
8. Moller V., Williams-Jones A.T. (2016) Petrogenesis of the Nechalacho Layered Suite, Canada: Magmatic Evolution of a REE–Nb-rich Nepheline Syenite Intrusion. Journal of Petrology 57:229–276
9. Torsvik T. H., Burke K., Steinberger B., Webb S. J., Ashwal L. D. (2010) Diamonds sampled by plumes from the core–mantle boundary. Nature 466:352-355
10. Vladykin N.V., Kotov A. B., Borisenko A. S. et al. (2014) Age Boundaries of Formation of the Tomtor Alkaline–Ultramafic Pluton: U–Pb and $^{40}Ar/^{39}Ar$ Geochronological Studies. Doklady Earth Sciences 454:7-11

ГРАНИТОИДНЫЙ МАГМАТИЗМ НА ТЕРРИТОРИИ ФРОЛОВСКОЙ МЕГАВПАДИНЫ ЗАПАДНО-СИБИРСКОЙ НЕФТЕГАЗОНОСНОЙ ПРОВИНЦИИ

Мороз М. Л., Белова Е. В., Тугарева А. В., Чернова Г. А.

АУ «НАЦ РН им. В.И. Шпильмана»

В пределах Фроловской мегавпадины пробурено порядка 240 поисково-разведочных скважин, большинство из которых вскрыли доюрскую часть разреза на глубину менее 50 м. Хорошо изучена бурением центральная часть впадины, в северной её части только одиночные скважины вскрыли доюрские отложения.

Территория Фроловской мегавпадины имеет блоковое строение. Фроловский геоблок сформировался в палеозое над погребенными уралидами. В палеозойское время он не был вовлечен в орогенез, здесь господствовал спокойный платформенный режим и накапливались преимущественно терригенно-карбонатные осадки девона. Все отложения палеозоя подвергнуты складчатости в верхнем карбоне - нижней перми. Этот период связан с метаморфическими преобразованиями пород, складчатостью, внедрением гранитоидов и т.д. [3].

Фроловская мегавпадина является наложенной впадиной, сформировавшейся в сеноманское и постсеноманское время на относительно приподнятой части Среднеобской антеклизы [2].

Гранитоидные массивы, как правило, приурочены к эрозионно-тектоническим выступам фундамента, для их выделения используются карты потенциальных полей (грави- и магниторазведка), результаты сейсмических исследований и данные бурения. В потенциальных полях им соответствуют отрицательные гравитационные и магнитные аномалии. Контуры гранитных тел довольно хорошо совпадают с участками пониженного магнитного поля. В некоторых случаях магнитное поле над гранитами может быть повышенным и дифференцированным. Это, в основном, связано со сложным составом гранитного комплекса.

Гранитоидные массивы, включающие граниты, гранодиориты и плагиограниты; интрузии диоритов выявлены в пределах Фроловской мегавпадины на Верхнепомутской, Унлорской, Ольховской, Восточно-Мытаяхинской, Западно-Нялинской, Северо-Селияровской и др. площадях.

На рис.1А показаны массивы гранитоидов и диоритов, выделенные на Схематической структурно-формационной карте фундамента центральной части Западно-Сибирской плиты (под ред. Суркова В.С. и др., 2005, 2014), а также на Схеме геологического строения доюрского основания (Криночкин В.Г., 2005, 2011). На рис.1Б показаны гранитоидные массивы и интрузии диоритов, выделенные ранее и уточнённые нами по результатам проведённых работ, в том числе и по сейсморазведке.

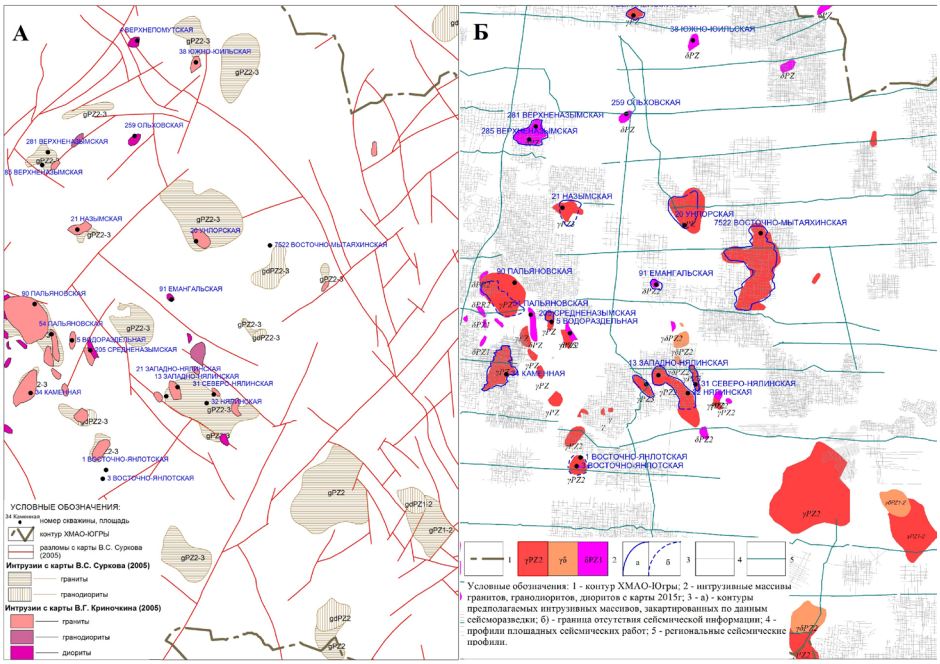


Рис. 1. Гранитоидные массивы в пределах Фроловской мегавпадины

По материалам сейсморазведки уточнены контуры Верхнепомутского, Унлорского, Верхнеляминского, Каменного, Пальяновского, Нялинского и др. массивов. Предполагаемый контур Северо-Нялинской гранитной интрузии, вскрытой скв.31 Северо-Нялинской и скорректированный по материалам площадной сейсмики, приведён на рис.2.

Картирование интрузивных массивов и их изучение является важным этапом при прогнозе нефтегазоносности. Это объекты тектонически мобильные, приуроченные к эрозионно-тектоническим выступам, обычно с повышенным тепловым потоком и поэтому являются благоприятными для формирования залежей УВ.

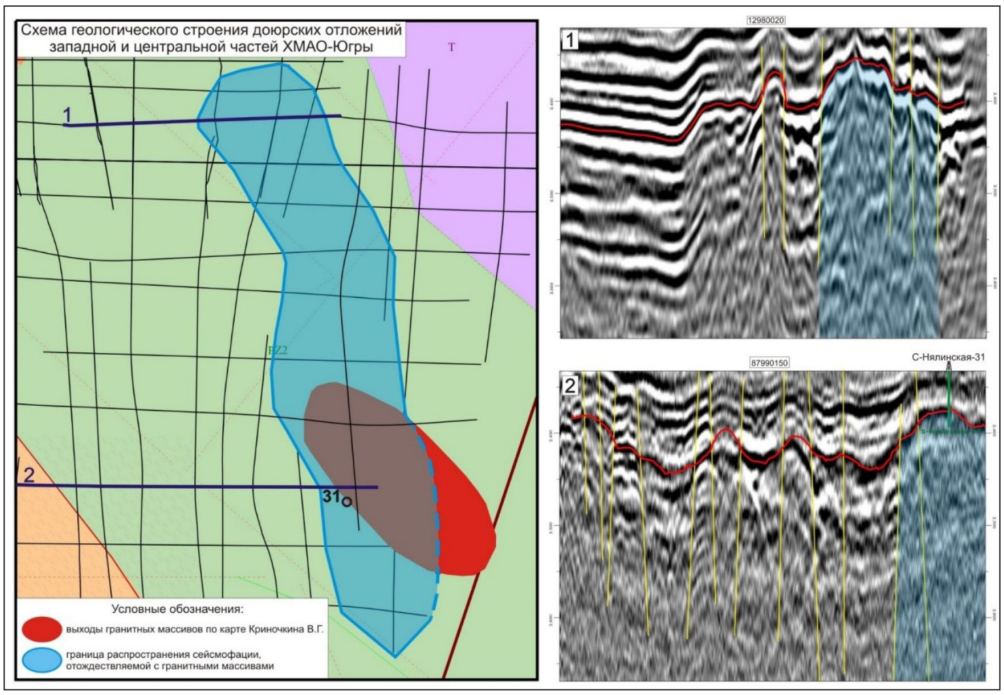


Рис.2. Уточнение границ гранитных массивов по сейсморазведке методом типизации сейсмической записи

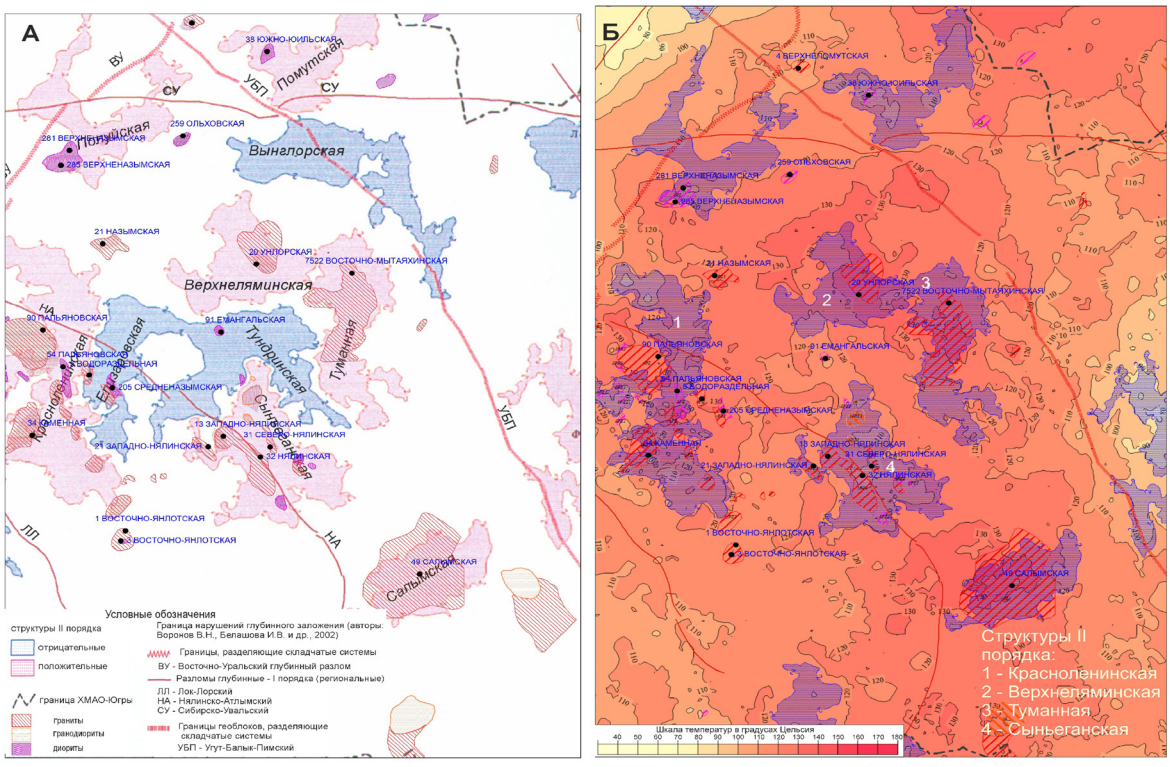


Рис. 3. А – Схема расположения тектонических структур II порядка. Б – Карта изотерм фундамента с тектоническими элементами II порядка

(Составили: В.А. Волков, А.А. Сидоров, В.Н. Гончарова, 2015)

ПАЛЕОЗОЙСКИЙ БАЗИТОВЫЙ МАГМАТИЗМ СЕВЕРНОГО УСТЮРТА

Попков В. И.

Кубанский государственный университет, г. Краснодар, Россия

Ключевые слова: *Северный Устюрт, палеозой. Базитовый магматизм*

Доверхнепермские отложения на значительных пространствах Туранской платформы дислоцированы, в той или иной степени метаморфизованы, прорваны гранитоидными интрузиями и входят в состав ее фундамента (Попков, 1992б). Лишь в северо-западной части платформы (Бузачи, Северный Устюрт, Приаралье) неметаморфизованные отложения девонско-каменноугольно-раннепермского возраста имеют широкое площадное распространение, слагая нижний структурный ярус чехла Северо-Устюртского докембрийского массива. Геофизические материалы и данные глубокого бурения позволяют предполагать широкое развитие в его составе вулканогенных и вулканогенно-осадочных толщ значительной мощности. В настоящей работе предпринята попытка обобщения геологического материала по данному комплексу отложений, рассматриваемому многими исследователями в качестве перспективного на нефть и газ.

Мощный разрез сероцветных отложений верхнего карбона-нижней перми под пестроцветными отложениями пермотриаса вскрыт на п-ове Бузачи скв. 1П Северный Карамандыбас (1755 – 4128 м), Г-7 Северные Бузачи (1954 – 3500 м) и Г-4 Култай (1950 – 2705 м). На максимальную толщину (2373 м) они вскрыты в скв. 1П Северный Каражанбас. Разрез имеет четко выраженное двухчленное строение: нижняя часть – вулканогенно-осадочная (интервал 2982 – 4128 м), верхняя – преимущественно карбонатно-глинистого состава. Андезитовые порфириты, распространенные в низах разреза, представляют собой плотные массивные породы с однообразной зеленовато-серой или мелкопятнистой зеленовато-темно-серой основной массой с многочисленными порфировыми вкраплениями плагиоклаза светло-серого. Толщина андезитовых порфиритов, залегающих параллельно напластованию осадочных пород, колеблется от 6 – 10 до 20 – 49 м.

В скв. 4 Култай под отложениями пермотриаса вскрыта нижняя вулканогенно-осадочная часть разреза.

В базальной пачке конгломератов пермотриаса содержатся обломки андезитовых порфиритов, а также карбонатных пород. Последние часто содержат фауну позднего карбона-ранней перми.

Более представительная информация о строении отложений карбона и нижней перми имеется для территории Барсакельмесского прогиба. Судя по имеющимся данным, здесь можно выделить два типа разрезов: карбонатный и эффузивно-осадочный. Первый из них вскрыт скважинами на Аламбек-Куанышском валу (Каракудукская, Центрально-Кушкаирская, Восточно- и Западно-Барсакельмесская площади). Так, карбонатный комплекс пород на Каракудукском поднятии вскрыт скважинами 10П, 2 и 5. Известняки светло-серые, серые, белые, местами с розовым оттенком, тонкоплитчатые. По составу подразделяются: 1) на органогенные, сложенные в основном остатками различных организмов, среди которых отмечены рифостроящие разности; 2) органогенно-обломочные, сложенные обломками микрофауны (мшанки, иглокожие, остракоды, строматопороидеи) и водорослевым материалом; 3) кристаллозернистые известняки (имеют подчиненное значение). Рассматриваемые отложения сформировались в морских мелководных условиях вдали от береговой линии. В известняках обнаружен комплекс фауны, датирующий раннекарбоновый (визейский, возможно, намюрский век) возраст вмещающих пород (Акрамходжаев и др., 1979).

На Южно-Кушкаирской площади разрез сложен в основном кристалло-зернистыми и органогенно-детритовыми известняками, содержащими фораминиферы серпуховского яруса нижнего карбона, а также комплекс микрофауны, свидетельствующий о раннекаменноугольном возрасте пород (визейский, намюрско-башкирский ярусы) (Акрамходжаев и др., 1979, Лабутина, 1978). Близкие в литологическом отношении отложения вскрыты на Центрально-Кушкаирской и скв. 1П на Западно-Барсакельмесской площадях. В известняках Центрально-Кушкаирской площади обнаружена микрофауна, указывающая на принадлежность пород к верхней части раннекарбонового разреза (визейский, намюрский и башкирский ярусы).

Значительная часть Барсакельмесского прогиба, судя по всему, заполнена продуктами герцинской вулканической деятельности, которая особенно активизировалась в конце карбона и ранней перми. Так, осадочно-эффузивные толщи встречены в разрезах скважин Аджибая, Тулея, Куаныша, Кибира, а также на севере и востоке Актумсукского выступа (Байтерек, Сарытекиз) и Байчагырской моноклинали (Курлук). В интервале 4077 – 3912 м опорной скважины 1-Тулей вскрыты туфы андезитовых и базальтовых порфиритов, мелко- и среднеобломочные туфы и туффиты, сложенные эффузивами основного и среднего состава, с прослоями глин, алевролитов, песчаников и известняков. В целом для данной толщи характерны зеленовато-серые, буровато-коричневые и темно-серые окраски. Определение абсолютного возраста эффузивных пород Тулейской площади дало цифры 249 ± 7 млн лет и 255 ± 10 млн лет (Акрамходжаев и др., 1979).

На Сарытекизской площади (скв. 1) осадочно-эффузивный комплекс вскрыт в интервале глубин 3243 – 2694 м и подразделяется на две пачки (Акрамходжаев и др., 1979). Нижняя (3243 – 2982 м), преимущественно пирокластическая пачка, сложена пестроцветными, плохо отсортированными пирокластическими породами (обломками базальтовых порфиритов, эффузивов основного и среднего состава, вулканического стекла основного состава), содержащими прослои эффузивов и терригенных пород со сгустками микрокристаллического карбонатного материала, а также обломками мшанок, фораминифер, иглокожих и брахиопод. В интервале 3022 – 3028 м обнаружен комплекс микрофауны, характерный для гжельского яруса верхнего карбона и ассельского яруса нижней перми (Акрамходжаев и др., 1979; Лабутина, 1978). Абсо-

лютный возраст порфиритов (3166 – 3174 м), определенный калий-аргоновым методом, составляет 223 ±10 млн лет (T_1). Однако залегание выше них фаунистически охарактеризованных пород верхнего карбона-нижней перми свидетельствует, скорее всего, о занижении абсолютного возраста эффузивов.

Верхняя пачка (2982 – 2694 м) представлена толщей эффузивных пород. В основании преобладают интенсивно преобразованные миндалекаменные диабазовые пироксен-оливиновые и плагиоклазовые порфириты, в верхней части – базальтовые порфириты. Определение химического состава порфиритов Сарытекизской площади указывает на принадлежность их к щелочным базальтам (Акрамходжаев и др., 1979).

Осадочно-эффузивные породы вскрыты также на Аджибайской (скв. 1, интервал 3805 – 3868 м), Кибирской (скв. 1, 3767 – 3800 м), Куанышской (скв. 2П, 3767 – 3770 м) и Курлукской (скв. 2, 2965 – 2970 м) площадях. Согласно данным абсоютной геохронологии, возраст курлукских андезитовых порфиритов составляет 197 ± 7 млн лет (Акрамходжаев и др., 1979),однако по аналогии с Сарытекизским разрезом наиболее вероятен их позднекаменноугольно-раннепермский возраст.

Изучение условий формирования вулканогенного комплекса показало (Попков, 1992а; Попков и др., 1993), что вулканическая деятельность в период образования нижней его части носит в основном подводный характер. В пользу этого свидетельствуют наличие пропластков нормально-осадочных пород, содержащих микрофауну, тонкая слоистость в отдельных частях разреза, хемогенный состав цемента туфопесчаников и туфоалевролитов и альбитизация эффузивов, объясняющаяся эпимагматическим изменением плагиоклазов в условиях подводного излияния. В этом отношении большой интерес представляет туфолава из верхней секции разреза скв. 2П Байтерек, обладающая типичными признаками, характерными для спилитов: шаровой текстурой, наличием ассоциации с кремнистыми радиоляриевыми и спикуловыми образованиями, интенсивной хлоритизацией стекла и вмещающей породы, кислым составом плагиоклаза. Формирование основной массы порфиритов Сарытекиза и Аджибая, пирокластов Тулея и Кибира имеет континентальный характер.

Примечательно, что в пределах западной части Северного Устюрта по материалам высокоточной аэромагнитной съемки также предполагается присутствие в домезозойском разрезе мощных и значительных по размерам эффузивных линз основного состава, совпадающих в плане с современными платформенными депрессиями. Как было показано ранее (Попков и др., 1993; Попков и др., 1985), отложения платформенного чехла не имеют достаточно интенсивных по активности магнитных горизонтов, которые могли бы создать в наблюдаемой структуре регионального магнитного поля значительные положительные аномалии. Выполненные количественные расчеты в комплексе с материалами сейсморазведки указывают на приуроченность аномалеобразующих тел к доверхнепермской части разреза. Следовательно, можно говорить о том, что на данном этапе геологической истории Северного Устюрта имели место интенсивные излияния магм основного состава. Для выяснения причины этого явления требуются дополнительные исследования.

Работа выполнена при поддержке РФФИ, грант 19-05-00165 а.

Список литературы

1. Акрамходжаев А.М., Авазходжаев Х.Х., Лабутина Л.И. Литология, условия образования и нефтегазоносность доюрских отложений Устюрта. Ташкент: ФАН, 1979. 160 с.
2. Лабутина Л.И. Распространение эффузивных пород в верхнем палеозое в Каракалпакской части Устюрта // Вопросы литологии, фаций, палеогеографии и геохимии нефтегазоносных отложений Узбекистана. Ташкент: ФАН, 1978. С. 66-72.
3. Попков В.И. Палеозойский вулканогенно-осадочный комплекс северо-запада Туранской платформы // Разработка нефтегазовых месторождений. М.: ВНИИОЭНГ, 1992а. Вып. 4. С. 11-16.
4. Попков В.И. Тектоника запада Туранской плиты. М.: ИГиРГИ, 1992б. 148 с.
5. Попков В.И., Воскобой В.А., Нурманов А.М. Глубинное строение Северного Устюрта. М.: ИГиРГИ, 1993. 94 с.
6. Попков В.И., Калинин М.И., Сейфуллин Ш.М. Глубинное строение запада Туранской плиты // Доклады АН СССР. 1985. Т. 284. № 4. С. 939-943.

ГРАНИТОИДНЫЕ ИНТРУЗИВНЫЕ КОМПЛЕКСЫ ЮГО-ЗАПАДА ТУРАНСКОЙ ПЛИТЫ

Попков И. В., Попков В. И.

Кубанский государственный университет, г. Краснодар, Россия

Ключевые слова: *Туранская плита, магматизм, интрузивные комплексы*

Выходы магматических пород на дневную поверхность известны в окрестностях города Туркменбаши (Красноводска), где они слагают возвышенности Шах-Адам и Кара-Даг, и в районе Большого Балхана. Вскрыты они многими скважинами и в пределах Карабогазского свода. Хорошая их изученность, позволяющая восстановить последовательность магматических инъекций, а также достаточно многочисленные данные абсолютной геохронологии дают возможность известные здесь интрузивные породы сгруппировать в четыре основные группы (Попков, 1992; Попков и др., 1989)..

1. Ордовикско-раннедевонский интрузивный комплекс. В западной части Шах-Адама и на п-ове Даг-Ада среди биотитовых гранитов обнажены гранито-гнейсы, представляющие собой ксенолит в первых, что послужило основанием для отнесения гранито-гнейсов к самым древним интрузивным образованиям /339/. Абсолютный возраст пород, определенный калий-аргоновым методом, составил 450-395 млн. лет /260/. Косвенным подтверждением их более древнего происхождения является наличие аплитовых жил в гранито-гнейсах, не переходящих в биотитовые граниты, и более интенсивная метаморфизация этих пород по сравнению с вмещающими их биотитовыми гранитами. К образованиям этого возраста, вероятно, могут быть отнесены и граниты, вскрытые на Каршинской площади, абсолютный возраст которых составляет 440 млн. лет.

2. Позднедевонско-среднекаменноугольный интрузивный комплекс. К нему принадлежат тоналиты, вскрытые бурением на площади Букбаш в северо-западном Прикарабогазье, габбро, биотитовые граниты и диориты Красноводска, гранитоиды Прикарабогазья и мыса Песчаный Южного Мангышлака (Попков и др., 1985).

В северо-восточном направлении на расстоянии 600 м от выхода массива на поверхность они вскрыты под юрскими отложениями буровыми скважинами до глубины 270 м от дневной поверхности. Широкое развитие подобных пород на юго-восточном крыле Кизылкиинской складки предполагается по данным магниторазведки, что подтверждается скважинами, пробуренными в 4 км юго-западнее Аман-Булака.

На Туаркырской брахискладке первоначально магниторазведкой, а затем буровыми работами установлена узкая полоса габброидных пород, простирание которой совпадает с направлением регионального западного разлома. По составу - это основные породы типа габбро, как правило, сильно катаклазированные, измененные, часто превращенные в грязно-зеленые рухляковые хлоритизированные разности. Среди них установлены также серпентинизированные пироксениты и диориты. Контакт их с отложениями юры и перми тектонический. В зоне разлома с глубины выведены на поверхность отдельные клинья и глыбы перми и магматических пород. В непосредственной близости от контакта с пермскими породами габбро превращены в типичный тектонит, среди которого в перетертой массе встречены обломки плотного габбро и пермских пород.

Допермский возраст основных и ультраосновных пород доказан бурением в районе г. Яшмовой, где под пестроцветными отложениями перми на глубину 160 и вскрыты габбриды. На контакте осадочных и магматических пород четко выделяется десятиметровая зона перемыва, сложенная остроугольными обломками пород, слабо сцементированных песчано-глинистым материалом, содержащим сильно разрушенные хлоритизированные рухляковые разности габброидов. Следы активного воздействия основных пород и ультрамафитов отсутствуют.

Е.А. Худобина (Худобина, 1961), детально изучавшая этот комплекс пород, пришла к выводу о первичном мономинеральном пироксенитовом составе ультраосновных пород, не содержащих полевых шпатов, об их древности и глубинности. Известные здесь протрузивные ультрабазиты, габброиды и зеленокаменные породы, обнажающиеся совместно с кремнисто-сланцевыми и яшмовыми образованиями могут быть отнесены к комплексу пород палеозойской океанической коры.

Наиболее молодыми в ряду позднедевонско-среднекзменноугольных интрузий являются микроклиновые граниты, вскрытые глубокими скважинами в пределах северо-западного и южного Прикарабогазья, возраст которых, по данным калий-аргонового метода, оценен как среднекаменноугольный.

3. Позднекамениоугольно-раннеиермский интрузивный комплекс объединяет в себя группу жильных пород, в которой выделяются образования кислого, среднего и основного состава. Кислые разности представлены дайками гранит-порфира, кварцевого порфира, сферолит-порфира, |фельзит-порфира и фельзита, окрашенными в красные и палевые тона. Детально изучены в Красноводском районе и на Большом Балхане в обнажениях, установлены также и на закрытых площадях по буровым данным. Возраст их определен по характеру взаимоотношения с более древними интрузиями, а также по немногочисленным определениям абсолютного возраста. Мощность жил не превышает 25-30 см.

Дайки основного и среднего состава рвут описанные выше разности. Окрашены в различные оттенки зеленого цвета. Мощность от нескольких сантиметров до 1-2, реже 3-4 м. Представлены плагиоклазовыми, диабазовыми и диоритовыми порфиритами. Наиболее молодыми из них являются дайки диабазового порфирита, секущие весь комплекс магматических пород.

Сравнительно редко встречаются дайки щелочного ряда. Отличаются интенсивно зеленым цветом и хорошей

В корах выветривания гранитоидов в пределах ХМАО-Югры открыты залежи газа на Пунгинском, Верхнекондинском месторождениях, нефти – на Назымском, Каменном и др. месторождениях, расположенных в западной части округа. При выветривании интрузивных пород кислого состава формируются коллекторы преимущественно трещинно-порового типа. Эти породы содержат в своем составе большое количество устойчивых к выветриванию минералов (кварц, калиевые полевые шпаты и др.), кроме того являются довольно хрупкими и формируют, как правило, значительные по мощности и хорошо проницаемые зоны дезинтеграции, где возможно накопление кварц-полевошпатовых песков [3].

Признаки нефтегазоносности гранитоидов отмечены в северной и центральной частях Березовского НГР. Притоки газа в скважинах Березовского, Похромского, Чуэльского, Деминского и др. газовых месторождений, как правило, получены при совместном испытании пласта П и доюрского основания. В пределах Шаимского мегавала залежи нефти и газа в основном приурочены к сланцевому обрамлению гранитоидов.

Связь температуры, продуктивности с гранитоидами и блоками фундамента

Изучаемая территория осложнена региональными глубинными разломами. Основными из них являются Восточно-Уральский, Лок-Лорский, Нялинско-Атлымский, Угут-Балык-Пимский, осложнённый многочисленными телами серпентинитов и Сибирско-Увальский субширотного простирания (рис.3).

Геотермические условия и нефтегазоносность недр тесно взаимосвязаны. Сведения о термометрии пластов могут использоваться как весомый критерий для прогноза и поиска месторождений нефти и газа в глубокопогруженных горизонтах [1].

Определённой точки зрения на связь температур, продуктивности отложений с гранитоидами и блоками фундамента не выработано. Относительно изучаемой территории можно сформулировать следующие предположения.

Области сочленения Восточно-Уральского и Угут-Балык-Пимского глубинных разломов повторяют форму Уват-Ханты-Мансийской зоны каледонской покровно-складчатой системы, образуя «клин» или треугольник. В.С. Сурков в этой области по геофизическим и буровым данным выделял зоны преимущественно антиклинорного строения, которые интерпретировались как останцы байкальских антиклинориев с гранитами в ядерной части. Зоны устойчивых поднятий внутри его (останцы байкальских антиклинориев) подверглись вторичной гранитизации и в последующее время испытывали относительное воздымание [4].

В зоне сочленения Восточно-Уральского и Угут-Балык-Пимского глубинных разломов отмечается наличие кольцевой структуры (рис.3А), образованной поднятиями II порядка: Красноленинским, Вехнеляминским, Туманным и замыкающим Сыньеганским. На всех этих структурах выявлены гранитоидные массивы, выходящие на предъюрскую поверхность. В.А. Волков сделал предположение, что эта кольцевая структура, вероятно, является крупным гранитным батолитом. [2].

В пределах Красноленинского свода и Салымского мегавала отмечена следующая закономерность: чем ближе к глубинному разлому, тем выше температуры в фундаменте и больше продуктивность отложений фундамента и осадочного чехла. На Красноленинском своде отмечается большой этаж нефтеносности, связанный с меловыми, юрскими и доюрскими отложениями; на Салымском мегавале нефтеносность приурочена к неокомским и вехнеюрским (баженовско-абалакский НГК) отложениям.

Максимальные температуры (115-146°С) в фундаменте отмечены в пределах Красноленинского свода (Каменная, Пальяновская площади), Туманного вала (Верхнеляминская, Мытаяхинская и др. площади), Салымского и Верхнесалымского мегавалов (рис.3Б). Гранитоидные массивы выделяются на всех перечисленных структурах. Приуроченность повышенного теплового потока к гранитным массивам, обусловленную как внедрением высокотемпературной магмы, так и генерацией радиогенного тепла, можно считать весьма вероятным событием. Эта закономерность осложняется временем внедрения гранитоидов, глубиной залегания гранитного массива под поверхностью доюрского основания и т.д. Как правило, чем моложе породы, слагающие массив, тем соответственно должна быть выше их температура.

Список литературы

1. Беккина С.М., Куриленкова Г.А, Сиднев А.В. Основные геологические критерии нефтегазоносности доюрского фундамента Фроловской мегавпадины Широтного Приобья (в порядке обсуждения) // Нефтяное хозяйство – 2009. - №10. – С. 38-40.
2. Волков В.А., Гончарова В.Н. Об истории тектонического развития территории Фроловской мегавпадины// Вестник недропользователя. - №27. - 2015. – С. 4-11.
3. Криночкин В.Г., Муртаев И.С., Савин В.Г. Перспективы нефтегазоносности доюрских отложений центральной части ХМАО-Югры // Пути реализации нефтегазового потенциала Ханты-Мансийского автономного округа (Материалы восьмой научно-практической конференции).- Ханты-Мансийск.- 2005.- Т. 1.- С. 112-119.
4. Сурков В.С. Основные этапы тектонического развития фундамента Западно-Сибирской плиты // Геология и геофизика Западной Сибири. Избранные труды. – СНИИГГиМС. - Новосибирск. – 2007. – 552 с.

МОРФОЛОГИЯ ЦИРКОНА В ЩЕЛОЧНЫХ СИЕНИТАХ И ЩЕЛОЧНЫХ ГРАНИТОИДАХ АРЫСКАНСКОГО И АСТЫГСКОГО МАССИВОВ ВОСТОЧНОЙ ТУВЫ

Хертек А.К.

Тувинский институт комплексного освоения природных ресурсов СО РАН

Введение

Изучение акцессорных минералов является целесообразным подходом к решению вопросов об условиях образования гранитоидов, которые сопровождаются месторождений полезных ископаемых. Одним из самых информативных индикаторов условий петрогенеза является циркон. В статье приводятся результаты морфологических исследований циркона из щелочных гранитоидов Арысканского массива и расположенных вблизи него щелочных гранитов Астыгского массива, с которым тоже связаны рудопроявления редких металлов (Zr, Nb, U, REE).

Краткая геологическая характеристика

Общей чертой обоих массивов является их приуроченность к зонам крупнейших разломов. Они расположены в зоне сочленения Восточно-Саянского и Кандатского разломов. Арысканский массив щелочных гранитоидов и близлежащее тело щелочных гранитов Астыг, со слабо проявленным оруденением, относятся к единому Арысканскому интрузивному комплексу. Их тектоническая позиция определяется приуроченностью к зонам зачаточных нижнепалеозойских рифтов и упоминавшихся выше региональных разломов (Алтухов и др. 1991).

Арысканский массив длиной 375 м вытянут вдоль разлома, ширина его колеблется от 15–20м в западной части до 70 м в восточной части. В разрезе тело имеет дайкообразную форму, с глубиной оно расширяется. Апикальная часть Арысканского массива сложен рудными пегматитами. Наиболее древними породами района месторождения являются гнейсы, кристаллические известняки и черные сланцы, условно датируемые протерозоем. Они со структурным несогласием перекрыты осадочно-метаморфической вулканогенной толщей нижнего и среднего кембрия. Вмещающими породами для щелочных гранитоидов являются габбро-диориты, биотитовые граниты и амфиболовые сиениты. Впервые полученные результаты Sm-Nd исследований показало возраст валовых проб и монофракций 460 млн. лет. (Никифоров и др. 2017)

Последовательность образования щелочных гранитоидов, по данным ранних исследователей (Костицын и др. 1998) и собственным наблюдением автора, была следующей. Первоначально возникли щелочные сиениты Арысканского массива. После них образовались граниты Астыгского массива, а затем произошло образование редкометальных гранитоидов Арысканского массива. Последние представлены 3 типами пород: а) мелко- среднезернистыми микроклин-альбитовыми директивными щелочными гранитами с астрофиллитом, которые не обнажены на поверхности и вскрыты штольневым горизонтом и серией скважин; б) средне- крупнозернистыми микроклин-альбитовыми щелочными гранитами, развитыми в апикальной части массива; в) альбит-рибекит-малаконовыми жилами пегматитов с зонами массивных альбититов. Последние два типа пород вскрыты поверхностными горными выработками (Хертек и др. 2016).

Морфотипы циркона

В монофракциях циркона по цвету, морфологическим и текстурным признакам выделено 2 типа. Первый тип – прозрачные, темно-розовые и коричневые, короткопризматические и призматические кристаллы циркона (рис. 1 а, б, в). Второй тип – дипирамидальные кристаллы от красновато-бурого до почти темно-коричневого цвета. Размер зерен колеблется от 50 до 300 мкм. Средние размеры 0,07–0,05 мм, К.уд. 1,2–1,4. Для второго типа циркона характерно неотчетливо зональное строение, насыщение микровключений и метамиктизация. При кристаллизации пород изменение таких габитусных форм свидетельствует о колебании кислотности, щелочности и температуры. Кристаллы имеющие формы призмы являются более высокотемпературными (более ранние) по отношению к дипирамидальным (Носырев И.В.1989; Прощенко Е.Г.1964; Червинская и др.1982; Pupin J. P.1980).

Циркон во всех разновидностях пород района месторождения встречается часто. Он является либо главным, либо акцессорным минералом. В малом количестве циркон встречается в щелочных сиенитах.

По морфологическим характеристикам кристаллы циркона в щелочных сиенитах относятся к первому типу. Это в основном бесцветные, призматические и короткопризматические зерна, в которых редко присутствуют метамиктные ядра. Также в щелочных сиенитах встречаются угловатые кристаллы циркона. Как правило, они окружены каймой светлого (в CL) гомогенного циркона без видимых структур роста. Наличие светлой каймы вокруг большинства зерен циркона свидетельствует о фрагментации циркона в процессе тектонических деформаций самих вмещающих пород.

В мелко-среднезернистых щелочных гранитах Арысканского массива и щелочных гранитах Астыгского массива циркон относится ко второму морфологическому типу. Он образует структуру неправильных зерен реже дипирамидальные кристаллы без граней призмы. Размер кристаллов циркона варьирует от 0,05 до 0,2 мм. Четко выделяется ядро. Оно, как правило, мутное и окрашено в бурые темно-бурые тона. Минерал в основном ассоциируется с альбитом, калиевым полевым шпатом, пироксеном. Мельчайшие включения редкоземельных, ториевых и урановых минералов диагностированы на электронном микроскопе с ЭДС спектрометром.

В средне-крупнозернистых гранитах и альбит-рибекит-малаконовых жил пегматитов Арысканского массива в основном встречается метамиктный циркон. Он представляет собой крупнозернистую форму с сильно искривленными и дипирамидальными гранями кристаллов, который относится ко второму типу. Цвет циркона изменяется от красновато-бурого до темно-серого. Размер его варьирует от 0,05 до 0,25 мм. Некоторые зерна обладают каемками, отличающимися более чистой и светлой окраской. Зерна циркона, как правило, сильно изотропизированы.

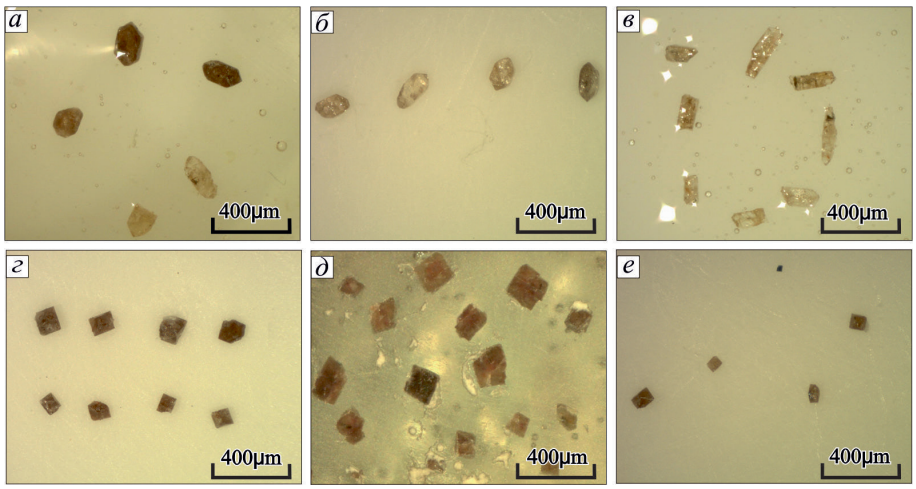


Рис. 1. Типичный циркон в щелочных сиенитах и щелочных гранитоидах Арысканского и Астыгского массивов. Размер зерен 100–300мкм. Короткопризматические (а, б); призматические – в, дипирамидальные (г – е).

Процесс его изотропизации можно проследить на отдельных зернах. Обычно начинающийся с центра зерна. В первую очередь, изотропия зерен, сказывается в значительном помутнении зерен резком снижении двупреломления от синевато-зеленых до серых, желтовато-серых тонов вплоть до полной изотропии зерен. Такая зональность циркона и неполная изотропия зерен свидетельствует о частичном неполном переходе циркона в метамиктное состояние.

При подробном исследовании циркона под микроскопом в средне-крупнозернистых щелочных гранитах и альбит-рибекит-малаконовых жилах было обнаружено, что почти все кристаллы циркона имеют центральную часть – «ядро» и апикальную часть – «кайму», граница между ними неровная, сильно корродированно. Центральная часть пересыщена радиоактивными минералами. Внутренняя неоднородность, может быть, свидетельствует о реликтовом цирконе. Рост циркона происходил быстро, с захватом большого количества включений. В работе Corfu (Corfu F et.al. 2003) более подробно обсуждается происхождение зональности роста и пришли к выводу, что эпизодический рост является результатом взаимодействий между стадией роста кристалла, степенью перенасыщения (расплава), природой жидкой межфазной границы кристалла, скоростями диффузии и состоянием окисления. Возможно, цирконы этой группы начали образовываться при больших скоростях роста в газоводонасыщенных условиях, что способствовало захвату многочисленных минеральных и газово-жидких включений. Внешние зоны чистые и почти не содержат включений, что, возможно связано с уменьшением скорости роста в спокойных условиях кристаллизации.

Вывод

Изученные цирконы из щелочных сиенитов показывают, что они магматического происхождения, а их морфология характерна для слабо дифференцированных пород. В щелочных гранитоидах Арысканского и Астыгского массивов, цирконы представляют общие морфологические черты, внутреннего строения, а также аналогический набор минеральных включений. В целом является свидетельством единого генезиса двух массивов.

Список литературы:

1. Алтухов Е.Н. Бородин Л.С., Брызгова Т.М. и др. геолого-геохимические критерии выявления редкометально-редкоземельных рудных районов и полей щелочногранитоидного типа. М.: Изд. ИМГРЭ, 1991. 109 с.
2. Костицын Ю.А., Алтухов Е.Н., Филина Н.П. Rb-Sr изохронное датирование щелочных гранитов Северо-Восточной Тувы. / Геология и геофизика, 1998, т. 39, № 7, С. 917–923.
3. Носырев И.В. Генерационный анализ акцессорного циркона / М: Наука, 1989. 204 с.
4. Никифоров А.В., Хертек А.К., Козловский А.М. Арысканское редкоземельное месторождение: первые результаты Sm-Nd изотопных исследований, Восточная Тува / Материалы III Всероссийской школы – конференции с международным – Кызыл: Тувинский институт комплексного освоения природных ресурсов СО РАН, 2017. С. 99–102.
5. Прощенко Е.Г. Отношение Zr/Hf и типоморфизм кристаллов циркона в щелочных гранитных пегматитах и альбититах / Минералогия и генетические особенности щелочных массивов. М.: Наука, 1964. С. 49–55.
6. Хертек А.К., Никифоров А.В., Козловский А.М. Минеральный состав и геохимические характеристики щелочных гранитоидов Арысканского редкометального (REE, Zr) месторождения, Восточная Тува / Шестая Российская молодежная конференция научно-практической Школы с международным участием «Новое в познании процессов рудообразования», М.: ИГЕМ РАН, 2016. С. 369–373.
7. Червинская А.Д., Тархов Ю. А. Морфология кристаллов акцессорного циркона и химические особенности материнских горных пород. Акцессорные минералы магматических и метаморфических пород / М.: Наука, 1982. С. 161–176.
8. Corfu F., Hanchar J.M., Hoskin P.W.O., Kinny P. Atlas ofzircon textures / Zircon. J.M. Hanchar, P.W.O. Hoskin (eds). Mineralogical Society of America, Spec. Publ. 2003 V. 53 P. 469–500.
9. Pupin J. P. Zircon and granite petrology / Contrib. Miner. Petrol. 1980. Vol. 73. P. 207–220.

О ВЛИЯНИИ МАГМАТИЗМА НА ФОРМИРОВАНИЕ МЕСТОРОЖДЕНИЙ ВОСТОЧНО-БАРЕНЦЕВСКОГО МЕГАБАССЕЙНА

Шипилов Э. В.

Полярный геофизический институт КНЦ РАН, Мурманск, Россия

Ключевые слова: *Восточно-Баренцевский мегабассейн, базальтоидный магматизм, сейсмические разрезы, антиклинальные структуры, месторождения углеводородов, тектономагматический фактор.*

Проявления базальтоидного магматизма отмечены геологическим картированием в различных стратиграфических подразделениях разрезов близлежащего сухопутного (материкового и островного) обрамления исследуемого региона. Фиксируются они в осадочных комплексах и морскими геолого-геофизическими работами. Наиболее широко проявился ареал, связанный с юрско-меловым тектономагматическим этапом. Распространение этих магматогенных образований отмечается на архипелагах Шпицберген и Земля Франца-Иосифа (ЗФИ) и окружающем их шельфе, в Южно - и Северо-Баренцевской впадинах, в троге Святой Анны и других районах. Очевидно, что изучение этого тектономагматического фактора имеет первостепенное значение для реконструкции истории геологического развития как самой окраины, так и раннего периода становления Арктического океана. Кроме того, это важно в плане его стрессового влияния на созревание $C_{орг}$ в нефтематеринских толщах, фазовый состав углеводородов, формирование ловушек и скопление в них флюидов (Шипилов, 2015; 2018).

На многочисленных сейсмических разрезах через Южно - и Северо-Баренцевскую впадины достаточно отчетливо наблюдается, что пакеты отражений, обусловленные интрузивными базальтоидными телами, проявляются во всем диапазоне отложений вплоть до нижнемелового комплекса. Экспозиция их сохранившихся от эрозии останцов (даек) наблюдается на поверхности дна моря вблизи архипелага ЗФИ. Геологическое подтверждение этому было получено после того, как скважиной Лудловской (на одноименном поднятии в центральной части Восточно-Баренцевского мегапрогиба) были вскрыты в разрезе триаса два самых верхних прослоя базальтов. Изучение показало, что силлы представлены преимущественно габбро-диабазовыми и габбро-долеритовыми породами. По химическому составу они аналогичны траповым образованиям архипелагов ЗФИ и Шпицберген.

Таким образом, по результатам анализа геологических и геофизических данных был оконтурен ареал Баренцеворской магматической провинции. В плане она имеет близкую к Т-образной конфигурацию с размахом с юга на север около 1300-1400 км, а с запада на восток (от Западного Шпицбергена до желоба Святой Анны) – около 1300 км. Интервал насыщения интрузиями разреза палеозойско-мезозойского осадочного чехла в депоцентре Восточно-Баренцевского бассейна может достигать 12-14 км. При этом следует отметить, что мощность пластовых тел базальтов изменяется от нескольких до десятков и сотен метров, судя по их обнажениям и результатам бурения параметрических скважин на островах архипелагов Шпицберген и ЗФИ. Число пластов базальтов может достигать здесь, по меньшей мере, нескольких десятков. Наиболее интенсивный и значительный по объему магматизм связывается с интервалом валанжин - апт (ранний мел). Учитывая общий объем и временной отрезок проявления магматизма (в целом от J_1 по K_1 включительно) он может рассматриваться как своеобразный природный «термоэлемент» периодически разогревавший осадочное выполнение бассейнов.

Среди открытых в Восточно-Баренцевском бассейне месторождений УВ особый интерес вызывает группа месторождений связанная с, так называемым, Лудловским (или Штокманско-Лунинским) порогом (поднятием), разделяющим Южно - и Северо-Баренцевскую впадины. Газоконденсатные месторождения Штокманское и Ледовое относятся к уникальным по запасам, а Лудловское газовое месторождение - к крупным. Продуктивными здесь являются юрские отложения.

Обычно, при характеристике и иллюстрации строения месторождения рассматриваются лишь комплексы пород, которые вскрыты бурением. Ниже залегающая часть разреза, уже после открытия месторождений, хотя и освещенная сейсморазведкой, чаще всего выпадает из поля зрения. А между тем, судя по материалам МОВ ОГТ, антиклинальные поднятия отмеченных выше месторождений не имеют соответствия в подстилающих допозднетриасовых отложениях. Опорные отражающие горизонты, относимые к средне-верхнепалезойскому комплексу под рассматриваемыми структурами, залегают субгоризонтально либо моноклинально. При этом видимого углового несогласия между верхнепалеозойскими и мезозойскими отложениями не зафиксировано. Вместе с тем на сводовых частях рассматриваемых структур отмечаются следы размыва, начавшегося, по меньшей мере, в конце юры – начале мела, а возможно, и несколько ранее. Это, вне сомнения, свидетельствует о том, что к позднеюрско-раннемеловому времени (неоком) в структурном плане эти поднятия уже начали намечаться и продолжали расти. Если это так, тогда можно говорить о том, что с этого периода началось формирование месторождений и заполнение ловушек УВ флюидами. Многочисленные тела силлов в триасовых отложениях под локальными структурами месторождений УВ – Штокманским, Ледовым и Лудловским образуют как бы подушкообразные раздувы за счет увеличения числа пластовых тел (рис. 1). Учитывая их число, суммарная мощность базальтовых прослоев примерно соответствует амплитуде рассматриваемых локальных поднятий по кровле юры. Бурением на Лудловской структуре были вскрыты два самых верхних пласта габбро-диабазов, залегающих в верхней половине разреза триаса. Как показало определение их абсолютного возраста K-Ar методом, они принадлежат разным генерациям: верхний силл имеет возраст 131-139 млн. лет (неоком: готерив-валанжин), а второй, расположенный на 143 метра ниже, - 159 млн. лет (оксфорд).

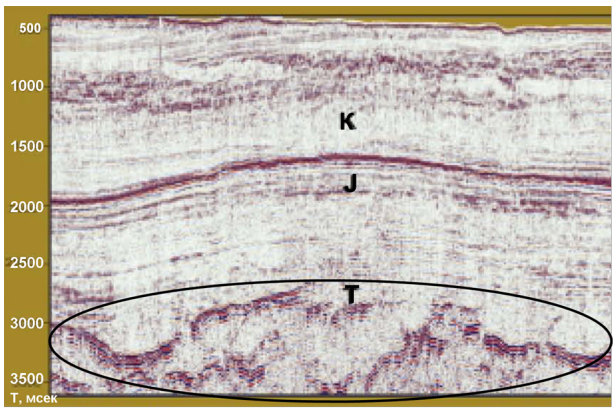


Рис. 1. Сейсмический «портрет» структуры Штокманского месторождения, иллюстрирующий поведение «аномальных» отражающих горизонтов, обусловленных интрузиями силлов (обведено овалом).

Мощность этих пластов базальтов оценивается соответственно 27 и 5 м. Новейшие определения абсолютного возраста образцов пород трапповой формации, отобранных нами на островах Земли Франца-Иосифа, $^{40}Ar/^{39}Ar$ методом показали более широкий разброс его значений – от 125 до 189 млн. лет (Шипилов, 2015; 2018).

Результаты сейсмостратиграфического анализа и определения возраста проявлений базальтоидного магматизма с большой вероятностью указывают на то, что формирование и рост локальных структур рассматриваемых месторождений УВ, впрочем, как и самого Штокманско-Лунинского порога, и процесс интрузивной магматической деятельности проистекали практически одновременно.

Изложенное позволяет заключить, что юрско-меловой тектономагматический этап имел определяющее значение в создании условий для размещения месторождений, а, следовательно, и УВ потенциала Лудловского (Штокманско-Лунинского) поднятия. И проведенный в этом отношении анализ геолого-геофизического материала позволяет высказать следующие соображения:

- для рассматриваемых антиклинальных структур, к которым приурочены гигантские газоконденсатные месторождения, причиной формирования являлся тектономагматический фактор, т.е. внедрение силлов;

- преобладающий фазовый состав флюидов указанных месторождений и их громадный по запасам потенциал, в отличие от других нефтегазоносных структур Баренцевоморского региона, во многом определялся влиянием термальных процессов базальтоидного магматизма на газогенерационные свойства вмещающих пород верхнепермско-триасового и более древнего возраста;



Рис. 2. Каналы миграции флюидов (отмечены стрелками) в базальтах о-ва Земля Александры (арх. Земля Франца-Иосифа). Фото Э.В. Шипилова.

- магмоподводящие каналы, разломы и зоны трещиноватости (рис. 2) могли служить активными каналами миграции УВ флюидов, участвуя в «подкачке» и заполнении структурных ловушек;

- учитывая широкое развитие пластовых тел базальтов в плане и по разрезу, они могут быть промежуточными флюидоупорами для УВ, что не исключает возможности обнаружения месторождений-спутников.

Список литературы:

1. Шипилов Э.В. Базальтоидный магматизм и проблема газоносности Восточно-Баренцевского мегабассейна // Арктика: экология и экономика. 2018. № 2 (30). С. 94-106.
2. Шипилов Э.В. Позднемезозойский магматизм и кайнозойские тектонические деформации Баренцевоморской континентальной окраины: влияние на распределение углеводородного потенциала // Геотектоника. 2015. № 1. С. 60-85.
3. Шипилов Э.В., Моссур А.П. Об аномальных сейсмических горизонтах в осадочном чехле Баренцева моря // Геотектоника. 1990. № 1. С. 90-97.
4. Шипилов Э.В., Мурзин Р.Р. Месторождения углеводородного сырья западной части российского шельфа Арктики: геология и закономерности размещения // Геология нефти и газа. 2001. № 4. С. 6-19.
5. Шипилов Э.В., Юнов А.Ю. О генезисе антиклинальных структур месторождений углеводородов восточной части Баренцева моря // ДАН. 1995. Т. 342. №. 1. С. 87-88.

ГИГАНТСКИЕ БАТОЛИТЫ ЦЕНТРАЛЬНОЙ АЗИИ И РОЛЬ МАНТИЙНЫХ ПЛЮМОВ В ИХ ФОРМИРОВАНИИ: ПО РЕЗУЛЬТАТАМ ИЗОТОПНЫХ (ND, PB) И ГЕОХИМИЧЕСКИХ ИССЛЕДОВАНИЙ

Ярмолюк В.В.[1], Козловский А.М.[1], Саватенков В.М.[2]

[1]*Институт геологии рудных месторождений петрографии, минералогии и геохимии РАН, Москва*
[2]*Институт геологии и геохронологии докембрия РАН, Санкт-Петербург*

В строении Центрально-Азиатского складчатого пояса выделяется ряд гигантских батолитов (Ангаро-Витимский, Хангайский и Хэнтей-Даурский), возникших в сходных геологических условиях в интервале между 300 и 200 млн лет (Fig.1). Для них характерны сравнительно узкие диапазоны формирования (~20-30 млн лет); соразмеримые объемы (~ 1000000 км^3); разнообразие составов пород, варьирующих от тоналитов и гранодиоритов до щелочных гранитов и сиенитов; широкое развитие синплутонических интрузий базитов; положение в центре зональных магматических ареалов, внешние зоны которых формировались под влиянием рифтогенных процессов.

Геологическая позиция батолитов определяется приуроченностью к молодым складчатым областям, что поднимает вопрос о природе столь масштабного плавления коры. Ответ на него строится на основе результатов изотопно-геохимических исследований Хангайского батолита.

Хангайский батолит является крупнейшим (> 150 тыс. км^2) скоплением гранитных плутонов, возникших в Центральной Азии в поздней перми – раннем триасе в интервале времени между 270 и 240 млн. лет назад. Батолит образует ядро более крупной Хангайской зонально построенной магматической области. В ее строении батолит обрамляется рифтовыми зонами с характерным для них магматизмом.

Батолит возник в пределах Хангайской группы докембрийских террейнов, включающей блоки раннедокембрийской коры (Дзабханский и Тарбагатайский), а также ранне- и поздненеопротерозойские комплексы Сонгинского блока. Осевая зона этой группы террейнов осложнена Хангайским позднепалеозойским прогибом. В строении батолита участвуют граниты нормального ряда щелочности, субщелочные граниты, более редкие щелочные граниты. Породы основного состава представлены синплутоническими телами, нередко с минглинговыми границами. В рифтовом обрамлении батолита развиты бимодальные базальт-трахириолитовые (комендитовые) ассоциации, а также массивы щелочных гранитоидов.

Геохимические характеристики большинства гранитоидов имеют сходство с составом континентальной коры. Гранитоиды рифтовых зон выделяются высокими содержаниями большинства микроэлементов. Субщелочные гранитоиды батолита (гранитоиды А-типа), обладающие повышенными значениями коэффициента агпаитности, имеют промежуточные характеристики между типичными гранитоидами батолита и гранитоидами рифтовых зон. Базиты рифтовых зон и, прежде всего, высоко-Ti базальты близки к базальтами OIB типа.

Геологические характеристики, а также результаты изотопно-геохимических исследований свидетельствуют об участии в образовании зонального магматического ареала как вмещающей континентальной коры, так и мантийных магм из зон рифтогенеза. Коровые субстраты плавления характеризуются неоднородностью изотопных составов Pb и Nd, связанной с их возрастными различиями.

Источники магматизма (Nd изотопная систематика). Изотопные составы Nd пород рифтовых зон и синплутонических базитов батолита тяготеют к диапазону $\varepsilon_{Nd}(260) = -1 - +3$. Высоко-Ti базальты группируются вблизи величины $\varepsilon_{Nd}(260) = +1 - +2$, отражающей состав мантийного источника магматизма. Параметры коры, вмещающей граниты, определяются значениями $\varepsilon_{Nd}(260) = -3 - -20$ и варьируют в зависимости от ее принадлежности тому или иному террейну. Гранитоиды батолита характеризуется составами промежуточными между составами вмещающей их коры и составом мантийного источника, что свидетельствует об их образовании в результате взаимодействия мантийных и коровых источников.

Источники магматизма (Pb изотопная систематика). Pb-Pb изотопные составы гранитов Хангайского батолита варьируют в зависимости от принадлежности пород тому или иному блоку Хангайской группы террейнов (Fig.2). На изотопных диаграммах $^{206}Pb/^{204}Pb$-$^{207}Pb/^{204}Pb$ и $^{206}Pb/^{204}Pb$-$^{208}Pb/^{204}Pb$ фигуративные точки образуют тренды, свидетельствующие об участии в их образовании коровых источников с разной геологической историей, а также ювенильного источника. Корреляция изотопных составов Pb и Nd показывает, что коровые источники гранитов характеризуются менее радиогенным изотопным составом Pb, а ювенильный более радиогенным. При этом параметры корового источника согласуются с модельными составами нижней коры (по модели Крамерса и Толстихина), определяемыми временем ее образования. Так, в образовании гранитоидов Тарбагатайского блока участвовала кора с изотопными характеристиками, соответствующими 2.5 млрд лет, источником гранитоидов Сонгинского блока стала нижняя кора, образовавшаяся 800 млн лет назад. Pb изотопная система нижней коры Дзабханского микроконтинента была сформирована в результате ряда корообразующих процессов, которые протекали на рубежах 2.5, 1.9, 0.7 и 0.5 млрд лет. В гранитоидах Хангайского прогиба ювенильный ($\varepsilon Nd > 0$) источник имеет менее радиогенный состав Pb по сравнению с коровым. Это позволило говорить, что кора Хангайского прогиба к моменту формирования батолита еще не испытала дифференциации на верхнюю и нижнюю.

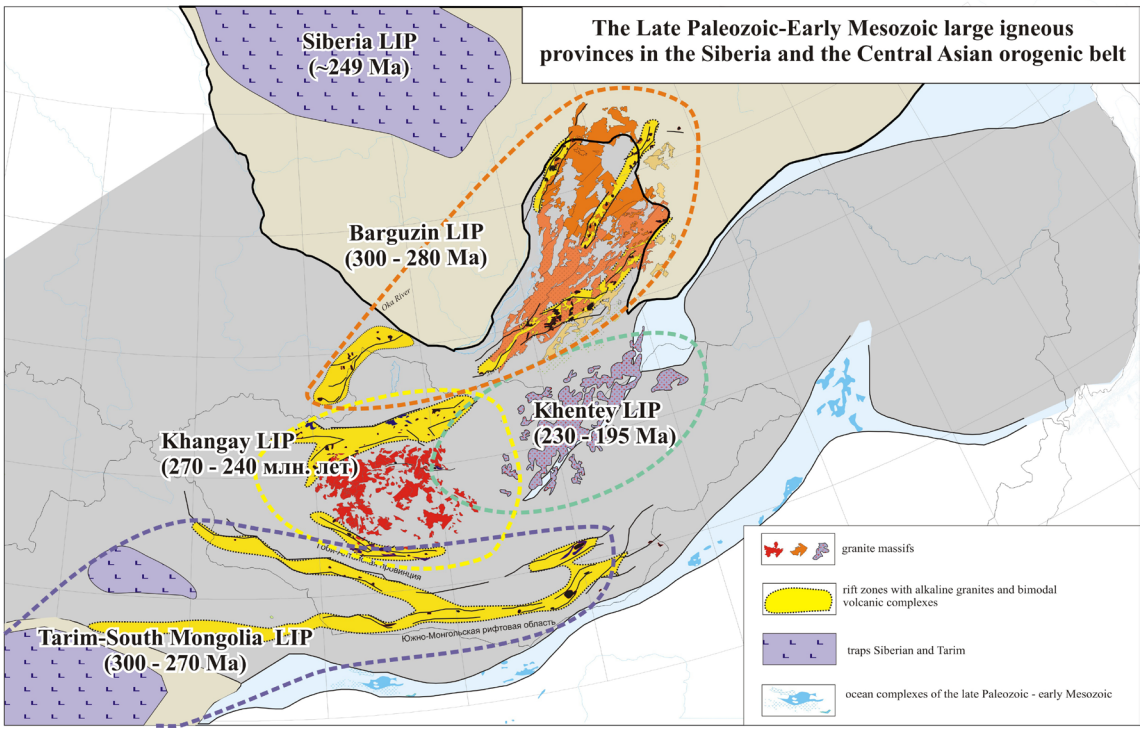


Fig.1. The Late Paleozoic-Early Mesozoic large igneous provinces in the Siberia and the Central Asian orogenic belt

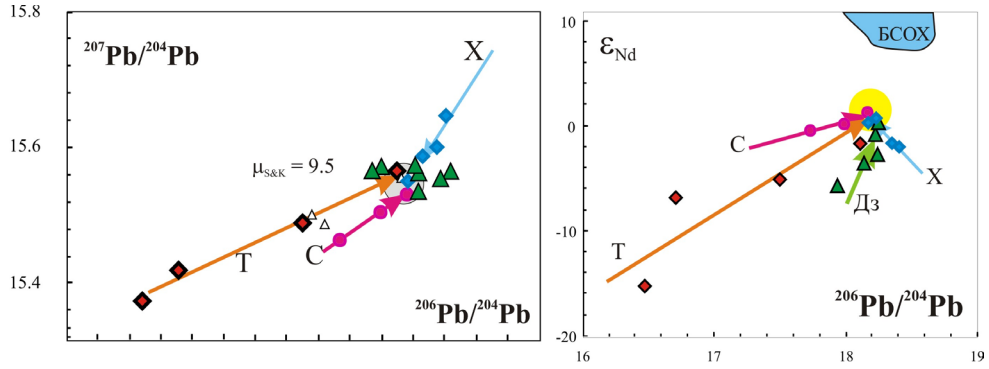


Fig.2. The Pb and Nd isotopic composition of the Khangai batholith granitoids. Blocks: C - Songinsky, T - Tarbagatai, Дз - Dzabkhansky, X - Khangaysky. The area of intersection of the variation lines determines the composition of the juvenile source.

Определены параметры ювенильного источника Хангайского батолита. На графике $^{206}Pb/^{204}Pb$ - $\varepsilon_{Nd}(260)$ он выделяется благодаря пересечению трендов вариаций составов гранитов из разных участков Хангайской группы террейнов. Его изотопные параметры: $^{206}Pb/^{204}Pb \sim 18.1$, $^{207}Pb/^{204}Pb \sim 15.5$ и $_{Nd} \sim +2$ соответствуют обогащённой мантии, обладающей более высоким отношением U/Pb и более низким отношением Sm/Nd по сравнению с деплетированной мантией.

Образование гигантских батолитов стало особенностью развития активной континентальной окраины Сибирского палеоконтинента в позднем палеозое и раннем мезозое. В то же время их связь с процессами рифтогенеза свидетельствует об участии в их формировании мантийных плюмов, которые, согласно изотопным данным несли характеристики обогащенной мантии. Предполагается, что столь масштабное и столь специфичное батолитообразование последовало за перекрытием активной континентальной окраиной позднепалеозойского Сибирского континента ряда горячих точек Палеоазиатского океана. В результате возникла крупнейшая анорогенная магматическая провинция, включавшая, помимо батолитов, трапповые области Тарима и Джунгарии и Центрально-Азиатскую рифтовую систему. Батолиты являются элементами ее структуры. Предполагается, что мантийные плюмы служили источником для пород щелочнобазитовых и щелочносалических ассоциаций в различных участках краевой части континента. В участках, подверженных стрессовым воздействиям, которые типичны для активных окраин, мантийные расплавы не поднимались выше низов коры. Их тепловое воздействие вызывало анатексис коры и, в конечном итоге, определяло образование батолитов.

Работа выполнена при финансовой поддержке РФФИ (проект 18-55-91004)

TABLE OF CONTENTS

Abersteiner A., Kamenetsky V. S., Goemann K., Kamenetsky M.
RECONSTRUCTING PRIMARY KIMBERLITE MELT COMPOSITIONS:
INSIGHTS FROM MELT INCLUSIONS *4*

Afonin I. V., Tishin P. A., Hitarova A. V., Ernst R. E., Kudamanov A. V.
PRELIMINARY DATA ON THE CONNECTION OF THE CA. 150 MA LIPS
WITH THE BAZHENOV FORMATION (WESTERN SIBERIA) *6*

Altermann W., Humbert F., de Kock M.
500 MILLION YEARS OF VOLCANISM AND SEDIMENTATION ON THE NEOARCHAEAN
TO EARLY PALAEOPROTEROZOIC KAAPVAAL CRATON: THE VENTERSDORP,
ONGELUK AND HEKPOORT LIPS *8*

Anosova M., Latyshev A., Khotylev A.
EMPLACEMENT OF BASHKIRIAN MEGAZONE RIPHEAN INTRUSIVE BODIES
(SOUTH URALS) BASED OF PALEOMAGNETIC DATA *10*

Ariskin A. A., Pshenitsyn I. V., Danyushevsky L. V., Fiorentini M. L., Nikolaev G. S., Kislov E. V.
THE EARLY STAGES OF SILICATE-SULFIDE IMMISCIBILITY AT CRYSTALLIZATION
OF PRIMITIVE CUMULATES IN LAYERED INTRUSIONS
(EXEMPLIFIED BY THE YOKO-DOVYREN MASSIF IN NORTHERN TRANSBAIKALIA)..... *11*

Artemieva I. M.
IS THERE A TRACK OF THE ICELAND PLUME BENEATH GREENLAND? *13*

Artemieva I. M.
KIMBERLITE MAGMATISM AND LITHOSPHERIC STRUCTURE *14*

Artemieva I. M., Dong S-W., Ernst R. E.
NEW ILP TASK FORCE (2019-2024): LITHOSPHERIC STRUCTURE AND MINERAL RESOURCES *15*

Bekker A.
GREAT OXIDATION EVENT IN THE EARLY PALEOPROTEROZOIC AND ITS IMPACT
ON THE SECULAR TRENDS IN SEDIMENT-HOSTED MINERAL DEPOSITS *16*

Belyaev V. A., Gornova M. A., Karimov A. A., Medvedev A. Y.
GEOCHEMISTRY OF SUPRA-SUBDUCTION, MORB AND OIB MAGMATISM IN OPHIOLITIC
FRAGMENTS OF THE DZHIDA TERRAIN (NORTHERN MONGOLIA AND SOUTHERN SIBERIA)..... *17*

Bethell E. M., Ernst R. E., Samson C.
LARGE IGNEOUS EVENTS IN THE ALPHA REGIO (V-32) QUADRANGLE, VENUS..... *18*

Chamberlain K. R., Khudoley A. K., Ernst R. E., Prokopiev A. V.
IMPROVED U-PB DATING OF THE CA. 450 MA SUORDAKH MAFIC EVENT
IN EASTERN SIBERIA WILL TEST WHETHER THIS IS THE MISSING LIP RELATED
TO END-ORDOVICIAN MASS EXTINCTION: PROGRESS REPORT..... *20*

Chen Y., Hedding D. W., Li G-J., Li X-M., Wu W-H.
CHEMICAL WEATHERING OF LESOTHO HIGHLANDS BASALT *21*

de Wit M. J., Linol B., Furnes H., Valashiya K.
PILLOW LAVAS OF KAROO LIP FORMED MANY LEAGUES UNDER THE SEA *22*

Diamond C. W., Ernst R. E., Zhang S-H., Lyons T. W.
MID-PROTEROZOIC LARGE IGNEOUS PROVINCES AND ENVIRONMENTAL PERTURBATION *24*

Djeutchou C., de Kock M.O., Wabo H.
A NEW KEY PALEOMAGNETIC POLE FOR THE ~1.8 GA KAAPVAAL CRATON: IMPLICATIONS FOR THE PALEOPROTEROZOIC APPARENT POLAR WANDER AND RECONSTRUCTIONS *24*

Egorova S. V., Stepanova A. V., Salnikova E. B., Larionova Y. O., Arzamastsev A. A., Samsonov A. V., Veselovskiy R. V.
2.5 GA MAFIC DYKES IN THE KOLA AND MURMANSK BLOCKS, EASTERN FENNOSCANDIA: COMPOSITION, PETROLOGY AND PALEOCONTINENTAL APPLICATION *25*

Ernst R. E.
FRONTIERS IN LARGE IGNEOUS PROVINCE RESEARCH *27*

Ernst R. E., Rodygin S. A., Grinev O. M.
DEVONIAN BIOTIC CRISES AND LINKS TO LIPS *29*

Fedoseev G. S.
EARLY-MIDDLE DEVONIAN KAZAKHSTAN-ALTAI-SAYAN IGNEOUS PROVINCE: FACIES AND TECTONIC ASPECTS *30*

Galinsky K., Zagorovsky Y., Kobylinsky D., Novikova L.
THE DENSITY OF FAULTS OVER TRIASSIC RIFTS AND PALEOZOIC BLOCKS AT DIFFERENT OIL AND GAS FIELDS IN WESTERN SIBERIA *32*

Gladkochub D. P., Donskaya T. V., Ernst R. E., Söderlund U., Kotov A. B., Mazukabzov A. M., Shokhonova M. N.
LATEST PALEOPROTEROZOIC DYKE SWARMS OF THE SIBERIAN CRATON *34*

Gogoleva S. S., Tomshin M. D., Kopylova A. G.
MIDDLE PALEOZOIC BASITES OF THE VILYUI PALEORIFT AS DERIVATIVES OF PLUME-MAGMATIC INTERACTION *35*

Golubeva I. I.
CARBONATITE FLUID-EXPLOSIVE SYSTEM OF THE MIDDLE TIMAN *37*

Gongalsky B. I., Krivolutskaya N. A., Belyatsky B. V., Dolgal A. S., Makarieva E. M.
GEOCHEMISTRY OF THE INTRUSIVE ROCKS OF THE SIBERIAN TRAP PROVINCE *38*

Gongalsky B. I., Krivolutskaya N. A., Safonov Y. G., Murashov K. Y., Timashkov A. N.
MULTI-DEPTH MAGMATIC CHAMBERS OF THE PALEOPROTEROZOIC ULTRAMAFIC-MAFIC MAGMATISM OF THE WESTERN PART OF THE ALDAN SHIELD. *40*

Goryachev N. A., Izokh A. E., Hoa T. T.
TECTONIC AND METALLOGENIC CONSEQUENCES OF THE EMEISHAN PLUME MANIFESTATION IN THE SOUTHEAST ASIA STRUCTURES *42*

Grinev O. M., Vorontsov A. A., Bogorodov A. A., Adylbaev R. R., Perfilova O. Y., Grinev R. O.
MORPHOTECTONICS AND THE EVOLUTION OF PLUM-RIFTOGENIC MAGMATISM OF GORYACHEGORSK VOLCANIC PLATEAU (KUZNETSKIY ALATAU) *43*

Grinev O. M., Vorontsov A. A., Ernst R. E., Perfilova O. Y.
PARAMETERS AND CLASSIFICATION OF THE DEVON RIFTOGENOUS ALTAI-SAYANSKY LIP *45*

Gumsley A., Sałacińska A., Knoper M., Mamuse A., Chew D., Söderlund U., Kamo S., Szopa K., Ernst R. E.
THE KALAHARI AND GRUNEHOGNA CRATONS, AND THEIR PLACEMENT WITHIN NEOPROTEROZOIC RODINIA, DEFINED BY NEW U-PB GEOCHRONOLOGY ON LARGE IGNEOUS PROVINCES *47*

Guryanov V. A., Ernst R. E.
ULKAN-BILYAKCHAN LIP (CA. 1.7 GA), SE SIBERIAN PLATFORM, ASSOCIATED TRIPLE JUNCTION RIFTING, AND ORE DEPOSITS *47*

Hollanda M. H. B. M., Macêdo Filho A. A., Oliveira A. L., Negri F. A., Archanjo C. J., de Castro D. L., Dantas A. R.
PRELIMINARY COMMENTS ON THE ELEMENTAL AND ISOTOPE GEOCHEMISTRY
OF THE EQUAMP MAFIC ROCKS (SOUTH AMERICA) *49*

Huang X-L., Yang F., Xu Y-G.
PLUME-RIDGE INTERACTION IN THE SOUTH CHINA SEA *50*

Huang Y., He C., Chen N-S., Xia B.
THE DIABASE SILLS IN THE OUTER ZONE OF THE EMEISHAN LARGE IGNEOUS
PROVINCE SW CHINA: PETROGENESIS AND TECTONIC IMPLICATIONS..... *51*

Izbrodin I. A., Doroshkevich A. G., Khubanov V. B., Rampilov M. O., Lastochkin E. I.
U-PB GEOCHRONOLOGY OF THE BAMBUYKA ALKALINE ROCKS (TRANSBAIKALIA, RUSSIA)..... *51*

Izokh A. E., Polyakov G. V., Hoa T. T.
SYNCOLLISION AND SYNSHEARING ULTRAMAFIC-MAFIC ASSOCIATIONS
OF WESTERN MONGOLIA, CHINE AND NORTH VIETNAM *52*

Jowitt S. M., Ernst R. E.
LARGE IGNEOUS PROVINCES (LIPS) AND METALLOGENY;
PUTTING LIP-RELATED MINERAL DEPOSITS INTO A LIP FRAMEWORK CONTEXT *54*

Kastek N., Ernst R. E., Cousens B. L.
GEOCHRONOLOGY, GEOCHEMISTRY AND EXTENT OF THE 1998 MA MINTO-POVUNGNITUK LIP *56*

Khawja S., Ernst R. E., Samson C.
DO TESSERA TERRAINS ON VENUS EXHIBIT EROSIONAL FEATURES? *58*

Khotylev A.O.
MESOPROTEROZOIC MAGMATISM OF THE WESTERN SLOPE OF THE SOUTHERN URALS *60*

Khromykh S. V., Izokh A. E., Kotler P. D., Semenova D. V.
EVOLUTION OF MANTLE MAGMATISM IN LATE PALEOZOIC IN EASTERN KAZAKHSTAN:
THE EVIDENCE OF TARIM LIP APPEARANCE *61*

Khubanov V. B., Tsygankov A. A., Burmakina G. N.
LATE PALEOZOIC WESTERN TRANSBAIKALIAN GRANITOID PROVINCE
(ANGARO-VITIM BATHOLITE): FORMATION STAGES AND GEODYNAMIC ENVIRONMENT..... *63*

Kingsbury C. G. , Altermann W., Ernst R. E., Söderlund U.
AN IDENTITY CRISIS SOLVED BY U-PB DATING: THE CASE OF THE CEDERBERG
DYKE SWARM, WESTERN AND NORTHERN CAPES, SOUTH AFRICA *64*

Kislov E. V., Kamenetskiy V. S., Vanteev V. V.
YOKO-DOVYREN MASSIF, IRKUTSK LIP: GENESIS OF CHROMITITES..... *66*

Kotler P. D., Khromykh S. V. , Oitseva T. A., D'yachkov B. A., Smirnov S. Z.
RARE METAL PEGMATITE MINERALIZATION OF THE KALBA RIDGE,
EASTERN KAZAKHSTAN - CONNECTION WITH THE TARIM LIP *68*

Krylova V. A., Gertner I. F., Gutierrez-Alonso G.
ORIGIN OF ULTRAMAFIC XENOLITHS FROM CANARY ISLANDS *70*

Latyshev A. V., Veselovskiy R. V., Fetisova A. M., Krivolutskaya N. A., Ulyakhina P. S.,
Pasenko A. M, Pavlov V. E.
PALEOMAGNETISM OF THE PERMIAN-TRIASSIC INTRUSIONS OF THE NORILSK REGION:
IMPLICATIONS OF THE SIBERIAN TRAPS EMPLACEMENT AND THE CU-NI-PGE DEPOSITS ORIGIN *71*

Li G-J., Börker J., Chen Y., Hedding D. W., Hartmann J., Li X-M., Romero-Mujalli G., Wu W-H.
CHEMICAL WEATHERING OF LARGE IGNEOUS PROVINCES:
AGE AND TEMPERATURE DEPENDENCE *72*

Liu J-M., Zhang S-H., Zhao Y., Li J-B.
METALLOGENY OF LIPS FROM SIBERIAN OF RUSSIA AND EMEISHAN OF CHINA..... *73*

Lu G-M., Wang W., Ernst R. E., Söderlund U.
PETROGENESIS OF PALEO-MESOPROTEROZOIC MAFIC ROCKS
IN THE SOUTHWESTERN YANGTZE BLOCK OF SOUTH CHINA:
IMPLICATIONS FOR TECTONIC EVOLUTION AND PALEOGEOGRAPHIC RECONSTRUCTION *75*

Lubnina N., Tarasov N.
EARLY PALEOPROTEROZOIC LARGE IGNEOUS PROVINCE
OF THE KARELIAN PROTOCRATON: PALEOMAGNETIC ASPECT *76*

Lyons T. W., Diamond C. W.
A RISE IN GLOBAL OXYGEN AT CA. 800 MA:
TECTONIC CAUSES AND BIOLOGICAL CONSEQUENCES *77*

MacLellan L. M., Ernst R. E.
THE DERCETO-KALLISTOS LIP EVENT, LADA TERRA, VENUS *78*

Manankov A.V.
FEATURES OF COMPOSITION AND PLASTICITY OF TWO ASTENOSPHERES OF PLANET EARTH *80*

Manankov A.V.
TRIGGER EFFECTS OF GEODYNAMICS AND GLOBAL TOXICATION OF THE ATMOSPHERE *81*

Manankov A.V.
TWO GENETIC TYPES OF METALLOGENIC ZONES IN WAVE GEODYNAMICS *83*

Marfin A.E., Yakich T. Yu., Abersteiner A., Ivanov A. V., Kamenetsky V. S.
SULFIDES OF IVAKINSKY FORMATION BASALTS, NORIL'SK ORE DISTRICT: REVISITED *85*

Mikhailenko D., Korsakov A., Golovin A., Rezvukhin D., Aulbach S.
HIGH-FERROUS OLIVINE IN ECLOGITE FROM KIMBERLITE PIPE UDACHNAYA:
METASOMATIC TRANSFORMATION OF ECLOGITE TO PYROXENITE-PERIDOTITE *87*

Muedi T., de Wit M. J., Linol B., Nengovhela V., Dhansay T.
SURFACE AND SUBSURFACE DESCRIPTIONS OF THE EARLY JURASSIC
KAROO DOLERITES: TOWARD A COMPREHENSIVE UNDERSTANDING
OF THE EMPLACEMENT MECHANISM AND POSSIBLE GAS MIGRATION..... *88*

Muedi T., MacLennan S., Schoene B., Linol B., de Wit M. J.
AGE-VARIATIONS OF DOLERITES INTRUDED AT DIFFERENT ELEVATIONS ACROSS THE KAROO LIP..... *88*

Mustafayev A. A., Gertner I. F., Serov P. A.
NEW SM-ND ISOTOPIC DATA ON THE UNIVERSITY ALKALINE-GABBRO MASSIF
(NE KUZNETSK ALATAU) *90*

Myshenkova M. S., Veselovskiy R. V., Zaitsev V. A., Thomson S., Latyshev A. V., Zakharov V. S.
THERMAL EVOLUTION OF THE NORTHERN SIBERIAN TRAPS LIP AS INFERRED
FROM APATITE FISSION TRACK DATING OF THE GULI PLUTON..... *93*

Okrugin A. V., Ernst R. E., Beryozkin V. I., Popov N. V.
LATE PRECAMBRIAN MAFIC DYKE SWARMS OF THE ALDAN SHIELD
AND THEIR IMPORTANCE IN ORE-MAGMATIC PROCESSES *94*

Okrugin A. V., Yakubovich O. V., Ernst R. E., Druzhinina Zh.Y.
PLATINUM-BEARING PLACERS OF THE SIBERIAN PLATFORM
AND THEIR POTENTIAL LINKS WITH LARGE IGNEOUS PROVINCES *96*

Okunlola O.
ANOROGENIC MAGMATISM OF NIGERIA: CHARACTERISTICS,
AGE TRENDS AND TECTONO STRUCTURAL CONSTRAINS *98*

Pavlov V. E., Veselovskiy R. V., Latyshev A. V., Fetisova A. M.
APPLICATION OF PALEOMAGNETIC RECORD OF GEOMAGNETIC
SECULAR VARIATIONS FOR CONSTRAINING THE RATE AND DURATION
OF VOLCANISM IN LARGE IGNEOUS PROVINCES *98*

Pavlov V. E., Tikhomirov P. L., Pasenko A. M, Gavryushkin D. A., Lebedev I. E.
PROSPECTS OF PALEOMAGNETIC RESEARCHES OF THE OKHOTSK-CHUKOTKA
VOLCANIC BELT FOR DECIPHERING THE TECTONIC HISTORY OF NORTHEASTERN ASIA
AND FOR STUDYING THE EVOLUTION OF THE EARTH MAGNETIC FIELD *99*

Pearce J. A., Ernst R. E., Rogers C., Peate D. W.
LIP PRINTING: A GEOCHEMiCAL PROXY APPROACH
TO THE CHARACTERIZATION OF LARGE IGNEOUS PROVINCES *99*

Pisarevsky S. A.
LIPS AND SUPERCONTINENT RECONSTRUCTIONS *100*

Polyansky O. P., Prokopiev A. V., Koroleva O. V., Babichev A. V.
THE MIDDLE PALAEOZOIC STAGE OF MAFIC MAGMATISM AND EVOLUTION
VILYUI PALEORIFT BASIN (EASTERN SIBERIAN PLATFORM): PLUME- OR EXTENSION-RELATED? *102*

Popov Yu. V., Grinev O. M.
GEOLOGY, MATERIAL COMPOSITION OF BREEDS AND ISSUES
OF GEODYNAMICS OF MATYSKEN BASIT-HYPERBASITE MASSIF (KORYAKIA) *104*

Puchkov V. N.
LIP RECORD OF THE URALS: RECOGNIZING PLUMES IN A FOLD BELT LIPS *106*

Rudmin M., Mazurov A.
POTENTIAL LINK BETWEEN UPPER CRETACEOUS LIPS
AND FORMATION OF OOIDAL IRONSTONE DEPOSIT *108*

Safonova I., Maruyama S., Perfilova A.
PACIFIC-TYPE CONVERGENT MARGINS AND MANTLE PLUMES *110*

Salnikova E. B., Stifeeva M. V., Kotov A. B.
LIP'S TIMING - WHAT'S NEW *113*

Samal A. K., Srivastava R. K., Ernst R. E., Söderlund U.
AN UPDATED OVERVIEW ON THE LARGE IGNEOUS PROVINCE (LIP)
RECORD OF THE INDIAN SHIELD *113*

Samsonov A. V., Stepanova A. V., Salnikova E. B., Larionova Y. O., Arzamastsev A. A.,
Egorova S. V., Veselovskiy R. V., Erofeeva K. G., Stifeeva M. V.
NEOARCHEAN MAFIC DYKE SWARMS IN THE MURMANSK CRATON:
PETROLOGY, TECTONIC SETTING, AND PALEOCONTINENTAL SIGNIFICANCE *115*

Savelev A. D., Khudoley A. K.
THE ORDOVICIAN MAGMATIC EVENTS IN THE SIBERIAN PLATFORM
AND MONGOLIAN TERRAINS – ARE THEY RELATED? *116*

Sedaeva K.M.
GLOBAL STRATALEVEL OF INCREASED AND INTENSIVE ORE-, OIL-, GAS-
AND SHALE FORMATION AS A CONSEQUENCE OF THE MANIFESTATION
OF GALACTIC, TECTONOMAGMATIC AND BIOTIC EVENTS AT THE TURN OF DEVONIAN
AND CARBONIFERIOUS PERIODS..... *118*

Serov P. A., Bayanova T. B., Kunakkuzin E. L., Steshenko E. N
ISOTOPIC ND-SR HETEROGENEITY NEAR THE ORE-BEARING ZONES OF "TERRASA"
DEPOSIT (MONCHEGORSK PGE-CR-CU-NI ORE REGION, KOLA PENINSULA)..... *120*

Shaldybin M. V., Kondrashova E. S.
THE JURASSIC GLOBAL VOLCANIC EVENTS RECORDED IN SEDIMENTARY
BLACK SHALE DEPOSITS (BAZHENOV FORMATION, WEST SIBERIA)..... *122*

Shapovalova M., Tolstykh N., Shelepaev R.
CU-NI-PGE MINERALIZATION OF MAFIC-ULTRAMAFIC INTRUSIONS
OF THE KHANGAY UPLAND (MONGOLIA) *124*

Sharkov E., Bogina M., Chistyakov A.
THREE MAJOR TYPES OF THE LIPS IN THE EARLY PRECAMBRIAN:
EVDENCE FROM THE EASTERN FENNOSCANDIAN SHIELD *126*

Shen J.
MERCURY CHEMICAL SPECIATION IN SEDIMENTS AND THEIR APPLICATIONS *128*

Silantyev S.
NEOGENE WITHINPLATE MAGMATISM OF DE LONG ISLANDS:
FOOTPRINT OF YOUNG MANTLE PLUME OF THE EASTERN ARCTIC BASIN *128*

Simonov V. A., Vasiliev Y. R., Kotlyarov A. V., Prihodko V. S.
ULTRABASIC IGNEOUS PROVINCE OF THE SIBERIAN PLATFORM:
PHYSICAL AND CHEMICAL CONDITIONS OF INTRUSIVE COMPLEXES FORMATION *130*

Stepanova A. V., Samsonov A. V., Salnikova E. B., Arzamastsev A. A., Egorova S. V.,
Larionova Yu. O., Veselovskiy R. V., Erofeeva K. G., Stifeeva M. V.
PRECAMBRIAN MAFIC DYKE SWARMS IN KOLA-MURMANSK AND KARELIAN PROVINCES,
EASTERN FENNOSCANDIA: BAR-CODE CORRELATIONS AND IMPLICATIONS FOR TECTONIC
RECONSTRUCTIONS *132*

Su X-D., Peng P., Wang C., Sun F-B., Zhang Z-Y., Zhou X-T.
PETROGENESIS OF TWO GENERATIONS OF SILLS IN THE XUHUAI RIFT:
IMPLICATIONS FOR THE EVOLUTION OF THE ~925-890 MA LARGE IGNEOUS PROVINCE
IN SE MARGIN OF THE NORTH CHINA CRATON..... *134*

Sedki T., Ali S., Mohamed H. A.
GEOCHEMICAL CHARACTERIZATION OF THE SOL HAMED NEOPROTEROZOIC
OPHIOLITIC SERPENTINITES, SOUTHERN EASTERN DESERT, EGYPT *136*

Thybo H.
INTERNATIONAL LITHOSPHERE PROGRAM (ILP) *138*

Thybo H., Artemieva I. M.
MAGMATIC UNDERPLATING IN CONTINENTAL LITHOSPHERE *138*

Tolstykh N., Zhitova L., Shapovalova M., Chayka I.
EVOLUTION OF SULPHIDE MELT IN THE LOW-SULPHIDE HORIZON OF THE NORIL'SK-1 DEPOSIT *139*

Tomshin M. D., Kopylova A. G., Vasilyeva A. E.
PETRO-GEOCHEMICAL COMPARISON OF TRAPS FROM THE NORTHEASTERN TUNGUSKA SYNECLISE AND THE SOUTHWESTERN OLENEK UPLIFT *141*

Travin A. V., Vladimirov A. G., Tsygankov A. A., Khanchuk A. I., Ernst R. E., Murzintsev N. G., Mikheev E. I., Khubanov V. B
THERMOCHRONOLOGY OF THE ANGARA-VITIM GRANITOID BATHOLITH AS A PROXY INDICATOR OF PLUME EVENTS?. *143*

Tsygankov A. A., Khubanov V. B., Burmakina G. N.
GIANT GRANITOID BATHOLITES OF CENTRAL AND NORTHEASTERN ASIA - A NEW TYPE OF SILICEOUS LARGE IGNEOUS PROVINCE (SLIP)?..... *145*

Turkina O.
MESOARCHEAN BIMODAL VOLCANICS OF SOUTHWESTERN SIBERIAN CRATON, ARE THEY RELATED TO MANTLE PLUME ACTIVITY? *146*

Turkina O. M., Kalugin V. M., Shevko A. Y., Gora M. P.
GEOCHEMISTRY OF BASALTS OF THE MOKULAEVSKY FORMATION (SIBERIAN TRAP): MANTLE SOURCES AND MAGMA EVOLUTION IN INTERMEDIATE MAGMA CHAMBER..... *148*

Veselovskiy R. V., Samsonov A. V., Stepanova A. V., Salnikova E. B., Larionova Y. O., Travin A. V., Arzamastsev A. A., Egorova S. V., Erofeeva K. G., Stifeeva M. V., Shcherbakova V. V., Shcherbakov V. P., Zhidkov G. V., Zakharov V. S.
NEW 1.86 GA EASTERN MURMAN SILL PROVINCE, THE KOLA PENINSULA: PALEOMAGNETISM, GEOCHRONOLOGY AND PETROLOGY..... *151*

Veselovskiy R. V., Thomson S. N., Arzamastsev A. A., Botsyun S. B., Travin A. V., Yudin D. S., Samsonov A. V., Stepanova A. V., Myshenkova M. S.
THERMOCHRONOLOGY AND EXHUMATION HISTORY OF THE NORTHEASTERN FENNOSCANDIAN SHIELD BEFORE AND AFTER THE KOLA DEVONIAN ALKALINE LIP FORMATION: EVIDENCE FROM 40Ar/39Ar AND APATITE FISSION TRACK DATA *152*

Vetrov E. V., Uvarov A. N., Vishnevskaya I. A., Vetrova N. I., Zhimulev F. I., Chervyakovskaya M. V.
ORDOVICIAN AND DEVONIAN STAGES OF VOLCANISM IN THE SW TUVA: SYNTHESIS OF GEOCHEMICAL, GEOCHRONOLOGICAL AND ISOTOPE-GEOCHEMICAL DATA..... *153*

Vorontsov A. A., Perfilova O. Y., Grinev O. M., Ernst R. E.
ORDOVICIAN–DEVONIAN VOLCANISM IN THE NORTH OF THE ALTAI–SAYAN FOLDED AREA (GEOLOGY, GEOCHEMISTRY, GEODYNAMICS) *155*

Vrublevskii V. V., Doroshkevich A. G., Izokh A. E.
MAIN STAGES OF THE PALEOZOIC ALKALINE MAGMATISM IN THE WESTERN CAOB: ISOTOPE AGE AND GEOCHEMISTRY OF PLUTONIC ROCKS ACCORDING THE PERIODIC MANTLE PLUMES ACTIVITY *157*

Wabo H., de Kock M., Belyanin G.
PALEOMAGNETIC CONSTRAINTS ON DURATION OF THE BUSHVELD LARGE IGNEOUS PROVINCE..... *159*

Wang Q.
SEISMIC PROPERTIES OF THE LOWER CRUST BENEATH LARGE IGNEOUS PROVINCES *160*

Wang W., Lu G-M., Cawood P., Ernst R. E., Huang S-F., Xue E-K.
LATE PALEO- TO EARLY MESOPROTEROZOIC MAFIC MAGMATISMIN SW YANGTZE BLOCK: A MANTLE PLUME ASSOCIATED WITH NUNA BREAKUP? *161*

Wu H-X., Zhang F-Q., Dilek Y., Li P., Chen X-X., Lin X-B., Cheng X-G., Chen H-L.
A POSSIBLE PLUME HEAD LOCATION OF THE PERMIAN LARGE IGNEOUS PROVINCE: CONSTRAINTS FROM MAFIC SILL PROVINCE AND DOMING STRUCTURE IN NW TARIM BLOCK..... *162*

Yong P-L.
A COMPARATIVE STUDY OF TWO LARGE IGNEOUS PROVINCES
(SIBERIA, EMEI MOUNTAIN) IN RUSSIA AND CHINA.....*162*

Youbi N., Söderlund U., Ernst R. E., Ait Lahna A., Gong Z., Evans D., Wen B., Jing X-Q., Ait Malek M., Palassia M., Boumehdi M. A., Bensalah M. K., Admou H., Ikenne M., Cousens B., El Bahat A.
U-PB BADDELEYITE AGE OF A NE TRENDING DOLERITIC DYKE SWARM
IN THE TAGRAGRA OF AKKA INLIER: ADDITIONAL CONSTRAINTS
ON THE CA. 1416-1360 MA MESOPROTEROZOIC MAGMATIC EVENT(S)
IN THE ANTI-ATLAS OF MOROCCO (WEST AFRICAN CRATON) *164*

Youbi N., Söderlund U., Ernst R. E., Ait Malek M., Barzouk A., Ait Lahna A., Palassia M., Gong Z., Evans D., Wen B., Jing X-Q., Boumehdi M. A., Ikenne M., Bensalah M. K., Admou H., Bajddi A., Maacha L.
CA. 1.65 GA MAFIC SILLS EMPLACED INTO THE QUARTZITE OF JBEL LKEST
FROM KERDOUS INLIER, ANTI-ATLAS, WEST AFRICAN CRATON, MOROCCO:
ADDITIONAL EVIDENCE THAT THE BASAL PART OF TAGHDOUT GROUP
IS NEARLY 1 GA OLDER THAN PREVIOUSLY THOUGHT *165*

Zagorovsky Y., Galinsky K., Kobylinsky D., Ufelman Z.
WESTERN SIBERIA - THE LAND OF NATURAL GAS, RIFTS
AND VOLCANOES SINCE TRIASSIC TO THIS DAY *166*

Zhang C-L., Li H-K., Ernst R. E.
CA.890 MA LIP FRAGMENT IN SOUTHERN TARIM, NW CHINA *168*

Zhang N., Ma C-Q.
PETROLOGY OF CALC-ALKALINE LAMPROPHYRES IN THE EAST KUNLUN
OROGENIC BELT, NORTHERN TIBET PLATEAU AND ITS IMPLICATIONS FOR MAGMA HISTORY *169*

Zhang Q-Q., Zhang S-H., Zhao Y.
IDENTIFICATION OF AN EARLY NEOPROTEROZOIC GABBRO SILL FROM
THE GUYANG AREA IN THE NORTHWESTERN NORTH CHINA CRATON:
IMPLICATIONS FOR BREAKUP OF THE NCC IN THE RODINIA SUPERCONTINENT *170*

Zhang S-H., Shui G-H., Hu G-H., Zhang Q-Q., Zhao Y., Pei J-L.
POTENTIAL ENVIRONMENTAL EFFECT OF LARGE-SCALE CA. 1.32 GA MAFIC SILL
EMPLACEMENT IN THE NORTH CHINA AND NORTHERN AUSTRALIAN CRATONS *172*

Zhao Y., Wang W., Pei J-L., Cai Y-H., Zhang S-H.
NORTH CHINA CRATON IN NUNA/COLUMBIA SUPERCONTINENT DURING
THE LATE PALEOPROTEROZOIC: IMPLICATIONS FROM THE LARGE IGNEOUS PROVINCE.....*173*

Zhao J-H.
TEMPORAL EVOLUTION OF THE PANXI-HANNAN ARC IN SOUTH CHINA *174*

Zhong Y-F., Wang L-X., Zhao J-H.
PARTIAL MELTING OF AN ANCIENT SUB-CONTINENTAL LITHOSPHERIC MANTLE
IN THE EARLY PALEOZOIC INTRACONTINENTAL REGIME AND ITS CONTRIBUTION
TO PETROGENESIS OF THE COEVAL PERALUMINOUS GRANITES IN SOUTH CHINA *175*

Арбузов С. И., Вергунов А. В.
ВУЛКАНОГЕННАЯ ПИРОКЛАСТИКА КАК ФАКТОР ФОРМИРОВАНИЯ
NB(TA)-ZR(HF)-REE-GA ОРУДЕНЕНИЯ В УГЛЯХ (НА ПРИМЕРЕ СИБИРИ).....*177*

Буслов М. М., Куликова А. В., Рубанова Е. С., Семенова Д. В.
ПОЗДНЕДОКЕБРИЙСКО-ДЕВОНСКИЙ ПЛЮМОВАЫЙ МАГМАТИЗМ
АЛТАЕ - САЯНСКОЙ СКЛАДЧАТОЙ ОБЛАСТИ: ЭВОЛЮЦИЯ ГОРЯЧЕЙ ТОЧКИ *179*

Добрецов Н. Л., Жмодик С. М., Лазарева Е. В., Толстов А. В., Белянин Д. К.,
Сурков О. Н., Добрецов Н. Н., Родионов Н. В.
U/Pb ВОЗРАСТ СФЕНОВ, ПЕТРОХИМИЧЕСКИЕ, МИНЕРАЛОГИЧЕСКИЕ И ГЕОХИМИЧЕСКИЕ
ОСОБЕННОСТИ ЩЕЛОЧНЫХ ПОРОД МАССИВА БОГДО (АРКТИЧЕСКАЯ СИБИРЬ) *181*

Мороз М. Л., Белова Е. В., Тугарева А. В., Чернова Г. А.
ГРАНИТОИДНЫЙ МАГМАТИЗМ НА ТЕРРИТОРИИ ФРОЛОВСКОЙ МЕГАВПАДИНЫ
ЗАПАДНО-СИБИРСКОЙ НЕФТЕГАЗОНОСНОЙ ПРОВИНЦИИ..... *183*

Попков В. И.
ПАЛЕОЗОЙСКИЙ БАЗИТОВЫЙ МАГМАТИЗМ СЕВЕРНОГО УСТЮРТА. *185*

Попков И. В., Попков В. И.
ГРАНИТОИДНЫЕ ИНТРУЗИВНЫЕ КОМПЛЕКСЫ ЮГО-ЗАПАДА ТУРАНСКОЙ ПЛИТЫ..... *187*

Хертек А. К.
МОРФОЛОГИЯ ЦИРКОНА В ЩЕЛОЧНЫХ СИЕНИТАХ И ЩЕЛОЧНЫХ
ГРАНИТОИДАХ АРЫСКАНСКОГО И АСТЫГСКОГО МАССИВОВ ВОСТОЧНОЙ ТУВЫ *189*

Шипилов Э. В.
О ВЛИЯНИИ МАГМАТИЗМА НА ФОРМИРОВАНИЕ МЕСТОРОЖДЕНИЙ
ВОСТОЧНО-БАРЕНЦЕВСКОГО МЕГАБАССЕЙНА *191*

Ярмолюк В.В., Козловский А.М., Саватенков В.М.
ГИГАНТСКИЕ БАТОЛИТЫ ЦЕНТРАЛЬНОЙ АЗИИ И РОЛЬ МАНТИЙНЫХ ПЛЮМОВ
В ИХ ФОРМИРОВАНИИ: ПО РЕЗУЛЬТАТАМ ИЗОТОПНЫХ (ND, PB)
И ГЕОХИМИЧЕСКИХ ИССЛЕДОВАНИЙ 193

LARGE IGNEOUS PROVINCES THROUGH EARTH HISTORY: MANTLE PLUMES, SUPERCONTINENTS, CLIMATE CHANGE, METALLOGENY AND OIL-GAS, PLANETARY ANALOGUES (LIP – 2019)

Abstract volume of the 7 International Conference
Tomsk, Russia, 28 August – 8 September 2019

КРУПНЫЕ ИЗВЕРЖЕННЫЕ ПРОВИНЦИИ В ИСТОРИИ ЗЕМЛИ: МАНТИЙНЫЕ ПЛЮМЫ, СУПЕРКОНТИНЕНТЫ, КЛИМАТИЧЕСКИЕ ИЗМЕНЕНИЯ, МЕТАЛЛОГЕНИЯ, ФОРМИРОВАНИЕ НЕФТИ И ГАЗА, ПЛАНЕТЫ ЗЕМНОЙ ГРУППЫ (КИП – 2019)

Тезисы VII Международной конференции
Томск, Россия 28 августа – 8 сентября 2019

Technical editors: Polezhaeva T.V., Tishin P.A., Mishenina Y.A.

Технические редакторы: Полежаева Т.В., Тишин П.А., Мишенина Ю.А.

Издательство Томского ЦНТИ. Бумага офсетная № 1. Печать офсетная.
Подписано в печать 26.08.2019 г. Заказ № 589. Тираж 150 экз.
Отпечатано в Томском ЦНТИ.
Россия, 634021, г. Томск, пр.Фрунзе, 115/3. Тел. (8-3822) 26-31-69